ISSN 1948-5204 (online)

World Journal of *Gastrointestinal Oncology*

World J Gastrointest Oncol 2022 November 15; 14(11): 2088-2301

Published by Baishideng Publishing Group Inc

World Journal of Gastrointestinal Oncology

Contents

Monthly Volume 14 Number 11 November 15, 2022

MINIREVIEWS

ORIGINAL ARTICLE

Basic Study

Clinical and Translational Research

World Journal of Gastrointestinal Oncology

Monthly Volume 14 Number 11 November 15, 2022

Contents

World Journal of Gastrointestinal Oncology

Monthly Volume 14 Number 11 November 15, 2022

Contents

ABOUT COVER

Associate Editor of *World Journal of Gastroenterology Oncology*, Keun-Yeong Jeong, PhD, Research Assistant Professor, Chief Executive Officer, PearlsinMires, Seoul 03690, South Korea. alvirus@naver.com

AIMS AND SCOPE

The primary aim of *World Journal of Gastrointestinal Oncology* (*WJGO*, *World J Gastrointest Oncol*) is to provide scholars and readers from various fields of gastrointestinal oncology with a platform to publish high-quality basic and clinical research articles and communicate their research findings online.

WJGO mainly publishes articles reporting research results and findings obtained in the field of gastrointestinal oncology and covering a wide range of topics including liver cell adenoma, gastric neoplasms, appendiceal neoplasms, biliary tract neoplasms, hepatocellular carcinoma, pancreatic carcinoma, cecal neoplasms, colonic neoplasms, colorectal neoplasms, duodenal neoplasms, esophageal neoplasms, gallbladder neoplasms, *etc*.

INDEXING/ABSTRACTING

The *WJGO* is now abstracted and indexed in PubMed, PubMed Central, Science Citation Index Expanded (SCIE, also known as SciSearch®), Journal Citation Reports/Science Edition, Scopus, Reference Citation Analysis, China National Knowledge Infrastructure, China Science and Technology Journal Database, and Superstar Journals Database. The 2022 edition of Journal Citation Reports® cites the 2021 impact factor (IF) for *WJGO* as 3.404; IF without journal self cites: 3.357; 5-year IF: 3.250; Journal Citation Indicator: 0.53; Ranking: 162 among 245 journals in oncology; Quartile category: Q3; Ranking: 59 among 93 journals in gastroenterology and hepatology; and Quartile category: Q3. The *WJGO*'s CiteScore for 2021 is 3.6 and Scopus CiteScore rank 2021: Gastroenterology is 72/149; Oncology is 203/360.

RESPONSIBLE EDITORS FOR THIS ISSUE

Production Editor: *Xiang-Di Zhang*; **Production Department Director:** *Xiang Li*; **Editorial Office Director:** *Jia-Ru Fan*.

NAME OF JOURNAL
World Journal of Gastrointestinal Oncology

ISSN
ISSN 1948-5204 (online)

LAUNCH DATE
February 15, 2009

FREQUENCY
Monthly

EDITORS-IN-CHIEF
Monjur Ahmed, Florin Burada

EDITORIAL BOARD MEMBERS
https://www.wjgnet.com/1948-5204/editorialboard.htm

PUBLICATION DATE
November 15, 2022

INSTRUCTIONS TO AUTHORS
https://www.wjgnet.com/bpg/gerinfo/204

GUIDELINES FOR ETHICS DOCUMENTS
https://www.wjgnet.com/bpg/GerInfo/287

GUIDELINES FOR NON-NATIVE SPEAKERS OF ENGLISH
https://www.wjgnet.com/bpg/gerinfo/240

PUBLICATION ETHICS
https://www.wjgnet.com/bpg/GerInfo/288

PUBLICATION MISCONDUCT
https://www.wjgnet.com/bpg/gerinfo/208

ARTICLE PROCESSING CHARGE
https://www.wjgnet.com/bpg/gerinfo/242

STEPS FOR SUBMITTING MANUSCRIPTS
https://www.wjgnet.com/bpg/GerInfo/239

ONLINE SUBMISSION
https://www.f6publishing.com

World Journal of Gastrointestinal Oncology

Submit a Manuscript: https://www.f6publishing.com

World J Gastrointest Oncol 2022 November 15; 14(11): 2088-2096

DOI: 10.4251/wjgo.v14.i11.2088

ISSN 1948-5204 (online)

MINIREVIEWS

Portal vein embolization failure: Current strategies and future perspectives to improve liver hypertrophy before major oncological liver resection

Gianluca Cassese, Ho-Seong Han, Boram Lee, Jai Young Cho, Hae Won Lee, Boris Guiu, Fabrizio Panaro, Roberto Ivan Troisi

Specialty type: Surgery

Provenance and peer review: Invited article; Externally peer reviewed.

Peer-review model: Single blind

Peer-review report's scientific quality classification

Grade A (Excellent): 0
Grade B (Very good): B, B, B
Grade C (Good): 0
Grade D (Fair): 0
Grade E (Poor): 0

P-Reviewer: Baba H, Japan; Jackson T, United States; Zhu X, China

Received: August 4, 2022
Peer-review started: August 4, 2022
First decision: September 30, 2022
Revised: October 1, 2022
Accepted: October 31, 2022
Article in press: October 31, 2022
Published online: November 15, 2022

Gianluca Cassese, Roberto Ivan Troisi, Clinical Medicine and Surgery, Federico II University, Naples 80131, Italy

Ho-Seong Han, Jai Young Cho, Department of Surgery, Seoul National University College of Medicine, Seongnam 13620, South Korea

Boram Lee, Hae Won Lee, Department of Surgery, Seoul National University Bundang Hospital, Seongnam 13620, South Korea

Boris Guiu, Department of Medical Imaging and Interventional Radiology, St-Eloi University Hospital, Montpellier 34295, France

Fabrizio Panaro, Digestive Surgery and Transplantation, CHU de Montpellier, Montpellier 34295, France

Corresponding author: Ho-Seong Han, MD, PhD, Professor, Department of Surgery, Seoul National University College of Medicine, 166 Gumi-ro, Bundang-gu, Seongnam-si, Gyeonggi-do, Seongnam 13620, South Korea. hanhs@snubh.org

Abstract

Portal vein embolization (PVE) is currently considered the standard of care to improve the volume of an inadequate future remnant liver (FRL) and decrease the risk of post-hepatectomy liver failure (PHLF). PHLF remains a significant limitation in performing major liver surgery and is the main cause of mortality after resection. The degree of hypertrophy obtained after PVE is variable and depends on multiple factors. Up to 20% of patients fail to undergo the planned surgery because of either an inadequate FRL growth or tumor progression after the PVE procedure (usually 6-8 wk are needed before surgery). The management of PVE failure is still debated, with a lack of consensus regarding the best clinical strategy. Different additional techniques have been proposed, such as sequential transarterial chemoembolization followed by PVE, segment 4 PVE, intra-portal administration of stem cells, dietary supplementation, and hepatic vein embolization. The aim of this review is to summarize the up-to-date strategies to overcome such difficult situations and discuss future perspectives on improving FRL hypertrophy.

Key Words: Portal vein embolization; Portal vein embolization failure; Rescue associating liver partition and portal vein ligation; Hepatic vein embolization; Liver venous deprivation; Segment 4 portal vein embolization

Core Tip: Portal vein embolization (PVE) is actually considered the standard of care for inducing volume augmentation of the future remnant liver. However, 20% of patients who have undergone PVE, reportedly never undergo curative resection, due to either insufficient future remnant liver (FRL) growth with an unacceptable risk of post-hepatectomy liver failure, or oncologic progression after PVE, while waiting for the adequate FRL hypertrophy (6-8 wk or more). The management of PVE failure is still highly debated, with different additional techniques that have been proposed, such as sequential transarterial chemoembolization followed by PVE, segment 4 PVE, intra-portal administration of stem cells, dietary supplementation, and hepatic vein embolization.

Citation: Cassese G, Han HS, Lee B, Cho JY, Lee HW, Guiu B, Panaro F, Troisi RI. Portal vein embolization failure: Current strategies and future perspectives to improve liver hypertrophy before major oncological liver resection. *World J Gastrointest Oncol* 2022; 14(11): 2088-2096
URL: https://www.wjgnet.com/1948-5204/full/v14/i11/2088.htm
DOI: https://dx.doi.org/10.4251/wjgo.v14.i11.2088

INTRODUCTION

The main goal of hepatic surgical oncology is to perform a R0 resection, by preserving a sufficient future remnant liver (FRL) to prevent post-hepatectomy liver failure (PHLF). Indeed, PHLF is still a major cause of mortality after major liver surgery[1]. To reduce the risk of PHLF it is necessary to preserve not only a sufficient amount of liver parenchyma, but also ensure adequate liver function[2]. Owing to advances in preoperative evaluation and optimization of the FRL, the postoperative mortality rate for major liver resections (≥ 3 segments) is currently showed to be less than 5%[3,4]. The FRL volume is the only factor that can be acted on, depending on the surgery and liver condition. An FRL ≥ 20% of the volume is considered safe in cases of healthy liver, ≥ 30% after chemotherapy, 40% in case of steatosis or cholestasis, and ≥ 50% in case of cirrhosis[5]. Prior to performing major hepatectomy, multiple patient factors should also be considered to optimize FRL growth, such as an age higher than 65 years, obesity or malnutrition, diabetes, chronic renal failure[4]. The degree of liver hypertrophy is also affected by many liver related factors, with the eventual presence of chronic liver disease or previous chemotherapy playing a fundamental role[6,7]. However, pooled data from a recent meta-analysis showed no difference in the degree of hypertrophy between patients receiving neo-adjuvant chemotherapy compared to patients who did not receive pre-procedural systemic treatment[8], despite a very high degree of heterogeneity in the studies included[9,10].

Portal vein embolization (PVE) is seen as the standard of care for inducing hypertrophy of the FRL. However, 20% of patients who have undergone PVE, reportedly never undergo curative resection, due to either insufficient FRL growth with an unacceptable risk of PHLF, or oncologic progression after the PVE procedure (6 wk or more before surgery)[11]. For patients with insufficient liver hypertrophy following PVE, adjunctive techniques such as hepatic vein embolization, segment 4 embolization, intra-portal administration of stem cells, dietary supplementation, and sequential transarterial embolization followed by PVE, have been proposed. However, evidence regarding the appropriate management of these patients after PVE failure is still lacking.

This review aims to summarize the up-to-date strategies available and future perspectives on the management of patients scheduled for major hepatic resection with insufficient FRL hypertrophy after PVE.

PVE: TECHNIQUE, INFLUENCING FACTORS AND LIMITATIONS

PVE was first described by Makuuchi *et al*[12] in 1984, in patients with cholangiocarcinoma (CCA) undergoing major hepatectomy[13]. However, the principle of contralateral liver lobe hypertrophy after hepatic vessel obliteration was first identified by James Cantlie 100 years before[14]. Currently, PVE is the standard of care procedure to obtain FRL hypertrophy in patients requiring major liver surgery, in case of marginal FRL. Reportedly, about 80% of patients are able to undergo the planned liver surgery

after 6-8 wk[15].

PVE is a technique of interventional radiology, carried out under local anesthesia. Three approaches have been classically reported for this procedure: trans-hepatic, trans-splenic and trans-ileocolic. The trans-hepatic technique involves percutaneous access to the portal branches. The trans-ileocolic technique consists of a mini-laparotomy to isolate and cannulate the ileocolic vein, to access the portal vein. As it is a more invasive procedure, it is used when interventional radiology is not feasible. The trans-splenic technique is more recent, providing the advantage of eliminating the risk of tumor seeding. This access was initially thought to have a higher risk of bleeding complications; however, such concerns have been addressed and this approach is being increasingly used[16]. In contrast, a meta-analysis by Abulkhir *et al*[17] found that FRL hypertrophy was significantly higher using the trans-hepatic technique. Recently, Yamao *et al*[18] described for the first time the round ligament approach, suggesting its usefulness in elective cases for which it is difficult to safely perform trans-hepatic or trans-ileocecal approaches. In their study on 50 patients undergoing major hepatectomy, the authors observed no morbidity, neither mortality, related to the round ligament approach. The median functional hepatic remnant rate before and after the procedure was 55.6% and 63.2%, respectively.

Response to PVE has been found to be an important predictor of PHLF. Abdalla *et al*[19] proposed a degree of hypertrophy (DOH) cutoff of > 5% in case of healthy liver and > 10% in cirrhotic patients, to safely perform a major hepatectomy. Chapelle *et al*[20] investigated the hypertrophic response after PVE using hepatobiliary scintigraphy (HBS) and found a cut-off value of 1.72%/min/m^2 of pre-PVE FRL-F for safe resection (81.3% sensitivity and 82.4% specificity). The increase in volume after PVE is not proportional to the increase in liver function (FRL-F), with a greater increase in FRL-F up to 3-4 wk after PVE procedure[21]. All previous studies agree that the smaller the FRL pre-PVE, the larger the FRL hypertrophy post-PVE[8,22,23].

PVE is contraindicated in cases of tumor invasion into the ipsilateral portal vein. A relative contraindication is portal hypertension since PVE may increase portal vein pressure and worsen the liver function and the clinical state[24].

Some previous studies suggested a negative impact of liver regeneration on long-term oncological outcomes, as regard to both disease-free survival (DFS) and overall survival (OS). Margonis *et al*[25] reported that a kinetic growth rate (KGR) higher than 1% could be related to an increased risk of recurrence. However, a meta-analysis focusing on the oncological outcomes of PVE showed that the procedure does not worsen the long term results of major liver surgery, without any higher risk in terms of hepatic recurrence, 3-year OS, and 5-year OS after PVE[26].

The true weight of most factors involved in PVE failure remains unclear, apart from the presence of the underlying liver disease. The main drawback of unresolved PVE: The 15%-25% rate of failure due to inadequate FRL hypertrophy or oncologic progression[11].

Risk factors for PVE failure

Several factors can influence the efficacy of PVE procedure. Regarding embolization materials that can be used for PVE, the combination of N-butil-cyanoacrylate (NBCA) with lipiodol is the most widely used, leading to reliable FRL hypertrophy with efficient embolization, and low rate of vascular recanalization[27]. Furthermore, recent reports showed similar results with resorbable materials, hypothesizing the advantage to prevent an accidental contralateral embolization[28]. A recent meta-analysis by Soykan *et al*[8] reported a significant difference in the degree of hypertrophy in favor of NBCA compared to the other agents. In the same study, other risk factors were investigated, and showed that sex and previous chemotherapy were not associated with a lower degree of hypertrophy, contrary to what has been previously reported. It is reported that five predictive factors for insufficient FRL growth: Age, FRL%, plasma indocyanine green detection rate (ICG-PDR), total bilirubin level, and a history of chemotherapy. A prediction formula was created using these parameters, and had a 100% sensitivity and 90.9% specificity for predicting an FRL < 20% after PVE. However, this finding has not been validated in larger cohorts.

MANAGEMENT STRATEGIES AFTER PVE FAILURE

Insufficient FRL augmentation after PVE is a difficult issue to overcome because of two reasons: The need to act quickly to avoid tumor progression and the need to prevent PHLF. Different strategies have been suggested without consensus. In Figure 1, the authors propose their algorithm, which is discussed below.

Segment 4 PVE

When right trisectionectomy is planned, additional embolization of segment 4 (S4) can be performed. The first encouraging experience with this procedure was published by Kishi *et al*[29], which showed a higher FRL hypertrophy, resulting in a median volumetric increase of 54% *vs* 26% after PVE alone, without affecting post-procedural morbidity or perioperative outcomes. Recently, a larger Scandinavian study showed similar results (median increase of 47% *vs* 38%, respectively; $P = 0.02$), but with a hetero-

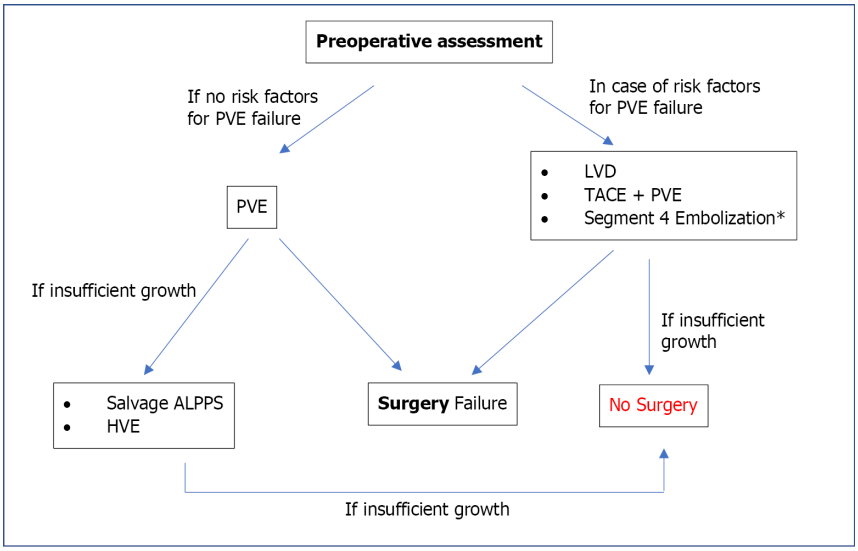

DOI: 10.4251/wjgo.v14.i11.2088 **Copyright** ©The Author(s) 2022.

Figure 1 Proposed algorithm for future remnant liver augmentation and portal vein embolization failure. The asterisk (*) represents only if right trisectionectomy is planned. PVE: Portal vein embolization; ALPPS: Associated liver partition with portal vein ligation for staged hepatectomy; LVD: Liver venous deprivation; TACE: Trans-arterial chemoembolization; HVE: Hepatic vein embolization.

geneous cohort, including patient with cirrhosis, CCA, and colorectal liver metastases (CRLM)[30]. Furthermore, the pre-PVE FRL was smaller in the S4 group (333 mL *vs* 380 mL; $P = 0.01$), which is associated with a higher DOH. A Japanese, propensity score-matched study in patients with biliary carcinoma also reported an improved FRL after PVE with S4 embolization[31]. In contrast, three other studies showed no significant differences between PVE alone and PVE with S4 embolization[22,32,33]. Studies have always considered the time interval needed to obtain FRL increase after S4 portal embolization similar to that after PVE, without the advantage of faster hypertrophy. Furthermore, when the scheduled surgery is not a right trisectionectomy, this technique is useless[34].

Hepatic vein embolization

Hepatic vein embolization (HVE) was introduced to obtain an additional increase in FRL after PVE failure. The first experience with sequential HVE after ipsilateral PVE was reported by Hwang *et al*[35] in 2004, in order to obtain an additional FRL hypertrophy in 42 patients. Another study reported an FRL augmentation rate of 28.9% after HVE (*vs* 13.3% after PVE alone), without significant complications[36]. The mechanism of action probably consists of a higher stress on the liver due to a major outflow obstruction, showing at the same time a protective effect of the residual arterial flow against any dangerous biliary ischemia. Similar outcomes were recently reported by Niekamp *et al*[37] in nine patients with CRLM who underwent salvage HVE following PVE failure. The standardized FRL increased from 16% to 26% after HVE and 22% after PVE ($P = 0.0005$). HVE was performed after a median of 40 d from PVE, and only four of the nine patients underwent hepatectomy. Thus, even though HVE is safer and more effective, the sequential association of PVE and HVE requires a long interval between them, without counteracting a possible progression of tumor disease. Hence, Guiu *et al* [38] published the first reports about the liver venous deprivation (LVD) technique, consisting in a simultaneous embolization of the hepatic vein(s) and ipsilateral portal vessels. LVD requires that both the ipsilateral portal and venous branch (+/− accessory veins) are occluded with an Amplatzer plug, placed approximately 1 cm from the ostium. NBCA is injected beyond the plug to close the intrahepatic part of the vein(s), as well as any collaterals. The extended LVD (e-LVD) is a variation of the technique in which the middle hepatic vein is also treated[39]. First data after 99 m-Tc mebrofenin hepatobiliary scintigraphy (HBS) reported a 66% improvement in FRL-F 7 d after e-LVD procedure. After 3 wk, the median volumetric gain was 63.3%, while the functional increase was 64.3%. Furthermore, subsequent studies have shown also safe perioperative and oncological results after the completion surgery[40-42]. Thus, preliminary studies have shown that LVD can induce a higher FRL hypertrophy than PVE, without adding additional periprocedural risks. However, to reach stronger conclusions, randomized studies comparing LVD and PVE are awaited (HyperLiv 01 and Dragon 1 are currently still ongoing).

In essence, HVE seems to be a safe salvage option after PVE failure, but carries the risk of tumor progression during the long waiting times. The LVD technique seems to be a better substitute for PVE, and aims to replace PVE owing to its higher and faster hypertrophic effects[43].

Salvage associating liver partition and portal vein ligation

Associating liver partition and portal vein ligation (ALPPS) was first described by Schnitzbauer *et al*[44] in 2012 as a novel two-staged hepatectomy, with the main advantage of remarkably reducing the delay between the first and second procedure. During the first stage, the lesions in the FRL are treated, and an anticipated line of resection is transected with ligation of the contralateral first order portal branch. After only 1-2 wk, completion surgery is performed after a sufficient FRL is confirmed using CT-based volumetry[45]. The reported successful rate for the completion surgery was 99%, while the traditional two staged hepatectomy reached only about 75%[46,47]. The shorter interval needed for FRL augmentation could significantly decrease the risk of tumor progression. Furthermore, the two surgeries could possibly be performed during the same hospitalization, affecting the costs and the organization. However, there has been concern regarding the effective increase in FRL-F. Olthof *et al*[48] showed a median increase of 29% in the FRL-F 7 d after ALPPS stage 1, compared to a volumetric increase of 78%, in a study involving patients with perihilar cholangiocarcinoma ($P < 0.01$). Similar results have been reported in patients with CRLM[49]. To this end, the efficacy of HBS in predicting PHLF after ALPPS was proven by Tomassini *et al*[50]; patients presenting with a daily gain in FRL-F of ≤ 2.7%/min/m^2 indicated a high risk of PHLF development, which requires re-discussion of the second stage. The ALPPS registry shows a mortality rate of 5% in a series which included only patients treated for colorectal liver metastasis aged < 60 years old[45]. The main disadvantage of this fast post-procedural hypertrophy is the risk for higher rates of perioperative morbidity and mortality[45].

ALPPS was proposed as a salvage procedure by Enne *et al*[51]. The study reported a mean FRL increase of 88% in 20 patients who underwent ALPPS after PVE failure, with an exceptional 100% success rate and no 90-d mortality. Similar results were reported by Sparrelid *et al*[49] in 11 patients with CRLM: A median FRL growth of 61.8%, with no 90-d mortality or high-grade complications (≥ 3b-complication according to Clavien-Dindo). Many variations of the original ALPPS procedure have been reported in the literature (mini ALPPS, partial ALPPS, radio-frequency-assisted liver partition with portal vein ligation, and Tourniquet modification), with the aim of reducing postoperative morbidity and bring some technical advantages. However, none of these ones have been proposed as salvage procedures. It may be beneficial to obtain data on this in the future. Additionally, Dondorf *et al*[52] reported the possibility of obtaining a significant further increase in FRL after additional ligation of the middle hepatic vein in combination with ALPPS (a sort of "surgical LVD"). Though higher morbidity and mortality were observed, they were most likely associated with the underlying liver conditions.

Although the actual role of salvage ALPPS is still debated, we believe that it can be considered a viable salvage option.

Sequential trans arterial chemoembolization and PVE

Herein, we present an option that can't be performed after PVE failure, but in addition to PVE when there are risk factors of failure, as proposed in our flow-chart. Indeed, the presence of an underlying chronic liver disease is a risk factor for poor hypertrophy after PVE. One of the reasons could be the presence of arterio-portal tumoral shunts, typical of hepatocellular carcinoma (HCC), which could counteract the hemodynamic effect of PVE. Sequential trans arterial chemoembolization (TACE) followed by PVE has been shown to achieve a higher DOH than PVE alone[53]. Ipsilateral PVE is performed 7-10 d after the initial TACE, once the blood parameters have normalized. The benefits of this dual technique include improved FRL hypertrophy relative to PVE alone and induction of an anti-tumor effect in the embolized lobe[54,55]. Ogata *et al*[54] reported a mean FRL increase in the TACEPVE group of 12% *vs* 8% for the PVE alone group ($P = 0.022$), with a DOH of 10% *vs* 5%, respectively ($P = 0.044$). In the same study, the TACE + PVE group had a higher complete tumor necrosis incidence (83.00% *vs* 0.05%; $P < 0.001$) and 5-year DFS (37% *vs* 19%; $P = 0.041$), owing to better local control of the HCC nodule. A limitation of this strategy is the consequent inflammation of the hepatic pedicle, which makes subsequent surgery more challenging. Furthermore, areas of residual segmental infarction were found within the non-cancerous liver on histopathology; thus, TACE should be performed carefully, since many of these patients have pre-existing liver dysfunction[55].

Intra-portal administration of stem cells

Fürst *et al*[56] first reported caries in six patients undergoing PVE with CD133 (+) bone marrow stem cells (BMSC) administration to improve FRL hypertrophy following PVE. In their study, a significantly higher mean increase in FRL volume was reported (77.3% *vs* 39.1%, $P = 0.039$). The time to surgery was also shorter in patients who received stem cell infusion (27 d *vs* 45 d, $P = 0.057$). Similarly, am Esch *et al* [57] showed a median absolute gain of 138.66 in the PVE-BMSC group compared to 62.95 mL in the PVE-alone group ($P = 0.004$). Post hoc analysis revealed better survival in the PVE-BMSC group ($P = 0.028$) than in the PVE-alone group ($P = 0.094$) and controls.

Despite the encouraging results, further issues need to be investigated prior to their routine use. Stem cells have been reported to stimulate tumor growth in murine models of CRLM[58,59]. Furthermore, the effectiveness of this technique in patients with chronic liver disease and prolonged chemotherapy remains unknown[60].

CONCLUSION

Owing to tremendous technological advances, appropriate FRL optimization can reduce the risk of PHLF. Although PVE is considered the standard of care for FRL volume augmentation, up to 20% of patients fail to undergo the planned surgery. An in-depth knowledge of all the risk factors for PVE failure can help us to choose the most effective procedure. In our opinion, LVD could replace PVE in the future, particularly in cases with negative predictive factors for FRL hypertrophy, once its validity has been confirmed. Other strategies, such as the combination of PVE and TACE or segment 4 embolization, can be carefully considered when appropriate. To date, after PVE failure, ALPPS is reportedly the most effective salvage procedure to obtain a volumetric gain with only a short delay, thus preventing tumor progression. However, prospective and large-scale studies on this challenging scenario are still needed.

FOOTNOTES

Author contributions: Cassese G, Han HS, Panaro F, and Troisi RI conceived and designed the study; Lee HW, Cho JY, Guiu B, and Troisi RI critically revised the manuscript; Cassese G and Lee B wrote the manuscript.

Conflict-of-interest statement: The authors declare that they have no conflict of interest.

Country/Territory of origin: South Korea

ORCID number: Gianluca Cassese 0000-0001-9185-2054; Ho-Seong Han 0000-0001-9659-1260; Fabrizio Panaro 0000-0001-8200-4969; Roberto Ivan Troisi 0000-0001-6280-810X.

S-Editor: Chen YL
L-Editor: A
P-Editor: Chen YL

REFERENCES

1 **Pulitano C**, Crawford M, Joseph D, Aldrighetti L, Sandroussi C. Preoperative assessment of postoperative liver function: the importance of residual liver volume. *J Surg Oncol* 2014; **110**: 445-450 [PMID: 24962104 DOI: 10.1002/jso.23671]
2 **Kishi Y**, Vauthey JN. Issues to be considered to address the future liver remnant prior to major hepatectomy. *Surg Today* 2021; **51**: 472-484 [PMID: 32894345 DOI: 10.1007/s00595-020-02088-2]
3 **Xu HW**, Liu F, Li HY, Wei YG, Li B. Outcomes following laparoscopic *vs* open major hepatectomy for hepatocellular carcinoma in patients with cirrhosis: a propensity score-matched analysis. *Surg Endosc* 2018; **32**: 712-719 [PMID: 28726140 DOI: 10.1007/s00464-017-5727-2]
4 **Cassese G**, Han HS, Al Farai A, Guiu B, Troisi RI, Panaro F. Future remnant liver optimization: preoperative assessment, volume augmentation procedures and management of PVE failure. *Minerva Surg* 2022; **77**: 368-379 [PMID: 35332767 DOI: 10.23736/S2724-5691.22.09541-7]
5 **Clavien PA**, Petrowsky H, DeOliveira ML, Graf R. Strategies for safer liver surgery and partial liver transplantation. *N Engl J Med* 2007; **356**: 1545-1559 [PMID: 17429086 DOI: 10.1056/NEJMra065156]
6 **Yokoyama Y**, Nagino M, Nimura Y. Mechanisms of hepatic regeneration following portal vein embolization and partial hepatectomy: a review. *World J Surg* 2007; **31**: 367-374 [PMID: 17219273 DOI: 10.1007/s00268-006-0526-2]
7 **Beal IK**, Anthony S, Papadopoulou A, Hutchins R, Fusai G, Begent R, Davies N, Tibballs J, Davidson B. Portal vein embolisation prior to hepatic resection for colorectal liver metastases and the effects of periprocedure chemotherapy. *Br J Radiol* 2006; **79**: 473-478 [PMID: 16714748 DOI: 10.1259/bjr/29855825]
8 **Soykan EA**, Aarts BM, Lopez-Yurda M, Kuhlmann KFD, Erdmann JI, Kok N, van Lienden KP, Wilthagen EA, Beets-Tan RGH, van Delden OM, Gomez FM, Klompenhouwer EG. Predictive Factors for Hypertrophy of the Future Liver Remnant After Portal Vein Embolization: A Systematic Review. *Cardiovasc Intervent Radiol* 2021; **44**: 1355-1366 [PMID: 34142192 DOI: 10.1007/s00270-021-02877-3]
9 **Tanaka K**, Kumamoto T, Matsuyama R, Takeda K, Nagano Y, Endo I. Influence of chemotherapy on liver regeneration induced by portal vein embolization or first hepatectomy of a staged procedure for colorectal liver metastases. *J Gastrointest Surg* 2010; **14**: 359-368 [PMID: 19888636 DOI: 10.1007/s11605-009-1073-6]
10 **Covey AM**, Brown KT, Jarnagin WR, Brody LA, Schwartz L, Tuorto S, Sofocleous CT, D'Angelica M, Getrajdman GI, DeMatteo R, Kemeny NE, Fong Y. Combined portal vein embolization and neoadjuvant chemotherapy as a treatment strategy for resectable hepatic colorectal metastases. *Ann Surg* 2008; **247**: 451-455 [PMID: 18376189 DOI: 10.1097/SLA.0b013e31815ed693]

11 **Alvarez FA**, Castaing D, Figueroa R, Allard MA, Golse N, Pittau G, Ciacio O, Sa Cunha A, Cherqui D, Azoulay D, Adam R, Vibert E. Natural history of portal vein embolization before liver resection: a 23-year analysis of intention-to-treat results. *Surgery* 2018; **163**: 1257-1263 [PMID: 29502872 DOI: 10.1016/j.surg.2017.12.027]

12 **Makuuchi M**, Takayasu K, Takuma T. Preoperative Transcatheter Embolization of the Portal Venous Branch for Patients Receiving Extended Lobectomy Due to the Bile Duct Carcinoma. *J Jpn Pract Surg Soc* 1984; **45**: 1558-1564 [DOI: 10.3919/ringe1963.45.1558]

13 **Makuuchi M**, Thai BL, Takayasu K, Takayama T, Kosuge T, Gunvén P, Yamazaki S, Hasegawa H, Ozaki H. Preoperative portal embolization to increase safety of major hepatectomy for hilar bile duct carcinoma: a preliminary report. *Surgery* 1990; **107**: 521-527 [PMID: 2333592]

14 **Wellcome collection**. "On a new arrangement of the right and left lobes of the liver". Anatomical Society of Great Britain and Ireland. Wellcome Collection. [cited June 30, 2022]. Available from: https://wellcomecollection.org/works/jrwbtbys [DOI: 10.2307/2842821]

15 **Sugawara Y**, Yamamoto J, Higashi H, Yamasaki S, Shimada K, Kosuge T, Takayama T, Makuuchi M. Preoperative portal embolization in patients with hepatocellular carcinoma. *World J Surg* 2002; **26**: 105-110 [PMID: 11898042 DOI: 10.1007/s00268-001-0189-y]

16 **Zurcher KS**, Smith MV, Naidu SG, Saini G, Patel IJ, Knuttinen MG, Kriegshauser JS, Oklu R, Alzubaidi SJ. Transsplenic Portal System Catheterization: Review of Current Indications and Techniques. *Radiographics* 2022; **42**: 1562-1576 [PMID: 35984753 DOI: 10.1148/rg.220042]

17 **Abulkhir A**, Limongelli P, Healey AJ, Damrah O, Tait P, Jackson J, Habib N, Jiao LR. Preoperative portal vein embolization for major liver resection: a meta-analysis. *Ann Surg* 2008; **247**: 49-57 [PMID: 18156923 DOI: 10.1097/SLA.0b013e31815f6e5b]

18 **Yamao T**, Tamura Y, Hayashi H, Takematsu T, Higashi T, Yamamura K, Imai K, Yamashita YI, Ikeda O, Baba H. Novel Approach *via* the Round Ligament in Portal Vein Embolization. *World J Surg* 2021; **45**: 2878-2885 [PMID: 34085093 DOI: 10.1007/s00268-021-06145-w]

19 **Abdalla EK**, Denys A, Chevalier P, Nemr RA, Vauthey JN. Total and segmental liver volume variations: implications for liver surgery. *Surgery* 2004; **135**: 404-410 [PMID: 15041964 DOI: 10.1016/j.surg.2003.08.024]

20 **Chapelle T**, Op De Beeck B, Huyghe I, Francque S, Driessen A, Roeyen G, Ysebaert D, De Greef K. Future remnant liver function estimated by combining liver volumetry on magnetic resonance imaging with total liver function on (99m)Tc-mebrofenin hepatobiliary scintigraphy: can this tool predict post-hepatectomy liver failure? *HPB (Oxford)* 2016; **18**: 494-503 [PMID: 27317953 DOI: 10.1016/j.hpb.2015.08.002]

21 **de Graaf W**, van Lienden KP, van den Esschert JW, Bennink RJ, van Gulik TM. Increase in future remnant liver function after preoperative portal vein embolization. *Br J Surg* 2011; **98**: 825-834 [PMID: 21484773 DOI: 10.1002/bjs.7456]

22 **Zeile M**, Bakal A, Volkmer JE, Stavrou GA, Dautel P, Hoeltje J, Stang A, Oldhafer KJ, Brüning R. Identification of cofactors influencing hypertrophy of the future liver remnant after portal vein embolization-the effect of collaterals on embolized liver volume. *Br J Radiol* 2016; **89**: 20160306 [PMID: 27730840 DOI: 10.1259/bjr.20160306]

23 **Kohno S**, Isoda H, Ono A, Furuta A, Taura K, Shibata T, Togashi K. Portal Vein Embolization: Radiological Findings Predicting Future Liver Remnant Hypertrophy. *AJR Am J Roentgenol* 2020; **214**: 687-693 [PMID: 31642696 DOI: 10.2214/AJR.19.21440]

24 **Vauthey JN**, Dixon E, Abdalla EK, Helton WS, Pawlik TM, Taouli B, Brouquet A, Adams RB; American Hepato-Pancreato-Biliary Association; Society of Surgical Oncology; Society for Surgery of the Alimentary Tract. Pretreatment assessment of hepatocellular carcinoma: expert consensus statement. *HPB (Oxford)* 2010; **12**: 289-299 [PMID: 20590901 DOI: 10.1111/j.1477-2574.2010.00181.x]

25 **Margonis GA**, Sasaki K, Andreatos N, Pour MZ, Shao N, Ghasebeh MA, Buettner S, Antoniou E, Wolfgang CL, Weiss M, Kamel IR, Pawlik TM. Increased kinetic growth rate during late phase liver regeneration impacts the risk of tumor recurrence after colorectal liver metastases resection. *HPB (Oxford)* 2017; **19**: 808-817 [PMID: 28602644 DOI: 10.1016/j.hpb.2017.05.002]

26 **Giglio MC**, Giakoustidis A, Draz A, Jawad ZAR, Pai M, Habib NA, Tait P, Frampton AE, Jiao LR. Oncological Outcomes of Major Liver Resection Following Portal Vein Embolization: A Systematic Review and Meta-analysis. *Ann Surg Oncol* 2016; **23**: 3709-3717 [PMID: 27272106 DOI: 10.1245/s10434-016-5264-6]

27 **de Baere T**, Roche A, Vavasseur D, Therasse E, Indushekar S, Elias D, Bognel C. Portal vein embolization: utility for inducing left hepatic lobe hypertrophy before surgery. *Radiology* 1993; **188**: 73-77 [PMID: 8511321 DOI: 10.1148/radiology.188.1.8511321]

28 **Tranchart H**, Koffi GM, Gaillard M, Lainas P, Poüs C, Gonin P, Nguyen TH, Dubart-Kupperschmitt A, Dagher I. Liver regeneration following repeated reversible portal vein embolization in an experimental model. *Br J Surg* 2016; **103**: 1209-1219 [PMID: 27256140 DOI: 10.1002/bjs.10153]

29 **Kishi Y**, Madoff DC, Abdalla EK, Palavecino M, Ribero D, Chun YS, Vauthey JN. Is embolization of segment 4 portal veins before extended right hepatectomy justified? *Surgery* 2008; **144**: 744-751 [PMID: 19081016 DOI: 10.1016/j.surg.2008.05.015]

30 **Björnsson B**, Hasselgren K, Røsok B, Larsen PN, Urdzik J, Schultz NA, Carling U, Fallentin E, Gilg S, Sandström P, Lindell G, Sparrelid E. Segment 4 occlusion in portal vein embolization increase future liver remnant hypertrophy - A Scandinavian cohort study. *Int J Surg* 2020; **75**: 60-65 [PMID: 32001330 DOI: 10.1016/j.ijsu.2020.01.129]

31 **Ito J**, Komada T, Suzuki K, Matsushima M, Nakatochi M, Kobayashi Y, Ebata T, Naganawa S, Nagino M. Evaluation of segment 4 portal vein embolization added to right portal vein for right hepatic trisectionectomy: A retrospective propensity score-matched study. *J Hepatobiliary Pancreat Sci* 2020; **27**: 299-306 [PMID: 32030904 DOI: 10.1002/jhbp.723]

32 **de Baere T**, Teriitehau C, Deschamps F, Catherine L, Rao P, Hakime A, Auperin A, Goere D, Elias D, Hechelhammer L. Predictive factors for hypertrophy of the future remnant liver after selective portal vein embolization. *Ann Surg Oncol* 2010; **17**: 2081-2089 [PMID: 20237856 DOI: 10.1245/s10434-010-0979-2]

33 **Massimino KP**, Kolbeck KJ, Enestvedt CK, Orloff S, Billingsley KG. Safety and efficacy of preoperative right portal vein embolization in patients at risk for postoperative liver failure following major right hepatectomy. *HPB (Oxford)* 2012; **14**:

14-19 [PMID: 22151446 DOI: 10.1111/j.1477-2574.2011.00402.x]
34 **Nagino M**, Kanai M, Morioka A, Yamamoto H, Kawabata Y, Hayakawa N, Nimura Y. Portal and arterial embolization before extensive liver resection in patients with markedly poor functional reserve. *J Vasc Interv Radiol* 2000; **11**: 1063-1068 [PMID: 10997472 DOI: 10.1016/s1051-0443(07)61340-2]
35 **Hwang S**, Lee SG, Park KM, Kim KH, Ahn CS, Lee YJ, Sung KB, Moon DB, Ha TY, Cho SH, Oh KB, Han JM, Kim MH. Hepatic venous congestion in living donor liver transplantation: preoperative quantitative prediction and follow-up using computed tomography. *Liver Transpl* 2004; **10**: 763-770 [PMID: 15162471 DOI: 10.1002/Lt.20178]
36 **Hwang S**, Ha TY, Ko GY, Kwon DI, Song GW, Jung DH, Kim MH, Lee SK, Lee SG. Preoperative Sequential Portal and Hepatic Vein Embolization in Patients with Hepatobiliary Malignancy. *World J Surg* 2015; **39**: 2990-2998 [PMID: 26304608 DOI: 10.1007/s00268-015-3194-2]
37 **Niekamp AS**, Huang SY, Mahvash A, Odisio BC, Ahrar K, Tzeng CD, Vauthey JN. Hepatic vein embolization after portal vein embolization to induce additional liver hypertrophy in patients with metastatic colorectal carcinoma. *Eur Radiol* 2020; **30**: 3862-3868 [PMID: 32144462 DOI: 10.1007/s00330-020-06746-4]
38 **Guiu B**, Chevallier P, Denys A, Delhom E, Pierredon-Foulongne MA, Rouanet P, Fabre JM, Quenet F, Herrero A, Panaro F, Baudin G, Ramos J. Simultaneous trans-hepatic portal and hepatic vein embolization before major hepatectomy: the liver venous deprivation technique. *Eur Radiol* 2016; **26**: 4259-4267 [PMID: 27090112 DOI: 10.1007/s00330-016-4291-9]
39 **Guiu B**, Quenet F, Escal L, Bibeau F, Piron L, Rouanet P, Fabre JM, Jacquet E, Denys A, Kotzki PO, Verzilli D, Deshayes E. Extended liver venous deprivation before major hepatectomy induces marked and very rapid increase in future liver remnant function. *Eur Radiol* 2017; **27**: 3343-3352 [PMID: 28101681 DOI: 10.1007/s00330-017-4744-9]
40 **Khayat S**, Cassese G, Quenet F, Cassinotto C, Assenat E, Navarro F, Guiu B, Panaro F. Oncological Outcomes after Liver Venous Deprivation for Colorectal Liver Metastases: A Single Center Experience. *Cancers (Basel)* 2021; **13** [PMID: 33429913 DOI: 10.3390/cancers13020200]
41 **Kobayashi K**, Yamaguchi T, Denys A, Perron L, Halkic N, Demartines N, Melloul E. Liver venous deprivation compared to portal vein embolization to induce hypertrophy of the future liver remnant before major hepatectomy: A single center experience. *Surgery* 2020; **167**: 917-923 [PMID: 32014304 DOI: 10.1016/j.surg.2019.12.006]
42 **Cassese G**, Troisi RI, Khayat S, Quenet F, Tomassini F, Panaro F, Guiu B. Liver venous deprivation *vs* associating liver partition and portal vein ligation for staged hepatectomy for colo-rectal liver metastases: a comparison of early and late kinetic growth rates, and perioperative and oncological outcomes. *Surg Oncol* 2022; **43**: 101812 [PMID: 35820263 DOI: 10.1016/j.suronc.2022.101812]
43 **Laurent C**, Fernandez B, Marichez A, Adam JP, Papadopoulos P, Lapuyade B, Chiche L. Radiological Simultaneous Portohepatic Vein Embolization (RASPE) Before Major Hepatectomy: A Better Way to Optimize Liver Hypertrophy Compared to Portal Vein Embolization. *Ann Surg* 2020; **272**: 199-205 [PMID: 32675481 DOI: 10.1097/SLA.0000000000003905]
44 **Schnitzbauer AA**, Lang SA, Goessmann H, Nadalin S, Baumgart J, Farkas SA, Fichtner-Feigl S, Lorf T, Goralcyk A, Hörbelt R, Kroemer A, Loss M, Rümmele P, Scherer MN, Padberg W, Königsrainer A, Lang H, Obed A, Schlitt HJ. Right portal vein ligation combined with in situ splitting induces rapid left lateral liver lobe hypertrophy enabling 2-staged extended right hepatic resection in small-for-size settings. *Ann Surg* 2012; **255**: 405-414 [PMID: 22330038 DOI: 10.1097/SLA.0b013e31824856f5]
45 **Lang H**, Baumgart J, Mittler J. Associated Liver Partition and Portal Vein Ligation for Staged Hepatectomy (ALPPS) Registry: What Have We Learned? *Gut Liver* 2020; **14**: 699-706 [PMID: 32036644 DOI: 10.5009/gnl19233]
46 **Eshmuminov D**, Raptis DA, Linecker M, Wirsching A, Lesurtel M, Clavien PA. Meta-analysis of associating liver partition with portal vein ligation and portal vein occlusion for two-stage hepatectomy. *Br J Surg* 2016; **103**: 1768-1782 [PMID: 27633328 DOI: 10.1002/bjs.10290]
47 **Lam VW**, Laurence JM, Johnston E, Hollands MJ, Pleass HC, Richardson AJ. A systematic review of two-stage hepatectomy in patients with initially unresectable colorectal liver metastases. *HPB (Oxford)* 2013; **15**: 483-491 [PMID: 23750490 DOI: 10.1111/j.1477-2574.2012.00607.x]
48 **Olthof PB**, Coelen RJS, Wiggers JK, Groot Koerkamp B, Malago M, Hernandez-Alejandro R, Topp SA, Vivarelli M, Aldrighetti LA, Robles Campos R, Oldhafer KJ, Jarnagin WR, van Gulik TM. High mortality after ALPPS for perihilar cholangiocarcinoma: case-control analysis including the first series from the international ALPPS registry. *HPB (Oxford)* 2017; **19**: 381-387 [PMID: 28279621 DOI: 10.1016/j.hpb.2016.10.008]
49 **Sparrelid E**, Jonas E, Tzortzakakis A, Dahlén U, Murquist G, Brismar T, Axelsson R, Isaksson B. Dynamic Evaluation of Liver Volume and Function in Associating Liver Partition and Portal Vein Ligation for Staged Hepatectomy. *J Gastrointest Surg* 2017; **21**: 967-974 [PMID: 28283924 DOI: 10.1007/s11605-017-3389-y]
50 **Tomassini F**, D'Asseler Y, Linecker M, Giglio MC, Castro-Benitez C, Truant S, Axelsson R, Olthof PB, Montalti R, Serenari M, Chapelle T, Lucidi V, Sparrelid E, Adam R, Van Gulik T, Pruvot FR, Clavien PA, Bruzzese D, Geboes K, Troisi RI. Hepatobiliary scintigraphy and kinetic growth rate predict liver failure after ALPPS: a multi-institutional study. *HPB (Oxford)* 2020; **22**: 1420-1428 [PMID: 32057681 DOI: 10.1016/j.hpb.2020.01.010]
51 **Enne M**, Schadde E, Björnsson B, Hernandez Alejandro R, Steinbruck K, Viana E, Robles Campos R, Malago M, Clavien PA, De Santibanes E, Gayet B; ALPPS Registry Group. ALPPS as a salvage procedure after insufficient future liver remnant hypertrophy following portal vein occlusion. *HPB (Oxford)* 2017; **19**: 1126-1129 [PMID: 28917644 DOI: 10.1016/j.hpb.2017.08.013]
52 **Dondorf F**, Deeb AA, Bauschke A, Felgendreff P, Tautenhahn HM, Ardelt M, Settmacher U, Rauchfuss F. Ligation of the middle hepatic vein to increase hypertrophy induction during the ALPPS procedure. *Langenbecks Arch Surg* 2021; **406**: 1111-1118 [PMID: 33970336 DOI: 10.1007/s00423-021-02181-1]
53 **Esposito F**, Lim C, Lahat E, Shwaartz C, Eshkenazy R, Salloum C, Azoulay D. Combined hepatic and portal vein embolization as preparation for major hepatectomy: a systematic review. *HPB (Oxford)* 2019; **21**: 1099-1106 [PMID: 30926329 DOI: 10.1016/j.hpb.2019.02.023]
54 **Ogata S**, Belghiti J, Farges O, Varma D, Sibert A, Vilgrain V. Sequential arterial and portal vein embolizations before right hepatectomy in patients with cirrhosis and hepatocellular carcinoma. *Br J Surg* 2006; **93**: 1091-1098 [PMID: 16779884

DOI: 10.1002/bjs.5341]
55 **Aoki T**, Imamura H, Hasegawa K, Matsukura A, Sano K, Sugawara Y, Kokudo N, Makuuchi M. Sequential preoperative arterial and portal venous embolizations in patients with hepatocellular carcinoma. *Arch Surg* 2004; **139**: 766-774 [PMID: 15249411 DOI: 10.1001/archsurg.139.7.766]
56 **Fürst G**, Schulte am Esch J, Poll LW, Hosch SB, Fritz LB, Klein M, Godehardt E, Krieg A, Wecker B, Stoldt V, Stockschläder M, Eisenberger CF, Mödder U, Knoefel WT. Portal vein embolization and autologous CD133+ bone marrow stem cells for liver regeneration: initial experience. *Radiology* 2007; **243**: 171-179 [PMID: 17312278 DOI: 10.1148/radiol.2431060625]
57 **am Esch JS**, Schmelzle M, Fürst G, Robson SC, Krieg A, Duhme C, Tustas RY, Alexander A, Klein HM, Topp SA, Bode JG, Häussinger D, Eisenberger CF, Knoefel WT. Infusion of CD133+ bone marrow-derived stem cells after selective portal vein embolization enhances functional hepatic reserves after extended right hepatectomy: a retrospective single-center study. *Ann Surg* 2012; **255**: 79-85 [PMID: 22156926 DOI: 10.1097/SLA.0b013e31823d7d08]
58 **Audollent R**, Eveno C, Contreres JO, Hainaud P, Rampanou A, Dupuy E, Brouland JP, Pocard M. Bone marrow-derived endothelial and hematopoietic precursors cells enhance the metastasis of colon cancer in an orthotopic murine model. *Int J Cancer* 2011; **129**: 2304-2305 [PMID: 22736413 DOI: 10.1002/ijc.25882]
59 **Alison MR**, Islam S, Lim S. Stem cells in liver regeneration, fibrosis and cancer: the good, the bad and the ugly. *J Pathol* 2009; **217**: 282-298 [PMID: 18991329 DOI: 10.1002/path.2453]
60 **Huang SY**, Aloia TA. Portal Vein Embolization: State-of-the-Art Technique and Options to Improve Liver Hypertrophy. *Visc Med* 2017; **33**: 419-425 [PMID: 29344515 DOI: 10.1159/000480034]

World Journal of Gastrointestinal Oncology

Submit a Manuscript: https://www.f6publishing.com

World J Gastrointest Oncol 2022 November 15; 14(11): 2097-2107

DOI: 10.4251/wjgo.v14.i11.2097

ISSN 1948-5204 (online)

ORIGINAL ARTICLE

Basic Study

Proteomic signatures of infiltrative gastric cancer by proteomic and bioinformatic analysis

Li-Hua Zhang, Hui-Qin Zhuo, Jing-Jing Hou, Yang Zhou, Jia Cheng, Jian-Chun Cai

Specialty type: Oncology

Provenance and peer review: Unsolicited article; Externally peer reviewed.

Peer-review model: Single blind

Peer-review report's scientific quality classification

Grade A (Excellent): 0
Grade B (Very good): B, B
Grade C (Good): C
Grade D (Fair): 0
Grade E (Poor): 0

P-Reviewer: Menendez-Menendez J, Spain; M'Koma AE, United States; Nakaji K, Japan

Received: March 25, 2022
Peer-review started: March 25, 2022
First decision: June 2, 2022
Revised: June 16, 2022
Accepted: October 17, 2022
Article in press: October 17, 2022
Published online: November 15, 2022

Li-Hua Zhang, Hui-Qin Zhuo, Jing-Jing Hou, Yang Zhou, Jia Cheng, Jian-Chun Cai, Department of Gastrointestinal Surgery, Zhongshan Hospital of Xiamen University, School of Medicine, Xiamen University, Xiamen 361004, Fujian Province, China

Li-Hua Zhang, Yang Zhou, Jian-Chun Cai, Institute of Gastrointestinal Oncology, Zhongshan Hospital of Xiamen University, School of Medicine, Xiamen University, Xiamen 361004, Fujian Province, China

Hui-Qin Zhuo, Jing-Jing Hou, Jia Cheng, Jian-Chun Cai, Xiamen Municipal Key Laboratory of Gastrointestinal Oncology, Xiamen 361004, Fujian Province, China

Corresponding author: Jian-Chun Cai, PhD, Professor, Department of Gastrointestinal Surgery, Zhongshan Hospital of Xiamen University, School of Medicine, Xiamen University, No. 201 Hubin Road, Siming Street, Xiamen 361004, Fujian Province, China. jianchunfh2@sina.com

Abstract

BACKGROUND

Proteomic signatures of Ming's infiltrative gastric cancer (IGC) remain unknown.

AIM

To elucidate the molecular characteristics of IGC at the proteomics level.

METHODS

Twelve pairs of IGC and adjacent normal tissues were collected and their proteomes were analyzed by high performance liquid chromatography tandem mass spectrometry. The identified peptides were sequenced de novo and matched against the SwissProt database using Maxquant software. The differentially expressed proteins (DEPs) were screened using $|\log2(\text{Fold change})| > 1$ and $P\text{-adj} < 0.01$ as the thresholds. The expression levels of selected proteins were verified by Western blotting. The interaction network of the DEPs was constructed with the STRING database and visualized using Cytoscape with cytoHubba software. The DEPs were functionally annotated using clusterProfiler, STRING and DAVID for Gene Ontology (GO) and Kyoto Encyclopedia of Genes and Genomes (KEGG) pathways. $P < 0.05$ was considered statistically significant.

RESULTS

A total of 7361 DEPs were identified, of which 94 were significantly up-regulated and 223 were significantly down-regulated in IGC relative to normal gastric

tissues. The top 10 up-regulated proteins were MRTO4, BOP1, PES1, WDR12, BRIX1, NOP2, POLR1C, NOC2L, MYBBP1A and TSR1, and the top 10 down-regulated proteins were NDUFS8, NDUFS6, NDUFA8, NDUFA5, NDUFC2, NDUFB8, NDUFB5, NDUFB9, UQCRC2 and UQCRC1. The up-regulated proteins were enriched for 9 biological processes including DNA replication, ribosome biogenesis and initiation of DNA replication, and the cellular component MCM complex. Among the down-regulated proteins, 17 biological processes were enriched, including glucose metabolism, pyruvic acid metabolism and fatty acid β-oxidation. In addition, the mitochondrial inner membrane, mitochondrial matrix and mitochondrial proton transport ATP synthase complex were among the 6 enriched cellular components, and 11 molecular functions including reduced nicotinamide adenine dinucleotide dehydrogenase activity, acyl-CoA dehydrogenase activity and nicotinamide adenine dinucleotide binding were also enriched. The significant KEGG pathways for the up-regulated proteins were DNA replication, cell cycle and mismatch repair, whereas 18 pathways including oxidative phosphorylation, fatty acid degradation and phenylalanine metabolism were significantly enriched among the down-regulated proteins.

CONCLUSION

The proteins involved in cell cycle regulation, DNA replication and mismatch repair, and metabolism were significantly altered in IGC, and the proteomic profile may enable the discovery of novel biomarkers.

Key Words: Infiltrative gastric cancer; Proteomics; Molecular biological characteristics; Ming's classification; Bioinformatic analysis

Core Tip: A total of 7361 proteins were identified and 317 proteins were significantly abnormally expressed in infiltrative gastric cancer (IGC). Twenty hub proteins were found and some of them were verified in IGC. Cell cycle regulation, DNA replication and mismatch repair, and metabolism were significantly altered in IGC.

Citation: Zhang LH, Zhuo HQ, Hou JJ, Zhou Y, Cheng J, Cai JC. Proteomic signatures of infiltrative gastric cancer by proteomic and bioinformatic analysis. *World J Gastrointest Oncol* 2022; 14(11): 2097-2107
URL: https://www.wjgnet.com/1948-5204/full/v14/i11/2097.htm
DOI: https://dx.doi.org/10.4251/wjgo.v14.i11.2097

INTRODUCTION

Gastric cancer (GC) is the fourth most prevalent malignancy worldwide and ranks third in terms of mortality, especially in Asia[1,2]. It is divided into infiltrative GC (IGC) and expanding GC (EGC) according to Ming's system of classification, which is related to Bormann classification (protrusion and ulcer type), Lauren classification (intestinal and diffuse type) and World Health Organization classification (papillary adenocarcinoma, adenosquamous carcinoma, squamous cell carcinoma, carcinoid, *etc.*). The incidence of IGC is 61.5%, and its prognosis is worse than that of EGC[3-5]. Although the IGC classification is relevant in clinical diagnosis, treatment and prognosis assessment[6], the molecular mechanism of IGC is not completely understood. In this study, we analyzed the proteomes of IGC and normal gastric tissues using high performance liquid chromatography tandem mass spectrometry (HPLC-MS/MS), and identified the differentially expressed proteins (DEPs). The key proteins were screened and functionally annotated by Gene Ontology (GO) and Kyoto Encyclopedia of Genes and Genomes (KEGG) pathway analyses. This study is the first to profile the IGC proteome, and may help unravel the molecular mechanisms and novel biomarkers of IGC.

MATERIALS AND METHODS

Clinical samples

Twelve pairs of IGC tissues and normal resection margin tissues were obtained from Zhongshan Hospital Affiliated to Xiamen University. The samples were fixed in formalin and snap frozen at -80 °C. The frozen tissue sections were stained with hematoxylin and eosin as per standard protocols, and

examined by the chief surgeon and chief physician of the pathology department. All patients signed an informed consent form, and the study was approved by the ethics committee of Zhongshan Hospital affiliated to Xiamen University.

Peptide preparation

The frozen tissue samples were homogenized in liquid nitrogen, and ultrasonicated with lysis buffer (8 mol/L urea, 1% protease inhibitor and 2 mmol/L EDTA). The protein samples were reduced with 5 mmol/L dithiothreitol at 56 °C for 30 min, and then incubated with 11 mmol/L iodoacetamide for 15 min at room temperature in the dark. The urea concentration of the sample was diluted to less than 2 mol/L.

HPLC-MS/MS

The peptides were fractionated by high pH reverse HPLC using an Agilent 300 Extend C18 column (5 μm particle size, 4.6 mm inner diameter, 250 mm length), and a step gradient of 8% to 32% acetonitrile at pH 9. Sixty components were separated in 60 min. The peptides were pooled into 6 components and freeze-dried under vacuum. The lyophilized peptides were dissolved in 0.1% v/v aqueous formic acid and then separated using the EASY-nLC 1000 ultra-high performance liquid system. Mobile phase A consisted of 0.1% formic acid and 2% acetonitrile, and mobile phase B was an aqueous solution of 0.1% formic acid and 90% acetonitrile. The gradient setting was as follows: 0-62 min, 5%-22% B; 62-82 min, 22%-35% B; 82-86 min, 35%-80% B; 86-90 min, 80% B. The flow rate was maintained at 450 nL/min.

The separated peptides were then injected into the NSI ion source and analyzed by the Q Exactive™ Plus mass spectrometer. The ion source voltage was set to 2 kV, and the peptide precursor ions and their secondary fragments were detected and analyzed by high-resolution Orbitrap. The scanning range of the primary mass spectrometer was set to 350-1800 m/z, the scanning resolution to 70000, and the secondary scanning resolution to 17500. Data were acquired using a data-dependent scanning program. The entire process of HPLC-MS/MS is briefly summarized and shown in Figure 1.

Database search

The secondary mass spectrum data were searched against the SwissProtHuman (20317 sequences) database using Maxquant (version 1.5.2.8). The search parameters were as follows: restriction enzyme: Trypsin/P; number of missing cleavage sites: 2; mass error tolerance of the primary precursor ion of the first search and the main search: 20 ppm and 5 ppm, respectively; mass error tolerance of the secondary fragment ion: 0.02 Da; fixed modification: cysteine alkylation; and variable modification: oxidation of methionine and acetylation of the N-terminus. The false discovery rate for protein identification and PSM identification was set to 1%.

Western blotting

Total protein was extracted using RIPA lysis buffer (Thermo Scientific, United Kingdom), and its concentration was determined with an enhanced bicinchoninic acid assay kit (CWBio, China). Around 40 mg protein per sample was separated by sodium dodecyl sulfate-polyacrylamide gel electrophoresis, and transferred to polyvinylidene difluoride membranes (CWBio, China). After blocking with 5% non-fat milk for 1 h at room temperature, the membranes were incubated overnight with primary antibodies targeting MRTO4 (1:2000, ab212044, Abcam, United States), BOP1 (1:3000, ab32053, Abcam, United States), PES1 (1:5000, ab56701, Abcam, United States), NDUFS8 (1:3000, ab226760, Abcam, United States), NDUFS6 (1:3000, ab226760, Abcam, United States), NDUFA8 (1:3000, ab226760, Abcam, United States) and β-actin (1:5000, ab8226, Abcam, United States) at 4 °C. The membranes were washed thrice with TBST (Tris-buffered saline with Tween 60), and probed with horseradish peroxidase-conjugated secondary antibody (1:5000) for 1.5 h at room temperature. The protein bands were visualized using an enhanced chemiluminescence system, and the membranes were exposed to X-ray films (Bio-Rad, United States). Densitometric analysis was performed using Image Pro-Plus software (Media Cybernetics, United States), and relative protein expression levels were normalized to β-actin.

Protein-protein interaction network and hub protein screening

The protein-protein interaction (PPI) network was analyzed using STRING (https://string-db.org/, version 11.0)[7] with Homo sapiens as the species. The DEPs were imported into the STRING website, and the Cytoscape plug-in cytoHubba was used to screen for hub proteins. The data were from experiments, databases, co-expression and co-occurrence, and the interaction score was 0.4. The TSV format file of PPI results was imported into Cytoscape (version 3.8.2) software for visual editing and network display.

GO and KEGG pathway enrichment analysis

ClusterProfiler enrichment analysis: The bioconductor, org.Hs.eg.db and clusterProfiler packages[8] were simultaneously installed in the R software. The gene names of the DEPs were converted to the ENTERZID format using org.Hs.eg.db package. The enrichGO software was used for GO (biological processes, BP; cell components, CC; molecular functions, MF) enrichment analysis and enrichKEGG for

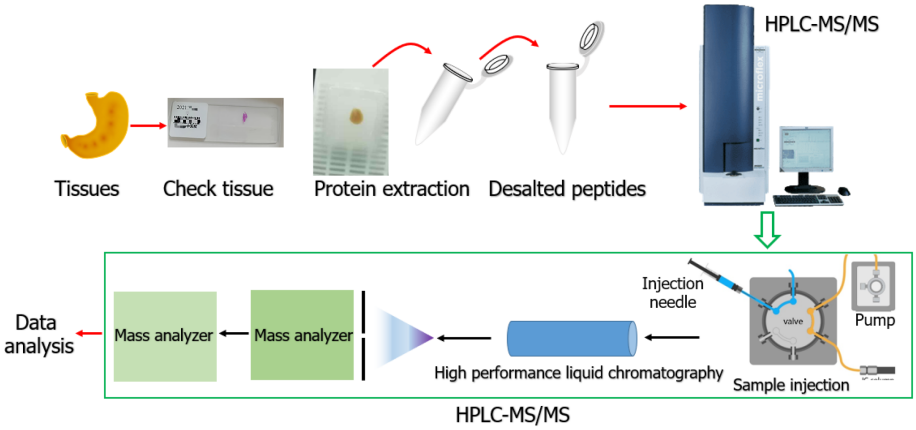

DOI: 10.4251/wjgo.v14.i11.2097

Figure 1 Schematic diagram illustrating the procedure of high performance liquid chromatography tandem mass spectrometry for proteomic analysis. HPLC-MS/MS: High performance liquid chromatography tandem mass spectrometry.

KEGG pathway enrichment analysis. *P* value < 0.05 was considered as a significant enrichment.

STRING enrichment analysis: The selected proteomic gene names were enriched and analyzed on the STRING website (https://string-db.org/, version 11.0) using the full network mode with Homo sapiens as the enriched species. The type of interactions between the proteins was indicated by the network connection line. The data were retrieved from experiments, databases, and co-expression and co-occurrence analyses. The interaction score was set at 0.4, and *P* value < 0.05 was considered significant.

DAVID enrichment analysis: The selected proteomic genes were enriched in DAVID version 6.8 (The Database for Annotation, Visualization and Integrated Discovery; https://david.ncifcrf.gov/)[9,10] with Homo sapiens as the selected species. GO enrichment was analyzed by Gene_Ontology, and KEGG pathways by KEGG_PATHWAY. *P* value < 0.05 was considered statistically significant.

Statistical methods and software

The difference in protein expression levels between IGC and normal tissues was analyzed by the paired *t* test using R (version R4.0.3, https://www.r-project.org/). The volcano graph was plotted using the ggplot and ggrepel packages. The protein interaction network was visualized in Cytoscape (version 3.8.2, https://cytoscape.org/) software[11]. The pictures were edited using Adobe Photoshop CS6 software.

RESULTS

Proteomic signature of IGC relative to normal gastric tissues

The proteomes of 12 pairs of histo-pathologically confirmed IGC and adjacent normal gastric tissues (Figure 2A and B) were profiled. The representative MS/MS fragments are shown in Figure 2C, and the expanded region of a single FTMS full scan with a mass range of 400-1800 m/z is shown in Figure 2D. There were a total of 7361 DEPs between IGC and normal tissues ($P < 0.01$), of which 94 were up-regulated and 223 were downregulated in the IGC samples (Figure 2E).

Proteomic signature of IGC tissues

The interaction networks of the upregulated and downregulated proteins in IGC are shown in Figure 3A and C, respectively. According to the MCC algorithm, the top 10 up-regulated proteins were MRTO4, BOP1, PES1, WDR12, BRIX1, NOP2, POLR1C, NOC2L, MYBBP1A and TSR1 (Figure 3B), whereas NDUFS8, NDUFS6, NDUFA8, NDUFA5, NDUFC2, NDUFB8, NDUFB5, NDUFB9, UQCRC2 and UQCRC1 were the key down-regulated proteins (Figure 3D). The expression levels of MRTO4, BOP1, PES1 (Figure 3E), NDUFS8, NDUFS6 and NDUFA8 (Figure 3F) were verified in IGC tissues by western blotting.

Proteomic signatures of GO analysis in IGC

The significantly enriched GO terms for the up-regulated and down-regulated proteins and their interactive networks are shown in Figure 4A-D. The biological processes enriched in the upregulated proteins included DNA replication, ribosome biogenesis, and DNA replication initiation (Figure 4E), and MCM complex was the key cellular component (Figure 4F). The molecular functions did not show

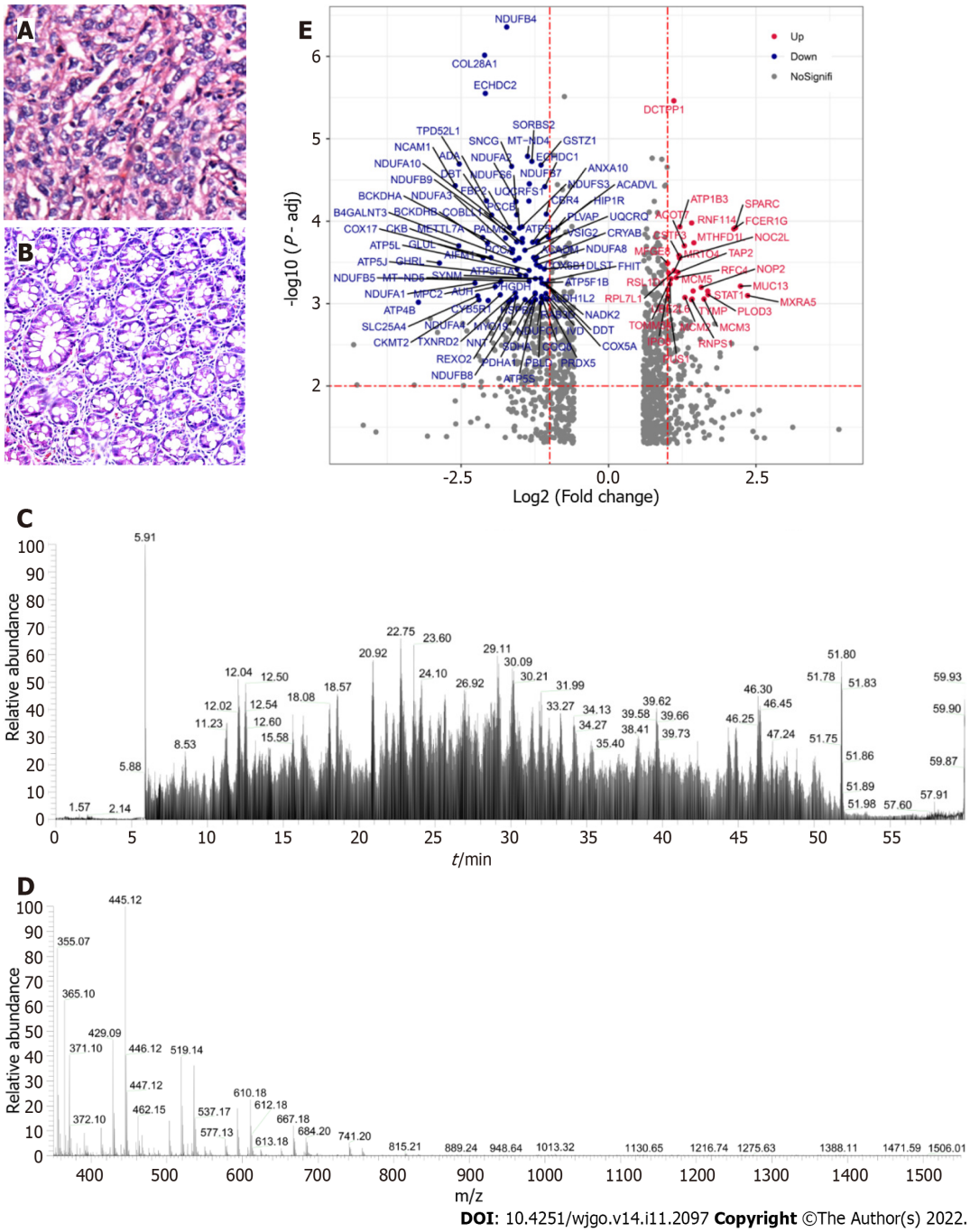

DOI: 10.4251/wjgo.v14.i11.2097 **Copyright** ©The Author(s) 2022.

Figure 2 Volcano map of significant differentially expressed proteins. A and B: Representative images of hematoxylin and eosin stained infiltrative gastric cancer (IGC) (A) and normal gastric tissues (B); C: Base peak chromatogram of tissue sample on Orbitrap LTQ-LC/MS-CID activation; D: Expanded region of a single FTMS full scan with a mass range of m/z 350-1800, and ion peaks with double or higher charge (612.30, *Z* = 3); E: Volcano map showing differentially expressed proteins between IGC and normal tissues. *P*-adj: Corrected *P* value; Fold change: Ratio of expression levels in cancer and adjacent tissues.

co-enrichment (Figure 4G). Among the significantly down-regulated proteins, 17 biological processes including glucose metabolism, pyruvate metabolism and fatty acid β-oxidation were significantly enriched (Figure 4H). In addition, 6 cell components including the mitochondrial inner membrane, mitochondrial matrix and mitochondrial proton-transporting ATP synthase complex (Figure 4I), and 11 molecular functions including reduced nicotinamide adenine dinucleotide (NADH) dehydrogenase activity, acyl-CoA dehydrogenase activity and nicotinamide adenine dinucleotide (NAD) binding (Figure 4J) were enriched.

Proteomic signatures of KEGG pathways in IGC

Three KEGG pathways were significantly enriched in the up-regulated proteins (Figure 5A), including DNA replication, cell cycle and mismatch repair (Figure 5B). Among the down-regulated proteins, 18 KEGG pathways were enriched (Figure 5C), such as oxidative phosphorylation, fatty acid degradation,

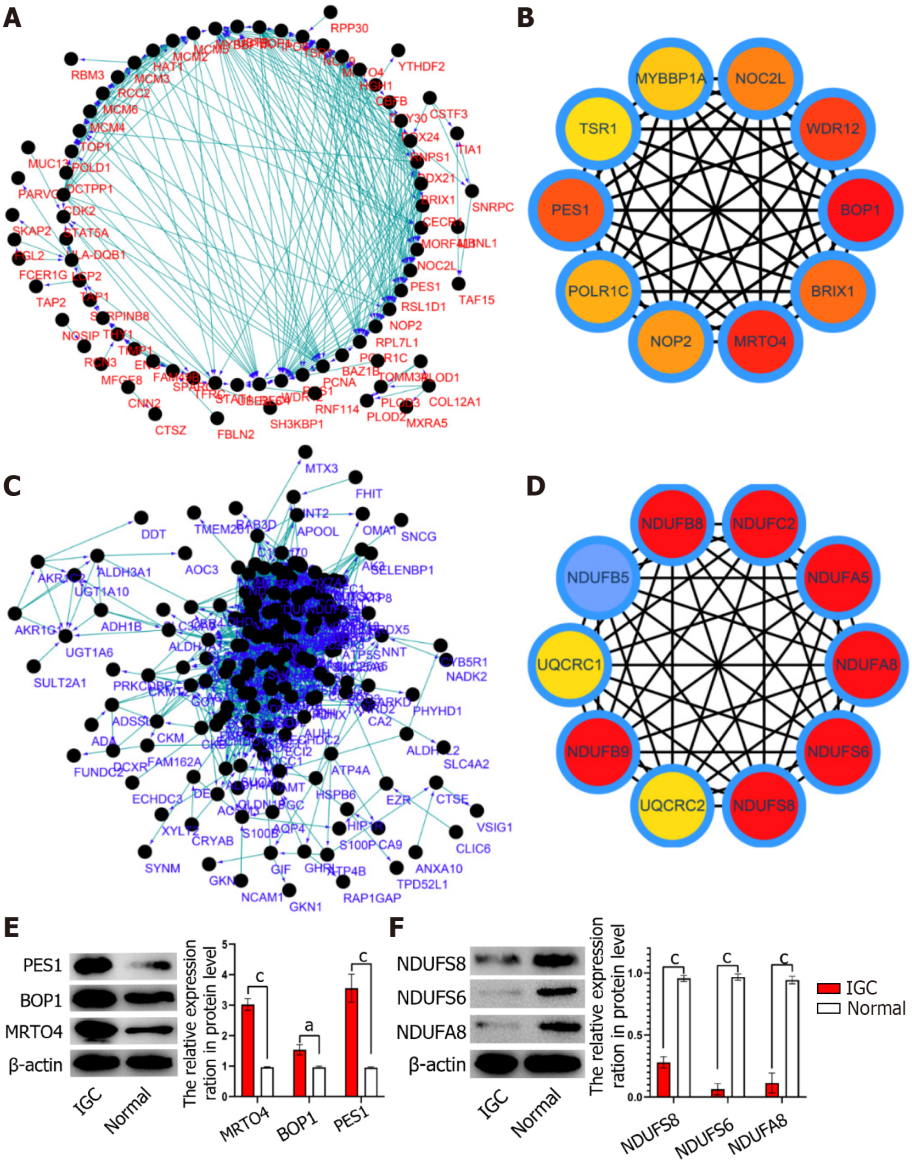

DOI: 10.4251/wjgo.v14.i11.2097 **Copyright** ©The Author(s) 2022.

Figure 3 Protein interaction networks of differentially expressed proteins. A and B: The interaction network of the significantly up-regulated proteins (A) in infiltrative gastric cancer (IGC) and the top 10 proteins (B); C: The interaction network of the significantly down-regulated proteins (C) in IGC and the top 10 proteins (D); E and F: Representative immunoblots showing the expression levels of specific up-regulated (E) and down-regulated (F) proteins in IGC tissues. $^{a}P < 0.05$; $^{c}P < 0.001$.

and phenylalanine metabolism (Figure 5D).

DISCUSSION

The top 20 hub proteins identified in the IGC tissues were MRTO4, BOP1, PES1, WDR12, BRIX1, NOP2, POLR1C, NOC2L, MYBBP1A, TSR1, NDUFS8, NDUFS6, NDUFA8, NDUFA5, NDUFC2, NDUFB8, NDUFB5, NDUFB9, UQCRC2 and UQCRC1. PES1 is highly expressed in GC tissues, and knocking down PES1 in GC cells inhibited their proliferation[12]. On the other hand, UQCRC2 is downregulated in GC and its overexpression inhibited the migration and invasion of the tumor cells[13]. Therefore, these proteins are promising prognostic biomarkers of IGC.

The proteins that were upregulated in IGC tissues showed significant enrichment of DNA replication, ribosome biogenesis and DNA replication initiation, MCM complex, and the cell cycle and mismatch repair signal pathways. This strongly suggests that these proteins exert a pro-proliferative and oncogenic function in IGC, most likely by promoting DNA replication, cell cycle progression and mismatch repair. Changes in the MCM complex have been previously reported in IGC cells, and are regulated by miRNAs[14]. In addition, DNA replication and cell cycle signaling pathways are key factors involved in the proliferation of GC cells[15,16], whereas the mismatch repair pathway affects

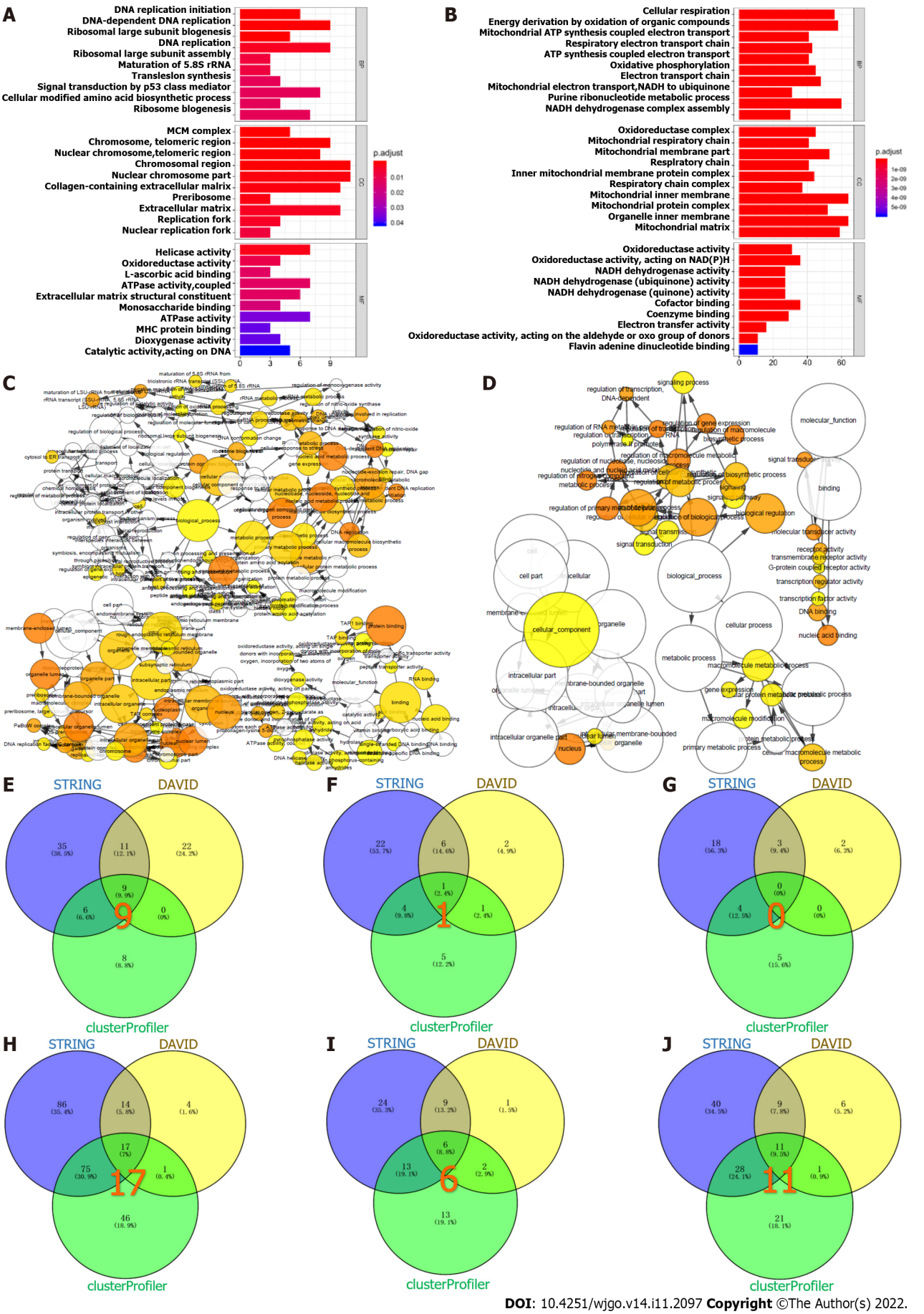

DOI: 10.4251/wjgo.v14.i11.2097

Figure 4 Gene Ontology of differentially expressed proteins. A and B: Histograms showing the significant Gene Ontology (GO) terms of up-regulated (A)

and down-regulated (B) proteins; C and D: Topological network diagram of the GO terms of up-regulated (C) and down-regulated (D) proteins; E-G: Venn diagrams showing significantly enriched BP (E), CC (F) and MF (G) terms in the up-regulated proteins; H-J: Venn diagrams showing significantly enriched BP (H), CC (I) and MF (J) terms in the down-regulated proteins.

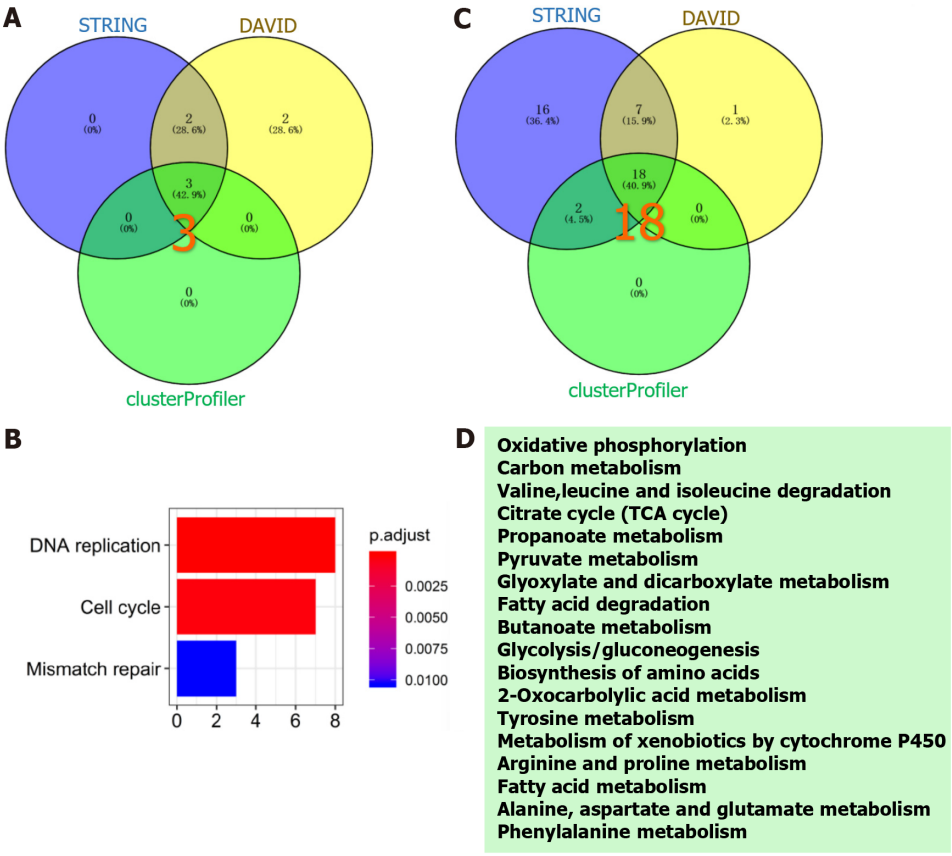

DOI: 10.4251/wjgo.v14.i11.2097

Figure 5 Enriched Kyoto Encyclopedia of Genes and Genomes pathways in differentially expressed proteins. A and B: Venn diagram of Kyoto Encyclopedia of Genes and Genomes (KEGG) enrichment in the up-regulated protein group (A) and significantly enriched KEGG pathways (B); C and D: Venn diagram of KEGG enrichment in the down-regulated protein group (C) and significantly enriched KEGG pathways (D).

drug resistance and metastasis[17-21].

The down-regulated proteins were enriched in glucose metabolism, pyruvate metabolism, phenylalanine metabolism, fatty acid β-oxidation, oxidative phosphorylation, mitochondrial inner membrane, mitochondrial matrix, mitochondrial proton transport ATP synthase complex, NADH dehydrogenase activity, acyl-CoA dehydrogenase activity and NAD binding. This is indicative of aberrant mitochondrial metabolism in the IGC cells. Consistent with our findings, a previous study reported dysregulated oxidative phosphorylation in GC[22].

The significant DEPs identified in our study are potential diagnostic and prognostic markers, as well as therapeutic targets in IGC, and will have to be validated in a large cohort from multiple centers. Furthermore, the proteomic signatures of IGC provide insights into the possible mechanisms underlying IGC progression, which likely involve DNA replication, cell cycle, mismatch repair, and energy metabolism pathways, and will also contribute to precision medicine for more accurate diagnosis and better treatment effect.

CONCLUSION

This study has several limitations that ought to be considered. First, only 12 paired IGC and adjacent normal tissues were analyzed, and the sample size will have to be increased by involving multiple centers in the follow-up study. Second, few proteins could be verified, and the number will have to be increased in future studies by mass spectrometry.

ARTICLE HIGHLIGHTS

Research background

The prognosis of infiltrative gastric cancer (IGC) patients remains relatively poor. Therefore, it is necessary to explore the molecular mechanisms underlying the occurrence and development of IGC.

Research motivation

The proteomic signatures of IGC remain unknown.

Research objectives

To profile the proteome of IGC.

Research methods

The proteins from IGC and normal tissue samples were analyzed by high performance liquid chromatography tandem mass spectrometry and searched against the database *via* Maxquant software. The differentially expressed proteins (DEPs) were screened using $|\log2(\text{Fold Change})| > 1$ and $P\text{-adj} < 0.01$ as the thresholds. The expression levels of some proteins were verified by Western blotting. The interaction network of DEPs was constructed using the STRING database, and the key proteins were visualized using Cytoscape cytoHubba software. Finally, clusterProfiler, STRING and DAVID were used for Gene Ontology (GO) and Kyoto Encyclopedia of Genes and Genomes (KEGG) pathway enrichment analysis of DEPs, with $P < 0.05$ as the threshold.

Research results

A total of 7361 DEPs were identified, of which 94 were significantly up-regulated and 223 were significantly down-regulated in IGC relative to normal gastric tissues. The top 10 up-regulated proteins were MRTO4, BOP1, PES1, WDR12, BRIX1, NOP2, POLR1C, NOC2L, MYBBP1A and TSR1, and the top 10 down-regulated proteins were NDUFS8, NDUFS6, NDUFA8, NDUFA5, NDUFC2, NDUFB8, NDUFB5, NDUFB9, UQCRC2 and UQCRC1. The up-regulated proteins were enriched for 9 biological processes including DNA replication, ribosome biogenesis and initiation of DNA replication, and the cellular component MCM complex. Among the down-regulated proteins, 17 biological processes were enriched, including glucose metabolism, pyruvic acid metabolism and fatty acid β-oxidation. In addition, the mitochondrial inner membrane, mitochondrial matrix and mitochondrial proton transport ATP synthase complex were among the 6 enriched cellular components among the down-regulated proteins, and 11 molecular functions including reduced nicotinamide adenine dinucleotide dehydrogenase activity, acyl-CoA dehydrogenase activity and nicotinamide adenine dinucleotide binding were also enriched. The significant KEGG pathways for the up-regulated proteins were DNA replication, cell cycle and mismatch repair, whereas 18 pathways including oxidative phosphorylation, fatty acid degradation and phenylalanine metabolism were significantly enriched among the down-regulated proteins.

Research conclusions

The proteins involved in cell cycle regulation, DNA replication and mismatch repair, and metabolism were significantly altered in IGC, which provides a basis for the future identification of novel biomarkers.

Research perspectives

This study reveals the proteomic signature of IGC.

FOOTNOTES

Author contributions: Cai JC, Zhang LH and Zhuo HQ contributed conceptualization; Zhang LH, Zhuo HQ, Hou JJ, Zhou Y and Cheng J contributed methodology; Hou JJ and Cheng J contributed data curation; Zhang LH, Hou JJ, Zhou Y and Cheng J contributed formal analysis; Zhang LH and Zhou Y contributed visualization; Zhang LH and Zhuo HQ wrote the manuscript; Zhang LH, Zhuo HQ, Hou JJ, Zhou Y, Cheng J and Cai JC contributed manuscript review; Cai JC, Zhuo HQ and Hou JJ contributed supervision.

Supported by National Natural Science Foundation of China, No. 81871979; Natural Science Foundation of Fujian Province, No. 2021J02056, No. 2021J05276 and No. 2020CXB048; and Medical and Health Sciences Foundation of Xiamen, No. 3502Z20199171 and No. 3502Z20204002.

Institutional review board statement: This research was conducted with the approval of the ethical review committee of Zhongshan Hospital of Xiamen University (approval No. 2022-178) and in accordance with the guidelines of the Declaration of Helsinki.

Informed consent statement: All study participants, or their legal guardian, provided informed written consent prior to study enrollment.

Conflict-of-interest statement: All the authors report no relevant conflicts of interest for this article.

Data sharing statement: Technical appendix, statistical code, and dataset available from the corresponding author at jianchunfh2@sina.com.

Country/Territory of origin: China

ORCID number: Li-Hua Zhang 0000-0002-0931-5039; Hui-Qin Zhuo 0000-0001-8322-4197; Jing-Jing Hou 0000-0001-9984-9386; Yang Zhou 0000-0003-0406-3175; Jia Cheng 0000-0003-3116-4035; Jian-Chun Cai 0000-0002-0931-503X.

S-Editor: Gao CC
L-Editor: Webster J
P-Editor: Zhao S

REFERENCES

1 **Bray F**, Ferlay J, Soerjomataram I, Siegel RL, Torre LA, Jemal A. Global cancer statistics 2018: GLOBOCAN estimates of incidence and mortality worldwide for 36 cancers in 185 countries. *CA Cancer J Clin* 2018; **68**: 394-424 [PMID: 30207593 DOI: 10.3322/caac.21492]
2 **Chen W**, Zheng R, Baade PD, Zhang S, Zeng H, Bray F, Jemal A, Yu XQ, He J. Cancer statistics in China, 2015. *CA Cancer J Clin* 2016; **66**: 115-132 [PMID: 26808342 DOI: 10.3322/caac.21338]
3 **Cimerman M**, Repse S, Jelenc F, Omejc M, Bitenc M, Lamovec J. Comparison of Lauren's, Ming's and WHO histological classifications of gastric cancer as a prognostic factor for operated patients. *Int Surg* 1994; **79**: 27-32 [PMID: 8063551]
4 **Garnier P**, Vielh P, Asselain B, Durand JC, Girodet J, Pilleron JP, Salmon RJ. [Prognostic value of the Lauren and Ming classifications in gastric adenocarcinoma. Multidimensional analysis]. *Gastroenterol Clin Biol* 1988; **12**: 553-558 [PMID: 3417082]
5 **Ribeiro MM**, Sarmento JA, Sobrinho Simões MA, Bastos J. Prognostic significance of Lauren and Ming classifications and other pathologic parameters in gastric carcinoma. *Cancer* 1981; **47**: 780-784 [PMID: 7226025 DOI: 10.1002/1097-0142(19810215)47:4<780::aid-cncr2820470424>3.0.co;2-g]
6 **Luebke T**, Baldus SE, Grass G, Bollschweiler E, Thiele J, Dienes HP, Hoelscher AH, Moenig SP. Histological grading in gastric cancer by Ming classification: correlation with histopathological subtypes, metastasis, and prognosis. *World J Surg* 2005; **29**: 1422-7; discussion 1428 [PMID: 16222448 DOI: 10.1007/s00268-005-7795-z]
7 **Szklarczyk D**, Gable AL, Lyon D, Junge A, Wyder S, Huerta-Cepas J, Simonovic M, Doncheva NT, Morris JH, Bork P, Jensen LJ, Mering CV. STRING v11: protein-protein association networks with increased coverage, supporting functional discovery in genome-wide experimental datasets. *Nucleic Acids Res* 2019; **47**: D607-D613 [PMID: 30476243 DOI: 10.1093/nar/gky1131]
8 **Yu G**, Wang LG, Han Y, He QY. clusterProfiler: an R package for comparing biological themes among gene clusters. *OMICS* 2012; **16**: 284-287 [PMID: 22455463 DOI: 10.1089/omi.2011.0118]
9 **Huang da W**, Sherman BT, Lempicki RA. Systematic and integrative analysis of large gene lists using DAVID bioinformatics resources. *Nat Protoc* 2009; **4**: 44-57 [PMID: 19131956 DOI: 10.1038/nprot.2008.211]
10 **Huang da W**, Sherman BT, Lempicki RA. Bioinformatics enrichment tools: paths toward the comprehensive functional analysis of large gene lists. *Nucleic Acids Res* 2009; **37**: 1-13 [PMID: 19033363 DOI: 10.1093/nar/gkn923]
11 **Otasek D**, Morris JH, Bouças J, Pico AR, Demchak B. Cytoscape Automation: empowering workflow-based network analysis. *Genome Biol* 2019; **20**: 185 [PMID: 31477170 DOI: 10.1186/s13059-019-1758-4]
12 **Li J**, Zhou X, Lan X, Zeng G, Jiang X, Huang Z. Repression of PES1 expression inhibits growth of gastric cancer. *Tumour Biol* 2016; **37**: 3043-3049 [PMID: 26423399 DOI: 10.1007/s13277-015-4069-8]
13 **Wang DW**, Su F, Zhang T, Yang TC, Wang HQ, Yang LJ, Zhou FF, Feng MH. The *miR-370*/UQCRC2 axis facilitates tumorigenesis by regulating epithelial-mesenchymal transition in Gastric Cancer. *J Cancer* 2020; **11**: 5042-5055 [PMID: 32742452 DOI: 10.7150/jca.45553]
14 **Cheng J**, Zhuo H, Wang L, Zheng W, Chen X, Hou J, Zhao J, Cai J. Identification of the Combinatorial Effect of miRNA Family Regulatory Network in Different Growth Patterns of GC. *Mol Ther Oncolytics* 2020; **17**: 531-546 [PMID: 32637572 DOI: 10.1016/j.omto.2020.03.012]
15 **Rozacky J**, Nemec AA, Sweasy JB, Kidane D. Gastric cancer associated variant of DNA polymerase beta (Leu22Pro) promotes DNA replication associated double strand breaks. *Oncotarget* 2015; **6**: 24474-24487 [PMID: 26090616 DOI: 10.18632/oncotarget.4426]
16 **Zhu L**, Wang C, Lin S, Zong L. CircKIAA0907 Retards Cell Growth, Cell Cycle, and Autophagy of Gastric Cancer In

Vitro and Inhibits Tumorigenesis In Vivo *via* the miR-452-5p/KAT6B Axis. *Med Sci Monit* 2020; **26**: e924160 [PMID: 32722658 DOI: 10.12659/MSM.924160]

17 **An JY**, Choi YY, Lee J, Hyung WJ, Kim KM, Noh SH, Choi MG, Cheong JH. A Multi-cohort Study of the Prognostic Significance of Microsatellite Instability or Mismatch Repair Status after Recurrence of Resectable Gastric Cancer. *Cancer Res Treat* 2020; **52**: 1153-1161 [PMID: 32599987 DOI: 10.4143/crt.2020.173]

18 **Dislich B**, Blaser N, Berger MD, Gloor B, Langer R. Preservation of Epstein-Barr virus status and mismatch repair protein status along the metastatic course of gastric cancer. *Histopathology* 2020; **76**: 740-747 [PMID: 31898331 DOI: 10.1111/his.14059]

19 **Kim SM**, An JY, Byeon SJ, Lee J, Kim KM, Choi MG, Lee JH, Sohn TS, Bae JM, Kim S. Prognostic value of mismatch repair deficiency in patients with advanced gastric cancer, treated by surgery and adjuvant 5-fluorouracil and leucovorin chemoradiotherapy. *Eur J Surg Oncol* 2020; **46**: 189-194 [PMID: 31500870 DOI: 10.1016/j.ejso.2019.08.025]

20 **Sugimoto R**, Endo M, Osakabe M, Toya Y, Yanagawa N, Matsumoto T, Sugai T. Immunohistochemical Analysis of Mismatch Repair Gene Proteins in Early Gastric Cancer Based on Microsatellite Status. *Digestion* 2021; **102**: 691-700 [PMID: 33053554 DOI: 10.1159/000510679]

21 **Verma R**, Agarwal AK, Sakhuja P, Sharma PC. Microsatellite instability in mismatch repair and tumor suppressor genes and their expression profiling provide important targets for the development of biomarkers in gastric cancer. *Gene* 2019; **710**: 48-58 [PMID: 31145962 DOI: 10.1016/j.gene.2019.05.051]

22 **Su F**, Zhou FF, Zhang T, Wang DW, Zhao D, Hou XM, Feng MH. Quantitative proteomics identified 3 oxidative phosphorylation genes with clinical prognostic significance in gastric cancer. *J Cell Mol Med* 2020; **24**: 10842-10854 [PMID: 32757436 DOI: 10.1111/jcmm.15712]

World Journal of Gastrointestinal Oncology

Submit a Manuscript: https://www.f6publishing.com

World J Gastrointest Oncol 2022 November 15; 14(11): 2108-2121

DOI: 10.4251/wjgo.v14.i11.2108

ISSN 1948-5204 (online)

ORIGINAL ARTICLE

Basic Study

Potential role of long noncoding RNA RP5-881L22.5 as a novel biomarker and therapeutic target of colorectal cancer

Hua Zong, Jian-Qiang Zou, Jian-Peng Huang, Shi-Ting Huang

Specialty type: Gastroenterology and hepatology

Provenance and peer review: Unsolicited article; Externally peer reviewed.

Peer-review model: Single blind

Peer-review report's scientific quality classification

Grade A (Excellent): 0
Grade B (Very good): B
Grade C (Good): C, C
Grade D (Fair): 0
Grade E (Poor): 0

P-Reviewer: Batyrbekov K, Kazakhstan; Ezenkwa US; Manojlovic N, Serbia

Received: June 25, 2022
Peer-review started: June 25, 2022
First decision: August 30, 2022
Revised: September 13, 2022
Accepted: October 19, 2022
Article in press: October 19, 2022
Published online: November 15, 2022

Hua Zong, Jian-Qiang Zou, Jian-Peng Huang, Shi-Ting Huang, Department of Gastrointestinal Surgery, The Third People's Hospital of Shenzhen, Shenzhen 518000, Guangdong Province, China

Corresponding author: Hua Zong, Doctor, Department of Gastrointestinal Surgery, The Third People's Hospital of Shenzhen, No. 29 Bulan Road, Shenzhen 518000, Guangdong Province, China. zonghua@mail.sustech.edu.cn

Abstract

BACKGROUND

The incidence of colorectal cancer in humans is high, and it is in the top five for cancer-related morbidity and mortality. It is one of the main threats to human health. The function of long noncoding RNAs in tumor occurrence and development has gradually gained attention in recent years. In increasing numbers of studies, researchers have demonstrated that it plays an important role in the pathogenesis of colorectal cancer.

AIM

To find out if long noncoding RNA RP5-881L22.5 played a role in the pathogenesis of colorectal cancer in relation to the tumor microenvironment.

METHODS

We analyzed the transcriptome data and clinical data in The Cancer Genome Atlas-colon adenocarcinoma. The CIRBERSORT algorithm was applied to evaluate these tumor-infiltrating immune cells in The Cancer Genome Atlas-colon adenocarcinoma cancer tissue samples. Using the "estimate" package in R, we assessed the tumor immune microenvironment. The expression level of RP5-881L22.5 in tumor tissue and adjacent normal tissue samples from 4 pairs of colorectal cancer patients was determined by quantitative reverse transcription PCR. Colorectal cancer cells were tested for invasiveness using a transwell invasion assay after RP5-881L22.5 expression was knocked down.

RESULTS

The expression of lncRNA RP5-881L22.5 was related to the clinical characteristics of the tumors, and it was negatively related to the infiltration level of immune cells in the tumor microenvironment and the expression of T cell inhibitory receptors. A major function of its coexpressed mRNA was to regulate tumor immunity, such as the immune response. When quantitative reverse transcription

PCR was performed on tumor tissues from 4 pairs of colorectal cancer patients, the results showed that RP5-881L22.5 was highly expressed. Subsequently, knocking down the expression of RP5-881L22.5, the invasiveness of colorectal cancer cell lines was reduced, and the apoptosis rate was increased.

CONCLUSION

RP5-881L22.5 plays a crucial role in the microenvironment of tumors as well as in the pathogenesis of colorectal cancer. The relationship between RP5-881L22.5 and the tumor immune microenvironment deserves further study.

Key Words: Colorectal cancer; Long noncoding RNA RP5-881L22.5; Tumor immune microenvironment; Biomarker; Therapeutic target

Core Tip: Long noncoding RNA RP5-881L22.5 is related to the clinical characteristics of tumors, and it is negatively related to the infiltration level of immune cells in the tumor microenvironment and the expression of T cell inhibitory receptors. RP5-881L22.5 may play an important role in the tumor immune microenvironment as well as in the pathogenesis of colorectal cancer. The relationship between RP5-881L22.5 and the tumor immune microenvironment deserves further study.

Citation: Zong H, Zou JQ, Huang JP, Huang ST. Potential role of long noncoding RNA RP5-881L22.5 as a novel biomarker and therapeutic target of colorectal cancer. *World J Gastrointest Oncol* 2022; 14(11): 2108-2121
URL: https://www.wjgnet.com/1948-5204/full/v14/i11/2108.htm
DOI: https://dx.doi.org/10.4251/wjgo.v14.i11.2108

INTRODUCTION

Among all malignant tumors, colorectal cancer is the most common worldwide. In total, 1148515 new cases were diagnosed worldwide in 2020[1]. Although the diagnosis and treatment of colorectal cancer have been continuously improved in recent years, the 5-year survival rate of colorectal cancer patients has not changed significantly. Greater than 20% of patients have already experienced metastasis at diagnosis, and approximately 50% of patients experience metastases during treatment[2]. Therefore, more research on the pathogenesis, early diagnosis, early treatment and prognosis of colorectal cancer is needed.

With the progression of research, it is increasingly recognized that tumors are a systemic disease, and the tumor immune microenvironment is a key factor involved in the pathogenesis and mechanism of tumors[3,4]. Innate immunity and adaptive immunity run through the whole disease process[5,6]. In the early stage of tumorigenesis, natural killer (NK) cells can recognize specific ligands on the surface of tumor cells, even if there are only a few tumor cells[3]. On the other hand, the activation of macrophages and dendritic cells, especially T cells and B cells, in the tumor immune microenvironment produces a large amount of additional cytokines, which further promotes the activation of $CD8^+$ cytotoxic T cells and promotes immune memory[7]. However, given the long-term presence of tumors in the body, tumor cells can resist or suppress anti-tumor immune responses, leading to immune evasion and promoting tumor progression, which also represents a challenge for immunotherapy[8].

Long noncoding RNAs (lncRNAs) have a length over 200 nucleotides and are involved in many normal human physiological functions and pathogenic processes of disease[9,10]. In addition, extensive studies have found that lncRNAs have a pivotal function in the formation of the tumor immune microenvironment[11]. Therefore, we designed this study to explore whether lncRNAs can be used as molecular markers for a more accurate prediction of colorectal cancer prognosis and whether the molecular mechanisms of lncRNAs are the reasons for the differences in colorectal cancer prognosis as well as their impact on the tumor immune microenvironment.

MATERIALS AND METHODS

Data preparation

We downloaded the transcriptome sequencing data and clinical data from the Colon Adenocarcinoma (COAD) project in The Cancer Genome Atlas (TCGA) from the UCSC Xena (https://xenabrowser.net/)

website[12,13]. The data included HTseq-FPKM data [log2 (FPKM+1)] (https://gdc-hub.s3.us-east-1.amazonaws.com/download/TCGA-COAD.htseq_fpkm.tsv.gz), survival data (https://gdc-hub.s3.us-east-1.amazonaws.com/download/TCGA-COAD.survival.tsv) and clinical data (Phenotype including pathological staging and other data) (https://gdc-hub.s3.us-east-1.amazonaws.com/download/TCGA-COAD.GDC_phenotype.tsv.gz). The dataset contains 512 colon cancer tissues and adjacent normal tissues, of which 448 colon cancer tissues have complete survival data and pathological stage data (tumor stage was determined according to the UICC and AJCC TNM classification system).

Gene annotation and dataset construction

According to the human reference genome GRch38 file (release 22) provided on the GENCODE website (https://www.gencodegenes.org), we converted gene IDs from Ensembl to symbols. Then, according to the annotation files provided by GENCODE, we extracted the mRNA and lncRNA expression datasets from the TCGA-COAD sequencing data[14].

Differential expression analysis of mRNA and lncRNA

Genes with extremely low expression levels [log2 (FKPM+1) < 0.5] were removed, and the differential expression of HTseq-FPKM data was analyzed with "limma" (R language, V4.1.1)[15]. We compared mRNA and lncRNA expression differences between 471 COAD tumor specimens and 41 adjacent normal tissue specimens. The lncRNA RP5-881L22.5 was selected as the research object, and a comparison of RP5-881L22.5 expression across different stages of COAD was conducted. Kaplan-Meier survival curves were drawn for patients grouped by different expression levels, and the survival differences of all patients grouped by expression levels as well as the effect of the expression differences of RP5-881L22.5 in different stages on survival were compared.

Online analysis at the bioinformatics website

The expression of RP5-881L22.5 in 33 cancers in TCGA was acquired from the GEPIA2 (http://gepia2.cancer-pku.cn/). The differential expression of RP5-881L22.5 between colon cancer tissue (TCGA-COAD) and normal colon tissue (data involved the TCGA-COAD project and Genotype-Tissue Expression (GTEx) database) were analyzed[16,17].

Assessment of immune infiltration

We downloaded the benchmark database file (LM22.txt) of 22 tumor-infiltrating immune cells ($CD8^+$ T cells, CD4 naive T cells, regulatory reg cells, naïve B cells, memory B cells, plasma cells, CD4 memory resting T cells, CD4 memory activated T cells, follicular helper T cells, gamma delta T cells, resting NK cells, activated NK cells, monocytes, macrophages M0/M1/M2, resting dendritic cells, activated dendritic cells, resting mast cells, activated mast cells, eosinophils and neutrophils). The CIRBERSORT algorithm was applied to evaluate these tumor-infiltrating immune cells in TCGA-COAD cancer tissue samples[18]. Using the "estimate" package in the R language, we evaluated the tumor immune microenvironment[19]. All TCGA-COAD cancer tissue samples were divided into high expression and low expression groups according to the median expression of RP5-881L22.5, and the differences in immune components and immune cell infiltration between the two groups were compared. In addition, the expression levels of the coinhibitory receptors LAG3, CTLA4, HAVCR2, TIGIT and CD244 were compared between the two groups[20].

Functional enrichment analysis

Pearson correlation analysis was performed using the "cor.test" function of the basic R package. Among the differentially expressed mRNAs (logFC > 1 or logFC < -1, and adj.P.val < 0.05), the mRNAs coexpressed with RP5-881L22.5 were screened out. Gene set enrichment analysis of coexpressed mRNAs was performed using the "clusterProfiler" package in R language[21].

Clinical specimens

Colorectal cancer tissue specimens were obtained from the radical surgery specimens of colorectal cancer patients admitted to the Gastrointestinal Surgery Department of the Second Affiliated Hospital of Southern University of Science and Technology (Shenzhen Third People's Hospital) in August 2021. All patients were diagnosed by pathological diagnosis of colonoscopy biopsy: (1) Patients with acute infection, such as intestinal obstruction or intestinal perforation, were excluded; (2) Patients with HIV infection, autoimmune diseases, inflammatory bowel disease and other immune system-related diseases were excluded; (3) Preoperative neoadjuvant treatment patients were excluded; and (4) Patients with severe heart and lung insufficiency who could not tolerate surgery were excluded. Finally, eight tissue samples were obtained, which were colorectal cancer (3 cases of colon cancer, 1 case of rectal cancer), and four tumor tissues and four adjacent normal intestinal tissues were saved and transferred to a -80 °C freezer for storage. The experiment was ethically approved by the Ethics Committee of Shenzhen Third People's Hospital (Shenzhen, China; license no. HE2022177).

Cell culture and siRNA transfection

The colorectal cancer cell line DLD-1 was obtained from ATCC (Manassas, VA, United States). 1640 medium supplemented with 10% fetal bovine serum, 1% penicillin-streptomycin and 3% glucose (HyClone, Logan, UT, United States) was used to incubate DLD-1 cells. Control siRNA and RP5-881L22.5 siRNA were purchased from RiboBio Co., Ltd. (GuangZhou, China). Lipofectamine 2000 Transfection Reagent (Invitrogen, CA, United States) was used to transfect siRNA into DLD-1 cells.

RNA extraction and quantitative real-time PCR

TRIzol reagent (ELK Biotechnology, Wuhan, China) was used to isolate total RNA from colorectal cancer tissues. On 1% agarose gels, degradation and contamination of RNA were monitored after isolation. Synthesis of first-strand cDNA was performed using an M-MLV Reverse Transcriptase kit (ELK Biotechnology, Wuhan, China). Quantitative real-time PCR was completed on a StepOne™ Real-Time PCR machine (Life Technologies, CA, United States) with 3 replicate per sample using QuFast SYBR Green PCR Master Mix kit (ELK Biotechnology, Wuhan, China). GAPDH was used as an endogenous control gene. The reactions were incubated at 95 °C for 1 min, followed by 40 cycles at 95 °C for 15 s, 58 °C for 20 s and 72 °C for 45 s. Calculation of relative expression levels was performed using the $2^{-\Delta\Delta CT}$ value relative quantification. The primer sequences were as follows: RP5-881L22.5 (ENSG00000226812) Sense: 5′- TATTGAGCACCTACTATGTACCAGG -3′ and Antisense: 5′- GTTAGAGCTCAGTCTCTCACAGCTC -3′; and GAPDH Sense: 5′- CATCATCCCTGCCTCTACTGG -3′ and Antisense: 5′- GTGGGTGTCGCTGTTGAAGTC -3′.

Transwell invasion assay

To prepare the transwell chamber for use, 50 μL of Matrigel (Corning, United States) and medium were diluted 1:3 and added to the chamber. Cell suspension (1 mL) was centrifuged at 1500 rpm for 5 min after being diluted to 105 cells/mL. The cell suspension was pipetted into a transwell chamber with 1 mL of serum-free medium. In a 24-well plate, 500 μL of complete medium containing 10% fetal bovine serum was added, and the chamber was inserted. The plate was incubated at 37 °C in a CO_2 (5% content) incubator for 24 h (adjusted according to the experiment). A 0.5% crystal violet solution (1:4) was diluted into a 0.1% crystal violet staining solution with PBS solution. The medium was washed with PBS, and the glue and cells in the upper chamber were wiped off with a cotton swab, fixed with paraformaldehyde for 20 min, washed twice with PBS, stained with crystal violet for 10 min, and washed to remove the crystal violet on the surface. The side devoid of cell seeding was photographed under an inverted microscope (OLYMPUS).

Apoptosis assay

Precooled PBS was added at 4 °C, and an appropriate amount of binding buffer was diluted for use. After washing with PBS once, the cells in the 6-well plate were digested with 400 μL of 0.25% trypsin. The digestion was terminated by adding complete medium once the cells had become round and some had fallen off. We collected samples in 1.5 mL EP tubes and centrifuged them at 300 × g for 5 min, discarding the supernatant. One milliliter of PBS was added to resuspend the cells, they were centrifuged at 300 × g for 5 min, and the supernatant was discarded. A 200 μL solution of Binding Buffer was used to resuspend the pellet. Following this, 5 μL of Annexin V-FITC (Sungene Biotech, Tianjin, China) were added, mixed well and incubated for 10 min in the dark. Next, 5 μL propidium iodide was added, mixed well and incubated in the dark for 5 min. On-board inspection was performed within 1 h.

Statistical analysis

Comparing survival rates between groups was carried out using Kaplan-Meier survival curves and log-rank tests. The immune scores, the infiltration of immune cells and the expression levels of each gene were compared between groups using Wilcoxon tests. Differences were considered statistically significant when $P < 0.05$. All statistical procedures and graphs were completed using R programmer language (V4.1.1).

RESULTS

Differential expression analysis of mRNAs and lncRNAs

According to the GENCODE annotation file, we identified a total of 19712 mRNAs and 15878 lncRNAs in TCGA-COAD database. Genes with very low expression levels [log2 (FKPM+1) < 0.5] were deleted, and differential expression analysis was performed on the remaining 13285 mRNAs and 1850 lncRNAs. There were 1612 differentially expressed mRNAs and 122 differentially expressed lncRNAs (logFC > 1 or < -1 and adjusted *P* value < 0.05) (Figure 1A and B).

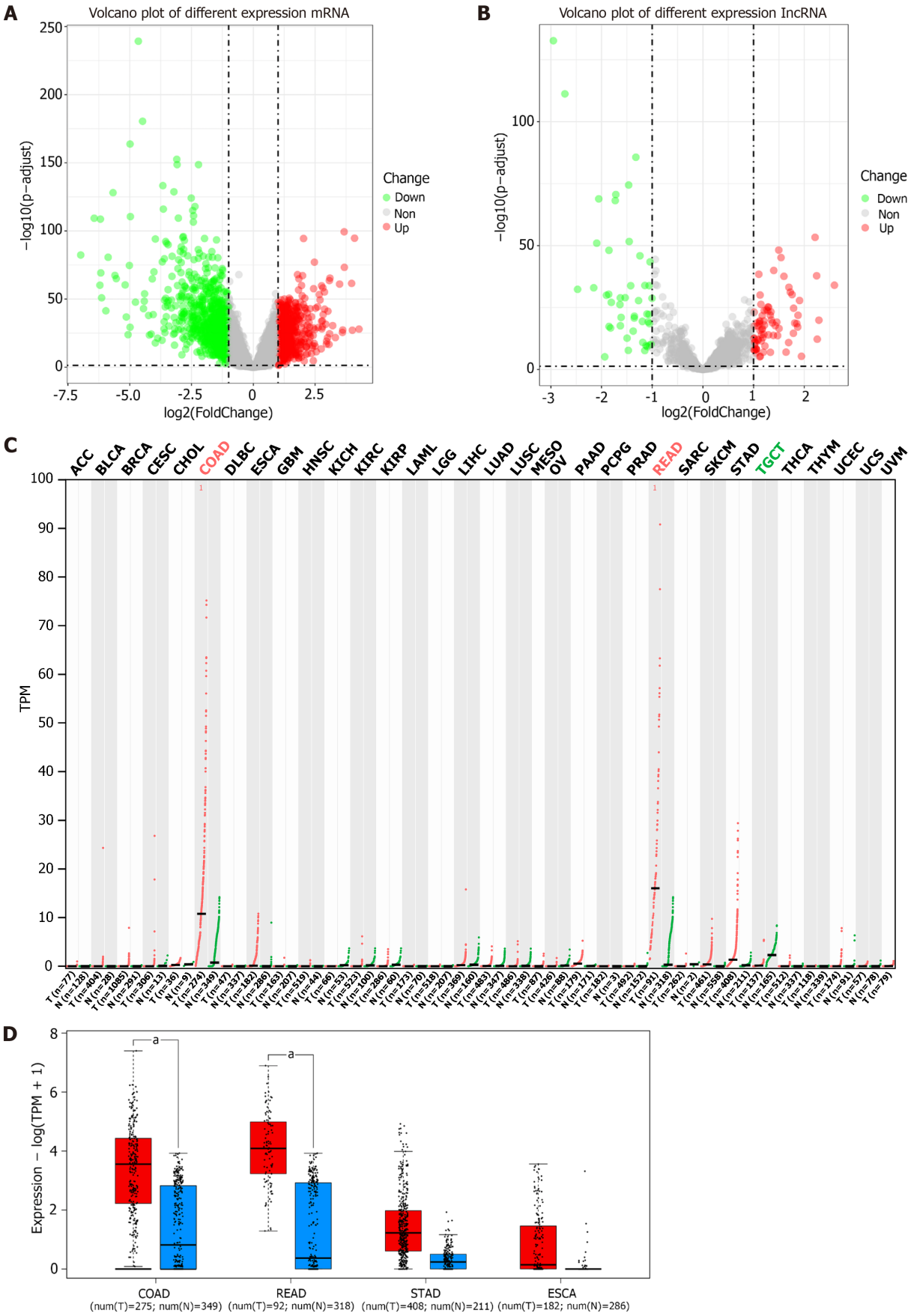

DOI: 10.4251/wjgo.v14.i11.2108 **Copyright** ©The Author(s) 2022.

Figure 1 Volcano plot of the differentially expressed genes in The Cancer Genome Atlas-colon adenocarcinoma (LogFC > 1 or < -1 and adjust *P* value < 0.05 were defined as significant difference) and results from GEPIA2 website query. A: Volcano plot of mRNA differential

expression; B: Volcano plot of long noncoding (lnc) RNA differential expression. Red points referred to upregulated differentially expressed genes; green points referred to downregulated differentially expressed genes; grey points referred to non-differentially expressed genes; C: RP5-881L22.5 expression in the 33 cancers of The Cancer Genome Atlas. Log2FC > 1.0 or < -1.0 and *q* value < 0.05 were defined as a significant difference. Red points referred to tumor tissues; green points referred to normal tissues; D: Expression level of RP5-881L22.5 among colon adenocarcinoma, rectum adenocarcinoma, stomach adenocarcinoma and esophageal carcinoma (The Cancer Genome Atlas). Red referred to tumor tissues; blue referred to normal tissues (include data of GTEx); "a" referred to log2FC > 1.0 and *q* value < 0.01. ACC: Adrenocortical carcinoma; BLCA: Bladder urothelial carcinoma; BRCA: Breast invasive carcinoma; CESC: Cervical squamous cell carcinoma and endocervical adenocarcinoma; CHOL: Cholangiocarcinoma; COAD: Colon adenocarcinoma; DLBC: Lymphoid Neoplasm Diffuse Large B-cell Lymphoma; ESCA: Esophageal carcinoma; GBM: Glioblastoma multiforme; HNSC: Head and neck squamous cell carcinoma; KICH: Kidney chromophobe; KIRC: Clear cell renal cell carcinoma; KIRP: Kidney renal papillary cell carcinoma; LAML: Acute myeloid leukemia; LGG: Brain lower grade glioma; LIHC: Liver hepatocellular carcinoma; LUAD: Lung adenocarcinoma; LUSC: Lung squamous cell carcinoma; MESO: Mesothelioma; N: Normal; OV: Ovarian serous cystadenocarcinoma; PAAD: Pancreatic adenocarcinoma; PCPG: Pheochromocytoma and Paraganglioma; PRAD: Prostate adenocarcinoma; READ: Rectum adenocarcinoma; SARC: Sarcoma; SKCM: Skin Cutaneous Melanoma; STAD: Stomach adenocarcinoma; T: Tumor; TGCT: Testicular Germ Cell Tumors; THCA: Thyroid carcinoma; THYM: Thymoma; UCEC: Uterine corpus endometrial carcinoma; UCS: Uterine carcinosarcoma; UVM: Uveal melanoma.

RP5-881L22.5 expression in TCGA pan-cancer analysis

By querying the expression of RP5-881L22.5 in all tumor tissues from the TCGA database on the GEPIA2 website, we found that among all 33 malignant tumors, only COAD and READ had significant differential expression (log2FC > 1.0, *q* value < 0.01) (Figure 1C) between cancer and normal tissues. Additionally, we found similar differences in gastric and esophageal cancers, both of which are malignant tumors of the digestive tract (Figure 1D).

Association between RP5-881L22.5 expression and clinical features

Based on the median expression of RP5-881L22.5 in 448 colon cancer tissue, we divided all samples into two groups with 224 samples in each. The 62 specimens of patients in stage IV were divided into two groups according to the median expression of RP5-881L22.5 with 31 samples in each group. Eighty specimens of patients in the N2 stage were divided into two groups according to the median expression of RP5-881L22.5 with 40 samples in each group. A positive correlation was found between RP5-881L22.5 expression and TNM stage (UICC and AJCC TNM staging system) as well as N stage and M stage, although no association was found with T stage (Figure 2A-D). However, after dividing all COAD samples into high and low groups according to RP5-881L22.5 expression levels, no difference in survival was noted between the two groups. For stage IV patients and patients with lymph node metastasis stage N2, high expression was associated with better survival. No differences in survival were noted among the other stages (Figure 2E-G).

Association between RP5-881L22.5 expression and the tumor immune microenvironment

To explore whether the expression of RP5-881L22.5 is related to the tumor immune microenvironment, we divided all samples from TCGA-COAD into high and low groups according to the median expression of RP5-881L22.5 and compared the immune microenvironment differences. According to our findings, the immune score and tumor stroma score in the high expression group were lower than those in the low expression group, and the differences were significant (Figure 3A-C). Comparing the infiltration of 22 types of immune cells in the high and low groups, four types of immune cells showed significant differences, including CD8 T cells, M0 macrophages, activated NK cells and neutrophils (P < 0.05) (Figure 3D). T cell exhaustion is one of the reasons for the formation of a tumor suppressive immune microenvironment, and the coinhibitory receptors PDCD1 (PD-1), LAG3, CTLA4, HAVCR2, TIGIT, CD244, *etc*, related to T cell exhaustion were also significantly different between the two groups. The expression levels of these genes in the RP5-881L22.5 high expression group were lower, and statistically significant differences were found (Figure 3E-J).

Afterward, coexpression analysis was performed on the transcriptome data from TCGA-COAD, and the genes coexpressed with RP5-881L22.5 among the differentially expressed mRNAs were selected. Through gene set enrichment analysis, it was found that the genes coexpressed with RP5-881L22.5 among the differentially expressed mRNAs were mainly involved in immune biological processes or pathways such as the immune response (Figure 4).

Quantitative reverse transcription PCR and cell function assay results using clinical specimens

Four pairs of tissue samples from colorectal cancer patients were assessed by quantitative reverse transcription PCR. We found that RP5-881L22.5 was generally highly expressed in tumor tissues compared with adjacent normal tissues (Figure 5A), which was consistent with the aforementioned bioinformatics analysis results. The apoptosis assay showed that the apoptosis rate of colorectal cancer cells increased after RP5-881L22.5 knockdown (Figure 5B-D). The transwell invasion assay revealed reduced invasiveness (Figure 5E). These results indicated that RP5-881L22.5 is a significant contributor to the occurrence and development of colorectal cancer.

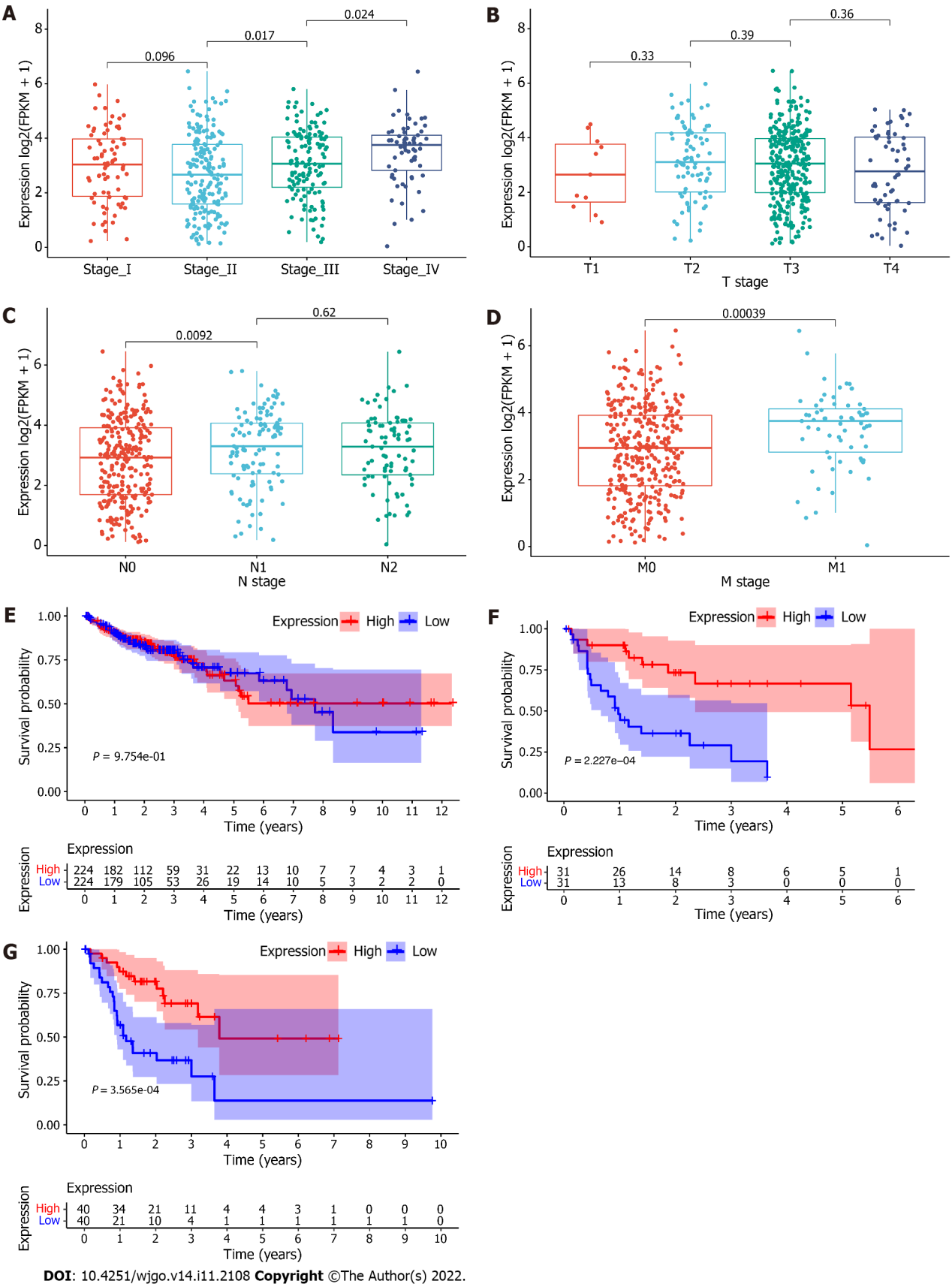

DOI: 10.4251/wjgo.v14.i11.2108 **Copyright** ©The Author(s) 2022.

Figure 2 Association between the expression level of RP5-881L22.5 and clinical characteristics. A: Association between expression and TNM stage; B: Association between expression and T stage; C: Association between expression and N stage; D: The association between expression and M stage; E: Kaplan-Meier survival curve of the population at all stages; F: Stage IV; G: N2 stage. Red referred to the higher expression group, and blue referred to the lower expression group (grouped by median expression of RP5-881L22.5).

DISCUSSION

LncRNAs play important functions in many regulatory mechanisms, such as transcriptional silencing, transcriptional activation, chromosome modification and intranuclear transport and play important roles in the occurrence and development of cancer[22,23]. Liu *et al*[24] found that three lncRNAs, LINC00114, LINC00261 and HOTAIR, can accurately judge the prognosis of colorectal cancer. Zhang *et al*[25] found that lncRNA-NEAT1 interacts with DDX5 to activate Wnt/β-catenin signaling, thereby promoting the progression of colorectal cancer. Ni *et al*[26] found that lncRNA-GAS5 controls colorectal cancer progression by regulating the phosphorylation and interpretation of YAP. This process is also negatively regulated by the m6A methylation reader protein YTHDF3.

We observed significant differences in lncRNA expression between colon cancer tumor tissues and normal colon tissues based on the analysis of TCGA dataset. This expression difference was also observed in rectal cancer, gastric cancer and esophageal cancer. Moreover, its expression was correlated with clinical features, such as the pathological stage of patients, and exhibited a significant correlation with survival in specific populations. These findings illustrate that RP5-881L22.5 may be a unique molecular marker in digestive tract cancer and may be involved in some important processes in the pathogenic process of digestive tract cancer. Subsequent clinical specimen detection and cell function experiments also verified this conclusion. All of these findings indicate that this lncRNA is likely to be related to the pathogenic process of colorectal cancer.

In addition to tumor cell characteristics, the microenvironment of the tumor also plays a substantial role in cancer[27]. Many lncRNAs show strong cell type-specific expression phenomena. Most mRNAs are expressed in the vast majority of cell types, whereas more than half of the cells contain only a few lncRNAs[28]. Cells with malignant characteristics had 9% of lncRNAs, lymphocytes had 11%, myeloid cells had 6%, and epithelial cells had 5%[29]. In particular, immune-specific lncRNAs recruit proteins to specific genomic loci to regulate target gene expression epigenetically and transcriptionally in most cases, thereby controlling the activity and differentiation of immune cells. For example, H19, ROCKI, lnc13 and HOXA-AS2 regulate target genes in immune cells by exerting protein recruitment functions or controlling chromatin accessibility[30-33]. At the same time, the tumor immune microenvironment can also be regulated by lncRNAs by targeting macrophages, dendritic cells, regulatory T cells and $CD8^+$ T lymphocytes through a competing endogenous RNA mechanism, such as the SNHG1/miR-448/IDO regulator network[34], the SNHG16/miR-16-5p/SMAD5 regulator network[35], the FENDR/miR-423-5p/GADD45B regulator network[36], the SBF2-AS1miR-122-5p/XIAP regulator network[37] and the NEAT1/miR-155/Tim-3 regulator network[38].

Of course, in addition to their role in immune cells, lncRNAs also modulate the presentation of antigen or PD-L1 in tumor cells[39,40]. Li *et al*[41] identified a lncRNA, lncRNA inducing major histocompatibility complex I and immunogenicity of tumor, in humans and mice. They proposed the lncRNA inducing major histocompatibility complex I and immunogenicity of tumor-GBP-HSF1 axis as a therapeutic target for immunotherapy to modulate major histocompatibility complex I expression based on experimental validation *in vivo* and *in vitro*. In conclusion, increasing evidence indicates that the key mechanisms by which lncRNAs regulate tumor immunity involve various aspects, such as antigen presentation and T cell exhaustion.

In our study, RP5-881L22.5 expression in colorectal cancer was also strongly related to the tumor immune microenvironment. There was a negative correlation between its expression and the presence of $CD8^+$ T lymphocytes and activated NK cells in the tumor microenvironment, and it was negatively correlated with the expression of various coinhibitory receptors on the surface of T lymphocytes. In addition, RP5-881L22.5 coexpressed genes were more involved in the pathways of tumor immune microenvironment formation, such as immune response and immune signal transmission.

In particular, TCGA data analysis revealed that RP5-881L22.5 expression was related to some clinical features of colorectal cancer patients but not to the T stage of the tumor, and no difference in survival was noted between the high expression group and the low expression group. Furthermore, a subset of advanced stage tumors showed better survival despite high marker expression. The expression of inhibitory receptors in the RP5-881L22.5 high expression group decreased. Therefore, T cells showed relatively stronger antitumor immune activity in the high expression group. This finding may explain why advanced tumors with higher RP5-881L22.5 expression showed a better survival rate. Further research on immunotherapy of advanced tumors using RP5-881L22.5 as a marker should be explored.

CONCLUSION

RP5-881L22.5 expression levels were significantly different between colorectal cancer tissues and nontumor tissues , and RP5-881L22.5 expression in tumor samples was considerably higher. RP5-881L22.5 expression levels were significantly correlated with clinicopathological stage and could predict prognosis for colorectal cancer. Moreover, RP5-881L22.5 showed an obvious immune correlation in colorectal cancer and might be a key molecule in the formation of the immunosuppressive microenvironment, which deserves further research. The relationship between RP5-881L22.5 and the tumor

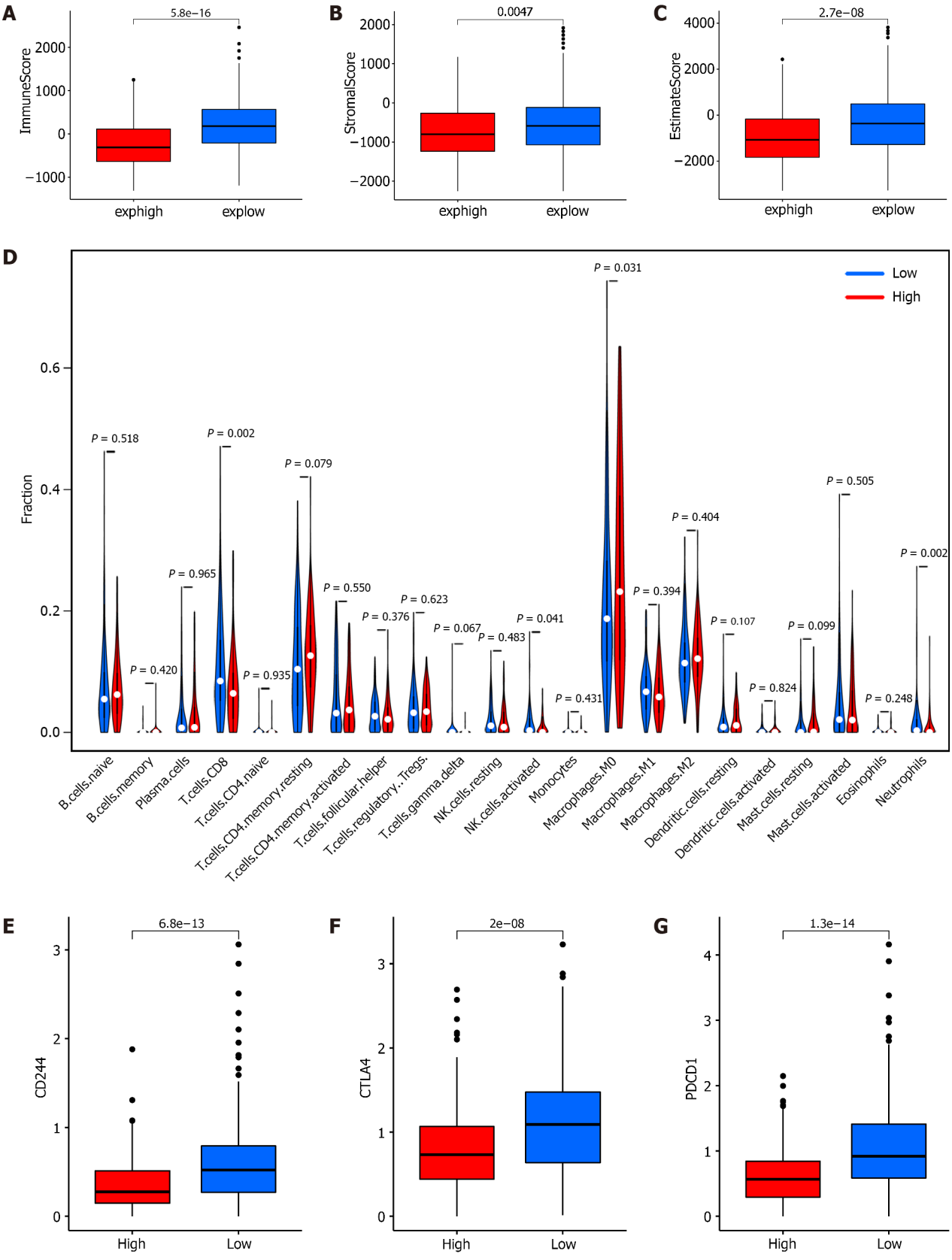
A
5.8e−16
ImmuneScore
exphigh
explow
B
0.0047
StromalScore
exphigh
explow
C
2.7e−08
EstimateScore
exphigh
explow
D
Low
High
Fraction
P = 0.518
P = 0.420
P = 0.965
P = 0.002
P = 0.935
P = 0.079
P = 0.550
P = 0.376
P = 0.623
P = 0.067
P = 0.483
P = 0.041
P = 0.431
P = 0.031
P = 0.394
P = 0.404
P = 0.107
P = 0.824
P = 0.099
P = 0.505
P = 0.248
P = 0.002
B.cells.naive
B.cells.memory
Plasma.cells
T.cells.CD8
T.cells.CD4.naive
T.cells.CD4.memory.resting
T.cells.CD4.memory.activated
T.cells.follicular.helper
T.cells.regulatory..Tregs.
T.cells.gamma.delta
NK.cells.resting
NK.cells.activated
Monocytes
Macrophages.M0
Macrophages.M1
Macrophages.M2
Dendritic.cells.resting
Dendritic.cells.activated
Mast.cells.resting
Mast.cells.activated
Eosinophils
Neutrophils
E
6.8e−13
CD244
High
Low
F
2e−08
CTLA4
High
Low
G
1.3e−14
PDCD1
High
Low

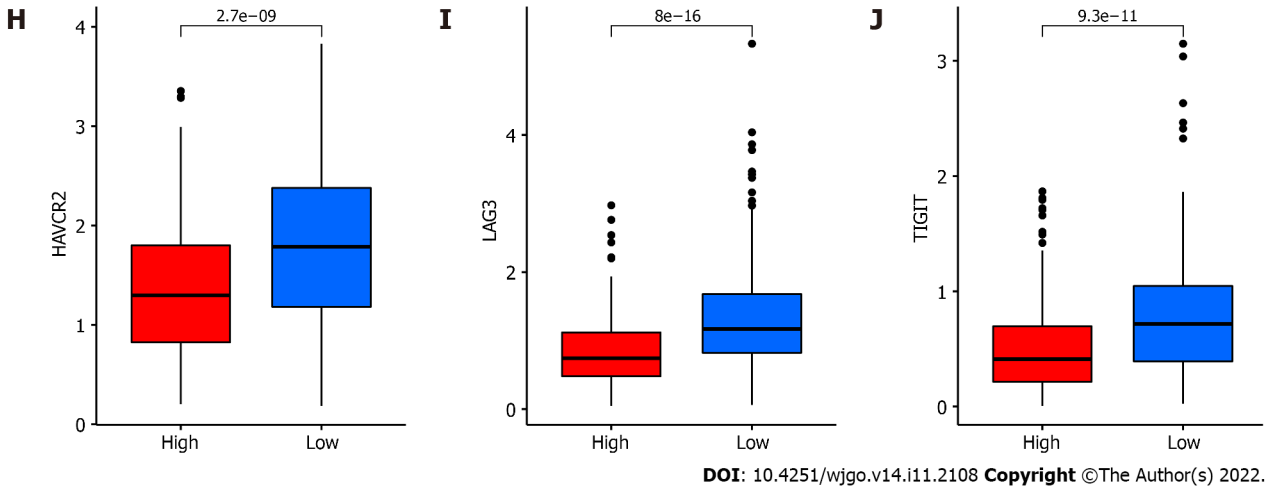

DOI: 10.4251/wjgo.v14.i11.2108 **Copyright** ©The Author(s) 2022.

Figure 3 Distribution of tumor microenvironment scores, 22 types of immune cells and expression of T lymphocyte coinhibitory receptor genes between different groups. A: ImmuneScore, $P = 5.8 \times 10^{-16}$; B: StromalScore, $P = 0.0047$; C: EstimateScore, $P = 2.7 \times 10^{-8}$; D: The 22 immune cell types were represented in columns, and the proportions of immune cells were represented in rows; E: Expression of CD244, $P = 6.8 \times 10^{-13}$; F: Expression of CTLA4, $P = 2.0 \times 10^{-8}$; G: Expression of PDCD1, $P = 1.3 \times 10^{-14}$; H: Expression of HAVCR2, $P = 2.7 \times 10^{-9}$; I: Expression of LAG3, $P = 8.0 \times 10^{-16}$; J: Expression of TIGIT, $P = 9.3 \times 10^{-11}$. Red referred to the high expression group, and blue referred to the low expression group (grouped by median of RP5-881L22.5 expression). NK: Natural killer; exphigh: Expression high; explow: Expression low.

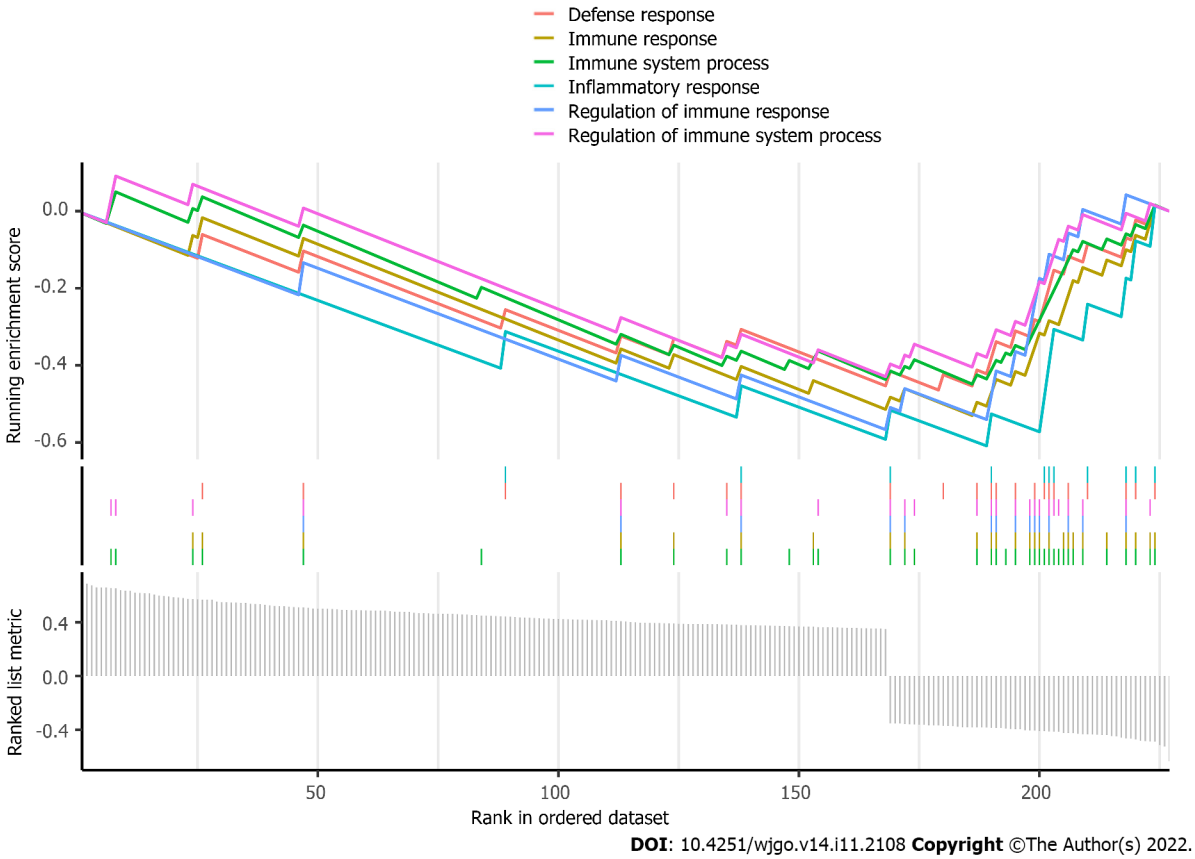

DOI: 10.4251/wjgo.v14.i11.2108 **Copyright** ©The Author(s) 2022.

Figure 4 Gene set enrichment analysis for the differentially expressed mRNAs.

immune microenvironment, as well as the different prognostic differences it represents in tumors with different clinical characteristics, needs to further investigated in clinical tissue samples.

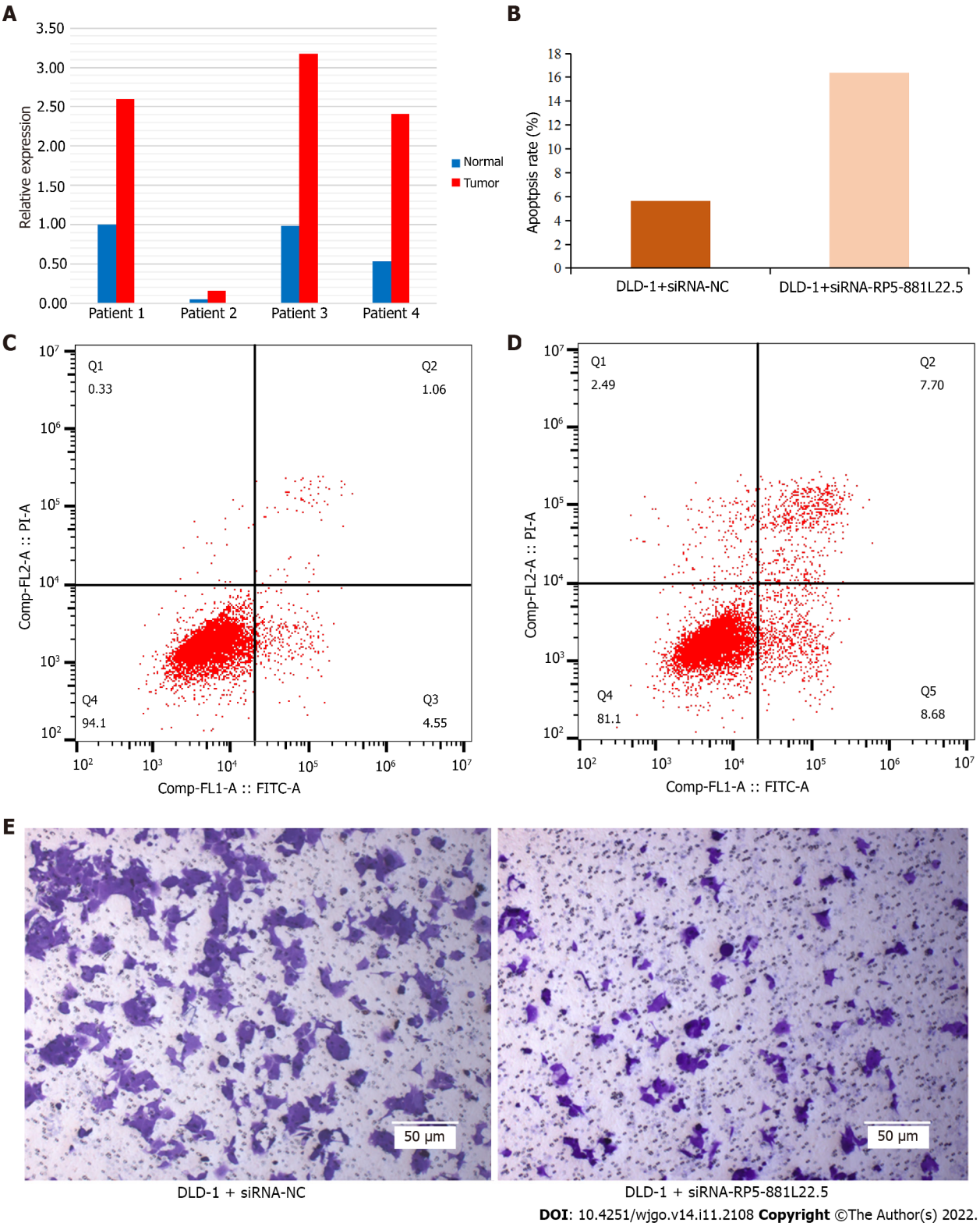

DOI: 10.4251/wjgo.v14.i11.2108

Figure 5 Results of quantitative reverse transcription PCR for clinical specimens and cellular experiments. A: Expression level of RP5-881L22.5 in tumor tissues and normal tissues among 4 patients' surgical samples. Red referred to tumor tissues, and blue referred to adjacent normal tissues; B: The apoptosis ratio difference between siRNA + negative control (NC) group and siRNA + RP5-881L22.5; C: Representative image of the siRNA + NC by flow cytometry; D: Representative image of the siRNA+RP5-881L22.5 by flow cytometry; E: Effect of knockdown of RP5-881L22.5 on the transwell invasion assay of colorectal cancer cells. Scale bars: 50 μm. The magnification is 100 times the original size. Left: Representative image of the siRNA + NC; Right: Representative image of the siRNA + RP5-881L22.5.

ARTICLE HIGHLIGHTS

Research background

Colorectal cancer is one of the most common malignant tumors in the world. Long noncoding RNAs (lncRNAs) are involved in many normal human physiological functions and pathogenic processes of diseases.

Research motivation

LncRNAs may be used as molecular markers for more accurate prediction of colorectal cancer prognosis. The molecular mechanisms of lncRNAs involved can impact colorectal cancer prognosis and impact the tumor immune microenvironment. Further research into these questions is needed.

Research objectives

To explore the differential expression analysis of mRNAs and lncRNAs in the colorectal cancer and to determine the association between RP5-881L22.5 expression and the tumor immune microenvironment.

Research methods

We analyzed the immune cell microenvironment through the bioinformatics combined with clinical data and cell experiments to verify the results.

Research results

RP5-881 L22.5 expression led to a difference in prognosis, which warrants further research on immunotherapy of advanced tumors with RP5-881 L22.5 as a marker.

Research conclusions

RP5-881 L22.5 plays an important role in the pathogenesis of colorectal cancer.

Research perspectives

RP5-881 L22.5 may be an important research target for the treatment of colorectal cancer.

FOOTNOTES

Author contributions: Zong H designed the project, wrote the paper and acquired the data; Zou JQ and Huang JP analyzed and interpreted the data; Huang ST modified the language of the article.

Supported by the Shenzhen Third People's Hospital, No. G2022117.

Institutional review board statement: The study was reviewed and approved by the Shenzhen Third People's Hospital (Approval No. G2022117).

Informed consent statement: Patients were not required to give informed consent to the study.

Conflict-of-interest statement: All authors declare that there is no conflict of interest in this work.

Data sharing statement: All data are publicly available for sharing use.

Country/Territory of origin: China

ORCID number: Hua Zong 0000-0002-5330-0096; Jian-Qiang Zou 0000-0002-3811-3452; Jian-Peng Huang 0000-0001-5974-2322; Shi-Ting Huang 0000-0003-2525-1132.

S-Editor: Chen YL
L-Editor: Filipodia
P-Editor: Li X

REFERENCES

1 **Sung H**, Ferlay J, Siegel RL, Laversanne M, Soerjomataram I, Jemal A, Bray F. Global Cancer Statistics 2020: GLOBOCAN Estimates of Incidence and Mortality Worldwide for 36 Cancers in 185 Countries. *CA Cancer J Clin* 2021; **71**: 209-249 [PMID: 33538338 DOI: 10.3322/caac.21660]

2 **Siegel RL**, Miller KD, Fuchs HE, Jemal A. Cancer Statistics, 2021. *CA Cancer J Clin* 2021; **71**: 7-33 [PMID: 33433946 DOI: 10.3322/caac.21654]

3 **Hinshaw DC**, Shevde LA. The Tumor Microenvironment Innately Modulates Cancer Progression. *Cancer Res* 2019; **79**: 4557-4566 [PMID: 31350295 DOI: 10.1158/0008-5472.CAN-18-3962]

4 **Pansy K**, Uhl B, Krstic J, Szmyra M, Fechter K, Santiso A, Thüminger L, Greinix H, Kargl J, Prochazka K, Feichtinger J, Deutsch AJ. Immune Regulatory Processes of the Tumor Microenvironment under Malignant Conditions. *Int J Mol Sci* 2021; **22** [PMID: 34948104 DOI: 10.3390/ijms222413311]

5 **Gajewski TF**, Schreiber H, Fu YX. Innate and adaptive immune cells in the tumor microenvironment. *Nat Immunol* 2013; **14**: 1014-1022 [PMID: 24048123 DOI: 10.1038/ni.2703]

6 **Jordan SC**. Innate and adaptive immune responses to SARS-CoV-2 in humans: relevance to acquired immunity and vaccine responses. *Clin Exp Immunol* 2021; **204**: 310-320 [PMID: 33534923 DOI: 10.1111/cei.13582]

7 **Lei X**, Lei Y, Li JK, Du WX, Li RG, Yang J, Li J, Li F, Tan HB. Immune cells within the tumor microenvironment: Biological functions and roles in cancer immunotherapy. *Cancer Lett* 2020; **470**: 126-133 [PMID: 31730903 DOI: 10.1016/j.canlet.2019.11.009]

8 **O'Donnell JS**, Teng MWL, Smyth MJ. Cancer immunoediting and resistance to T cell-based immunotherapy. *Nat Rev Clin Oncol* 2019; **16**: 151-167 [PMID: 30523282 DOI: 10.1038/s41571-018-0142-8]

9 **Statello L**, Guo C J, Chen L L, Huarte M. Gene regulation by long non-coding RNAs and its biological functions. *Nat Rev Mol Cell Biol* 2021; **22**: 96-118

10 **Arraiano CM**. Regulatory noncoding RNAs: functions and applications in health and disease. *FEBS J* 2021; **288**: 6308-6309 [PMID: 34153158 DOI: 10.1111/febs.16027]

11 **Pi YN**, Qi WC, Xia BR, Lou G, Jin WL. Long Non-Coding RNAs in the Tumor Immune Microenvironment: Biological Properties and Therapeutic Potential. *Front Immunol* 2021; **12**: 697083 [PMID: 34295338 DOI: 10.3389/fimmu.2021.697083]

12 **Goldman MJ**, Craft B, Hastie M, Repečka K, McDade F, Kamath A, Banerjee A, Luo Y, Rogers D, Brooks AN, Zhu J, Haussler D. Visualizing and interpreting cancer genomics data *via* the Xena platform. *Nat Biotechnol* 2020; **38**: 675-678 [PMID: 32444850 DOI: 10.1038/s41587-020-0546-8]

13 **Tomczak K**, Czerwińska P, Wiznerowicz M. The Cancer Genome Atlas (TCGA): an immeasurable source of knowledge. *Contemp Oncol (Pozn)* 2015; **19**: A68-A77 [PMID: 25691825 DOI: 10.5114/wo.2014.47136]

14 **Frankish A**, Diekhans M, Ferreira AM, Johnson R, Jungreis I, Loveland J, Mudge JM, Sisu C, Wright J, Armstrong J, Barnes I, Berry A, Bignell A, Carbonell Sala S, Chrast J, Cunningham F, Di Domenico T, Donaldson S, Fiddes IT, García Girón C, Gonzalez JM, Grego T, Hardy M, Hourlier T, Hunt T, Izuogu OG, Lagarde J, Martin FJ, Martínez L, Mohanan S, Muir P, Navarro FCP, Parker A, Pei B, Pozo F, Ruffier M, Schmitt BM, Stapleton E, Suner MM, Sycheva I, Uszczynska-Ratajczak B, Xu J, Yates A, Zerbino D, Zhang Y, Aken B, Choudhary JS, Gerstein M, Guigó R, Hubbard TJP, Kellis M, Paten B, Reymond A, Tress ML, Flicek P. GENCODE reference annotation for the human and mouse genomes. *Nucleic Acids Res* 2019; **47**: D766-D773 [PMID: 30357393 DOI: 10.1093/nar/gky955]

15 **Ritchie ME**, Phipson B, Wu D, Hu Y, Law CW, Shi W, Smyth GK. limma powers differential expression analyses for RNA-sequencing and microarray studies. *Nucleic Acids Res* 2015; **43**: e47 [PMID: 25605792 DOI: 10.1093/nar/gkv007]

16 **Tang Z**, Kang B, Li C, Chen T, Zhang Z. GEPIA2: an enhanced web server for large-scale expression profiling and interactive analysis. *Nucleic Acids Res* 2019; **47**: W556-W560 [PMID: 31114875 DOI: 10.1093/nar/gkz430]

17 **eGTEx Project**. Enhancing GTEx by bridging the gaps between genotype, gene expression, and disease. *Nat Genet* 2017; **49**: 1664-1670 [PMID: 29019975 DOI: 10.1038/ng.3969]

18 **Newman AM**, Liu CL, Green MR, Gentles AJ, Feng W, Xu Y, Hoang CD, Diehn M, Alizadeh AA. Robust enumeration of cell subsets from tissue expression profiles. *Nat Methods* 2015; **12**: 453-457 [PMID: 25822800 DOI: 10.1038/nmeth.3337]

19 **Yoshihara K**, Shahmoradgoli M, Martínez E, Vegesna R, Kim H, Torres-Garcia W, Treviño V, Shen H, Laird PW, Levine DA, Carter SL, Getz G, Stemke-Hale K, Mills GB, Verhaak RG. Inferring tumour purity and stromal and immune cell admixture from expression data. *Nat Commun* 2013; **4**: 2612 [PMID: 24113773 DOI: 10.1038/ncomms3612]

20 **Wherry EJ**, Kurachi M. Molecular and cellular insights into T cell exhaustion. *Nat Rev Immunol* 2015; **15**: 486-499 [PMID: 26205583 DOI: 10.1038/nri3862]

21 **Wu T**, Hu E, Xu S, Chen M, Guo P, Dai Z, Feng T, Zhou L, Tang W, Zhan L, Fu X, Liu S, Bo X, Yu G. clusterProfiler 4.0: A universal enrichment tool for interpreting omics data. *Innovation (Camb)* 2021; **2**: 100141 [PMID: 34557778 DOI: 10.1016/j.xinn.2021.100141]

22 **Bhan A**, Soleimani M, Mandal SS. Long Noncoding RNA and Cancer: A New Paradigm. *Cancer Res* 2017; **77**: 3965-3981 [PMID: 28701486 DOI: 10.1158/0008-5472.CAN-16-2634]

23 **Lorenzi L**, Avila Cobos F, Decock A, Everaert C, Helsmoortel H, Lefever S, Verboom K, Volders PJ, Speleman F, Vandesompele J, Mestdagh P. Long noncoding RNA expression profiling in cancer: Challenges and opportunities. *Genes Chromosomes Cancer* 2019; **58**: 191-199 [PMID: 30461116 DOI: 10.1002/gcc.22709]

24 **Liu S**, Cao Q, An G, Yan B, Lei L. Identification of the 3-lncRNA Signature as a Prognostic Biomarker for Colorectal Cancer. *Int J Mol Sci* 2020; **21** [PMID: 33302562 DOI: 10.3390/ijms21249359]

25 **Zhang M**, Weng W, Zhang Q, Wu Y, Ni S, Tan C, Xu M, Sun H, Liu C, Wei P, Du X. The lncRNA NEAT1 activates Wnt/β-catenin signaling and promotes colorectal cancer progression *via* interacting with DDX5. *J Hematol Oncol* 2018; **11**: 113 [PMID: 30185232 DOI: 10.1186/s13045-018-0656-7]

26 **Ni W**, Yao S, Zhou Y, Liu Y, Huang P, Zhou A, Liu J, Che L, Li J. Long noncoding RNA GAS5 inhibits progression of colorectal cancer by interacting with and triggering YAP phosphorylation and degradation and is negatively regulated by

the m^{6}A reader YTHDF3. *Mol Cancer* 2019; **18**: 143 [PMID: 31619268 DOI: 10.1186/s12943-019-1079-y]

27 **Grassi L**, Izuogu OG, Jorge NAN, Seyres D, Bustamante M, Burden F, Farrow S, Farahi N, Martin FJ, Frankish A, Mudge JM, Kostadima M, Petersen R, Lambourne JJ, Rowlston S, Martin-Rendon E, Clarke L, Downes K, Estivill X, Flicek P, Martens JHA, Yaspo ML, Stunnenberg HG, Ouwehand WH, Passetti F, Turro E, Frontini M. Cell type-specific novel long non-coding RNA and circular RNA in the BLUEPRINT hematopoietic transcriptomes atlas. *Haematologica* 2021; **106**: 2613-2623 [PMID: 32703790 DOI: 10.3324/haematol.2019.238147]

28 **Jarroux J**, Morillon A, Pinskaya M. History, Discovery, and Classification of lncRNAs. *Adv Exp Med Biol* 2017; **1008**: 1-46 [PMID: 28815535 DOI: 10.1007/978-981-10-5203-3_1]

29 **Park EG**, Pyo SJ, Cui Y, Yoon SH, Nam JW. Tumor immune microenvironment lncRNAs. *Brief Bioinform* 2022; **23** [PMID: 34891154 DOI: 10.1093/bib/bbab504]

30 **Zhou J**, Xu J, Zhang L, Liu S, Ma Y, Wen X, Hao J, Li Z, Ni Y, Li X, Zhou F, Li Q, Wang F, Wang X, Si Y, Zhang P, Liu C, Bartolomei M, Tang F, Liu B, Yu J, Lan Y. Combined Single-Cell Profiling of lncRNAs and Functional Screening Reveals that H19 Is Pivotal for Embryonic Hematopoietic Stem Cell Development. *Cell Stem Cell* 2019; **24**: 285-298.e5 [PMID: 30639035 DOI: 10.1016/j.stem.2018.11.023]

31 **Zhang Q**, Chao TC, Patil VS, Qin Y, Tiwari SK, Chiou J, Dobin A, Tsai CM, Li Z, Dang J, Gupta S, Urdahl K, Nizet V, Gingeras TR, Gaulton KJ, Rana TM. The long noncoding RNA *ROCKI* regulates inflammatory gene expression. *EMBO J* 2019; **38** [PMID: 30918008 DOI: 10.15252/embj.2018100041]

32 **Castellanos-Rubio A**, Fernandez-Jimenez N, Kratchmarov R, Luo X, Bhagat G, Green PH, Schneider R, Kiledjian M, Bilbao JR, Ghosh S. A long noncoding RNA associated with susceptibility to celiac disease. *Science* 2016; **352**: 91-95 [PMID: 27034373 DOI: 10.1126/science.aad0467]

33 **Zhao H**, Zhang X, Frazão JB, Condino-Neto A, Newburger PE. HOX antisense lincRNA HOXA-AS2 is an apoptosis repressor in all trans retinoic acid treated NB4 promyelocytic leukemia cells. *J Cell Biochem* 2013; **114**: 2375-2383 [PMID: 23649634 DOI: 10.1002/jcb.24586]

34 **Pei X**, Wang X, Li H. LncRNA SNHG1 regulates the differentiation of Treg cells and affects the immune escape of breast cancer *via* regulating miR-448/IDO. *Int J Biol Macromol* 2018; **118**: 24-30 [PMID: 29886172 DOI: 10.1016/j.ijbiomac.2018.06.033]

35 **Ni C**, Fang QQ, Chen WZ, Jiang JX, Jiang Z, Ye J, Zhang T, Yang L, Meng FB, Xia WJ, Zhong M, Huang J. Breast cancer-derived exosomes transmit lncRNA SNHG16 to induce CD73+γδ1 Treg cells. *Signal Transduct Target Ther* 2020; **5**: 41 [PMID: 32345959 DOI: 10.1038/s41392-020-0129-7]

36 **Yu Z**, Zhao H, Feng X, Li H, Qiu C, Yi X, Tang H, Zhang J. Long Non-coding RNA FENDRR Acts as a miR-423-5p Sponge to Suppress the Treg-Mediated Immune Escape of Hepatocellular Carcinoma Cells. *Mol Ther Nucleic Acids* 2019; **17**: 516-529 [PMID: 31351327 DOI: 10.1016/j.omtn.2019.05.027]

37 **Yin Z**, Zhou Y, Ma T, Chen S, Shi N, Zou Y, Hou B, Zhang C. Down-regulated lncRNA SBF2-AS1 in M2 macrophage-derived exosomes elevates miR-122-5p to restrict XIAP, thereby limiting pancreatic cancer development. *J Cell Mol Med* 2020; **24**: 5028-5038 [PMID: 32301277 DOI: 10.1111/jcmm.15125]

38 **Zhang M**, Zheng Y, Sun Y, Li S, Chen L, Jin X, Hou X, Liu X, Chen Q, Li J, Liu M, Zheng X, Zhang Y, Wu J, Yu B. Knockdown of NEAT1 induces tolerogenic phenotype in dendritic cells by inhibiting activation of NLRP3 inflammasome. *Theranostics* 2019; **9**: 3425-3442 [PMID: 31281488 DOI: 10.7150/thno.33178]

39 **Hu Q**, Ye Y, Chan LC, Li Y, Liang K, Lin A, Egranov SD, Zhang Y, Xia W, Gong J, Pan Y, Chatterjee SS, Yao J, Evans KW, Nguyen TK, Park PK, Liu J, Coarfa C, Donepudi SR, Putluri V, Putluri N, Sreekumar A, Ambati CR, Hawke DH, Marks JR, Gunaratne PH, Caudle AS, Sahin AA, Hortobagyi GN, Meric-Bernstam F, Chen L, Yu D, Hung MC, Curran MA, Han L, Lin C, Yang L. Oncogenic lncRNA downregulates cancer cell antigen presentation and intrinsic tumor suppression. *Nat Immunol* 2019; **20**: 835-851 [PMID: 31160797 DOI: 10.1038/s41590-019-0400-7]

40 **Jiang W**, Pan S, Chen X, Wang ZW, Zhu X. The role of lncRNAs and circRNAs in the PD-1/PD-L1 pathway in cancer immunotherapy. *Mol Cancer* 2021; **20**: 116 [PMID: 34496886 DOI: 10.1186/s12943-021-01406-7]

41 **Li G**, Kryczek I, Nam J, Li X, Li S, Li J, Wei S, Grove S, Vatan L, Zhou J, Du W, Lin H, Wang T, Subramanian C, Moon JJ, Cieslik M, Cohen M, Zou W. LIMIT is an immunogenic lncRNA in cancer immunity and immunotherapy. *Nat Cell Biol* 2021; **23**: 526-537 [PMID: 33958760 DOI: 10.1038/s41556-021-00672-3]

World Journal of Gastrointestinal Oncology

Submit a Manuscript: https://www.f6publishing.com

World J Gastrointest Oncol 2022 November 15; 14(11): 2122-2137

DOI: 10.4251/wjgo.v14.i11.2122

ISSN 1948-5204 (online)

ORIGINAL ARTICLE

Basic Study

Synaptophysin-like 2 expression correlates with lymph node metastasis and poor prognosis in colorectal cancer patients

Zong-Xian Zhao, Qin-Lingfei Liu, Yao Yuan, Fu-Sheng Wang

Specialty type: Oncology

Provenance and peer review: Unsolicited article; Externally peer reviewed.

Peer-review model: Single blind

Peer-review report's scientific quality classification

Grade A (Excellent): 0
Grade B (Very good): B, B
Grade C (Good): C
Grade D (Fair): 0
Grade E (Poor): 0

P-Reviewer: Hamaya Y, Japan; Herold M, Hungary

Received: July 4, 2022
Peer-review started: July 4, 2022
First decision: August 13, 2022
Revised: August 24, 2022
Accepted: October 11, 2022
Article in press: October 11, 2022
Published online: November 15, 2022

Zong-Xian Zhao, Yao Yuan, Fu-Sheng Wang, Department of Anorectal Surgery, Fuyang People's Hospital, Fuyang 236000, Anhui Province, China

Qin-Lingfei Liu, Department of Digestive Internal Medicine, Tianjin Medical University General Hospital, Tianjin 300070, China

Corresponding author: Zong-Xian Zhao, MD, Researcher, Surgeon, Department of Anorectal Surgery, Fuyang People's Hospital, No. 501 Sanqing Road, Yingzhou District, Fuyang 236000, Anhui Province, China. 461901590@qq.com

Abstract

BACKGROUND

Colorectal cancer (CRC) is one of the most common and fatal cancers worldwide. Synaptophysin-like 2 (SYPL2) is a neuroendocrine-related protein highly expressed in skeletal muscle and the tongue. The involvement of SYPL2 in CRC, including its level of expression and function, has not been evaluated.

AIM

To evaluate the correlations of SYPL2 expression with lymph node metastasis (LNM) and prognosis in patients with CRC.

METHODS

The levels of expression of SYPL2 in CRC and normal colorectal tissues were analyzed in multiple public and online databases. The associations between clinical variables and SYPL2 expression were evaluated statistically, and the associations between SYPL2 expression and prognosis in patients with CRC were analyzed using the Kaplan-Meier method and univariate/multivariate Cox regression analyses. SYPL2 expression was assessed in 20 paired CRC tissue and adjacent normal colorectal tissue samples obtained from Fuyang People's Hospital, and the associations between SYPL2 expression and the clinical characteristics of these patients were investigated. Correlations between the levels of expression of SYPL2 and key targeted genes were determined by Pearson's correlation analysis. The distribution of immune cells in these samples was calculated using the CIBERSORT algorithm. Gene set enrichment analysis (GSEA) was performed to evaluate the biofunction and pathways of SYPL2 in CRC.

RESULTS

SYPL2 expression was significantly lower in CRC tissue samples than in normal

colorectal tissue samples ($P < 0.05$). High SYPL2 levels in CRC tissues correlated significantly with LNM ($P < 0.05$) and a poorer patient prognosis, including significantly shorter overall survival (OS) [hazard ratio (HR) = 1.9, $P < 0.05$] and disease-free survival (HR = 1.6, $P < 0.05$). High SYPL2 expression was an independent risk factor for OS in both univariate (HR = 2.078, $P = 0.014$) and multivariate (HR = 1.754, $P = 0.018$) Cox regression analyses. In addition, SYPL2 expression correlated significantly with the expression of KDR ($P < 0.0001$, $r = 0.47$) and the $BRAF^{V600E}$ mutation ($P < 0.05$). Higher SYPL2 expression was associated with the enrichment of CD8 T-cells and M0 macrophages in the tumor microenvironment. GSEA revealed that SYPL2 was associated with the regulation of epithelial cell migration, vasculature development, pathways in cancer, and several vital tumor-related pathways.

CONCLUSION

SYPL2 expression was lower in CRC tissue than in normal colorectal tissue. Higher SYPL2 expression in CRC was significantly associated with LNM and poorer survival.

Key Words: Synaptophysin-like 2; Colorectal cancer; Lymph node metastasis; Prognosis; Immune microenvironment; Bevacizumab

Core Tip: In this research, we reported the expression and biofunctions of synaptophysin-like 2 (SYPL2) in colorectal cancer (CRC) for the first time. SYPL2 correlated with lymph node metastasis and a poor prognosis (both overall and disease-free survival) in CRC. SYPL2 mainly influence CD8 T-cell and M0 macrophage enrichment in the tumor microenvironment. Gene set enrichment analysis indicated that SYPL2 might also influence the tumor vasculature development. In addition, we found that SYPL2 was correlated with the effect of bevacizumab therapy.

Citation: Zhao ZX, Liu QL, Yuan Y, Wang FS. Synaptophysin-like 2 expression correlates with lymph node metastasis and poor prognosis in colorectal cancer patients. *World J Gastrointest Oncol* 2022; 14(11): 2122-2137
URL: https://www.wjgnet.com/1948-5204/full/v14/i11/2122.htm
DOI: https://dx.doi.org/10.4251/wjgo.v14.i11.2122

INTRODUCTION

Colorectal cancer (CRC), which is responsible for an estimated 8% of new cancer diagnoses and 8% of cancer deaths annually, is the third-most common cause of cancer deaths worldwide[1]. The stage at diagnosis is the most important predictor of survival, with 5-year relative survival rates of 90% for patients diagnosed with localized disease compared to 14% for patients diagnosed with distant-stage disease[2]. Complete mesocolic excision is the cornerstone of CRC treatment, showing good pathological outcomes as well as improvements in overall survival (OS), disease-free survival (DFS) and local recurrence[3]. Lymph node metastasis (LNM) is important in CRC staging and patient prognosis [4], with regional LNM being one of the most important indications for adjuvant chemotherapy[5,6]. Risk factors for LNM include lymphovascular invasion, histological grade, submucosal invasion depth, and tumor budding[7-9]. Although LNM of CRC is usually evaluated by radiologic methods, including computed tomography, magnetic resonance imaging, and positron emission tomography/computed tomography, these imaging methods cannot accurately evaluate LNM using criteria like short-axis diameter, signal heterogeneity, shape, and boundaries[10,11]. Several key biomarkers, however, have been reported to be predictive of LNM and prognosis in patients with CRC[12,13].

Immunotherapy and targeted therapy play important roles in the management of CRC. The molecular targets of CRC identified to date include epithelial growth factor receptor (EGFR), vascular endothelial growth factor (VEGF), human EGFR2, V-raf murine sarcoma viral oncogene homolog B1 (BRAF), Kirsten rat sarcoma (KRAS), P53 mutation, programmed cell death protein 1, and cytotoxic T-lymphocyte–associated protein 4[14,15]. Targeting these proteins in clinical practice has provided survival benefits for patients.

Synaptophysin-like 2 (SYPL2) is a neuroendocrine-related cytosolic protein enriched primarily in skeletal muscles and the tongue. The role of SYPL2 in cancer, including CRC, has not been determined. Thus, the present study comprehensively and systematically compared SYPL2 expression in CRC and normal colorectal tissues. Survival (Cox regression) analyses were also performed to assess the prognostic value of SYPL2 expression, along with other clinicopathological features. The correlation

between SYPL2 expression and the expression of key targeted genes in CRC was analyzed. Moreover, gene set enrichment analysis (GSEA) was performed to evaluate the SYPL2-associated biological pathways involved in CRC pathogenesis, providing clues about the function of SYPL2.

MATERIALS AND METHODS

Data collection

The gene-expression profiles and associated clinicopathological data of patients with CRC were downloaded from the Cancer Genome Atlas (TCGA) Genomic Data Commons Data Portal (https://portal.gdc.cancer.gov/repository) on March 25, 2022. RNA-sequencing gene-expression HTSeq-FPKM data for 571 CRC tissue samples and 44 normal adjacent tissue samples were collected for further analysis. The GSE87211, GSE44076, GSE60331, and GSE103479 datasets were obtained from Gene Expression Omnibus microarrays. In addition, CRC and normal adjacent tissue samples were collected from 20 patients who underwent surgery for CRC at the Fuyang People's Hospital. Demographic and clinical characteristics of these patients, including their age, sex, cancer stage, and lymph node status, were also recorded and analyzed. All participating patients provided written informed consent, and the study protocol was approved by the ethics review committees of Fuyang People's Hospital.

Gene Expression Profiling Interactive Analysis

Gene Expression Profiling Interactive Analysis (GEPIA) is a newly developed, interactive web server that includes the RNA-sequencing expression data of 9736 tumors and 8587 normal samples from the TCGA and Genotype-Tissue Expression datasets, utilizing a standard processing pipeline. GEPIA offers customizable functions, such as tumor/normal differential expression analysis, profiling according to cancer type or pathological stage, patient survival analysis, detection of similar genes, correlation analysis, and dimensional reduction analysis. In the present study, GEPIA was used to perform differential expression, survival, and correlation analyses, the latter of which was performed with key targeted genes using Pearson's test.

Quantitative real-time polymerase chain reaction

Total RNA extracted from cells using RNAprep Pure Tissue kits (Tiangen, Beijing, China) was reverse-transcribed to complementary DNA using the FastKing gDNA Dispelling RT SuperMix for quantitative polymerase chain reaction (qPCR) (Tiangen). The samples were subjected to quantitative real-time PCR (qRT-PCR) using 2 × SYBR Green qPCR Master Mix (Tiangen) and primers specific for SYPL2 (forward, 5′-CGCTGGTGGACTTCTGTG-3′; reverse, 5′-GCTGGATGGTCGTGTGG-3′) and GAPDH (forward, 5′-AAGGTCGGAGTCAACGGA-3′; reverse, 5′-TTAAAAGCAGCCCTGGTGA-3′), with all gene primers obtained from Aoke Dingsheng Biotechnology (Beijing, China). Thermal cycling conditions consisted of an initial denaturation at 95 °C for 15 s, followed by 40 cycles of denaturation at 95 °C for 15 s, annealing at 55 °C for 30 s, and extension at 72 °C for 30 s. Relative messenger RNA expression levels were calculated using the $2^{-\Delta\Delta CT}$ method, with the average level of SYPL2 expression in the 20 normal colorectal tissues defined as the reference for normalization and comparison with the 20 CRC tissues.

Cox regression analyses and immune cell enrichment analyses

Univariate and multivariate Cox analyses were used to investigate the association between SYPL2 expression and other clinical characteristics, such as age, sex, cancer stage, distant metastasis status, and lymph node status. OS was assessed by univariate Cox regression analyses, with factors significantly associated with OS subsequently entered into a multivariate Cox model. In addition, survival was directly analyzed using the Kaplan-Meier method (KM plotter: http://kmplot.com). The presence of 22 types of immune cells in the CRC microenvironment was assessed using the CIBERSORT algorithm[16].

GSEA

Datasets and phenotype label files from TCGA were generated and uploaded into the GSEA software program. The phenotype labels were SYPL2 high expression and SYPL2 low expression (grouped relative to the median SYPL2 expression). Gene set permutations were conducted 1000 times for each analysis. Gene sets with ES > 0.6 and FWER $P < 0.05$ were considered enriched.

Statistical analysis

Survival curves were plotted using the Kaplan-Meier method and compared using the log-rank test. Cox regression analyses were performed using the R "survival" package. Correlation analyses were performed by determining Pearson's correlation coefficients. Categorical variables were compared using the chi-squared and Fisher's exact tests, parametric continuous variables were compared using Student's *t* tests, and non-parametric continuous variables were compared using Mann-Whitney *U* tests. Statistical analyses were performed using R version 4.1.0 (R Foundation for Statistical Computing, Vienna, Austria), Bioconductor (https://www.bioconductor.org/), and GraphPad Prism 8 (GraphPad

Software, San Diego, CA, United States), with $P < 0.05$ defined as statistically significant.

RESULTS

Expression of SYPL2 and its association with prognosis in CRC

GEPIA showed that the mean expression of SYPL2 was significantly lower in 275 colon cancer tissue samples than in 349 normal colon tissue samples and was lower in 92 rectal cancer tissue samples compared to 318 normal rectal tissue samples ($P < 0.05$, Figure 1A). Similar findings were observed when SYPL2 expression was compared between 203 CRC and 160 normal colorectal tissue samples (GSE87211) ($P < 0.001$, Figure 1B) and between 98 CRC samples, 98 adjacent normal colorectal tissue samples, and 50 healthy normal tissue samples ($P < 0.0001$, Figure 1C). These findings were confirmed by comparing SYPL2 expression by qRT-PCR in 20 freshly obtained CRC and adjacent normal tissue samples ($P < 0.05$, Figure 1D). A high expression of SYPL2 was significantly associated with poorer OS and DFS ($P < 0.05$, Figures 1E and 1F), with these results confirmed by Kaplan-Meier analysis ($P < 0.05$, Figures 1G and 1H). Furthermore, high expression of SYPL2 was significantly associated with a worse OS in both stage II and III CRC (Figures 1I and 1J).

Correlations of SYPL2 expression with clinicopathological characteristics of patients with CRC

Associations between SYPL2 expression and the clinicopathological characteristics of patients with CRC were assessed by dividing CRC patients into two groups based on the median SYPL2 expression. High expression of SYPL2 was significantly associated with greater tumor depth ($P = 0.0140$, $\chi^2 = 6.078$), LNM ($P = 0.0312$, $\chi^2 = 4.644$), and greater American Joint Committee on Cancer stage ($P = 0.0228$, $\chi^2 = 5.182$) (Table 1). An analysis of the 20 paired CRC and normal colon tissue samples showed that SYPL2 expression was significantly correlated with LNM ($P < 0.001$, Figure 2B). Univariate Cox regression analysis showed that high expression of SYPL2 was associated with poorer OS [hazard ratio (HR) = 2.078; 95% confidence interval (CI): 1.162-3.716; $P = 0.014$], older age ($P < 0.05$), and higher TNM stage ($P < 0.05$) (Table 2), with multivariate Cox analysis revealing that high SYPL2 expression remained an independent risk factor for OS (HR = 1.754; 95%CI: 1.103-2.790; $P = 0.018$).

Correlation between SYPL2 expression and the expression of key target genes

Correlation analyses were performed to determine whether SYPL2 could act as a biomarker to predict the outcomes of targeted therapy in patients with CRC. SYPL2 expression correlated significantly with the mutation of $BRAF^{V600E}$ ($P < 0.05$) (Figure 3A) and the expression levels of *KDR* ($P < 0.0001$, $r = 0.47$), *EGFR* ($P < 0.0001$, $r = 0.33$), *CTLA4* ($P < 0.01$, $r = 0.15$), and *PDCD1* ($P < 0.01$, $r = 0.15$) (Figure 3B). We collected a total of 16 tumor samples entered into GSE60331 prior to undergoing treatment with bevacizumab; the responder group included seven samples and the non-responder group contained nine samples. Some detailed information can be retrieved from GSE60331[17]. Moreover, high SYPL2 expression was found to correlate with the response to bevacizumab treatment ($P < 0.05$, Figure 4). Taken together, these findings indicate that SYPL2 may be a potential biomarker of response of CRC to targeted therapy.

SYPL2 predicts the infiltration of immune cells into the CRC microenvironment

To assess the roles of SYPL2 in the tumor immune microenvironment, it was necessary to investigate the types of infiltrating immune cells in CRC patients. CIBERSORT evaluation of the relative proportions of 22 types of immune cells in all CRC specimens from TCGA showed high infiltration of regulatory T-cells and M0 macrophages in tumors with high SYPL2 expression (Figure 5A) and high infiltration of CD8 T-cells, activated CD4 memory T-cells, activated natural killer cells, and activated dendritic cells in tumors with low SYPL2 expression (Figure 5A). The level of SYPL2 expression had no effect on OS in tumors enriched with CD8 T-cells ($P > 0.05$, Figure 5B), whereas high expression of SYPL2 was closely associated with poorer OS in tumors unenriched with CD8 T-cells ($P < 0.05$, Figure 5C). High expression of SYPL2 was also associated with poorer OS in tumors both enriched ($P < 0.05$, Figure 5D) and unenriched ($P < 0.05$, Figure 5E) with M0 macrophages. Collectively, these findings show that SYPL2 expression correlates with the level of infiltration of most immune cells, possibly indicating the state of the tumor immune microenvironment and suggesting that SYPL2 might play different roles in different immune microenvironments.

GSEA identified functions and signaling pathways

GSEA was performed to determine the biological characteristics shared by tissue samples displaying different levels of SYPL2 expression and to identify the functions and pathways in which SYPL2 may be involved. Gene Ontology (GO) enrichment analyses indicated that SYPL2 was associated with the enrichment of genes involved in the positive regulation of vasculature development, epithelial cell migration, development growth, JUN kinase activity, MAP kinase activity, phospholipase activity, and single-organism cell adhesion (Figure 6A). In addition, Kyoto Encyclopedia of Genes and Genomes

Table 1 Correlation between synaptophysin-like 2 level and clinicopathological characteristics in colorectal cancer

Characteristics	SYPL2 level		*P* value
	Low (*n* = 285)	High (*n* = 286)	
Age (yr)	68.00 ± 12.14	65.31 ± 13.37	0.1148
Gender			
Female	125	128	0.8273
Male	145	143	
Unknow	20	15	
T			
T1 + T2	61	37	0.0140[a]
T3 + T4	179	192	
Unknow	45	57	
N			
N0	153	123	0.0312[a]
N1-2	87	105	
Unknow	45	56	
M			
M0	185	164	0.0955
M1	29	39	
Unknow	71	83	
AJCC stage			
I-II	146	114	0.0228[a]
III-IV	88	106	
Unknow	51	66	

[a]$P < 0.05$.

AJCC: American Joint Commission on Cancer; SYPL2: Synaptophysin-like 2.

(KEGG) analysis found that genes involved in basal cell carcinoma; cell-adhesion molecules; extracellular matrix receptor interactions; the epidermal growth factor receptor, hedgehog, mitogen-activated protein kinases (MAPK), NOTCH, transforming growth factor (TGF)-β, and WNT signaling pathways; GAP junctions; and vascular smooth muscle contraction were significantly enriched in CRC samples expressing high levels of SYPL2 (Figure 6B).

DISCUSSION

Members of the synaptophysin-like family, including SYPL1 and SYPL2, are synaptic vesicle membrane proteins. SYPL1 was originally considered a neuroendocrine-related protein but was found to be expressed in both neuronal and non-neuronal tissues[18]. A recent immunohistochemistry-based study showed that SYPL1 was prognostic of poor outcomes in patients with hepatocellular carcinoma and was associated with the epithelial-mesenchymal transition[19]. SYPL1 is also upregulated in pancreatic ductal adenocarcinoma, with higher SYPL1 expression being associated with tumor cell proliferation and poorer prognosis[20]. Serum SYPL1 may be a diagnostic marker for CRC, especially in patients with low serum carcinoembryonic antigen concentrations[21]. SYPL2, also called MG29, is primarily expressed in skeletal muscles and the tongue and is functionally thought to participate in cellular calcium ion homeostasis[22]. In addition, the SYPL2 gene has been associated with morbid obesity and may be involved in the development of excess body fat[23]. However, the roles and functions of SYPL2 in cancer and its related molecular mechanisms remain unknown.

The present study, using multiple public databases and donor-matched CRC and adjacent normal tissues, showed that the level of SYPL2 expression was lower in cancerous tissues than in normal tissues. An analysis of the associations between SYPL2 expression and clinical pathologic features

Table 2 Cox regression analysis of synaptophysin-like 2 expression and clinical pathological characteristics

Characteristics	Univariate Cox			Multivariate Cox		
	HR	95%CI	*P* value	HR	95%CI	*P* value
Age	1.037	1.015-1.059	0.0001[a]	1.051	1.027-1.075	0.0001[a]
Gender (male)	1.160	0.746-1.803	0.509	0.987	0.621-1.571	0.957
T						
T1	1			1		
T2	0.819	0.169-3.953	0.804	0.354	0.069-1.805	0.212
T3	1.324	0.322-5.456	0.697	0.424	0.096-1.863	0.256
T4	4.661	1.082-20.075	0.039[a]	0.906	0.189-4.348	0.901
N						
N0	1			1		
N1	2.547	1.484-4.368	0.0001[a]	1.988	1.048-3.770	0.035[a]
N2	4.195	2.479-7.099	0.0001[a]	2.253	1.179-4.304	0.014[a]
M (M1)	4.482	2.829-7.100	0.0001[a]	2.585	1.468-4.660	0.001[a]
ACJJ						
I	1					
II	1.474	0.548-3.961	0.442			
III	2.858	1.086-7.627	0.033[a]			
IV	8.096	3.135-20.903	0.0001[a]			
SYPL2 (high)	2.078	1.162-3.716	0.014[a]	1.754	1.103-2.790	0.018[a]

[a]$P < 0.05$.

AJCC: American Joint Commission on Cancer; SYPL2: Synaptophysin-like 2; HR: Hazards ratio; CI: Confidence interval.

revealed that higher SYPL2 levels in CRC patients were associated with lymph node metastases (N stage) and more advanced tumors (T stage), although qRT-PCR analysis found that higher SYPL2 expression was associated only with LNM. Univariate and multivariate Cox analyses and survival analyses indicated that SYPL2 expression level is a potential independent marker of poor prognosis in patients with CRC. Correlation analyses showed that the SYPL2 gene-expression level was significantly associated with the expression of *KDR* (also called *VEGFR*) (R > 0.4) and *EGFR* (R > 0.3) and with $BRAF^{V600E}$ mutation ($P < 0.05$). Carvalho *et al*[24] reported that *VEGFR* expression is associated with the effect of bevacizumab therapy, and Szablewski *et al*[25] found that *EGFR* overexpression and mutations in *KRAS* and *BRAF* contribute to colorectal carcinogenesis. Moreover *EGFR*-directed molecular treatments could be investigated in a subset of patients affected by intestinal-type adenocarcinoma. These results of above studies were consistent with our research.

Agents targeting *VEGFR* or *EGFR* and multiple tyrosine kinase inhibitors play an important role in CRC management[26]. The mutation of $BRAF^{V600E}$ residue occurs in approximately 10% of CRCs, constituting a group with a particularly poor prognosis. And our result also found that SYPL2 was higher expression in the $BRAF^{V600E}$ mutation group, and associated with poor prognosis. The mutation of $BRAF^{V600E}$ is also extremely associated with targeted therapy of metastatic CRC[27]. Our result suggests that SYPL2 may be a biomarker for predicting targeted treatment of CRC patients. We collected a total of 16 tumor samples prior to bevacizumab treatment from GSE60331 for validation because there is greater clinical practice value in predicting the treatment response by considering pre-treatment genes. Our result revealed that the SYPL2 higher-expression group seemed more likely to respond to bevacizumab. Existing evidence indicates that tumor progression may result from the escape of cancer cells from host immunosurveillance[28]. Therefore, clarifying the infiltrating immune cells in the tumor microenvironment may help to elucidate the underlying mechanism involving SYPL2 in CRC. Moreover, SYPL2 may be involved in the immune microenvironment by enriching CD8 T-cells and M0 macrophages. These data indicate that SYPL2 might influence the infiltration of immunocytes and lead to a worse prognosis in CRC.

GO enrichment analysis of the biological functions of SYPL2 in CRC indicated that SYPL2 might regulate epithelial cell migration, vasculature development, MAPK kinase activity, and cell adhesion. Furthermore, KEGG enrichment analysis found that SYPL2 might participate in cell adhesion; several

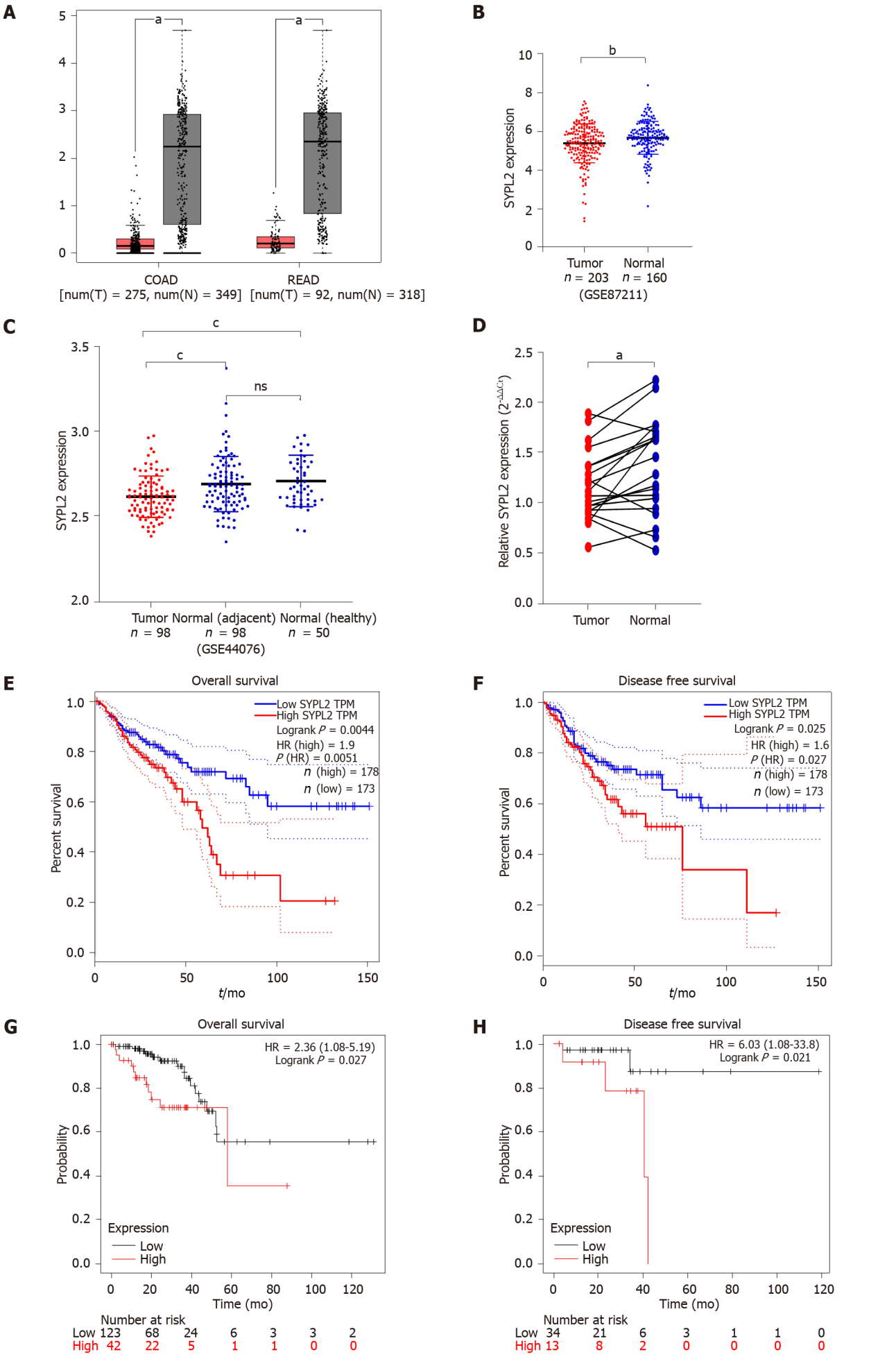
A
a
a
COAD
READ
[num(T) = 275, num(N) = 349]
[num(T) = 92, num(N) = 318]
B
b
SYPL2 expression
Tumor
Normal
n = 203
n = 160
(GSE87211)
C
c
c
ns
SYPL2 expression
Tumor
Normal (adjacent)
Normal (healthy)
n = 98
n = 98
n = 50
(GSE44076)
D
a
Relative SYPL2 expression (2^-ΔΔCt)
Tumor
Normal
E
Overall survival
Low SYPL2 TPM
High SYPL2 TPM
Logrank P = 0.0044
HR (high) = 1.9
P (HR) = 0.0051
n (high) = 178
n (low) = 173
Percent survival
t/mo
F
Disease free survival
Low SYPL2 TPM
High SYPL2 TPM
Logrank P = 0.025
HR (high) = 1.6
P (HR) = 0.027
n (high) = 178
n (low) = 173
Percent survival
t/mo
G
Overall survival
HR = 2.36 (1.08-5.19)
Logrank P = 0.027
Probability
Expression
Low
High
Time (mo)
Number at risk
Low 123 68 24 6 3 3 2
High 42 22 5 1 1 0 0
H
Disease free survival
HR = 6.03 (1.08-33.8)
Logrank P = 0.021
Probability
Expression
Low
High
Time (mo)
Number at risk
Low 34 21 6 3 1 1 0
High 13 8 2 0 0 0 0

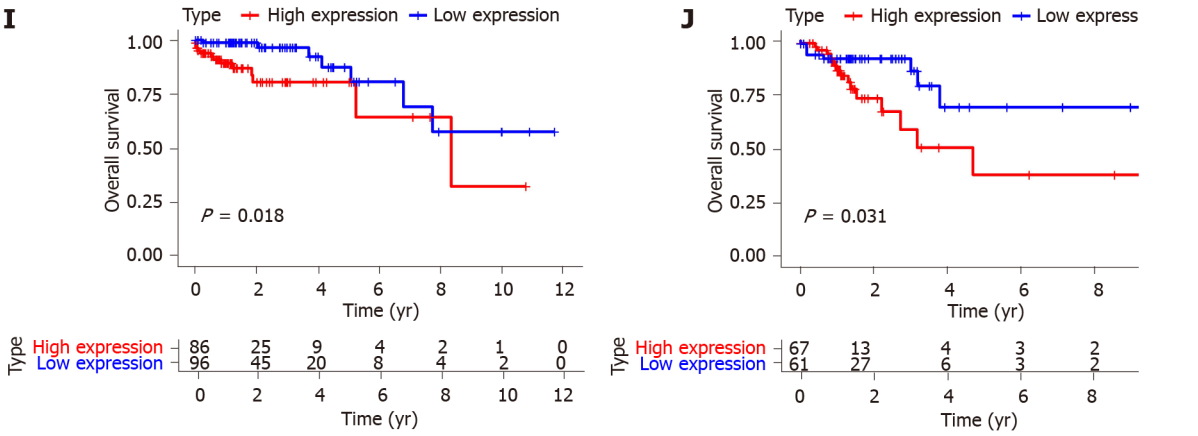

DOI: 10.4251/wjgo.v14.i11.2122 **Copyright** ©The Author(s) 2022.

Figure 1 Synaptophysin-like 2 expression levels and survival analyses in colorectal cancer. A: Synaptophysin-like 2 (SYPL2) expression in 275 colon cancer tissue and 349 normal colon tissue samples and in 92 rectal cancer tissue and 318 normal rectal tissue samples from Gene Expression Profiling Interactive Analysis (GEPIA) ($P < 0.05$); B: SYPL2 expression in 203 colorectal cancer (CRC) tissue and 160 normal colorectal tissue samples from GSE87211 ($P < 0.01$); C: SYPL2 expression in 98 CRC samples, 98 adjacent normal samples, and 50 healthy colon tissue samples from GSE44076 ($P < 0.001$); D: SYPL2 expression in tumor tissues and adjacent normal colon tissue samples from 20 CRC patients who underwent tumor resection at Fuyang People's Hospital ($P < 0.05$). The average expression of SYPL2 in the 20 normal tissue samples was regarded as a reference; E: Associations of SYPL2 expression with the overall survival (OS) of CRC patients from GEPIA ($P < 0.05$); F: Associations of SYPL2 expression with the disease-free survival (DFS) of CRC patients from GEPIA ($P < 0.05$); G: Associations of SYPL2 expression with the OS of CRC patients from the Kaplan-Meier plotter ($P < 0.05$); H: Associations of SYPL2 expression with the DFS of CRC patients from the Kaplan-Meier plotter ($P < 0.05$); I: Associations of SYPL2 expression with the OS of stage II CRC patients from TCGA (P < 0.05); J: Associations of SYPL2 expression with the OS of stage III CRC patients from TCGA ($P < 0.05$). $^{a}P < 0.05$, $^{b}P < 0.01$, $^{c}P < 0.001$. SYPL2: Synaptophysin-like 2; HR: Hazards ratio.

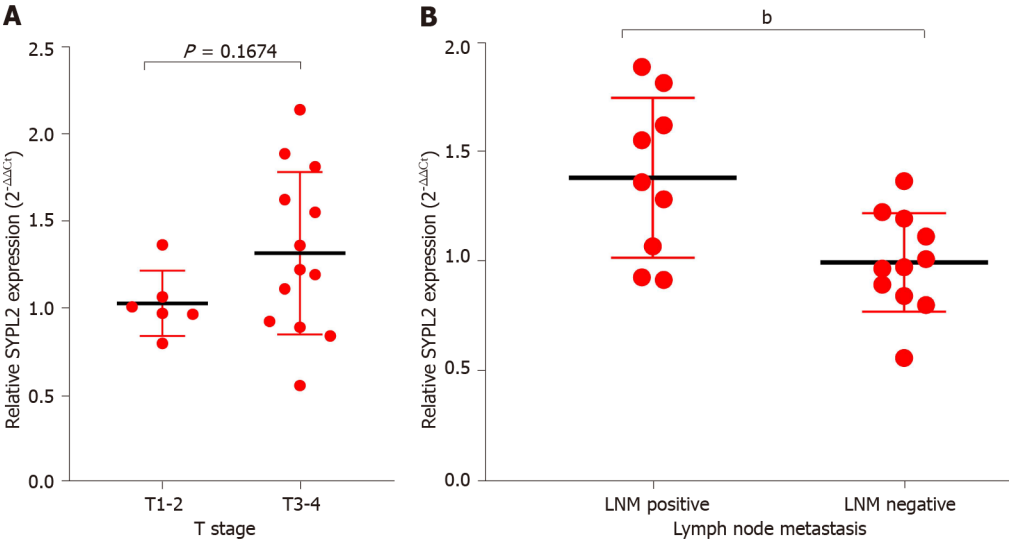

DOI: 10.4251/wjgo.v14.i11.2122 **Copyright** ©The Author(s) 2022.

Figure 2 Correlations of tumor expression of synaptophysin-like 2 among the 20 colorectal cancer patients who underwent tumor resection at Fuyang People's Hospital. A: T stage; B: Lymph node metastasis. SYPL2: Synaptophysin-like 2; LNM: Lymph node metastasis. $^{b}P < 0.01$.

cancer-related pathways, including pathways in basal cell carcinoma, renal cancer, and small-cell lung cancer; and several vital tumor-related signaling pathways, including the hedgehog, MAPK, NOTCH, and TGF-β signaling pathways.

In this study, SYPL2 expression in tumor tissues was significantly lower than that in normal tissue. However, higher SYPL2 expression was associated with worse survival in CRC. The paradox of the opposite effect of SYPL2 expression might be due to the following reasons. First, compared to normal tissue, tumor tissue can abnormally activate a series of signaling pathways and have special tumor microenvironment[29,30]. Some genes (including SYPL2) may play roles in promoting or suppressing cancer in specific signal pathways in the tumor microenvironment. Second, SYPL2 might work as a biomarker in CRC. Higher expression of SYPL2 could be associated with some specific and powerful activated oncogenic genes and enhanced malignant behavior of tumors. Finally, tumor-infiltrating immune cells are closely related to tumorigenesis, angiogenesis, and tumor cell growth and metastasis,

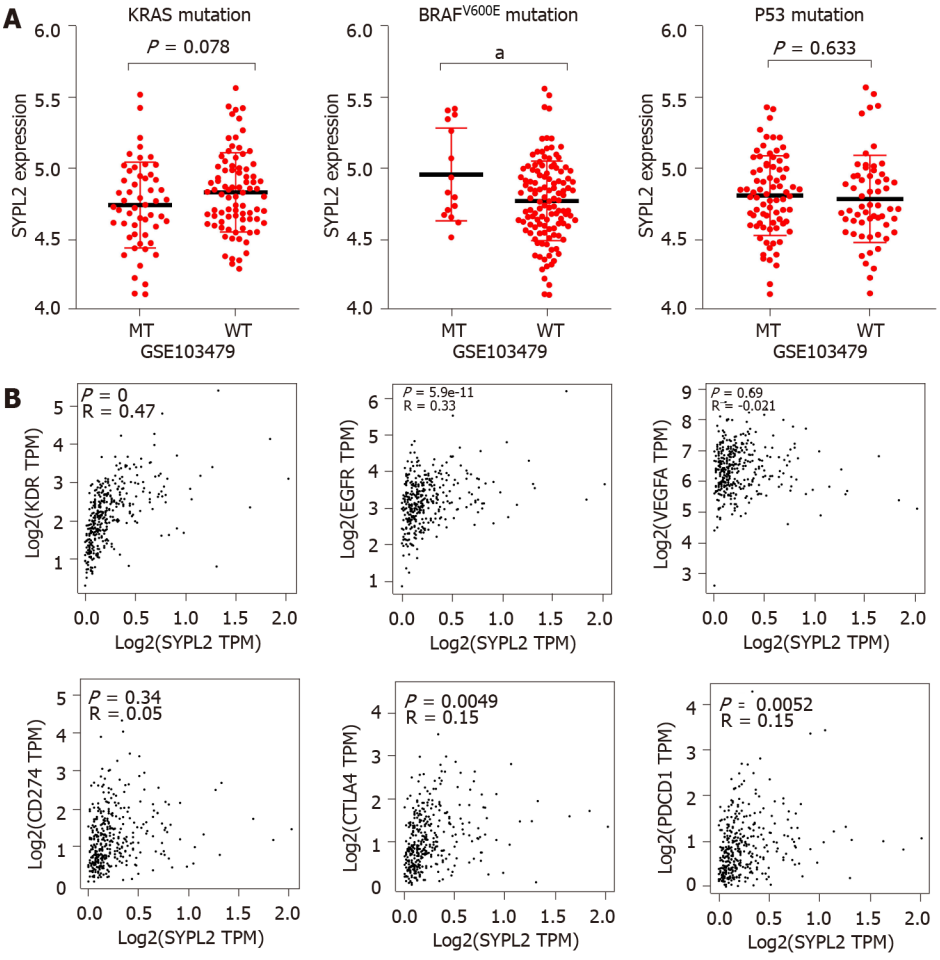

DOI: 10.4251/wjgo.v14.i11.2122 **Copyright** ©The Author(s) 2022.

Figure 3 Correlations of levels of synaptophysin-like 2 expression with Kirsten rat sarcoma *BRAF*^{V600E}, and *P53* mutations from GSE103479 and levels of expression of the key target genes *KDR*, epidermal growth factor receptor, vascular endothelial growth factor A, *CD274*, *PDCD1*, and *CTLA4* from Gene Expression Profiling Interactive Analysis. A: Association of synaptophysin-like 2 (SYPL2) expression with *KRAS*, *BRAF*^{V600E}, *P53* mutation; B: Association of SYPL2 expression with KDR, epidermal growth factor receptor, vascular endothelial growth factor A, CD274, PDCD1, cytotoxic T-lymphocyte-associated protein 4. SYPL2: Synaptophysin-like 2; MT: Mutation type; WT: Wild type; EGFR: Epidermal growth factor receptor; VEGFA: Vascular endothelial growth factor A; CTLA4: Cytotoxic T-lymphocyte-associated protein 4.

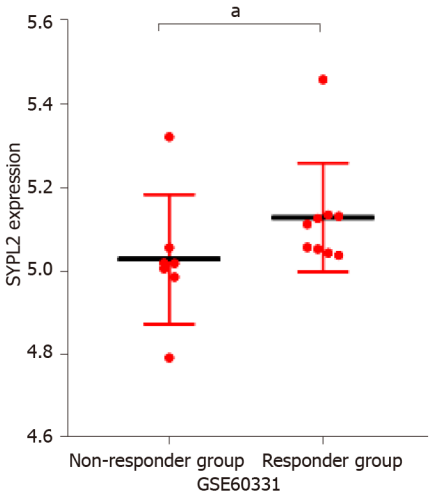

DOI: 10.4251/wjgo.v14.i11.2122 **Copyright** ©The Author(s) 2022.

Figure 4 Levels of synaptophysin-like 2 expression in colorectal cancer patients from GSE60331 who did and did not respond to bevacizumab treatment. $^{a}P < 0.05$.

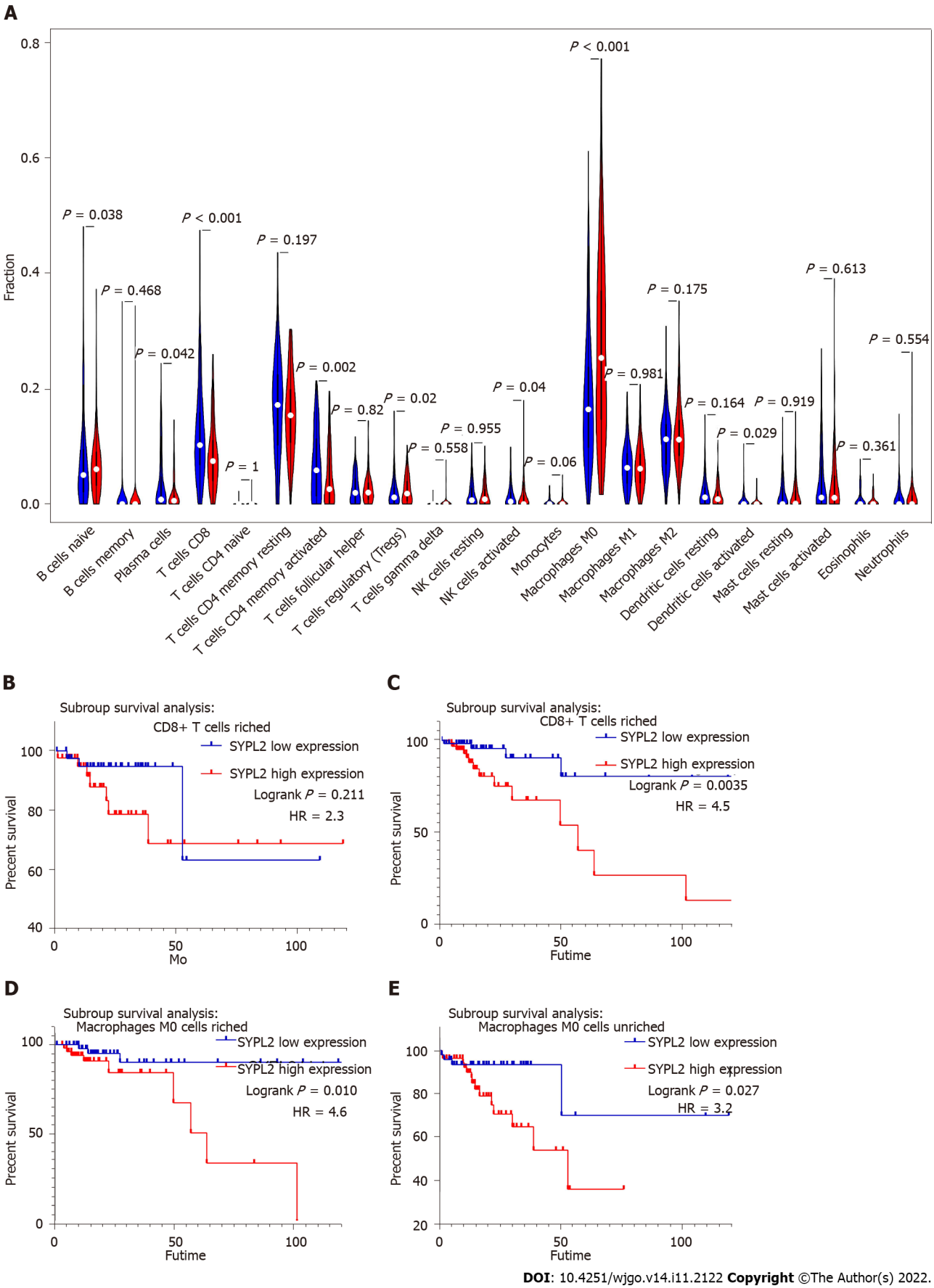

DOI: 10.4251/wjgo.v14.i11.2122

Figure 5 Effects of synaptophysin-like 2 expression level on the immune microenvironment in colorectal cancer from the Cancer Genome Atlas. A: Statistical chart after using the CIBERSORT method, showing the different proportions of immune cells in groups of patients with high (red) and low (blue) synaptophysin-like 2 expression; B-E: Survival analyses of patient subgroups. SYPL2: Synaptophysin-like 2; HR: Hazards ratio.

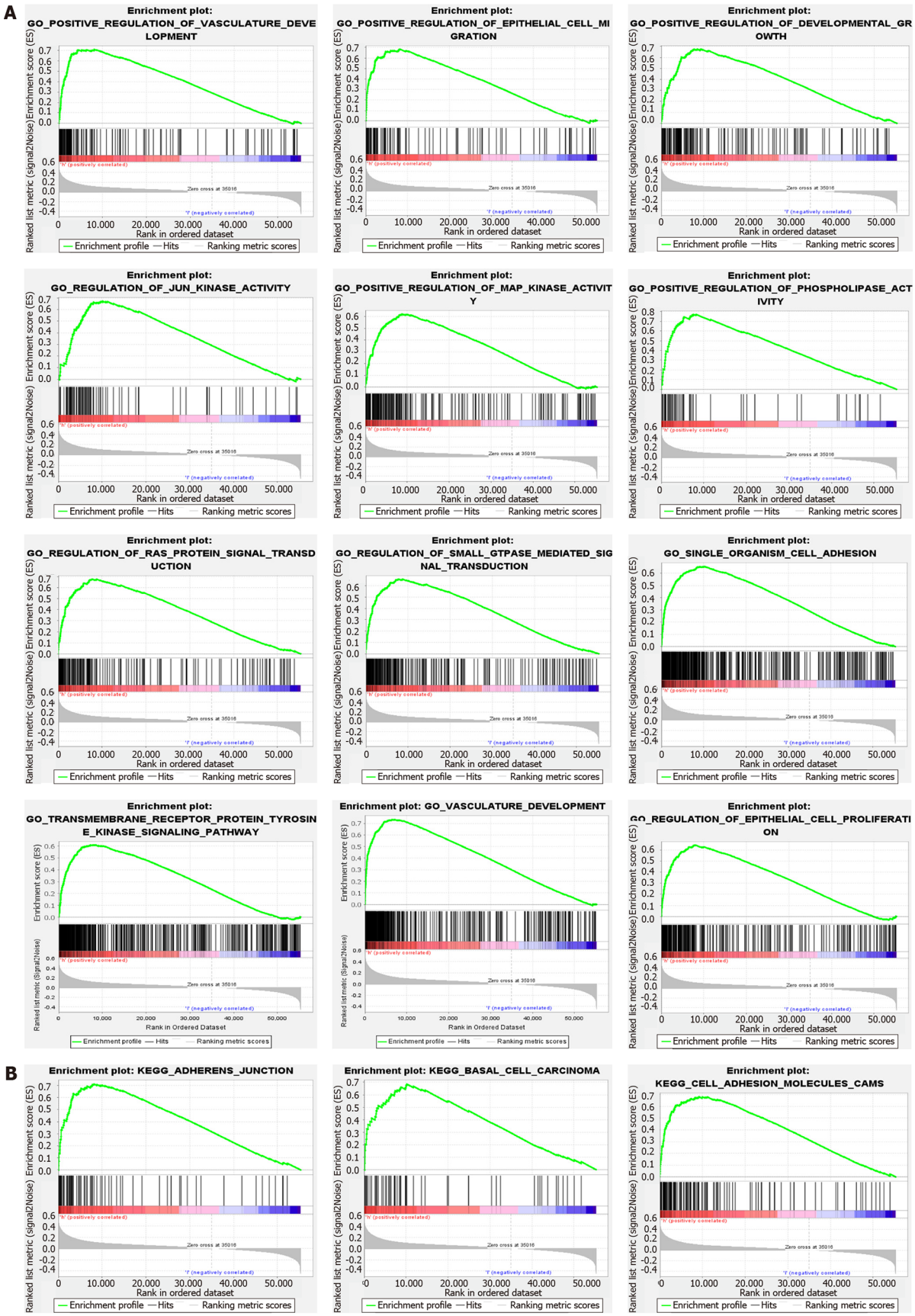
A
Enrichment plot: GO_POSITIVE_REGULATION_OF_VASCULATURE_DEVELOPMENT
Enrichment plot: GO_POSITIVE_REGULATION_OF_EPITHELIAL_CELL_MIGRATION
Enrichment plot: GO_POSITIVE_REGULATION_OF_DEVELOPMENTAL_GROWTH
Enrichment plot: GO_REGULATION_OF_JUN_KINASE_ACTIVITY
Enrichment plot: GO_POSITIVE_REGULATION_OF_MAP_KINASE_ACTIVITY
Enrichment plot: GO_POSITIVE_REGULATION_OF_PHOSPHOLIPASE_ACTIVITY
Enrichment plot: GO_REGULATION_OF_RAS_PROTEIN_SIGNAL_TRANSDUCTION
Enrichment plot: GO_REGULATION_OF_SMALL_GTPASE_MEDIATED_SIGNAL_TRANSDUCTION
Enrichment plot: GO_SINGLE_ORGANISM_CELL_ADHESION
Enrichment plot: GO_TRANSMEMBRANE_RECEPTOR_PROTEIN_TYROSINE_KINASE_SIGNALING_PATHWAY
Enrichment plot: GO_VASCULATURE_DEVELOPMENT
Enrichment plot: GO_REGULATION_OF_EPITHELIAL_CELL_PROLIFERATION
B
Enrichment plot: KEGG_ADHERENS_JUNCTION
Enrichment plot: KEGG_BASAL_CELL_CARCINOMA
Enrichment plot: KEGG_CELL_ADHESION_MOLECULES_CAMS
Enrichment profile
Hits
Ranking metric scores
Rank in ordered dataset
Enrichment score (ES)
Ranked list metric (signal2Noise)

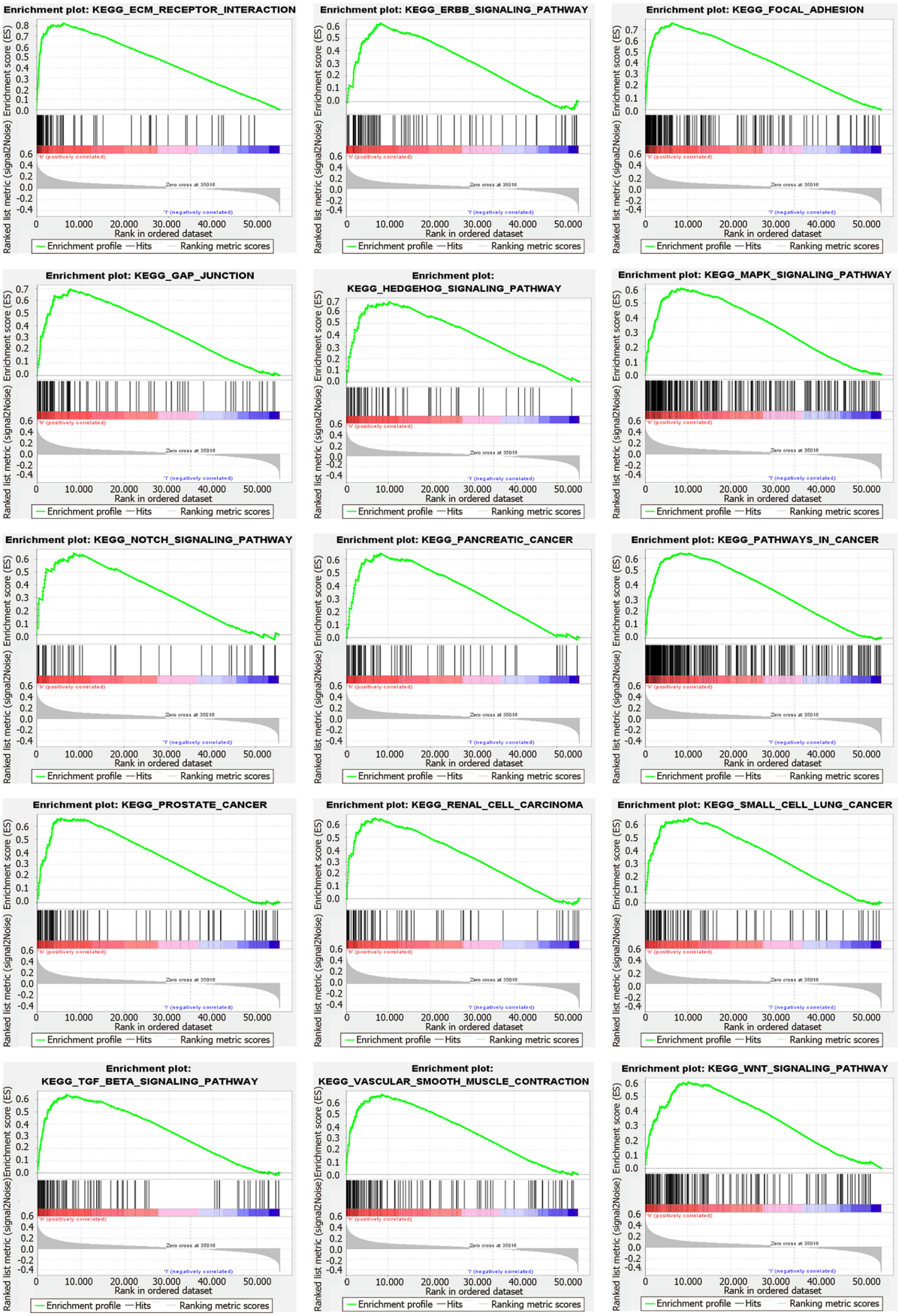

DOI: 10.4251/wjgo.v14.i11.2122

Figure 6 Enrichment plots from the Gene set enrichment analysis. A: Gene Ontology; B: Kyoto Encyclopedia of Genes and Genomes.

which may in turn regulate the quantity and differentiation of immune cells[31]. $CD8^+$ T-cells are typically thought to be a homogenous group of cytotoxic cells that produce interferon-γ[32]. In addition, $CD8^+$ T lymphocytes are the major anti-tumor effector cells[33]. In this study, $CD8^+$ T-cell counts in the SYPL2 high-expression group were significantly lower than those in the SYPL2 low-expression group. Therefore, SYPL2 might contribute to the poor prognosis of CRC by affecting immune cell infiltration. However, the relevant molecular and pathway mechanisms still necessitate further experiments for verification.

The present study was designed to evaluate SYPL2 gene expression in CRC and reveal the associations of SYPL2 with pathologic features and survival outcomes. This study used only GSEA to analyze biological functions and the molecular mechanism of SYPL2 in CRC. Further studies of SYPL2 protein expression and its associations with biological functions and molecular mechanisms in CRC are warranted.

CONCLUSION

SYPL2 expression was lower in CRC than in adjacent normal tissue, suggesting that SYPL2 may be a potential diagnostic and prognostic CRC-specific molecular marker. High SYPL2 expression was significantly associated with lymph node metastases and poorer survival.

ARTICLE HIGHLIGHTS

Research background

Colorectal cancer (CRC) is the third-most common cause of cancer deaths worldwide and lymph node metastasis (LNM) is important in CRC staging and patient prognosis. Risk factors for LNM include lymphovascular invasion, histological grade, submucosal invasion depth, and tumor budding. In addition, LNM of CRC is usually evaluated by radiologic methods, including computed tomography, magnetic resonance imaging *etc*. However, these imaging methods cannot accurately evaluate LNM. It was necessary to investigate key biomarkers to predict LNM and prognosis in patients with CRC. Moreover, synaptophysin-like 2 (SYPL2) is a neuroendocrine-related cytosolic protein enriched primarily in skeletal muscles and the tongue. The role of SYPL2 in cancer, including CRC, has not been determined.

Research motivation

The role of SYPL2 in CRC has not been studied. The present study comprehensively and systematically compared SYPL2 expression and potential functions. The relationship between SYPL2 expression and clinicopathological characteristics was completed. And we found that high expression of SYPL2 was significantly associated with LNM and worse prognosis. And we verified the results by experiment. In addition, we analyzed the correlation between SYPL2 expression and the expression and mutation of target genes.

Research objectives

This study aimed to investigate the SYPL2 expression, potential biological functions and pathways, correlation clinicopathological characteristics and prognosis in CRC.

Research methods

The gene expression profiles and associated clinicopathological data of patients with CRC were downloaded from multiple public and online databases {The Cancer Genome Atlas, GEO, Gene Expression Profiling Interactive Analysis [gene set enrichment analysis (GSEA)]}. The associations between clinical variables, prognosis and SYPL2 expression were analyzed statistically using the Kaplan-Meier method, univariate/multivariate Cox regression analyses, chi-squared and Fisher's exact tests. In addition, we collected 20 paired CRC tissue and adjacent normal colorectal tissue samples for validation by quantitative real-time polymerase chain reaction (qRT-PCR). GSEA was performed to evaluate the biofunction and pathways of SYPL2 in CRC.

Research results

SYPL2 expression was significantly lower in CRC tissue samples than in normal colorectal tissue samples. High SYPL2 levels in CRC tissues correlated significantly with LNM and worse prognosis. High SYPL2 expression was an independent risk factor for overall survival in both univariate and multivariate Cox regression analyses. SYPL2 expression correlated significantly with the expression of KDR and high SYPL2 expression was correlate with the response to bevacizumab treatment. Higher SYPL2 expression was associated with the enrichment of CD8 T-cells and M0 macrophages. GSEA

revealed that SYPL2 was associated with the regulation of epithelial cell migration, vasculature development, pathways in cancer, and several vital tumor-related pathways.

Research conclusions

SYPL2 expression was lower in CRC than in adjacent normal tissue. However, high SYPL2 expression was significantly associated with lymph node metastases and poorer survival.

Research perspectives

The SYPL2 gene expression and the correlations between clinical variables, prognosis were analyzed by multiple public and online databases. Furthermore, we collected 20 paired CRC tissue and adjacent normal colorectal tissue samples for validation by qRT-PCR.

FOOTNOTES

Author contributions: Zhao ZX and Liu QL collected data and completed the manuscript; Yuan Y collected relevant reference and completed a part of experiment; Wang FS designed the study and assisted in writing the manuscript; and all authors read and approved the final manuscript.

Institutional review board statement: The study was reviewed and approved for publication by our Institutional Reviewer.

Informed consent statement: All study participants or their legal guardian provided informed written consent about personal and medical data collection prior to study enrolment.

Conflict-of-interest statement: All the authors report no relevant conflicts of interest for this article.

Data sharing statement: The original anonymous dataset is available on request from the corresponding author at 461901580@qq.com.

Country/Territory of origin: China

ORCID number: Zong-Xian Zhao 0000-0001-7553-2085.

S-Editor: Wang JJ
L-Editor: A
P-Editor: Wang JJ

REFERENCES

1 **Siegel RL**, Miller KD, Fuchs HE, Jemal A. Cancer statistics, 2022. *CA Cancer J Clin* 2022; **72**: 7-33 [PMID: 35020204 DOI: 10.3322/caac.21708]
2 **Siegel RL**, Miller KD, Goding Sauer A, Fedewa SA, Butterly LF, Anderson JC, Cercek A, Smith RA, Jemal A. Colorectal cancer statistics, 2020. *CA Cancer J Clin* 2020; **70**: 145-164 [PMID: 32133645 DOI: 10.3322/caac.21601]
3 **Brenner H**, Kloor M, Pox CP. Colorectal cancer. *Lancet* 2014; **383**: 1490-1502 [PMID: 24225001 DOI: 10.1016/S0140-6736(13)61649-9]
4 **Provenzale D**, Ness RM, Llor X, Weiss JM, Abbadessa B, Cooper G, Early DS, Friedman M, Giardiello FM, Glaser K, Gurudu S, Halverson AL, Issaka R, Jain R, Kanth P, Kidambi T, Lazenby AJ, Maguire L, Markowitz AJ, May FP, Mayer RJ, Mehta S, Patel S, Peter S, Stanich PP, Terdiman J, Keller J, Dwyer MA, Ogba N. NCCN Guidelines Insights: Colorectal Cancer Screening, Version 2.2020. *J Natl Compr Canc Netw* 2020; **18**: 1312-1320 [PMID: 33022639 DOI: 10.6004/jnccn.2020.0048]
5 **Benson AB**, Venook AP, Al-Hawary MM, Arain MA, Chen YJ, Ciombor KK, Cohen S, Cooper HS, Deming D, Garrido-Laguna I, Grem JL, Gunn A, Hoffe S, Hubbard J, Hunt S, Kirilcuk N, Krishnamurthi S, Messersmith WA, Meyerhardt J, Miller ED, Mulcahy MF, Nurkin S, Overman MJ, Parikh A, Patel H, Pedersen K, Saltz L, Schneider C, Shibata D, Skibber JM, Sofocleous CT, Stoffel EM, Stotsky-Himelfarb E, Willett CG, Johnson-Chilla A, Gurski LA. NCCN Guidelines Insights: Rectal Cancer, Version 6.2020. *J Natl Compr Canc Netw* 2020; **18**: 806-815 [PMID: 32634771 DOI: 10.6004/jnccn.2020.0032]
6 **Benson AB**, Venook AP, Al-Hawary MM, Arain MA, Chen YJ, Ciombor KK, Cohen S, Cooper HS, Deming D, Farkas L, Garrido-Laguna I, Grem JL, Gunn A, Hecht JR, Hoffe S, Hubbard J, Hunt S, Johung KL, Kirilcuk N, Krishnamurthi S,

Messersmith WA, Meyerhardt J, Miller ED, Mulcahy MF, Nurkin S, Overman MJ, Parikh A, Patel H, Pedersen K, Saltz L, Schneider C, Shibata D, Skibber JM, Sofocleous CT, Stoffel EM, Stotsky-Himelfarb E, Willett CG, Gregory KM, Gurski LA. Colon Cancer, Version 2.2021, NCCN Clinical Practice Guidelines in Oncology. *J Natl Compr Canc Netw* 2021; **19**: 329-359 [PMID: 33724754 DOI: 10.6004/jnccn.2021.0012]

7 **Argilés G**, Tabernero J, Labianca R, Hochhauser D, Salazar R, Iveson T, Laurent-Puig P, Quirke P, Yoshino T, Taieb J, Martinelli E, Arnold D; ESMO Guidelines Committee. Localised colon cancer: ESMO Clinical Practice Guidelines for diagnosis, treatment and follow-up. *Ann Oncol* 2020; **31**: 1291-1305 [PMID: 32702383 DOI: 10.1016/j.annonc.2020.06.022]

8 **Glynne-Jones R**, Wyrwicz L, Tiret E, Brown G, Rödel C, Cervantes A, Arnold D; ESMO Guidelines Committee. Rectal cancer: ESMO Clinical Practice Guidelines for diagnosis, treatment and follow-up. *Ann Oncol* 2017; **28**: iv22-iv40 [PMID: 28881920 DOI: 10.1093/annonc/mdx224]

9 **Hashiguchi Y**, Muro K, Saito Y, Ito Y, Ajioka Y, Hamaguchi T, Hasegawa K, Hotta K, Ishida H, Ishiguro M, Ishihara S, Kanemitsu Y, Kinugasa Y, Murofushi K, Nakajima TE, Oka S, Tanaka T, Taniguchi H, Tsuji A, Uehara K, Ueno H, Yamanaka T, Yamazaki K, Yoshida M, Yoshino T, Itabashi M, Sakamaki K, Sano K, Shimada Y, Tanaka S, Uetake H, Yamaguchi S, Yamaguchi N, Kobayashi H, Matsuda K, Kotake K, Sugihara K; Japanese Society for Cancer of the Colon and Rectum. Japanese Society for Cancer of the Colon and Rectum (JSCCR) guidelines 2019 for the treatment of colorectal cancer. *Int J Clin Oncol* 2020; **25**: 1-42 [PMID: 31203527 DOI: 10.1007/s10147-019-01485-z]

10 **Li M**, Zhang J, Dan Y, Yao Y, Dai W, Cai G, Yang G, Tong T. A clinical-radiomics nomogram for the preoperative prediction of lymph node metastasis in colorectal cancer. *J Transl Med* 2020; **18**: 46 [PMID: 32000813 DOI: 10.1186/s12967-020-02215-0]

11 **Yang L**, Liu D, Fang X, Wang Z, Xing Y, Ma L, Wu B. Rectal cancer: can T2WI histogram of the primary tumor help predict the existence of lymph node metastasis? *Eur Radiol* 2019; **29**: 6469-6476 [PMID: 31278581 DOI: 10.1007/s00330-019-06328-z]

12 **Huang D**, Sun W, Zhou Y, Li P, Chen F, Chen H, Xia D, Xu E, Lai M, Wu Y, Zhang H. Mutations of key driver genes in colorectal cancer progression and metastasis. *Cancer Metastasis Rev* 2018; **37**: 173-187 [PMID: 29322354 DOI: 10.1007/s10555-017-9726-5]

13 **Yang C**, Cao F, Huang S, Zheng Y. Follistatin-Like 3 Correlates With Lymph Node Metastasis and Serves as a Biomarker of Extracellular Matrix Remodeling in Colorectal Cancer. *Front Immunol* 2021; **12**: 717505 [PMID: 34335633 DOI: 10.3389/fimmu.2021.717505]

14 **Biller LH**, Schrag D. Diagnosis and Treatment of Metastatic Colorectal Cancer: A Review. *JAMA* 2021; **325**: 669-685 [PMID: 33591350 DOI: 10.1001/jama.2021.0106]

15 **Piawah S**, Venook AP. Targeted therapy for colorectal cancer metastases: A review of current methods of molecularly targeted therapy and the use of tumor biomarkers in the treatment of metastatic colorectal cancer. *Cancer* 2019; **125**: 4139-4147 [PMID: 31433498 DOI: 10.1002/cncr.32163]

16 **Ciavarella S**, Vegliante MC, Fabbri M, De Summa S, Melle F, Motta G, De Iuliis V, Opinto G, Enjuanes A, Rega S, Gulino A, Agostinelli C, Scattone A, Tommasi S, Mangia A, Mele F, Simone G, Zito AF, Ingravallo G, Vitolo U, Chiappella A, Tarella C, Gianni AM, Rambaldi A, Zinzani PL, Casadei B, Derenzini E, Loseto G, Pileri A, Tabanelli V, Fiori S, Rivas-Delgado A, López-Guillermo A, Venesio T, Sapino A, Campo E, Tripodo C, Guarini A, Pileri SA. Dissection of DLBCL microenvironment provides a gene expression-based predictor of survival applicable to formalin-fixed paraffin-embedded tissue. *Ann Oncol* 2018; **29**: 2363-2370 [PMID: 30307529 DOI: 10.1093/annonc/mdy450]

17 **Verstraete M**, Debucquoy A, Dekervel J, van Pelt J, Verslype C, Devos E, Chiritescu G, Dumon K, D'Hoore A, Gevaert O, Sagaert X, Van Cutsem E, Haustermans K. Combining bevacizumab and chemoradiation in rectal cancer. Translational results of the AXEBeam trial. *Br J Cancer* 2015; **112**: 1314-1325 [PMID: 25867261 DOI: 10.1038/bjc.2015.93]

18 **Windoffer R**, Borchert-Stuhlträger M, Haass NK, Thomas S, Hergt M, Bulitta CJ, Leube RE. Tissue expression of the vesicle protein pantophysin. *Cell Tissue Res* 1999; **296**: 499-510 [PMID: 10370136 DOI: 10.1007/s004410051310]

19 **Chen DH**, Wu QW, Li XD, Wang SJ, Zhang ZM. SYPL1 overexpression predicts poor prognosis of hepatocellular carcinoma and associates with epithelial-mesenchymal transition. *Oncol Rep* 2017; **38**: 1533-1542 [PMID: 28731154 DOI: 10.3892/or.2017.5843]

20 **Song Y**, Sun X, Duan F, He C, Wu J, Huang X, Xing K, Sun S, Wang R, Xie F, Mao Y, Wang J, Li S. SYPL1 Inhibits Apoptosis in Pancreatic Ductal Adenocarcinoma *via* Suppression of ROS-Induced ERK Activation. *Front Oncol* 2020; **10**: 1482 [PMID: 33042794 DOI: 10.3389/fonc.2020.01482]

21 **Liu L**, He Q, Li Y, Zhang B, Sun X, Shan J, Pan B, Zhang T, Zhao Z, Song X, Guo Y. Serum SYPL1 is a promising diagnostic biomarker for colorectal cancer. *Clin Chim Acta* 2020; **509**: 36-42 [PMID: 32502495 DOI: 10.1016/j.cca.2020.05.048]

22 **Kurebayashi N**, Takeshima H, Nishi M, Murayama T, Suzuki E, Ogawa Y. Changes in Ca2+ handling in adult MG29-deficient skeletal muscle. *Biochem Biophys Res Commun* 2003; **310**: 1266-1272 [PMID: 14559251 DOI: 10.1016/j.bbrc.2003.09.146]

23 **Pan Z**, Yang D, Nagaraj RY, Nosek TA, Nishi M, Takeshima H, Cheng H, Ma J. Dysfunction of store-operated calcium channel in muscle cells lacking mg29. *Nat Cell Biol* 2002; **4**: 379-383 [PMID: 11988740 DOI: 10.1038/ncb788]

24 **Carvalho B**, Lopes JM, Silva R, Peixoto J, Leitão D, Soares P, Fernandes AC, Linhares P, Vaz R, Lima J. The role of c-Met and VEGFR2 in glioblastoma resistance to bevacizumab. *Sci Rep* 2021; **11**: 6067 [PMID: 33727583 DOI: 10.1038/s41598-021-85385-1]

25 **Szablewski V**, Solassol J, Poizat F, Larrieux M, Crampette L, Mange A, Bascoul-Mollevi C, Costes V. EGFR Expression and KRAS and BRAF Mutational Status in Intestinal-Type Sinonasal Adenocarcinoma. *Int J Mol Sci* 2013; **14**: 5170-5181 [PMID: 23459231 DOI: 10.3390/ijms14035170]

26 **Khotskaya YB**, Holla VR, Farago AF, Mills Shaw KR, Meric-Bernstam F, Hong DS. Targeting TRK family proteins in cancer. *Pharmacol Ther* 2017; **173**: 58-66 [PMID: 28174090 DOI: 10.1016/j.pharmthera.2017.02.006]

27 **Grothey A**, Fakih M, Tabernero J. Management of BRAF-mutant metastatic colorectal cancer: a review of treatment options and evidence-based guidelines. *Ann Oncol* 2021; **32**: 959-967 [PMID: 33836264 DOI:

10.1016/j.annonc.2021.03.206]

28 **Wang C**, Li Y, Jia L, Kim JK, Li J, Deng P, Zhang W, Krebsbach PH, Wang CY. CD276 expression enables squamous cell carcinoma stem cells to evade immune surveillance. *Cell Stem Cell* 2021; **28**: 1597-1613.e7 [PMID: 33945793 DOI: 10.1016/j.stem.2021.04.011]

29 **Derynck R**, Turley SJ, Akhurst RJ. TGFβ biology in cancer progression and immunotherapy. *Nat Rev Clin Oncol* 2021; **18**: 9-34 [PMID: 32710082 DOI: 10.1038/s41571-020-0403-1]

30 **Hernández Borrero LJ**, El-Deiry WS. Tumor suppressor p53: Biology, signaling pathways, and therapeutic targeting. *Biochim Biophys Acta Rev Cancer* 2021; **1876**: 188556 [PMID: 33932560 DOI: 10.1016/j.bbcan.2021.188556]

31 **Li B**, Severson E, Pignon JC, Zhao H, Li T, Novak J, Jiang P, Shen H, Aster JC, Rodig S, Signoretti S, Liu JS, Liu XS. Comprehensive analyses of tumor immunity: implications for cancer immunotherapy. *Genome Biol* 2016; **17**: 174 [PMID: 27549193 DOI: 10.1186/s13059-016-1028-7]

32 **St Paul M**, Ohashi PS. The Roles of $CD8^+$ T Cell Subsets in Antitumor Immunity. *Trends Cell Biol* 2020; **30**: 695-704 [PMID: 32624246 DOI: 10.1016/j.tcb.2020.06.003]

33 **Mami-Chouaib F**, Blanc C, Corgnac S, Hans S, Malenica I, Granier C, Tihy I, Tartour E. Resident memory T cells, critical components in tumor immunology. *J Immunother Cancer* 2018; **6**: 87 [PMID: 30180905 DOI: 10.1186/s40425-018-0399-6]

World Journal of Gastrointestinal Oncology

Submit a Manuscript: https://www.f6publishing.com

World J Gastrointest Oncol 2022 November 15; 14(11): 2138-2156

DOI: 10.4251/wjgo.v14.i11.2138

ISSN 1948-5204 (online)

ORIGINAL ARTICLE

Basic Study

Comprehensive analysis of the potential role and prognostic value of sine oculis homeobox homolog family in colorectal cancer

Ze-Xuan Fang, Chun-Lan Li, Zheng Wu, Yan-Yu Hou, Hua-Tao Wu, Jing Liu

Specialty type: Oncology

Provenance and peer review: Invited article; Externally peer reviewed.

Peer-review model: Single blind

Peer-review report's scientific quality classification

Grade A (Excellent): 0
Grade B (Very good): B
Grade C (Good): C, C, C
Grade D (Fair): D
Grade E (Poor): 0

P-Reviewer: Brkanović S, Croatia; Janmohammadi P, Iran; Jeong KY, South Korea

Received: July 9, 2022
Peer-review started: July 9, 2022
First decision: July 31, 2022
Revised: August 30, 2022
Accepted: October 31, 2022
Article in press: October 31, 2022
Published online: November 15, 2022

Ze-Xuan Fang, Chun-Lan Li, Zheng Wu, Yan-Yu Hou, Jing Liu, Guangdong Provincial Key Laboratory for Diagnosis and Treatment of Breast Cancer, Cancer Hospital of Shantou University Medical College, Shantou 515041, Guangdong Province, China

Hua-Tao Wu, Department of General Surgery, The First Affiliated Hospital of Shantou University Medical College, Shantou 515041, Guangdong Province, China

Corresponding author: Jing Liu, MD, PhD, Academic Research, Associate Professor, Research Scientist, Senior Scientist, Guangdong Provincial Key Laboratory for Diagnosis and Treatment of Breast Cancer, Cancer Hospital of Shantou University Medical College, No. 22 Xinling Road, Shantou 515041, Guangdong Province, China. jliu12@stu.edu.cn

Abstract

BACKGROUND

Several genes, important for development, are reduced or silenced in adulthood, and their abnormal expression has been related to the occurrence and development of malignant tumors. Human sine oculis homeobox homolog (SIX) proteins belong to the homeobox family and play important roles in the development of different organs. Importantly, SIXs are predicted to have chromatin-binding and DNA-binding transcription factor activity with reported roles in cancers. However, a comprehensive analysis of SIXs in colorectal cancers (CRCs) has not been performed.

AIM

To explore the expression pattern of six SIX proteins in CRCs and their relationship with the clinicopathological parameters of CRC patients as well as investigate the potential utilization of SIXs as novel prognostic indicators in CRCs.

METHODS

The expression level of SIXs in normal tissues of different organs and related cancerous tissues was analyzed in the Human Protein Atlas. Kaplan-Meier Plotter and GEPIA2 were used to analyze the prognostic values of SIXs. To analyze the potential signaling pathways with SIX family involvement, LinkedOmics was used to perform Gene Ontology and Kyoto Encyclopedia of Genes and Genomes analyses of SIX4-related genes. Subsequently, immunohistochemical experiments were performed on CRC tissues and adjacent normal tissues, and we examined the SIX4 expression level in 87 pairs of patients with tissue microarray. The relationship between SIX4 and clinicopathological parameters in CRC patients

was tested using the χ^2 test and Fisher's exact probability to verify the results of the database analysis.

RESULTS

The RNA levels of *SIX1-4* and *SIX6* were relatively low in normal human tissues, while SIX5 was highly expressed at both the RNA and protein levels. However, the protein level of SIX4 was found to be elevated in various malignancies. In CRC tissues, SIX1, SIX2 and SIX4 were elevated in cancer tissues compared with adjacent normal tissue. Among all SIXs, a high level of SIX4 was found to be associated with poor overall and disease-free survival in patients with CRC. For different clinicopathological parameters, increased SIX4 expression was positively correlated with advanced CRC. The top 50 SIX4-related genes were involved with oxidative phosphorylation and the respiratory chain signaling pathways.

CONCLUSION

The current results provided a comprehensive analysis of the expression and prognostic values of SIX family members in CRC. Among different SIXs, SIX4 plays an oncogenic role in CRC to promote the development of malignancy. In CRC, SIX4 mRNA and protein expression is higher than that in normal tissues and associated with shorter CRC patient survival, suggesting that SIX4 may be a potential therapeutic target for treatment of CRC patients.

Key Words: Sine oculis homeobox homolog; Colorectal cancer; Development; Treatment; Expression; Prognostic indicator

Core Tip: This study systematically analyzed the expression pattern and prognostic value of sine oculis homeobox homolog (SIX) family members in colorectal cancer (CRC). It was found that the expression of SIX4 in CRC tissues positively correlated with the development of CRC and negatively correlated with overall survival. The top 50 SIX4-related genes were involved with oxidative phosphorylation and the respiratory chain signaling pathways. SIX4 may be a novel and potential therapeutic target for CRC.

Citation: Fang ZX, Li CL, Wu Z, Hou YY, Wu HT, Liu J. Comprehensive analysis of the potential role and prognostic value of sine oculis homeobox homolog family in colorectal cancer. *World J Gastrointest Oncol* 2022; 14(11): 2138-2156

URL: https://www.wjgnet.com/1948-5204/full/v14/i11/2138.htm

DOI: https://dx.doi.org/10.4251/wjgo.v14.i11.2138

INTRODUCTION

Although the study of early human development is limited due to the small number of samples, it is well known how the genome activates or silences transcriptional programs to govern organ formation [1]. Gerrard *et al*[2] focused on histone modifications during human organogenesis and found that key developmental gene sets are actively repressed outside of the appropriate organ. Interestingly, the abnormal expression of organogenesis-related genes at inappropriate developmental stages has been reported in different diseases, especially malignant tumors[3].

Human sine oculis homeobox homolog (SIX) proteins comprise a group of six family members that act as key regulators of organogenesis in the kidney, limbs, eye, brain and craniofacial structure[4-7]. Defects in these genes result in hypoplastic disorders, such as autosomal dominant deafness type 23, branchiootic syndrome type 3, holoprosencephaly type 2, branchiootorenal syndrome type 2 and isolated microphthalmia with cataract type 2[8-12].

Colorectal cancer (CRC) is ranked third in incidence among malignant tumors worldwide and is the second leading cause of cancer-related mortality[13]. In China, the annual average increase of new CRC cases has been estimated to be 4.2%[14]. Although sex and regional differences are reported to be the prognostic factors for CRC patients[15], the etiology of CRC oncogenesis and development is still complex and unclear. The high mortality of patients with CRC and the limitations of the traditional tumor-node-metastasis staging emphasize the need to explore key genes closely associated with CRC development and prognosis[16].

Unsurprisingly, abnormal SIX levels have been reported to participate in the regulation of human cancers. Several studies report that mutations or aberrant expression of the SIX family play an important

role in colorectal tumorigenesis through multiple processes, such as transformation, proliferation, angiogenesis, migration and metastasis[17-19]. Song *et al*[20] showed that SIX1 was highly expressed in CRC patients who have short overall survival (OS) and enhances proliferation and migration of CRC cells through activation of Wnt/β-catenin signaling. Human SIX2 levels are higher in non-metastatic CRC, and targeting this gene can modulate CRC metastasis and immunity, thereby improving the survival of CRC patients[18]. In glioblastoma, where SIX3 is transcriptionally silenced by DNA hypermethylation, SIX3 functions as a tumor suppressor[21], and SIX4 promotes development and progression in CRC through the PI3K-AKT signaling pathways[17]. SIX5 is an important paralog of SIX4 and promotes lung adenocarcinoma progression through transcriptional activation of LINC01468 and its downstream pathways[22], and SIX5 cooperates with hypoxia-induced EYA3 and P3000 to mediate tumorigenesis and cancer progression[19]. However, SIX6 is poorly studied in CRC than in other tumor types. Hence, the current study conducted a comprehensive evaluation of the potential roles of SIX family members and provided novel therapeutic targets for further investigation.

MATERIALS AND METHODS

The expression levels of SIXs in normal tissues and different types of cancers

The Human Protein Atlas (HPA) (https://www.proteinatlas.org/), a rich resource database with more than 5000 types of human protein expression data and high-definition images of human normal and cancerous cells[23], was used to obtain and analyze the mRNA and protein levels of SIX family members in normal tissues and different types of cancers. RNA expression levels were evaluated using consensus normalized expression (NX) combined with three transcriptome datasets (HPA, GTEx and FANTOM5), as described before[24]. RNA expression was divided into four levels: Not detected (NX < 1), low expression (1 ≤ NX < 15), medium expression (15 ≤ NX < 30) and high expression (NX ≥ 30)[24]. Similarly, protein expression was also categorized into four groups: Negative (-), low expression (+), medium expression (++) and high expression (+++). The Cancer Genome Atlas (TCGA) datasets were evaluated through the Tumor Immune Estimation Resource 2.0 online resource (http://timer.cistrome.org/) for pan-cancer analysis[25] and the UCSC Xena database (https://genome-cancer.ucsc.edu/)[26] for colon and rectal adenocarcinomas and related normal tissues.

The prognostic values of SIXs in patients with CRC

Kaplan-Meier Plotter (http://kmplot.com/analysis/), a dataset containing gene expression and survival of cancer patients[27], was assessed for the prognostic value regarding OS of SIXs in patients with CRC. For disease-free survival (DFS) analysis, GEPIA2 (http://gepia2.cancerpku.cn/) information, containing 9736 tumors and 8587 normal samples[28], was used to detect the correlation between SIX levels and DFS in CRC patients.

Signaling pathways involving SIX4

LinkedOmics (http://www.linkedomics.org), a multi-omics dataset that includes data from 32 TCGA tumor types and 10 clinical proteomic tumor analysis cohorts[29], was used to predict potential SIX4-related genes and explore their related signaling pathways through the Kyoto Encyclopedia of Genes and Genomes (KEGG) and Gene Ontology (GO) analyses. The LinkFinder module in the LinkedOmics dataset was applied to analyze the correlation between the expression level of SIX4 and clinicopathological parameters of CRC patients.

Patient information and ethics statement

A tissue microarray with 87 matched primary colon cancer tissues and their corresponding adjacent normal colon tissue samples and 6 extra samples of cancer cases were purchased from the Shanghai OUTDO Biotech Company (Shanghai, China). This study was approved by the Ethics Committee of Shantou University Medical college (SUMC-2022-045).

Immunohistochemistry

Immunohistochemical staining of SIX4 was performed as described previously[30]. Deparaffinization in xylene, hydration in graded alcohols and epitope retrieval by microwaving in EDTA (Fuzhou Maixin Biotechnology Development Co. LTD, Fuzhou, China) was conducted sequentially on the tissue microarray slide. After blocking endogenous peroxidase with 3% H_2O_2, the slide was incubated with anti-SIX4 antibody (dilution: 1:400, bs-17503R, Bioss, China,) at 4 °C overnight. Stained tissues were mounted by nuclear counterstaining with hematoxylin for visualization.

The sections were visualized and evaluated independently under a bright-field microscope (PerkinElmer Vectra, PerkinElmer, United States) by two investigators with no prior knowledge of the patient information. For evaluating SIX4 expression, the staining intensities with colorless, light yellow, brown yellow and dark brown were labeled as 0, 1, 2 and 3, respectively, while the percentage of positive cells corresponding to 0%, 1%-25%, 26%-50%, 51%-75% and 76%-100% were recorded as 0, 1, 2,

Table 1 Expression levels of sine oculis homeobox homolog family members in human normal tissues

Organs	SIX1		SIX2		SIX3		SIX4		SIX5		SIX6	
	RNA	Protein	RNA	Protein	RNA	Protein	RNA	Protein	RNA	Protein	RNA	Protein
Cerebral cortex	+	-	+	NE	++	NE	+	NE	+	+	-	-
Thyroid gland	+	-	+	NE	-	NE	+	NE	++	++	-	-
Lung	+	-	+	NE	-	NE	+	NE	+	-	-	-
Esophagus	+	-	+	NE	-	NE	+	NE	+	+	-	-
Stomach	+	-	+	NE	-	NE	+	NE	++	++	-	-
Colon/rectum	-	-	+	NE	-	NE	+	NE	+++	++	-	-
Liver	-	-	-	NE	-	NE	+	NE	++	++	-	-
Pancreas	+	+	+	NE	+	NE	+	NE	+++	+	-	-
Kidney	-	-	+	NE	+	NE	+	NE	++	++	-	-
Urinary bladder	+	+	+	NE	-	NE	+	NE	++	++	-	-
Testis	+	++	+	NE	+	NE	+	NE	+	++	+	-
Prostate	+	++	+	NE	-	NE	+	NE	+++	++	-	-
Ovary	+	-	+	NE	-	NE	+	NE	+++	-	-	-
Endometrium	-	-	+	NE	-	NE	+	NE	+++	++	-	-
Uterine cervix	+	+++	+	NE	+	NE	+	NE	+++	-	-	-
Breast	+	-	+	NE	+	NE	+	NE	++	++	-	-
Skin	-	-	+	NE	-	NE	+	NE	+	-	-	-
Lymph node	+	-	+	NE	+	NE	-	NE	+	-	-	-
Bone marrow	-	-	-	NE	-	NE	+	NE	+	-	-	-

-: Not detected; +: Low levels; ++: Medium levels; +++: High levels; NE: Not examined; SIX: Sine oculis homeobox homolog.

3 and 4, respectively. The final staining score for SIX4 expression was calculated as the sum of staining intensity and percentage of positive cells and divided into low (0-4) and high (5-7) expression groups.

Statistical analyses

SPSS 25.0 statistical software was used to do the statistical analyses. The relationship between expression levels of SIX4 in 87 paired CRC and paracancerous tissues was performed using the χ^2 test. A total of 93 case numbers from the tissue microarrays were recruited to analyze the relationship between SIX4 and clinicopathological parameters of CRC patients using the χ^2 or Fisher's exact probability test. To investigate the prognostic value of SIX4 in CRC patients, the Kaplan-Meier survival curve and log-rank test were used. The difference was considered statistically significant at $P < 0.05$.

RESULTS

Expression of SIXs in normal tissues

As shown in Table 1, the results from the HPA database revealed that in normal tissues, SIX1-4 and SIX6 were expressed at relatively low levels, except for SIX1 in the testis, prostate and uterine cervix. SIX5 RNA and protein were highly expressed in the thyroid gland, stomach, colon/rectum, kidney, urinary bladder, prostate, endometrium and breast tissues. The protein levels of SIX2-4 have yet to be examined.

Expression of SIXs in different types of malignant tumors

To explore the different expression patterns of SIXs in normal and malignant tissues, the expression levels of SIXs in different types of malignant tumors was collected from the HPA (Table 2). Interestingly, the levels of SIX1-3 and SIX6 were still relatively low in different types of cancers, except for SIX1 in prostate, cervix uterine and breast cancers. It was found that the RNA levels of *SIX5* were low, but the protein levels of SIX5 were quite high in cancers of the thyroid gland, prostate, ovary and breast and moderately in cancers of the colon/rectum, liver and endometrium. Although there is still no data on

Table 2 Expression levels of sine oculis homeobox homolog family members in different types of malignant tumors

Organs	SIX1		SIX2		SIX3		SIX4		SIX5		SIX6	
	RNA	Protein	RNA	Protein	RNA	Protein	RNA	Protein	RNA	Protein	RNA	Protein
Cerebral cortex	-	-	-	NE	-	NE	-	-	-	-	-	-
Thyroid gland	+	-	+	NE	+	NE	+	+++	+	+++	+	-
Lung	+	+	+	NE	+	NE	+	+	+	+	+	-
Esophagus	-	-	-	NE	-	NE	-	-		-	-	-
Stomach	-	-	+	NE	+	NE	+	-	+	+	+	-
Colon/rectum	+	-	+	NE	+	NE	+	++	+	++	+	-
Liver	+	-	+	NE	+	NE	+	++	+	++	+	-
Pancreas	+	+	+	NE	+	NE	+	+	+	++	+	-
Kidney	+	-	+	NE	+	NE	+	+	+	+	+	-
Urinary bladder	+	-	+	NE	+	NE	+	+	+	+	+	-
Testis	+	-	+	NE	+	NE	+	+	+	+	+	-
Prostate	+	++	+	NE	+	NE	+	++	+	+++	+	-
Ovary	+	-	+	NE	+	NE	+	+	+	+++	+	+
Endometrium	+	+	+	NE	+	NE	+	+	+	++	+	-
Cervix uterine	+	++	+	NE	+	NE	+	++	+	+	+	-
Breast	+	++	+	NE	+	NE	+	+++	+	+++	+	-
Skin	-	-	-	NE	-	NE	-	+++	-	-	-	-
Lymph node	-	-	-	NE	-	NE	-	+	-	-	-	-
Bone marrow	-	-	-	NE	-	NE	-	-	-	-	-	

-: Not detected; +: Low levels; ++: Medium levels; +++: High levels; NE: Not examined; SIX: Sine oculis homeobox homolog.

the protein level of SIX2 and SIX3, the protein level of SIX4 has been evaluated in a series of studies and found to be high in cancers of the thyroid gland, breast and skin, moderately in cancers of the colon/rectum, liver, prostate and uterine cervix and low in cancers of the lung, pancreas, kidney, urinary bladder, testis, ovary, endometrium and lymph node.

To confirm the above findings, the Tumor Immune Estimation Resource 2.0 with TCGA datasets was used to evaluate the expression of SIXs in different cancerous tissues and corresponding normal tissues (Figure 1). SIX1 and SIX4 were highly expressed in almost all types of cancer tissues compared with their corresponding normal tissues ($P < 0.001$), except for SIX1 in head and neck squamous cell carcinoma, kidney renal papillary cell carcinoma and thyroid carcinoma and SIX4 in kidney renal clear cell carcinoma, kidney renal papillary cell carcinoma and thyroid carcinoma. In contrast, almost no difference was found in the expression of SIX6 in cancers, except for lung adenocarcinoma and lung squamous cell carcinoma ($P < 0.05$). The expressions of SIX2, SIX3 and SIX5 were inconsistent in the different types of cancer tissues compared with their corresponding normal tissues.

SIX1, SIX2 and SIX4 were highly expressed in CRC tissues compared with normal tissues

The expression patterns of SIXs in CRC were verified with the UCSC Xena database (Figure 2). In TCGA colon and rectal cancer cohort ($n = 736$), the expression of SIX1, SIX2 and SIX4 in CRC tissues was higher than that in normal tissues ($P < 0.001$), while no significant difference was found for the levels of SIX3 and SIX6.

Prognostic value of SIXs in CRC patients

To estimate the prognostic function of SIXs in CRC patients, OS and DFS were analyzed. CRC patients with high SIX4 levels had poor OS, with hazard ratio = 2.28 (1.04-4.99), predicting a potential oncogenic role for SIX4 in CRC development (Figure 3). Although no statistical significance was found for the other SIXs, CRC patients with high SIX1 or SIX5 tended to display poor OS, and the hazard ratio was predicted to be 2.11 (0.96-4.6) and 2.54 (0.94-6.86), respectively.

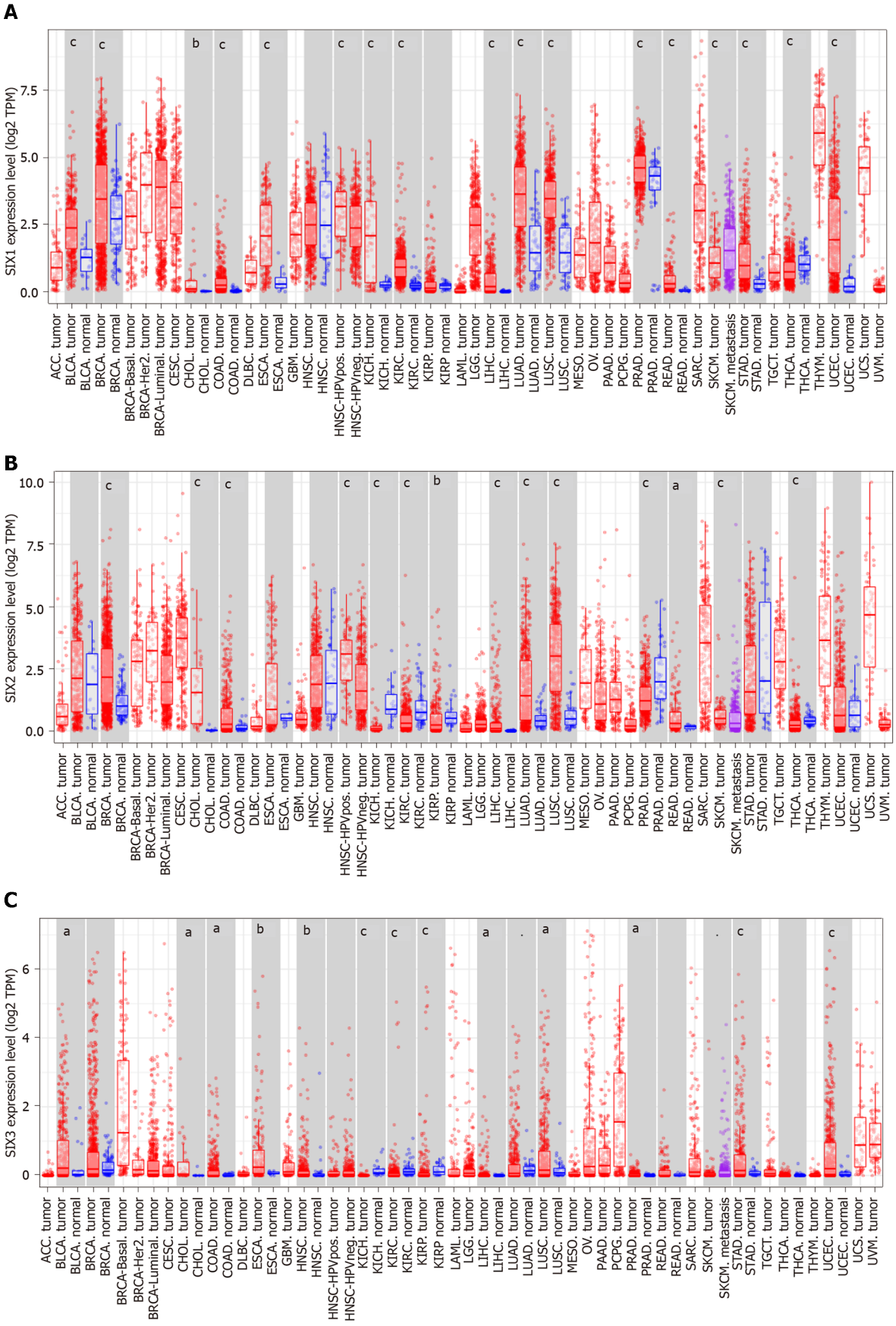
A
SIX1 expression level (log2 TPM)
B
SIX2 expression level (log2 TPM)
C
SIX3 expression level (log2 TPM)
ACC. tumor
BLCA. tumor
BLCA. normal
BRCA. tumor
BRCA. normal
BRCA-Basal. tumor
BRCA-Her2. tumor
BRCA-Luminal. tumor
CESC. tumor
CHOL. tumor
CHOL. normal
COAD. tumor
COAD. normal
DLBC. tumor
ESCA. tumor
ESCA. normal
GBM. tumor
HNSC. tumor
HNSC. normal
HNSC-HPVpos. tumor
HNSC-HPVneg. tumor
KICH. tumor
KICH. normal
KIRC. tumor
KIRC. normal
KIRP. tumor
KIRP normal
LAML. tumor
LGG. tumor
LIHC. tumor
LIHC. normal
LUAD. tumor
LUAD. normal
LUSC. tumor
LUSC. normal
MESO. tumor
OV. tumor
PAAD. tumor
PCPG. tumor
PRAD. tumor
PRAD. normal
READ. tumor
READ. normal
SARC. tumor
SKCM. tumor
SKCM. metastasis
STAD. tumor
STAD. normal
TGCT. tumor
THCA. tumor
THCA. normal
THYM. tumor
UCEC. tumor
UCEC. normal
UCS. tumor
UVM. tumor

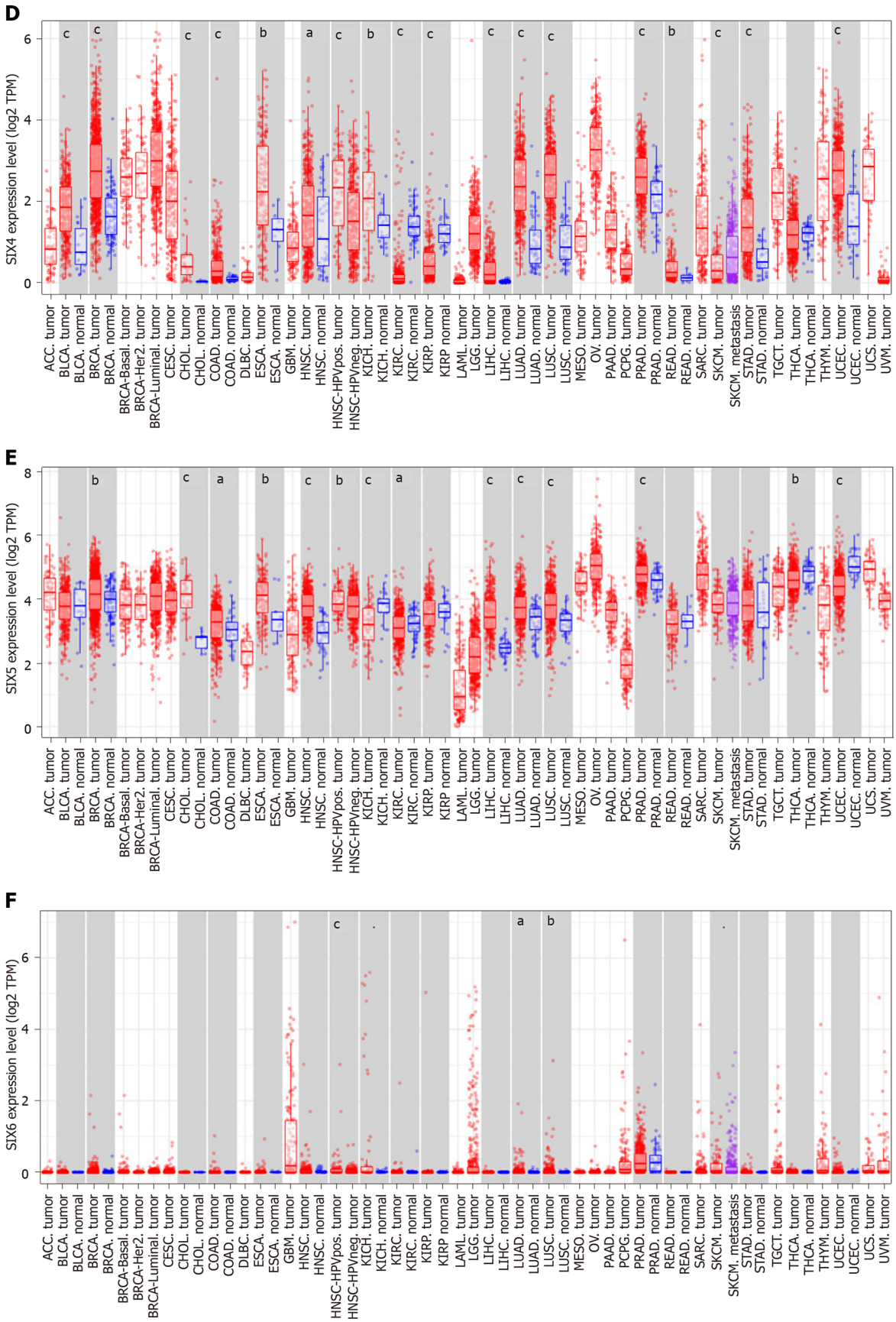

DOI: 10.4251/wjgo.v14.i11.2138

Figure 1 Sine oculis homeobox homologs in different cancerous tissues and corresponding normal tissues in the Tumor Immune Estimation Resource 2.0 database. A: Sine oculis homeobox homolog (SIX)1; B: SIX2; C: SIX3; D: SIX4; E: SIX5; F: SIX6. [a]*P* < 0.05, [b]*P* < 0.01, [c]*P* < 0.001. SIX: Sine oculis homeobox homolog; TPM: Transcript count per million.

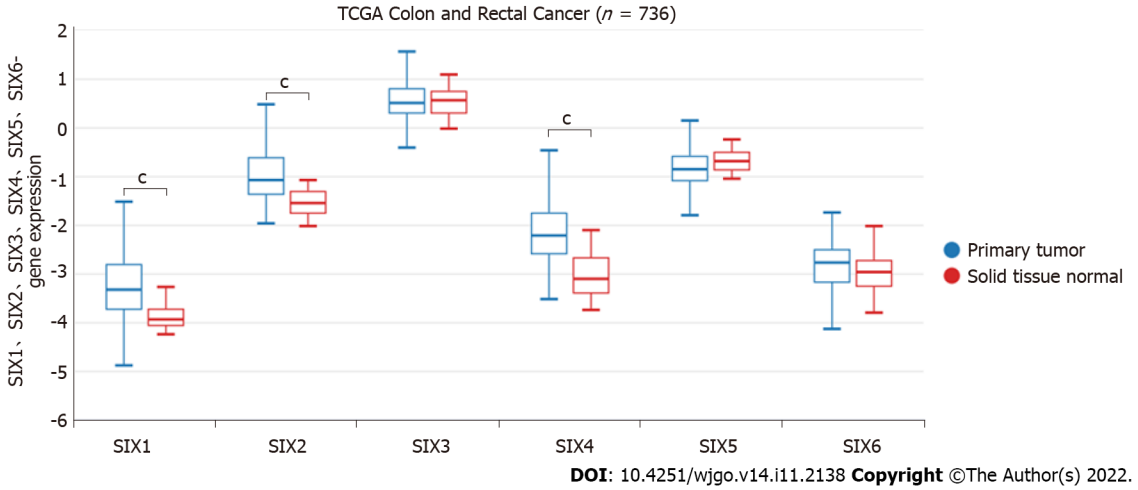

DOI: 10.4251/wjgo.v14.i11.2138 **Copyright** ©The Author(s) 2022.

Figure 2 Expression of sine oculis homeobox homolog family members in The Cancer Genome Atlas colon and rectal cancer tissues in the UCSC Xena database. Red: Normal tissue; Blue: Cancerous tissue. One-way analysis of variance was utilized for statistical significance. °P < 0.001. SIX: Sine oculis homeobox homolog; TCGA: The Cancer Genome Atlas.

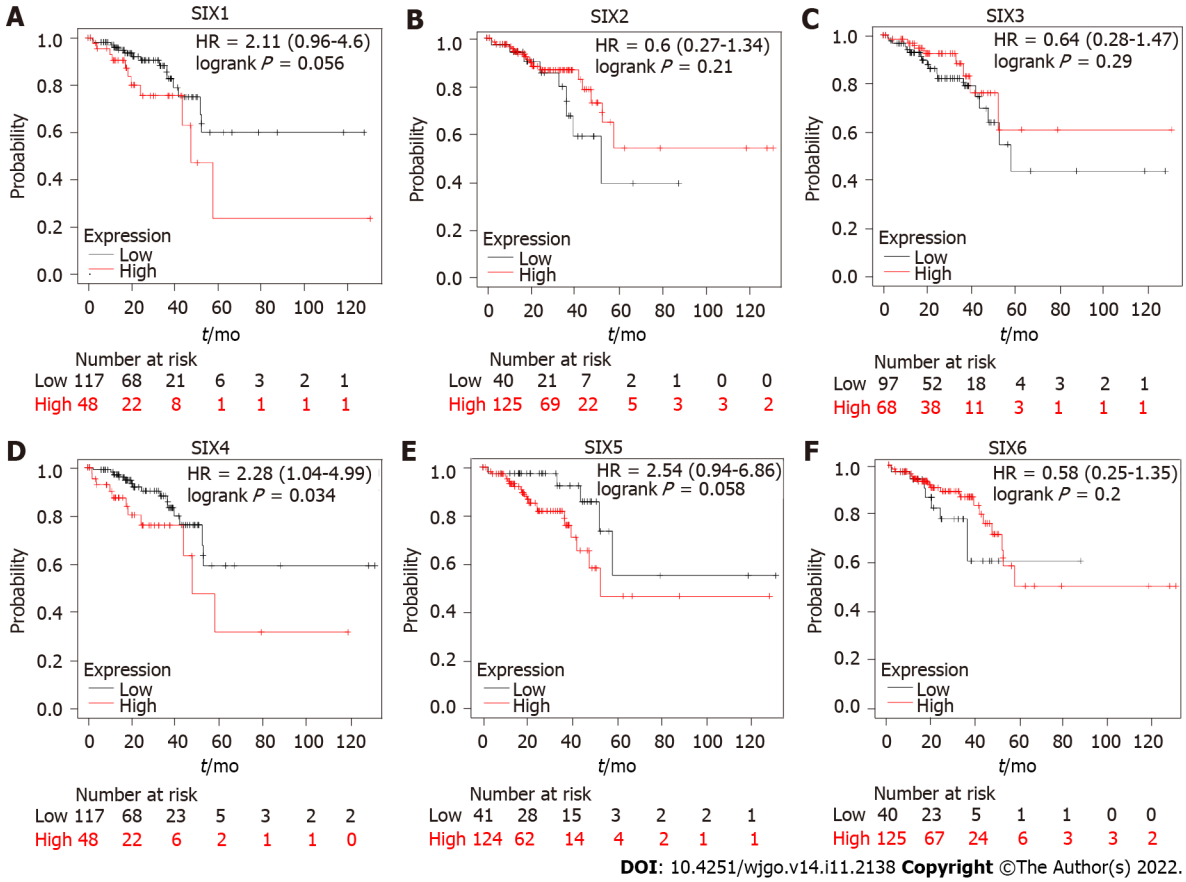

DOI: 10.4251/wjgo.v14.i11.2138 **Copyright** ©The Author(s) 2022.

Figure 3 Overall survival of colorectal cancer patients estimated by individual expression of sine oculis homeobox homolog family members. A: Sine oculis homeobox homolog (SIX)1; B: SIX2; C: SIX3; D: SIX4; E: SIX5; F: SIX6. HR: Hazard ratio; SIX: Sine oculis homeobox homolog.

As shown in Figure 4, only the SIX4 expression level was found to be associated with progression of CRC. High levels of SIX4 in CRC patients predicted short DFS, indicating that the expression of SIX4 might promote the recurrence or relapse of CRC. Interestingly, CRC patients with high SIX1 or SIX5 also tended to have short DFS but were without statistical significance. As of now, no results have been collected for SIX6.

Table 3 The etiological and demographic information of colorectal cancer patients

Characteristic	
Patients, *n* (M/F)	93 (44/49)
Type of tumor (colon tumor/others)	93 (93/0)
age in yr, mean ± SD (range)	67.7 ± 9.8 (43-90)
Histologic type, *n* (carcinoma/adjacent)	93 (93/87)
Pathological stage, *n* (I/II/III)	93 (1/77/15)
Primary tumor, *n* (T1/T2/T3/T4)[1]	92 (1/4/70/15)
Lymph node status, *n* (N0/N1/N2)	93 (58/26/9)
Survival state, *n* (life/death)	93 (48/45)

[1]One patient with an undetected primary tumor was excluded.
F: Female; M: Male; SD: Standard deviation.

Table 4 Expression of sine oculis homeobox homolog 4 in colorectal cancer tissues and paired adjacent tissue

Tissue type	*n*	Low (%)	High (%)	χ^2	*P* value
Adjacent tissues	87	60 (69.0)	27 (31.0)	22.10	< 0.0001
CRC tissues	87	29 (33.3)	58 (66.7)		

CRC: Colorectal cancer.

Table 5 Relationship between the expression of sine oculis homeobox homolog 4 and clinicopathological parameters of colon cancer patients

Clinicopathological parameter	*n*	SIX4 expression		χ^2	*P* value
		Low	High		
Age					
≤ 60 yr	22	10 (45.5%)	12 (54.5%)	1.558	0.2120
> 60 yr	71	22 (31.0%)	49 (69.0%)		
Sex					
Male	44	17 (38.6%)	27 (61.4%)	0.6614	0.4161
Female	49	15 (30.6%)	34 (69.4%)		
Maximum tumor diameter[1]					
< 5 cm	37	13 (35.1%)	24 (64.9%)	0.0034	0.9563
≥ 5 cm	55	19 (34.5%)	36 (65.5%)		
Pathological stage					
I-II	78	29 (37.2%)	49 (62.8%)	-	0.2470
III	15	3 (20.0%)	12 (80.0%)		
Primary tumor					
T1-T2	5	2 (40.0%)	3 (60.0%)	0.0696	0.9658
T3	70	24 (34.3%)	46 (65.7%)		
T4	17	6 (35.3%)	11 (64.7%)		
N					
N0	58	24 (41.4%)	34 (58.6%)	3.318	0.0685

N1-N2	35	8 (22.9%)	27 (77.1%)

[1]One patient with an undetected primary tumor was excluded.
SIX: Sine oculis homeobox homolog.

SIX4-related signaling pathways

The above results indicated that SIX4 could have a potential oncogenic role in CRC. Therefore, further investigation was conducted to delineate potential roles. Potential SIX4-related genes were collected through LinkedOmics (Figure 5A), and the top 50 positively- and negatively-correlated genes were recruited for KEGG and GO analysis to identify related signaling pathways (Figures 5B and C).

In Figure 6, the top 50 positively- and negatively-correlated genes were analyzed. KEGG analysis revealed that SIX4-related genes were mainly involved in oxidative phosphorylation, peroxisome, pyruvate metabolism and carbon metabolism pathways (Figure 6A). For biological process annotation, SIX4-related genes were associated with mitochondrial respiratory chain complex assembly, mitochondrial gene expression, NADH dehydrogenase complex assembly and tricarboxylic acid metabolic process (Figure 6B). In cellular component analysis, the respiratory chain was the significant category for SIX4-related genes (Figure 6C), whereas for molecular function, structural constituent of ribosome and rRNA binding were found to be associated with SIX4-related genes (Figure 6D).

Relationship between SIX4 mRNA level and clinicopathological parameters of CRC patients

Using the LinkFinder module in the LinkedOmics dataset, expression of SIX4 was found to be positively related to tumor size and lymph node metastasis in CRC, meaning that the progression of CRC may be driven by high expression of SIX4 (Figures 7A and B). However, no association was found between SIX4 expression and CRC patient metastasis status (Figure 7C). Importantly, considering the progression of CRC, the expression of SIX4 was positively correlated with the stage of CRC patients, consistent with the results for tumor size and lymph node status (Figure 7D).

The etiological and demographic information of CRC patients

The tissue microarray included 93 colon cancer patients, 87 of whom had corresponding adjacent tissue (Table 3). There were 44 male patients and 49 female patients. The average age of the patients was 67.7 ± 9.8 years-old. Among the pathological stages, stage II patients accounted for the largest proportion (82.8%). Most patients did not have lymph node metastasis. During long-term follow-up, 45 of the patients died of CRC.

SIX4 was highly expressed in CRC compared with adjacent normal tissues

As an important transcription factor involved in development, SIX4 was predicted to be subcellularly located mainly in the nucleus but also in the cytosol. Immunohistochemical staining confirmed the subcellular location of SIX4 (Figure 8). The protein level of SIX4 was consistently high in CRC tissues compared with adjacent normal tissues ($P < 0.0001$) (Table 4).

SIX4 protein tends to promote lymph node metastasis in CRC patients

Further analysis of the expression pattern of SIX4 was conducted in 93 CRC patients (Table 5). However, no statistical significance was found between SIX4 levels and clinicopathological parameters, such as the onset age, sex, primary tumor characteristics and lymph node status ($P > 0.05$). Although no difference was found, the percentage of patients with high SIX4 levels tended to be increased at advanced pathological stage, while high expression of SIX4 tended to promote lymph node metastasis, which is similar to the results from analysis of *SIX4* mRNA levels.

SIX4 protein level is a predictor of poor OS for CRC patients

Survival analysis, based on the expression level of SIX4, was also conducted in 93 CRC patients (Figure 9). Unsurprisingly, high levels of SIX4 predicted poor OS for patients with CRC, suggesting that the SIX4 level is negatively correlated with the survival of CRC patients ($P = 0.0263$).

DISCUSSION

The SIX family members were originally identified as members of the homeobox family, SIX subfamily and are required for organogenesis during human development. Previous reports have demonstrated that members of the SIX family not only regulate progenitor cell proliferation and differentiation but also contribute to tumorigenesis[31]. In this study, bioinformatics was used to comprehensively analyze the expression and clinical significance of the SIX family in CRC.

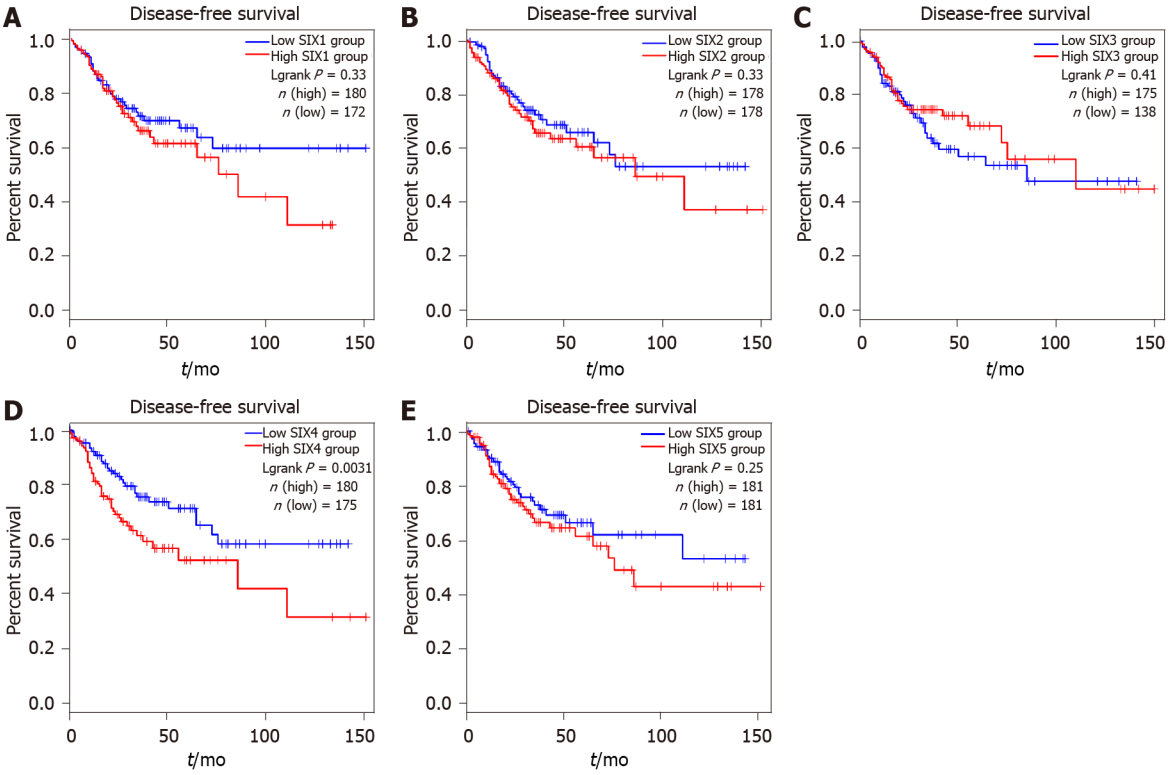

DOI: 10.4251/wjgo.v14.i11.2138

Figure 4 Disease-free survival of colorectal cancer patients estimated by individual expression of sine oculis homeobox homolog family members. A: Sine oculis homeobox homolog (SIX)1; B: SIX2; C: SIX3; D: SIX4; E: SIX5. SIX: Sine oculis homeobox homolog.

Members of the SIX family are homologs of the *Drosophila sine oculis*, *optix* and *Dsix4* genes, which play important roles in organ formation and mesoderm derivatives in *Drosophila*[32]. Interestingly, the genes encoding SIXs are located at three loci:14q23.1 for SIX1, SIX4 and SIX6, 2q21 for SIX2 and SIX3 and 19q13.32 for SIX5, although they can be divided into three subgroups (SIX1 and SIX2, SIX3 and SIX6 and SIX4 and SIX5) based on their SIX-type homeodomains and SIX domains[33]. All SIX proteins are predicted to have DNA-binding transcription factor and chromatin-binding activity[34].

SIX1 has been reported to be a strong factor for many diseases, with important roles in tumorigenesis [35]. Jiang *et al*[36] showed that SIX1 was highly expressed in gastric cancer patients who have short OS and is the target by which the ginsenocide Rh4 suppresses metastasis of gastric cancer through inhibition of the SIX1-stimulated transforming growth factor-β/Smad2/Smad3 signaling pathway. The transforming growth factor-β/Smad2/3 signaling pathway also has been found to be the downstream target of SIX2, which is strongly expressed in hepatocellular carcinoma and negatively related to the prognosis of hepatocellular carcinoma patients[37].

In glioblastoma, where SIX3 is transcriptionally silenced by DNA hypermethylation, SIX3 functions as a tumor suppressor. Elevated expression of SIX4 has been found in human hepatocellular carcinoma and to be positively correlated with loss of tumor encapsulation, microvascular invasion, higher tumor-node-metastasis stage and poor prognosis[38]. SIX5 is an important paralog of SIX4 and promotes lung adenocarcinoma progression through transcriptional activation of LINC01468 and its downstream pathways[22]. In T cell acute lymphoblastic leukemia, SIX6 has been shown to belong to a relevant regulatory transcription factor in T cell acute lymphoblastic leukemia to regulate gene networks[39]. However, research about the function of the SIX family members is still limited, especially for the novel family members.

The present study systematically analyzes the expression pattern of SIXs in normal and cancerous tissues. It is interesting that the expression level of SIXs is relatively low in a majority of organs, indicating they are relatively silent or suppressed in adults. In contrast, the expression of SIX1, SIX2 and SIX4 was found to be higher in CRC than in corresponding normal tissues, based on analysis of the UCSC Xena database, while the expression levels of SIX3 and SIX6 were not significantly different. Further survival analysis, using Kaplan-Meier Plotter, showed that the OS and DFS of CRC patients with high SIX4 expression were significantly worse, and there was no significant difference in other members. Previous studies simply demonstrated that SIX4 promoted the development of CRC cells by activating the PI3K-AKT pathway at the cellular level. To better understand the functional mechanism of SIX4, we used the LinkedOmics database to show that SIX4 expression was positively correlated with clinical stage, T stage and N stage in CRC, and the top 50 SIX4-related genes were involved in oxidative

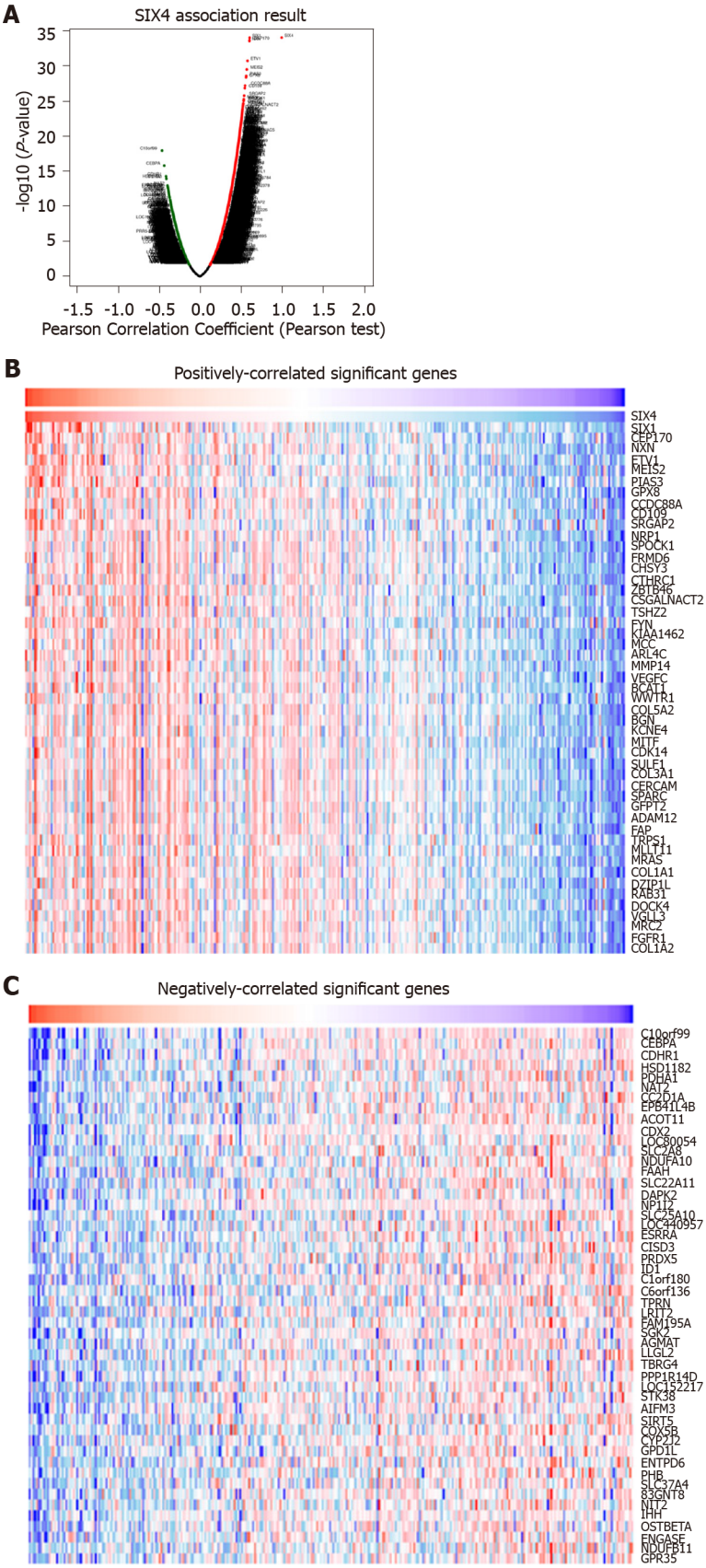

DOI: 10.4251/wjgo.v14.i11.2138

Figure 5 Sine oculis homeobox homolog 4-associated genes. A: All associated genes; B: Top 50 positively-correlated genes; C: Top 50 negatively-correlated genes. SIX4: Sine oculis homeobox homolog 4.

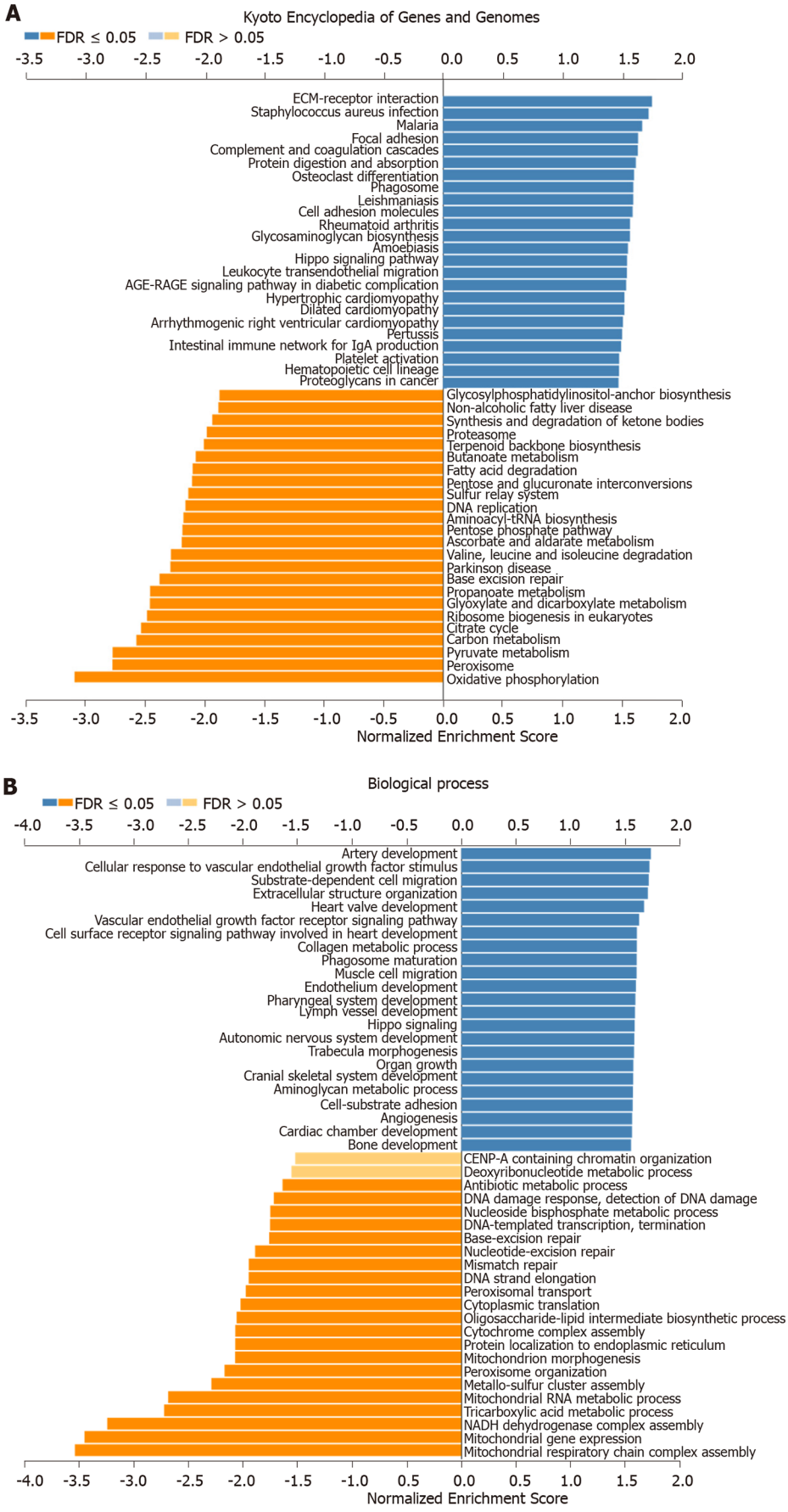
A
Kyoto Encyclopedia of Genes and Genomes
FDR ≤ 0.05
FDR > 0.05
-3.5 -3.0 -2.5 -2.0 -1.5 -1.0 -0.5 0.0 0.5 1.0 1.5 2.0
ECM-receptor interaction
Staphylococcus aureus infection
Malaria
Focal adhesion
Complement and coagulation cascades
Protein digestion and absorption
Osteoclast differentiation
Phagosome
Leishmaniasis
Cell adhesion molecules
Rheumatoid arthritis
Glycosaminoglycan biosynthesis
Amoebiasis
Hippo signaling pathway
Leukocyte transendothelial migration
AGE-RAGE signaling pathway in diabetic complication
Hypertrophic cardiomyopathy
Dilated cardiomyopathy
Arrhythmogenic right ventricular cardiomyopathy
Pertussis
Intestinal immune network for IgA production
Platelet activation
Hematopoietic cell lineage
Proteoglycans in cancer
Glycosylphosphatidylinositol-anchor biosynthesis
Non-alcoholic fatty liver disease
Synthesis and degradation of ketone bodies
Proteasome
Terpenoid backbone biosynthesis
Butanoate metabolism
Fatty acid degradation
Pentose and glucuronate interconversions
Sulfur relay system
DNA replication
Aminoacyl-tRNA biosynthesis
Pentose phosphate pathway
Ascorbate and aldarate metabolism
Valine, leucine and isoleucine degradation
Parkinson disease
Base excision repair
Propanoate metabolism
Glyoxylate and dicarboxylate metabolism
Ribosome biogenesis in eukaryotes
Citrate cycle
Carbon metabolism
Pyruvate metabolism
Peroxisome
Oxidative phosphorylation
-3.5 -3.0 -2.5 -2.0 -1.5 -1.0 -0.5 0.0 0.5 1.0 1.5 2.0
Normalized Enrichment Score
B
Biological process
FDR ≤ 0.05
FDR > 0.05
-4.0 -3.5 -3.0 -2.5 -2.0 -1.5 -1.0 -0.5 0.0 0.5 1.0 1.5 2.0
Artery development
Cellular response to vascular endothelial growth factor stimulus
Substrate-dependent cell migration
Extracellular structure organization
Heart valve development
Vascular endothelial growth factor receptor signaling pathway
Cell surface receptor signaling pathway involved in heart development
Collagen metabolic process
Phagosome maturation
Muscle cell migration
Endothelium development
Pharyngeal system development
Lymph vessel development
Hippo signaling
Autonomic nervous system development
Trabecula morphogenesis
Organ growth
Cranial skeletal system development
Aminoglycan metabolic process
Cell-substrate adhesion
Angiogenesis
Cardiac chamber development
Bone development
CENP-A containing chromatin organization
Deoxyribonucleotide metabolic process
Antibiotic metabolic process
DNA damage response, detection of DNA damage
Nucleoside bisphosphate metabolic process
DNA-templated transcription, termination
Base-excision repair
Nucleotide-excision repair
Mismatch repair
DNA strand elongation
Peroxisomal transport
Cytoplasmic translation
Oligosaccharide-lipid intermediate biosynthetic process
Cytochrome complex assembly
Protein localization to endoplasmic reticulum
Mitochondrion morphogenesis
Peroxisome organization
Metallo-sulfur cluster assembly
Mitochondrial RNA metabolic process
Tricarboxylic acid metabolic process
NADH dehydrogenase complex assembly
Mitochondrial gene expression
Mitochondrial respiratory chain complex assembly
-4.0 -3.5 -3.0 -2.5 -2.0 -1.5 -1.0 0.5 0.0 0.5 1.0 1.5 2.0
Normalized Enrichment Score

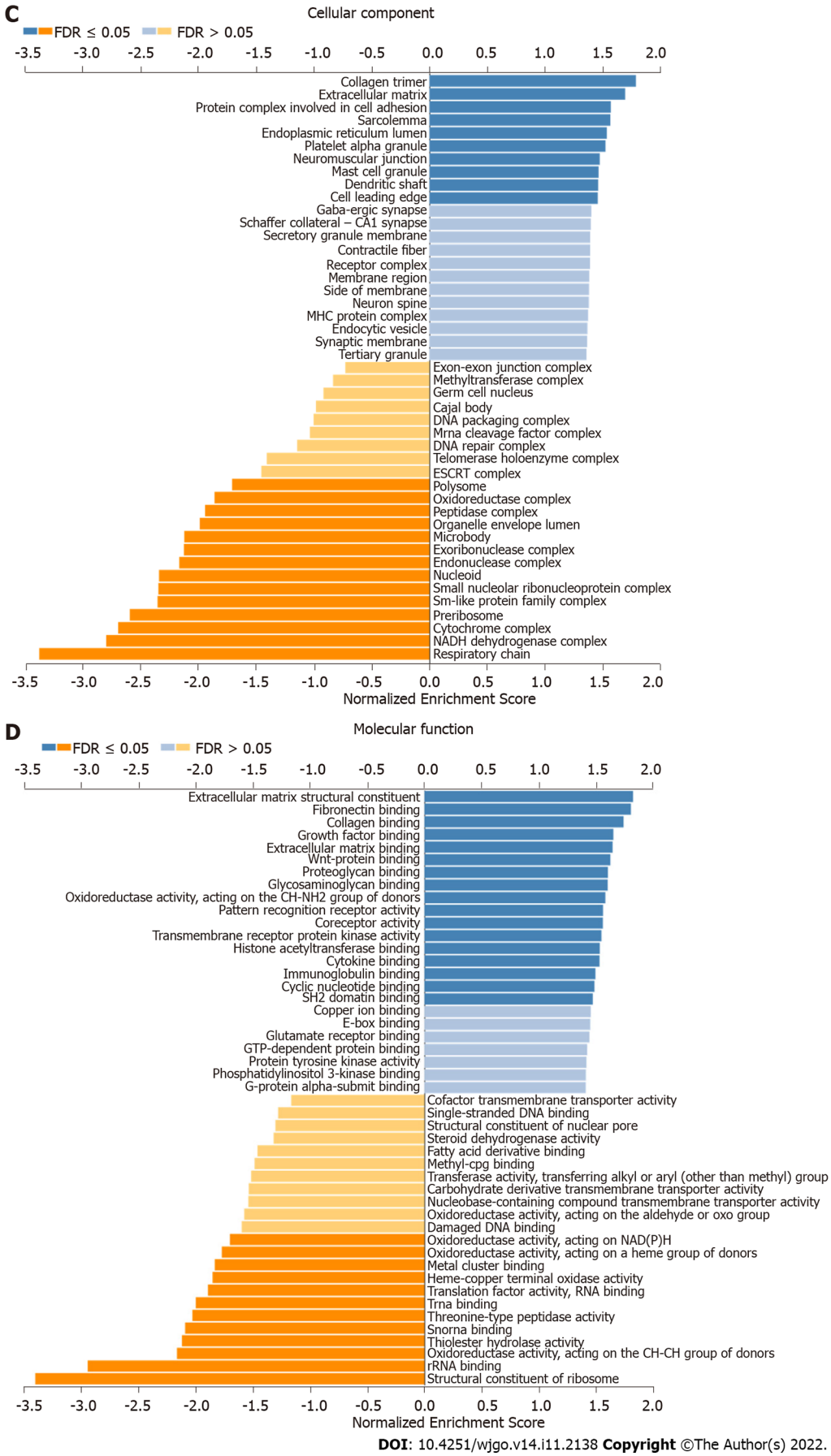

DOI: 10.4251/wjgo.v14.i11.2138

Figure 6 Kyoto Encyclopedia of Genes and Genomes and Gene Ontology analyses of sine oculis homeobox homolog 4-associated genes. A: Kyoto Encyclopedia of Genes and Genomes; B: Biological process; C: Cellular component; D: Molecular function.

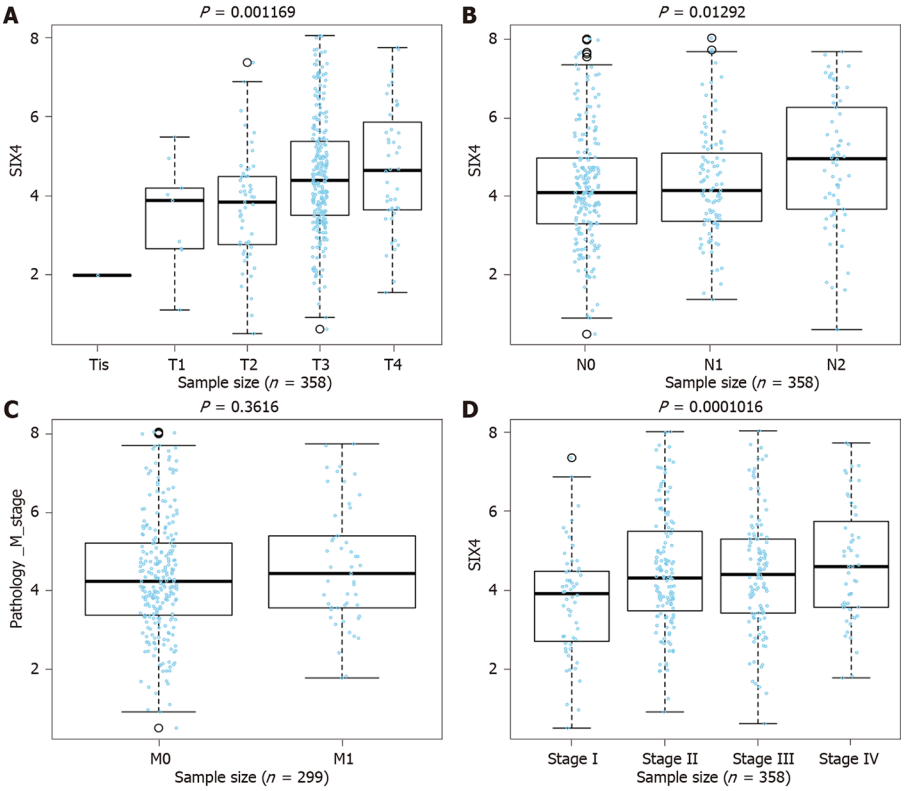

DOI: 10.4251/wjgo.v14.i11.2138 **Copyright** ©The Author(s) 2022.

Figure 7 Relationship between sine oculis homeobox homolog 4 level and clinicopathological parameters of colorectal cancer patients. A: Tumor size; B: Lymph node status; C: Metastasis; D: Stage. SIX: Sine oculis homeobox homolog.

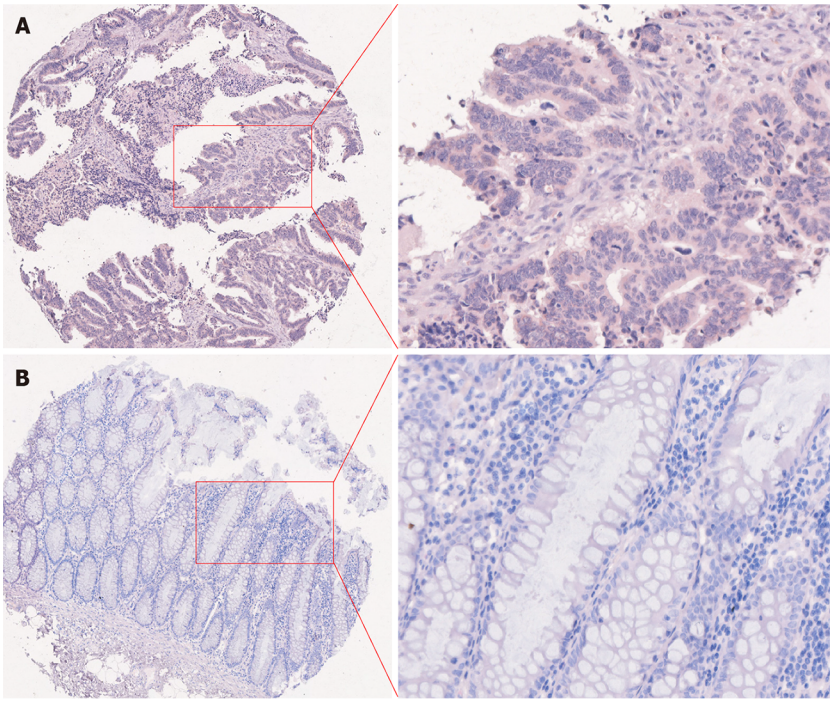

DOI: 10.4251/wjgo.v14.i11.2138 **Copyright** ©The Author(s) 2022.

Figure 8 Representative sine oculis homeobox homolog 4 staining in colorectal cancer and adjacent normal tissues from a patient. A: Colorectal cancer tissue; B: Adjacent normal tissue.

phosphorylation and respiratory chain signaling pathways, suggesting that SIX4 is involved in promoting the growth and metastasis of CRC.

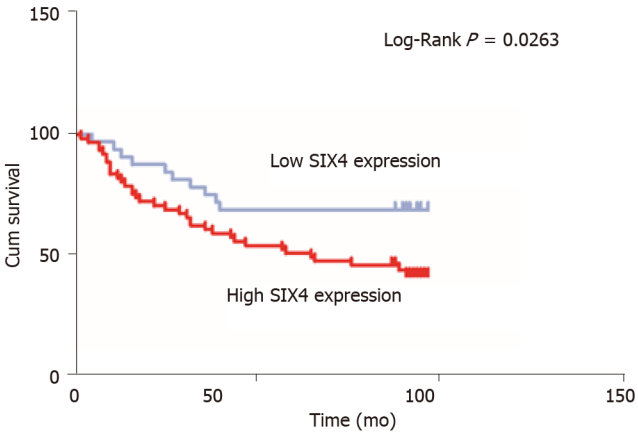

DOI: 10.4251/wjgo.v14.i11.2138

Figure 9 Kaplan-Meier analysis of sine oculis homeobox homolog 4 expression on overall survival of colorectal cancer patients. SIX: Sine oculis homeobox homolog.

CRC threatens the health and life quality of patients and needs more specific therapeutic targets and novel treatment strategies[40]. Using different databases, the expression of SIX4 was found to be increased in CRC tissues compared with adjacent normal ones. As a transcription factor, abnormal increases in SIX4 may enhance the expression of downstream oncogenes, such as AKT, YAP1 and c-MET[38,41]. SIX4 promotes activation of the STAT3 signaling pathway in breast cancer and plays an important role in epithelial-mesenchymal transition. Furthermore, SIX4 has been reported to play a carcinogenic role in CRC by activating the Akt signaling pathway[17]. KEGG and GO annotation predicted SIX4 and its correlated genes to be involved in oxidative phosphorylation, respiratory chain and metabolism, which are also related to classical signaling pathways, including AKT and YAP1. Therefore, the Akt signaling pathway is extremely likely to be the mechanism of SIX4-enhanced development of CRC.

The expression of SIX4 was also evaluated in clinical trials to provide solid evidence for the use of SIX4 in clinical testing. Significantly, lymph node metastasis was found to be positively associated with SIX4 level in CRC patients. The development of CRC may be at least partially due to high SIX4 expression and its transcription of downstream genes, subsequently promoting the migratory ability of tumor cells through the lymph node. As a solid tumor, the recurrence and relapse of CRC could severely affect patient survival[42]. The present study demonstrated that CRC patients with low SIX4 expression have longer survival, suggesting a novel therapy to inhibit or suppress SIX4 activity would be useful in prolonging CRC patient survival. This study provides the first comprehensive analysis of the potential role and prognostic value of the SIX family in CRC. However, the current study is limited to analyzing the expression and clinicopathological parameters of SIXs in CRC, and the sample size is relatively limited. Therefore, further in-depth analysis will be conducted in future studies. Although SIX4 may be involved in oxidative phosphorylation, respiratory chain activity and metabolism, further studies on these can be investigated.

CONCLUSION

Among the SIX family members, SIX4 was found to be a tumor-promoting factor in the intestinal tract and could be a prognostic indicator and treatment target for patients with CRC. Further investigation of novel therapeutic strategies targeting SIX4 in CRC patients could provide important potential for treatment of CRC.

ARTICLE HIGHLIGHTS

Research background

Human sine oculis homeobox homolog (SIX) protein belongs to the homeobox family, which plays an important role in different developmental organs, and the abnormal expression of most development-related genes is closely related to the occurrence and development of malignant tumors. However, no studies have comprehensively analyzed SIXs in colorectal cancer (CRC).

Research motivation
SIXs has been found to be closely related to the occurrence and development of cancer. However, there are few studies on SIXs in CRC. SIXs may become a new potential prognostic indicator of CRC.

Research objectives
To comprehensively analyze the expression and the prognosis of the SIX family in CRC tissues and to explore the potential role of the SIX family as a new prognostic indicator of CRC.

Research methods
In this study, the RNA and protein expression levels of the SIX family in CRC were analyzed by various online databases and immunohistochemically. Then the relationship between the SIX family and the prognosis of CRC was further analyzed. In order to better understand the mechanism of SIX4, the positive correlation between SIX4 expression and tumor-node-metastasis stage of CRC was analyzed. Then, the relationship between *SIX4* mRNA levels and clinicopathological parameters in CRC patients was analyzed.

Research results
The expression levels of SIXs in most organs were relatively low in the Human Protein Atlas. UCSC Xena database analysis showed that the expression levels of SIX1, SIX2 and SIX4 in CRC were higher than those in corresponding normal tissue. Further survival analysis with Kaplan-Meier Plotter showed that the relation between poor overall survival and disease-free survival of CRC patients and high SIX4 expression were significant. Using the LinkedOmics database, the expression of SIX4 was positively correlated with the clinical stage, T stage and N stage of CRC, and the top 50 SIX4-related genes were involved in oxidative phosphorylation and respiratory chain signaling pathway, suggesting that SIX4 was involved in promoting the growth and metastasis of CRC.

Research conclusions
As a member of the SIX family, SIX4 played a role in promoting tumor development in the intestine, which may serve as a potential prognostic indicator and therapeutic target for CRC patients. Therefore, targeting SIX4 may serve as a new therapeutic strategy for CRC patients, providing important potential for the treatment of CRC.

Research perspectives
This is the first comprehensive analysis of the potential role and prognostic value of the SIX family in CRC. However, the current research is limited, and future studies need to further explore the oxidative phosphorylation, respiratory chain activity and metabolism of SIX4 in CRC.

FOOTNOTES

Author contributions: Liu J and Wu HT designed the research study; Fang ZX performed the research; Fang ZX, Li CL, Wu Z, Hou YY and Wu HT analyzed the research and wrote the manuscript; Liu J revised the manuscript critically; and all authors have read and approved the final manuscript.

Supported by the National Natural Science Foundation of China, No. 81501539; the Natural Science Foundation of Guangdong Province, No. 2021A1515012180 and 2016A030312008; Special Grant for Key Area Programs of Guangdong Department of Education, No. 2021ZDZX2004; Science and Technology Special Project of Guangdong Province, No. 210715216902829; "Dengfeng Project" for the construction of high-level hospitals in Guangdong Province-First Affiliated Hospital of Shantou University College Supporting Funding, No. 202003-10.

Institutional review board statement: The current study was reviewed and approved by the Ethics Committee of Shantou University Medical College.

Conflict-of-interest statement: All the authors report no relevant conflicts of interest for this article.

Data sharing statement: No additional data are available.

Country/Territory of origin: China

ORCID number: Ze-Xuan Fang 0000-0002-6100-9012; Chun-Lan Li 0000-0002-1649-9059; Zheng Wu 0000-0002-1393-7586; Yan-Yu Hou 0000-0002-4249-8770; Hua-Tao Wu 0000-0002-1640-6094; Jing Liu 0000-0002-7483-4572.

S-Editor: Wang JJ
L-Editor: Filipodia
P-Editor: Wang JJ

REFERENCES

1 **Töhönen V**, Katayama S, Vesterlund L, Jouhilahti EM, Sheikhi M, Madissoon E, Filippini-Cattaneo G, Jaconi M, Johnsson A, Bürglin TR, Linnarsson S, Hovatta O, Kere J. Novel PRD-like homeodomain transcription factors and retrotransposon elements in early human development. *Nat Commun* 2015; **6**: 8207 [PMID: 26360614 DOI: 10.1038/ncomms9207]
2 **Gerrard DT**, Berry AA, Jennings RE, Birket MJ, Zarrineh P, Garstang MG, Withey SL, Short P, Jiménez-Gancedo S, Firbas PN, Donaldson I, Sharrocks AD, Hanley KP, Hurles ME, Gomez-Skarmeta JL, Bobola N, Hanley NA. Dynamic changes in the epigenomic landscape regulate human organogenesis and link to developmental disorders. *Nat Commun* 2020; **11**: 3920 [PMID: 32764605 DOI: 10.1038/s41467-020-17305-2]
3 **Hong S**, Shen X, Luo C, Sun F. Comparative analysis of the testes from wild-type and Alkbh5-knockout mice using single-cell RNA sequencing. *G3 (Bethesda)* 2022; **12** [PMID: 35652742 DOI: 10.1093/g3journal/jkac130]
4 **Xu PX**, Zheng W, Huang L, Maire P, Laclef C, Silvius D. Six1 is required for the early organogenesis of mammalian kidney. *Development* 2003; **130**: 3085-3094 [PMID: 12783782 DOI: 10.1242/dev.00536]
5 **Xu J**, Li J, Ramakrishnan A, Yan H, Shen L, Xu PX. Six1 and Six2 of the Sine Oculis Homeobox Subfamily are Not Functionally Interchangeable in Mouse Nephron Formation. *Front Cell Dev Biol* 2022; **10**: 815249 [PMID: 35178390 DOI: 10.3389/fcell.2022.815249]
6 **Ghanbari H**, Seo HC, Fjose A, Brändli AW. Molecular cloning and embryonic expression of Xenopus Six homeobox genes. *Mech Dev* 2001; **101**: 271-277 [PMID: 11231090 DOI: 10.1016/s0925-4773(00)00572-4]
7 **Chen R**, Hou Y, Connell M, Zhu S. Homeodomain protein Six4 prevents the generation of supernumerary Drosophila type II neuroblasts and premature differentiation of intermediate neural progenitors. *PLoS Genet* 2021; **17**: e1009371 [PMID: 33556050 DOI: 10.1371/journal.pgen.1009371]
8 **Mosrati MA**, Hammami B, Rebeh IB, Ayadi L, Dhouib L, Ben Mahfoudh K, Hakim B, Charfeddine I, Mnif J, Ghorbel A, Masmoudi S. A novel dominant mutation in SIX1, affecting a highly conserved residue, result in only auditory defects in humans. *Eur J Med Genet* 2011; **54**: e484-e488 [PMID: 21700001 DOI: 10.1016/j.ejmg.2011.06.001]
9 **Ruf RG**, Xu PX, Silvius D, Otto EA, Beekmann F, Muerb UT, Kumar S, Neuhaus TJ, Kemper MJ, Raymond RM Jr, Brophy PD, Berkman J, Gattas M, Hyland V, Ruf EM, Schwartz C, Chang EH, Smith RJ, Stratakis CA, Weil D, Petit C, Hildebrandt F. SIX1 mutations cause branchio-oto-renal syndrome by disruption of EYA1-SIX1-DNA complexes. *Proc Natl Acad Sci U S A* 2004; **101**: 8090-8095 [PMID: 15141091 DOI: 10.1073/pnas.0308475101]
10 **Geng X**, Speirs C, Lagutin O, Inbal A, Liu W, Solnica-Krezel L, Jeong Y, Epstein DJ, Oliver G. Haploinsufficiency of Six3 fails to activate Sonic hedgehog expression in the ventral forebrain and causes holoprosencephaly. *Dev Cell* 2008; **15**: 236-247 [PMID: 18694563 DOI: 10.1016/j.devcel.2008.07.003]
11 **Wang SH**, Wu CC, Lu YC, Lin YH, Su YN, Hwu WL, Yu IS, Hsu CJ. Mutation screening of the EYA1, SIX1, and SIX5 genes in an East Asian cohort with branchio-oto-renal syndrome. *Laryngoscope* 2012; **122**: 1130-1136 [PMID: 22447252 DOI: 10.1002/lary.23217]
12 **Panagiotou ES**, Fernandez-Fuentes N, Farraj LA, McKibbin M, Elçioglu NH, Jafri H, Cerman E, Parry DA, Logan CV, Johnson CA, Inglehearn CF, Toomes C, Ali M. Novel *SIX6* mutations cause recessively inherited congenital cataract, microcornea, and corneal opacification with or without coloboma and microphthalmia. *Mol Vis* 2022; **28**: 57-69 [PMID: 35693420]
13 **Siegel RL**, Miller KD, Fuchs HE, Jemal A. Cancer Statistics, 2021. *CA Cancer J Clin* 2021; **71**: 7-33 [PMID: 33433946 DOI: 10.3322/caac.21654]
14 **Xing XL**, Yao ZY, Zhang T, Zhu N, Liu YW, Peng J. MicroRNA-Related Prognosis Biomarkers from High-Throughput Sequencing Data of Colorectal Cancer. *Biomed Res Int* 2020; **2020**: 7905380 [PMID: 32964043 DOI: 10.1155/2020/7905380]
15 **Zahnd WE**, Josey MJ, Schootman M, Eberth JM. Spatial accessibility to colonoscopy and its role in predicting late-stage colorectal cancer. *Health Serv Res* 2021; **56**: 73-83 [PMID: 32954527 DOI: 10.1111/1475-6773.13562]
16 **Gong B**, Kao Y, Zhang C, Sun F, Gong Z, Chen J. Identification of Hub Genes Related to Carcinogenesis and Prognosis in Colorectal Cancer Based on Integrated Bioinformatics. *Mediators Inflamm* 2020; **2020**: 5934821 [PMID: 32351322 DOI: 10.1155/2020/5934821]
17 **Li G**, Hu F, Luo X, Hu J, Feng Y. SIX4 promotes metastasis *via* activation of the PI3K-AKT pathway in colorectal cancer. *PeerJ* 2017; **5**: e3394 [PMID: 28584719 DOI: 10.7717/peerj.3394]
18 **Yang Y**, Feng M, Bai L, Liao W, Zhou K, Zhang M, Wu Q, Wen F, Lei W, Zhang P, Zhang N, Huang J, Li Q. Comprehensive analysis of EMT-related genes and lncRNAs in the prognosis, immunity, and drug treatment of colorectal cancer. *J Transl Med* 2021; **19**: 391 [PMID: 34526059 DOI: 10.1186/s12967-021-03065-0]
19 **Yang C**, Liu H. Both a hypoxia-inducible EYA3 and a histone acetyltransferase p300 function as coactivators of SIX5 to mediate tumorigenesis and cancer progression. *Ann Transl Med* 2022; **10**: 752 [PMID: 35957720 DOI: 10.21037/atm-22-2663]
20 **Song W**, Ma J, Lei B, Yuan X, Cheng B, Yang H, Wang M, Feng Z, Wang L. Sine oculis homeobox 1 promotes proliferation and migration of human colorectal cancer cells through activation of Wnt/β-catenin signaling. *Cancer Sci* 2019; **110**: 608-616 [PMID: 30548112 DOI: 10.1111/cas.13905]

21 **Yu Z**, Feng J, Wang W, Deng Z, Zhang Y, Xiao L, Wang Z, Liu C, Liu Q, Chen S, Wu M. The EGFR-ZNF263 signaling axis silences SIX3 in glioblastoma epigenetically. *Oncogene* 2020; **39**: 3163-3178 [PMID: 32051553 DOI: 10.1038/s41388-020-1206-7]

22 **Yuan Y**, Zhou D, Chen F, Yang Z, Gu W, Zhang K. SIX5-activated LINC01468 promotes lung adenocarcinoma progression by recruiting SERBP1 to regulate SERPINE1 mRNA stability and recruiting USP5 to facilitate PAI1 protein deubiquitylation. *Cell Death Dis* 2022; **13**: 312 [PMID: 35387981 DOI: 10.1038/s41419-022-04717-9]

23 **Uhlén M**, Fagerberg L, Hallström BM, Lindskog C, Oksvold P, Mardinoglu A, Sivertsson Å, Kampf C, Sjöstedt E, Asplund A, Olsson I, Edlund K, Lundberg E, Navani S, Szigyarto CA, Odeberg J, Djureinovic D, Takanen JO, Hober S, Alm T, Edqvist PH, Berling H, Tegel H, Mulder J, Rockberg J, Nilsson P, Schwenk JM, Hamsten M, von Feilitzen K, Forsberg M, Persson L, Johansson F, Zwahlen M, von Heijne G, Nielsen J, Pontén F. Proteomics. Tissue-based map of the human proteome. *Science* 2015; **347**: 1260419 [PMID: 25613900 DOI: 10.1126/science.1260419]

24 **Wu HT**, Chen WJ, Xu Y, Shen JX, Chen WT, Liu J. The Tumor Suppressive Roles and Prognostic Values of STEAP Family Members in Breast Cancer. *Biomed Res Int* 2020; **2020**: 9578484 [PMID: 32802887 DOI: 10.1155/2020/9578484]

25 **Li T**, Fan J, Wang B, Traugh N, Chen Q, Liu JS, Li B, Liu XS. TIMER: A Web Server for Comprehensive Analysis of Tumor-Infiltrating Immune Cells. *Cancer Res* 2017; **77**: e108-e110 [PMID: 29092952 DOI: 10.1158/0008-5472.CAN-17-0307]

26 **Goldman M**, Craft B, Swatloski T, Cline M, Morozova O, Diekhans M, Haussler D, Zhu J. The UCSC Cancer Genomics Browser: update 2015. *Nucleic Acids Res* 2015; **43**: D812-D817 [PMID: 25392408 DOI: 10.1093/nar/gku1073]

27 **Lánczky A**, Győrffy B. Web-Based Survival Analysis Tool Tailored for Medical Research (KMplot): Development and Implementation. *J Med Internet Res* 2021; **23**: e27633 [PMID: 34309564 DOI: 10.2196/27633]

28 **Tang Z**, Kang B, Li C, Chen T, Zhang Z. GEPIA2: an enhanced web server for large-scale expression profiling and interactive analysis. *Nucleic Acids Res* 2019; **47**: W556-W560 [PMID: 31114875 DOI: 10.1093/nar/gkz430]

29 **Vasaikar SV**, Straub P, Wang J, Zhang B. LinkedOmics: analyzing multi-omics data within and across 32 cancer types. *Nucleic Acids Res* 2018; **46**: D956-D963 [PMID: 29136207 DOI: 10.1093/nar/gkx1090]

30 **Liu J**, Wei XL, Huang WH, Chen CF, Bai JW, Zhang GJ. Cytoplasmic Skp2 expression is associated with p-Akt1 and predicts poor prognosis in human breast carcinomas. *PLoS One* 2012; **7**: e52675 [PMID: 23300741 DOI: 10.1371/journal.pone.0052675]

31 **Ronca R**, Benkheil M, Mitola S, Struyf S, Liekens S. Tumor angiogenesis revisited: Regulators and clinical implications. *Med Res Rev* 2017; **37**: 1231-1274 [PMID: 28643862 DOI: 10.1002/med.21452]

32 **Kumar JP**. The sine oculis homeobox (SIX) family of transcription factors as regulators of development and disease. *Cell Mol Life Sci* 2009; **66**: 565-583 [PMID: 18989625 DOI: 10.1007/s00018-008-8335-4]

33 **Laclef C**, Hamard G, Demignon J, Souil E, Houbron C, Maire P. Altered myogenesis in Six1-deficient mice. *Development* 2003; **130**: 2239-2252 [PMID: 12668636 DOI: 10.1242/dev.00440]

34 **Rafiq A**, Aashaq S, Jan I, Beigh MA. SIX1 transcription factor: A review of cellular functions and regulatory dynamics. *Int J Biol Macromol* 2021; **193**: 1151-1164 [PMID: 34742853 DOI: 10.1016/j.ijbiomac.2021.10.133]

35 **Wu W**, Ren Z, Li P, Yu D, Chen J, Huang R, Liu H. Six1: a critical transcription factor in tumorigenesis. *Int J Cancer* 2015; **136**: 1245-1253 [PMID: 24488862 DOI: 10.1002/ijc.28755]

36 **Jiang H**, Ma P, Duan Z, Liu Y, Shen S, Mi Y, Fan D. Ginsenoside Rh4 Suppresses Metastasis of Gastric Cancer *via* SIX1-Dependent TGF-β/Smad2/3 Signaling Pathway. *Nutrients* 2022; **14** [PMID: 35458126 DOI: 10.3390/nu14081564]

37 **Wan ZH**, Ma YH, Jiang TY, Lin YK, Shi YY, Tan YX, Dong LW, Wang HY. Six2 is negatively correlated with prognosis and facilitates epithelial-mesenchymal transition *via* TGF-β/Smad signal pathway in hepatocellular carcinoma. *Hepatobiliary Pancreat Dis Int* 2019; **18**: 525-531 [PMID: 31564506 DOI: 10.1016/j.hbpd.2019.09.005]

38 **He Q**, Lin Z, Wang Z, Huang W, Tian D, Liu M, Xia L. SIX4 promotes hepatocellular carcinoma metastasis through upregulating YAP1 and c-MET. *Oncogene* 2020; **39**: 7279-7295 [PMID: 33046796 DOI: 10.1038/s41388-020-01500-y]

39 **Laukkanen S**, Oksa L, Nikkilä A, Lahnalampi M, Parikka M, Seki M, Takita J, Degerman S, de Bock CE, Heinäniemi M, Lohi O. SIX6 is a TAL1-regulated transcription factor in T-ALL and associated with inferior outcome. *Leuk Lymphoma* 2020; **61**: 3089-3100 [PMID: 32835548 DOI: 10.1080/10428194.2020.1804560]

40 **Biller LH**, Schrag D. Diagnosis and Treatment of Metastatic Colorectal Cancer: A Review. *JAMA* 2021; **325**: 669-685 [PMID: 33591350 DOI: 10.1001/jama.2021.0106]

41 **Sun X**, Hu F, Hou Z, Chen Q, Lan J, Luo X, Wang G, Hu J, Cao Z. SIX4 activates Akt and promotes tumor angiogenesis. *Exp Cell Res* 2019; **383**: 111495 [PMID: 31301290 DOI: 10.1016/j.yexcr.2019.111495]

42 **Dueland S**, Smedman TM, Røsok B, Grut H, Syversveen T, Jørgensen LH, Line PD. Treatment of relapse and survival outcomes after liver transplantation in patients with colorectal liver metastases. *Transpl Int* 2021; **34**: 2205-2213 [PMID: 34792825 DOI: 10.1111/tri.13995]

World Journal of Gastrointestinal Oncology

Submit a Manuscript: https://www.f6publishing.com

World J Gastrointest Oncol 2022 November 15; 14(11): 2157-2169

DOI: 10.4251/wjgo.v14.i11.2157

ISSN 1948-5204 (online)

ORIGINAL ARTICLE

Basic Study

KLF16 promotes pancreatic adenocarcinoma cell proliferation and migration by positively regulating SMAD6

Wei Mi, Zhi Zheng, Jiong-Di Lu, Shu-Quan Duan, Jie Zhang, Hai-Qiao Zhang, Yi-Xuan Ding, Jie Yin, Feng Cao, Jun Zhang, Fei Li

Specialty type: Oncology

Provenance and peer review: Unsolicited article; Externally peer reviewed.

Peer-review model: Single blind

Peer-review report's scientific quality classification

Grade A (Excellent): 0
Grade B (Very good): 0
Grade C (Good): C, C
Grade D (Fair): 0
Grade E (Poor): 0

P-Reviewer: Miceli V, Italy; Tantau AI, Romania

Received: July 15, 2022
Peer-review started: July 15, 2022
First decision: July 28, 2022
Revised: September 10, 2022
Accepted: October 18, 2022
Article in press: October 18, 2022
Published online: November 15, 2022

Wei Mi, Zhi Zheng, Hai-Qiao Zhang, Jie Yin, Jun Zhang, Department of General Surgery, Beijing Friendship Hospital, Capital Medical University, Beijing 100050, China

Jiong-Di Lu, Yi-Xuan Ding, Feng Cao, Fei Li, Department of General Surgery, Xuanwu Hospital, Capital Medical University, Beijing 100053, China

Shu-Quan Duan, Department of Digestive Minimally Invasive Surgery, The Second Affiliated Hospital of Baotou Medical College, Baotou 014030, Inner Mongolia Autonomous Region, China

Jie Zhang, Department of Radiology, Beijing Friendship Hospital, Capital Medical University, Beijing 100050, China

Corresponding author: Jun Zhang, MD, PhD, Chief Doctor, General Surgery Department, Beijing Friendship Hospital, Capital Medical University, No. 95 Yongan Road, Xi-Cheng District, Beijing 100050, China. zhangjun5986@ccmu.edu.cn

Abstract

BACKGROUND

Pancreatic adenocarcinoma (PAAD) is a cancerous tumor with an extremely poor 5-year survival rate. The exploration of biomarkers for the diagnosis and treatment of PAAD is crucial in clinical practice. Krüppel-like factors (KLFs) are involved in a variety of biological functions in cells. According to multiple studies, KLF16 behave as an oncogene in prostate, breast and gastric cancers. However, no research has been done on the significance of KLF16 in PAAD.

AIM

To explore the molecular mechanisms of KLF16 in PAAD.

METHODS

KLF16 was identified in the tumor specimens and normal tissues by GEPIA database and verified by quantitative real-time PCR (qRT-PCR). Knockdown or exogenous expression of KLF16, combined with *in vitro* and *in vivo* assays, was performed to show the functional significance of KLF16. The molecular mechanism of KLF16 was demonstrated by qRT-PCR, western blotting, immunoprecipitation assay and flow cytometry.

RESULTS

We showed that KLF16 was highly expressed in PAAD patients based on the GEPIA database. KLF16 silencing suppressed while KLF16 overexpression promoted the malignant function of PAAD cells. Based on RNA sequencing, we discovered that KLF16 potentiated the expression of SMAD6 in PAAD cells. SMAD6 transcript abundance was increased and positively correlated with KLF16 expression in PAAD samples. In addition, inhibiting SMAD6 was able to mitigate the effects of KLF16 overexpression on PAAD cell processes, suggesting the importance of SMAD6 in the development of KLF16-triggered PAAD.

CONCLUSION

KLF16/SMAD6 axis might be explored as a therapeutic target for PAAD therapy.

Key Words: KLF16; Pancreatic adenocarcinoma; SMAD6; Tumorigenesis; Therapeutic target

Core Tip: Our study provided the evidence that KLF16 acted as an oncogene in pancreatic adenocarcinoma (PAAD). We also identified that SMAD6 served as the downstream substrate of KLF16 and this signaling cascade has never been reported. This mechanism indicated a novel insight into the pathological events during the development of PAAD.

Citation: Mi W, Zheng Z, Lu JD, Duan SQ, Zhang J, Zhang HQ, Ding YX, Yin J, Cao F, Zhang J, Li F. KLF16 promotes pancreatic adenocarcinoma cell proliferation and migration by positively regulating SMAD6. *World J Gastrointest Oncol* 2022; 14(11): 2157-2169

URL: https://www.wjgnet.com/1948-5204/full/v14/i11/2157.htm

DOI: https://dx.doi.org/10.4251/wjgo.v14.i11.2157

INTRODUCTION

Pancreatic adenocarcinoma (PAAD) ranks fourteenth in incidence with about 496000 new cases (2.6%) per year, but seventh in mortality with roughly 466000 (4.7%) deaths per year, according to GLOBOCAN 2020[1]. Due to its dismal prognosis, experts expect that pancreatic cancer will rank third in terms of fatality by 2025[2]. Currently, the only way to improve the outcomes of this condition is to diagnose it early[3]. However, since the early signs of PAAD are not well-defined, it is difficult to diagnose, even when it progresses fast to neighboring organs[4]. As a result, new unique and useful biomarkers for the diagnosis and prognosis of PAAD are required.

Three zinc finger DNA binding domains distinguish the Krüppel-like factor (KLF) which belongs to the SP/KLF transcription factor family[5]. KLF binds to GT or GC-rich regions and regulates transcription as an activator or repressor, depending on the promoter type[6]. The KLF16 gene is located on chromosome 19 that participates in various cellular activities such as proliferation, metabolism and death[7]. Various studies on the role of KLF16 in cancer have been published in recent years with mixed results. It has been reported that KLF16 promoted progression of breast cancer *via* activating MAGT1 [8]. Ma *et al*[9] found that KLF16 enhanced colorectal carcinoma progression by modulating nucleolar homeostasis and translational reprogramming. On the other hand, in some malignancies, KLF16 functions as an oncogenic suppressor. It has been reported that KLF16 suppressed human glioma cell proliferation and tumorigenesis by regulating TFAM[10]. Nevertheless, understanding the molecular mechanisms of KLF16 in PAAD is still limited.

MATERIALS AND METHODS

The Cancer Genome Atlas provided clinical samples

A total of 350 cases which encompassed 171 normal and 179 tumor specimens were analyzed from the database of Gene Expression Profiling Interactive Analysis (GEPIA) (http://gepia.cancer-pku.cn/index.html) database, which combines the TCGA database and GEO database.

Cell culture

Shanghai Institutes for Biological Sciences (Shanghai, China) provided the AsPC-1 and MIA PaCa-2 cell lines. Cells were incubated in Eagle's minimal essential medium (MEM) with 10% fetal bovine serum

(FBS), in a 37°C incubator supplemented with 5% CO_2. L-glutamine and sodium pyruvate were both supplied by Gibco and added to the medium to ensure constant cell growth.

Quantitative real-time PCR (qRT-PCR)

Cultivated cell lines were lysed in TRIzol (Ambion, Austin, TX, United States). To reverse transcribe 500 ng of RNA template, the Takara PrimeScript RT Reagent Kit was employed. The following primers were used: KLF16-F: 5'-TGGGCAAACCCTGAAGACA-3' and KLF16-R, 5′-GTTGCACAGATGGGAAGAAA-3′; SMAD6-F:5′- CCTCCCTACTCTCGGCTGTC-3′, and SMAD6-R, 5′- GGTAGCCTCCGTTTCAGTGTA-3′; and β-actin-F: 5′-CATGTACGTTGCTATCCAGGC-3′, β-actin-R, 5′-CTCCTTAATGTCACGCACGAT-3′. RT-qPCR was conducted on real-time PCR system (7500 Fast; Life Technologies Holdings Pte Ltd, Singapore). The expression of targeted genes was adjusted to β-actin.

Knockdown and overexpression assay

Specific small interfering RNAs (siRNAs) targeting KLF16 (siKLF16#1, siKIF16#2) and SMAD6 (siSMAD6#1, siSMAD6#2) and negative controls siRNA (siCtrl) were provided by Genechem (Shanghai, China). For transient transfection, Invitrogen's Lipofectamine RNAiMAX transfection reagent was employed. The sequences used were as follows: siKLF16#1 (5′-GGGUUCUUC-CAAAGAACAU-3′), siKLF16#2 (5′-GGUAUCACGUGACAAUCAA-3′), siSMAD6#1 (5′-CCACAT-TGTCTTACACTGAAA-3′), siSMAD6#2 (5′-CTCCATCAAGGTGTTCGACTT-3′) and siCtrl (5′-UUCUCCGAACGUGUCACGU-3′).

KLF16-pCDNA3.1 was overexpressed using Lipofectamine 3000 (Thermo Fisher Scientific, Waltham, MA, United States). shRNA targeting SMAD6 (shSMAD6) purchased from Genechem (Shanghai, China) was used for lentiviral transduction.

Western blotting

To lyse the cells, the RIPA lysis buffer (Beyotime, Jiangsu, China) was used. This solution contains the protease inhibitor cocktail (Roche, Basel, Switzerland). To detect protein amount present in the lysates, a Bradford reagent manufactured by Sigma was used. After that, 30 μg of protein per row was run on SDS-PAGE gels and then immunoblotted onto a 0.22 m polyvinylidene fluoride membrane (Roche). The membranes were incubated for an hour with 5% nonfat milk solution that dissolved in TBST. After adding primary antibodies against KLF16 (1:1000; sc-377519; Santa Cruz Biotechnology, Dallas, TX, United States), SMAD6 (1:1000; ab273106; Abcam), and GAPDH (1:1000; ab8245; Abcam), the membrane was incubated at 4°C overnight. After that, the secondary antibody specific to primary antibody was added. An Odessey CLx system uncovered evidence of the presence of protein bands (LI-COR, Lincoln, NE, United States).

Cell Counting Kit-8 and cell colony

The CCK-8 (Beyotime) was applied to determine cell proliferation rate. In all, 1×10^3 transfected cells were planted in 200 μL complete medium. A total of 20 μL of CCK-8 was used to treat the cells and cultured for a further two hours at 37°C, followed by OD450 measurement. For cell colony assay, 1.2×10^3 transfected cells were planted in six-well plates with 2 mL of complete media and cultivated for 14 d. Every 3 d, the medium was replaced. The cells were fixed with methanol and stained with 0.1% crystal violet (Solarbio, Beijing, China).

Flow cytometry

In a six-well plate, 2×10^5 AsPC-1 and MIApaca-2 cells were planted per well. Flow cytometry was performed on cells 48 h after transfection with siKLF16#1, siKLF16#2, siCtrl, or KLF16 overexpressed plasmid and Ctrl plasmid.

A cell cycle staining kit (Cat No. 4040301; Yeasen, Shanghai, China) was used to detect the cell cycle. The cells were fixed for two hours at 4°C in 75% ethanol. The cells were stained with a staining solution containing 10 μL propidium iodide and 10 μL RNaseA in a volume of 0.5 mL. The cells were stained for 30 mins at 25°C and then subjected to analysis with the Guava easyCyte HT system (Millipore) after passing through a screen with a mesh size of 400. The cell cycle was analyzed by a flow cytometry system.

The Annexin V Apoptosis Detection Kit (Cat No. 88-8007; Invitrogen, Waltham, MA, United States) was used to examine apoptosis. The cells (1 to 5×10^5) were collected in 1X binding buffer and were incubated with staining solution in the dark for 15 min. The samples were analyzed using the Guava easyCyte HT system (Millipore, Burlington, MA, United States) within 1 h.

Cell migration

5.0×10^4 AsPC-1 or MIApaca-2 cells in 300 μL medium were planted in the upper chambers of 24-well Corning® FluoroBlokTM Cell Culture Inserts (Corning, NY, United States). The bottom chamber was added to 600 μL medium which contained 10% FBS. The migrating cells were stained by 0.1% crystal violet. Images of migrating cells were collected under a microscope.

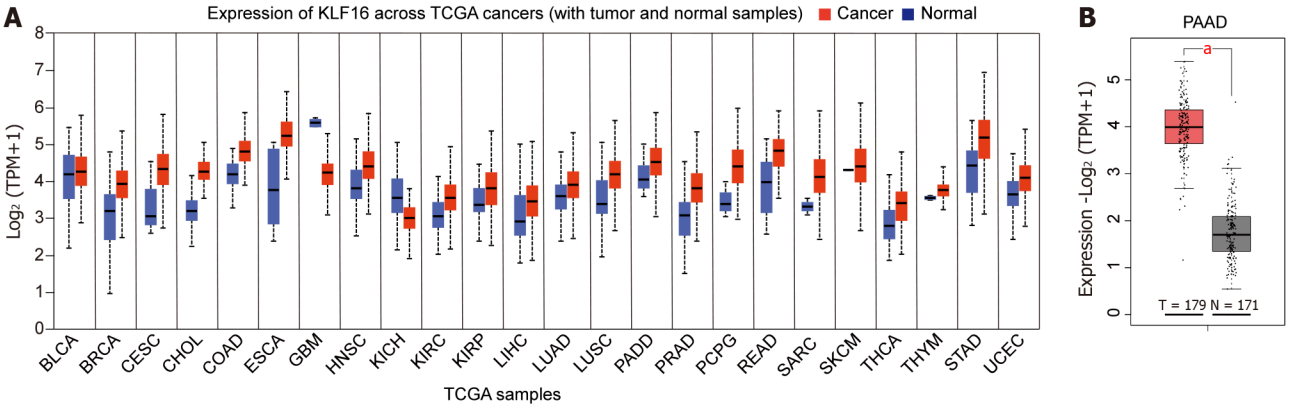

Figure 1 Krüppel-like factor 16 expression in pancreatic adenocarcinoma. A: Expression of Krüppel-like factor (KLF)16 in various The Cancer Genome Atlas (TCGA) cancers; B: Expression of KLF16 in pancreatic adenocarcinoma (PAAD) from the Gene Expression Profiling Interactive Analysis (GEPIA) database. [a]*P* < 0.05.

RNA sequencing

RNA sequencing (RNA-seq) was carried out on MIA PaCa-2 cells using the Illumina HiSeq TM 4000 (Illumina, San Diego, CA, United States. The sequencing reads were processed using the Fast-QC program. The investigation of the signaling pathway was carried out by KEGG after the KLF16 knockdown.

Tumor xenograft

Vital River Company (Beijing, China) provided the Balb/c nude mice (4-6 wk, female). MIA PaCa-2 cells were subcutaneously implanted into three different groups of nude mice (n = 5). On days 20, 25, 29, 33, 38, and 43, the tumor's volume was assessed. Tumor volume = 4/3 × π × [(length (l) + width (w)) / 4][3][11]. The mice were euthanized after 43 d, and the tumor tissues were surgically removed and studied. Every experiment that included animals was carried out in compliance with the Principles on the Protection of Experimental Animals that are outlined by the Beijing Friendship Hospital.

Analysis of the data

Data were presented as mean standard deviation and analyzed by using GraphPad Prism 8.0 software (La Jolla, CA, United States). When comparing the difference between one or more groups, Student's t test or one-way ANOVA followed by Tukey's multiple comparison test was applied. Statistical significance was considered when $P < 0.05$.

RESULTS

KLF16 is upregulated in pancreatic adenocarcinoma samples

To examine the functions of KLF16 in PAAD, we interrogated the GEPIA database (http://gepia.cancer-pku.cn) and assessed the expression of KLF16 across different tumor histocytes. We found that KLF16 was overexpressed in almost all tumors (Figure 1A). More importantly, we found that KLF16 upregulation was observed in 179 PAAD patients compared with 171 healthy subjects ($P < 0.05$; Figure 1B).

KLF16 regulates pancreatic adenocarcinoma cell proliferation

To examine if KLF16 could influence the progression of PAAD cells, we performed knockdown and overexpression studies. Firstly, we showed that KLF16 expression was significantly reduced in PAAD cells transfected with siRNAs against KLF16, indicating that the knockdown was effective (Figure 2A and 2B). The number of cell colonies and viability of PAAD cells were significantly reduced when KLF16 was knocked down (Figure 2C-F). Then overexpression experiments were conducted. The results showed that KLF16 overexpression was successful (Figure 2G and 2H). When KLF16 was overexpressed in AsPC-1 and MIA PaCa-2 cells, both the cell viability and the number of cell colonies considerably increased (Figure 2I-L). These findings indicated that KLF16 accelerated the proliferation of PAAD cells.

KLF16 regulates apoptosis and the cell cycle

We then investigated the impact of KLF16 on the PAAD cell cycle as well as the apoptotic process. Following KLF16 knockdown, an enhanced number of the cells at G0/G1 phase and a reduced number of the cells at G2/M phase were observed (Figure 3A). When KLF16 was overexpressed in cells, the opposite effects were found (Figure 3B). Apoptosis in the cells was inhibited after KLF16 overex-

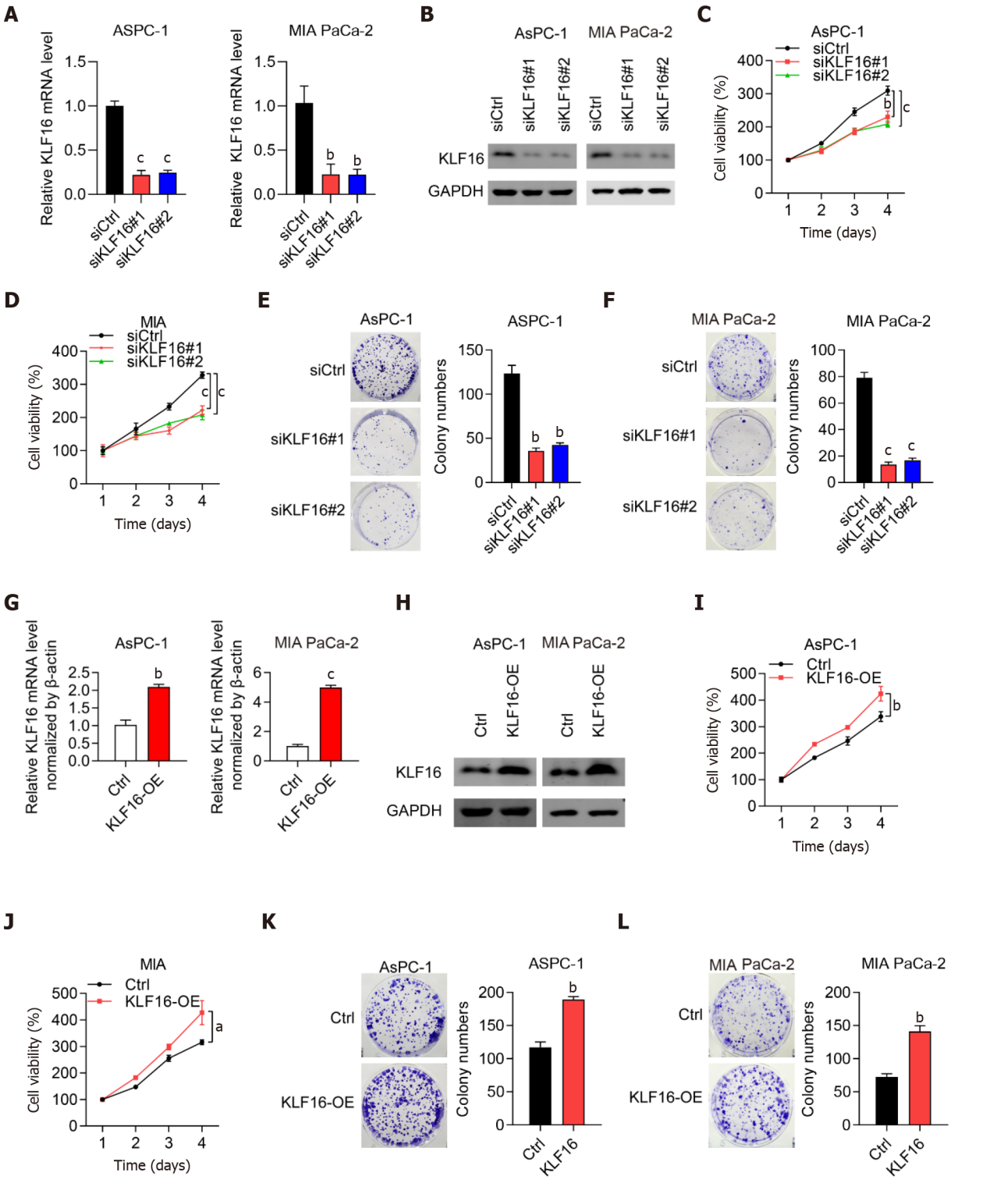

Figure 2 Krüppel-like factor 16 regulates pancreatic adenocarcinoma cell proliferation. A, B: The efficiency of Krüppel-like factor (KLF)16 knockdown in pancreatic adenocarcinoma (PAAD) cells by (A) qPCR and (B) western blotting. GAPDH used as the internal control; C, D: Cell proliferation of PAAD cells after KLF16 knockdown. (E, F) Colony numbers of PAAD cells after KLF16 knockdown; G, H: The efficiency of KLF16 overexpression in the cells by (G) qPCR and (H) western blotting. GAPDH used as the internal control; I, J: Cell proliferation of PAAD cells after KLF16 overexpression by the CCK-8 assay; K, L: Colony numbers of PAAD cells after KLF16 overexpression by colony formation assay. $^{a}P < 0.05$; $^{b}P < 0.01$; $^{c}P < 0.001$.

pression, whereas it was significantly promoted by KLF16 downregulation (Figure 3C and 3D).

KLF16 regulates pancreatic adenocarcinoma cell migration

Following that, we investigated whether KLF16 influenced the migration of cells. After KLF16 was knocked down, the amount of cell migration was dramatically reduced (Figure 4A). When KLF16 was overexpressed, the number of migrating cells increased (Figure 4B). According to these findings, KLF16 could regulate the migration of the PAAD cell.

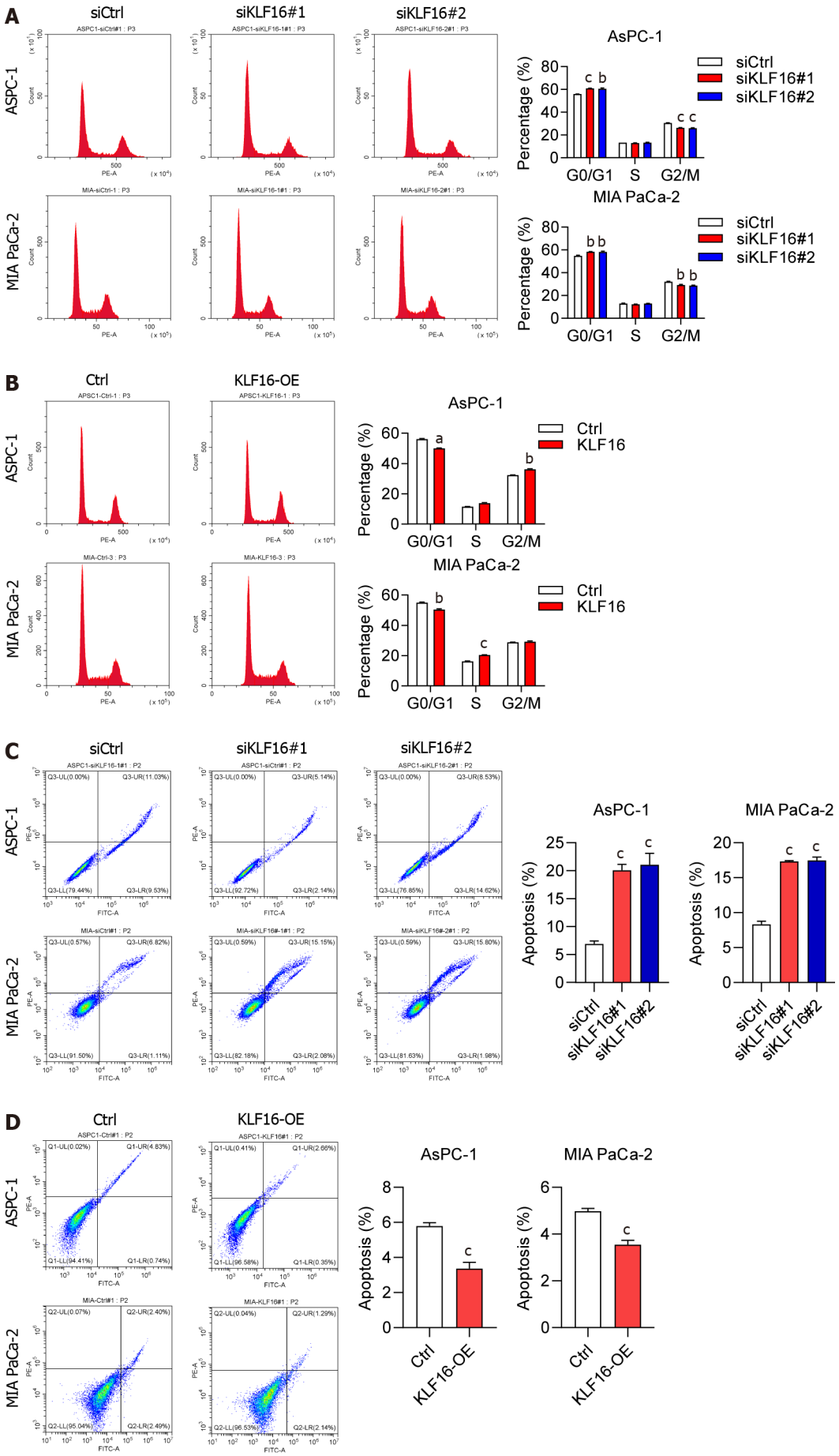

Figure 3 Krüppel-like factor 16 regulates the cell cycle progression and apoptosis in pancreatic adenocarcinoma cells. A, B: Cell cycle

progression of pancreatic adenocarcinoma (PAAD) cells with (A) Krüppel-like factor (KLF)16 knockdown or (B) KLF16 overexpression; C, D: Cell apoptosis of PAAD cells with (C) KLF16 knockdown or (D) KLF16 overexpression. $^{a}P < 0.05$; $^{b}P < 0.01$; $^{c}P < 0.001$.

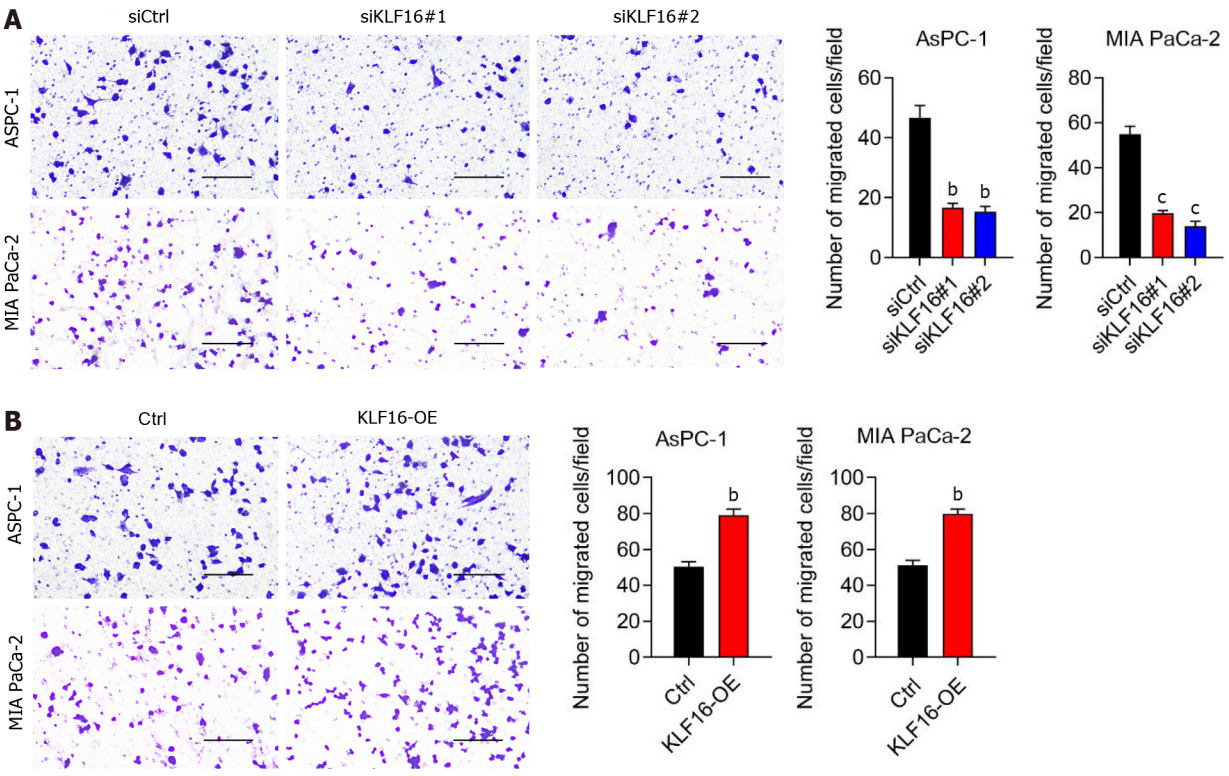

Figure 4 Krüppel-like factor 16 regulates pancreatic adenocarcinoma cell migration. A, B: Cell migration of pancreatic adenocarcinoma (PAAD) cells with (A) knockdown of Krüppel-like factor (KLF16) or (B) overexpression of KLF16 by transwell assay. Bar, 100 μm. $^{b}P < 0.01$, $^{c}P < 0.001$.

SMAD6 participates in the tumor promoting function of KLF16 in pancreatic adenocarcinoma cells

RNA-seq studies were carried out so that we could determine the pathways that KLF16 is responsible for in the development of PAAD. As shown in Figure 5A, the suppression of KLF16 in MIA PaCa-2 cells resulted in downregulation and upregulation of several genes. Figure 5B displays the top ten pathways that were discovered by cluster analysis to be associated with these genes. Autophagy-related genes were found to be among the most highly upregulated genes, while ribosome-related genes were the most highly downregulated. A highly expressed SMAD6 gene that had not been characterized before was found in PAAD. As a result, we investigated the connection between KLF16 and SMAD6. After KLF16 was either knocked down or overexpressed, respectively, we found that there was either a considerable rise or reduction in the levels of SMAD6 (Figure 5C and 5D). In addition, SMAD6 expression was increased in PAAD tissues retrieved from the TCGA database (Figure 5E). According to the findings of the study of correlation, the level of expression of KLF16 was shown to have a positive association with the level of expression of SMAD6 ($r = 0.37$; Figure 5F). Collectively, KLF16 promoted the expression of SMAD6 in PAAD cells and tissues.

SMAD6 regulated PAAD cell proliferation and migration

Following that, we explored the impact of SMAD6 on PAAD cells. qPCR was used to test the efficiency of SMAD6 knockdown or overexpression, as shown in Figure 6A. The ability of PAAD cells was suppressed by SMAD6 downregulation, while it was increased when SMAD6 was overexpressed (Figure 6B). This oncogenic function of SMAD6 was further validated by the findings that the number of migrating cells was greatly inhibited by downregulation of SMAD6 (Figure 6C) but was stimulated after SMAD6 overexpression (Figure 6D). According to these findings, SMAD6 was responsible for PAAD cell proliferation and migration.

SMAD6 knockdown rescues the effects of KLF16 overexpression in pancreatic adenocarcinoma cells

To understand how SMAD6 interacted with KLF16 overexpression, we investigated the impact of SMAD6 knockdown on KLF16-mediated PAAD. The protein level of SMAD6 was moderately elevated in MIA PaCa-2 cells transfected with KLF16 and was drastically reduced in cells transfected with KLF16+shSMAD6 (Figure 7A). The viability of MIA PaCa-2 cells improved when KLF16 was overex-

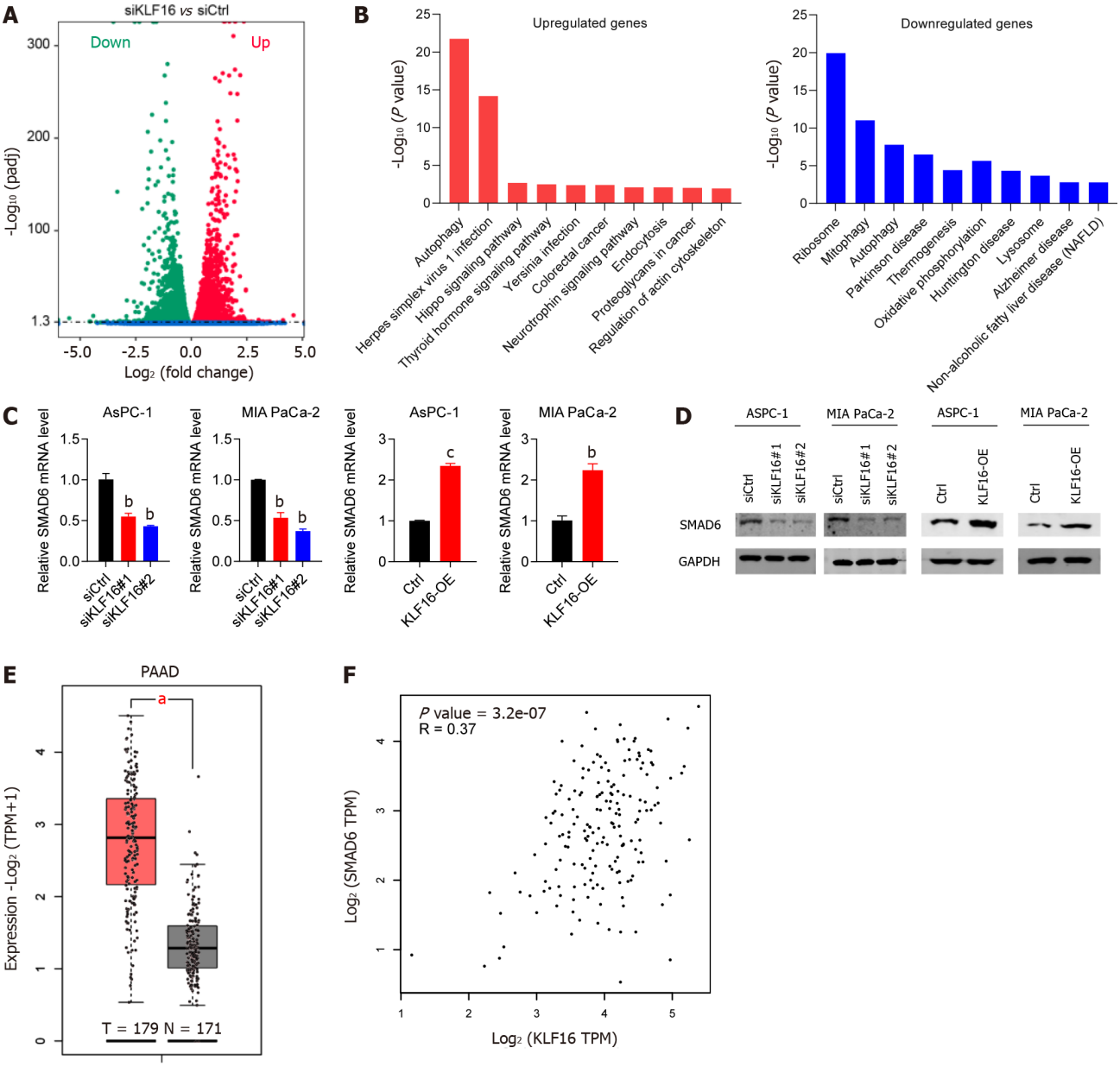

Figure 5 SMAD6 is a downstream target of Krüppel-like factor 16 in pancreatic adenocarcinoma. A: Volcano analysis of differentially expressed genes with Krüppel-like factor (KLF)16 knockdown in MIA PaCa-2 cells by RNA-seq; B: The top 10 pathways or biological processes of upregulated or downregulated genes; C and D: SMAD6 mRNA and protein levels in pancreatic adenocarcinoma (PAAD) cells with KLF16 knockdown or overexpression. GAPDH used as the internal control; E: The expression of SMAD6 in PAAD from The Cancer Genome Atlas; F: Spearman relationship between KLF16 and SMAD6 in PAAD. $^{b}P < 0.01$; $^{c}P < 0.001$.

pressed, but SMAD6 knockdown had a significant adverse effect on that viability (Figure 7B). Moreover, we overexpressed SMAD6 in the KLF16 knockdown AsPC1 cells. SMAD6 was significantly downregulated in the KLF16 knockdown cells, while the protein level of SMAD6 was rescued after SMAD6 overexpression (Figure 7C). The viability of AsPC1 cells was impaired when KLF16 was knocked down, but SMAD6 overexpression had a significant adverse effect on that viability (Figure 7D). *In vivo* tumor transplantation investigations validated these results as well, showing that the tumor size and volume of xenografts increased after KLF16 overexpression in nude mice injected with MIA PaCa-2 cells, but decreased following SMAD6 knockdown (Figure 7E-G). Overall, SMAD6 knockdown rescued the effects of KLF16 overexpression in PAAD cells.

DISCUSSION

KLF16 was highly expressed in PAAD patients based on the GEPIA database. KLF16 silencing suppressed, while KLF16 overexpression promoted the malignant function of PAAD cells. Based on RNA sequencing, we discovered that KLF16 potentiated the expression of SMAD6 in PAAD cells. SMAD6 transcript abundance was increased and positively correlated with KLF16 expression in PAAD

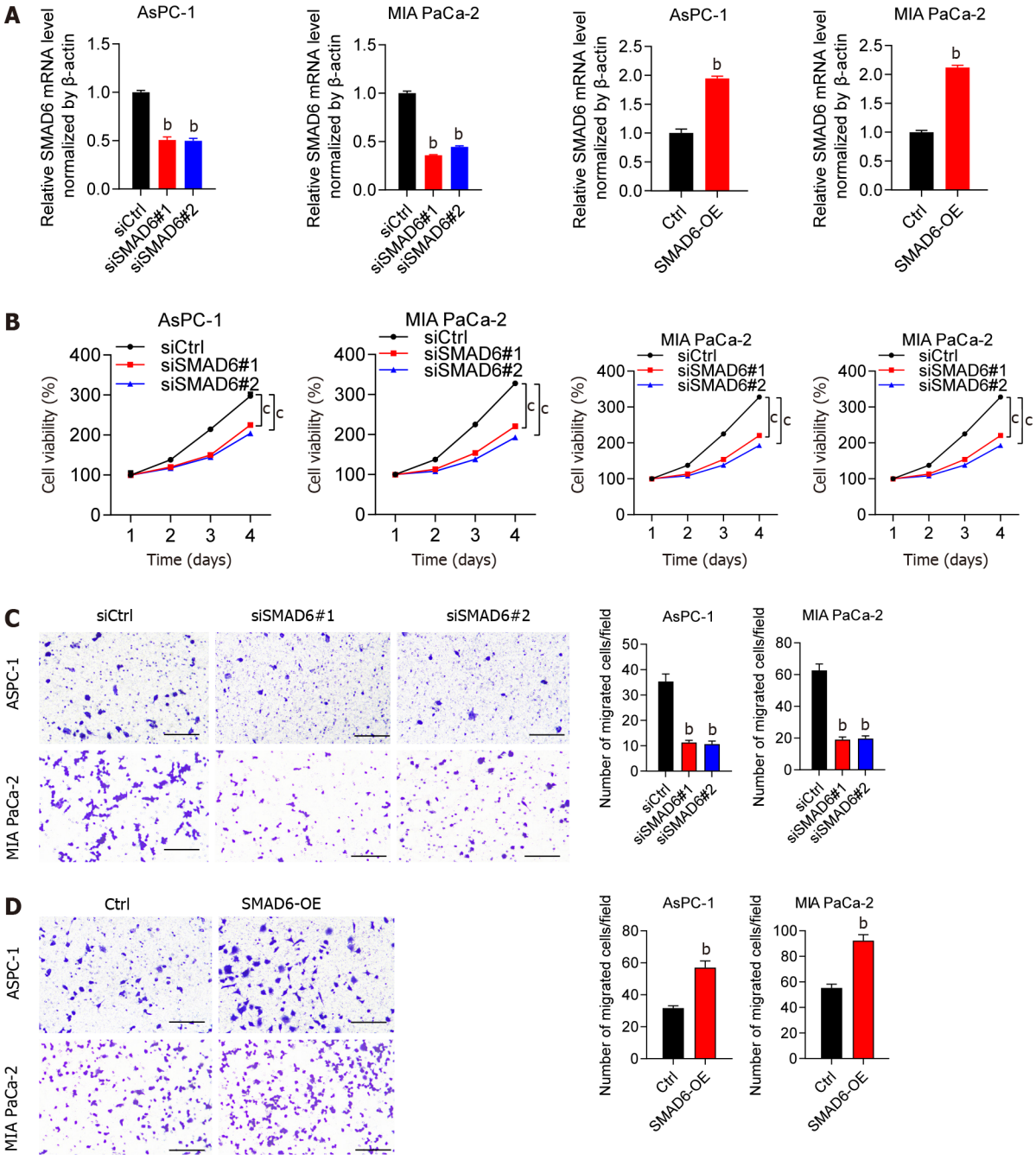

Figure 6 SMAD6 regulates pancreatic adenocarcinoma cell malignancy. A: The efficiency of SMAD6 knockdown or SMAD6 overexpression in pancreatic adenocarcinoma (PAAD) cells by qPCR; B: Cell proliferation of PAAD cells with knockdown or overexpression of SMAD6; C, D: The migration capacity of PAAD cells with (C) SMAD6 knockdown or (D) SMAD6 overexpression by transwell assay. Bar, 100 μm. $^{b}P < 0.01$; $^{c}P < 0.001$.

samples, and inhibiting SMAD6 was able to mitigate the effects of KLF16 overexpression on PAAD cell processes, suggesting the importance of SMAD6 in the development of KLF16-triggered PAAD.

Pancreatic adenocarcinoma, a very aggressive tumor of the digestive system, is difficult to diagnose and treat. PAAD is also known as pancreatic ductal adenocarcinoma, a kind of pancreatic cancer that accounts for the vast majority of cases (95%)[12]. Accumulation of genetic alterations, such as KRAS, CDKN2A/P16, TP53 and SMAD4 contributes to the progression of PAAD[13,14]. These abnormalities may be used to develop a novel effective therapy targeting PAAD.

KLFs refer to zinc finger transcription factors involved in various developmental processes through enhancing and/or repressing the expression of several genes[15]. KLF3, KLF4, KLF12 and KLF15 are only a few of the KLFs that participate in the formation and advancement of PAAD. KLF3 is a pancreatic cancer cell growth inhibitor, according to the study conducted by Wan *et al*[16]. KLF12 was found to be a miR-137 target and inhibited the cancer stem cell phenotype in pancreatic cancer cells[17]. In contrast, Zhu *et al*[18] found that downregulated Caveolin-1 by KLF4 maintained pancreatic cancer epithelial-mesenchymal transition and metastasis. As a member of KLFs, KLF16's function in PAAD is less clear. During our research, we observed that pancreatic adenocarcinoma samples and cells had

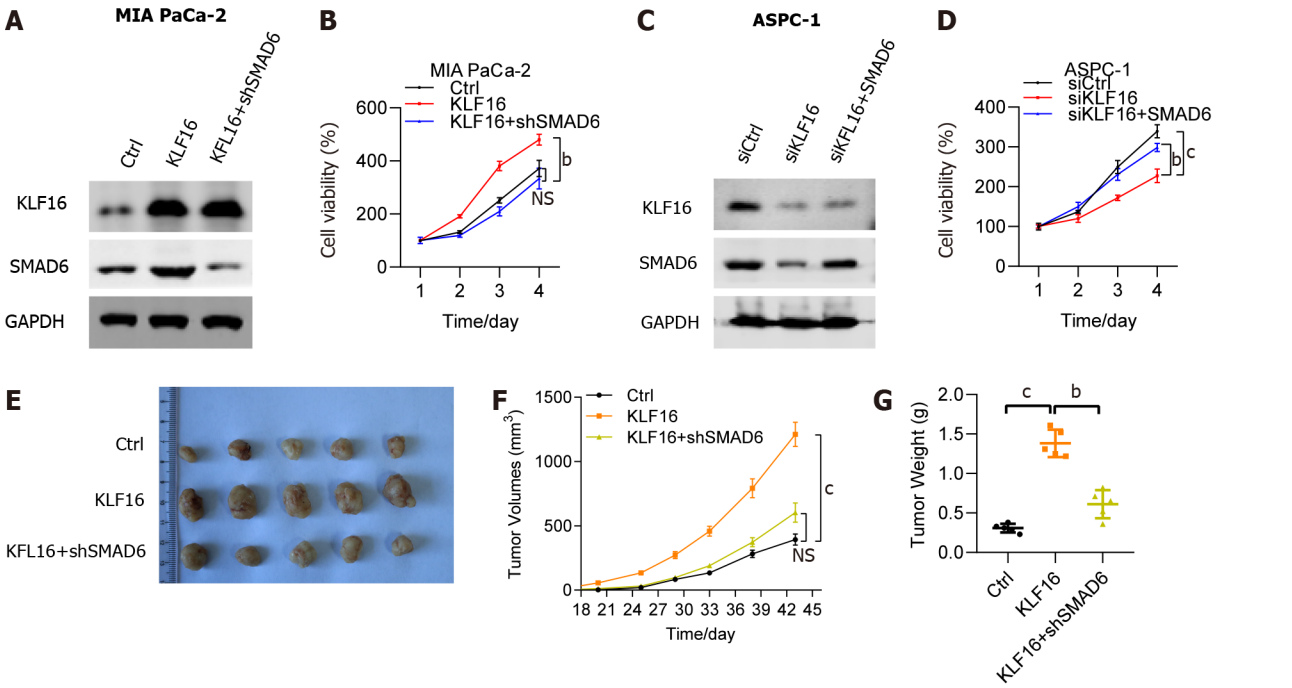

Figure 7 SMAD6 knockdown rescues the effects of Krüppel-like factor 16 overexpression on pancreatic adenocarcinoma. (A) Protein levels of Krüppel-like factor (KLF)16 and SMAD6 in control (Ctrl), KLF16, and KLF16+shSAMD6 cells by western blotting in MIA PaCa-2 cells. GAPDH used as the internal control; B: Cell viability of Ctrl, KLF16, and KLF16+shSAMD6 cells by CCK-8 assay in MIA PaCa-2 cells; C: Protein levels of KLF16 and SMAD6 in siCtrl, siKLF16, and siKLF16+SAMD6 cells by western blotting in AsPC-1 cells. GAPDH used as the internal control; D: Cell viability of siCtrl, siKLF16, and siKLF16+SAMD6 cells by the CCK-8 assay in AsPC-1 cells; E: Tumor size from three groups of nude mice that were injection with MIA PaCa-2 cells transfected with Ctrl, KLF16, and KLF16+shSAMD6, separately; F: Tumor growth curve in three groups; G: Tumor weight among the three groups. NS: Not significant. $^{b}P < 0.01$; $^{c}P < 0.001$.

elevated levels of KLF16. By completing knockdown and overexpression studies on KLF16, we were able to show that it controlled PAAD cell malignancy. These studies were carried out using PAAD cells.

SMAD6, a member of the SMAD family, was discovered in the 1990s and serves as a key mediator of the TGF signaling pathway[19,20]. In mammalian cells, eight SMAD have been discovered[21]. SMAD4 Loss predicts poor prognosis in PAAD[14], while SMAD7 has been discovered to be adversely regulated in PAAD[22]. SMAD6 was shown to be downregulated in patients with colorectal cancer[23], while its upregulation was associated with poor patient survival from lung cancer[24]. Experiments using RNA sequencing were carried out so that we could determine the specific mechanism by which KLF16 is involved in the development of PAAD. It has been reported that KLF16 acted as a transcriptional repressor[25]. In the present study, KLF16 expression was discovered to have a favorable positive correlation with SMAD6, which was considerably upregulated. In this context, it was suggested that SMAD6 is not the directed target gene of KLF16. Hence, the role of KLF16 in regulating SMAD6 expression required further experimentation. Finally, we showed that SMAD6 expression was elevated in PAAD samples as well. SMAD6 knockdown inhibited PAAD cell proliferation and migration, but SMAD6 overexpression increased PAAD cell advancement. In addition, inhibiting SMAD6 in PAAD cells reversed the effects of KLF16 overexpression. Overall, KLF16 is an oncogenic protein in PAAD that positively influence SMAD6 expression.

Although this study can fully explain the mechanism of KLF16 on the proliferation and migration of PAAD cells, the lack of prognosis information of patients makes this study limited to a certain extent. It will be further verified in human pancreatic cancer tissues in the future, so as to better support the experimental results and enhance the credibility of the study.

CONCLUSION

The role that KLF16 and SMAD6 play in PAAD was investigated in this work. Both genes carried out their oncogenic functions and contributed to the development of PAAD. Furthermore, we identified a strong correlation between KLF16 and SMAD6 expression levels. KLF16 and SMAD6 appear to have the potential to act as both a novel prognostic marker and a potential therapeutic target for PAAD, based on our findings.

ARTICLE HIGHLIGHTS

Research background

Pancreatic adenocarcinoma (PAAD) is a cancerous tumor with an extremely poor 5-year survival rate. The exploration of biomarkers for the diagnosis and treatment of PAAD is crucial in clinical practice.

Research motivation

KLF16 behaves as an oncogene in prostate, breast and gastric cancers. However, no research has been done on the significance of Krüppel-like factor 16 (KLF16) in PAAD.

Research objectives

This study aimed to explore the molecular mechanisms of KLF16 in PAAD.

Research methods

KLF16 was identified in the tumor specimens and normal tissues by GEPIA database and verified by quantitative real-time PCR (qRT-PCR). Knockdown or exogenous expression of KLF16, combined with *in vitro* and *in vivo* assays, was performed to show the functional significance of KLF16. The molecular mechanism of KLF16 was demonstrated by qRT-PCR, western blotting, immunoprecipitation assay and flow cytometry.

Research results

KLF16 was highly expressed in PAAD patients based on the GEPIA database. KLF16 silencing suppressed, while KLF16 overexpression promoted the malignant function of PAAD cells. Based on RNA sequencing, we discovered that KLF16 potentiated the expression of SMAD6 in PAAD cells. SMAD6 transcript abundance was increased and positively correlated with KLF16 expression in PAAD samples. In addition, inhibiting SMAD6 was able to mitigate the effects of KLF16 overexpression on PAAD cell processes, suggesting the importance of SMAD6 in the development of KLF16-triggered PAAD.

Research conclusions

KLF16/SMAD6 axis might be explored as a therapeutic target for PAAD therapy.

Research perspectives

KLF16 and SMAD6 appear to have the potential to act as both a novel prognostic marker and a potential therapeutic target for PAAD, based on our findings.

ACKNOWLEDGEMENTS

We would like to thank the Clinical Data and Biobank Resource of Beijing Friendship Hospital for their help with data processing.

FOOTNOTES

Author contributions: Mi W, Zheng Z, Lu JD, Duan SQ, Zhang J and Zhang HQ all contributed equally to this work; Mi W, Zheng Z, Lu JD and Duan SQ designed the study; Zhang HQ, Yin J and Zhang J performed the experiments; Zheng Z and Lu JD wrote the manuscript; Ding YX and Cao F performed statistical analysis; Li F and Zhang J revised the manuscript; All authors read and approved the final manuscript.

Institutional review board statement: The research was approved by the Ethics Committee of Beijing Friendship Hospital, Capital Medical University (No. 2018-P2-015-02). The principles outlined in the Declaration of Helsinki were adhered to throughout the course of this research project (as revised in 2013).

Institutional animal care and use committee statement: Every experiment that included animals was carried out in compliance with the Principles on the Protection of Experimental Animals that are outlined by the Beijing Friendship Hospital.

Conflict-of-interest statement: All authors report having no relevant conflict of interest for this article.

Data sharing statement: Data are available from the corresponding authors upon request.

ARRIVE guidelines statement: The authors have read the ARRIVE guidelines, and the manuscript was prepared and revised according to the ARRIVE guidelines.

Country/Territory of origin: China

ORCID number: Wei Mi 0000-0002-1330-9926; Zhi Zheng 0000-0003-0390-9466; Hai-Qiao Zhang 0000-0002-4224-7146; Jie Yin 0000-0003-2708-0111; Jun Zhang 0000-0001-5411-1273.

S-Editor: Wu YXJ
L-Editor: Filipodia
P-Editor: Yuan YY

REFERENCES

1 **Sung H**, Ferlay J, Siegel RL, Laversanne M, Soerjomataram I, Jemal A, Bray F. Global Cancer Statistics 2020: GLOBOCAN Estimates of Incidence and Mortality Worldwide for 36 Cancers in 185 Countries. *CA Cancer J Clin* 2021; **71**: 209-249 [PMID: 33538338 DOI: 10.3322/caac.21660]
2 **Ferlay J**, Partensky C, Bray F. More deaths from pancreatic cancer than breast cancer in the EU by 2017. *Acta Oncol* 2016; **55**: 1158-1160 [PMID: 27551890 DOI: 10.1080/0284186X.2016.1197419]
3 **Ottenhof NA**, Milne AN, Morsink FH, Drillenburg P, Ten Kate FJ, Maitra A, Offerhaus GJ. Pancreatic intraepithelial neoplasia and pancreatic tumorigenesis: of mice and men. *Arch Pathol Lab Med* 2009; **133**: 375-381 [PMID: 19260743 DOI: 10.5858/133.3.375]
4 **Goral V**. Pancreatic Cancer: Pathogenesis and Diagnosis. *Asian Pac J Cancer Prev* 2015; **16**: 5619-5624 [PMID: 26320426 DOI: 10.7314/apjcp.2015.16.14.5619]
5 **Philipsen S**, Suske G. A tale of three fingers: the family of mammalian Sp/XKLF transcription factors. *Nucleic Acids Res* 1999; **27**: 2991-3000 [PMID: 10454592 DOI: 10.1093/nar/27.15.2991]
6 **Pearson R**, Fleetwood J, Eaton S, Crossley M, Bao S. Krüppel-like transcription factors: a functional family. *Int J Biochem Cell Biol* 2008; **40**: 1996-2001 [PMID: 17904406 DOI: 10.1016/j.biocel.2007.07.018]
7 **Sun N**, Shen C, Zhang L, Wu X, Yu Y, Yang X, Yang C, Zhong C, Gao Z, Miao W, Yang Z, Gao W, Hu L, Williams K, Liu C, Chang Y, Gao Y. Hepatic Krüppel-like factor 16 (KLF16) targets PPARα to improve steatohepatitis and insulin resistance. *Gut* 2021; **70**: 2183-2195 [PMID: 33257471 DOI: 10.1136/gutjnl-2020-321774]
8 **Bang S**, Li J, Zhang M, Cui R, Wu X, Xin Z, Ma D, Zhang J, Zhang H. The Clinical Relevance and Function of Krüppel-Like Factor 16 in Breast Cancer. *Cancer Manag Res* 2020; **12**: 6373-6383 [PMID: 32821156 DOI: 10.2147/CMAR.S256490]
9 **Ma XD**, Xu SD, Hao SH, Han K, Chen JW, Ling H, Chen RX, Jin XH, Cao JH, Lin JL, Ou QJ, Fang YJ, Pan ZZ, Xie D, Wang FW. KLF16 enhances stress tolerance of colorectal carcinomas by modulating nucleolar homeostasis and translational reprogramming. *Mol Ther* 2022; **30**: 2828-2843 [PMID: 35524408 DOI: 10.1016/j.ymthe.2022.04.022]
10 **Chen X**, Li S, Ke Y, Wu S, Huang T, Hu W, Fu H, Guo X. KLF16 suppresses human glioma cell proliferation and tumourigenicity by targeting TFAM. *Artif Cells Nanomed Biotechnol* 2018; **46**: 608-615 [PMID: 29374989 DOI: 10.1080/21691401.2018.1431654]
11 **Lee MD**, She Y, Soskis MJ, Borella CP, Gardner JR, Hayes PA, Dy BM, Heaney ML, Philips MR, Bornmann WG, Sirotnak FM, Scheinberg DA. Human mitochondrial peptide deformylase, a new anticancer target of actinonin-based antibiotics. *J Clin Invest* 2004; **114**: 1107-1116 [PMID: 15489958 DOI: 10.1172/JCI22269]
12 **Tanaka S**. Molecular Pathogenesis and Targeted Therapy of Pancreatic Cancer. *Ann Surg Oncol* 2016; **23** Suppl 2: S197-S205 [PMID: 25749932 DOI: 10.1245/s10434-015-4463-x]
13 **Vincent A**, Herman J, Schulick R, Hruban RH, Goggins M. Pancreatic cancer. *Lancet* 2011; **378**: 607-620 [PMID: 21620466 DOI: 10.1016/S0140-6736(10)62307-0]
14 **Jones S**, Zhang X, Parsons DW, Lin JC, Leary RJ, Angenendt P, Mankoo P, Carter H, Kamiyama H, Jimeno A, Hong SM, Fu B, Lin MT, Calhoun ES, Kamiyama M, Walter K, Nikolskaya T, Nikolsky Y, Hartigan J, Smith DR, Hidalgo M, Leach SD, Klein AP, Jaffee EM, Goggins M, Maitra A, Iacobuzio-Donahue C, Eshleman JR, Kern SE, Hruban RH, Karchin R, Papadopoulos N, Parmigiani G, Vogelstein B, Velculescu VE, Kinzler KW. Core signaling pathways in human pancreatic cancers revealed by global genomic analyses. *Science* 2008; **321**: 1801-1806 [PMID: 18772397 DOI: 10.1126/science.1164368]
15 **Swamynathan SK**. Krüppel-like factors: three fingers in control. *Hum Genomics* 2010; **4**: 263-270 [PMID: 20511139 DOI: 10.1186/1479-7364-4-4-263]
16 **Wan Y**, Luo H, Yang M, Tian X, Peng B, Zhan T, Chen X, Ding Y, He J, Cheng X, Huang X, Zhang Y. miR-324-5p Contributes to Cell Proliferation and Apoptosis in Pancreatic Cancer by Targeting KLF3. *Mol Ther Oncolytics* 2020; **18**: 432-442 [PMID: 32913892 DOI: 10.1016/j.omto.2020.07.011]
17 **He Z**, Guo X, Tian S, Zhu C, Chen S, Yu C, Jiang J, Sun C. MicroRNA-137 reduces stemness features of pancreatic cancer cells by targeting KLF12. *J Exp Clin Cancer Res* 2019; **38**: 126 [PMID: 30866999 DOI: 10.1186/s13046-019-1105-3]
18 **Zhu Z**, Yu Z, Wang J, Zhou L, Zhang J, Yao B, Dou J, Qiu Z, Huang C. Krüppel-Like Factor 4 Inhibits Pancreatic Cancer Epithelial-to-Mesenchymal Transition and Metastasis by Down-Regulating Caveolin-1 Expression. *Cell Physiol Biochem*

2018; **46**: 238-252 [PMID: 29587259 DOI: 10.1159/000488426]

19 **Sekelsky JJ**, Newfeld SJ, Raftery LA, Chartoff EH, Gelbart WM. Genetic characterization and cloning of mothers against dpp, a gene required for decapentaplegic function in Drosophila melanogaster. *Genetics* 1995; **139**: 1347-1358 [PMID: 7768443 DOI: 10.1093/genetics/139.3.1347]

20 **Derynck R**, Gelbart WM, Harland RM, Heldin CH, Kern SE, Massagué J, Melton DA, Mlodzik M, Padgett RW, Roberts AB, Smith J, Thomsen GH, Vogelstein B, Wang XF. Nomenclature: vertebrate mediators of TGFbeta family signals. *Cell* 1996; **87**: 173 [PMID: 8861901 DOI: 10.1016/s0092-8674(00)81335-5]

21 **Singh P**, Wig JD, Srinivasan R. The Smad family and its role in pancreatic cancer. *Indian J Cancer* 2011; **48**: 351-360 [PMID: 21921337 DOI: 10.4103/0019-509X.84939]

22 **Wang Y**, Yang Y, Wang Y, Li X, Xiao Y, Wang W. High Cancer Susceptibility Candidate 8 Expression Is Associated With Poor Prognosis of Pancreatic Adenocarcinoma: Validated Analysis Based on Four Cancer Databases. *Front Cell Dev Biol* 2020; **8**: 392 [PMID: 32582694 DOI: 10.3389/fcell.2020.00392]

23 **Zhang Z**, Wang L, Wang Q, Zhang M, Wang B, Jiang K, Ye Y, Wang S, Shen Z. Molecular Characterization and Clinical Relevance of RNA Binding Proteins in Colorectal Cancer. *Front Genet* 2020; **11**: 580149 [PMID: 33193701 DOI: 10.3389/fgene.2020.580149]

24 **Jeon HS**, Dracheva T, Yang SH, Meerzaman D, Fukuoka J, Shakoori A, Shilo K, Travis WD, Jen J. SMAD6 contributes to patient survival in non-small cell lung cancer and its knockdown reestablishes TGF-beta homeostasis in lung cancer cells. *Cancer Res* 2008; **68**: 9686-9692 [PMID: 19047146 DOI: 10.1158/0008-5472.CAN-08-1083]

25 **Yao W**, Jiao Y, Zhou Y, Luo X. KLF13 suppresses the proliferation and growth of colorectal cancer cells through transcriptionally inhibiting HMGCS1-mediated cholesterol biosynthesis. *Cell Biosci* 2020; **10**: 76 [PMID: 32523679 DOI: 10.1186/s13578-020-00440-0]

World Journal of Gastrointestinal Oncology

Submit a Manuscript: https://www.f6publishing.com

World J Gastrointest Oncol 2022 November 15; 14(11): 2170-2182

DOI: 10.4251/wjgo.v14.i11.2170

ISSN 1948-5204 (online)

ORIGINAL ARTICLE

Basic Study

MiR-30e-3p inhibits gastric cancer development by negatively regulating THO complex 2 and PI3K/AKT/mTOR signaling

Xiao-Jing Gu, Ya-Jun Li, Fang Wang, Ting Ye

Specialty type: Gastroenterology and hepatology

Provenance and peer review: Unsolicited article; Externally peer reviewed.

Peer-review model: Single blind

Peer-review report's scientific quality classification

Grade A (Excellent): 0
Grade B (Very good): B
Grade C (Good): C, C
Grade D (Fair): 0
Grade E (Poor): 0

P-Reviewer: Liu YQ, United States; Tanabe S, Japan

Received: July 15, 2022
Peer-review started: July 15, 2022
First decision: August 8, 2022
Revised: September 5, 2022
Accepted: October 12, 2022
Article in press: October 12, 2022
Published online: November 15, 2022

Xiao-Jing Gu, Ya-Jun Li, Fang Wang, Ting Ye, Department of Gastroenterology, General Hospital of Ningxia Medical University, Yinchuan 750004, Ningxia Hui Autonomous Prefecture, China

Corresponding author: Ya-Jun Li, Doctor, DPhil, Chief Doctor, Department of Gastroenterology, General Hospital of Ningxia Medical University, No. 804 Shengli South Street, Xingqing District, Yinchuan 750004, Ningxia Hui Autonomous Prefecture, China. lyajundoc@126.com

Abstract

BACKGROUND

Gastric cancer (GC) is a common type of digestive cancer with high morbidity and mortality rates worldwide. Considerable effort has been expended in understanding the mechanism of GC development and metastasis. The current study therefore explores the involvement of microRNAs in the regulation of GC progression.

AIM

To explore the expression and function of miR-30e-3p in GC development.

METHODS

MiR-30e-3p was found to be downregulated in GC, with low levels thereof predicting poor outcomes among patients with GC. Functionally, we revealed that miR-30e-3p suppressed cell growth and metastatic behaviors of GC cells. Bioinformatics analysis predicted that THO complex 2 (THOC2) was a direct target of miR-30e-3p, and the interaction between miR-30e-3p and THOC2 was further validated by a luciferase reporter assay.

RESULTS

Our findings revealed that knockdown of THOC2 inhibited the growth and metastatic behaviors of GC cells. After investigating signaling pathways involved in miR-30e-3p regulation, we found that the miR-30e-3p/THOC2 axis regulated the PI3K/AKT/mTOR pathway in GC.

CONCLUSION

Our findings suggest the novel functional axis miR-30e-3p/THOC2 is involved in GC development and progression. The miR-30e-3p/THOC2 axis could be utilized to develop new therapies against GC.

Key Words: Gastric cancer; MiR-30e-3p; THO complex2; PI3K/AKT/mTOR signaling

Core Tip: Gastric cancer (GC) is a common digestive cancer with high morbidity and mortality rates worldwide. Considerable effort has been expended in understanding the mechanism of GC development and metastasis. Given that microRNAs have been found to participate in the regulation of GC progression, we explored the expression and function of miR-30e-3p in GC development and revealed that knockdown of THO complex 2 (THOC2) inhibited the growth and metastatic behaviors of GC cells. After investigating signaling pathways involved in miR-30e-3p regulation were investigated, we found that the miR-30e-3p/THOC2 axis regulated the PI3K/AKT/mTOR pathway in GC.

Citation: Gu XJ, Li YJ, Wang F, Ye T. MiR-30e-3p inhibits gastric cancer development by negatively regulating THO complex 2 and PI3K/AKT/mTOR signaling. *World J Gastrointest Oncol* 2022; 14(11): 2170-2182
URL: https://www.wjgnet.com/1948-5204/full/v14/i11/2170.htm
DOI: https://dx.doi.org/10.4251/wjgo.v14.i11.2170

INTRODUCTION

Gastric cancer (GC) is a common type of digestive cancer with high morbidity and mortality rates worldwide[1]. *Helicobacter pylori* (*H. pylori*) infection has been considered the most significant risk factor for GC, especially in China[2,3]. Nonetheless, the incidence of GC has substantially declined with improvements in the treatment of *H. pylori* infection over the past decades[4]. Technical advances of diagnosis and therapy improve the survival of patients with GC[5,6]. However, the prognosis remains unsatisfactory as patients with GC are mostly diagnosed at later stages and develop drug-resistance after treatment. Thus, it is essential to understand the tumorigenesis of GC and identify novel early diagnostic biomarkers and therapeutic targets for its treatment.

MicroRNAs (miRNAs) are small non-coding RNAs that participate in various biological processes[7]. Mounting evidence has shown that miRNA regulates tumorigenesis of multiple cancers, including GC [8,9]. MiRNAs exert their functions in GC development and metastasis by modulating tumor cell growth and malignancy[10]. For instance, miR-181a acts as an oncogenic miRNA in GC by negatively regulating caprin-1 expression, and overexpression of miR-181a predicts poor patient survival[11]. In contrast, microRNA profiling has identified that miR-6165 is a tumor suppressor and inhibits GC progression by regulating STRN4[12]. Moreover, miRNAs can be utilized as biomarkers for GC diagnosis and patient prognosis[13]. Our preliminary screening identified low miR-30e-3p expression in GC tissues. It has been reported that miR-30e-3p suppressed clear cell renal cell carcinoma (ccRCC) development and metastasis *via* targeting snail 1[14]. Nevertheless, the function of miR-30e-3p in GC has yet to be studied.

THO complex 2 (THOC2) is an RNA-binding protein involved in mRNA export, genomic stability, and mitotic progression[15]. THOC2 is essential for the early embryonic development of zebrafish[16]. Zhou *et al*[17] reported that THOC2 serves as an oncogene in melanoma and that knockdown of THOC2 inhibits the growth and metastasis of melanoma. Nevertheless, the function and regulation of THOC2 in GC remain unclear.

In the current study, we showed that miR-30e-3p was downregulated in GC tissues and cell lines, and low miR-30e-3p levels predicted unfavorable prognosis in patients with GC. Overexpression of miR-30e-3p suppressed the malignant behaviors of GC cells by negatively regulating THOC2. We also confirmed that the miR-30e-3p/THOC2 axis regulated the PI3K/AKT/mTOR pathway in GC. These findings indicate that miR-30e-3p/THOC2 could serve as a novel diagnosis biomarker and therapeutic target for GC treatment.

MATERIALS AND METHODS

Patient tissues

Human GC tissues and matched adjacent tissues (20 pair) were obtained during surgery on patients with GC at General Hospital of Ningxia Medical University. The primary clinicopathological features of the patients are summarized in Supplementary Table 1. The tissues were stored in liquid nitrogen until further use. All tissue samples were validated by two independent pathologists. All patients participating in the study provided written informed consent. The Institutional Review Board and ethics

committee of Ningxia Medical University reviewed and approved the protocol.

Cell culture

Human GC cells (MGC803, AGS, MKN45, and BGC-823) and control human GES-1 cells were obtained from American Type Culture Collection (ATCC, VA, United States) and cultured following the guidelines provided by ATCC in an incubator at 37 °C and 5% CO_2.

Quantitative real-time polymerase chain reaction

RNA from tissue specimens or cells were extracted using Trizol (Thermo Scientific, United States) and reverse-transcribed into cDNA using the TaqMan microRNA RT Kit (Thermo Scientific, United States). Quantitative real-time polymerase chain reaction (qRT-PCR) was conducted using the PowerUP SYBR Master Mix (Applied Biosystems, United States). The $2^{-\Delta\Delta CT}$ method was used to calculate the relative expression of miR-30e-3p or THOC2. The sequences of primers were as follows: miR-30e-3p: 5′-GCGTCTTTCAGTCGGATGTTTACAGC-3′; COLEC12: 5′-TCTCCTCCGTCAGTAACCGT-3′, and 5′-CAGGCTTGATTGACACTGGC-3′; CNPY2: 5′-GGCCACTCCTATTCTACGGC-3′, and 5′-CATCC-AAAGCCAGAGTGAGC-3′; YTHDF3: 5′-CGAGAAGCAGAGAGCGAGAG-3′, and 5′-TACTG-CTAATGCCAGGCACC-3′; SLC25A33: 5′-TGTGCCTCCTGCATTGCTTA-3′, and 5′-TCTGC-AGTTCTA-GGGCAGGT-3′; NPY2R: 5′-CGAGGTCCAGGTCAGTTGTA-3′, and 5′-TACTGTGCGCATGCTCTTGA-3′; CDKN1B: 5′-AGTGTCTAACGGGAGCCCTA-3′, and 5′-AAGAATCGTCGGTTGCAGGT-3′; C20orf202: 5′-GTGCTCTAGTGCTCTGGCAA-3′, and 5'-CATCTGTTGTGTGGCCCTCT-3′; THOC2: 5′-TATGGGCTACTCTGGGCAGT-3′, and 5'-TAAGTCCGGTGGCACTTCAC-3′.

Transfection

MiR-30e-3p mimics (5′-CUUUCAGUCGGAUGUUUACAGC-3′), miR-30e-3p inhibitors (5′-CTGTAAA-CATCCGACTGAAA-3′), and the relative negative controls (5′-UCACAACCUCCUAGAAA-GAGUAGA-3′) were purchased from GenePharma (Shanghai, China). SiRNA targeting THOC2 (siRNA1: CGAAUUUUUGCAUUUAUGUCG-3′, siRNA1: 5′-CAUGAUAGUUCAACAUACAGA-3′) and scramble negative control (5′-UUCUCCGAACGUGUCACGUTT-3′) were obtained from Gene-Copoeia (Shanghai, China). Transfection was conducted using FuGene HD (Roche, Switzerland).

Cell growth assays

Cell growth was assessed using a colony formation assay and CCK-8 assay as previously described[18].

Transwell assay

Transwell assay was conducted using a transwell 24-well plate (Corning, United States) with or without matrigel precoating (BD Bioscience, United States). Cells were suspended in medium without serum and added into the upper chamber. The bottom chamber was filled with 500 μL complete medium. After 48 h, the migration or invasive cells were fixed, stained with crystal violet, and then calculated.

Luciferase reporter assay

The putative WT or mutated 3′-UTR of THOC2 was cloned into the pGL3 plasmid (Promega, United States). The luciferase reporter vector and control Renilla vector were co-transfected into AGS or BGC-823 cells with miR-30e-3p mimics or control. The relative luciferase activity was assessed 48 h later using the Dual-Glo kit (Promega, United States).

Western blot

Protein lysate preparation, SDS-PAGE, and Western blot were performed following the standard protocol. The following primary antibodies were used: THOC2 (ab129485) from Abcam, United States and mTOR (#2983), Akt (#4685), and PI3K (#17366) from Cell Signaling Technology, United States. E-cadherin (20874-1-AP), N-cadherin (22018-1-AP), vimentin (10366-1-AP), CNPY2 (14635-1-AP), YTHDF3 (25537-1-AP), SLC25A33 (17794-1-AP), CDKN1B (25614-1-AP), and β-actin (81115-1-RR) were purchased from Proteintech; COLEC12 (SAB1403383) was purchased from Sigma; and was purchased from NPY2R (PA5-102110) from Invitrogen.

Tumor implantation in vivo

Four-week-old male BALB/c nude mice were obtained from Jiangsu Aniphe Biolaboratory Inc. The guidelines for the animal studies were approved by the Animal Care Committee of Ningxia Medical University Hospital. BGC-823 cells were selected for tumor implantation. Around 48 h after transfection of miR-30e-3p mimic, approximately 1 ×10^7 BGC-823 cells were harvested and implanted subcutaneously into the nude mice.

Statistical analysis

All results were presented as mean ± SD. Statistical analysis was conducted using GraphPad Prism V6.0 (GraphPad, United States). Student *t*-test or one-way ANOVA was used as necessary. A $P < 0.05$

indicated statistical significance.

RESULTS

MiR-30e-3p expression is downregulated in patients with GC and low expression of miR-30e-3p predicts poor outcome

We first examined the miR-30e-3p expression in several GC cell lines. As detailed in Figure 1A, miR-30e-3p levels were lower in GC cells (MGC803, AGS, MKN45, and BGC-823) than in control GES-1 cells. Additionally, we demonstrated that miR-30e-3p expression was much lower in GC tissues than in matched adjacent non-tumor tissues (Figure 1B). Kaplan–Meier survival analysis suggested that patients with low miR-30e-3p expression had worse overall survival rate compared to those with high miR-30e-3p expression (Figure 1C). Thus, miR-30e-3p might function as a tumor suppressor in GC.

Overexpression of miR-30e-3p suppresses the malignant behaviors of GC cells

To explore miR-30e-3p function in GC, we transfected miR-30e-3p mimics into AGS or BGC-823 cells, after which the overexpression of miR-30e-3p was validated using qRT-PCR (Figure 2A). Functionally, we found that miR-30e-3p overexpression suppressed cell proliferation and colony formation of AGS or BGC-823 (Figure 2B and C). Furthermore, transfection of miR-30e-3p mimics resulted in decreased metastatic abilities of GC cells, with lesser cell migration or invasion (Figure 2D and E). In addition, transfection of miR-30e-3p mimics increased E-cadherin expression but decreased the expression of N-cadherin and vimentin (Figure 2F). These findings suggest that overexpression of miR-30e-3p suppresses the growth and metastatic behaviors of GC cells.

Inhibition of miR-30e-3p promotes the malignant behaviors of GC cells

Conversely, we utilized miR-30e-3p inhibitors to suppress miR-30e-ep expression in GC cells (Figure 3A). MiR-30e-3p inhibitors also dampened the cell proliferation of GC cells (Figure 3B). Inhibition of miR-30e-3p promoted a higher colony number in AGC or SGC-823 cells compared with the control or negative control group (Figure 3C). Consistently, inhibition of miR-30e-3p enhanced GC cell migration and invasion (Figure 3D and E). In addition, transfection of miR-30e-3p inhibitors suppressed E-cadherin expression but promoted N-cadherin and Vimentin expression (Figure 3F). Taken together, both the overexpression and knockdown experiments demonstrated that miR-30e-3p negatively regulated GC cell growth and metastasis.

THOC2 is a direct target of miR-30e-3p in GC cells

Bioinformatics analysis identified THOC2 as a top candidate of miR-30e-3p (Figure 4A and Supplementary Table 2). Overexpression of miR-30e-3p inhibitor significantly promoted CNPY2, YTHDF3, SLC25A33, C20orf202, and THOC2 expression, among which THOC2 demonstrated the greatest upregulation (Figure 4B). After also detecting the protein levels of these potential target genes, we found that the results were consistent with the mRNA expression level of these genes (Figure 4C and D). Moreover, suppression of miR-30e-3p also upregulated THOC2 expression in GES-1 cells (Figure 4E), suggesting that miR-30e-3p could bind to the 3′-URT of THOC2 (Figure 4F). Luciferase reporter assay further confirmed the binding between miR-30e-3p and the wild-type 3′-UTR of THOC2 (Figure 4F). We found that THOC2 expression was significantly higher in GC cells than in GES-1 cells (Figure 4G). Furthermore, both THOC2 mRNA and protein levels were markedly enhanced in GC tissues (Figure 4H–J). THOC2 expression was negatively associated with miR-30e-3p expression in GC tissues (Figure 4J). Hence, THOC2 is a direct target of miR-30e-3p in GC cells.

Knockdown of THOC2 suppresses the malignant behaviors of GC cells

To evaluate the function of THOC2 in GC, we silenced THOC2 expression in AGS or BGC-823 cells using siRNA targeting THOC2 (Figure 5A). THOC2 knockdown significantly dampened colony formation and cell viability of GC cells (Figure 5B and 5C). The CCK-8 assay showed that knockdown of THOC2 significantly inhibited GC cells proliferation (Figure 5D). Furthermore, the metastasis behaviors of GC cells transfected with siTHOC2 were drastically inhibited (Figure 5E-H). In addition, silencing THOC2 significantly increase E-cadherin expression but decreased the expression of N-cadherin and Vimentin in AGS and BGC-823 cells (Figure 5I). In summary, the provided data indicated that knockdown of THOC2 suppresses the malignant behaviors of GC cells.

MiR-30e-3p/THOC2 axis regulates the PI3K/AKT/mTOR pathway in GC cells

A previous study has demonstrated that the THO complex participates in the modulation of the *p53* and PI3K/AKT pathways[19]. As such, we examined the PI3K/AKT/mTOR pathway in GC and analyzed the functional role of miR-30e-3p/THOC2. As shown in Figure 6A and B, inhibition of miR-30e-3p enhanced PI3K/AKT/mTOR expression, whereas overexpression of miR-30e-3p using miR-30e-3p mimics significantly decreased the expression of PI3K/AKT/mTOR in AGS or BGC-823 cells.

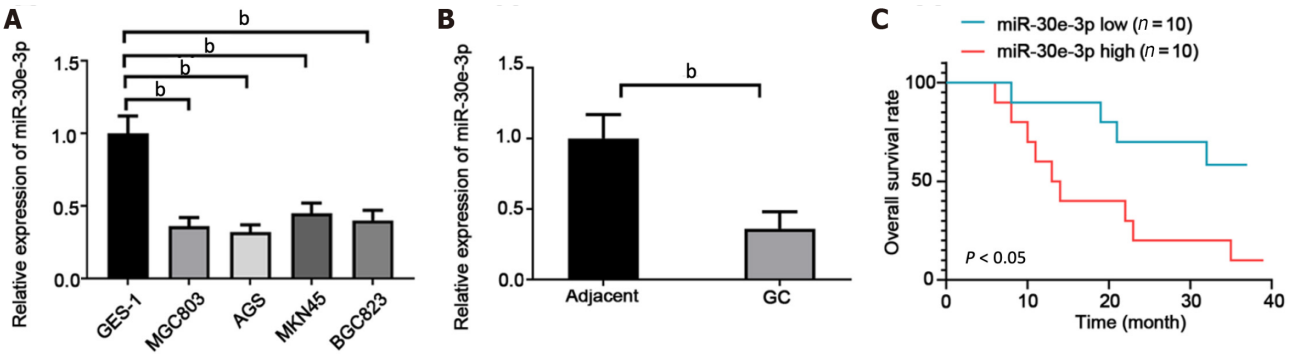

Figure 1 MiR-30e-3p expression is downregulated in gastric cancer and low expression of miR-30e-3p predicts poor outcome of gastric cancer patients. A: Quantitative real-time polymerase chain reaction (RT-PCR) was performed to analyze the expression of miR-30e-3p in normal human gastric epithelium cell line and four human gastric cancer (GC) cell lines (AGS, MGC803, BGC-823, and MKN45). n = 3 for each group; B: Quantitative RT-PCR was performed to analyze the expression of miR-30e-3p in GC and adjacent non-cancerous tissues. n = 20 for each group; C: Kaplan-Meier survival analysis of prognosis in GC patients with high or low expression of miR-30e-3p. n = 10 for each group. Error bars represented the mean ± SD of more than two independent experiments. $^{b}P < 0.01$.

Additionally, we demonstrated that THOC2 knockdown inhibited the expression of PI3K/AKT/mTOR (Figure 6C and D). Moreover, a restoration assay designed by our group showed that inhibition of miR-30e-3p interfered with THOC2 siRNA and that miR-30e-3p played a regulatory role by directly targeting THOC2 to regulate PI3K/AKT/mTOR signaling pathway in gastric cancer (Figure 6E and F). Thus, miR-30e-3p/THOC2 might regulate GC cell growth and metastasis by modulating the PI3K/AKT/mTOR signaling pathway.

MiR-30e-3p inhibits GC cells growth in vivo

To investigate the function of miR-30e-3p on GC cell growth *in vivo,* BGC-823 cells transfected with miR-30e-3p mimics after 48 h were injected subcutaneously into BALB/c nude mice. After 16 d, the growth status of the tumor was analyzed. The tumor diameter of the miR-30e-3p mimic group was significantly smaller than that of the control group (Figure 7A). The tumor volume and weight of the miRNA mimic group were smaller than that of the control group (Figure 7B and C). In addition, we also detected the protein expression of THOC2, the target gene of miR-30e-3p, and genes associated with the PI3K/AKT/mTOR signaling pathway (Figure 7D). Accordingly, we found that the protein expression of these genes was consistent with that *in vitro*. Taken together, the presented data showed that miR-30e-3p inhibits GC cells growth *in vivo*.

DISCUSSION

Accumulating evidence has revealed that miRNAs play important regulatory roles in GC development and metastasis[20]. MiRNAs can also serve as non-invasive diagnostic biomarkers for GC[21]. In line with this, the current study sought to further investigate the expression and function of miR-30e-3p. Notably, we found that miRNA-30e-3p functioned as a tumor suppressor in GC and that miR-30e-3p overexpression inhibited GC cell growth and invasion. Additionally, we identified that THOC2 was a target of miR-30e-3p and that knockdown of THOC2 suppressed the malignant behaviors of GC cells. Taken together, our results demonstrated that miR-30e-3p/THOC2 could be utilized to develop new diagnostic biomarker and therapeutic target for GC treatment.

The current study found that GC tissues and cells had lower miR-30e-3p levels compared to matched normal tissues and control cells. Previous studies have shown that miR-30e-3p expression decreased in hepatocellular carcinoma (HCC) and that miR-30e-3p regulated HCC development by modulating MDM2/TP53 signaling[22]. Moreover, low expression of miR-30e-3p in HCC predicted drug-resistance to sorafenib treatment[22]. Similarly, evidence has shown that miR-30e inhibited breast cancer development and progression by targeting IRS1, and low miR-30e expression mediated the chemosensitivity of paclitaxel treatment in breast cancer[23]. We also showed that miR-30e-3p decreased GC cell proliferation, migration, and invasion. Low levels of miR-30e-3p in patients with GC indicated poor prognosis. Thus, miR-30e-3p functions as a tumor suppressor in GC. However, further investigations are needed to determine whether miR-30e-3p exerts regulatory effects on drug sensitivity during GC treatment. One intriguing finding of the current stud was the regulation of miR-30e-3p expression in GC. In ovarian cancer, lncRNA MEG3 had been found to sponge miR-30e-3p and regulate LAMA4 expression[24].

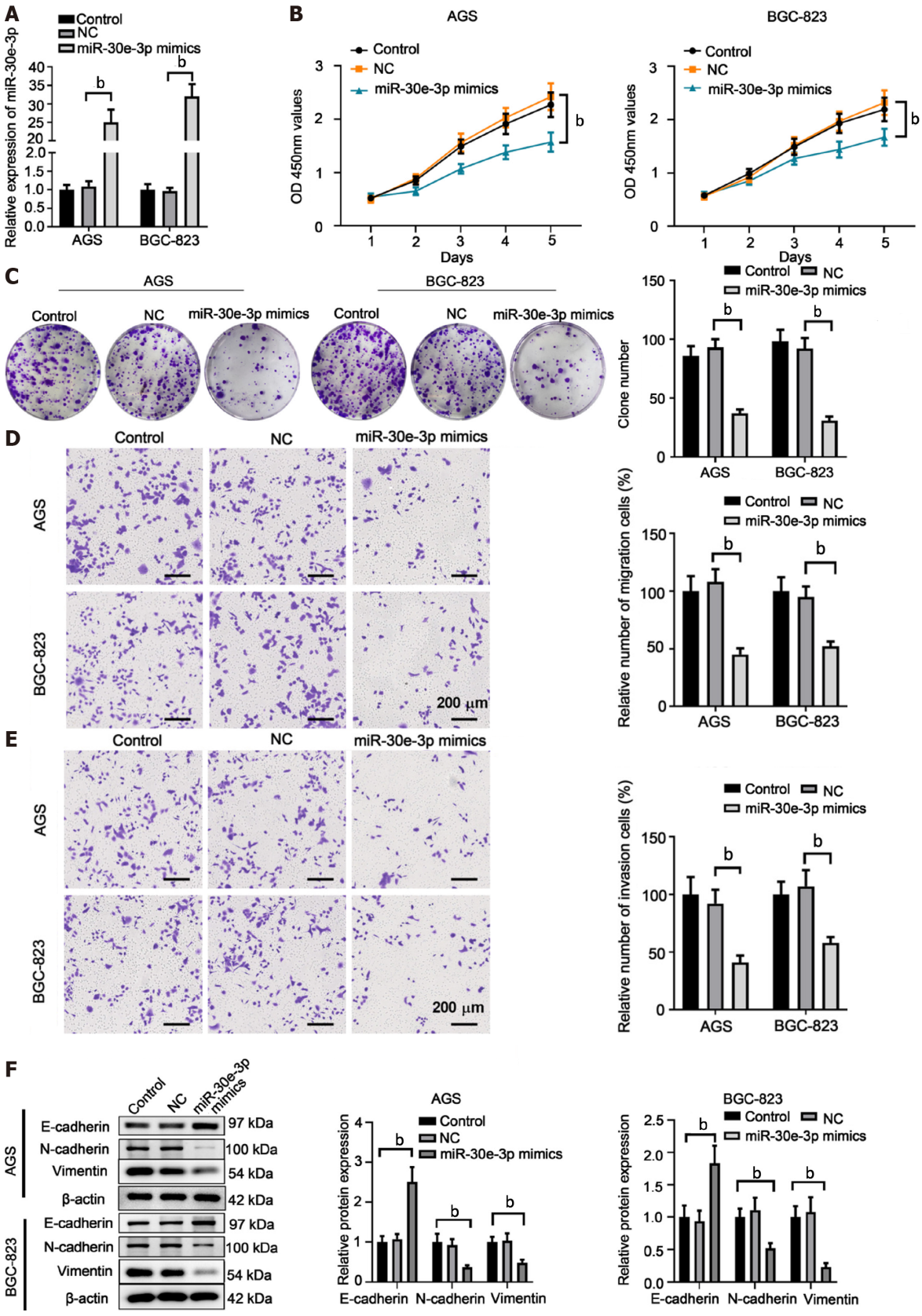

Figure 2 Overexpression of miR-30e-3p suppresses the malignant behaviors of gastric cancer cells. AGS or BGC-823 cells were transfected with negative control, miR-30e-3p mimics, or left untreated (control). A: Quantitative real-time polymerase chain reaction was performed to analyze miR-30e-3p expression levels in AGS or BGC-823 cells 48 h post transfection; B: CCK-8 assay was conducted to evaluate cell viability; C: Colony formation assay was conducted to evaluate the cell proliferation; D and E: Transwell assay was conducted using transwell chamber with or without matrigel to evaluate the cell migration (D) and invasion (E); F: Expression of E-cadherin, N-cadherin, and vimentin in AGS or BGC-823 was determined using western blotting. $n = 3$ for each group. $^{b}P < 0.01$.

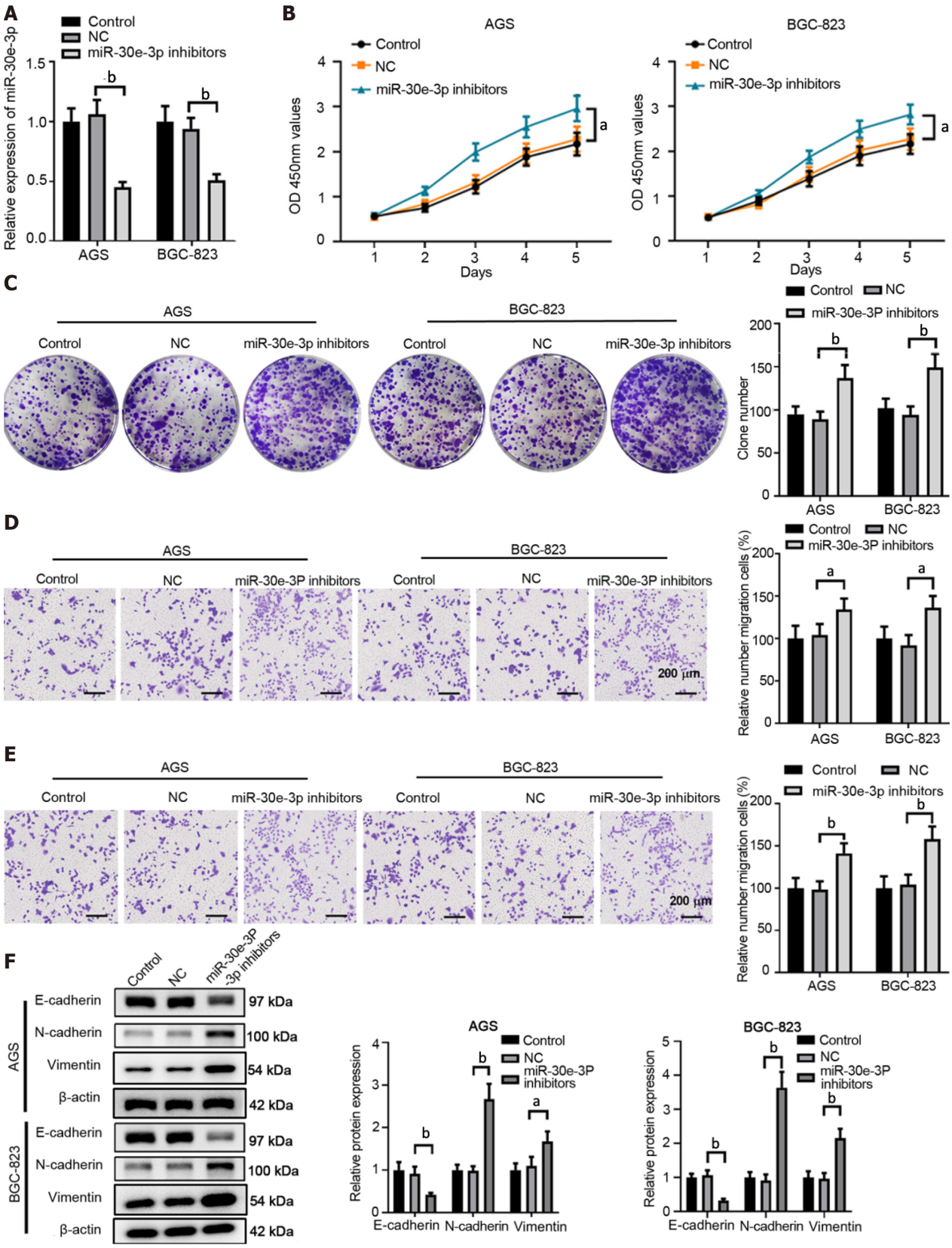

Figure 3 Inhibition of miR-30e-3p promotes the malignant behaviors of gastric cancer cells. AGS or BGC-823 cells were transfected with negative control, miR-30e-3p inhibitors, or left untreated (control). A: Quantitative real-time polymerase chain reaction was performed to analyze miR-30e-3p expression levels in AGS or BGC-823 cells 48 hours post transfection; B: CCK-8 assay was conducted to evaluate cell viability; C: Colony formation assay was conducted to evaluate the cell proliferation; D and E: Transwell assay was conducted using transwell chamber with or without matrigel to evaluate the cell migration (D) and invasion (E); F: Expression of E-cadherin, N-cadherin, and vimentin in AGS or BGC-823 was determined using western blotting. n = 3 for each group. $^{a}P < 0.05$, $^{b}P < 0.01$.

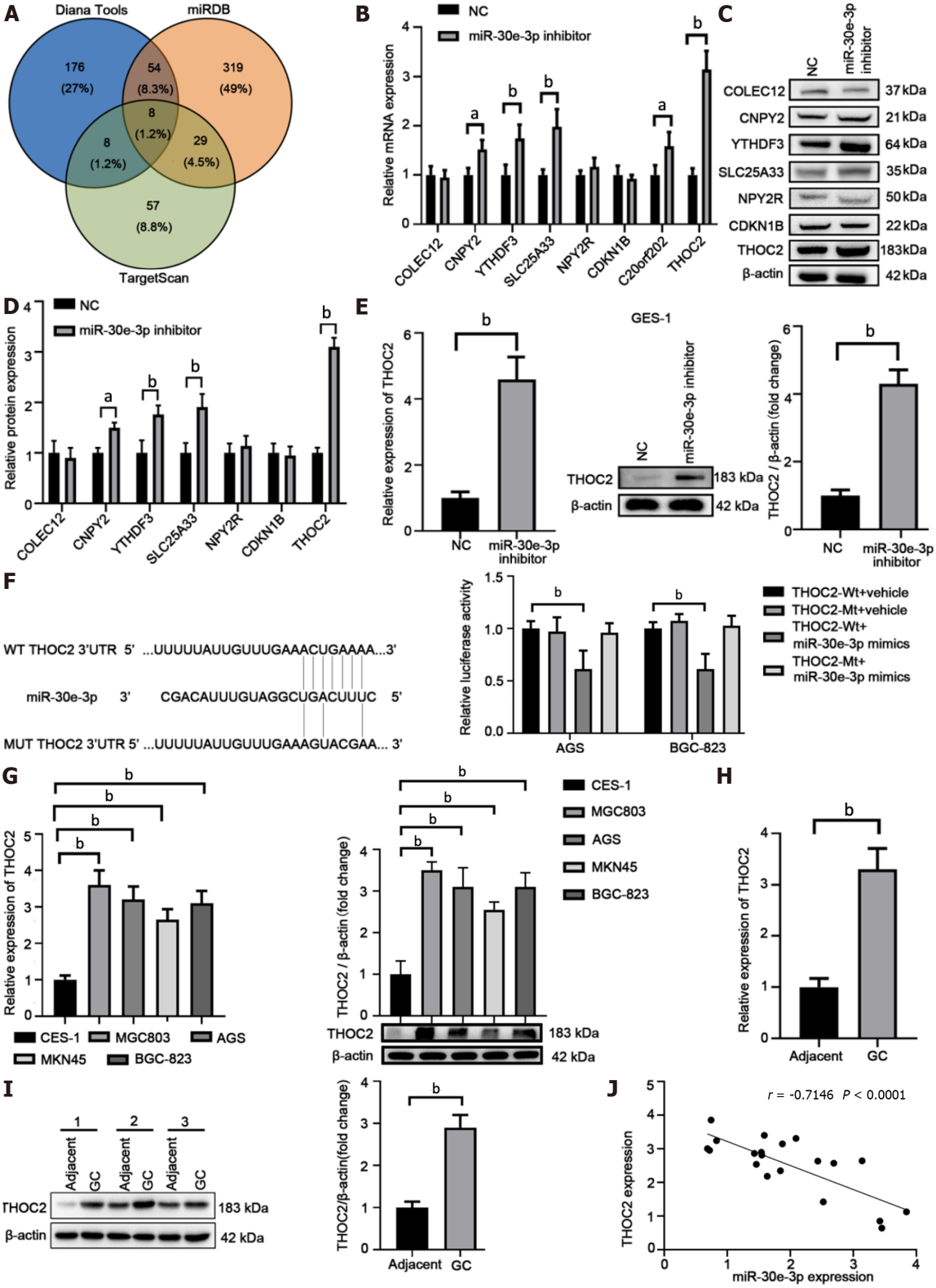

Figure 4 THO complex 2 is a direct target of miR-30e-3p in gastric cancer cells. A: Bioinformatics analysis predicted the potential targets of miR-30e-3p in gastric cancer (GC) cells; B: The mRNA expression level of candidate genes in GC after transfecting with miR-30e-3p inhibitor; C and D: The protein expression level of candidate genes in GC after transfecting with miR-30e-3p inhibitor; E: The expression of THO complex 2 (THOC2) in GSE-1 cells after transfecting with miR-30e-3p; F: The putative binding sequences between miR-30e-3p and 3'-UTR of THOC2 was shown. AGS or BGC-823 cells were co-transfected with luciferase reporter vector, with or without miR-30e-3p mimics. The relative luciferase activity in AGS or BGC-823 cells was analyzed 48 hours later. *n* = 3 for each group. G: The expression of THOC2 in human GC cell lines and control GES-1 cells were analyzed by quantitative real-time polymerase chain reaction (qRT-PCR) and western blot. *n* = 3 for each group; H: The expression of THOC2 in GC tissues and adjacent non-tumor normal tissues were analyzed by qRT-PCR. *n* = 20 for each group; I: Western blot was performed to examine THOC2 protein expression in human GC tissues and adjacent non-tumor normal tissues. *n* = 20 for each group. J: Pearson correlation analysis was performed to evaluate the relationship between THOC2 mRNA and miR-30e-3p expression in GC tissues. *n* = 20. $^{b}P < 0.01$.

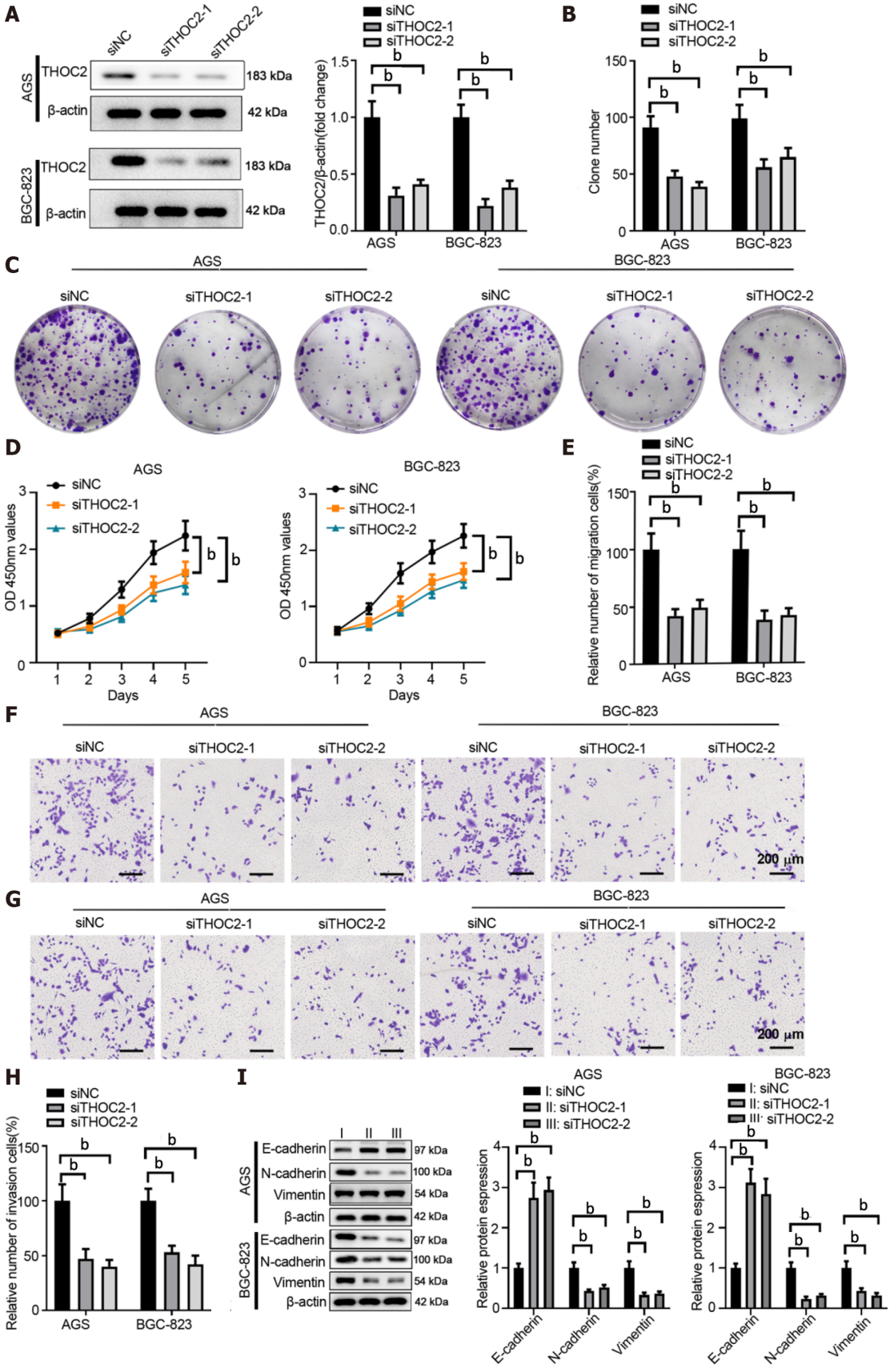

Figure 5 Knockdown of THO complex 2 suppresses malignant behaviors of gastric cancer cells. AGS or BGC-823 cells were transfected with siNC or siTHO complex 2 (siTHOC2)-1/2 to knockdown the expression of THOC2. A: The protein expression of THOC2 was analyzed by western blotting 48 hours later; B and C: Colony formation assay was conducted to evaluate the cell proliferation; D: CCK-8 assay was conducted to evaluate cell viability; E-H: Transwell assay was conducted using transwell chamber with or without Matrigel to evaluate the cell migration (E and F) and invasion (G and H); I: Expression of E-cadherin, N-cadherin, and vimentin in AGS or BGC-823 was determined using western blotting. $n = 3$ for each group. $^{b}P < 0.01$.

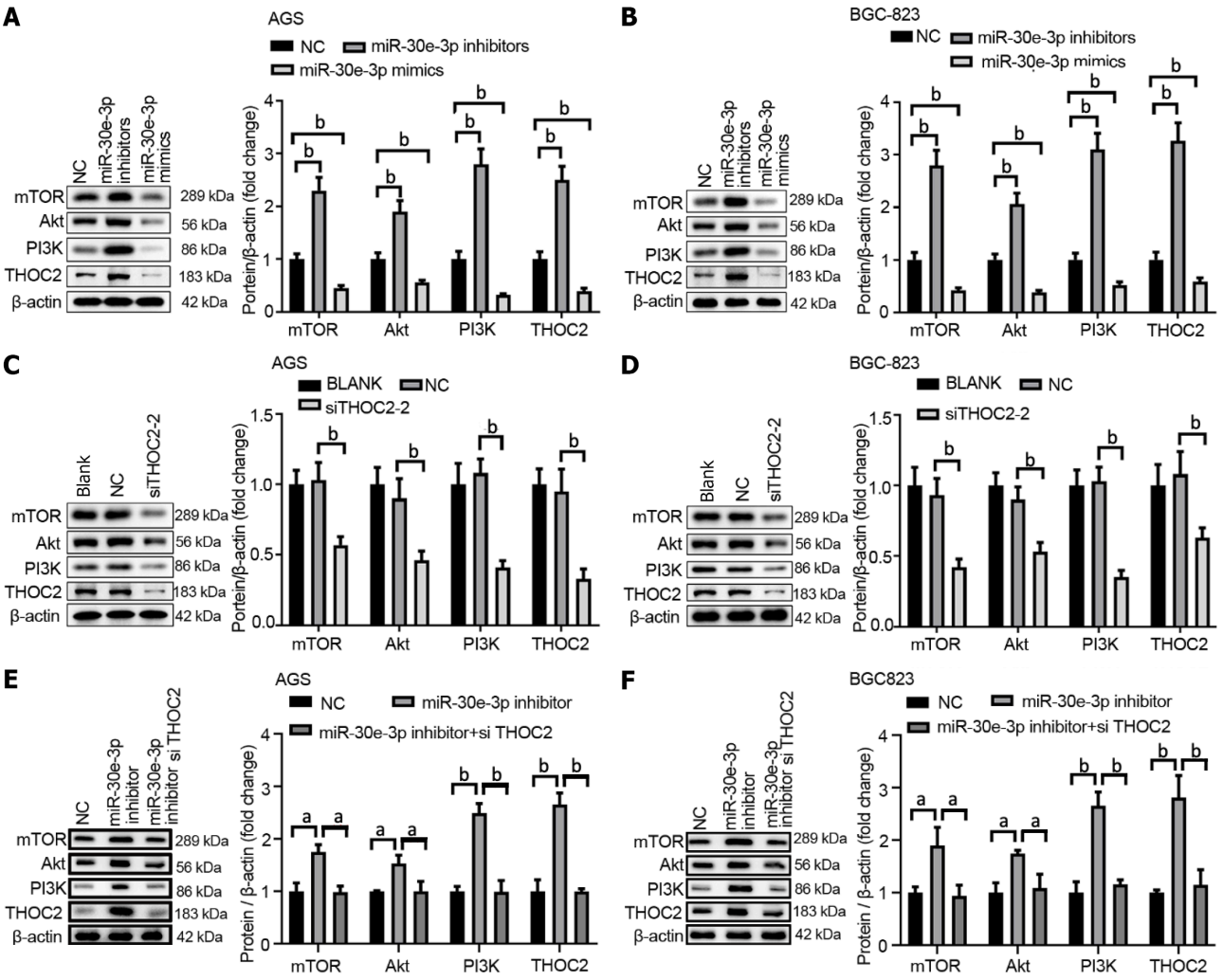

Figure 6 MiR-30e-3p regulates the PI3K/AKT/mTOR signaling pathway *via* inhibiting THO complex 2 expression in gastric cancer cells. A and B: AGS or BGC-823 cells were transfected with NC, miR-30e-3p inhibitors or miR-30e-3p mimics. The relative protein expression of THO complex 2 (THOC2), PI3K, AKT and mTOR was detected by western blot after 48 h; C and D: AGS or BGC-823 cells were transfected with NC, siTHOC2 or left untreated (blank). The relative protein expression of THOC2, PI3K, AKT and mTOR was detected by western blot after 48 h; E and F: AGS or BGC-823 cells were transfected with NC, miR-30e-3p inhibitor, miR-30e-3p inhibitor and si-THOC2. The relative protein expression of THOC2, PI3K, AKT and mTOR was detected by western blot after 48 h. $n = 3$ for each group. $^{b}P < 0.01$.

Multiple targets of miR-30e-3p have been identified, including Ubc9, P4HA1, IRS1, and ATG5[23,25-27]. We found that THOC2 was directly targeted by miR-30e-3p. Studies on the function of THOC2 in patients with psychomotor retardation showed that THOC2 was involved in mRNA-Export pathway in X-linked intellectual disability[28,29]. The dysregulated expression of THOC2 has been reported in severe neurocognitive and growth disorders[30]. Recently, the oncogenic function of THOC2 has been revealed in malignancies such as melanoma[17]. To the best of our knowledge, this has been the first study to demonstrated that THOC2 exhibited oncogenic function in GC development. Knockdown of THOC2 suppressed GC cell growth and metastasis. The regulatory axis of miR-30e-3p/THOC2 has been validated using the luciferase reporter assay, and Pearson analysis indicated that miR-30e-3p expression was negatively associated with THOC2 expression. Although our data confirmed that THOC2 was regulated by miR-30e-3p, other miRNAs might regulate THOC2, which could suppress GC development and progression.

Bioinformatics analysis was conducted to study the signaling pathways involved in miR-30e-3p/THOC2 regulation in GC. One study showed that the THO complex participates in the regulation of p53 and PI3K/AKT signaling[19]. The PI3K/AKT pathway is critical for cancer cell survival, proliferation, and apoptosis[31,32]. Consistently, we also found that the PI3K/AKT/mTOR signaling pathway was regulated by miR-30e-3p/THOC2 axis *in vitro* and *in vivo*. Thus, our findings provide a new approach in regulating the PI3K/AKT/mTOR pathway.

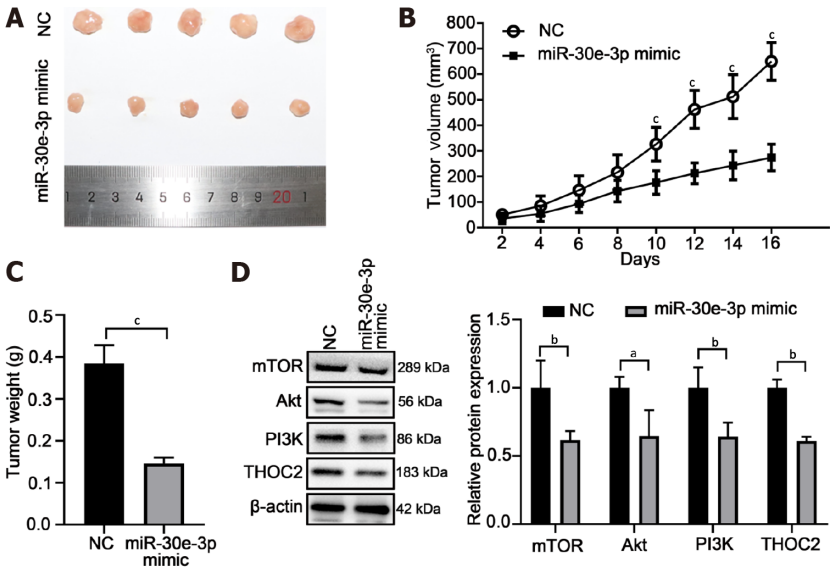

Figure 7 MiR-30e-3p inhibits gastric cancer cells growth *in vivo*. A: BGC-823 cells were transfected with NC, miR-30e-3p mimic and injected subcutaneously into BALB/c nude mice. Sixteen days later, the tumors diameter were analyzed. $n = 5$ for each group; B: The tumor volume (mm^3) was measured after the tumor implantation every other day; C: Sixteen days after the tumor implantation, the tumor weight (g) was measured; D: Sixteen days after the tumor implantation, the relative protein expression of THOC2, PI3K, AKT and mTOR was detected by Western blot. $^aP < 0.05$, $^bP < 0.01$.

CONCLUSION

In conclusion, our findings suggested that miR-30e-3p directly targets THOC2 and that THOC2 mediates the tumor suppression function of miR-30e-3p in GC. Low expression of miR-30e-3p or upregulation of THOC2 predicts poor prognosis of patients with GC. The diagnostic and therapeutic value of miR-30e-3p/THOC2 in GC should be further investigated in future studies.

ARTICLE HIGHLIGHTS

Research background

Gastric cancer (GC) is a common type of digestive cancer with high morbidity and mortality rates worldwide.

Research motivation

Considerable effort has been expended in understanding the mechanism of GC development and metastasis.

Research objectives

We explored the expression and function of miR-30e-3p in GC development.

Research methods

We conducted quantitative real-time polymerase chain reaction, transfection, cell growth assays, transwell assay, luciferase reporter assay, western blot assays to explore the expression and function of miR-30e-3p.

Research results

Our findings revealed that knockdown of THO complex 2 (THOC2) inhibited the growth and metastatic behaviors of GC cells. After investigating signaling pathways involved in miR-30e-3p regulation, we found that the miR-30e-3p/THOC2 axis regulated the PI3K/AKT/mTOR pathway in GC.

Research conclusions

Our findings suggested that miR-30e-3p directly targets THOC2 and that THOC2 mediates the tumor suppression function of miR-30e-3p in GC. Low expression of miR-30e-3p or upregulation of THOC2 predicts poor prognosis of patients with GC. The diagnostic and therapeutic value of miR-30e-3p/THOC2 in GC should be further investigated in future studies.

Research perspectives

Considerable effort has been expended in understanding the mechanism of GC development and metastasis. Given that microRNAs have been found to participate in the regulation of GC progression.

FOOTNOTES

Author contributions: Gu XJ and Li YJ conceived, designed the experiments, wrote and revised the manuscript; Gu XJ, Li YJ, Wang F and Ye T performed the experiments; Wang F and Ye T analyzed and interpreted the data; All the authors have read and approved the final version of the manuscript.

Supported by National Natural Science Foundation of China, No. 81860442; and Ningxia Natural Science Foundation Project, No. 2022AAC03525.

Institutional review board statement: The study was reviewed and approved by the Institutional Review Board of Ningxia Medical University.

Institutional animal care and use committee statement: All animal experiments conformed to the internationally accepted principles for the care and use of laboratory animals.

Conflict-of-interest statement: The authors declare that they have no competing interests.

Data sharing statement: No additional data are available.

ARRIVE guidelines statement: The authors have read the ARRIVE guidelines, and the manuscript was prepared and revised according to the ARRIVE guidelines.

Country/Territory of origin: China

ORCID number: Ya-Jun Li 0000-0002-2728-3237; Ting Ye 0000-0003-3497-0737.

S-Editor: Zhang H
L-Editor: A
P-Editor: Zhang XD

REFERENCES

1 **Rawla P**, Barsouk A. Epidemiology of gastric cancer: global trends, risk factors and prevention. *Prz Gastroenterol* 2019; **14**: 26-38 [PMID: 30944675 DOI: 10.5114/pg.2018.80001]
2 **Khasag O**, Boldbaatar G, Tegshee T, Duger D, Dashdorj A, Uchida T, Matsuhisa T, Yamaoka Y. The prevalence of *Helicobacter pylori* infection and other risk factors among Mongolian dyspeptic patients who have a high incidence and mortality rate of gastric cancer. *Gut Pathog* 2018; **10**: 14 [PMID: 29636824 DOI: 10.1186/s13099-018-0240-2]
3 **Fuccio L**, Eusebi LH, Bazzoli F. Gastric cancer, Helicobacter pylori infection and other risk factors. *World J Gastrointest Oncol* 2010; **2**: 342-347 [PMID: 21160805 DOI: 10.4251/wjgo.v2.i9.342]
4 **Balakrishnan M**, George R, Sharma A, Graham DY. Changing Trends in Stomach Cancer Throughout the World. *Curr Gastroenterol Rep* 2017; **19**: 36 [PMID: 28730504 DOI: 10.1007/s11894-017-0575-8]
5 **Necula L**, Matei L, Dragu D, Neagu AI, Mambet C, Nedeianu S, Bleotu C, Diaconu CC, Chivu-Economescu M. Recent advances in gastric cancer early diagnosis. *World J Gastroenterol* 2019; **25**: 2029-2044 [PMID: 31114131 DOI: 10.3748/wjg.v25.i17.2029]
6 **Xu HM**, Wang X. [Current status and prospects of clinical research on diagnosis and treatment of gastric cancer in China]. *Zhonghua Wei Chang Wai Ke Za Zhi* 2020; **23**: 109-114 [PMID: 32074788 DOI: 10.3760/cma.j.issn.1671-0274.2020.02.003]
7 **O'Brien J**, Hayder H, Zayed Y, Peng C. Overview of MicroRNA Biogenesis, Mechanisms of Actions, and Circulation. *Front Endocrinol (Lausanne)* 2018; **9**: 402 [PMID: 30123182 DOI: 10.3389/fendo.2018.00402]
8 **Zheng Q**, Chen C, Guan H, Kang W, Yu C. Prognostic role of microRNAs in human gastrointestinal cancer: A systematic review and meta-analysis. *Oncotarget* 2017; **8**: 46611-46623 [PMID: 28402940 DOI: 10.18632/oncotarget.16679]
9 **Peng Y**, Croce CM. The role of MicroRNAs in human cancer. *Signal Transduct Target Ther* 2016; **1**: 15004 [PMID: 29263891 DOI: 10.1038/sigtrans.2015.4]
10 **Yoda Y**, Takeshima H, Niwa T, Kim JG, Ando T, Kushima R, Sugiyama T, Katai H, Noshiro H, Ushijima T. Integrated

analysis of cancer-related pathways affected by genetic and epigenetic alterations in gastric cancer. *Gastric Cancer* 2015; **18**: 65-76 [PMID: 24510342 DOI: 10.1007/s10120-014-0348-0]

11 **Lu Q**, Chen Y, Sun D, Wang S, Ding K, Liu M, Zhang Y, Miao Y, Liu H, Zhou F. MicroRNA-181a Functions as an Oncogene in Gastric Cancer by Targeting Caprin-1. *Front Pharmacol* 2018; **9**: 1565 [PMID: 30687106 DOI: 10.3389/fphar.2018.01565]

12 **Wang Z**, Li Y, Cao J, Zhang W, Wang Q, Zhang Z, Gao Z, Ye Y, Jiang K, Wang S. MicroRNA Profile Identifies miR-6165 Could Suppress Gastric Cancer Migration and Invasion by Targeting STRN4. *Onco Targets Ther* 2020; **13**: 1859-1869 [PMID: 32184620 DOI: 10.2147/OTT.S208024]

13 **Yuan HL**, Wang T, Zhang KH. MicroRNAs as potential biomarkers for diagnosis, therapy and prognosis of gastric cancer. *Onco Targets Ther* 2018; **11**: 3891-3900 [PMID: 30013369 DOI: 10.2147/OTT.S156921]

14 **Wang D**, Zhu C, Zhang Y, Zheng Y, Ma F, Su L, Shao G. MicroRNA-30e-3p inhibits cell invasion and migration in clear cell renal cell carcinoma by targeting Snail1. *Oncol Lett* 2017; **13**: 2053-2058 [PMID: 28454361 DOI: 10.3892/ol.2017.5690]

15 **Francisco-Mangilet AG**, Karlsson P, Kim MH, Eo HJ, Oh SA, Kim JH, Kulcheski FR, Park SK, Manavella PA. THO2, a core member of the THO/TREX complex, is required for microRNA production in Arabidopsis. *Plant J* 2015; **82**: 1018-1029 [PMID: 25976549 DOI: 10.1111/tpj.12874]

16 **Amsterdam A**, Nissen RM, Sun Z, Swindell EC, Farrington S, Hopkins N. Identification of 315 genes essential for early zebrafish development. *Proc Natl Acad Sci U S A* 2004; **101**: 12792-12797 [PMID: 15256591 DOI: 10.1073/pnas.0403929101]

17 **Zhou X**, Liu X, Zhang G, Zhang Q, Chen H, Wang Y, Fang F, Sun J. Knockdown THOC2 suppresses the proliferation and invasion of melanoma. *Bioengineered* 2019; **10**: 635-645 [PMID: 31680623 DOI: 10.1080/21655979.2019.1685727]

18 Recent advances in the management of children with Wilms' tumor. *Prog Clin Biol Res* 1983; **132E**: 153-158 [PMID: 6316364]

19 **Moon S**, Chung YD. p53 and PI3K/AKT signalings are up-regulated in flies with defects in the THO complex. *Mol Cells* 2013; **35**: 261-268 [PMID: 23475424 DOI: 10.1007/s10059-013-0009-x]

20 **Hwang J**, Min BH, Jang J, Kang SY, Bae H, Jang SS, Kim JI, Kim KM. MicroRNA Expression Profiles in Gastric Carcinogenesis. *Sci Rep* 2018; **8**: 14393 [PMID: 30258124 DOI: 10.1038/s41598-018-32782-8]

21 **Link A**, Kupcinskas J. MicroRNAs as non-invasive diagnostic biomarkers for gastric cancer: Current insights and future perspectives. *World J Gastroenterol* 2018; **24**: 3313-3329 [PMID: 30122873 DOI: 10.3748/wjg.v24.i30.3313]

22 **Gramantieri L**, Pollutri D, Gagliardi M, Giovannini C, Quarta S, Ferracin M, Casadei-Gardini A, Callegari E, De Carolis S, Marinelli S, Benevento F, Vasuri F, Ravaioli M, Cescon M, Piscaglia F, Negrini M, Bolondi L, Fornari F. MiR-30e-3p Influences Tumor Phenotype through *MDM2*/*TP53* Axis and Predicts Sorafenib Resistance in Hepatocellular Carcinoma. *Cancer Res* 2020; **80**: 1720-1734 [PMID: 32015093 DOI: 10.1158/0008-5472.CAN-19-0472]

23 **Liu MM**, Li Z, Han XD, Shi JH, Tu DY, Song W, Zhang J, Qiu XL, Ren Y, Zhen LL. MiR-30e inhibits tumor growth and chemoresistance *via* targeting IRS1 in Breast Cancer. *Sci Rep* 2017; **7**: 15929 [PMID: 29162879 DOI: 10.1038/s41598-017-16175-x]

24 **Liu Y**, Xu Y, Ding L, Yu L, Zhang B, Wei D. LncRNA MEG3 suppressed the progression of ovarian cancer *via* sponging miR-30e-3p and regulating LAMA4 expression. *Cancer Cell Int* 2020; **20**: 181 [PMID: 32489317 DOI: 10.1186/s12935-020-01259-y]

25 **Wu F**, Zhu S, Ding Y, Beck WT, Mo YY. MicroRNA-mediated regulation of Ubc9 expression in cancer cells. *Clin Cancer Res* 2009; **15**: 1550-1557 [PMID: 19223510 DOI: 10.1158/1078-0432.CCR-08-0820]

26 **Feng G**, Shi H, Li J, Yang Z, Fang R, Ye L, Zhang W, Zhang X. MiR-30e suppresses proliferation of hepatoma cells *via* targeting prolyl 4-hydroxylase subunit alpha-1 (P4HA1) mRNA. *Biochem Biophys Res Commun* 2016; **472**: 516-522 [PMID: 26966067 DOI: 10.1016/j.bbrc.2016.03.008]

27 **Ye Y**, Fang Y, Xu W, Wang Q, Zhou J, Lu R. 3,3'-Diindolylmethane induces anti-human gastric cancer cells by the miR-30e-ATG5 modulating autophagy. *Biochem Pharmacol* 2016; **115**: 77-84 [PMID: 27372603 DOI: 10.1016/j.bcp.2016.06.018]

28 **Kumar R**, Corbett MA, van Bon BW, Woenig JA, Weir L, Douglas E, Friend KL, Gardner A, Shaw M, Jolly LA, Tan C, Hunter MF, Hackett A, Field M, Palmer EE, Leffler M, Rogers C, Boyle J, Bienek M, Jensen C, Van Buggenhout G, Van Esch H, Hoffmann K, Raynaud M, Zhao H, Reed R, Hu H, Haas SA, Haan E, Kalscheuer VM, Gecz J. THOC2 Mutations Implicate mRNA-Export Pathway in X-Linked Intellectual Disability. *Am J Hum Genet* 2015; **97**: 302-310 [PMID: 26166480 DOI: 10.1016/j.ajhg.2015.05.021]

29 **Di Gregorio E**, Bianchi FT, Schiavi A, Chiotto AM, Rolando M, Verdun di Cantogno L, Grosso E, Cavalieri S, Calcia A, Lacerenza D, Zuffardi O, Retta SF, Stevanin G, Marelli C, Durr A, Forlani S, Chelly J, Montarolo F, Tempia F, Beggs HE, Reed R, Squadrone S, Abete MC, Brussino A, Ventura N, Di Cunto F, Brusco A. A de novo X;8 translocation creates a PTK2-THOC2 gene fusion with THOC2 expression knockdown in a patient with psychomotor retardation and congenital cerebellar hypoplasia. *J Med Genet* 2013; **50**: 543-551 [PMID: 23749989 DOI: 10.1136/jmedgenet-2013-101542]

30 **Kumar R**, Gardner A, Homan CC, Douglas E, Mefford H, Wieczorek D, Lüdecke HJ, Stark Z, Sadedin S; Broad CMG, Nowak CB, Douglas J, Parsons G, Mark P, Loidi L, Herman GE, Mihalic Mosher T, Gillespie MK, Brady L, Tarnopolsky M, Madrigal I, Eiris J, Domènech Salgado L, Rabionet R, Strom TM, Ishihara N, Inagaki H, Kurahashi H, Dudding-Byth T, Palmer EE, Field M, Gecz J. Severe neurocognitive and growth disorders due to variation in THOC2, an essential component of nuclear mRNA export machinery. *Hum Mutat* 2018; **39**: 1126-1138 [PMID: 29851191 DOI: 10.1002/humu.23557]

31 **Zhang H**, Xu W, Li B, Zhang K, Wu Y, Xu H, Wang J, Zhang J, Fan R, Wei J. Curcumin Promotes Cell Cycle Arrest and Inhibits Survival of Human Renal Cancer Cells by Negative Modulation of the PI3K/AKT Signaling Pathway. *Cell Biochem Biophys* 2015; **73**: 681-686 [PMID: 27259310 DOI: 10.1007/s12013-015-0694-5]

32 **Zhou C**, Qiu L, Sun Y, Healey S, Wanebo H, Kouttab N, Di W, Yan B, Wan Y. Inhibition of EGFR/PI3K/AKT cell survival pathway promotes TSA's effect on cell death and migration in human ovarian cancer cells. *Int J Oncol* 2006; **29**: 269-278 [PMID: 16773209]

World Journal of Gastrointestinal Oncology

Submit a Manuscript: https://www.f6publishing.com

World J Gastrointest Oncol 2022 November 15; 14(11): 2183-2194

DOI: 10.4251/wjgo.v14.i11.2183

ISSN 1948-5204 (online)

ORIGINAL ARTICLE

Basic Study

E3 ubiquitin ligase *TRIM55* promotes metastasis of gastric cancer cells by mediating epithelial-mesenchymal transition

Wei-Wei Li, Hao Yuan, Shuai Kong, Shu-Bo Tian

Specialty type: Oncology

Provenance and peer review: Unsolicited article; Externally peer reviewed.

Peer-review model: Single blind

Peer-review report's scientific quality classification

Grade A (Excellent): 0
Grade B (Very good): 0
Grade C (Good): C, C, C
Grade D (Fair): 0
Grade E (Poor): 0

P-Reviewer: Liu YQ, United States; Qin Y, China

Received: August 21, 2022
Peer-review started: August 21, 2022
First decision: September 13, 2022
Revised: September 28, 2022
Accepted: October 27, 2022
Article in press: October 27, 2022
Published online: November 15, 2022

Wei-Wei Li, Department of Pulmonary and Critical Care Medicine, Shandong Provincial Hospital, Cheeloo College of Medicine, Shandong University, Jinan 250021, Shandong Province, China

Wei-Wei Li, Department of Critical Care Medicine, The 960th Hospital of the People's Liberation Army Joint Logistics Support Force, Jinan 250031, Shandong Province, China

Hao Yuan, Shuai Kong, Shu-Bo Tian, Department of Gastrointestinal Surgery, Shandong Provincial Hospital Affiliated to Shandong First Medical University, Jinan 250021, Shandong Province, China

Shuai Kong, Shu-Bo Tian, Department of Gastrointestinal Surgery, Shandong Provincial Hospital, Cheeloo College of Medicine, Shandong University, Jinan 250021, Shandong Province, China

Corresponding author: Shu-Bo Tian, PhD, Chief Doctor, Surgeon, Department of Gastrointestinal Surgery, Shandong Provincial Hospital Affiliated to Shandong First Medical University, No. 324 Jingwuweiqi Road, Jinan 250021, Shandong Province, China.
ttkl_bo@126.com

Abstract

BACKGROUND

Gastric cancer (GC) is considered a major global health problem. The role of TRIM55, a member of the three-domain protein family, in GC is unknown.

AIM

To determine the expression of *TRIM55* in GC tissues and its relationship with clinicopathological characteristics, and to investigate the effects of *TRIM55* on the malignant biological behavior of GC cells.

METHODS

Differential expression of *TRIM55* in GC and para-cancer tissues was detected by immunohistochemistry, and the relationship between *TRIM55* level and clinicopathological characteristics and prognosis was analyzed. Gain-of-function, loss-of-function, cell counting kit-8 assay, colony formation, transwell assay, wound healing assay, and western blot analysis were used to assess the potential role of *TRIM55* in the development of GC.

RESULTS

TRIM55 expression was significantly increased in GC tissues compared with adjacent normal tissues. High expression of *TRIM55* was associated with advanced pathological stage and poor prognosis. Overexpression of *TRIM55* promoted invasion and metastasis of GC cells *in vitro* by regulating epithelial-mesenchymal transition (EMT), whereas knockdown of *TRIM55* had the opposite effect. Our data showed that *TRIM55* is highly expressed in GC tissues, and is associated with poor prognosis. *TRIM55* plays the role of an oncogene in GC, and it promotes metastasis of GC through the regulation of EMT.

CONCLUSION

TRIM55 may be a possible target for the diagnosis and prognosis of GC patients.

Key Words: *TRIM55*; Gastric cancer; Prognosis; Epithelial-mesenchymal transition

Core Tip: *TRIM55* expression was elevated in gastric cancer (GC) cancer tissues. Depletion of *TRIM55* in GC cells suppressed proliferation, migration and invasion of cells. Knockdown of *TRIM55* affected the expression of cell epithelial-mesenchymal transition-related proteins. *TRIM55* may serve as an oncogene in GC.

Citation: Li WW, Yuan H, Kong S, Tian SB. E3 ubiquitin ligase *TRIM55* promotes metastasis of gastric cancer cells by mediating epithelial-mesenchymal transition. *World J Gastrointest Oncol* 2022; 14(11): 2183-2194
URL: https://www.wjgnet.com/1948-5204/full/v14/i11/2183.htm
DOI: https://dx.doi.org/10.4251/wjgo.v14.i11.2183

INTRODUCTION

Gastric cancer (GC) is one of the most common tumors and seriously affects patients' health[1]. Comprehensive treatment based on surgery is the preferred strategy for GC[2]. Postoperative metastasis is the leading cause of death from GC; however, the mechanisms underlying the occurrence and the development of GC have not been fully elucidated, and there is a lack of effective markers for early diagnosis[3]. Therefore, identifying molecular markers of GC is important for the early diagnosis, treatment, and prognostic evaluation of GC. The three-domain protein (TRIM) family is composed of many members, including the tripartite motif, which consists of a RING domain, 1 or 2 Box motifs, and a coiled-coil region[4]. Some TRIM proteins are involved in the regulation of cellular transcription, cell proliferation, and tumor development; thus, they play a role in either promoting or inhibiting cancer[5]. The structural diversity of TRIM family proteins underpins their functional diversity. TRIM55, also known as muscle-specific RING zinc finger protein 2, maintains muscle development and cardiac function. *TRIM55* plays an important role in early skeletal muscle differentiation and the generation of muscle fibers[6]. Studies have shown that mir-30-5p can inhibit muscle cell differentiation and regulate the alternative splicing of *TRIM55* by targeting Muscleblind-like Protein[7]. *TRIM55* can regulate the TNF-α-CCL2 pathway and promote an inflammatory response in the development of mesangial proliferative glomerulonephritis[8]; however, the role of *TRIM55* in GC has not been fully elucidated.

In this study, we determined the differential expression of *TRIM55* in GC patients and investigated the relationship between *TRIM55* and clinicopathological characteristics. We found that *TRIM55* induced proliferation, migration, and invasion of GC cells. We also investigated the mechanism underlying these effects.

MATERIALS AND METHODS

Tissue samples

Tissues were obtained from 91 GC patients admitted to the Department of Gastrointestinal Surgery of Shandong Provincial Hospital Affiliated to Shandong First Medical University between July 2014 and December 2015. The tumor tissue samples and adjacent normal gastric mucosal tissue samples were validated by pathologists. Of the 91 patients, 61 were male and 30 were female, with an average age of 63.6 years. Data such as gender and age of the patient, tumor location, tumor pathological stage, and lymph node metastasis, were also collected. In addition, five fresh GC tissue samples and matched

adjacent normal gastric tissues were obtained from our hospital. The research protocols were approved by the Ethics Committee of the Provincial Hospital Affiliated to Shandong First Medical University, and all the patients signed an informed consent form before surgery.

Cell culture and transfection

Human GC cell lines (AGS, MKN28, MGC803, SGC7901, HGC27, and MKN45) and the immortalized gastric mucosa cell line (GES-1) were provided by the Cell Center of the Chinese Academy of Medical Sciences. All the cell lines were cultured in RPMI-1640 medium containing 10% fetal bovine serum (FBS, Gibco, United States). Cells were cultured in an incubator at 37 °C and 5% CO_2. According to the CDS coding sequence of *TRIM55*, small interfering RNAs (siRNA) to knock down *TRIM55* were designed and synthesized by RiboBio (Guangzhou, China), and the scramble nonsense sequence was used as the negative control (si-control). The targeting *TRIM55* siRNA sequence was as follows: *TRIM55* siRNA, 5′-AUCAAACUUCUCACAAAGCUC-3′. The control siRNA was not homologous to any human genome sequence. For the overexpression assay, the coding sequence of *TRIM55* was amplified and cloned into a pcDNA3.1-HA vector to construct the *TRIM55* overexpression system (*TRIM55* plasmid). The pcDNA3.1-HA empty vector was used as the negative control in HGC27 cells.

Immunohistochemical staining

The GC tissue and adjacent tissue were embedded in paraffin and sliced into 4-μm-thick sections. Xylene was used for dewaxing and citrate buffer was used for antigen repair. After washing with PBS 4 times, the samples were sealed with BSA blocking solution at 37 °C. TRIM55 primary antibody (Novus, United States) was added and incubated overnight at 4 °C. According to the instructions of the immunohistochemical test kit, the secondary antibody was added and incubated for 20 min at room temperature. Then, streptavidin-peroxidase conjugate was added and the samples were incubated for 20 min. DAB was used for staining and hematoxylin was used for redyeing and dehydration. The sections were observed and photographed under a microscope and analyzed with Image analysis software. According to the staining intensity, no staining was scored as 0, light yellow was scored as 1, brownish yellow was scored as 2, and brown was scored as 3. According to the percentage of positive cells, the score for no positive cells was 0, 1%–10% was 1, 11%–50% was 2, 51–75% was 3, and 76%–100% was 4. The expression of TRIM55 was considered to be high if the multiple of the two scores was ≥ 5.

Quantitative real-time polymerase chain reaction

Total RNA was extracted using TRIzol reagent (Invitrogen) and reverse transcribed to cDNA using a reverse transcription kit (Takara, Dalian, China) following the manufacturer's instructions. The quantitative real-time polymerase chain reaction three-step method was used, and the $2^{-\Delta\Delta Ct}$ method was used to calculate the relative expression levels of *TRIM55*. GAPDH was used as the endogenous control. The upstream primer sequence of *TRIM55* was 5 '-GGTTTTGGATAGACATGGGGT-3', and the downstream primer sequence was 5 '-TTCTCCTCTTGGGTTCGGGT-3'.

Cell counting kit-8 assay

Cells were seeded in 96-well plates (2000 cells/well) and placed into an incubator for further culture. Ten microliters of cell counting kit-8 (CCK-8) reagent (Dojindo, Mashikimachi, Japan) was added to each well on days 1, 2, 3, and 4. After 4 h incubation, the absorbance value at 450 nm (OD450) was measured with a microplate reader. The growth curve of cells was drawn according to the OD value. Three independent assays were performed for each time point.

Colony formation assay

Two thousand cells/well were plated in a six-well plate and allowed to grow in complete growth medium for 14 d. The colonies were then fixed with 4% paraformaldehyde for 15 min, followed by staining with 0.1% crystal violet solution for 10 min. The number of colonies was counted, and the average value was calculated from three independent experiments.

Transwell migration and invasion assay

GC cells at the logarithmic growth stage were trypsinized and suspended in serum-free media at a concentration of 1×10^6 cells/mL. Two hundred microliters of the cell suspension was added to the upper transwell chamber. Culture medium containing 10% FBS was added to the lower chamber. For the invasion assay, the transwell membrane was coated with Matrigel. After 48 h incubation, the cells that did not pass through the membrane in the upper chamber were removed with cotton swabs. The migrated/invaded cells were fixed with paraformaldehyde for 30 min and stained with 0.1% crystal violet solution. The cells were observed under a microscope and five random fields were selected to count the number of migrated or invaded cells.

Wound healing assay

GC cells were inoculated into a six-well plate at a density of 5×10^5 cells/well until 90% confluence was reached. Then, a sterile 100-μL pipette tip was used to scrape the bottom surface of the plate to form a

wound vertically. The cells were washed with 1× PBS, and complete growth medium was added. The wound margins were observed at 0 and 24 h in 5 randomly selected microscopic regions, and the mean cell spacing was calculated.

Western blot assays

GC cells were collected and lysed in immunoprecipitation lysis buffer. After protein quantification by the BCA method, 30 μg of protein sample was used for electrophoresis. After transfer and blocking, the membrane was incubated overnight at 4 °C with the primary antibody. Horseradish peroxidase-labeled secondary antibody was added and incubated for 1 h. The bands were visualized using chemiluminescence reagent.

Statistical analysis

Statistical analyses were performed using GraphPad Prism software version 7.0 (CA, United States). All the data are represented as mean ± SD from three independent experiments. Differences among groups were compared using student's t-test and one-way analysis of variance. The prognostic factors were analyzed by univariate and multivariate Cox regression models. The Kaplan-Meier method was used to calculate the survival rate, and the log-rank test was used to compare different survival curves. A value of $P < 0.05$ was considered to indicate a statistically significant difference.

RESULTS

TRIM55 is highly expressed in GC samples

Immunohistochemical results showed that *TRIM55* was mainly expressed in the nucleus. Figure 1A-D shows the representative immunohistochemical staining images of *TRIM55* in normal gastric mucosa tissue and cancer tissue. The expression of *TRIM55* was significantly high in 91 GC tissues and low in para-cancer tissues (Table 1, $P < 0.001$). There was no significant correlation between *TRIM55* expression and age at diagnosis, gender, tumor location, or Lauren type ($P > 0.05$, Table 2). However, a significant relationship was found between *TRIM55* expression and tumor stage, lymph node metastasis, and T stage ($P < 0.05$, Table 2).

To further confirm the results, we performed western blotting using five GC specimens and matched normal tissues. The results showed that protein levels of *TRIM55* in GC tissues were up-regulated compared to non-tumor tissues (Figure 1E).

Relationship between TRIM55 expression and prognosis of GC

The 5-year survival rate of patients with high *TRIM55* expression was lower than that of those with low expression ($P = 0.026$, Figure 1F). The median overall survival of patients with high and low expression of *TRIM55* was 34 mo [95% confidence interval (CI): 13.3–62.8] and 57 mo (95%CI: 25.5–84.5), respectively. Similarly, patients with high *TRIM55* gene expression had a poor prognosis in the TCGA database (Figure 1G). Univariate Cox regression analysis showed that T stage, lymph node metastasis, TNM stage, and *TRIM55* expression level were the influencing factors for the prognosis of GC patients (Table 3). Further multivariate Cox regression analysis showed that lymph node metastasis, TNM stage, and *TRIM55* expression level were independent factors affecting the prognosis of GC (Table 3).

TRIM55 protein is upregulated in GC cell lines

The protein level of *TRIM55* was analyzed in the immortalized gastric mucosal epithelial cell line GES-1 and six GC cell lines (AGS, MKN28, MGC803, SGC7901, HGC27, and MKN45). The results showed that the expression level of *TRIM55* in GC cell lines was significantly higher than that in GES-1 cells (Figure 2A). Among them, the expression level of *TRIM55* was highest in SGC7901 and lowest in the HGC27 cell line.

Transfection efficiency of TRIM55 siRNA and TRIM55 overexpressed plasmid

To analyze the effects of *TRIM55* knockdown, SGC7901 (cells with high *TRIM55* expression) GC cells were transfected with *TRIM55* siRNA. The results showed that both mRNA and protein expressions of *TRIM55* were significantly lower in cells transfected with *TRIM55* siRNA compared to those in the control group (Figure 2B and C). HGC27 cells with low endogenous *TRIM55* expression were transfected with *TRIM55* overexpressed plasmid to determine the effects. We found that cells transfected with the overexpressed plasmid had higher mRNA and protein levels of *TRIM55* compared to those transfected with the empty vector (Figure 2D and E).

TRIM55 promotes proliferation of GC cells

The CCK-8 assay was used to determine the proliferation of GC cells. The results showed that SGC7901 cell proliferation was significantly inhibited on days 2, 3, and 4 after *TRIM55* knockdown ($P < 0.001$, Figure 3A). However, the proliferation of HGC27 cells was significantly increased on days 2, 3, and 4 (P

Table 1 Immunohistochemical expression of *TIRM55* in gastric cancer and normal tissues

Tissue	*N*	High expression	Low expression	*P* value
Gastric cancer	91	40	51	< 0.001
Normal	91	3	89	

Table 2 Association between *TRIM55* expression and clinicopathological characteristics

Variables	No. of case	*TRIM55* expression		χ^2	*P* value
		High (*n* = 40)	Low (*n* = 51)		
Gender				0.284	0.594
Male	61	28	33		
Female	30	12	18		
Age (*n*)				0.216	0.642
≤ 65	48	20	28		
> 65	43	20	23		
Tumor location				0.008	0.928
Proximal	14	6	8		
Dismatal	77	34	43		
pT stage				6.232	0.013
T1 + T2	43	13	30		
T3 + T4	48	27	21		
Lymph node metastasis				5.506	0.019
Negative	49	16	33		
Positive	42	24	18		
TNM stage				5.146	0.023
I + II	53	18	35		
III	38	22	16		
Lauren histotype				3.366	0.067
Intestinal	47	25	22		
Diffuse	44	15	29		

< 0.001, Figure 3B) when *TRIM55* was overexpressed in these cells. These results suggest that *TRIM55* can promote the proliferation of GC cells.

The colony formation assay showed that the colony number was significantly reduced after siRNA transfection in SGC7901 cells (Figure 3C). Similarly, overexpression of *TRIM55* in HGC27 cells enhanced the ability of cells to form colonies (Figure 3D).

TRIM55 promotes invasion and migration of GC cells

The transwell migration and invasion assay results showed that *TRIM55* knockdown significantly reduced the migration and invasion of SGC7901 cells (Figure 4A). Furthermore, the number of migrated and invaded HGC27 cells was significantly increased after *TRIM55* overexpression (Figure 4B). The wound-healing assay revealed that knockdown of *TRIM55* significantly impaired the migration ability of SGC7901 cells (Figure 5A), while HGC27 migration ability was enhanced after overexpression of *TRIM55* (Figure 5B). These results suggest that *TRIM55* could promote the invasion and migration of GC cells.

TRIM55 promotes the migration and invasive growth of GC cells by inducing epithelial-mesenchymal transition

To further explore the potential mechanism of how *TRIM55* promotes the progression of GC, we

Table 3 Univariate and multivariate Cox regression models for estimating the overall survival

Variable	Univariate analysis			Multivariate analysis		
	HR	95%CI	*P* value	HR	95%CI	*P* value
Gender	0.79	0.12–1.38	0.463			
Age	0.56	0.38–1.50	0.517			
Tumor location	1.67	0.53–2.27	0.770			
pT stage	0.85	0.61–0.93	0.041			
Lymph node metastasis	3.29	2.07–5.44	0.005	2.64	1.35–3.08	0.021
TNM stage	2.18	1.32–2.89	0.016	1.20	1.06–1.88	0.028
Lauren histotype	1.45	0.39–2.46	0.433			
TRIM55	2.37	1.53–3.81	0.028	1.48	1.17–1.92	0.035

HR: Hazard ratio; CI: Confidence interval.

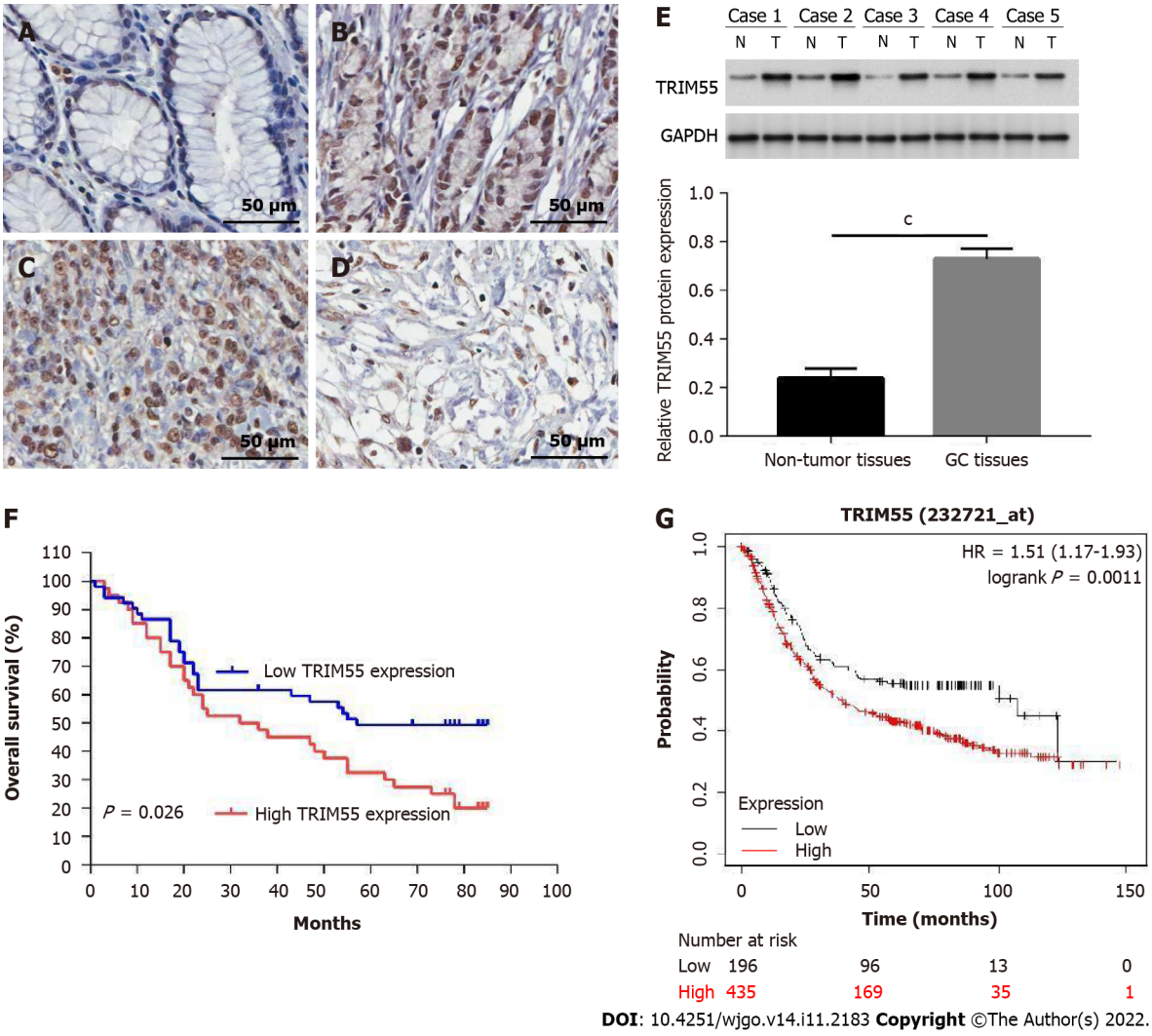

DOI: 10.4251/wjgo.v14.i11.2183

Figure 1 Representative images of immunohistochemical staining for *TRIM55* in human gastric cancer tissue and its prognostic significance. A: Low expression of *TRIM55* in gastric normal mucosa tissue; B: *TRIM55* expression in well-differentiated adenocarcinoma; C: *TRIM55* expression in poorly differentiated adenocarcinoma; D: Overexpression of *TRIM55* in signet-ring cell carcinoma. Original magnification, 400 ×; E: TRIM55 protein levels in five tumor samples and their matched normal tissues; F: Overall survival curves for 91 gastric cancer (GC) patients according to TRIM55 protein expression ($P = 0.026$); G: Overall survival curves of TCGA GC patients with different *TRIM55* expression. $^cP < 0.001$. HR: Hazard ratio; GC: Gastric cancer.

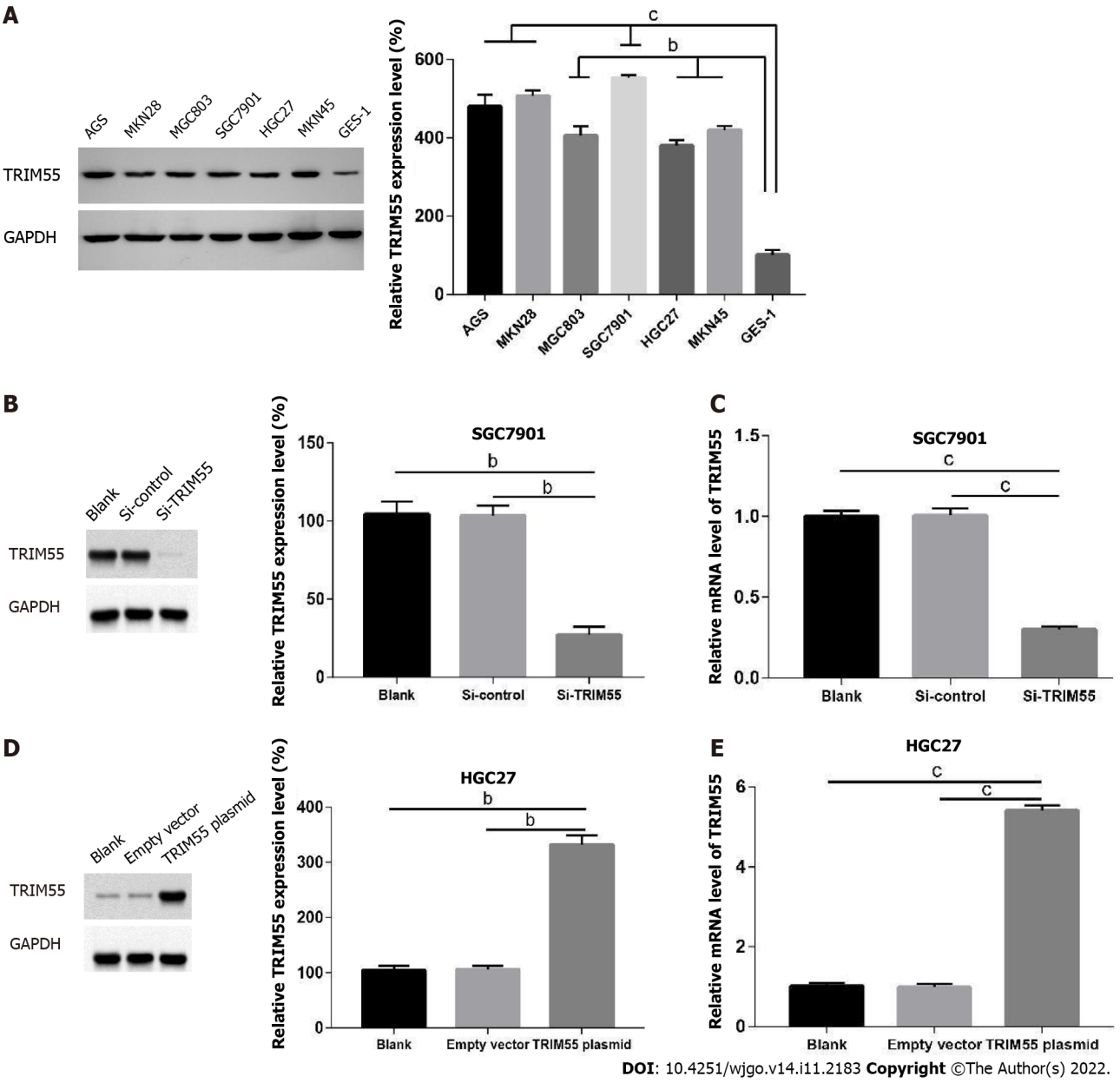

DOI: 10.4251/wjgo.v14.i11.2183 **Copyright** ©The Author(s) 2022.

Figure 2 *TRIM55* expression in gastric cancer cells. A: The expression of TRIM protein was detected in gastric cancer (GC) cells by western blot. The histogram shows the expression of *TRIM55* in GC cells was stronger than that in gastric mucosa cell line; B: The interference efficiency of *TRIM55* small interfering RNA (siRNA) in SGC7901 cells was detected by Western blot; C: Quantitative real-time-polymerase chain reaction assay was performed to determine *TRIM55* expression after transfection with siRNA; D: The up-regulation of *TRIM55* expression in HGC27 cells was detected by Western blot; E: *TRIM55* mRNA expression level in HGC27 after transfection with the *TRIM55* plasmid. $^{b}P < 0.01$; $^{c}P < 0.001$.

analyzed the expression of epithelial-mesenchymal transition (EMT)-related proteins by western blot analysis (Figure 6). The results showed that in the SGC7901 cell line, E-cadherin expression was significantly up-regulated after *TRIM55* knockdown, while N-cadherin, Vimentin, ZEB1, and Snail expression were significantly down-regulated compared with the control group (Figure 6A). Furthermore, the opposite results were observed when *TRIM55* was overexpressed in the HGC27 cell line (Figure 6B). These results confirmed that *TRIM55* promotes the invasion and metastasis of GC cells by inducing EMT.

DISCUSSION

TRIM55 belongs to the TRIM protein family, which plays an important role in the development and progression of tumors. TRIM proteins have three characteristic domains and function as an E3 ligase; they also mediate ubiquitination and regulate intracellular pathophysiological and tumor-related processes by degrading target molecules. TRIM family members exhibit oncogenic and tumor-

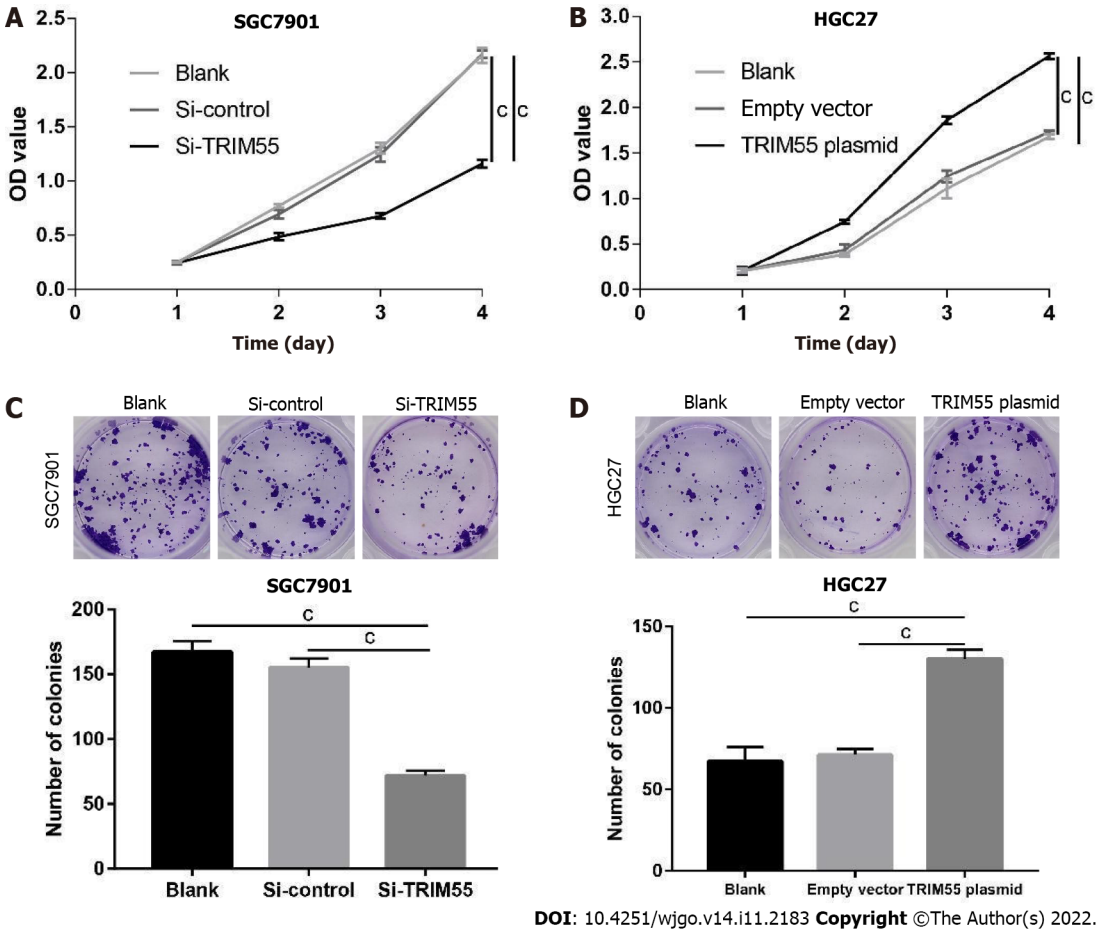

DOI: 10.4251/wjgo.v14.i11.2183 **Copyright** ©The Author(s) 2022.

Figure 3 *TRIM55* regulates gastric cancer cell proliferation. A and B: Cell viability detected by cell counting kit-8 assay in SGC7901 cells after knockdown of TRIM55 and in HGC27 cells after overexpression of *TRIM55*; C and D: Colony formation analysis of TRIM55 knockdown-treated SGC7901 cells and *TRIM55* overexpression-treated HGC27 cells. °$P < 0.001$.

suppressive capacities in different human cancer types by regulating signal transduction pathways[9,10]. EMT is a transitional process in which epithelial cells lose intercellular adhesion and polarity, and they acquire mesenchymal cell characteristics, enhanced cell motility, and migration ability[11,12].

The progression of EMT is regulated by translational factors and epigenetic modification[13]. Also, microRNAs and long non-coding RNAs are also involved in EMT regulation as post-translational regulators[14]. The tumor cells or other stromal cells can secret exosomes. Exosomes are extracellular vesicles with a lipid bilayer containing proteins, lipids and functional RNAs, which can transfer information between tumor cells or between tumor cells and the tumor microenvironment, thereby regulating the EMT process[15,16]. As EMT plays essential physiological roles, EMT-targeted therapy combined with conventional chemotherapy can improve the sensitivity of tumor cells to drugs.

TRIM proteins were found to be associated with EMT in various types of cancer. TRIM11 protein was upregulated in GC tissue and cell lines, and it could promote cell proliferation, migration, invasion, and EMT of GC by activating β-catenin signaling[17]. TRIM47 mainly influenced the EMT signaling pathway, was highly expressed in GC, and was associated with poor prognosis of patients[18]. In GC, *TRIM44* expression was also increased in GC tissues and cell lines, and it regulated GC cell metastasis by altering the expression of EMT-associated factors[19].

Previous studies have demonstrated that the role of *TRIM55* in tumors is tissue specific. For example, a study revealed that *TRIM55* expression was significantly suppressed in lung adenocarcinoma tissues and tumor cells. *TRIM55* exerted its tumor-suppressive effect by increasing the degradation of Snail protein *via* ubiquitination[20]. *TRIM55* was downregulated in hepatocellular carcinoma (HCC) tissue and associated with tumor stage and poor prognosis. Overexpression of *TRIM55* can suppress the migration and invasion of HCC cells through EMT and the MMP2 pathways[21].

To the best of our knowledge, our study is the first to determine the expression levels and biological functions of *TRIM55* in GC. We demonstrated that *TRIM55* could be a potential new biomarker for diagnosing and evaluating GC patients. First, we performed immunohistochemical staining, and the results showed that *TRIM55* was highly expressed in GC tissues and that *TRIM55* expression was related to the T stage, lymph node metastasis, and TNM stage of GC. Survival analysis showed that the 5-year survival rate of GC patients with high expression of *TRIM55* was significantly reduced. Cox

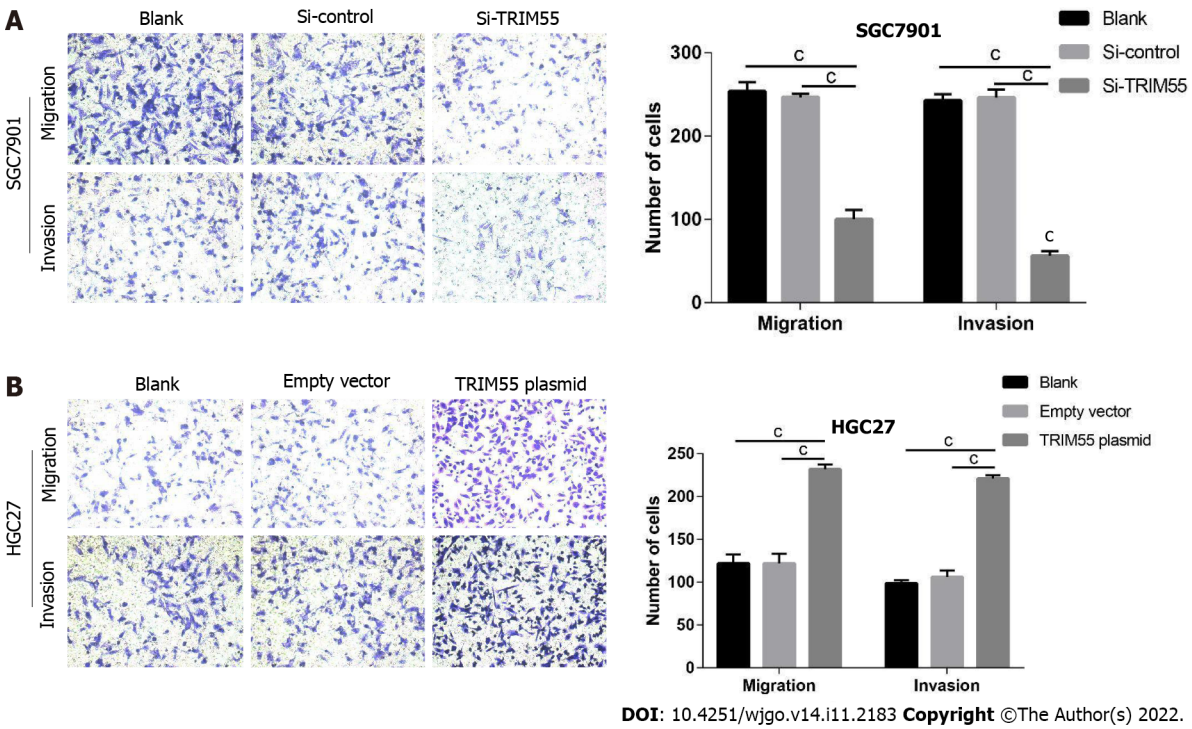

DOI: 10.4251/wjgo.v14.i11.2183 **Copyright** ©The Author(s) 2022.

Figure 4 *TRIM55* promotes metastasis of gastric cancer cells. A: Migration and invasion analysis of *TRIM55* knockdown-treated SGC7901 cells; B: Migration and invasion analysis of *TRIM55* overexpression treated-HGC27 cells. °*P* < 0.001.

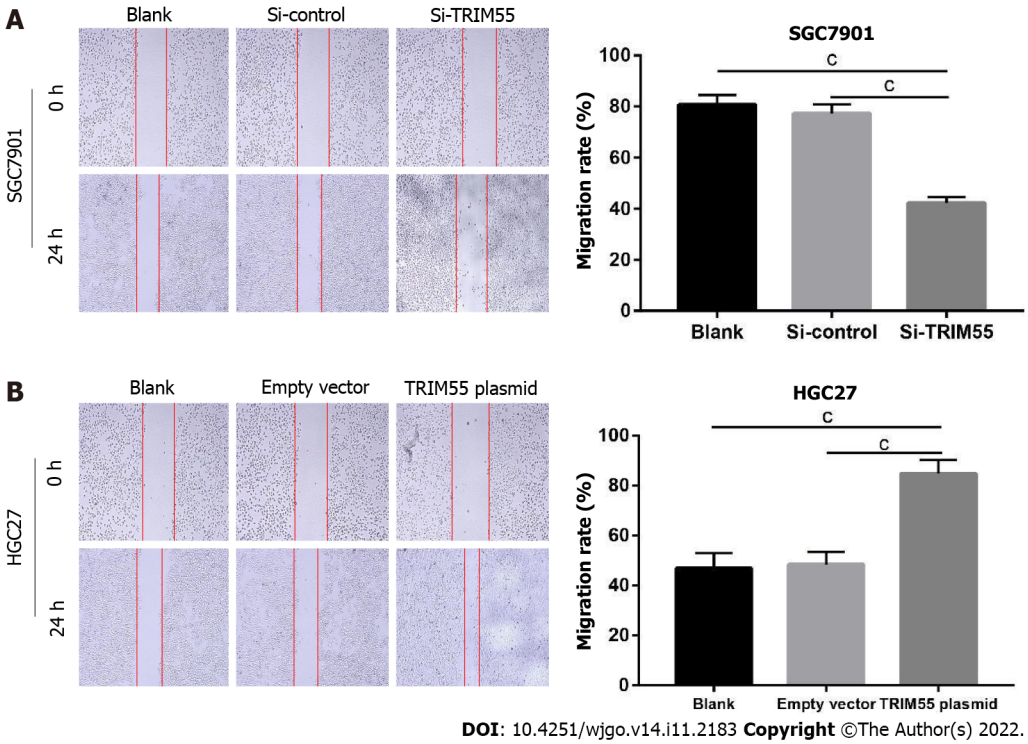

DOI: 10.4251/wjgo.v14.i11.2183 **Copyright** ©The Author(s) 2022.

Figure 5 Wound healing assays were performed in gastric cancer cells. A: Migration rates of SGC7901 cells at 24 h were lower than that in control groups after knockdown of *TRIM55*; B: Migration rates of HGC27 cells at 24 h were higher than that in control groups after overexpression of *TRIM55*. °*P* < 0.001.

regression analysis also confirmed that *TRIM55* expression was an independent prognostic factor in GC. These results suggest that *TRIM55* may be involved in the occurrence and development of GC. Furthermore, to confirm the biological functions of *TRIM55* in GC, we performed a gain and loss of function experiment *in vitro*. Results from the CCK-8 assay, colony formation assay, transwell, and wound healing assays indicated that inhibition of *TRIM55* decreases the proliferation and invasion of GC cells, whereas the overexpression of *TRIM55* promotes these processes in GC cells. Finally, we used

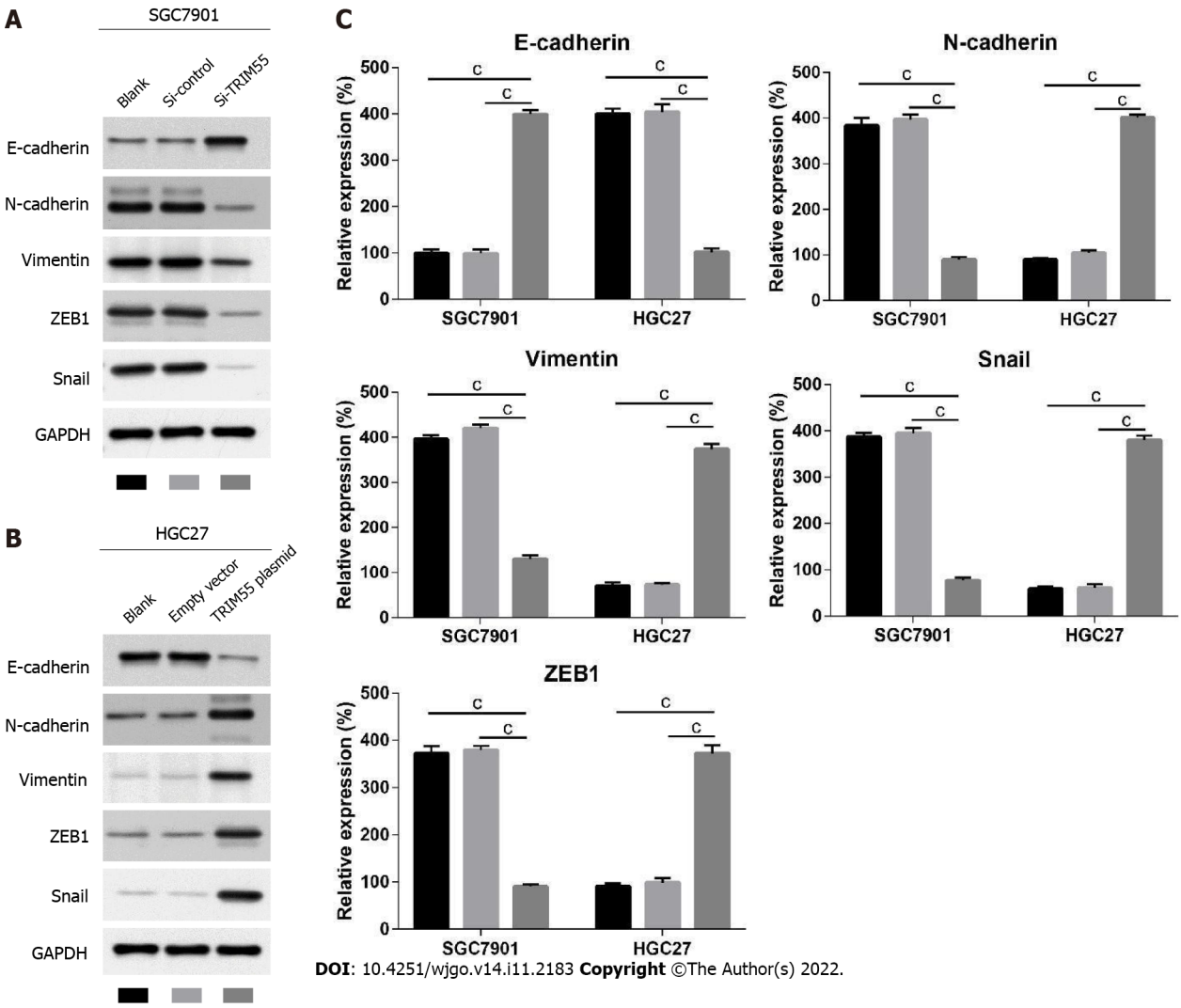

DOI: 10.4251/wjgo.v14.i11.2183 **Copyright** ©The Author(s) 2022.

Figure 6 Western blot results of epithelial-mesenchymal transition pathway-related proteins in gastric cancer cells. A and B: Western blot analysis of E-cadherin, N-cadherin, Vimentin, ZEB1, and Snail after *TRIM55* knockdown and overexpression in SGC7901 and HGC27 cells; C: Histogram of the expression of E-cadherin, N-cadherin, Vimentin, Snail, and ZEB1 proteins related to metastasis after knockdown or overexpression of *TRIM55*. $^{c}P < 0.001$.

western blot analysis to confirm that knockdown or overexpression of *TRIM55* could alter the EMT-related protein, suggesting that *TRIM55* could regulate the EMT process. TRIM proteins could serve the ubiquitination function to stabilize or dislocate target proteins in various cellular compartments[4]. Ubiquitination is a post-transcriptional modification that labels the target proteins to be degraded at the proteasome level. Thus, TRIM family members determine both tumor suppressor and oncogenic roles by affecting the signal pathways in cancer development and progression. For example, TRIM29 and TRIM8 exhibited contextual function in different cancers[22-24]. They negatively or positively regulate tumorigenesis and tumor progression by affecting pathways. In our study, we showed that *TRIM55* is highly expressed in gastric tumors and cultured tumor cells. *TRIM55* has E3 ubiquitin ligase activity and whether it can regulate the EMT-related proteins through ubiquitination requires further investigation.

However, some limitations exist in our study. First, the detection of *TRIM55* was based on a single-center clinical cohort, and the functional experiments were only performed *in vitro*. Future studies should enroll more patients and utilize animal models to confirm our conclusions. Second, *TRIM55* has E3 ubiquitin ligase activity and whether it can regulate the EMT-related proteins through ubiquitination requires further study.

CONCLUSION

In summary, our study analyzed the expression of *TRIM55* in GC and demonstrated that *TRIM55* could promote GC cell proliferation, migration, and invasion *via* the EMT process. Overexpression of *TRIM55* could be an independent factor predicting poor survival, and *TRIM55* may serve as a potential therapeutic target for GC. In addition, whether *TRIM55* can affect EMT through other molecular

mechanisms remains to be examined in future studies.

ARTICLE HIGHLIGHTS

Research background

TRIM55 plays important role in hepatocellular carcinoma and lung adenocarcinoma. However, little is known about the role of *TRIM55* in gastric cancer (GC).

Research motivation

To discover the targets for the diagnosis, treatment and prognosis prediction of GC.

Research objectives

To explore the biological function of *TRIM55* and its underlying molecular mechanism in GC.

Research methods

The expression of *TRIM55* was determined by quantitative real-time polymerase chain reaction and Western blot. Cell counting kit-8 assay, colony formation, wound healing assay and transwell assay were used to investigate the *TRIM55* function.

Research results

TRIM55 expression levels were significantly increased in GC cell lines and tissues. High expression of *TRIM55* was correlated with poor prognosis of GC patients. Knockdown of *TRIM55* in GC cell lines inhibited proliferation, colony formation, migration and invasion in vitro. *TRIM55* can regulate the expression of epithelial-mesenchymal transition-related proteins in GC cells.

Research conclusions

TRIM55 functions as an oncogene through promoting cell proliferation, migration and invasion in GC.

Research perspectives

TRIM55 may be a new potential target in GC treatment.

FOOTNOTES

Author contributions: Li WW and Yuan H contributed equally to this work; Tian SB and Li WW designed the study; Li WW and Yuan H performed all experiments; Kong S and Tian SB analyzed the data and drafted the article; All authors read and approved the final manuscript.

Supported by Shandong Province Medicine and Health Science and Technology Development Plan Project, No. 2019WS477.

Institutional review board statement: The study was reviewed and approved by the Shandong Provincial Hospital Affiliated to Shandong First Medical University Institutional Review Board.

Institutional animal care and use committee statement: No animal subjects were involved in our experiments.

Informed consent statement: All study participants or their legal guardian provided informed written consent about personal and medical data collection prior to study enrolment.

Data sharing statement: Technical appendix, statistical code, and dataset available from the corresponding author at ttkl_bo@126com.

Country/Territory of origin: China

ORCID number: Wei-Wei Li 0000-0003-3201-6739; Shu-Bo Tian 0000-0001-6022-6288.

S-Editor: Fan JR

L-Editor: A
P-Editor: Yuan YY

REFERENCES

1 **Rahman R**, Asombang AW, Ibdah JA. Characteristics of gastric cancer in Asia. *World J Gastroenterol* 2014; **20**: 4483-4490 [PMID: 24782601 DOI: 10.3748/wjg.v20.i16.4483]
2 **Tung I**, Sahu A. The treatment of resectable gastric cancer: a literature review of an evolving landscape. *J Gastrointest Oncol* 2022; **13**: 871-884 [PMID: 35557598 DOI: 10.21037/jgo-21-721]
3 **Xia JY**, Aadam AA. Advances in screening and detection of gastric cancer. *J Surg Oncol* 2022; **125**: 1104-1109 [PMID: 35481909 DOI: 10.1002/jso.26844]
4 **Mohammadi A**, Pour Abbasi MS, Khorrami S, Khodamoradi S, Mohammadi Goldar Z, Ebrahimzadeh F. The TRIM proteins in cancer: from expression to emerging regulatory mechanisms. *Clin Transl Oncol* 2022; **24**: 460-470 [PMID: 34643877 DOI: 10.1007/s12094-021-02715-5]
5 **Hatakeyama S**. TRIM proteins and cancer. *Nat Rev Cancer* 2011; **11**: 792-804 [PMID: 21979307 DOI: 10.1038/nrc3139]
6 **Perera S**, Holt MR, Mankoo BS, Gautel M. Developmental regulation of MURF ubiquitin ligases and autophagy proteins nbr1, p62/SQSTM1 and LC3 during cardiac myofibril assembly and turnover. *Dev Biol* 2011; **351**: 46-61 [PMID: 21185285 DOI: 10.1016/j.ydbio.2010.12.024]
7 **Zhang BW**, Cai HF, Wei XF, Sun JJ, Lan XY, Lei CZ, Lin FP, Qi XL, Plath M, Chen H. miR-30-5p Regulates Muscle Differentiation and Alternative Splicing of Muscle-Related Genes by Targeting MBNL. *Int J Mol Sci* 2016; **17** [PMID: 26840300 DOI: 10.3390/ijms17020182]
8 **Lu Y**, Mei Y, Chen L, Wu L, Wang X, Zhang Y, Fu B, Chen X, Xie Y, Cai G, Bai X, Li Q. The role of transcriptional factor D-site-binding protein in circadian CCL2 gene expression in anti-Thy1 nephritis. *Cell Mol Immunol* 2019; **16**: 735-745 [PMID: 29568121 DOI: 10.1038/s41423-018-0020-4]
9 **Cambiaghi V**, Giuliani V, Lombardi S, Marinelli C, Toffalorio F, Pelicci PG. TRIM proteins in cancer. *Adv Exp Med Biol* 2012; **770**: 77-91 [PMID: 23631001 DOI: 10.1007/978-1-4614-5398-7_6]
10 **Mantovani F**, Walerych D, Sal GD. Targeting mutant p53 in cancer: a long road to precision therapy. *FEBS J* 2017; **284**: 837-850 [PMID: 27808469 DOI: 10.1111/febs.13948]
11 **Xu R**, Won JY, Kim CH, Kim DE, Yim H. Roles of the Phosphorylation of Transcriptional Factors in Epithelial-Mesenchymal Transition. *J Oncol* 2019; **2019**: 5810465 [PMID: 31275381 DOI: 10.1155/2019/5810465]
12 **Yeung KT**, Yang J. Epithelial-mesenchymal transition in tumor metastasis. *Mol Oncol* 2017; **11**: 28-39 [PMID: 28085222 DOI: 10.1002/1878-0261.12017]
13 **Lu W**, Kang Y. Epithelial-Mesenchymal Plasticity in Cancer Progression and Metastasis. *Dev Cell* 2019; **49**: 361-374 [PMID: 31063755 DOI: 10.1016/j.devcel.2019.04.010]
14 **Huang Y**, Hong W, Wei X. The molecular mechanisms and therapeutic strategies of EMT in tumor progression and metastasis. *J Hematol Oncol* 2022; **15**: 129 [PMID: 36076302 DOI: 10.1186/s13045-022-01347-8]
15 **Jiang J**, Li J, Zhou X, Zhao X, Huang B, Qin Y. Exosomes Regulate the Epithelial-Mesenchymal Transition in Cancer. *Front Oncol* 2022; **12**: 864980 [PMID: 35359397 DOI: 10.3389/fonc.2022.864980]
16 **Kim H**, Lee S, Shin E, Seong KM, Jin YW, Youn H, Youn B. The Emerging Roles of Exosomes as EMT Regulators in Cancer. *Cells* 2020; **9** [PMID: 32252322 DOI: 10.3390/cells9040861]
17 **Lan Q**, Tan X, He P, Li W, Tian S, Dong W. TRIM11 Promotes Proliferation, Migration, Invasion and EMT of Gastric Cancer by Activating β-Catenin Signaling. *Onco Targets Ther* 2021; **14**: 1429-1440 [PMID: 33658804 DOI: 10.2147/OTT.S289922]
18 **Xia Y**, Wei Z, Huang W, Wei X, He Y. Trim47 overexpression correlates with poor prognosis in gastric cancer. *Neoplasma* 2021; **68**: 307-316 [PMID: 33350849 DOI: 10.4149/neo_2020_200708N706]
19 **Wang F**, Ruan L, Yang J, Zhao Q, Wei W. TRIM14 promotes the migration and invasion of gastric cancer by regulating epithelialtomesenchymal transition *via* activation of AKT signaling regulated by miR1955p. *Oncol Rep* 2018; **40**: 3273-3284 [PMID: 30272351 DOI: 10.3892/or.2018.6750]
20 **Guo T**, Zhang Z, Zhu L, Chen W, Ding Y, Li W, Huang Y, Huang J, Pan X. TRIM55 suppresses malignant biological behavior of lung adenocarcinoma cells by increasing protein degradation of Snail1. *Cancer Biol Ther* 2022; **23**: 17-26 [PMID: 34974792 DOI: 10.1080/15384047.2021.2004835]
21 **Li X**, Huang L, Gao W. Overexpression of Tripartite Motif Conaining 55 (TRIM55) Inhibits Migration and Invasion of Hepatocellular Carcinoma (HCC) Cells *via* Epithelial-Mesenchymal Transition and Matrix Metalloproteinase-2 (MMP2). *Med Sci Monit* 2019; **25**: 771-777 [PMID: 30685767 DOI: 10.12659/MSM.910984]
22 **Esposito JE**, De Iuliis V, Avolio F, Liberatoscioli E, Pulcini R, Di Francesco S, Pennelli A, Martinotti S, Toniato E. Dissecting the Functional Role of the TRIM8 Protein on Cancer Pathogenesis. *Cancers (Basel)* 2022; **14** [PMID: 35565438 DOI: 10.3390/cancers14092309]
23 **Deng X**, Fu X, Teng H, Fang L, Liang B, Zeng R, Chen L, Zou Y. E3 ubiquitin ligase TRIM29 promotes pancreatic cancer growth and progression *via* stabilizing Yes-associated protein 1. *J Transl Med* 2021; **19**: 332 [PMID: 34353343 DOI: 10.1186/s12967-021-03007-w]
24 **Xu M**, Hu J, Zhou B, Zhong Y, Lin N, Xu R. TRIM29 prevents hepatocellular carcinoma progression by inhibiting Wnt/β-catenin signaling pathway. *Acta Biochim Biophys Sin (Shanghai)* 2019; **51**: 68-77 [PMID: 30566565 DOI: 10.1093/abbs/gmy151]

World Journal of Gastrointestinal Oncology

Submit a Manuscript: https://www.f6publishing.com

World J Gastrointest Oncol 2022 November 15; 14(11): 2195-2207

DOI: 10.4251/wjgo.v14.i11.2195

ISSN 1948-5204 (online)

ORIGINAL ARTICLE

Clinical and Translational Research

Missed colorectal cancers in a fecal immunochemical test-based screening program: Molecular profiling of interval carcinomas

Manon van der Vlugt, Beatriz Carvalho, Joelle Fliers, Nahid Montazeri, Christian Rausch, Esmée J Grobbee, Manon van Engeland, Manon C W Spaander, Gerrit A Meijer, Evelien Dekker

Specialty type: Gastroenterology and hepatology

Provenance and peer review: Unsolicited article; Externally peer reviewed.

Peer-review model: Single blind

Peer-review report's scientific quality classification

Grade A (Excellent): 0
Grade B (Very good): B
Grade C (Good): C
Grade D (Fair): 0
Grade E (Poor): 0

P-Reviewer: Bustamante-Balen M, Spain; Gu GL, China

Received: July 26, 2022
Peer-review started: July 26, 2022
First decision: August 19, 2022
Revised: September 6, 2022
Accepted: October 2, 2022
Article in press: October 2, 2022
Published online: November 15, 2022

Manon van der Vlugt, Joelle Fliers, Evelien Dekker, Department of Gastroenterology and Hepatology, Amsterdam University Medical Center, Amsterdam 1105 AZ, Netherlands

Beatriz Carvalho, Christian Rausch, Gerrit A Meijer, Department of Pathology, Netherlands Cancer Institute, Amsterdam 1066 CX, Netherlands

Nahid Montazeri, Biostatistics Unit, Department of Gastroenterology and Hepatology, Amsterdam University Medical Center, Amsterdam 1105 AZ, Netherlands

Esmée J Grobbee, Manon C W Spaander, Department of Gastroenterology and Hepatology, Erasmus MC University Medical Center, Rotterdam 3015 CN, Netherlands

Manon van Engeland, Department of Pathology, GROW-School for Oncology and Developmental Biology, Maastricht University Medical Center, Maastricht 6202 AZ, Netherlands

Corresponding author: Manon van der Vlugt, MD, PhD, Doctor, Department of Gastroenterology and Hepatology, Amsterdam University Medical Center, Meibergdreef 9, Amsterdam 1105 AZ, Netherlands. m.vandervlugt@amsterdamumc.nl

Abstract

BACKGROUND

For optimizing fecal immunochemical test (FIT)-based screening programs, reducing the rate of missed colorectal cancers (CRCs) by FIT (FIT-interval CRCs) is an important aspect. Knowledge of the molecular make-up of these missed lesions could facilitate more accurate detection of all (precursor) lesions.

AIM

To compare the molecular make-up of FIT-interval CRCs to lesions that are detected by FIT [screen-detected CRCs (SD-CRCs)].

METHODS

FIT-interval CRCs observed in a Dutch pilot-program of FIT-based screening were compared to a control group of SD-CRCs in a 1:2 ratio, resulting in 27 FIT-interval CRC and 54 SD-CRCs. Molecular analyses included microsatellite instability (MSI), CpG island methylator phenotype (CIMP), DNA sequence mutations and copy number alterations (CNAs).

RESULTS
Although no significant differences were reached, FIT-interval CRCs were more often CIMP positive and MSI positive (33% CIMP in FIT-interval CRCs *vs* 21% in SD-CRCs (P = 0.274); 19% MSI in FIT-interval CRCs *vs* 12% in SD-CRCs (P = 0.469)), and showed more often serrated pathway associated features such as *BRAF* (30% *vs* 12%, P = 0.090) and *PTEN* (15% *vs* 2.4%, P = 0.063) mutations. *APC* mutations, a classic feature of the adenoma-carcinoma-sequence, were more abundant in SD-CRCs (68% *vs* 40% in FIT-interval CRCs P = 0.035). Regarding CNAs differences between the two groups; FIT-interval CRCs less often showed gains at the regions 8p11.22-q24.3 (P = 0.009), and more often gains at 20p13-p12.1 (P = 0.039).

CONCLUSION
Serrated pathway associated molecular features seem to be more common in FIT-interval CRCs, while classic adenoma carcinoma pathway associated molecular features seem to be more common in SD-CRCs. This indicates that proximal serrated lesions may be overrepresented among FIT-interval CRCs.

Key Words: Fecal immunochemical test-interval colorectal cancer; Mutation analysis; Colorectal cancer screening; Serrated pathway; Adenoma-carcinoma pathway

Core Tip: Fecal immunochemical test (FIT) is effective in reducing colorectal cancer (CRC) but FIT testing is not perfect. FIT interval cancers, *i.e.* CRCs diagnosed after a negative FIT but before the next FIT invitation, still occur. Previous studies have shown that FIT sensitivity for sessile serrated lesions (SSLs) is low, but a correlation between the occurrence of FIT interval cancers and the serrated pathway has not been established. In our study, the serrated pathway-associated molecular features were more common in FIT-interval CRCs as compared to screen detected CRCs. This indicates that proximal serrated lesions may be overrepresented among FIT interval CRCs. The findings of this study can provide guidance on strategies to further improve stool-based CRC screening with incorporating biomarkers for SSLs, thereby reducing the number of screening interval CRCs.

Citation: van der Vlugt M, Carvalho B, Fliers J, Montazeri N, Rausch C, Grobbee EJ, Engeland MV, Spaander MCW, Meijer GA, Dekker E. Missed colorectal cancers in a fecal immunochemical test-based screening program: Molecular profiling of interval carcinomas. *World J Gastrointest Oncol* 2022; 14(11): 2195-2207
URL: https://www.wjgnet.com/1948-5204/full/v14/i11/2195.htm
DOI: https://dx.doi.org/10.4251/wjgo.v14.i11.2195

INTRODUCTION

Fecal immunochemical test (FIT)-based screening worldwide has had a major impact on reducing colorectal cancer (CRC)-related mortality. Despite this success, the issue of false negative tests giving rise to FIT interval CRCs (*e.g.*, CRCs diagnosed after a negative FIT but before the next FIT invitation) leaves room for improvement[1]. Monitoring the incidence of FIT-interval CRCs is a key quality indicator of a FIT-based screening program, and any CRC that occurs in spite of recent screening can be regarded as an unwanted program outcome. The sensitivity of FIT for CRC is approximately 75%-85%, which indicates that still 1 in 4-5 CRCs will be missed in any single screening round[2-4]. Possible reasons for FIT-interval CRCs are the limited sensitivity of FIT for specific molecular types of CRCs that were already present at the time of FIT-screening, or rapid progression of premalignant lesions during the interval between two screening rounds. Both of these causes may be the consequence of differences in tumor biology between FIT-interval CRCs and screen-detected CRCs (SD-CRCs). Such biological differences may translate *e.g.*, into a lower bleeding tendency of colorectal lesions or an increased progression rate.

CRC has several precursor lesions reflecting different tumor-biology. Adenomas are well-known precursors of CRC. Adenomas may follow the canonical adenoma-carcinoma sequence with *APC* and *KRAS* mutations and subsequent typical patterns of chromosomal copy number alterations (CNAs) as classic features to develop into CRC[5-7]. More recently, also sessile serrated lesions (SSLs) have been identified as precursors of CRC. SSLs may follow the serrated neoplasia pathway resulting in CRCs that are more often microsatellite instable (MSI), CpG island methylator phenotype (CIMP) high and harbor *BRAF* mutations[8,9]. As a consequence of a different tumor biology, colorectal lesions can have

different morphology. Most SSLs are non-polypoid (flat or slightly elevated) lesions located in the proximal colon, whereas adenomas can be either non-polypoid or polypoid (*e.g.*, stalked or sessile). Previous studies have shown that FIT sensitivity for SSLs is low[10]. Also, non-polypoid colorectal neoplasms (NP-CRNs) have a flat morphology and are associated with more aggressive biologic behavior when compared to polypoid precursor lesions[11]. These NP-CRNs are usually located in the proximal colon. As they are more challenging to detect during colonoscopy, these NP-CRNs are thought to be a major contributor to post-colonoscopy CRCs (PC-CRCs)[12]. In a study on molecular characterization, NP-CRNs were more often found to harbor 5q-loss and *BRAF* mutations and have less *APC* and *KRAS* mutations[11,12]. It was hypothesized that NP-CRNs bleed less intensely and/or not continuously, which could lead to a falsely negative FIT and FIT-interval CRCs.

Generating more insight in the molecular features of FIT-interval CRCs may help to optimize screening strategies, aiming to reduce their incidence. The aim of the present study therefore was to compare the molecular composition of FIT-interval CRCs to that of SD-CRCs.

MATERIALS AND METHODS

Population and study design

From 2006 onwards, two cohort studies of biennial FIT-based CRC screening have been conducted in the southwest and northwest regions of the Netherlands. After three screening rounds, these two cohorts were combined in 2014 to conduct a fourth round of FIT screening. A threshold of 10 μg hemoglobin (Hb) per gram feces was used. Screenees with a fecal Hb concentration above this threshold were referred for colonoscopy. Colonoscopies were performed according to international quality guidelines[13]. Details about the design of this study have been reported previously[2,14,15]. After finishing the fourth screening round in 2015, the total cohort was linked to the Netherlands Cancer Registry, managed by the Netherlands Comprehensive Cancer Organization (Utrecht, The Netherlands), in order to identify CRC missed by FIT testing during the three completed screening rounds including 2 years of follow up.

Definitions

All CRCs detected during colonoscopy after a positive FIT (threshold ≥ 10 μg Hb/g feces) were recorded and labeled as SD-CRC.

FIT-interval CRCs were defined as a CRC diagnosed after a negative FIT (threshold < 10 μg Hb/g feces) and before the date of the next invitation for FIT-screening[16]. If a participant had a negative FIT and was not invited for a consecutive round (for having passed the upper age limit or after moving out of the target area) but developed CRC within the 2.37 years interval (median time between invitations), this CRC was also defined as a FIT-interval CRC.

Persons who had been inconsistent in participating in FIT screening and developed CRC outside the screening interval (median 2.37 years) were not defined as an interval CRC and not included in this study. Data on tumor stage and location (at time of resection) were collected for both FIT-interval CRC and SD-CRCs. With regard to tumor location, the colon was divided into proximal (cecum, ascending, hepatic flexure, and transverse colon) and distal colon (splenic flexure, descending colon, sigmoid colon, and rectum). All cancers were staged according to the 7th edition of the American Joint Committee on Cancer[17]. In the three intervals between four screening rounds, including the 2.37 years follow up for individuals that had reached the upper age limit after any of the first three rounds, in total 27 FIT-interval CRCs were identified. Besides, a total of 116 SD-CRCs was detected in the four screening rounds. All 27 FIT-interval CRCs were included in the study, and a random sample of SD-CRCs in a 1:2 ratio to SD-CRCs, yielding a control group of 54 SD-CRCs.

Sample collection and DNA isolation

All tissue samples of FIT-interval CRCs and SD-CRCs were collected from 11 departments of pathology through the Dutch National Pathology Registry[18]. DNA from formalin-fixed, paraffin-embedded material was isolated as previously described[19]. Good quality DNA could be obtained from 25 of 27 FIT-interval CRCs and 46 of 54 SD-CRCs (see Supplementary Figure 1).

CIMP status analysis

CIMP status was analyzed in the Pathology Department at the University of Maastricht. The CIMP panel (CACNA1G, IGF2, NEUROG1, RUNX3 and SOCS1)[20] was determined by nested methylation-specific polymerase chain reaction (PCR) using sodium bisulfite modified genomic DNA (EZ DNA methylation kit (ZYMO research Co., Orange, CA, United States) as described before[21,22], and CIMP positive was defined when ≥ 3 of the 5 CIMP markers were methylated. In some samples DNA was no longer available, in other samples the analysis was performed but failed, leaving CIMP-analysis results available for 21 of 27 FIT-interval CRCs and 39 of 54 SD-CRCs (see Supplementary Figure 1).

MSI status analysis

MSI status analysis was performed using the multiplex marker PCR panel from Promega (MSI Multiplex System Version 1.2, Promega, Madison, WI, United States). When two or more markers were unstable, the sample was interpreted as MSI. All other samples were classified as microsatellite stable. In some samples insufficient DNA was left, while in others the results obtained did not meet the quality criteria, leaving results for MSI analysis available for 21 of 27 FIT-interval CRCs and 41 of 54 SD-CRCs (see Supplementary Figure 1).

Mutation analysis

For mutation analysis, targeted sequencing was performed. DNA libraries were prepared using the KAPA HyperPrep Kit (KAPA Biosystems, Wilmington, MA, United States) as described in the KAPA HyperPrep Kit protocol (KR0961-v5.16). Target enrichment was performed using a custom 48 gene xGen® Predesigned Gene Capture Pools (Integrated DNA Technologies, San Diego, CA, United States), as previously described[23]. In some samples, DNA was no longer available, and one sample was analyzed but sequencing was not sufficiently deep to draw conclusions for almost all genes, leaving mutation analysis results available for 20 of 27 FIT-interval CRCs and 42 of 54 SD-CRCs (see Supplementary Figure 1). Genes and/or samples with ≥ 50% of low-quality reads, were excluded from analysis, as the results were not reliable. Mutation calling was done as previously described[23]. Raw mutation data have been deposited in the European Genome-Phenome Archive (EGA)[24], with the study ID: EGAS00001004683.

DNA copy number analysis

DNA CNAs were analyzed with low-coverage whole genome sequencing as described previously[23]. Briefly, DNA was fragmented by sonication (Covaris S2, Woburn, MA, United States) and run on the HiSeq 2500 (Illumina, San Diego, CA, United States) on a 65 basepairs single-read modus using the KAPA HyperPrepKit (KAPA Biosystems, KK8504, Wilmington, MA, United States). This yielded a coverage of 0.13x (IQR 0.12-0.14) genome coverage. To compare the frequencies of alterations in the two groups, the R-package CGHtest was used[25]. Good quality DNA copy number profiles were obtained for 19 of 27 FIT-interval CRCs and for 44 of 54 SD-CRCs (see Supplementary Figure 1). Raw DNA copy number data has been deposited in the EGA[24], with the study ID: EGAS00001004683.

Statistical analysis

Differences between groups were evaluated for statistical significance using the Chi square-test statistic, Fisher's exact test statistic, linear-by-linear test or Mann-Whitney-U test where appropriate. Two-sided P values < 0.05 were considered to indicate statistically significant differences. Differences between proportions were reported as mean with 95%CI.

Ethics approval and tissue handling

Ethics approval for performing FIT-based screening including linkage to the Netherlands Cancer Registry was provided by the Dutch National Health Council (WBO 2642467, 2832758, 3049078 and 161536-112008, The Hague, The Netherlands). No separate ethics approval was necessary for the additional molecular analysis, as judged by the scientific ethics board of the AMC University Hospital. Collection and use of tissue and patient data were performed in compliance with the 'Code for Proper Secondary Use of Human Tissue in the Netherlands' (www.federa.org). All authors had access to the study data and reviewed and approved the final manuscript.

Patient and public involvement

It was not appropriate or possible to involve patients or the public in the design, or conduct, or reporting, or dissemination plans of our research.

RESULTS

Clinicopathological characteristics

Demographic and clinicopathological characteristics of the patients with FIT-interval CRCs and SD-CRCs are shown in Table 1. No significant differences were found between both groups. Almost 60% of all patients were men. Among the FIT-interval CRCs, 21 patients (77.8%) were estimated to have a "normal/average" socioeconomic status, compared to 33 patients (61.1%) in the SD-CRC group. In the group of FIT-interval CRCs, fecal Hb concentrations were undetectable (n = 12, 44%) or below the threshold (n = 12, 44%). For three screenees (11%), the precise level of Hb/g feces was not available. Supplementary Table 1 shows per patient and per CRC type (SD-CRC or FIT-interval CRC) how many rounds of FIT participation had been completed prior to the diagnosis of CRC.

Table 1 Clinicopathological characteristics of all selected persons with fecal immunochemical test-interval and screen-detected colorectal cancers

Characteristics	FIT-interval CRC	SD-CRC	*P* value
Patients, *n*	27	54	
Age at diagnosis, mean (min-max)	65.9 yr (53-76)	65.2 yr (50-75)	NS
Male sex, *n* (%)	16 (59.3)	33 (61.1)	NS
Socio-economic status, *n* (%)			NS
Low	2 (7.4)	10 (18.5)	
Normal	21 (77.8)	33 (61.1)	
High	4 (14.8)	11 (20.4)	
Tumor location, *n* (%)			
Proximal	10 (37)	17 (31.5)	NS
Tumor stage, *n* (%)			
Stage I	8 (29.6)	25 (46.3)	NS
Stage II	6 (22.2)	8 (14.8)	
Stage III	9 (33.3)	20 (37.0)	
Stage IV	4 (14.8)	1 (1.9)	
Time interval between FIT and CRC			
Mean	1.4 yr		
Min-max	0.4-2.3 yr		
IQR	0.9-2.0 yr		
Mean Hb concentration last FIT in μg Hb/g feces, mean ± SD	2.7 ± 3.4[a]	167.8 ± 168.7	< 0.001

[a]3 cases missing.

All values expressed as number and % with respect to fecal immunochemical test-interval and screen-detected colorectal cancers. FIT: Fecal immunochemical test; CRC: Colorectal cancer; SD-CRC: Screen-detected colorectal cancer; IQR: Interquartile range; Hb: Hemoglobin; NS: Not significant.

MSI and CIMP analysis

MSI was more common among patients with FIT-interval CRCs compared to patients with SD-CRCs: 19% (4/21) *vs* 12% (5/41) [6.85% (95%CI: -12.7, 26.4); *P* = 0.469], respectively. Furthermore, CIMP was more prevalent in FIT-interval CRCs than in SD-CRCs, 33% (7/21) and 21% (8/39) [12.82% (95%CI: -11.36, 36.6); *P* = 0.274], respectively. However, differences for both variables did not reach statistical significance (Table 2).

Mutation analysis

Results of the mutation analysis in FIT-interval CRCs and SD-CRCs are shown in Figure 1. Of the 48 genes tested, 37 genes were mutated in at least one sample (see Figure 1). No mutations were detected in *FGFR1*, *FLT3*, *GNA11*, *GNAQ*, *HRAS*, *NPM1*, *PTPN11*, *SMARCB1*, *SMO*, *SRC* and *STK11*.

APC and *PIK3CA* were more often mutated in SD-CRC compared to FIT-interval CRC [*APC*: 68% *vs* 40%, 28.29% (95%CI: 2.53, 54.1); *P* = 0.035; *PIK3CA*: 27% *vs* 0%, 26.83% (95%CI: 13.27, 40.39); *P* = 0.011]. *KRAS* was mutated in 37% of SD-CRC compared to 30% in FIT-interval CRC [5% (95%CI: -20.57, 30.58); *P* =0.705]. *TP53* was mutated in 51% of SD-CRC compared to 40% in FIT-interval CRC [11.22% (95%CI: -15.14, 37.58); *P* = 0.410).

The following genes were significantly more often mutated in FIT-interval CRCs; *ALK* [20% *vs* 2.4%; 17.56% (95%CI: -0.59, 35.72); *P* = 0.019], *CSF-1R* [20% *vs* 2.4%; 17.56% (95%CI: -0.59, 35.72); *P* = 0.019], *EGFR* [10% *vs* 0%; 10% (95%CI: -3.15, 23.15); *P* = 0.037], *FGFR2* [10% *vs* 0%; 10% (95%CI: -3.15, 23.15); *P* = 0.040], *MET* [10% *vs* 0%; 10% (95%CI: -3.15, 23.15); *P* = 0.040], *MPL* [15% *vs* 0%; 15% (95%CI: -0.65, 30.65); *P* = 0.010].

BRAF [30% *vs* 12%; 17.8% (95%CI: -4.64, 40.25); *P* = 0.090], *KDR* [20% *vs* 5%; 15.12% (95%CI: -3.61, 33.85); *P* = 0.063] and *PTEN* [15% *vs* 2.4%; 12.56% (95%CI: -3.78, 28.9); *P* = 0.063] mutations were more abundant in FIT-interval CRCs compared to SD-CRC but this difference did not reach statistical significance (see Figure 1).

Table 2 Microsatellite instability analysis and CpG island methylator phenotype analysis

	FIT-interval CRC	SD-CRC	*P* value
MSI analysis[a]			
MSI	4 (19%)	5 (12%)	0.469
MSS	17 (81%)	36 (88%)	
CIMP analysis[b]			
Methylated, positive	7 (33%)	8 (21%)	0.274
Unmethylated, negative	14 (66%)	31 (79%)	

[a]*n* = 62.
[b]*n* = 60.
All values expressed as number and % with respect to fecal immunochemical test-interval and screen-detected colorectal cancers. FIT: Fecal immunochemical test; CRC: Colorectal cancer; SD-CRC: Screen-detected colorectal cancer; MSI: Microsatellite instability; MSS: Microsatellite stable; CIMP: CpG island methylator phenotype.

DNA copy number analysis

Figure 2 and Table 3 show the results of the DNA copy number analysis for FIT-interval CRC and SD-CRC. When comparing both groups, the only significantly different alterations were less frequent gains in FIT-interval CRCs at chromosome 8 region p11.22-q24.3 (P = 0.009) and more frequent gains in FIT-interval CRCs at chromosome 20 region p13-p12.1 (P = 0.039).

DISCUSSION

Of all interventions currently available, screening is one of the most powerful approaches for reducing CRC-related mortality[1]. Nevertheless, like all screening programs, CRC screening is facing the challenges of overdiagnosis and underdiagnosis. The latter mainly manifests as interval cancers. In the Dutch CRC screening program with a target population of 2.2M screenees, per screening round 544 interval cancers are observed, consistent with a FIT sensitivity of approximately 85%[26]. Theoretically, these FIT interval cancers consist of cancers that were present at the time the FIT was performed, but were missed, as well as cancer precursors missed at the time FIT was performed and that showed a rapid progression to a symptomatic cancer. On one hand sensitivity and specificity are simply determined by the cut off chosen, given the characteristics of the test. On the other hand, specific tumor characteristics driven by the underlying biology may differ between screened detected and interval cancers, a subject that so far has received little attention.

To address that question, the aim of the present study was to investigate the molecular characteristics between both categories. While we had access to a large well documented cohort of individuals followed over multiple screening rounds, the absolute number of interval cancers still was limited, which we consider to be the main reason why for most variables, differences were not statistically significant. Moreover, due to inherent formalin-fixed, paraffin-embedded associated artifacts, like DNA cross-links, the quality reads of some of the downstream analyses was poor and therefore some of the selected cases were further excluded from the final analysis (Supplementary Figure 1). Inherently these findings are exploratory in nature, yet they provide important indications on a major healthcare issue.

Indeed, the results of this exploratory study indicate that FIT-interval CRCs seem to more frequently carry the molecular features of the serrated neoplasia pathway and NP-CRNs than SD-CRCs do. FIT interval CRCs present more often CIMP high, MSI high and carry mutations like *ALK*, *BRAF*, *CSF1R*, *EGFR*, *FGR2*, *PTEN*, *KDR*, *MET* and *MPL* compared to SD-CRC. *PTEN* and *KDR* were previously described mutations detected in SSLs with high-grade dysplasia[27]. Furthermore, *APC* and *KRAS* mutations, which classically are part of the canonical adenoma-carcinoma sequence[5-7,27], were less frequently found in FIT-interval CRCs. Regarding DNA CNAs, FIT-interval CRCs showed very similar profiles to SD-CRCs, with only differences observed in the frequency of two genomic regions, namely, less often gains at 8p11.22-q24.3, and more often gains in FIT-interval CRCs at 20p13-p12.1. So, these results suggest that FIT-interval cancers are a mixed group of classical pathway and serrated pathway cancers, although with more commonly serrated pathway features and less commonly classical pathway features (both mutations and CNAs) in comparison with SD-CRCs. The overall pattern is striking, even if the individual variables do not reach statistical significance. Levin *et al*[28] also evaluated whether FIT-interval CRCs differed from FIT-positive patients with CRC by analyzing 7 *KRAS* mutations and 10 aberrantly methylated DNA biomarkers. They did not find any differences in their DNA profiles. In our study, however we investigated other genomic features and additional genes and did find differences as

Table 3 Copy number alterations

CGH-test[a]	Chr	Type	Band	Length basepairs	Group comparison	*P* value[b]
2.50%	8	Gain	p11.22-q24.3	106890001	Less in FIT-interval CRCs	0.009
2.50%	20	Gain	p13-p12.1	14520001	More in FIT-interval CRCs	0.039

[a]Percentage of information loss accepted at CGH-comparison test.
[b]Frequency of altered region in FIT-interval CRCs compared to screen-detected CRCs.
CGH: Comparative genomic hybridization; FIT: Fecal immunochemical test; CRC: Colorectal cancer.

described above[29].

FIT is a good test to detect cancers. However, it does not perform so well in the detection of precursor lesions, in particular sessile serrated polyps. In a study that compared sensitivities of several FITs in a screening population, FIT sensitivity for SSLs of > 1 cm was only 5.1%[10]. One possible explanation might be the result of less bleeding tendency due to the low vessel density in serrated lesions in combination with their flat morphology and proximal location. Another explanation could be that serrated pathway lesions may show faster progression to cancer than classic adenomas. This indicates that in FIT-screening, a substantial number of serrated polyps will be missed, and therefore cancers derived from these precursor lesions might be overrepresented in FIT-interval CRCs.

NP-CRNs also show distinct molecular features compared to classical polypoid adenomas, are frequently located in the right colon and might bleed less[11,30,31]. In previous studies, NP-CRNs have been described as being less often APC and KRAS-mutated[11]. In a study comparing PC-CRCs and prevalent CRCs, *KRAS* mutation was inversely associated with PC-CRCs[32]. Comparably, FIT-interval CRCs were less often APC mutated in the present study (40% in FIT-interval CRCs *vs* 68% in SD-CRCs, $P = 0.035$). However, although KRAS was less often mutated in FIT-interval CRCs, the difference was not significant (30% in FIT-interval CRCs *vs* 37% in SD-CRCs, $P = 0.705$). In the previously mentioned study on PC-CRCs, *BRAF*-mutation was present in 28% of PC-CRCs *vs* 19% of prevalent CRCs (not significant)[32]. These percentages are comparable to our findings on FIT-interval CRCs (*BRAF* mutated in 30% of FIT-interval CRCs *vs* 12% of SD-CRCs, not significant). Previously, it has been shown that PC-CRCs were more likely CIMP positive and MSI than sporadic CRCs[33,34]. A separate study in a large PC-CRC cohort in the Netherlands also shows PC-CRCs to be more likely CIMP positive, *MSI* and *BRAF* mutated than prevalent CRCs[35]. This suggests that the molecular patterns observed in the interval cancers suggest that these cancers arose *via* non-polypoid precursors and/or serrated precursors. This may reflect that interval cancers, both FIT interval CRCs and PC-CRCs, indeed have a different biology compared to prevalent CRCs but at the same time pose technical challenges because of their morphology (difficult to be detected during colonoscopy) as well their lack of bleeding (difficult to be detected by FIT).

Some CNAs are associated to progression of adenoma to carcinoma chromosomal instability canonical pathway, and these are labeled as cancer associated events[19]. As of yet, no CNAs have been well characterized in the CRCs originating from SSLs. A study of serrated polyps, with data on a set of 38 serrated polyps (12 traditional serrated adenomas and 26 SSLs) found gains at chromosome 7, 13 and 15q[36]. The present study did not show any differences at these specific regions. However, FIT-interval CRCs had less frequent gains at chromosome 8q, and more frequent gains at chromosome 20p then SD-CRCs. As 8q is one of the genomic regions associated with the canonical adenoma-to-carcinoma progression, this finding could mean that to a certain extent, FIT-interval CRCs follow a different progression pathway.

As stated above, FIT-interval CRCs identified in multiple screening rounds represent a case-mix of cancers originated from, not only the difficult to detect NP-CRNs and sessile serrated polyps, but also classic adenomas. Precursor lesions could simply be missed by FIT just because of the low sensitivity of this test to detect advanced adenomas and not representing a different biology as reason for missing the lesion. Yet, while molecular differences were observed between FIT-interval CRCs and SD-CRCs, not all of these were statistically significant. Still these findings provide an indication that FIT-interval CRCs are a heterogeneous mixture of phenotypes and underlying molecular biology, including CRCs from flat serrated lesions, from flat adenomas, and others, that for whatever reason shed blood in a way that levels are, at least intermittently, below the limit of detection of the FIT test. In view of this, there is a clinical need to improve in screening tests for CRC early detection.

Multi-target molecular stool DNA (mt-sDNA) testing has recently been recognized as a valid CRC screening option by the American Cancer Society[37], and its test characteristics seem especially favorable for the detection of serrated lesions. In a large trial, mt-sDNA testing showed a higher detection rate of larger serrated sessile polyps than FIT (sensitivity of 42.4% for mt-sDNA-test and 5.1% for FIT, for serrated polyps > 1 cm)[10]. The combined sensitivity for advanced precancerous lesions was also higher for mt-sDNA testing than for FIT (42.4% *vs* 23.8%). However, although the sensitivities are better compared to FIT, the mt-sDNA test shows lower specificity, compared to FIT, which is very

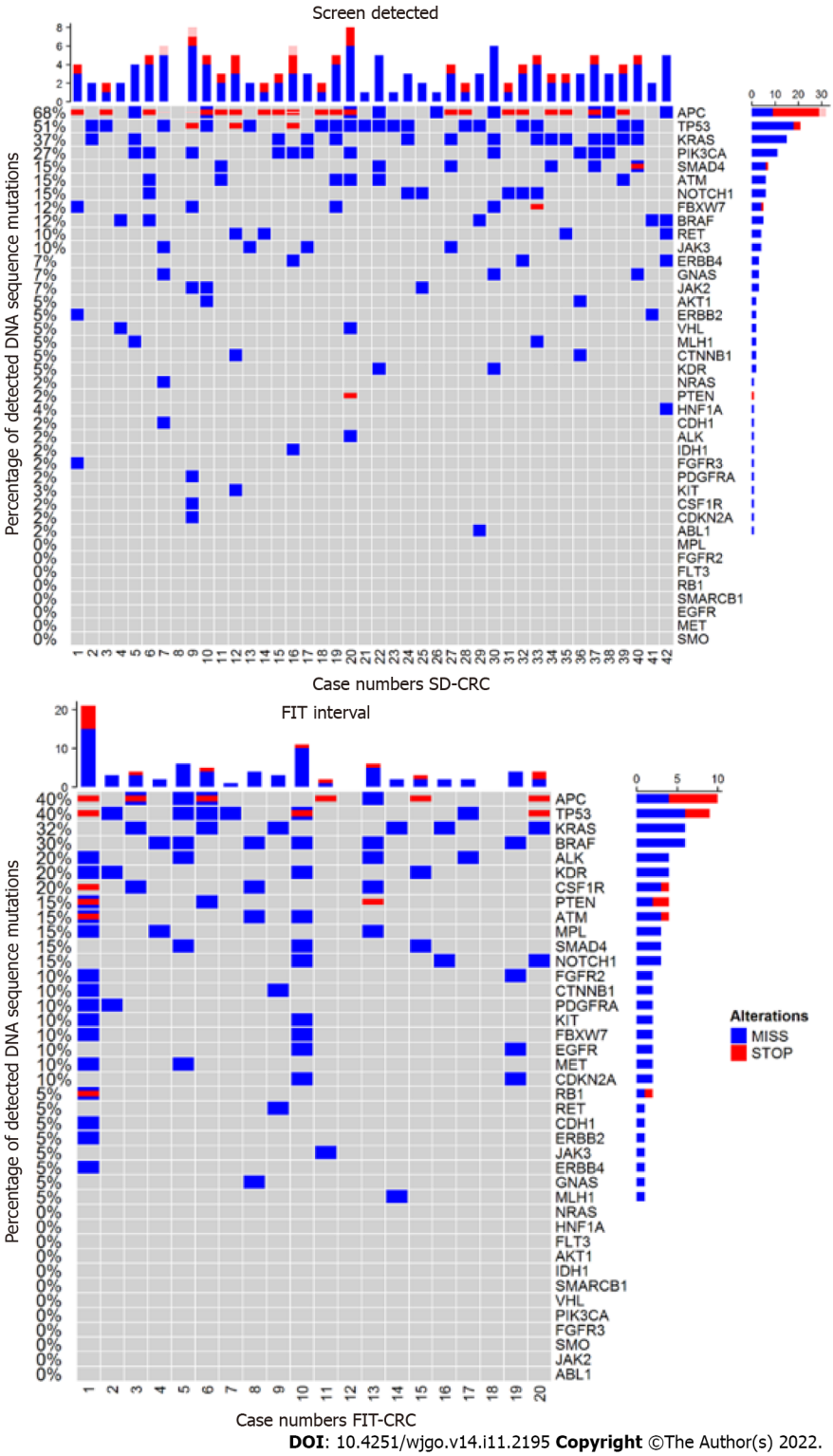

DOI: 10.4251/wjgo.v14.i11.2195 **Copyright** ©The Author(s) 2022.

Figure 1 DNA sequence mutation analysis. A and B: Overview of mutations detected in screen-detected colorectal cancer (CRC) (A) and in fecal immunochemical test-CRC (B). SD-CRC: Screen-detected colorectal cancer; FIT-CRC: Fecal immunochemical test- colorectal cancer.

important in programmatic screening. Recently, a panel of protein markers detected in stool showed also a higher sensitivity for advanced adenomas without losing in specificity, in comparison to FIT. This protein-based approach would have the potential to improve effectivity of FIT screening without major impact for program logistics or cost effectivity[38]. Implementation of a more accurate test could have the potential to detect a substantial number of CRCs or precursor lesions that would otherwise result in FIT-interval CRCs.

Strengths of our study include that FIT-interval CRCs were identified over multiple rounds in a biennial FIT-based screening cohort, and tissue specimens of each tumor could be obtained. We were able to compare FIT-interval CRCs to a control group of SD-CRCs within the same screening

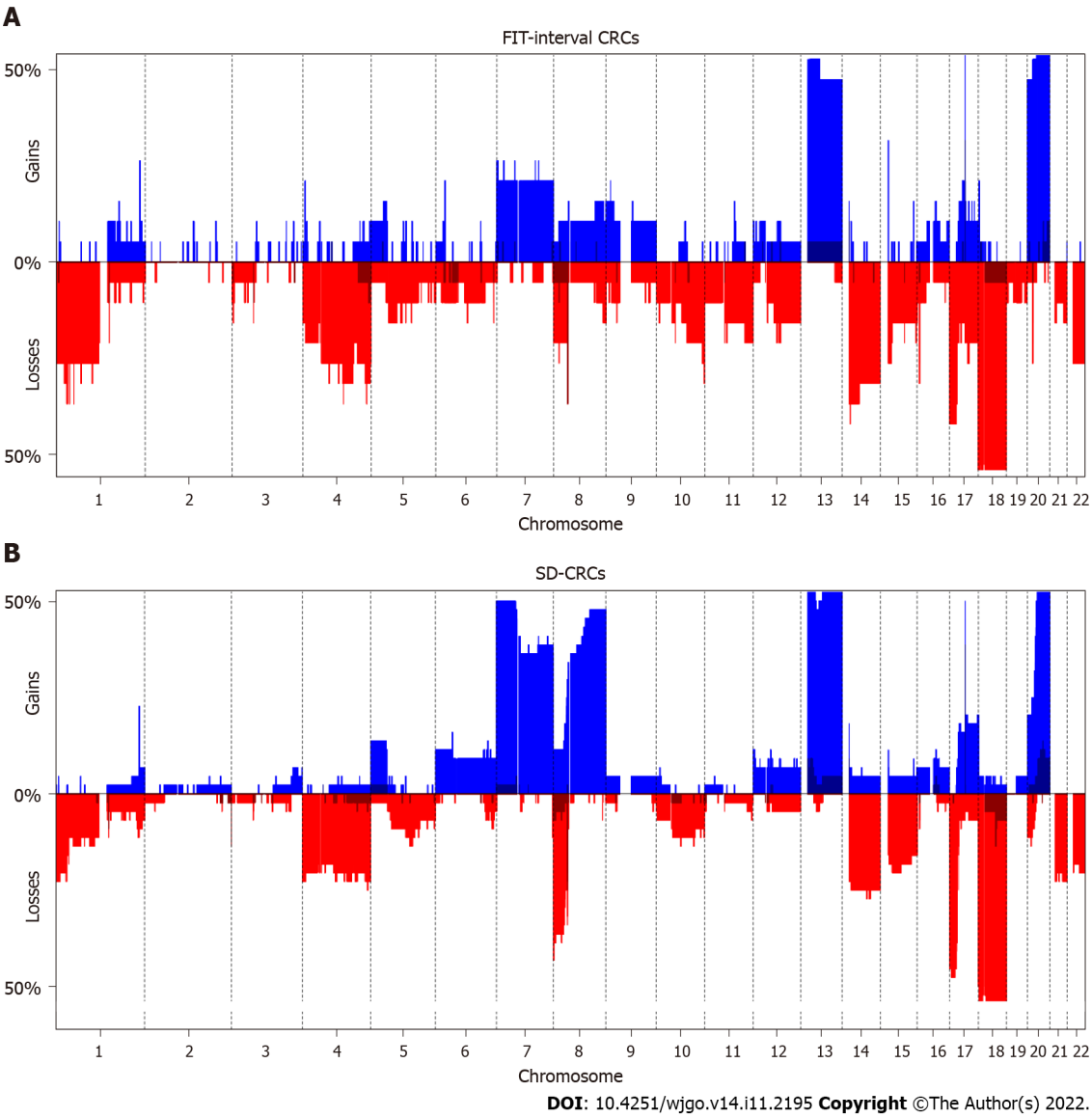

DOI: 10.4251/wjgo.v14.i11.2195

Figure 2 DNA copy number alterations in fecal immunochemical test-interval and screen-detected colorectal cancers, scale at 50%. A: Fecal immunochemical test-interval colorectal cancers (CRCs); B: Screen-detected CRCs. SD-CRC: Screen-detected colorectal cancer; FIT-CRC: Fecal immunochemical test- colorectal cancer.

population, region and time-span. However, an important limitation is the sample size. A total of 27 FIT-interval CRCs is still a limited number, reflecting the rarity of this entity, with inherent consequences for the statistical power of the study. To address this issue, a larger control group was composed through random selection in a 1:2 ratio. Due to budgetary and logistical constraints, we were not able to enlarge the control group. Also, we were not informed about the family history for cancer among the persons included in the study. Although rare, some of the FIT-interval CRCs might be related to familial CRC. So, although the findings of our study are suggestive for a difference in molecular make-up, further studies are needed to support our findings. We did not report tumor size and morphology of all CRCs, as this is not easy to determine in cancers (as compared to adenomas or SSLs). We were, therefore, not able to correlate size or morphology to the molecular analysis.

CONCLUSION

In conclusion, the present study provides evidence that SD-CRCs and FIT interval CRCs differ in the distribution of molecular tumor profiles. These findings can provide guidance on strategies for further improving stool-based CRC screening strategies. Future research should focus on the role of incorporating biomarkers in screening for identifying more CRCs during screening, thereby reducing the number of screening interval CRCs.

ARTICLE HIGHLIGHTS

Research background

Fecal immunochemical test (FIT) is effective in reducing colorectal cancer (CRC) but FIT testing is not perfect. FIT interval cancers, *i.e.* CRCs diagnosed after a negative FIT but before the next FIT invitation, still occur. FIT sensitivity for CRC is approximately 75%-85% and sensitivity drops to low detection rates for adenomas and even more so for sessile serrated lesions (SSLs).

Research motivation

In order to lower the number of missed lesions, we need to understand which lesions are more often missed by FIT in order to improve the screening strategy. Previous studies have shown that FIT sensitivity for SSLs is low, but a correlation between the occurrence of FIT interval cancers and the serrated pathway has not been established.

Research objectives

Our aim was to generate more insight in the molecular features of FIT-interval CRCs, as this could help in developing a more optimal screening strategy with the aim to reduce the incidence of FIT interval cancers.

Research methods

We compared the molecular make up of screen-detected CRCs (SD-CRCs) and FIT-interval CRCs, detected in a Dutch pilot-program of FIT-based screening. Molecular analyses included microsatellite instability (MSI), CpG island methylator phenotype (CIMP), DNA sequence mutations and copy number alterations.

Research results

FIT-interval CRCs were more often CIMP- and MSI-positive as compared to SD-CRCs. They also harbored more often *BRAF* and *PTEN* mutations as compared to SD-CRCs.

Research conclusions

The serrated pathway-associated molecular features seem to be more common in FIT-interval CRCs as compared to screen detected CRCs. This might indicate that proximal serrated lesions are overrepresented among FIT interval CRCs. Further research needs to be performed. Adding molecular markers of the serrated-pathway to the FIT needs to be further explored.

Research perspectives

These findings can provide guidance on strategies to further improve stool-based CRC screening with incorporating biomarkers for SSLs, thereby reducing the number of screening interval CRCs.

ACKNOWLEDGEMENTS

This work was performed within the framework of the COST Action (CA17118), supported by COST (European Cooperation in Science and Technology).

FOOTNOTES

Author contributions: van der Vlugt M, Carvalho B, Meijer GA and Dekker E contributed to the study concept and design, acquisition of data, analysis and interpretation of data; van der Vlugt M and Carvalho B contributed to drafting of the manuscript and statistical analysis; Fliers J contributed to the study concept and design; Fliers J, Montazeri N, Rausch C, Grobbee EJ, van Engeland M, Spaander MCW, Meijer GA and Dekker E contributed to critical revision of the manuscript for important intellectual content; Montazeri N and Rausch C contributed to study design and statistical analysis; Grobbee EJ, van Engeland M and Spaander MCW contributed to the study concept and acquisition of data.

Supported by Foundation of Population Screening Mid-West Netherlands, Amsterdam, The Netherlands (BoMW); Foundation of Population Screening South-West Netherlands, Rotterdam, The Netherlands (BoZW); Netherlands Comprehensive Cancer Organization (IKNL); Netherlands Organization for Health Research and Development of the Dutch Ministry of Health (ZonMW); PALGA, the Nationwide Network and Registry of Histo- and Cytopathology in the Netherlands.

Institutional review board statement: Ethics approval for performing FIT-based screening including linkage to the Netherlands Cancer Registry was provided by the Dutch National Health Council (WBO 2642467, 2832758, 3049078

and 161536-112008, The Hague, The Netherlands). No separate ethics approval was necessary for the additional molecular analysis, as judged by the scientific ethics board of the AMC University Hospital. Collection and use of tissue and patient data were performed in compliance with the 'Code for Proper Secondary Use of Human Tissue in the Netherlands' (www.federa.org).

Clinical trial registration statement: This study is registered at the Dutch Trial Registry. Registration number: NTR5874 (http://www.trialregister.nl).

Informed consent statement: All screenees participating in FIT screening filled in an informed consent form.

Conflict-of-interest statement: Meijer GA has research collaborations with Exact Sciences, Sysmex and Sentinel for other studies regarding early detection of colorectal cancer. The companies provide materials, equipment or (sample) analyses. Meijer GA is CSO and shareholder of CRCbioscreen BV. Carvalho B has several patents pending. Dekker E received a research grant from FujiFilm. She has received honorarium for consultancy from FujiFilm, Olympus, Tillots, GI Supply, CPP-FAP and PAION, and speakers' fees from Olympus, Roche, GI Supply and Norgine. Spaander MC received research support of Sysmex and Sentinel. All other coauthors don't have conflicts of interest.

Data sharing statement: Raw mutation data (concerning the mutation analysis and DNA copy number analysis) have been deposited in the European Genome-Phenome Archive with the study ID: EGAS00001004683.

Country/Territory of origin: Netherlands

ORCID number: Manon van der Vlugt 0000-0002-4472-7055; Manon C W Spaander 0000-0002-9103-9757.

S-Editor: Zhang H
L-Editor: Filipodia
P-Editor: Zhang H

REFERENCES

1 **Malila N**, Senore C, Armaroli P. International Agency for Research on C. European guidelines for quality assurance in colorectal cancer screening and diagnosis. First Edition--Organisation. *Endoscopy* 2012; **44**: SE31-48
2 **van der Vlugt M**, Grobbee EJ, Bossuyt PMM, Bos A, Bongers E, Spijker W, Kuipers EJ, Lansdorp-Vogelaar I, Spaander MCW, Dekker E. Interval Colorectal Cancer Incidence Among Subjects Undergoing Multiple Rounds of Fecal Immunochemical Testing. *Gastroenterology* 2017; **153**: 439-447.e2 [PMID: 28483499 DOI: 10.1053/j.gastro.2017.05.004]
3 **de Wijkerslooth TR**, Stoop EM, Bossuyt PM, Meijer GA, van Ballegooijen M, van Roon AH, Stegeman I, Kraaijenhagen RA, Fockens P, van Leerdam ME, Dekker E, Kuipers EJ. Immunochemical fecal occult blood testing is equally sensitive for proximal and distal advanced neoplasia. *Am J Gastroenterol* 2012; **107**: 1570-1578 [PMID: 22850431 DOI: 10.1038/ajg.2012.249]
4 **van Winden O**. Landelijke monitoring en evaluatie van het bevolkingsonderzoek naar darmkanker in Nederland 2014-2017. Accessed 3 March 2020. Available from: https://www.rivm.nl/sites/default/files/2019-03/monitor-evaluatie-darm-2014-2017.pdf
5 **Vogelstein B**, Fearon ER, Hamilton SR, Kern SE, Preisinger AC, Leppert M, Nakamura Y, White R, Smits AM, Bos JL. Genetic alterations during colorectal-tumor development. *N Engl J Med* 1988; **319**: 525-532 [PMID: 2841597 DOI: 10.1056/NEJM198809013190901]
6 **Fearon ER**, Cho KR, Nigro JM, Kern SE, Simons JW, Ruppert JM, Hamilton SR, Preisinger AC, Thomas G, Kinzler KW. Identification of a chromosome 18q gene that is altered in colorectal cancers. *Science* 1990; **247**: 49-56 [PMID: 2294591 DOI: 10.1126/science.2294591]
7 **Fearon ER**, Vogelstein B. A genetic model for colorectal tumorigenesis. *Cell* 1990; **61**: 759-767 [PMID: 2188735 DOI: 10.1016/0092-8674(90)90186-i]
8 **Kambara T**, Simms LA, Whitehall VL, Spring KJ, Wynter CV, Walsh MD, Barker MA, Arnold S, McGivern A, Matsubara N, Tanaka N, Higuchi T, Young J, Jass JR, Leggett BA. BRAF mutation is associated with DNA methylation in serrated polyps and cancers of the colorectum. *Gut* 2004; **53**: 1137-1144 [PMID: 15247181 DOI: 10.1136/gut.2003.037671]
9 **O'Brien MJ**, Yang S, Mack C, Xu H, Huang CS, Mulcahy E, Amorosino M, Farraye FA. Comparison of microsatellite instability, CpG island methylation phenotype, BRAF and KRAS status in serrated polyps and traditional adenomas indicates separate pathways to distinct colorectal carcinoma end points. *Am J Surg Pathol* 2006; **30**: 1491-1501 [PMID: 17122504 DOI: 10.1097/01.pas.0000213313.36306.85]
10 **Imperiale TF**, Ransohoff DF, Itzkowitz SH, Levin TR, Lavin P, Lidgard GP, Ahlquist DA, Berger BM. Multitarget stool

DNA testing for colorectal-cancer screening. *N Engl J Med* 2014; **370**: 1287-1297 [PMID: 24645800 DOI: 10.1056/NEJMoa1311194]

11 **Voorham QJ**, Carvalho B, Spiertz AJ, van Grieken NC, Mongera S, Rondagh EJ, van de Wiel MA, Jordanova ES, Ylstra B, Kliment M, Grabsch H, Rembacken BJ, Arai T, de Bruïne AP, Sanduleanu S, Quirke P, Mulder CJ, van Engeland M, Meijer GA. Chromosome 5q loss in colorectal flat adenomas. *Clin Cancer Res* 2012; **18**: 4560-4569 [PMID: 22761468 DOI: 10.1158/1078-0432.CCR-11-2385]

12 **le Clercq CM**, Bouwens MW, Rondagh EJ, Bakker CM, Keulen ET, de Ridder RJ, Winkens B, Masclee AA, Sanduleanu S. Postcolonoscopy colorectal cancers are preventable: a population-based study. *Gut* 2014; **63**: 957-963 [PMID: 23744612 DOI: 10.1136/gutjnl-2013-304880]

13 **Rembacken B**, Hassan C, Riemann JF, Chilton A, Rutter M, Dumonceau JM, Omar M, Ponchon T. Quality in screening colonoscopy: position statement of the European Society of Gastrointestinal Endoscopy (ESGE). *Endoscopy* 2012; **44**: 957-968 [PMID: 22987217 DOI: 10.1055/s-0032-1325686]

14 **Kapidzic A**, Grobbee EJ, Hol L, van Roon AH, van Vuuren AJ, Spijker W, Izelaar K, van Ballegooijen M, Kuipers EJ, van Leerdam ME. Attendance and yield over three rounds of population-based fecal immunochemical test screening. *Am J Gastroenterol* 2014; **109**: 1257-1264 [PMID: 24980879 DOI: 10.1038/ajg.2014.168]

15 **Stegeman I**, van Doorn SC, Mundt MW, Mallant-Hent RC, Bongers E, Elferink MA, Fockens P, Stroobants AK, Bossuyt PM, Dekker E. Participation, yield, and interval carcinomas in three rounds of biennial FIT-based colorectal cancer screening. *Cancer Epidemiol* 2015; **39**: 388-393 [PMID: 25910865 DOI: 10.1016/j.canep.2015.03.012]

16 **Sanduleanu S**, le Clercq CM, Dekker E, Meijer GA, Rabeneck L, Rutter MD, Valori R, Young GP, Schoen RE; Expert Working Group on 'Right-sided lesions and interval cancers', Colorectal Cancer Screening Committee, World Endoscopy Organization. Definition and taxonomy of interval colorectal cancers: a proposal for standardising nomenclature. *Gut* 2015; **64**: 1257-1267 [PMID: 25193802 DOI: 10.1136/gutjnl-2014-307992]

17 **Edge SB**, Compton CC. The American Joint Committee on Cancer: the 7th edition of the AJCC cancer staging manual and the future of TNM. *Ann Surg Oncol* 2010; **17**: 1471-1474 [PMID: 20180029 DOI: 10.1245/s10434-010-0985-4]

18 **Casparie M**, Tiebosch AT, Burger G, Blauwgeers H, van de Pol A, van Krieken JH, Meijer GA. Pathology databanking and biobanking in The Netherlands, a central role for PALGA, the nationwide histopathology and cytopathology data network and archive. *Cell Oncol* 2007; **29**: 19-24 [PMID: 17429138 DOI: 10.1155/2007/971816]

19 **Hermsen M**, Postma C, Baak J, Weiss M, Rapallo A, Sciutto A, Roemen G, Arends JW, Williams R, Giaretti W, De Goeij A, Meijer G. Colorectal adenoma to carcinoma progression follows multiple pathways of chromosomal instability. *Gastroenterology* 2002; **123**: 1109-1119 [PMID: 12360473 DOI: 10.1053/gast.2002.36051]

20 **Weisenberger DJ**, Siegmund KD, Campan M, Young J, Long TI, Faasse MA, Kang GH, Widschwendter M, Weener D, Buchanan D, Koh H, Simms L, Barker M, Leggett B, Levine J, Kim M, French AJ, Thibodeau SN, Jass J, Haile R, Laird PW. CpG island methylator phenotype underlies sporadic microsatellite instability and is tightly associated with BRAF mutation in colorectal cancer. *Nat Genet* 2006; **38**: 787-793 [PMID: 16804544 DOI: 10.1038/ng1834]

21 **Derks S**, Postma C, Moerkerk PT, van den Bosch SM, Carvalho B, Hermsen MA, Giaretti W, Herman JG, Weijenberg MP, de Bruïne AP, Meijer GA, van Engeland M. Promoter methylation precedes chromosomal alterations in colorectal cancer development. *Cell Oncol* 2006; **28**: 247-257 [PMID: 17167178 DOI: 10.1155/2006/846251]

22 **Herman JG**, Graff JR, Myöhänen S, Nelkin BD, Baylin SB. Methylation-specific PCR: a novel PCR assay for methylation status of CpG islands. *Proc Natl Acad Sci U S A* 1996; **93**: 9821-9826 [PMID: 8790415 DOI: 10.1073/pnas.93.18.9821]

23 **van Lanschot MCJ**, Carvalho B, Rausch C, Snaebjornsson P, van Engeland M, Kuipers EJ, Stoker J, Tutein Nolthenius CJ, Dekker E, Meijer GA. Molecular profiling of longitudinally observed small colorectal polyps: A cohort study. *EBioMedicine* 2019; **39**: 292-300 [PMID: 30555044 DOI: 10.1016/j.ebiom.2018.12.009]

24 **Lappalainen I**, Almeida-King J, Kumanduri V, Senf A, Spalding JD, Ur-Rehman S, Saunders G, Kandasamy J, Caccamo M, Leinonen R, Vaughan B, Laurent T, Rowland F, Marin-Garcia P, Barker J, Jokinen P, Torres AC, de Argila JR, Llobet OM, Medina I, Puy MS, Alberich M, de la Torre S, Navarro A, Paschall J, Flicek P. The European Genome-phenome Archive of human data consented for biomedical research. *Nat Genet* 2015; **47**: 692-695 [PMID: 26111507 DOI: 10.1038/ng.3312]

25 **van de Wiel MA**, Smeets SJ, Brakenhoff RH, Ylstra B. CGHMultiArray: exact P-values for multi-array comparative genomic hybridization data. *Bioinformatics* 2005; **21**: 3193-3194 [PMID: 15879450 DOI: 10.1093/bioinformatics/bti489]

26 **Toes-Zoutendijk E**, Kooyker AI, Dekker E, Spaander MCW, Opstal-van Winden AWJ, Ramakers C, Buskermolen M, van Vuuren AJ, Kuipers EJ, van Kemenade FJ, Velthuysen MF, Thomeer MGJ, van Veldhuizen H, van Ballegooijen M, Nagtegaal ID, de Koning HJ, van Leerdam ME, Lansdorp-Vogelaar I; Dutch National Colorectal Cancer Screening Working Group. Incidence of Interval Colorectal Cancer After Negative Results From First-Round Fecal Immunochemical Screening Tests, by Cutoff Value and Participant Sex and Age. *Clin Gastroenterol Hepatol* 2020; **18**: 1493-1500 [PMID: 31442598 DOI: 10.1016/j.cgh.2019.08.021]

27 **Murakami T**, Akazawa Y, Yatagai N, et al Molecular characterization of sessile serrated adenoma/polyps with dysplasia/carcinoma based on immunohistochemistry, next-generation sequencing, and microsatellite instability testing: a case series study. Diagn Pathol. 2018 Nov 20;13(1):88.

28 **Levin TR**, Corley DA, Jensen CD, Marks AR, Zhao WK, Zebrowski AM, Quinn VP, Browne LW, Taylor WR, Ahlquist DA, Lidgard GP, Berger BM. Genetic Biomarker Prevalence Is Similar in Fecal Immunochemical Test Positive and Negative Colorectal Cancer Tissue. *Dig Dis Sci* 2017; **62**: 678-688 [PMID: 28044229 DOI: 10.1007/s10620-016-4433-6]

29 **Cancer Genome Atlas Network**. Comprehensive molecular characterization of human colon and rectal cancer. *Nature* 2012; **487**: 330-337 [PMID: 22810696 DOI: 10.1038/nature11252]

30 **Nakama H**, Zhang B, Kamijo N. Sensitivity of immunochemical fecal occult blood test for colorectal flat adenomas. *Hepatogastroenterology* 2004; **51**: 1333-1336 [PMID: 15362746]

31 **van Doorn SC**, Stegeman I, Stroobants AK, Mundt MW, de Wijkerslooth TR, Fockens P, Kuipers EJ, Bossuyt PM, Dekker E. Fecal immunochemical testing results and characteristics of colonic lesions. *Endoscopy* 2015; **47**: 1011-1017 [PMID: 26126163 DOI: 10.1055/s-0034-1392412]

32 **Shaukat A**, Arain M, Anway R, Manaktala S, Pohlman L, Thyagarajan B. Is KRAS mutation associated with interval

colorectal cancers? *Dig Dis Sci* 2012; **57**: 913-917 [PMID: 22138963 DOI: 10.1007/s10620-011-1974-6]

33 **Sawhney MS**, Farrar WD, Gudiseva S, Nelson DB, Lederle FA, Rector TS, Bond JH. Microsatellite instability in interval colon cancers. *Gastroenterology* 2006; **131**: 1700-1705 [PMID: 17087932 DOI: 10.1053/j.gastro.2006.10.022]

34 **Arain MA**, Sawhney M, Sheikh S, Anway R, Thyagarajan B, Bond JH, Shaukat A. CIMP status of interval colon cancers: another piece to the puzzle. *Am J Gastroenterol* 2010; **105**: 1189-1195 [PMID: 20010923 DOI: 10.1038/ajg.2009.699]

35 **Bogie RMM**, le Clercq CMC, Voorham QJM, Cordes M, Sie D, Rausch C, van den Broek E, de Vries SDJ, van Grieken NCT, Riedl RG, Sastrowijoto P, Speel EJ, Vos R, Winkens B, van Engeland M, Ylstra B, Meijer GA, Masclee AAM, Carvalho B. Molecular pathways in post-colonoscopy versus detected colorectal cancers: results from a nested case-control study. *Br J Cancer* 2022; **126**: 865-873 [PMID: 34912077 DOI: 10.1038/s41416-021-01619-z]

36 **Gaiser T**, Meinhardt S, Hirsch D, Killian JK, Gaedcke J, Jo P, Ponsa I, Miró R, Rüschoff J, Seitz G, Hu Y, Camps J, Ried T. Molecular patterns in the evolution of serrated lesion of the colorectum. *Int J Cancer* 2013; **132**: 1800-1810 [PMID: 23011871 DOI: 10.1002/ijc.27869]

37 **Wolf AMD**, Fontham ETH, Church TR, Flowers CR, Guerra CE, LaMonte SJ, Etzioni R, McKenna MT, Oeffinger KC, Shih YT, Walter LC, Andrews KS, Brawley OW, Brooks D, Fedewa SA, Manassaram-Baptiste D, Siegel RL, Wender RC, Smith RA. Colorectal cancer screening for average-risk adults: 2018 guideline update from the American Cancer Society. *CA Cancer J Clin* 2018; **68**: 250-281 [PMID: 29846947 DOI: 10.3322/caac.21457]

38 **Bosch LJW**, de Wit M, Pham TV, Coupé VMH, Hiemstra AC, Piersma SR, Oudgenoeg G, Scheffer GL, Mongera S, Sive Droste JT, Oort FA, van Turenhout ST, Larbi IB, Louwagie J, van Criekinge W, van der Hulst RWM, Mulder CJJ, Carvalho B, Fijneman RJA, Jimenez CR, Meijer GA. Novel Stool-Based Protein Biomarkers for Improved Colorectal Cancer Screening: A Case-Control Study. *Ann Intern Med* 2017; **167**: 855-866 [PMID: 29159365 DOI: 10.7326/M17-1068]

World Journal of Gastrointestinal Oncology

Submit a Manuscript: https://www.f6publishing.com

World J Gastrointest Oncol 2022 November 15; 14(11): 2208-2223

DOI: 10.4251/wjgo.v14.i11.2208

ISSN 1948-5204 (online)

ORIGINAL ARTICLE

Case Control Study

Oxidative imbalance increases the risk for colonic polyp and colorectal cancer development

Dimitrios Tsounis, Vassiliki Villiotou, Angeliki Melpidou, Chara Pantsiou, Alexandra Argyrou, Charis Giannopoulou, Adriani Grigoratou, Dimitra Rontogianni, Gerassimos J Mantzaris, George Papatheodoridis

Specialty type: Gastroenterology and hepatology

Provenance and peer review: Unsolicited article; Externally peer reviewed.

Peer-review model: Single blind

Peer-review report's scientific quality classification

Grade A (Excellent): 0
Grade B (Very good): B
Grade C (Good): 0
Grade D (Fair): D
Grade E (Poor): 0

P-Reviewer: Jabbarpour Z, Iran; Jin CH, China

Received: May 4, 2022
Peer-review started: May 4, 2022
First decision: July 13, 2022
Revised: August 19, 2022
Accepted: September 21, 2022
Article in press: September 21, 2022
Published online: November 15, 2022

Dimitrios Tsounis, Alexandra Argyrou, Department of Gastroenterology, 251 General Hospital of Hellenic Air Force, Athens 11525, Greece

Vassiliki Villiotou, Department of Biochemistry, Metaxa Anticancer Hospital, Piraeus 18537, Greece

Angeliki Melpidou, Chara Pantsiou, Adriani Grigoratou, Department of Biochemistry, Evangelismos Hospital, Athens 10676, Greece

Charis Giannopoulou, Department of Nuclear Medicine and Positron Emission Tomography Computed Tomography, Evangelismos Hospital, Athens 10676, Greece

Dimitra Rontogianni, Department of Pathology, Evangelismos Hospital, Athens 10676, Greece

Gerassimos J Mantzaris, Department of Gastroenterology, Evangelismos, Ophthalmiatreion Athinon and Polyclinic Hospitals, Athens 10676, Greece

George Papatheodoridis, Academic Department of Gastroenterology, Athens University Medical School, Laikon General Hospital, Athens 11527, Greece

Corresponding author: Dimitrios Tsounis, FEBG, MD, MSc, Chief Doctor, Consultant Physician-Scientist, Department of Gastroenterology, 251 General Hospital of Hellenic Air Force, P. Kanellopoulou Avenue 3, Athens 11525, Greece. dim.tsoun69@gmail.com

Abstract

BACKGROUND

The role of oxidative stress in the pathogenesis of colorectal carcinoma (CRC) has garnered considerable interest recently. Specific oxidative factors have been implicated in the pathogenesis of adenomatous polyps and ultimately adenocarcinoma.

AIM

To evaluate the effect of oxidative imbalance as quantified by specific serological markers in the development of sporadic colon adenocarcinoma.

METHODS

A total of 170 patients that underwent endoscopy of the lower gastrointestinal tract in a tertiary center within 3 years were included in the study. They were

allocated in three groups; those with sporadic colon adenocarcinoma (n = 56, 32.9%), those with colonic polyps (n = 33, 19.4%) and healthy controls (n = 81, 47.7%). All patients were evaluated for oxidant activity and antioxidant capacity with serum measurements of specific markers such as vitamins A, 25(OH) D3, E, C, B12, folic acid, glutathione, selenium (Se), zinc (Zn), free iron (Fe^{2+}), and malondialdehyde and results were compared between groups.

RESULTS

Serum levels of vitamins C, E, D, Se, Zn, vitamin B12 and total antioxidant capacity were significantly lower in the combined neoplasia/polyp group than in the control group (P = 0.002, P = 0.009, P < 0.001, P < 0.001, P < 0.001, P = 0.020 and P < 0.001, correspondingly). Increased levels of vitamin E (P = 0.004), vitamin D (P < 0.001), Se (P < 0.001) and Zn (P < 0.001) seem to bestow a protective effect on the development of CRC. For vitamin D (P < 0.001) and Zn (P = 0.036), this effect seems to extend to the development of colon polyps as well. On the other hand, elevated serum levels of malondialdehyde are associated with a higher risk of CRC (OR = 2.09 compared to controls, P = 0.004). Regarding colonic polyp development, increased concentrations of vitamin A and Fe^{2+} are associated with a higher risk, whereas lower levels of malondialdehyde with a lower risk.

CONCLUSION

Increased oxidative stress may play an important role in the pathogenesis and progression of CRC. Antioxidants' presence may exert a protective effect in the very early stages of colon carcinogenesis.

Key Words: Oxidative imbalance; Reactive oxygen species; Colorectal adenocarcinoma; Colonic polyps; Antioxidant capacity

Core Tip: The role of oxidative stress in the pathogenesis of colorectal carcinoma (CRC) has garnered considerable interest recently. Here, we evaluated oxidant activity and antioxidant capacity of the patients with serum measurements of specific markers. Increased levels of vitamin E, vitamin D, selenium and zinc seem to bestow a protective effect regarding the development of CRC, whereas elevated serum levels of malondialdehyde are associated with a higher risk of CRC. Increased oxidative stress may play an important role in the pathogenesis and progression of CRC. Antioxidants' presence may exert a protective effect in the very early stages of colon carcinogenesis.

Citation: Tsounis D, Villiotou V, Melpidou A, Pantsiou C, Argyrou A, Giannopoulou C, Grigoratou A, Rontogianni D, Mantzaris GJ, Papatheodoridis G. Oxidative imbalance increases the risk for colonic polyp and colorectal cancer development. *World J Gastrointest Oncol* 2022; 14(11): 2208-2223
URL: https://www.wjgnet.com/1948-5204/full/v14/i11/2208.htm
DOI: https://dx.doi.org/10.4251/wjgo.v14.i11.2208

INTRODUCTION

The term oxidative stress or oxidative imbalance refers to a series of intracellular complex metabolic processes that lead to overproduction and accumulation of oxidative products, otherwise called free radicals or reactive oxygen species (ROS), including hydrogen peroxide, hydroxyl radical, superoxide anion and peroxynitrite[1]. These, in turn, collaborate to overcome the protective action of existing intracellular antioxidant mechanisms. The overproduction of ROS has been shown to ultimately result in toxicity inimical practically to every cellular macromolecule including all intracellular organelles with a special emphasis on membranes and mitochondria. The net effect of this process is local and eventually generalized impairment of human organ system function, either in the form of inflammation or carcinogenesis[1].

The pathogenesis of sporadic adenocarcinoma (adenoCa) of the large intestine is a complex process involving both genetic and epigenetic factors[2-4]. The genetic component refers to the gradual accumulation of multiple genetic mutations in key growth regulatory genes[5], leading to two main types of gene instability (chromosome and microsatellite) which characterize sporadic adenoCa and define its biological behavior[4]. Furthermore, multiple other conditions have been identified as implicated in the pathogenesis of large bowel adenoCa, possibly through chemical modification of DNA bases during the

replication process, especially in the stage of aberrant crypt foci (ACF) formation[5,6]. ACF represents the earliest histological alterations in the formation of colorectal neoplasia[6]. Risk factors associated with colorectal cancer include inflammatory bowel disease, nutrition habits (western type of diet), type II diabetes mellitus, sedentary (*e.g.*, low exercise) lifestyle, professional exposure to specific irritants (*e.g.*, mutagenic chemicals such as asbestos), previous medical procedures (*e.g.*, cholecystectomy, radiotherapy of the pelvis, ureterocolic anastomosis), as well as smoking and obesity.

Among the aforementioned risk factors, nutritional habits and their potential influence in particular on the equilibrium between oxidative and antioxidative substances have garnered a significant amount of interest recently. Epidemiological studies indicate that colon adenocarcinoma is observed more frequently among individuals with a diet characterized by a low intake of fiber and calcium and a higher consumption of saturated fatty acids and proteins, especially of bovine origin (red meat)[7-10]. This dietary profile has been associated with increased production of potentially carcinogenic substances such as toxic bile acids and free iron[11]. Furthermore, the resulting positive energy balance (due to the high accumulation of calories when following the western type of diet) and subsequent obesity have been suggested to lead to metabolic stress including overproduction of ROS or other organic compounds, such as malondialdehyde (MDA)[12]. Contrariwise, antioxidant substances including polyphenols, tocopherols, carotenoids, curcumin, vitamin A, vitamin C and vitamin D seem to obtain a protective role against colorectal cancer[1]. It is intriguing to ascertain the exact role of oxidative imbalance in the pathogenesis of initially precancerous lesions such as colonic polyps and ultimately colon cancer. To our knowledge, there are only a few studies that have tried to detect a pattern of total oxidant activity and antioxidant capacity among patients with established sporadic adenocarcinoma of the large intestine, as this may be assessed through the measurement of specific serum compounds and these studies have produced conflicting results[13,14]. Thus, we designed a prospective, case-control, single-center study aiming to evaluate the role of oxidative imbalance and its effect as a possible primary agent in the development of sporadic adenocarcinoma of the large intestine. We tried to achieve this by determining serum levels of specific markers that reflect oxidant capacity in patients with established colorectal carcinoma in comparison to patients with colonic polyps and healthy controls.

MATERIALS AND METHODS

Study population

A total of 6500 patients that were over 50-years-old and successfully underwent colonoscopy within 3 years in a major tertiary Greek hospital were screened for participation in the study. A set of specific exclusion criteria were used to curtail the influence of confounding risk factors in data analysis (Table 1). Ultimately 170 patients were included in our study. Among them, three specific groups were defined, those with a histologically confirmed sporadic adenoCa of the colon, those with a diagnosis of colonic polyps and a healthy control group consisting of patients with no significant findings or findings irrelevant to the development of CRC (*e.g.*, diverticula).

Study protocol

All patients gave informed consent for their participation in the study and were interviewed by a gastroenterologist not involved in their endoscopic management. Relevant demographic, epidemiological and clinical characteristics were recorded. Full colonoscopy was performed on all patients following the established sedation, preparation and safety protocols in our Centre following international guidelines. All procedures were performed by the same experienced gastroenterologist (with more than 2000 colonoscopies/year and a rate of over 98% for successful completion of the procedure). When endoscopic findings, suggestive of adenocarcinoma or polyps of the large intestine were identified, single or multiple biopsy samples were obtained and sent to the Pathology department of our hospital. Biopsy specimens were assessed by two independent and experienced pathologists, unaware of the endoscopic findings, with a high inter-observer agreement (> 90%). Sporadic adenocarcinoma was evaluated for the following parameters: (1) Staging according to the Astler-Coller system of classification[15]; (2) Grading according to a three-degree system of differentiation based on the architectural model of development of sporadic adenoCa defined by the presence of adenoCa blasts, as follows: poorly differentiated (0%-49% adenoCa blasts), moderately differentiated (50%-95% adenoCa blasts), well-differentiated (> 95% adenoCa blasts); (3) size of adenoCa (< 1 cm, 1 cm, > 1 cm); (4) the number of adenoCa (1, > 1–synchronous adenoCa); (5) pathologic classification as ulcerative, fungating and polyp-shaped (either with a stalk or not); and (6) location in the colon. Colonic polyps were evaluated for the following parameters: (1) Histological classification of adenoma according to World Health Organization (WHO) classification as tubular, villous, tubulovillous[16]; (2) grading of adenoma's dysplasia (mild, moderate and severe according to WHO criteria); (3) size of polyp (< 0.5 cm, > 0.5 cm); (4) number of polyps (1, > 1); (5) presence of stalk or not; and (6) location in the colon.

Table 1 Patients' main characteristics

	Adenocarcinoma, *n* = 56	Colon polyps, *n* = 33	Controls, *n* = 81
Age in yr, *n* (%)			
50-59	1 (1.8)	8 (24.2)	9 (11.1)
60-69	20 (35.7)	12 (36.4)	44 (54.3)
70-79	28 (50.0)	11 (33.3)	16 (19.8)
80-94	7 (12.5)	2 (6.1)	12 (14.8)
Sex			
Men	35 (62.5)	21 (63.6)	44 (54.3)
Women	21 (37.5)	12 (36.4)	37 (45.7)
Smoking			
Yes	50 (89.3)	17 (51.5)	68 (84.0)
No	6 (10.7)	16 (48.5)	13 (16.0)
Number of cigarettes/d			
< 20	4 ± 8.0	3 ± 17.6	0 ± 0.0
20	10 ± 20.0	6 ± 35.3	20 ± 29.4
> 20	36 ± 72.0	8 ± 47.1	48 ± 70.6
Smoking duration in yr (mean ± SD)	37.7 ± 10.0	33.5 ± 9.1	40.3 ± 6.2

Values are presented as *n* (%) or mean ± SD.

The definite diagnosis of either sporadic adenocarcinoma or colonic polyp was made within a maximum of 2 d from endoscopy. Until definite pathological diagnosis, patients underwent fasting (nil per os), after which blood samples were obtained.

The study protocol was approved by the Ethics Board of our Hospital.

Measurement of serum markers

Calculation of oxidative agents' levels took place as follows: Oxidant activity was measured by using a colorimetric test system for the quantitative determination of total lipid peroxides in serum (PerOx Assay, Immundiagnostik AG, Bensheim, Germany). Malondialdehyde was quantitatively measured using the reverse-phase high-performance liquid chromatography method (HPLC-Analytik, Immundiagnostik AG, Bensheim, Germany) and the Vp Series HPLC System (Series LC-10 ADVp Gradient pump, Series RF-10AXL Fluorescence detector, Series SPD-10ADVp UV detector, Shimadzu, Germany). Ferrum (Fe^{2+}) levels were calculated using a colorimetric assay [FerroZine, Roche Diagnostics GmbH (COBAS), Mannheim, Germany]. Triglycerides were quantitatively calculated by using a colorimetric enzymatic test [Trinder endpoint reaction, Roche Diagnostics GmbH (COBAS), Mannheim, Germany].

Calculation of antioxidative agents' concentrations took place as follows: Total antioxidant capacity was measured by using a colorimetric test system (Imanox Assay) for the quantitative determination of the residual exogenous provided hydrogen peroxide (H_2O_2) that could not be eliminated from the total antioxidants in serum, after having completed an eliminating reaction with a certain amount of exogenously provided hydrogen peroxide (Immundiagnostik AG, Bensheim, Germany). Fat-soluble vitamins A (retinol) and E (α-tocopherol) levels were determined simultaneously in human serum using the reverse-phase HPLC method with the 22000 ClinRep Kit (Recipe Chemicals + Instruments GmbH & Co KG Labortechnik, Munich, Germany). Retinol was monitored at 325 nm and α-tocopherol at 295 nm with the Up series HPLC System (Series LC-10ADVp Gradient pump, Series RF-10AXL Fluorescence detector, Series SPD-10ADVp UV detector, Shimadzu, Germany). Fat-soluble vitamin D (25-OH vitamin D) was measured using a chemiluminescent immunoassay method (DiaSorin LIAISON 25 OH Vitamin D Total Assay, DiaSorin S.p.A, Italy). Water soluble vitamin C was quantitatively measured using the reverse-phase HPLC method (Immundiagnostik AG, Bensheim, Germany). Glutathione (GSH) levels were calculated as the ratio between GSH reduced/GSH total using the reverse-phase HPLC method (Immundiagnostik AG, Bensheim, Germany). Cobalamin/vitamin B12 and folate acid concentrations were calculated using a radioimmunoassay method from MP Biomedicals Inc., New York, United States, with the Packard cobra autogamma g counter from Packard, United States. Selenium (Se) and zinc (Zn) serum levels were determined using a graphite furnace atomic absorption spectrophotometry method with the AA spectrophotometer model 2100 (Perkin Elmer, Norwalk CT, United States).

Statistical analysis

Statistical analyses were conducted using the SPSS statistical package (IBM Statistical Package for Social Sciences v. 19.0, Chicago, Illinois, United States). At first, cases were distributed according to demographic characteristics and smoking habits as well as levels of the studied compounds (median, 25th and 75th percentile for each compound and each patient category). As most variables measured followed a skewed distribution (with the notable exception of triglyceride levels), non-parametric tests (Mann-Whitney and Kruskal-Wallis) were used to compare means between different groups. In order to minimize the effect of possible confounding factors in our results, we then used multiple regression to compare log-transformed serum compound levels between patients with diagnosed pathology (either adenocarcinoma or polyp) *vs* controls (using two dummy variables for pathology diagnoses correspondingly), controlling for age (as a continuous variable), sex (male *vs* female), blood triglyceride (as a continuous variable) and smoking habits (as smokers *vs* non-smokers). Finally, we applied multiple logistic regression models to investigate the association between levels of the measured compounds and either risk of adenocarcinoma or risk of polyp development, controlling for the same variables as in the log-linear models. A two-tailed P value of < 0.05 was considered statistically significant for all comparisons.

RESULTS

The patients' main characteristics are summarized in Table 1. Briefly, our study included 56 patients with adenocarcinoma, 33 patients with colonic polyps and 81 patients in the control group (colonoscopy negative for cancer or precancerous lesions). Patients with adenocarcinoma tended to be relatively older (71.5 ± 6.6 years, mean ± SD), compared to those with colon polyps (66.1 ± 9.4 years) or with the control group (68.4 ± 8.5 years). Among patients with adenocarcinoma or polyps, men presented a clear majority (62.5% and 63.6% respectively) compared to women. In the adenocarcinoma subgroup, 89.3% of patients were smokers (from which 72% with a high rate of use, *e.g.*, more than 20 cigarettes per day) compared to 51.5% of patients who were smokers in the polyp group, whereas smoking habits in the control subgroup bore a close resemblance to those of the adenocarcinoma subgroup (84% smokers from which 70.6% smoked more than 20 cigarettes/day).

When comparing patients with adenocarcinoma or polyp(s) with the control group there were notable differences in practically all antioxidant markers (Table 2). Thus, serum levels of vitamins C, E, D, as well as Se, Zn and B12 and total antioxidant capacity were significantly lower in the combined neoplasia/polyp group than in the control group ($P = 0.002$, $P = 0.009$, $P < 0.001$, $P < 0.001$, $P < 0.001$, $P = 0.02$ and $P < 0.001$, correspondingly). For the antioxidant capacity, in particular, there is a clear picture of higher measurements in the control group when compared to a patient with neoplastic lesions (Figure 1). On the other hand, serum levels of oxidant activity presented the opposite pattern ($P < 0.001$ for the difference among the three groups) (Figure 2). In summary, all antioxidant substances were statistically significantly lower among patients with adenocarcinoma compared to controls, except vitamin A which did not present any differentiation (Table 3). Vitamin D presented the greatest difference since it was lower by 56.8% (95%CI: 50.2% to 62.6%). Although no statistically significant differences regarding the levels of each measured oxidant substance in isolation were observed, total oxidant activity was statistically significantly increased among adenocarcinoma patients.

In the group of patients with colonic polyps, most anti-oxidants did not present significant differences in serum concentration when compared to controls. Notable exceptions included, vitamin D which exhibited significantly lower levels by 46% (95%CI: 35.4% to 54.9%) (Figure 3) and total antioxidant capacity which was reduced by 40.1% (95%CI: 38.5% to 41.6%). Interestingly, vitamin A though nominally an anti-oxidant displayed significantly higher levels compared to controls. Finally, patients with colonic polyps, presented lower levels of malondialdehyde by 31.6% (95%CI: 22.3% to 39.8%), but higher Fe^{2+} concentrations by 43.5% (95%CI: 22.2% to 68.5%) (Figure 4), as well as total oxidant activity levels (95%CI: 111.7% to 128.9%).

Next, multivariate analyses were conducted to ascertain which variables presented a true correlation with the neoplastic process. Results were similar between univariate and multivariate analyses regarding the risk of adenoCa (Table 4, which presents the risk of adenocarcinoma in comparison to controls for change in the levels of the measured compounds equal to one standard deviation of its distribution). A significant protective effect was shown especially for vitamin D (OR = 0.04, 95%CI: 0.02 to 0.12) and Zn (OR = 0.16, 95%CI: 0.09 to 0.31) (Figure 5) but also for vitamin E (OR = 0.57, 95%CI: 0.39 to 0.84) and Se (OR = 0.35, 95%CI: 0.22 to 0.55). An increase of the levels of the abovementioned substances equal to one standard deviation reduced the risk of colon adenocarcinoma to about 50%. The relation between low levels of the aforementioned antioxidants and increased risk of adenocarcinoma remained significant after mutual adjustment, *e.g.*, OR for Se becomes 0.34 (95%CI: 0.13 to 0.88 $P = 0.027$). As far as the oxidant substances are concerned, the solitary finding was that a doubling of malondialdehyde serum concentration is associated with an approximately twofold increase in the risk for development of colon adenocarcinoma (OR = 2.09 95%CI: 1.27 to 3.45 $P = 0.004$).

Table 2 Distribution (median 25-75 percentile) of antioxidants and oxidants compounds in the plasma by group

	Adenocarcinoma, *n* = 56	Colon polyps, *n* = 33	Controls, *n* = 81
Antioxidants			
Antioxidant capacity in μmol/L	185.0 (177.0-190.0)	190.0 (182.0-196.2)	305.0 (298.0-324.0)
Vitamin A in μg/L	391.5 (288.3-493.8)	572.0 (480.0-609.0)	380.0 (350.0-416.0)
Vitamin C in μg/L	4.7 (3.9-6.5)	6.0 (4.7-10.0)	6.0 (4.5-9.0)
Vitamin E in mg/L	3.5 (2.4-3.9)	3.8 (3.5-4.2)	3.7 (3.2-4.0)
Vitamin D in ng/mL	9.0 (6.7-13.0)	9.0 (6.8-20.5)	24.0 (20.0-26.0)
Se in μg/L	62.0 (45.5-78.8)	78.0 (72.0-80.0)	76.0 (69.5-80.0)
Zn in μg/L	626.5 (594.5-782.5)	800.0 (711.0-840.0)	809.0 (780.5-842.5)
B12 in pg/L	211.0 (159.3-297.0)	250.0 (220.0-355.0)	289.0 (200.0-340.0)
Folic acid in ng/L	4.3 (3.3-4.6)	4.2 (3.9-4.6)	4.0 (3.8-4.4)
Oxidants			
Oxidant activity in μmol/L	368.8 (330.8-409.0)	378.0 (348.5-409.1)	172.0.0 (167.5-178.5)
Malondialdehyde in μmol/L)	1.9 (1.6-2.4)	1.2 (0.9-2.0)	1.8 (1.7-1.9)
Fe^{2+} in μg/dL)	64.0 (49.3-92.3)	110.0 (90.0-127.0)	68.0 (51.0-95.0)

Se: Selenium; Zn: Zinc; B12: Vitamin B12/cobalamin; Fe^{2+}: Ferum.

Table 3 Percent change (and 95%CIs respectively) in the levels of serum antioxidant and oxidant substances compared to the control group

	Colon polyps	Colon adenocarcinoma
	% Change (95%CI)	% Change (95%CI)
Antioxidants		
Antioxidant capacity	-40.1 (-41.6 to -38.5)	-40.7 (-41.8 to -39.5)
Vitamin A	32.2 (20.8 to 44.7)	0.1 (-6.9 to 7.6)
Vitamin C	-3.1 (-15.8 to 11.6)	-12.7 (-21.9 to -2.4)
Vitamin E	4.2 (-5.0 to 14.2)	-12.3 (-18.4 to -5.7)
Vitamin D	-46.0 (-54.9 to -35.4)	-56.8 (-62.6 to -50.2)
Se	1.7 (-6.3 to 10.4)	-19.4 (-24.5 to -14.0)
Zn	-6.7 (-12.9 to 0.0)	-20.2 (-24.5 to -15.7)
B12	6.0 (-11.7 to 27.2)	-15.0 (-26.5 to -1.8)
Folic acid	2.1 (-6.9 to 12.0)	-8.2 (-14.7 to -1.3)
Oxidants		
Oxidant activity	120.1 (111.7 to 128.9)	113.4 (106.8 to 120.2)
Malondialdehyde	-31.6 (-39.8 to -22.3)	10.1 (-0.6 to 21.9)
Fe^{2+}	43.5 (22.2 to 68.5)	-8.9 (-19.8 to 3.5)

Results from multiple log-linear regression models controlling for age, sex, serum triglycerides, and smoking habits.

Due to the small number of patients in the colon polyp subgroup, fewer associations retained their significance for the development of colon polyps (Table 5). Nevertheless, similarly to results from the CRC group increased levels of vitamin D (OR = 0.27, 95%CI: 0.15 to 0.48, $P < 0.001$) and Zn (OR = 0.39, 95%CI: 0.16 to 0.94, $P = 0.036$) exhibited an association with a reduced risk for colon polyp development, whereas it is worthy of note that increased levels of vitamin A were associated with almost 9 times higher risk of colon polyps compared to controls (OR = 8.84, 95%CI: 3.76 to 20.74, $P < 0.001$). Moreover,

Table 4 Results from multiple logistic regression models (odds ratios and 95%CIs) for the risk of colon adenocarcinoma in comparison to the control group[1]

	Odds ratio	95%CI	*P* value
Antioxidants			
Vitamin A, per 99.6 μg/L	1.20	0.77-1.88	0.430
Vitamin C, per 2.8 μg/L	0.71	0.44-1.15	0.168
Vitamin E, per 0.7 mg/L	0.57	0.39-0.84	0.004
Vitamin D, per 8.2 ng/mL	0.04	0.02-0.12	< 0.001
Se, per 13.6 μg/L	0.35	0.22-0.55	< 0.001
Zn, per 128.5 μg/L	0.16	0.09-0.31	< 0.001
B12, per 157.1 pg/L	0.80	0.51-1.26	0.337
Folic acid, per 38.1 ng/L	0.77	0.54-1.11	0.170
Oxidants			
Malondialdehyde, per 0.5 μmol/L	2.09	1.27-3.45	0.004
Fe^{2+}, per 33.9 μg/dL	0.73	0.47-1.13	0.154

[1]Controlling for age, sex, serum triglycerides, and smoking habits. Se: Selenium; Zn: Zinc; B12: Vitamin B12/cobalamin; Fe^{2+}: Ferum.

Table 5 Multiple logistic regression results (odds ratios and 95%CIs) for the risk of colon polyp development in comparison to the control group[1]

	Odds ratio	95%CI	*P* value
Antioxidants			
Vitamin A, per 99.6 μg/L	8.84	3.76-20.74	< 0.001
Vitamin C, per 2.8 μg/L	0.99	0.58-1.70	0.982
Vitamin E, per 0.7 mg/L	1.51	0.87-2.63	0.141
Vitamin D, per 8.2 ng/mL	0.27	0.15-0.48	< 0.001
Se, per 13.6 μg/L	1.68	0.82-3.42	0.157
Zn, per 128.5 μg/L	0.39	0.16-0.94	0.036
B12, per 157.1 pg/L	1.51	0.92-2.46	0.103
Folic acid, per 38.1 ng/L	1.42	0.74-2.72	0.299
Oxidants			
Malondialdehyde, per 0.5 μmol/L	0.35	0.20-0.60	< 0.001
Fe^{2+}, per 33.9 μg/dL	2.58	1.53-4.33	< 0.001

[1]Controlling for age, sex, serum triglycerides, and smoking habits. Se: Selenium; Zn: Zinc; B12: Vitamin B12/cobalamin; Fe^{2+}: Ferum.

regarding the oxidant group, elevated serum levels of Fe^{2+} seem to double the risk for the development of colon polyps, (OR = 2.58 95%CI: 1.53 to 4.33, $P < 0.001$). Interestingly, in contrast to results from the CRC group, higher malondialdehyde levels seem to exert a protective role (OR = 0.35 95%CI: 0.2 to 0.6 $P < 0.001$). These results remain stable after the mutual adjustment of the measured compounds.

DISCUSSION

CRC is the third cause of cancer-related mortality in both men and women worldwide[1,2]. Current therapeutic options including surgery, chemotherapy, radiotherapy and molecular-targeted therapy are still limited for advanced tumors. Thus, identifying new strategies that will increase the probability of early detection of this clinical modality while keeping the public health costs reasonable (as endoscopy

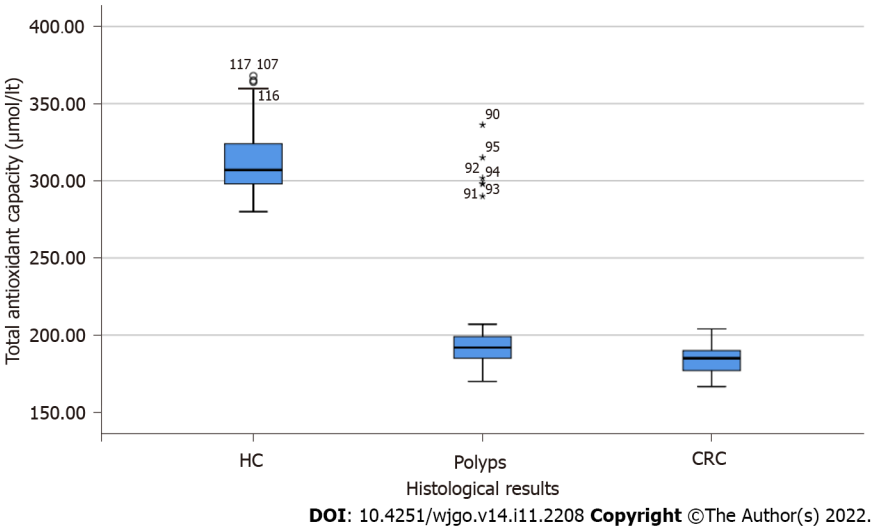

DOI: 10.4251/wjgo.v14.i11.2208 **Copyright** ©The Author(s) 2022.

Figure 1 Antioxidant capacity among control group, group of patients with colonic polyps and group of patients with neoplasia. HC: Healthy controls; CRC: Colorectal cancer.

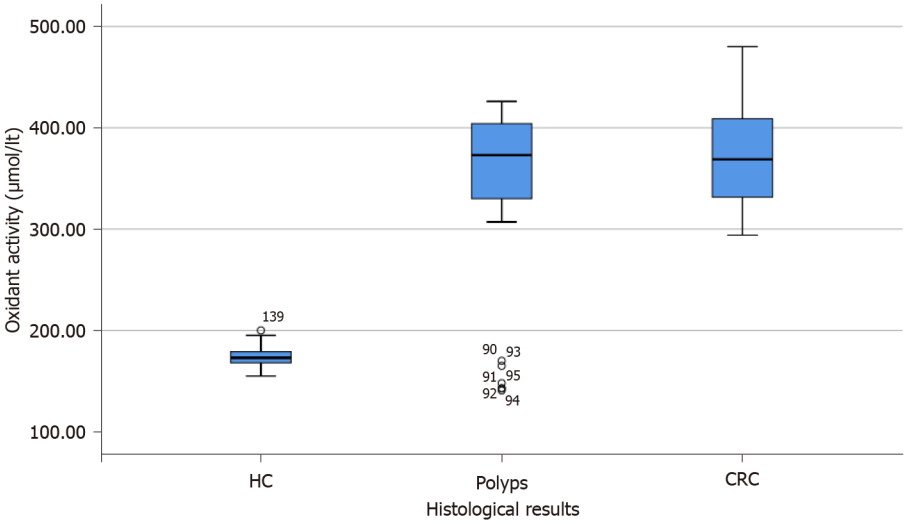

DOI: 10.4251/wjgo.v14.i11.2208 **Copyright** ©The Author(s) 2022.

Figure 2 Oxidant activity among the control group, group of patients with colonic polyps and group of patients with neoplasia. HC: Healthy controls; CRC: Colorectal cancer.

confers a significant financial burden on health budgets) remains an important challenge.

Comparative international epidemiological data indicate that the difference between the highest and lowest sporadic colon cancer incidence is approximately 10-fold, suggesting that environmental factors in the pathogenesis of colon cancer occupy a more prominent role than their genetic counterparts. The dominant environmental factor identified so far is the low-fiber, high-fat diet of Western industrialized countries[17,18].

Although numerous studies dedicated to elucidating the exact role of dietary factors in CRC pathogenesis, and research conducted in a variety of in-vitro and in-vivo animal models strongly hint in favor of a protective effect of antioxidants regarding CRC development, even in the stage of ACF formation, results derived from human populations are not as clear-cut in their results and are in fact at times conflicting[11,12,19,20].

In our study, a basic assumption was made that serum levels of oxidant/antioxidant compounds may accurately reflect the dietary intake habits of individuals and thus could be used to evaluate oxidative imbalance[12]. Over fifty natural and synthetic compounds have been shown to exert a relevant chemotherapeutic effect, but since for the majority of these agents, the literature concerning their role is comparatively scarce, we opted to focus on a variety of compounds with a reasonably established place in the management of the oxidative/anti-oxidative equilibrium[1].

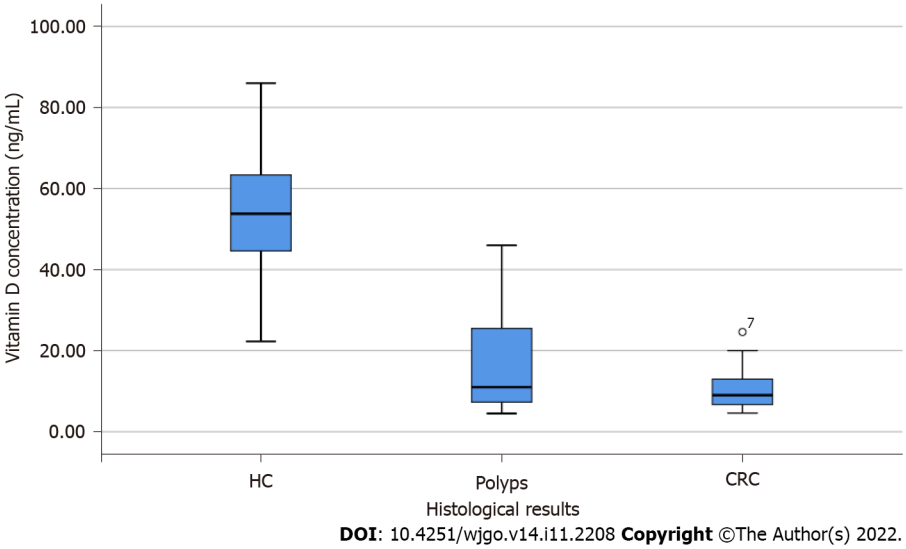

Figure 3 Vitamin D concentration among control group and group of patients with either colonic polyps or neoplasia. HC: Healthy controls.

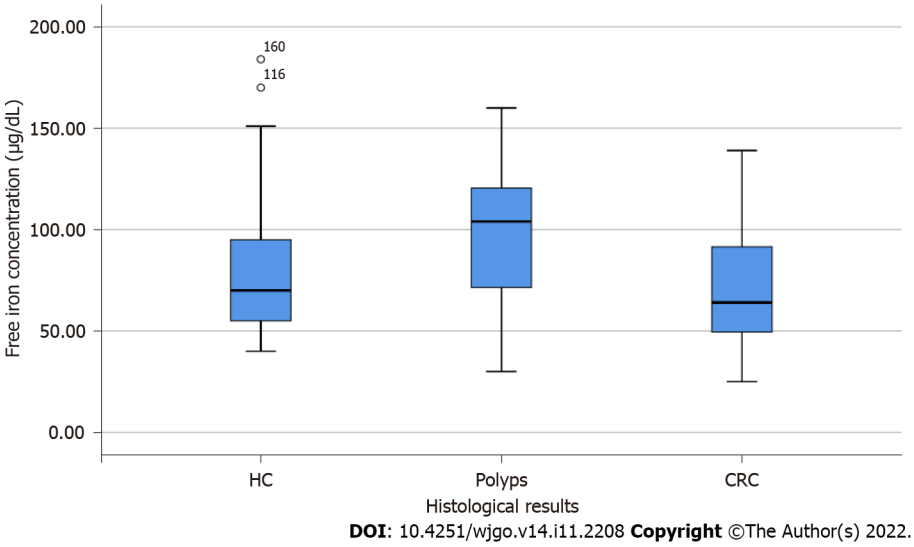

Figure 4 Free iron concentration among control group, group of patients with colonic polyps and group of patients with neoplasia. HC: Healthy controls; CRC: Colorectal cancer.

Regarding the oxidant markers, MDA is an endogenous genotoxic end product of lipid peroxidation by ROS and has been utilized *in vivo* as a bio-marker of oxidative stress (peroxidability index)[21]. It is thought to participate in harmful processes that lead to DNA damage and mutation mainly through the formation of DNA adducts[22]. MDA-induced DNA lesions, called DNA interstrand cross-link seems to be implicated in the gene-toxic effects associated with lipid peroxidation and oxidative stress[21]. Therefore, MDA has been suggested to be strongly associated with CRC pathogenesis, a suggestion that the results of our study strongly endorse. However, the results from the polyp subgroup present a different picture as MDA levels were significantly lower than those in the control group. This latter finding seems odd, considering the fact that colonic adenomas are established precursors of sporadic CRC, but firstly the small number of cases in this subgroup may skew the results in an unexpected direction, and secondly, this finding may account for a more prominent role of MDA in the second part of the neoplastic process that leads to the evolution of precancerous lesions such as polyps to adenoCa.

On the other hand, elevated levels of free iron (labile iron), another recognized strong oxidant, actually doubled the risk of colon polyp development in our cohort whereas no similar correlation was observed for the adenocarcinoma group of patients. Dietary iron can be consumed in the form of heme iron (Fe^{2+}) and nonheme iron (Fe^{3+})[23]. Heme iron contributes to colorectal cancer *via* the Fenton reaction. Hydroxyl radicals produced by the Fenton reaction can alter DNA leading to oxidative base damage[24]. Furthermore, heme iron contributes to cancer development by inducing colonic hyperproliferation through modulation of the intestinal microbiota and inducing mutations through DNA

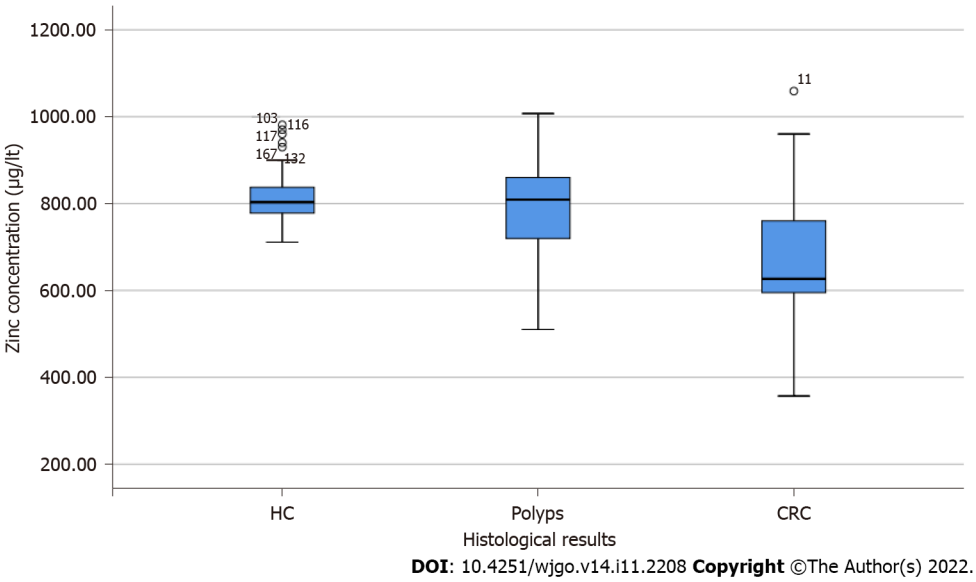

DOI: 10.4251/wjgo.v14.i11.2208 **Copyright** ©The Author(s) 2022.

Figure 5 Zinc concentration among control group, group of patients with colonic polyps and group of patients with neoplasia. HC: Healthy controls; CRC: Colorectal cancer.

adducts or by increasing the formation of lipid peroxyl radicals (ferroptosis), such as malondialdehyde and 4-hydroxynonenal which are potent carcinogens[24-26]**.** These findings provide a strong association between excessive intestinal heme iron and colorectal cancer. However, no sufficient evidence is available to our knowledge that links a mechanism of nonheme iron and colorectal cancer[25]. However, emerging evidence suggests that reduced iron intake and low systemic iron levels are also associated with the pathogenesis of colorectal cancer[25]. This is important because patients with colorectal cancer often present with iron deficiency. The mechanism supporting iron deficiency and colorectal cancer development is not fully understood; it may involve cellular functions' requirement for iron, which, when deficient, may hinder immune cells' ability to protect against cancer, providing the potential for a suppressed immunosurveillance response, affecting growth and differentiation of immune cells, as well as influencing cell-mediated immune response and cytokines activities which may contribute to tumor immune-cell evasion and inadequate tumor cell destruction[27]. On the contrary, the association between high iron concentration and the risk of formation of adenomatous (colonic) polyps is ambiguous[28]. Several studies suggest that the presence of high levels of Fe^{2+} may induce the formation of colonic polyps, suggesting a potent involvement in the early rather than later steps of colorectal carcinogenesis[1,28,29].

Regarding the antioxidant markers, Vitamin A (retinol) did not exhibit any protective role in our study population. Elevated vitamin A concentrations were associated with almost 9 times higher risk of colon polyps compared to controls with no significant effect observed in the adenoCa subgroup. This is not as confusing as it may seem as results regarding the role of vitamin A in the prevention or recurrence of adenomas have been conflicting so far. Several studies[30-32] suggested a protective effect of vitamin A and its derivatives (retinoids) against CRC, whereas Andersen *et al*[33] failed to establish a beneficial role for vitamin A in CRC. On the contrary, recent studies on the metabolism of vitamin A in CRC imply that despite the presence of high concentrations of retinol or all-trans-retinoic acid (ATRA), CRC has been promoted instead of obtaining decreasing cancer cell proliferation[34-36]. The growth and differentiation of the colonic epithelial cells are strongly controlled by retinoid-activated genes which contain retinoic acid receptors (RARs) in their promoter regions. RARs bind to ATRA to induce the transcription of these genes. In many epithelial-derived adenomas and carcinomas, the expression of one or more RAR is lost and the cell loses its ability to regulate normal growth, a phenomenon called "ATRA-resistance". In addition, as CRC progresses, colorectal tumor cells lose the ability to produce ATRA[34]. Kropotova *et al*[37] claimed that these dysregulated pathways were more observed in adenomas rather than in more advanced carcinomas[37]. Consequently, the high levels of vitamin A in the polyp group in our study might reveal the inadequate protective mechanism of retinol, possibly due to decreased ATRA production and the loss of RAR in the colonic epithelial cells.

On the other hand, Vitamin D was by far the compound with the most significant decrease in concentration among patients with adenocarcinoma or colorectal polyps when compared to controls in our analysis. It should be noted that we assessed vitamin D levels by measuring circulating 25(OH)D3 (calcidiol) levels, thus providing an overall estimate of vitamin D status, as described elsewhere[38]. Since 1980, a large number of epidemiological and experimental studies support the association of vitamin D deficiency with a large variety of human diseases, including an increased incidence of colorectal cancer[39]. The most active metabolite of vitamin D which is 1a,25-dihydroxy vitamin D3

[1,25(OH)2D3, (calcitriol)], is synthesized in a highly regulated multi-step process by mitochondrial 25(OH)D3-1a-hydroxylase[38]. Several cell types, including colon cells have been described to contain vitamin D receptors (VDRs)[38]. When these receptors are activated by calcitriol, they are thought to induce differentiation, regulate detoxification metabolism, sensitize cells to apoptosis and inhibit proliferation, invasiveness, angiogenesis and metastatic potential[39]. In general, according to epidemiological studies, vitamin D deficiency may be linked to a higher risk for neoplasia. A recent meta-analysis of case-control and cohort demonstrated a consistent inverse relationship between serum 25(OH)D3 levels and CRC risk[40]. Another systematic review of studies evaluating the association of vitamin D intake or serum levels of 25(OH)D3 and the risk of CRC suggests as well an inverse correlation between CRC risk and both serum 25(OH)D3 and vitamin D intake[41]. This mostly positive observational data have failed to be confirmed by human intervention studies in which supplemental vitamin D administration was found to be ineffective in reducing colon cancer risk in contrast with dietary sources of vitamin D. These disappointing results may be explained by the timing of administration indicating that colon lesions may progress to a stage where they become unresponsive to vitamin D, bearing, therefore, the hallmarks of an epigenetic change[42]. Moreover, gene expression and activity controlled by VDRs have been described as up-regulated at the early stages of colorectal tumorigenesis with a subsequent sharp decline in advanced CRC[43]. Further investigations of VDR expression at different stages of colon cancer development have come to a consensus that VDR expression is frequently increased at the pre-neoplastic ACF and the early stages before being lost in more advanced lesions, suggesting a possible role for vitamin D supplementation in early stages with no benefit conferred in advanced cases of this neoplasia[44,45].

Vitamin E is a generic term that describes a group of lipid-soluble chain-breaking antioxidants that exist in nature as eight structurally related forms with α-tocopherol as the isomer found in the highest concentrations in serum and dietary supplements[1]. The results of our study show a potent protective effect for vitamin E in the adenocarcinoma group of patients compared to controls, although studies focusing on vitamin E have produced conflicting results so far[46,47]. Non-significant trends toward reduced blood concentrations of α–tocopherol have been observed in subjects subsequently developing colorectal cancer when compared with controls[47]. Conversely, intakes of other forms of vitamin E (γ-tocopherol, δ-tocopherol, γ-tocotrienol and δ-tocotrienol) suggest a highly significant inverse trend between serum concentration of vitamin E and cancer risk ($P < 0.001$)[30,47]. In a recent interventional study, the administration of a combination of resveratrol and vitamin E to prevent the development of colonic adenomas exhibited clear benefits[48]. Therefore, our findings, though interesting, must be further evaluated within larger sample size studies.

Se, an essential trace element, is one of the most extensively studied anti-oxidant compounds[8]. A protective effect of Se for the prevention of colorectal adenomas development has been convincingly described[49-52]. Data from the European Prospective Investigation into Cancer and Nutrition cohort that evaluated the effect of Se supplementation according to the dose supplied, demonstrated a statistically significant decrease in the incidence of CRC, although only for a subgroup of subjects with baseline Se concentration < 100 μg/L[52]. These reports are in agreement with our results of a protective effect of higher Se levels regarding CRC risk. In summary, it can be concluded that an inverse dose-response correlation between the level of Se in serum and the risk of colorectal cancer may exist, albeit this association may be stronger in particular subgroups of patients.

Zn is another potent compound that has been found to play a crucial role mainly in antioxidant defense systems, as a specific activator of many enzymatic reactions (*e.g.*, CuZn Superoxide dismutases), in DNA synthesis as well as in immune functions[53]. Zn has also been shown to inhibit chemically induced neoplastic progression in the colon and to promote the cell cycle arrest of colon cancer cells in animal models[53,54]. Reports regarding Zn levels in biological fluids from CRC patients have been limited but encouraging[54]. In a large Mendelian randomization study, the analysis suggested that increased dietary Zn intake may be associated with a decreased risk of both proximal and distal colon cancer[55]. Similar findings were reported by a recent meta-analysis of nineteen studies that suggested a statistically significant inverse dose-response association of Zn intake with CRC risk[54]. The aforementioned findings are in agreement with our results that hint at a protective role for elevated serum levels of Zn in regards to CRC pathogenesis both in the early and later steps of this process.

There are several limitations to this study. From the antioxidant compounds analyzed in our study, we observed that vitamin D provided the strongest argument in favor of a protective role in the prevention of CRC. An important issue though, that should be taken into account concerning vitamin D assessment is the age of the participants as a potential confounder since it is known that vitamin D insufficiency is strongly associated with increasing age[56-59]. Of particular interest is also the finding that elevated serum levels of Fe^{2+} were associated with a twofold increase in the risk of colon polyp development suggesting a possible role in the formation of colonic polyps and more specifically involvement in early rather than late stages of colorectal carcinogenesis. To our knowledge, there are not many studies in the literature in favor of this association, probably because in most of them, bound - and not free- iron was under scrutiny[29]. In our analysis, we also noticed a trend for certain antioxidant substances to be associated with a lower risk of colonic polyp rather than CRC subgroups of patients. This possibly could be explained by a more prominent role in the protective effect of these antioxidants in the early stages of CRC pathogenesis, *i.e.* before the formation of precancerous cells. This effect, when

overcome by the sum of tumorigenic factors will then be attenuated when the adenoma stage is reached rendering interventions such as nutritional antioxidant supplementation incapable of stabilizing or reversing the neoplastic phenotype. This is an attractive theory, especially considering the often inconsistent and even negative results from intervention trials with antioxidant supplementation[1,60,61]. It is known that selecting the exact timing and duration of the intervention (*e.g.*, the age of the patient at enrollment and the supplementation period) is challenging[62,63]. It remains unclear if interventions given for a relatively short period, as in most of the trials due to practical reasons, have the potential to interrupt the tumorigenic sequence. Furthermore, it is difficult to ascertain the optimal follow-up duration for such a trial to detect an effect on the incidence of a disease such as CRC with a time-extensive pathogenetic process. Apart from that, clinical trials cannot provide evidence concerning the exact point at which chemoprevention begins to take effect concerning the start of treatment or concerning the precise nature of this effect (whether this is gradual or constant)[61,63-65]. In most studies, the relative risk predicted for the incidence of colonic polyp formation or CRC is assumed to be constant because of a lack of data to the contrary, thus suggesting that chemoprevention does not offer any cumulative protection[64,65]. Our study followed the "top-down" approach to studying the exosomal risk factors for CRC onset[2,66]. Thus, it suffers from the known limitations of this approach which we mentioned earlier, mainly that the time-points for specific marker measurements were limited and that the crucial pathophysiological effects regarding CRC pathogenesis may have already taken place. On the other hand, it presents a clear and unbiased approach to the biochemical serum profile of several factors important to the oxidative balance in a sizeable CRC cohort. Thus, while a causal effect can by no means be proven for these compounds, intriguing correlations emerge from our analysis that may be the trigger for further research and new insights.

CONCLUSION

In summary, we describe a possible protective effect for Se, Zn, vitamin E and vitamin D regarding CRC pathogenesis, while elevated levels of MDA were associated with a two-fold increase in the risk for CRC. Regarding the development of colonic polyps, higher serum levels of vitamin D and Zn correlated with a decreased risk of adenoma, whereas elevated levels of vitamin A and Fe^{2+} bestowed a higher risk. Interestingly, lower levels of MDA were found in patients with polyps when compared to controls. Our findings indicate that increased oxidative stress and a reduced antioxidant defense mechanism as assessed by a variety of serum compounds may participate in CRC pathogenesis and progression. Moreover, the possible protective effect of antioxidants may be more important in the very early stages of colon carcinogenesis, probably through an interactive mechanism in the early stages of ACF formation[1,6]. Total antioxidant intake may represent a better predictor of colorectal cancer risk as opposed to specific foods and nutrients[12]. Further trials are needed that should focus on the effect of total antioxidant intake in high-risk for CRC populations but prevention of CRC through manipulation of the oxidative balance in the human body *via* nutritional supplementation may represent a worthwhile future research target.

ARTICLE HIGHLIGHTS

Research background

The role of oxidative stress in the pathogenesis of colorectal cancer (CRC) has recently attracted considerable interest. Specific oxidative factors have been implicated in the pathogenesis of adenomatous polyps and ultimately adenocarcinoma.

Research motivation

Several studies have evaluated the association between oxidative imbalance and the development of colorectal adenocarcinoma although the results are conflicting. Thus, the study was designed to assess the correlation between the dietary intake habits of individuals with either colonic polyps or CRC through measurements of oxidant/antioxidant serological markers aiming to introduce novel serum indicators of colonic cancer even in the stage of aberrant crypt foci.

Research objectives

The main objective of the study was to evaluate the effect of total oxidant activity and antioxidant capacity in the development of sporadic colon adenocarcinoma.

Research methods

A total of 170 patients that underwent endoscopy of the lower gastrointestinal tract in a tertiary center within 3 years were included in the study. They were allocated in three groups; those with sporadic

colon adenocarcinoma (n = 56, 32.9%), those with colonic polyps (n = 33, 19.4%) and healthy controls (n = 81, 47.7%). All patients were evaluated for oxidant activity and antioxidant capacity with serum measurements of specific markers such as vitamins A, 25(OH) D3, E, C, B12, folic acid, glutathione, selenium (Se), zinc (Zn), free iron (Fe^{2+}) and malondialdehyde and results were compared between groups.

Research results

Serum levels of vitamins C, E, D, Se, Zn, vitamin B12 and total antioxidant capacity were significantly lower in the combined neoplasia/polyp group than in the control group (P = 0.002, P = 0.009, P < 0.001, P < 0.001, P < 0.001, P = 0.020 and P < 0.001, correspondingly). Increased levels of vitamin E (P = 0.004), vitamin D (P < 0.001), Se (P < 0.001) and Zn (P < 0.001) seem to bestow a protective effect on the development of CRC. For vitamin D (P < 0.001) and Zn (P = 0.036), this effect seems to extend to the development of colon polyps as well. On the other hand, elevated serum levels of malondialdehyde are associated with a higher risk of CRC (OR = 2.09 compared to controls, P = 0.004). Regarding colonic polyp development, increased concentrations of vitamin A and Fe^{2+} are associated with a higher risk whereas lower levels of malondialdehyde with a lower risk.

Research conclusions

In conclusion, increased oxidative stress may play an essential role in the pathogenesis and progression of CRC. Antioxidants' presence may exert a protective effect in the early stages of colon carcinogenesis.

Research perspectives

Further research in high-risk CRC populations is needed in order to assess the role of oxidative imbalance in the development of CRC and the potential for colonic cancer by dietary modifications regarding specific oxidative serum markers.

FOOTNOTES

Author contributions: All authors equally contributed to this paper with the conception and design of the study, literature review and analysis, drafting and critical revision and editing, and final approval of the final version.

Institutional review board statement: The study was approved by the ethics committee of Evangelismos Hospital (Athens, Greece).

Informed consent statement: All patients gave informed consent.

Conflict-of-interest statement: No benefits in any form have been received or will be received from a commercial party related directly or indirectly to the subject of this article.

Data sharing statement: Technical appendix, statistical code and dataset available from the corresponding author at dim.tsoun69@gmail.com.

STROBE statement: The authors have read the STROBE Statement and the manuscript was prepared and revised according to the STROBE Statement.

Country/Territory of origin: Greece

ORCID number: Dimitrios Tsounis 0000-0001-7453-7677; Vassiliki Villiotou 0000-0002-0990-7448; Angeliki Melpidou 0000-0002-2785-3789; Chara Pantsiou 0000-0002-6810-1743; Alexandra Argyrou 0000-0002-1569-5592; Charis Giannopoulou 0000-0002-4068-3120; Adriani Grigoratou 0000-0002-5765-5265; Dimitra Rontogianni 0000-0003-3723-2924; Gerassimos J Mantzaris 0000-0002-5302-5450; George Papatheodoridis 0000-0002-3518-4060.

Corresponding Author's Membership in Professional Societies: Hellenic Society of Gastroenterology; European Society of Gastrointestinal Endoscopy, No. 45909945; European Crohn's and Colitis Organization, No. 10007.

S-Editor: Zhang H
L-Editor: Filipodia
P-Editor: Zhang H

REFERENCES

1 **Carini F**, Mazzola M, Rappa F, Jurjus A, Geagea AG, Al Kattar S, Bou-Assi T, Jurjus R, Damiani P, Leone A, Tomasello G. Colorectal Carcinogenesis: Role of Oxidative Stress and Antioxidants. *Anticancer Res* 2017; **37**: 4759-4766 [PMID: 28870894 DOI: 10.21873/anticanres.11882]

2 **Burnett-Hartman AN**, Lee JK, Demb J, Gupta S. An Update on the Epidemiology, Molecular Characterization, Diagnosis, and Screening Strategies for Early-Onset Colorectal Cancer. *Gastroenterology* 2021; **160**: 1041-1049 [PMID: 33417940 DOI: 10.1053/j.gastro.2020.12.068]

3 **Nguyen LH**, Goel A, Chung DC. Pathways of Colorectal Carcinogenesis. *Gastroenterology* 2020; **158**: 291-302 [PMID: 31622622 DOI: 10.1053/j.gastro.2019.08.059]

4 **Pandurangan AK**, Divya T, Kumar K, Dineshbabu V, Velavan B, Sudhandiran G. Colorectal carcinogenesis: Insights into the cell death and signal transduction pathways: A review. *World J Gastrointest Oncol* 2018; **10**: 244-259 [PMID: 30254720 DOI: 10.4251/wjgo.v10.i9.244]

5 **Tiwari A**, Saraf S, Verma A, Panda PK, Jain SK. Novel targeting approaches and signaling pathways of colorectal cancer: An insight. *World J Gastroenterol* 2018; **24**: 4428-4435 [PMID: 30357011 DOI: 10.3748/wjg.v24.i39.4428]

6 **Clapper ML**, Chang WL, Cooper HS. Dysplastic Aberrant Crypt Foci: Biomarkers of Early Colorectal Neoplasia and Response to Preventive Intervention. *Cancer Prev Res (Phila)* 2020; **13**: 229-240 [PMID: 32132117 DOI: 10.1158/1940-6207.CAPR-19-0316]

7 **Ma H**, Brosens LAA, Offerhaus GJA, Giardiello FM, de Leng WWJ, Montgomery EA. Pathology and genetics of hereditary colorectal cancer. *Pathology* 2018; **50**: 49-59 [PMID: 29169633 DOI: 10.1016/j.pathol.2017.09.004]

8 **Cornish AJ**, Law PJ, Timofeeva M, Palin K, Farrington SM, Palles C, Jenkins MA, Casey G, Brenner H, Chang-Claude J, Hoffmeister M, Kirac I, Maughan T, Brezina S, Gsur A, Cheadle JP, Aaltonen LA, Tomlinson I, Dunlop MG, Houlston RS. Modifiable pathways for colorectal cancer: a mendelian randomisation analysis. *Lancet Gastroenterol Hepatol* 2020; **5**: 55-62 [PMID: 31668584 DOI: 10.1016/S2468-1253(19)30294-8]

9 **Gupta R**, Sinha S, Paul RN. The impact of microsatellite stability status in colorectal cancer. *Curr Probl Cancer* 2018; **42**: 548-559 [PMID: 30119911 DOI: 10.1016/j.currproblcancer.2018.06.010]

10 **Jung G**, Hernández-Illán E, Moreira L, Balaguer F, Goel A. Epigenetics of colorectal cancer: biomarker and therapeutic potential. *Nat Rev Gastroenterol Hepatol* 2020; **17**: 111-130 [PMID: 31900466 DOI: 10.1038/s41575-019-0230-y]

11 **Clinton SK**, Giovannucci EL, Hursting SD. The World Cancer Research Fund/American Institute for Cancer Research Third Expert Report on Diet, Nutrition, Physical Activity, and Cancer: Impact and Future Directions. *J Nutr* 2020; **150**: 663-671 [PMID: 31758189 DOI: 10.1093/jn/nxz268]

12 **Rafiee P**, Jafari Nasab S, Bahrami A, Rezaeimanesh N, Jalali S, Hekmatdoost A, Sadeghi A, Naja F, Houshyari M, Hejazi E. Dietary total antioxidant capacity and colorectal cancer and colorectal adenomatous polyps: a case-control study. *Eur J Cancer Prev* 2021; **30**: 40-45 [PMID: 32079892 DOI: 10.1097/CEJ.0000000000000577]

13 **Port J**, Muthalagu N, Raja M, Ceteci F, Monteverde T, Kruspig B, Hedley A, Kalna G, Lilla S, Neilson L, Brucoli M, Gyuraszova K, Tait-Mulder J, Mezna M, Svambaryte S, Bryson A, Sumpton D, McVie A, Nixon C, Drysdale M, Esumi H, Murray GI, Sansom OJ, Zanivan SR, Murphy DJ. Colorectal Tumors Require NUAK1 for Protection from Oxidative Stress. *Cancer Discov* 2018; **8**: 632-647 [PMID: 29500295 DOI: 10.1158/2159-8290.CD-17-0533]

14 **Taheri Z**, Asadzadeh Aghdaei H, Irani S, Modarressi MH, Zahra N. Evaluation of the Epigenetic Demethylation of NRF2, a Master Transcription Factor for Antioxidant Enzymes, in Colorectal Cancer. *Rep Biochem Mol Biol* 2020; **9**: 33-39 [PMID: 32821749 DOI: 10.29252/rbmb.9.1.33]

15 **Li Destri G**, Rinzivillo C, Vasquez E, Di Cataldo A, Puleo S, Licata A. Evaluation of the prognostic accuracy of Astler-Coller's and Jass' classifications of colorectal cancer. *Tumori* 2001; **87**: 127-129 [PMID: 11504364]

16 **Nagtegaal ID**, Odze RD, Klimstra D, Paradis V, Rugge M, Schirmacher P, Washington KM, Carneiro F, Cree IA; WHO Classification of Tumours Editorial Board. The 2019 WHO classification of tumours of the digestive system. *Histopathology* 2020; **76**: 182-188 [PMID: 31433515 DOI: 10.1111/his.13975]

17 **Bénard F**, Barkun AN, Martel M, von Renteln D. Systematic review of colorectal cancer screening guidelines for average-risk adults: Summarizing the current global recommendations. *World J Gastroenterol* 2018; **24**: 124-138 [PMID: 29358889 DOI: 10.3748/wjg.v24.i1.124]

18 **Costea T**, Hudiță A, Ciolac OA, Gălățeanu B, Ginghină O, Costache M, Ganea C, Mocanu MM. Chemoprevention of Colorectal Cancer by Dietary Compounds. *Int J Mol Sci* 2018; **19** [PMID: 30487390 DOI: 10.3390/ijms19123787]

19 **Roshani M**, Jafari A, Loghman A, Sheida AH, Taghavi T, Tamehri Zadeh SS, Hamblin MR, Homayounfal M, Mirzaei H. Applications of resveratrol in the treatment of gastrointestinal cancer. *Biomed Pharmacother* 2022; **153**: 113274 [PMID: 35724505 DOI: 10.1016/j.biopha.2022.113274]

20 **Guertin KA**, Li XS, Graubard BI, Albanes D, Weinstein SJ, Goedert JJ, Wang Z, Hazen SL, Sinha R. Serum Trimethylamine N-oxide, Carnitine, Choline, and Betaine in Relation to Colorectal Cancer Risk in the Alpha Tocopherol, Beta Carotene Cancer Prevention Study. *Cancer Epidemiol Biomarkers Prev* 2017; **26**: 945-952 [PMID: 28077427 DOI: 10.1158/1055-9965.EPI-16-0948]

21 **Tsikas D**. Assessment of lipid peroxidation by measuring malondialdehyde (MDA) and relatives in biological samples: Analytical and biological challenges. *Anal Biochem* 2017; **524**: 13-30 [PMID: 27789233 DOI: 10.1016/j.ab.2016.10.021]

22 **Ay A**, Gulyasar T, Alkanli N, Sipahi T, Cicin I, Kocak Z, Sut N. Investigation of the relationship between GSTM1 gene variations and serum trace elements, plasma malondialdehyde levels in patients with colorectal cancer. *Mol Biol Rep* 2021; **48**: 6911-6921 [PMID: 34498162 DOI: 10.1007/s11033-021-06694-2]

23 **Padmanabhan H**, Brookes MJ, Iqbal T. Iron and colorectal cancer: evidence from in vitro and animal studies. *Nutr Rev* 2015; **73**: 308-317 [PMID: 26011904 DOI: 10.1093/nutrit/nuu015]

24 **Xu C**, Liu Z, Xiao J. Ferroptosis: A Double-Edged Sword in Gastrointestinal Disease. *Int J Mol Sci* 2021; **22** [PMID: 34830285 DOI: 10.3390/ijms222212403]

25 **Phipps O**, Brookes MJ, Al-Hassi HO. Iron deficiency, immunology, and colorectal cancer. *Nutr Rev* 2021; **79**: 88-97

[PMID: 32679587 DOI: 10.1093/nutrit/nuaa040]
26 **Martin OCB**, Olier M, Ellero-Simatos S, Naud N, Dupuy J, Huc L, Taché S, Graillot V, Levêque M, Bézirard V, Héliès-Toussaint C, Estrada FBY, Tondereau V, Lippi Y, Naylies C, Peyriga L, Canlet C, Davila AM, Blachier F, Ferrier L, Boutet-Robinet E, Guéraud F, Théodorou V, Pierre FHF. Haem iron reshapes colonic luminal environment: impact on mucosal homeostasis and microbiome through aldehyde formation. *Microbiome* 2019; **7**: 72 [PMID: 31060614 DOI: 10.1186/s40168-019-0685-7]
27 **Ploug M**, Kroijer R, Qvist N, Lindahl CH, Knudsen T. Iron deficiency in colorectal cancer patients: a cohort study on prevalence and associations. *Colorectal Dis* 2021; **23**: 853-859 [PMID: 33253490 DOI: 10.1111/codi.15467]
28 **Bastide N**, Morois S, Cadeau C, Kangas S, Serafini M, Gusto G, Dossus L, Pierre FH, Clavel-Chapelon F, Boutron-Ruault MC. Heme Iron Intake, Dietary Antioxidant Capacity, and Risk of Colorectal Adenomas in a Large Cohort Study of French Women. *Cancer Epidemiol Biomarkers Prev* 2016; **25**: 640-647 [PMID: 26823477 DOI: 10.1158/1055-9965.EPI-15-0724]
29 **Constante M**, Fragoso G, Calvé A, Samba-Mondonga M, Santos MM. Dietary Heme Induces Gut Dysbiosis, Aggravates Colitis, and Potentiates the Development of Adenomas in Mice. *Front Microbiol* 2017; **8**: 1809 [PMID: 28983289 DOI: 10.3389/fmicb.2017.01809]
30 **Luo H**, Fang YJ, Lu MS, Pan ZZ, Huang J, Chen YM, Zhang CX. Dietary and serum vitamins A and E and colorectal cancer risk in Chinese population: a case-control study. *Eur J Cancer Prev* 2019; **28**: 268-277 [PMID: 29846268 DOI: 10.1097/CEJ.0000000000000452]
31 **Hunsu VO**, Facey COB, Fields JZ, Boman BM. Retinoids as Chemo-Preventive and Molecular-Targeted Anti-Cancer Therapies. *Int J Mol Sci* 2021; **22** [PMID: 34299349 DOI: 10.3390/ijms22147731]
32 **Zamzami MA**, Nasrullah M, Choudhry H, Khan MI. A Study on the Effect of Vitamins A and C to Modulate the Expression of NKG2D Ligands in Hepatic and Colon Cancer Cells. *Nutr Cancer* 2021; **73**: 2751-2762 [PMID: 33349056 DOI: 10.1080/01635581.2020.1860240]
33 **Andersen V**, Halekoh U, Bohn T, Tjønneland A, Vogel U, Kopp TI. No Interaction between Polymorphisms Related to Vitamin A Metabolism and Vitamin A Intake in Relation to Colorectal Cancer in a Prospective Danish Cohort. *Nutrients* 2019; **11** [PMID: 31242605 DOI: 10.3390/nu11061428]
34 **Applegate CC**, Lane MA. Role of retinoids in the prevention and treatment of colorectal cancer. *World J Gastrointest Oncol* 2015; **7**: 184-203 [PMID: 26483874 DOI: 10.4251/wjgo.v7.i10.184]
35 **Jin Y**, Teh SS, Lau HLN, Xiao J, Mah SH. Retinoids as anti-cancer agents and their mechanisms of action. *Am J Cancer Res* 2022; **12**: 938-960 [PMID: 35411232]
36 **Bauzone M**, Souidi M, Dessein AF, Wisztorski M, Vincent A, Gimeno JP, Monté D, Van Seuningen I, Gespach C, Huet G. Cross-talk between YAP and RAR-RXR Drives Expression of Stemness Genes to Promote 5-FU Resistance and Self-Renewal in Colorectal Cancer Cells. *Mol Cancer Res* 2021; **19**: 612-622 [PMID: 33472949 DOI: 10.1158/1541-7786.MCR-20-0462]
37 **Kropotova ES**, Zinovieva OL, Zyryanova AF, Dybovaya VI, Prasolov VS, Beresten SF, Oparina NY, Mashkova TD. Altered expression of multiple genes involved in retinoic acid biosynthesis in human colorectal cancer. *Pathol Oncol Res* 2014; **20**: 707-717 [PMID: 24599561 DOI: 10.1007/s12253-014-9751-4]
38 **Yuan C**, Sato K, Hollis BW, Zhang S, Niedzwiecki D, Ou FS, Chang IW, O'Neil BH, Innocenti F, Lenz HJ, Blanke CD, Goldberg RM, Venook AP, Mayer RJ, Fuchs CS, Meyerhardt JA, Ng K. Plasma 25-Hydroxyvitamin D Levels and Survival in Patients with Advanced or Metastatic Colorectal Cancer: Findings from CALGB/SWOG 80405 (Alliance). *Clin Cancer Res* 2019; **25**: 7497-7505 [PMID: 31548349 DOI: 10.1158/1078-0432.CCR-19-0877]
39 **Carlberg C**, Muñoz A. An update on vitamin D signaling and cancer. *Semin Cancer Biol* 2022; **79**: 217-230 [PMID: 32485310 DOI: 10.1016/j.semcancer.2020.05.018]
40 **Boughanem H**, Canudas S, Hernandez-Alonso P, Becerra-Tomás N, Babio N, Salas-Salvadó J, Macias-Gonzalez M. Vitamin D Intake and the Risk of Colorectal Cancer: An Updated Meta-Analysis and Systematic Review of Case-Control and Prospective Cohort Studies. *Cancers (Basel)* 2021; **13** [PMID: 34200111 DOI: 10.3390/cancers13112814]
41 **Vaughan-Shaw PG**, Buijs LF, Blackmur JP, Theodoratou E, Zgaga L, Din FVN, Farrington SM, Dunlop MG. The effect of vitamin D supplementation on survival in patients with colorectal cancer: systematic review and meta-analysis of randomised controlled trials. *Br J Cancer* 2020; **123**: 1705-1712 [PMID: 32929196 DOI: 10.1038/s41416-020-01060-8]
42 **Kim H**, Lipsyc-Sharf M, Zong X, Wang X, Hur J, Song M, Wang M, Smith-Warner SA, Fuchs C, Ogino S, Wu K, Chan AT, Cao Y, Ng K, Giovannucci EL. Total Vitamin D Intake and Risks of Early-Onset Colorectal Cancer and Precursors. *Gastroenterology* 2021; **161**: 1208-1217.e9 [PMID: 34245763 DOI: 10.1053/j.gastro.2021.07.002]
43 **El-Sharkawy A**, Malki A. Vitamin D Signaling in Inflammation and Cancer: Molecular Mechanisms and Therapeutic Implications. *Molecules* 2020; **25** [PMID: 32679655 DOI: 10.3390/molecules25143219]
44 **He L**, Liu T, Shi Y, Tian F, Hu H, Deb DK, Chen Y, Bissonnette M, Li YC. Gut Epithelial Vitamin D Receptor Regulates Microbiota-Dependent Mucosal Inflammation by Suppressing Intestinal Epithelial Cell Apoptosis. *Endocrinology* 2018; **159**: 967-979 [PMID: 29228157 DOI: 10.1210/en.2017-00748]
45 **Fang Y**, Song H, Huang J, Zhou J, Ding X. The clinical significance of vitamin D levels and vitamin D receptor mRNA expression in colorectal neoplasms. *J Clin Lab Anal* 2021; **35**: e23988 [PMID: 34651346 DOI: 10.1002/jcla.23988]
46 **Cheng WW**, Wang ZK, Shangguan HF, Zhu Q, Zhang HY. Are vitamins relevant to cancer risks? *Nutrition* 2020; **78**: 110870 [PMID: 32659681 DOI: 10.1016/j.nut.2020.110870]
47 **Jiang Q**. Natural Forms of Vitamin E as Effective Agents for Cancer Prevention and Therapy. *Adv Nutr* 2017; **8**: 850-867 [PMID: 29141970 DOI: 10.3945/an.117.016329]
48 **Wang C**, Wang N, Li N, Yu Q, Wang F. Combined Effects of Resveratrol and Vitamin E From Peanut Seeds and Sprouts on Colorectal Cancer Cells. *Front Pharmacol* 2021; **12**: 760919 [PMID: 34803703 DOI: 10.3389/fphar.2021.760919]
49 **Ullah H**, Liu G, Yousaf B, Ali MU, Abbas Q, Munir MAM, Mian MM. Developmental selenium exposure and health risk in daily foodstuffs: A systematic review and meta-analysis. *Ecotoxicol Environ Saf* 2018; **149**: 291-306 [PMID: 29268101 DOI: 10.1016/j.ecoenv.2017.11.056]
50 **Ala M**, Kheyri Z. The rationale for selenium supplementation in inflammatory bowel disease: A mechanism-based point of view. *Nutrition* 2021; **85**: 111153 [PMID: 33578241 DOI: 10.1016/j.nut.2021.111153]

51 **Hughes DJ**, Fedirko V, Jenab M, Schomburg L, Méplan C, Freisling H, Bueno-de-Mesquita HB, Hybsier S, Becker NP, Czuban M, Tjønneland A, Outzen M, Boutron-Ruault MC, Racine A, Bastide N, Kühn T, Kaaks R, Trichopoulos D, Trichopoulou A, Lagiou P, Panico S, Peeters PH, Weiderpass E, Skeie G, Dagrun E, Chirlaque MD, Sánchez MJ, Ardanaz E, Ljuslinder I, Wennberg M, Bradbury KE, Vineis P, Naccarati A, Palli D, Boeing H, Overvad K, Dorronsoro M, Jakszyn P, Cross AJ, Quirós JR, Stepien M, Kong SY, Duarte-Salles T, Riboli E, Hesketh JE. Selenium status is associated with colorectal cancer risk in the European prospective investigation of cancer and nutrition cohort. *Int J Cancer* 2015; **136**: 1149-1161 [PMID: 25042282 DOI: 10.1002/ijc.29071]

52 **Baker JR**, Umesh S, Jenab M, Schomburg L, Tjønneland A, Olsen A, Boutron-Ruault MC, Rothwell JA, Severi G, Katzke V, Johnson T, Schulze MB, Masala G, Agnoli C, Simeon V, Tumino R, Bueno-de-Mesquita HB, Gram IT, Skeie G, Bonet C, Rodriguez-Barranco M, Houerta JM, Gylling B, Van Guelpen B, Perez-Cornago A, Aglago E, Freisling H, Weiderpass E, Cross AJ, Heath AK, Hughes DJ, Fedirko V. Prediagnostic Blood Selenium Status and Mortality among Patients with Colorectal Cancer in Western European Populations. *Biomedicines* 2021; **9** [PMID: 34829750 DOI: 10.3390/biomedicines9111521]

53 **Luo H**, Fang YJ, Zhang X, Feng XL, Zhang NQ, Abulimiti A, Huang CY, Zhang CX. Association between Dietary Zinc and Selenium Intake, Oxidative Stress-Related Gene Polymorphism, and Colorectal Cancer Risk in Chinese Population - A Case-Control Study. *Nutr Cancer* 2021; **73**: 1621-1630 [PMID: 32777945 DOI: 10.1080/01635581.2020.1804950]

54 **Li P**, Xu J, Shi Y, Ye Y, Chen K, Yang J, Wu Y. Association between zinc intake and risk of digestive tract cancers: a systematic review and meta-analysis. *Clin Nutr* 2014; **33**: 415-420 [PMID: 24148607 DOI: 10.1016/j.clnu.2013.10.001]

55 **Tsilidis KK**, Papadimitriou N, Dimou N, Gill D, Lewis SJ, Martin RM, Murphy N, Markozannes G, Zuber V, Cross AJ, Burrows K, Lopez DS, Key TJ, Travis RC, Perez-Cornago A, Hunter DJ, van Duijnhoven FJB, Albanes D, Arndt V, Berndt SI, Bézieau S, Bishop DT, Boehm J, Brenner H, Burnett-Hartman A, Campbell PT, Casey G, Castellví-Bel S, Chan AT, Chang-Claude J, de la Chapelle A, Figueiredo JC, Gallinger SJ, Giles GG, Goodman PJ, Gsur A, Hampe J, Hampel H, Hoffmeister M, Jenkins MA, Keku TO, Kweon SS, Larsson SC, Le Marchand L, Li CI, Li L, Lindblom A, Martín V, Milne RL, Moreno V, Nan H, Nassir R, Newcomb PA, Offit K, Pharoah PDP, Platz EA, Potter JD, Qi L, Rennert G, Sakoda LC, Schafmayer C, Slattery ML, Snetselaar L, Schenk J, Thibodeau SN, Ulrich CM, Van Guelpen B, Harlid S, Visvanathan K, Vodickova L, Wang H, White E, Wolk A, Woods MO, Wu AH, Zheng W, Bueno-de-Mesquita B, Boutron-Ruault MC, Hughes DJ, Jakszyn P, Kühn T, Palli D, Riboli E, Giovannucci EL, Banbury BL, Gruber SB, Peters U, Gunter MJ. Genetically predicted circulating concentrations of micronutrients and risk of colorectal cancer among individuals of European descent: a Mendelian randomization study. *Am J Clin Nutr* 2021; **113**: 1490-1502 [PMID: 33740060 DOI: 10.1093/ajcn/nqab003]

56 **Ferrari D**, Lombardi G, Strollo M, Pontillo M, Motta A, Locatelli M. Association between solar ultraviolet doses and vitamin D clinical routine data in European mid-latitude population between 2006 and 2018. *Photochem Photobiol Sci* 2019; **18**: 2696-2706 [PMID: 31556901 DOI: 10.1039/c9pp00372j]

57 **McCullough ML**, Zoltick ES, Weinstein SJ, Fedirko V, Wang M, Cook NR, Eliassen AH, Zeleniuch-Jacquotte A, Agnoli C, Albanes D, Barnett MJ, Buring JE, Campbell PT, Clendenen TV, Freedman ND, Gapstur SM, Giovannucci EL, Goodman GG, Haiman CA, Ho GYF, Horst RL, Hou T, Huang WY, Jenab M, Jones ME, Joshu CE, Krogh V, Lee IM, Lee JE, Männistö S, Le Marchand L, Mondul AM, Neuhouser ML, Platz EA, Purdue MP, Riboli E, Robsahm TE, Rohan TE, Sasazuki S, Schoemaker MJ, Sieri S, Stampfer MJ, Swerdlow AJ, Thomson CA, Tretli S, Tsugane S, Ursin G, Visvanathan K, White KK, Wu K, Yaun SS, Zhang X, Willett WC, Gail MH, Ziegler RG, Smith-Warner SA. Circulating Vitamin D and Colorectal Cancer Risk: An International Pooling Project of 17 Cohorts. *J Natl Cancer Inst* 2019; **111**: 158-169 [PMID: 29912394 DOI: 10.1093/jnci/djy087]

58 **Kweder H**, Eidi H. Vitamin D deficiency in elderly: Risk factors and drugs impact on vitamin D status. *Avicenna J Med* 2018; **8**: 139-146 [PMID: 30319955 DOI: 10.4103/ajm.AJM_20_18]

59 **Keum N**, Lee DH, Greenwood DC, Manson JE, Giovannucci E. Vitamin D supplementation and total cancer incidence and mortality: a meta-analysis of randomized controlled trials. *Ann Oncol* 2019; **30**: 733-743 [PMID: 30796437 DOI: 10.1093/annonc/mdz059]

60 **Zhang C**, Cheng R, Ding J, Li X, Niu H. Serum Copper and Zinc Levels and Colorectal Cancer in Adults: Findings from the National Health and Nutrition Examination 2011-2016. *Biol Trace Elem Res* 2022; **200**: 2033-2039 [PMID: 34283364 DOI: 10.1007/s12011-021-02826-8]

61 **Song M**, Lee IM, Manson JE, Buring JE, Dushkes R, Gordon D, Walter J, Wu K, Chan AT, Ogino S, Fuchs CS, Meyerhardt JA, Giovannucci EL. No Association Between Vitamin D Supplementation and Risk of Colorectal Adenomas or Serrated Polyps in a Randomized Trial. *Clin Gastroenterol Hepatol* 2021; **19**: 128-135.e6 [PMID: 32062040 DOI: 10.1016/j.cgh.2020.02.013]

62 **Umezawa S**, Higurashi T, Komiya Y, Arimoto J, Horita N, Kaneko T, Iwasaki M, Nakagama H, Nakajima A. Chemoprevention of colorectal cancer: Past, present, and future. *Cancer Sci* 2019; **110**: 3018-3026 [PMID: 31361372 DOI: 10.1111/cas.14149]

63 **Katona BW**, Weiss JM. Chemoprevention of Colorectal Cancer. *Gastroenterology* 2020; **158**: 368-388 [PMID: 31563626 DOI: 10.1053/j.gastro.2019.06.047]

64 **Crockett SD**, Barry EL, Mott LA, Ahnen DJ, Robertson DJ, Anderson JC, Wallace K, Burke CA, Bresalier RS, Figueiredo JC, Snover DC, Baron JA. Calcium and vitamin D supplementation and increased risk of serrated polyps: results from a randomised clinical trial. *Gut* 2019; **68**: 475-486 [PMID: 29496722 DOI: 10.1136/gutjnl-2017-315242]

65 **Frugé AD**, Smith KS, Riviere AJ, Tenpenny-Chigas R, Demark-Wahnefried W, Arthur AE, Murrah WM, van der Pol WJ, Jasper SL, Morrow CD, Arnold RD, Braxton-Lloyd K. A Dietary Intervention High in Green Leafy Vegetables Reduces Oxidative DNA Damage in Adults at Increased Risk of Colorectal Cancer: Biological Outcomes of the Randomized Controlled Meat and Three Greens (M3G) Feasibility Trial. *Nutrients* 2021; **13** [PMID: 33917165 DOI: 10.3390/nu13041220]

66 **Vernia F**, Longo S, Stefanelli G, Viscido A, Latella G. Dietary Factors Modulating Colorectal Carcinogenesis. *Nutrients* 2021; **13** [PMID: 33401525 DOI: 10.3390/nu13010143]

World Journal of Gastrointestinal Oncology

Submit a Manuscript: https://www.f6publishing.com

World J Gastrointest Oncol 2022 November 15; 14(11): 2224-2237

DOI: 10.4251/wjgo.v14.i11.2224

ISSN 1948-5204 (online)

ORIGINAL ARTICLE

Retrospective Study

Predictive value of indirect bilirubin before neoadjuvant chemoradiotherapy in evaluating prognosis of local advanced rectal cancer patients

Shuo-Feng Li, Ran Wei, Guan-Hua Yu, Zheng Jiang

Specialty type: Oncology

Provenance and peer review: Unsolicited article; Externally peer reviewed.

Peer-review model: Single blind

Peer-review report's scientific quality classification

Grade A (Excellent): 0
Grade B (Very good): B
Grade C (Good): C, C
Grade D (Fair): 0
Grade E (Poor): 0

P-Reviewer: Aurello P, Italy; Bustamante-Lopez LA, Brazil; Preziosi F, Italy

Received: July 23, 2022
Peer-review started: July 23, 2022
First decision: August 18, 2022
Revised: August 25, 2022
Accepted: October 2, 2022
Article in press: October 2, 2022
Published online: November 15, 2022

Shuo-Feng Li, Ran Wei, Guan-Hua Yu, Zheng Jiang, Department of Colorectal Surgery, National Cancer Center/National Clinical Research Center for Cancer/Cancer Hospital, Chinese Academy of Medical Sciences and Peking Union Medical College, Beijing 100021, China

Corresponding author: Zheng Jiang, MD, Chief Physician, Professor, Department of Colorectal Surgery, National Cancer Center/National Clinical Research Center for Cancer/Cancer Hospital, Chinese Academy of Medical Sciences and Peking Union Medical College, No.17 Panjiayuan Nanli, Chaoyang District, Beijing 100021, China. jiangzheng@cicams.ac.cn

Abstract

BACKGROUND

Many biomarkers have predictive value for overall survival (OS) and disease-free survival (DFS) in tumor patients. However, the role of indirect bilirubin (IBIL) in local advanced rectal cancer (LARC) patients treated with neoadjuvant chemoradiotherapy (nCRT) has not been studied.

AIM

To explore the predictive value of IBIL before nCRT (pre-IBIL) for the OS and DFS of LARC patients treated with nCRT.

METHODS

A total of 324 LARC patients undergoing nCRT with total mesorectal excision (TME) were enrolled. Preoperative clinical features and postoperative pathological characteristics were collected. Cox regression analysis was performed, and a Cox-based nomogram was developed to predict OS and DFS. We also assessed the predictive performance of the nomogram with calibration plots and receiver operating characteristic (ROC) curves.

RESULTS

Among 324 patients, the median pre-IBIL was 6.2 μmol/L (interquartile range: 4.6 μmol/L-8.4 μmol/L). In the Cox multivariate regression analysis, we found that pre-IBIL, smoking history, tumor regression grade (TRG), vascular invasion, and carbohydrate antigen 19-9 before nCRT (pre-CA19-9) were predictors of OS. Additionally, pre-IBIL, body mass index (BMI), nCRT with surgery interval, TRG, and vascular invasion were predictors of DFS. Predictive nomograms were developed to predict 5-year OS and 5-year DFS with area under the ROC curve

values of 0.7518 and 0.7355, respectively. Good statistical performance on internal validation was shown by calibration plots and ROC curves.

CONCLUSION

This study demonstrated that pre-IBIL was an independent prognostic factor for OS and DFS in LARC patients treated with nCRT followed by TME. Nomograms incorporating pre-IBIL, BMI, smoking history, nCRT with surgery interval, TRG, vascular invasion, and pre-CA19-9 could be helpful to predict OS and DFS.

Key Words: Indirect bilirubin; Local advanced rectal cancer; Neoadjuvant chemoradiotherapy; Prognostic factor; Overall survival; Disease-free survival

Core Tip: Our study demonstrated that indirect bilirubin measurement before neoadjuvant chemoradiotherapy (nCRT) (pre-IBIL) is an independent and significant risk factor for survival in local advanced rectal cancer patients treated with nCRT followed by total mesorectal excision. In addition, nomograms based on pre-IBIL can predict 5-year overall survival and 5-year disease-free survival with good agreement.

Citation: Li SF, Wei R, Yu GH, Jiang Z. Predictive value of indirect bilirubin before neoadjuvant chemoradiotherapy in evaluating prognosis of local advanced rectal cancer patients. *World J Gastrointest Oncol* 2022; 14(11): 2224-2237

URL: https://www.wjgnet.com/1948-5204/full/v14/i11/2224.htm

DOI: https://dx.doi.org/10.4251/wjgo.v14.i11.2224

INTRODUCTION

According to the National Comprehensive Cancer Network guidelines, local advanced rectal cancer (LARC) patients should be treated with neoadjuvant chemoradiotherapy (nCRT) combined with surgery[1]. The nCRT can reduce the tumor burden, and local recurrence rate, as well as improve the R0 resection rate and anus preservation rate of LARC[2]. However, approximately 20%-46% of LARC patients with available postoperative pathological data had tumor cells that did not regress significantly or did not regress at all. These patients did not respond significantly to treatment and had poor prognoses[3-5]. Moreover, there are few studies on the changes in biological characteristics of tumors after nCRT treatment, so the current prognosis of this group of patients is still evaluated by TNM staging, which may not be accurate[6-8]. Combined with the results of existing studies, most of the studies evaluated the prognosis of this group of patients based on the pathological or anatomical characteristics of the tumor while ignoring some biological characteristics of the patients themselves, such as blood biochemistry status and underlying diseases[9-11].

Indirect bilirubin (IBIL) is bilirubin that is not bound to glucuronic acid. Elevated serum IBIL is mainly associated with various hemolytic diseases. After the destruction of a large number of red blood cells, a large amount of hemoglobin is converted into IBIL, which exceeds the processing capacity of the liver to convert all of it into direct bilirubin, resulting in elevated IBIL in the blood. Its concentration reflects the conversion function of hepatocytes and the catabolic state of red blood cells. In recent years, an increasing number of studies have found a relationship between IBIL and tumor prognosis. Some studies have shown that bilirubin is associated with prognosis in cancer patients, such as ovarian cancer, lung cancer, nasopharyngeal cancer, and oral squamous cell carcinoma[12-15]. However, the predictive values of the IBIL before nCRT (pre-IBIL) for prognostic outcomes in LARC patients treated with nCRT are unknown. In this retrospective study, we aimed to perform statistical analysis of the clinicopathological data of a large number of LARC patients who underwent nCRT was performed to investigate the predictive value of pre-IBIL in the prognosis and to create a nomogram that could predict the prognosis of patients.

MATERIALS AND METHODS

Patient population

We retrospectively identified 324 rectal cancer patients who received nCRT between November 1, 2012

and October 30, 2018 in the National Cancer Center/Cancer Hospital of the Chinese Academy of Medical Sciences and Peking Union Medical College (Beijing, P.R. China). The inclusion criteria were as follows: (1) Completion of long course nCRT followed by total mesorectal excision (TME); (2) Pathologically confirmed rectal adenocarcinoma by colonoscopic biopsy; and (3) Imaging suggested cTNM stage II-III without distant metastasis at initial diagnosis. The exclusion criteria were as follows: (1) Absence of some clinical features before nCRT treatment; (2) After nCRT, distant metastasis was found by imaging examinations; and (3) Synchronous tumors.

All the available detailed clinical characteristics and pathological parameters were enrolled, including pre-IBIL, age, sex, body mass index (BMI), smoking history, drinking history, chronic disease history, cTNM stage, nCRT with surgery interval, inferior margin, tumor regression grade (TRG), vascular invasion, neural invasion, radiotherapy type before surgery, chemotherapy type before surgery, adjuvant chemotherapy, carcinoembryonic antigen before nCRT (pre-CEA), and carbohydrate antigen 19-9 before nCRT (pre-CA19-9), in which TRG uses Dworak stage.

Treatment

All patients were treated with a 45-60 Gy dose of long-course nCRT. Three schemes of concurrent radiotherapy are volumetric modulated arc therapy (VMAT), intensity modulated radiation therapy (IMRT), and 3-dimensional conformal radiation therapy (3D-CRT). The concurrent chemotherapy schemes were capecitabine, capecitabine + platinum, capecitabine + bevacizumab, capecitabine + oxaliplatin and raltitrexed. All patients were treated with nCRT for at least 4 wk before undergoing TME.

Follow-up

All patients received postoperative reviews in the hospital every 3 mo for 2 years after surgery and every 6 mo for 3-5 years after surgery. The postoperative examinations included a physical examination, peripheral blood tumor markers, chest computed tomography (CT), abdominal CT, pelvic CT or magnetic resonance imaging, and a whole-body positron emission tomography-CT if necessary. Additionally, we followed up with patients at regular intervals until August 31, 2021. Overall survival (OS) was defined as the time from the date of diagnosis to the date of death due to any cause or the last follow-up. Disease-free survival (DFS) was defined as the time since radical surgery to disease recurrence, metastasis, the last follow-up, or patient death.

Statistical analysis

Fisher's exact test and χ^2 tests were employed to compare categorical data. Cox regression analysis was performed to evaluate the hazard ratio (HR) and 95% confidence interval (95%CI) of both OS and DFS. Parameters that were statistically significant in the univariate analysis were subsequently included in the multivariate analysis. Nomograms were constructed based on statistically significant factors identified by the multivariate analyses from the Cox regression model to predict 5-year OS and DFS. We assessed the predictive performance of the nomogram with calibration plots and receiver operating characteristic (ROC) curves. The Kaplan-Meier survival method was used to analyze OS and DFS, and survival differences were calculated by the log-rank test. All statistical analyses were performed using R version 4.1.0. Two-tailed *P* values less than 0.05 were considered statistically significant.

RESULTS

Patient characteristics

A total of 324 patients, 98 (30.25%) females and 226 (69.75%) males met the inclusion criteria for this study, and the median pre-IBIL (interquartile range) was 6.2 (4.6-8.4) μmol/L. Then, 6.2 μmol/L was used as cut-off value in grouping patients. Moreover, 48.46% (157/324) of patients had a smoking history, 41.67% (135/324) of patients had a drinking history and 37.04% (120/324) of patients had a chronic disease history. For radiotherapy type before surgery, 286 (88.27%) patients received the VMAT regimen, 30 (9.26%) patients received the IMRT regimen, and 8 (2.47%) patients received the 3D-CRT regimen. For chemotherapy type before surgery, 289 (89.20%) patients received the capecitabine regimen, and 18 (5.56%) patients received the capecitabine plus platinum regimen. The demographics and clinicopathological characteristics are presented in Table 1.

Cox regression analysis of prognostic factors for OS

All variables identified in Table 1 were selected for univariable Cox regression analysis to estimate OS in LARC patients treated with nCRT and TME. In the univariable analysis, there were many variables statistically significant for OS in these patients, including pre-IBIL, smoking history, TRG, vascular invasion, neural invasion, and pre-CA19-9. These statistically significant parameters in the univariate analysis were included in the multivariate model. In the multivariate analysis, we found that pre-IBIL (pre-IBIL > 6.2 μmol/L, adjusted HR = 1.77, 95%CI: 1.04-3.01, *P* = 0.035), smoking history (yes, adjusted

Table 1 Clinical characteristics and treatment strategies of local advanced rectal cancer patients

Characteristic	Pre-IBIL ≤ 6.2 μmol/L (*n* = 163)	Pre-IBIL > 6.2 μmol/L (*n* = 161)	*P* value	All patients (*n* = 324)
Age, yr			0.305	
< 60	88 (53.99)	97 (60.25)		185 (57.10)
≥ 60	75 (46.01)	64 (39.75)		139 (42.90)
Sex			0.007	
Female	61 (37.42)	37 (22.98)		98 (30.25)
Male	102 (62.58)	124 (77.02)		226 (69.75)
BMI, kg/m^2			0.317	
< 18.5	7 (4.29)	4 (2.48)		11 (3.40)
18.5-23.9	86 (52.76)	73 (45.34)		159 (49.07)
24.0-27.9	52 (31.90)	66 (40.99)		118 (36.42)
≥ 28.0	18 (11.04)	18 (11.18)		36 (11.11)
Smoking history			0.581	
No	87 (53.37)	80 (49.69)		167 (51.54)
Yes	76 (46.63)	81 (50.31)		157 (48.46)
Drinking history			0.925	
No	96 (58.90)	93 (57.76)		189 (58.33)
Yes	67 (41.10)	68 (42.24)		135 (41.67)
Chronic disease history			0.624	
No	100 (61.35)	104 (64.60)		204 (62.96)
Yes	63 (38.65)	57 (35.40)		120 (37.04)
cTNM stage			0.839	
II	23 (14.11)	25 (15.53)		48 (14.81)
III	140 (85.89)	136 (84.47)		276 (85.19)
nCRT with surgery interval, d			0.573	
31-60	88 (53.99)	79 (49.07)		167 (51.54)
61-90	63 (38.65)	66 (40.99)		129 (39.81)
> 90	12 (7.36)	16 (9.94)		28 (8.64)
Inferior margin			0.373	
≤ 5 cm	109 (66.87)	116 (72.05)		225 (69.44)
> 5 cm	54 (33.13)	45 (27.95)		99 (30.56)
TRG			0.160	
1	14 (8.59)	16 (9.94)		30 (9.26)
2	90 (55.21)	72 (44.72)		162 (50.00)
3	41 (25.15)	43 (26.71)		84 (25.93)
4	18 (11.04)	30 (18.63)		48 (14.81)
Vascular invasion			0.471	
Negative	155 (95.09)	149 (92.55)		304 (93.83)
Positive	8 (4.91)	12 (7.45)		20 (6.17)
Neural invasion			0.846	
Negative	130 (79.75)	126 (78.26)		256 (79.01)

Positive	33 (20.25)	35 (21.74)		68 (20.99)
Radiotherapy type before surgery			0.688	
VMAT	146 (89.57)	140 (86.96)		286 (88.27)
IMRT	14 (8.59)	16 (9.94)		30 (9.26)
3D-CRT	3 (1.84)	5 (3.11)		8 (2.47)
Chemotherapy type before surgery			0.975	
Capecitabine	145 (88.96)	144 (89.44)		289 (89.20)
Capecitabine + platinum	9 (5.52)	9 (5.59)		18 (5.56)
Other	9 (5.52)	8 (4.97)		17 (5.25)
Adjuvant chemotherapy			0.383	
No	57 (34.97)	48 (29.81)		105 (32.41)
Yes	106 (65.03)	113 (70.19)		219 (67.59)
Pre-CEA			0.832	
≤ 5 ng/mL	91 (55.83)	87 (54.04)		178 (54.94)
> 5 ng/mL	72 (44.17)	74 (45.96)		146 (45.06)
Pre-CA19-9			0.931	
≤ 27 U/mL	131 (80.37)	131 (81.37)		262 (80.86)
> 27 U/mL	32 (19.63)	30 (18.63)		62 (19.14)

nCRT: Neoadjuvant chemoradiotherapy; pre-IBIL: Indirect bilirubin before neoadjuvant chemoradiotherapy; BMI: Body mass index; TRG: Tumor regression grade; VMAT: Volumetric modulated arc therapy; IMRT: Intensity modulated radiation therapy; 3D-CRT: 3-dimensional conformal radiation therapy; pre-CEA: Carcinoembryonic antigen before neoadjuvant chemoradiotherapy; pre-CA19-9: Carbohydrate antigen 19-9 before neoadjuvant chemoradiotherapy.

HR = 0.58, 95%CI: 0.34-1.00. *P* = 0.048), TRG (TRG = 2, adjusted HR = 0.37, 95%CI: 0.18-0.75, *P* = 0.006; TRG = 3, adjusted HR = 0.27, 95%CI: 0.12-0.64, *P* = 0.003; TRG = 4, adjusted HR = 0.18, 95%CI: 0.06-0.53 *P* = 0.002), vascular invasion (positive, adjusted HR = 2.93, 95%CI: 1.39-6.21, *P* = 0.005), and pre-CA19-9 (pre-CA19-9 > 27 U/mL, adjusted HR = 2.05, 95%CI: 1.16-3.62, *P* = 0.014) were predictors of OS (Table 2).

Cox regression analysis of prognostic factors for DFS

All variables identified in Table 1 were selected for univariable Cox regression analysis to estimate DFS in LARC patients treated with nCRT and TME. Univariable analysis revealed that factors including pre-IBIL, BMI, nCRT with surgery interval, TRG, vascular invasion, and neural invasion were independently associated with DFS in these patients. All statistically significant predictors in the univariate analysis were included in the multivariate model. The multivariate analysis revealed that pre-IBIL (pre-IBIL > 6.2 μmol/L, adjusted HR = 1.86, 95%CI: 1.22-2.84, *P* = 0.004), BMI (BMI ≥ 28.0, adjusted HR = 0.19, 95%CI: 0.05-0.66, *P* = 0.009), nCRT with surgery interval (nCRT with surgery interval = 61-90 d, adjusted HR = 0.63, 95%CI: 0.40-0.99, *P* = 0.044), TRG (TRG = 2, adjusted HR = 0.43, 95%CI: 0.24-0.78, *P* = 0.005; TRG = 3, adjusted HR = 0.30, 95%CI: 0.15-0.62, *P* = 0.001; TRG = 4, adjusted HR = 0.31, 95%CI: 0.14-0.70, *P* = 0.005), and vascular invasion (positive, adjusted HR = 2.24, 95%CI: 1.13-4.44, *P* = 0.021) were predictors of DFS (Table 3).

Construction of nomograms to predict OS and DFS

We established nomograms for the prediction of the 5-year OS and DFS using the independent variables (Figure 1). Pre-IBIL, smoking history, TRG, vascular invasion, and pre-CA19-9 were statistically significant predictors of OS on Cox multivariate analysis. Pre-IBIL, BMI, nCRT with surgery interval, TRG, and vascular invasion were statistically significant predictors of DFS on Cox multivariate analysis. Therefore, these variables were subsequently included in the nomogram. A weighted total score is calculated from these factors, which is applied to predict the OS and DFS for the LARC patients who received nCRT. We found that patients with a lower pre-IBIL had better OS and DFS.

Evaluation of the nomogram

The nomogram for predicting OS and DFS in LARC patients treated with nCRT was developed based on the multivariate model in the cohort. The area under the ROC curve (AUC) was analyzed for the

Table 2 Cox regression analysis of prognostic factors for overall survival

Characteristic	Univariable analysis		Multivariable analysis	
	HR (95%CI)	*P* value	HR (95%CI)	*P* value
Pre-IBIL				
≤ 6.2 μmol/L	Reference		Reference	
> 6.2 μmol/L	1.71 (1.01-2.87)	0.045	1.77 (1.04-3.01)	0.035
Age, yr				
< 60	Reference			
≥ 60	1.39 (0.84-2.31)	0.199		
Sex				
Female	Reference			
Male	1.16 (0.66-2.04)	0.596		
BMI, kg/m^2				
< 18.5	Reference			
18.5-23.9	0.74 (0.23-2.43)	0.624		
24.0-27.9	0.57 (0.17-1.93)	0.370		
≥ 28.0	0.27 (0.05-1.32)	0.105		
Smoking history				
No	Reference		Reference	
Yes	0.57 (0.34-0.97)	0.039	0.58 (0.34-1.00)	0.048
Drinking history				
No	Reference			
Yes	0.72 (0.42-1.23)	0.227		
Chronic disease history				
No	Reference			
Yes	1.09 (0.65-1.82)	0.749		
cTNM stage				
II	Reference			
III	2.54 (0.92-6.99)	0.072		
nCRT with surgery interval, day				
31-60	Reference			
61-90	0.61 (0.35-1.07)	0.083		
> 90	0.68 (0.24-1.92)	0.469		
Inferior margin				
≤ 5 cm	Reference			
> 5 cm	0.91 (0.53-1.59)	0.752		
TRG				
1	Reference		Reference	
2	0.35 (0.18-0.67)	0.002	0.37 (0.18-0.75)	0.006
3	0.23 (0.10-0.52)	< 0.001	0.27 (0.12-0.64)	0.003
4	0.17 (0.06-0.48)	< 0.001	0.18 (0.06-0.53)	0.002
Vascular invasion				
Negative	Reference		Reference	

Positive	3.79 (1.86-7.74)	< 0.001	2.93 (1.39-6.21)	0.005
Neural invasion				
Negative	Reference		Reference	
Positive	2.15 (1.26-3.69)	0.005	1.27 (0.69-2.31)	0.442
Radiotherapy type before surgery				
VMAT	Reference			
IMRT	1.68 (0.85-3.35)	0.137		
3D-CRT	0.69 (0.09-4.98)	0.709		
Chemotherapy type before surgery				
Capecitabine	Reference			
Capecitabine + platinum	1.45 (0.57-3.66)	0.431		
Other	1.90 (0.76-4.78)	0.172		
Adjuvant chemotherapy				
No	Reference			
Yes	0.60 (0.36-1.00)	0.050		
Pre-CEA				
≤ 5 ng/mL	Reference			
> 5 ng/mL	1.44 (0.87-2.39)	0.158		
Pre-CA19-9				
≤ 27 U/mL	Reference		Reference	
> 27 U/mL	2.05 (1.19-3.54)	0.010	2.05 (1.16-3.62)	0.014

HR: Hazard ratio; 95%CI: 95% confidence interval; nCRT: Neoadjuvant chemoradiotherapy; pre-IBIL: Indirect bilirubin before neoadjuvant chemoradiotherapy; BMI: Body mass index; TRG: Tumor regression grade; VMAT: Volumetric modulated arc therapy; IMRT: Intensity modulated radiation therapy; 3D-CRT: 3-dimensional conformal radiation therapy; pre-CEA: Carcinoembryonic antigen before neoadjuvant chemoradiotherapy; pre-CA19-9: Carbohydrate antigen 19-9 before neoadjuvant chemoradiotherapy.

cohort, and the AUC values for the 5-year OS and DFS nomograms were 0.7518 and 0.7355, respectively (Figure 2). The model demonstrated good statistical performance for predicting OS and DFS, and calibration curves for the probability of 5-year OS and 5-year DFS indicated satisfactory consistency between actual observation and nomogram prediction (Figure 3).

Kaplan-Meier survival curves

In Kaplan-Meier survival analysis, we found that pre-IBIL was related to OS (Figure 4A**)** and DFS (Figure 4B**)** in LARC patients treated with nCRT. For OS, the median was 5.28 years. The patients in the pre-IBIL ≤ 6.2 μmol/L group had a significantly longer OS than patients in the pre-IBIL > 6.2 μmol/L group (P = 0.042). The 5-year survival rate of the patients in the pre-IBIL ≤ 6.2 μmol/L group was 87.27%, higher than that of the patients in the pre-IBIL > 6.2 μmol/L group, 78.48%. For DFS, the median DFS was 4.71 years. Additionally, the patients in the pre-IBIL ≤ 6.2 μmol/L group also had a significantly longer DFS than patients in the pre-IBIL > 6.2 μmol/L group (P = 0.012). The 5-year recurrence rates of patients in the pre-IBIL ≤ 6.2 μmol/L and pre-IBIL > 6.2 μmol/L groups were 76.90% and 64.39%, respectively.

DISCUSSION

The nCRT combined with TME is the standard treatment for patients with LARC[16]. Although this treatment regimen has been shown to improve the local control rate in some LARC patients, there are still considerable differences in prognoses among patients[17]. Tumor markers are substances that are synthesized or released by tumor cells themselves or produced by the body in response to tumor cells during the process of tumor development. When these substances reach a certain level, they can indicate the existence of a specific tumor, and the changes in the levels of these substances can be used to monitor the recurrence and progression of the tumor[18]. At present, common tumor markers are not

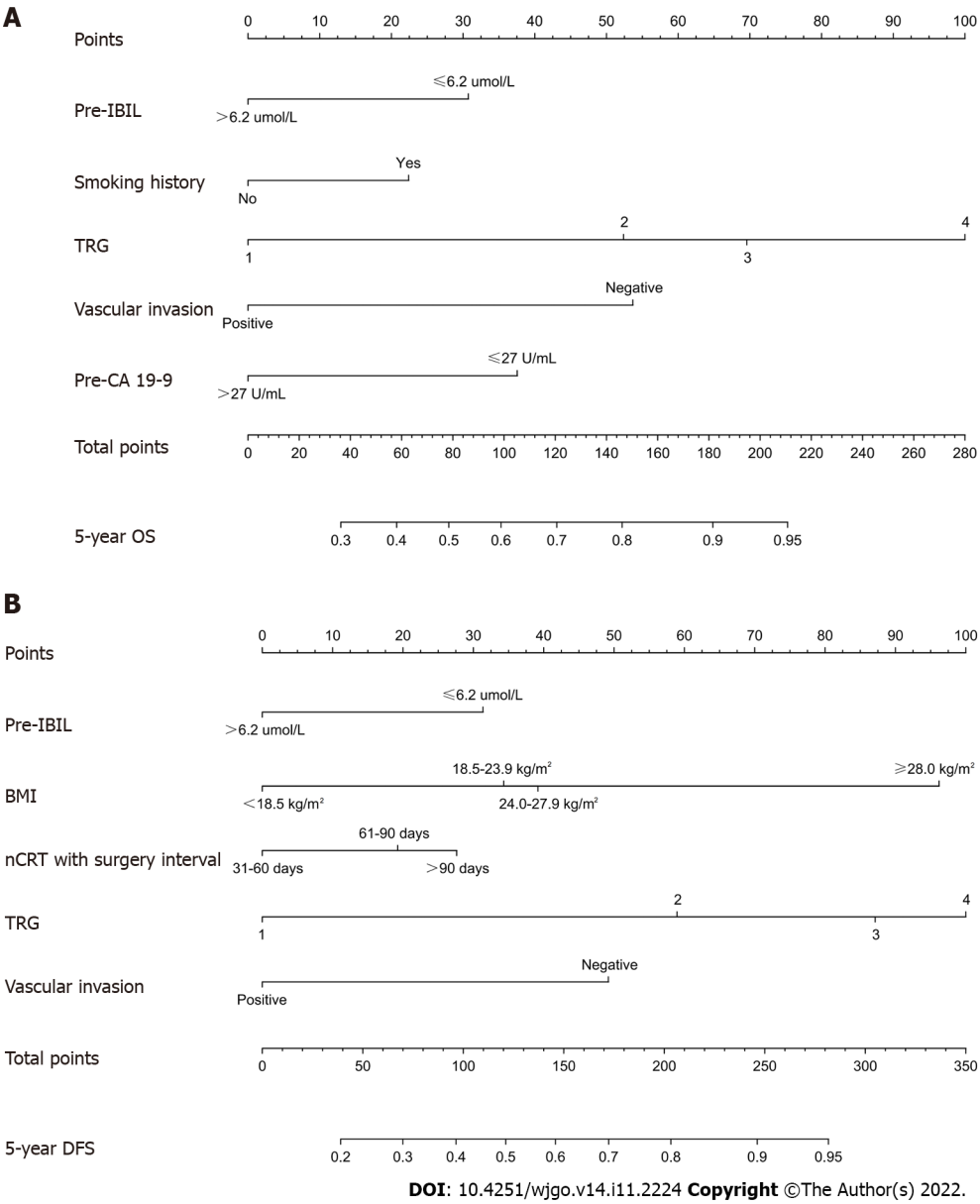

DOI: 10.4251/wjgo.v14.i11.2224

Figure 1 Nomograms. A: Overall survival; B: Disease-free survival. OS: Overall survival; DFS: Disease-free survival; nCRT: Neoadjuvant chemoradiotherapy; pre-IBIL: Indirect bilirubin before neoadjuvant chemoradiotherapy; BMI: Body mass index; TRG: Tumor regression grade; pre-CA19-9: Carbohydrate antigen 19-9 before neoadjuvant chemoradiotherapy.

routinely tested in health checkups, which often leads to the missed diagnosis of some patients with early malignant tumors, thus indicating that it is important to identify new tumor markers during routine checkups.

Previous studies have focused attention on identifying pretreatment blood-based biomarkers and traditional tumor biomarkers, including CEA, CA19-9 and the neutrophil-to-lymphocyte ratio. These biomarkers have been proven to have prognostic effects in predicting the response and survival in LARC[19]. In recent years, liquid biopsy has received increasing attention in cancer research, and biomarkers based on liquid biopsy have also shown favorable significance in treatment and prognosis prediction[20,21]. For example, a prospective study including 119 Chinese LARC patients identified circulating tumor DNA as a good predictor for risk stratification and for guiding the treatment strategy [22]. However, these new biomarkers are still under investigation, and their clinical application may need to be further studied to obtain a consensus.

Biochemical tests for blood samples are routinely performed for each hospitalized patient, and bilirubin is one of the most important markers of the biochemical test. Bilirubin is a major toxic metabolite of iron porphyrin compounds in the body, which can cause irreversible damage to the nervous system; however, it has antioxidant properties and can inhibit the oxidation of linoleic acid and phospholipids. Recent studies have shown that bilirubin, as an endogenous antioxidant, can moderately increase the ability of cancer patients to scavenge oxidative free radicals in the body and affect the prognoses of cancer patients. Therefore, bilirubin levels are of great clinical significance as a novel

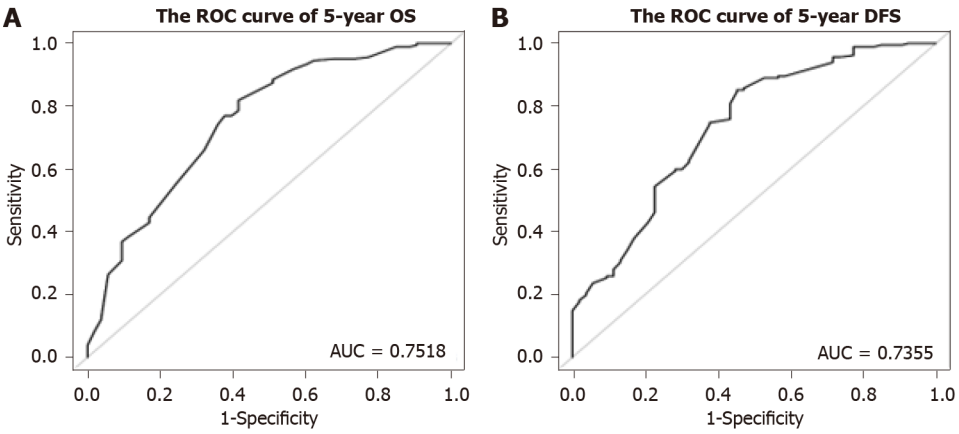

DOI: 10.4251/wjgo.v14.i11.2224 **Copyright** ©The Author(s) 2022.

Figure 2 Nomogram model receiver operating characteristic curve. A: 5-year overall survival; B: 5-year disease-free survival. ROC: Receiver operating characteristic; AUC: Area under the receiver operating characteristic curve; OS: Overall survival; DFS: Disease-free survival.

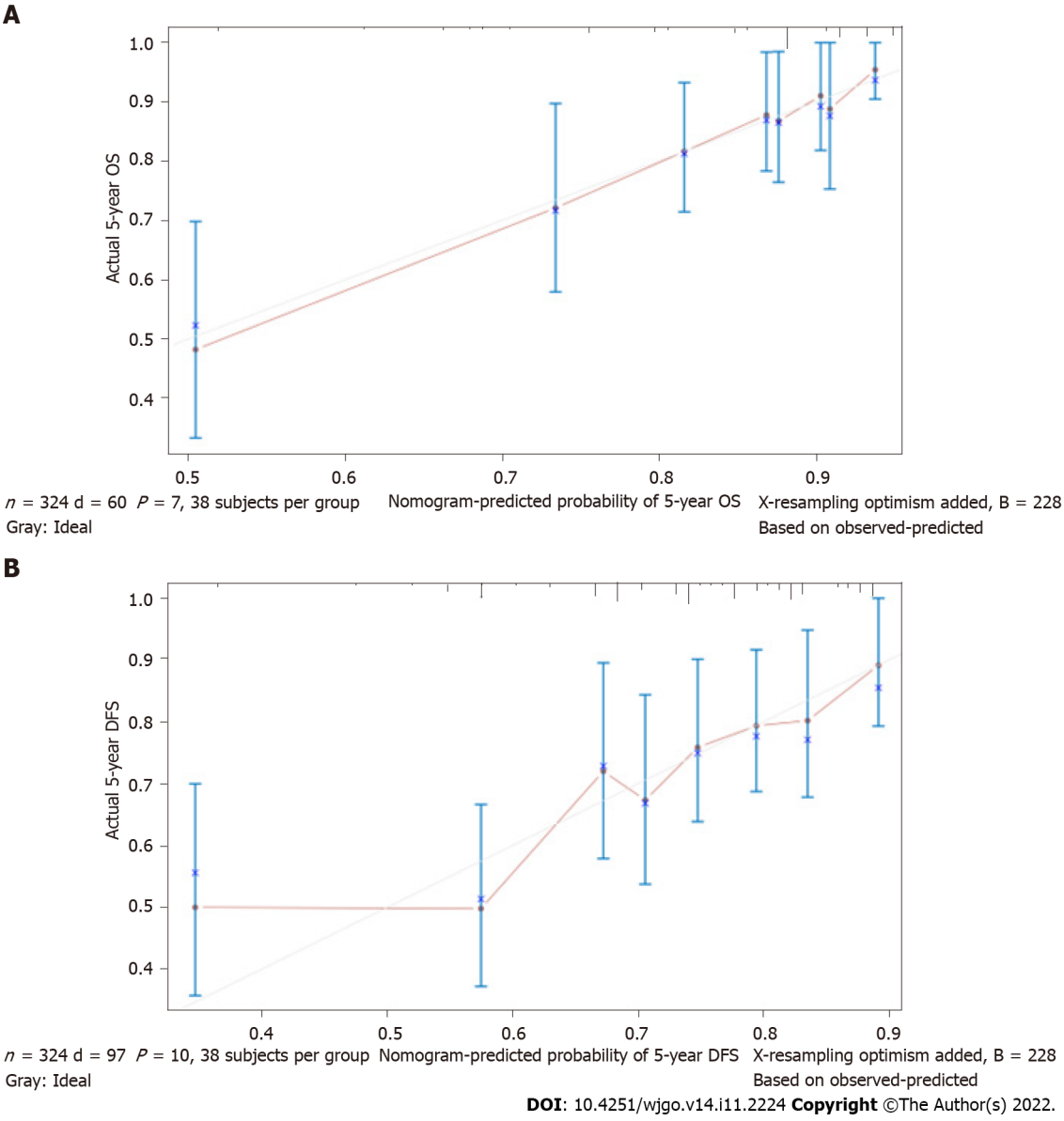

DOI: 10.4251/wjgo.v14.i11.2224 **Copyright** ©The Author(s) 2022.

Figure 3 Nomogram model calibration curves. A: 5-year overall survival; B: 5-year disease-free survival. OS: Overall survival; DFS: Disease-free survival.

Table 3 Cox regression analysis of prognostic factors for disease-free survival

Characteristic	Univariable analysis		Multivariable analysis	
	HR (95%CI)	*P* value	HR (95%CI)	*P* value
Pre-IBIL				
≤ 6.2 μmol/L	Reference		Reference	
> 6.2 μmol/L	1.68 (1.12-2.53)	0.013	1.86 (1.22-2.84)	0.004
Age, yr				
< 60	Reference			
≥ 60	1.16 (0.78-1.74)	0.456		
Sex				
Female	Reference			
Male	0.84 (0.55-1.28)	0.414		
BMI, kg/m^2				
< 18.5	Reference		Reference	
18.5-23.9	0.64 (0.26-1.61)	0.346	0.46 (0.18-1.17)	0.102
24.0-27.9	0.62 (0.24-1.57)	0.312	0.50 (0.19-1.30)	0.157
≥ 28.0	0.25 (0.07-0.87)	0.029	0.19 (0.05-0.66)	0.009
Smoking history				
No	Reference			
Yes	0.72 (0.48-1.08)	0.108		
Drinking history				
No	Reference			
Yes	0.71 (0.47-1.07)	0.103		
Chronic disease history				
No	Reference			
Yes	1.07 (0.72-1.61)	0.732		
cTNM stage				
II	Reference			
III	1.49 (0.80-2.80)	0.210		
nCRT with surgery interval, d				
31-60	Reference		Reference	
61-90	0.64 (0.41-0.99)	0.047	0.63 (0.40-0.99)	0.044
> 90	0.84 (0.40-1.77)	0.655	0.63 (0.29-1.35)	0.235
Inferior margin				
≤ 5 cm	Reference			
> 5 cm	0.80 (0.51-1.25)	0.318		
TRG				
1	Reference		Reference	
2	0.45 (0.26-0.79)	0.006	0.43 (0.24-0.78)	0.005
3	0.29 (0.15-0.57)	< 0.001	0.30 (0.15-0.62)	0.001
4	0.31 (0.15-0.66)	0.002	0.31 (0.14-0.70)	0.005
Vascular invasion				
Negative	Reference		Reference	

Positive	2.54 (1.32-4.90)	0.005	2.24 (1.13-4.44)	0.021
Neural invasion				
Negative	Reference		Reference	
Positive	1.82 (1.17-2.82)	0.008	1.34 (0.82-2.18)	0.238
Radiotherapy type before surgery				
VMAT	Reference			
IMRT	1.07 (0.57-2.01)	0.836		
3D-CRT	0.83 (0.20-3.37)	0.791		
Chemotherapy type before surgery				
Capecitabine	Reference			
Capecitabine + platinum	0.98 (0.43-2.26)	0.969		
Other	1.56 (0.72-3.37)	0.262		
Adjuvant chemotherapy				
No	Reference			
Yes	0.89 (0.59-1.35)	0.584		
Pre-CEA				
≤ 5 ng/mL	Reference			
> 5 ng/mL	1.33 (0.89-1.98)	0.158		
Pre-CA19-9				
≤ 27 U/mL	Reference			
> 27 U/mL	1.47 (0.92-2.33)	0.104		

HR: Hazard ratio; 95%CI: 95% confidence interval; nCRT: Neoadjuvant chemoradiotherapy; pre-IBIL: Indirect bilirubin before neoadjuvant chemoradiotherapy; BMI: Body mass index; TRG: Tumor regression grade; VMAT: Volumetric modulated arc therapy; IMRT: Intensity modulated radiation therapy; 3D-CRT: 3-dimensional conformal radiation therapy; pre-CEA: Carcinoembryonic antigen before neoadjuvant chemoradiotherapy; pre-CA19-9: Carbohydrate antigen 19-9 before neoadjuvant chemoradiotherapy.

tumor biomarker[23-27]. One study demonstrated that the direct bilirubin-to-IBIL ratio was an independent predictor of survival in resectable colorectal cancer patients[28]. Nevertheless, few studies have been conducted to explore the prognostic effect of bilirubin in LARC patients.

In this study, we collected clinical and pathological data of 324 LARC patients treated with nCRT combined with TME and followed up with each of these patients. We performed all factor Cox regression analyses in Table 1, and the characteristics with statistically significant results from the univariate analysis were included in the multivariate analysis. The multivariate analysis results showed that pre-IBIL, smoking history, TRG, vascular invasion and pre-CA19-9 were risk factors affecting OS. The multivariate analysis results showed that pre-IBIL, BMI, nCRT with surgery interval, TRG and vascular invasion were risk factors affecting DFS. In addition, we constructed nomograms to evaluate prognoses based on the above indicators.

Our research had the following advantages. First, we found a correlation of pre-IBIL with the prognosis of LARC patients after receiving nCRT, and the prognoses of those patients with pre-IBIL > 6.2 μmol/L were poorer, which indicated that pre-IBIL is a risk factor affecting the prognoses of patients. Second, we performed a Cox regression analysis of pre-IBIL with common characteristics and found that pre-IBIL was associated with the OS and DFS of LARC patients receiving nCRT. We also constructed nomograms that could predict OS and DFS. Third, we collected clinical characteristics, pathological characteristics, treatment information, hematological characteristics and sociological characteristics of patients and considered more comprehensive factors. However, our study had some limitations. First, this was a single-center study, the sample size was relatively small and the results need to be further validated by expanding the sample size. Second, in our study, with the limitations of the retrospective nature, we found an association between a blood sample and oncological outcomes in patients with LARC, and future prospective studies should be conducted to further explore the associations between pre-IBIL and the prognoses of LARC patients.

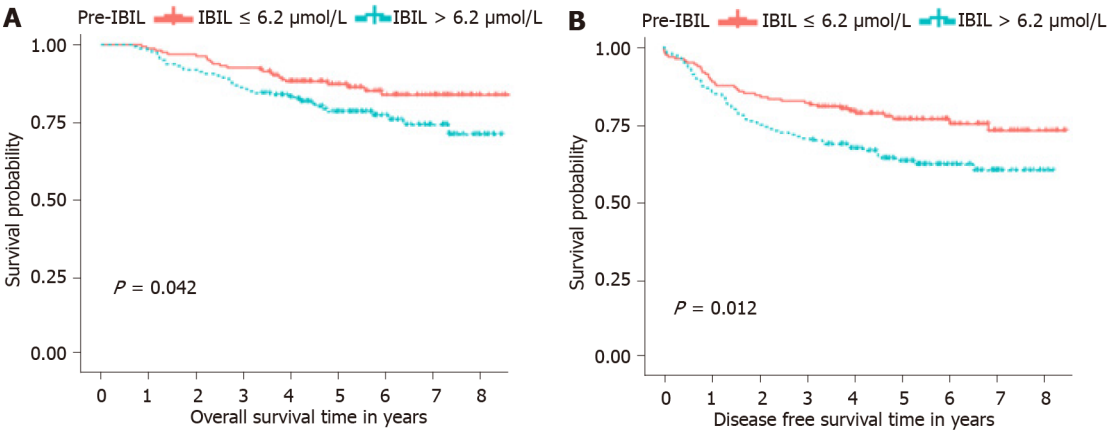

DOI: 10.4251/wjgo.v14.i11.2224

Figure 4 Kaplan-Meier curves. A: Overall survival; B: Disease-free survival. nCRT: Neoadjuvant chemoradiotherapy; pre-IBIL: Indirect bilirubin before neoadjuvant chemoradiotherapy.

CONCLUSION

In conclusion, this study demonstrated that pre-IBIL was an independent prognostic factor for OS and DFS in LARC patients treated with nCRT followed by TME. Nomograms incorporating pre-IBIL, BMI, smoking history, nCRT with surgery interval, TRG, vascular invasion, and pre-CA19-9 could be helpful to predict OS and DFS. These findings provide a new direction for future clinical precision treatment and scientific research.

ARTICLE HIGHLIGHTS

Research background

Neoadjuvant chemoradiotherapy (nCRT) has been regarded as the standard treatment for local advanced rectal cancer (LARC). Bilirubin has shown significance in the prognosis of various cancer types, including ovarian cancer and lung cancer. However, the predictive values of indirect bilirubin (IBIL) in the prognoses of LARC patients treated with nCRT remain unknown.

Research motivation

The present study attempted to identify the prognostic value of IBIL before nCRT (pre-IBIL) in LARC patients and to construct a nomogram based on pre-IBIL to predict the survival of the patients.

Research objectives

This study aimed to identify the prognostic value of pre-IBIL in LARC patients and to construct a nomogram to predict their 5-year overall survival (OS) and 5-year disease-free survival (DFS).

Research methods

A total of 324 LARC patients undergoing nCRT with total mesorectal excision (TME) were enrolled. Preoperative clinical features and postoperative pathological characteristics were collected. A Cox regression analysis was performed, and a Cox-based nomogram was developed to predict OS and DFS. We also assessed the predictive performance of the nomogram with receiver operating characteristic (ROC) and curves calibration plots.

Research results

In the Cox multivariate regression analysis, we found that pre-IBIL, smoking history, tumor regression grade (TRG), vascular invasion and carbohydrate antigen 19-9 before nCRT were predictors of OS. Furthermore, pre-IBIL, body mass index, nCRT with surgery interval, TRG and vascular invasion were predictors of DFS. Predictive nomograms were developed to predict 5-year OS and 5-year DFS with areas under the ROC curve of 0.7518 and 0.7355, respectively. Good statistical performance on internal validation was shown *via* the calibration plots and ROC curves.

Research conclusions

Pre-IBIL was an independent prognostic factor for OS and DFS in LARC patients treated with nCRT followed by TME. Nomograms based on pre-IBIL could be helpful for predicting survival in LARC

patients.

Research perspectives

Although our single-center study identified the prognostic value of pre-IBIL in LARC patients, a future prospective study with larger samples should be conducted to further explore the association between pre-IBIL and the prognosis of LARC patients.

FOOTNOTES

Author contributions: Li SF and Zheng J designed the study; Li SF, Wei R and Yu GH performed the research; Li SF, Wei R and Yu GH analyzed the data; Li SF and Wei R wrote the paper; Zheng J revised the manuscript for final submission.

Institutional review board statement: The study was reviewed and approved by the National Cancer Center/National Clinical Research Center for Cancer/Cancer Hospital, Chinese Academy of Medical Sciences and Peking Union Medical College.

Informed consent statement: This study was a retrospective non-interventional study, which did not affect any medical rights of patient and did not additionally increase patient risk. Some of the patients to be included in this study died or were lost to follow-up, and it is objectively impossible to obtain their informed consent. For these reasons, we have applied to the hospital ethics committee for a waiver of informed consent for all patients in this study at the time of project application, which has been approved.

Conflict-of-interest statement: All the authors report no relevant conflicts of interest for this article.

Data sharing statement: No additional data are available.

Country/Territory of origin: China

ORCID number: Shuo-Feng Li 0000-0003-2747-9501; Ran Wei 0000-0003-4293-6686; Guan-Hua Yu 0000-0003-4891-6993; Zheng Jiang 0000-0002-1369-3681.

S-Editor: Wang JJ
L-Editor: A
P-Editor: Wang JJ

REFERENCES

1 **Benson AB**, Venook AP, Al-Hawary MM, Arain MA, Chen YJ, Ciombor KK, Cohen S, Cooper HS, Deming D, Garrido-Laguna I, Grem JL, Gunn A, Hoffe S, Hubbard J, Hunt S, Kirilcuk N, Krishnamurthi S, Messersmith WA, Meyerhardt J, Miller ED, Mulcahy MF, Nurkin S, Overman MJ, Parikh A, Patel H, Pedersen K, Saltz L, Schneider C, Shibata D, Skibber JM, Sofocleous CT, Stoffel EM, Stotsky-Himelfarb E, Willett CG, Johnson-Chilla A, Gurski LA. NCCN Guidelines Insights: Rectal Cancer, Version 6.2020. *J Natl Compr Canc Netw* 2020; **18**: 806-815 [PMID: 32634771 DOI: 10.6004/jnccn.2020.0032]

2 **Li Y**, Wang J, Ma X, Tan L, Yan Y, Xue C, Hui B, Liu R, Ma H, Ren J. A Review of Neoadjuvant Chemoradiotherapy for Locally Advanced Rectal Cancer. *Int J Biol Sci* 2016; **12**: 1022-1031 [PMID: 27489505 DOI: 10.7150/ijbs.15438]

3 **Keller DS**, Berho M, Perez RO, Wexner SD, Chand M. The multidisciplinary management of rectal cancer. *Nat Rev Gastroenterol Hepatol* 2020; **17**: 414-429 [PMID: 32203400 DOI: 10.1038/s41575-020-0275-y]

4 **Sun Y**, Huang Z, Chi P. An inflammation index-based prediction of treatment response to neoadjuvant chemoradiotherapy for rectal mucinous adenocarcinoma. *Int J Clin Oncol* 2020; **25**: 1299-1307 [PMID: 32274615 DOI: 10.1007/s10147-020-01670-5]

5 **Sun Y**, Zhang Y, Huang Z, Chi P. Prognostic Implication of Negative Lymph Node Count in ypN+ Rectal Cancer after Neoadjuvant Chemoradiotherapy and Construction of a Prediction Nomogram. *J Gastrointest Surg* 2019; **23**: 1006-1014 [PMID: 30187336 DOI: 10.1007/s11605-018-3942-3]

6 **Li J**, Yi CH, Hu YT, Li JS, Yuan Y, Zhang SZ, Zheng S, Ding KF. TNM Staging of Colorectal Cancer Should be Reconsidered According to Weighting of the T Stage: Verification Based on a 25-Year Follow-Up. *Medicine (Baltimore)* 2016; **95**: e2711 [PMID: 26871810 DOI: 10.1097/MD.0000000000002711]

7 **Gunderson LL**, Jessup JM, Sargent DJ, Greene FL, Stewart AK. Revised TN categorization for colon cancer based on

national survival outcomes data. *J Clin Oncol* 2010; **28**: 264-271 [PMID: 19949014 DOI: 10.1200/JCO.2009.24.0952]

8 **Hashiguchi Y**, Hase K, Kotake K, Ueno H, Shinto E, Mochizuki H, Yamamoto J, Sugihara K. Evaluation of the seventh edition of the tumour, node, metastasis (TNM) classification for colon cancer in two nationwide registries of the United States and Japan. *Colorectal Dis* 2012; **14**: 1065-1074 [PMID: 22176600 DOI: 10.1111/j.1463-1318.2011.02917.x]

9 **Ji D**, Yi H, Zhang D, Zhan T, Li Z, Li M, Jia J, Qiao M, Xia J, Zhai Z, Song C, Gu J. Somatic Mutations and Immune Alternation in Rectal Cancer Following Neoadjuvant Chemoradiotherapy. *Cancer Immunol Res* 2018; **6**: 1401-1416 [PMID: 30282671 DOI: 10.1158/2326-6066.CIR-17-0630]

10 **Lee IH**, Kang K, Kang BW, Lee SJ, Bae WK, Hwang JE, Kim HJ, Park SY, Park JS, Choi GS, Kim JG. Genetic variations using whole-exome sequencing might predict response for neoadjuvant chemoradiotherapy in locally advanced rectal cancer. *Med Oncol* 2018; **35**: 145 [PMID: 30206710 DOI: 10.1007/s12032-018-1202-8]

11 **Tweedle EM**, Khattak I, Ang CW, Nedjadi T, Jenkins R, Park BK, Kalirai H, Dodson A, Azadeh B, Terlizzo M, Grabsch H, Mueller W, Myint S, Clark P, Wong H, Greenhalf W, Neoptolemos JP, Rooney PS, Costello E. Low molecular weight heat shock protein HSP27 is a prognostic indicator in rectal cancer but not colon cancer. *Gut* 2010; **59**: 1501-1510 [PMID: 20947885 DOI: 10.1136/gut.2009.196626]

12 **Geng Y**, Mei Y, Xi Y, Yu J, Meng K, Zhang T, Ma W. Bilirubin Can Be Used as a Prognostic Factor for Lung Adenocarcinoma Patients with EGFR Mutations. *Onco Targets Ther* 2020; **13**: 11089-11095 [PMID: 33149620 DOI: 10.2147/OTT.S266477]

13 **Xi XX**, Wang HL, Chen T, Dai JR, Hou SY, Chen YG. Prognostic value of preoperative serum bilirubin levels in ovarian cancer. *Am J Transl Res* 2020; **12**: 2267-2280 [PMID: 32509218]

14 **Yao JJ**, Kou J, Peng QH, Dong J, Zhang WJ, Lawrence WR, Zhang F, Zhou GQ, Wang SY, Sun Y. Prognostic value of serum bilirubin in southern Chinese patients with advanced nasopharyngeal carcinoma. *Clin Chim Acta* 2018; **484**: 314-319 [PMID: 29860034 DOI: 10.1016/j.cca.2018.05.058]

15 **Zhang H**, Li G, Zhu Z, Zheng Y, Wu Y, Zhang W, Gu N, Wang X, Song X. Serum bilirubin level predicts postoperative overall survival in oral squamous cell carcinoma. *J Oral Pathol Med* 2018; **47**: 382-387 [PMID: 29430757 DOI: 10.1111/jop.12693]

16 **Liu H**, Wei R, Li C, Zhao Z, Guan X, Yang M, Liu Z, Wang X, Jiang Z. BMI May Be a Prognostic Factor for Local Advanced Rectal Cancer Patients Treated with Long-Term Neoadjuvant Chemoradiotherapy. *Cancer Manag Res* 2020; **12**: 10321-10332 [PMID: 33116887 DOI: 10.2147/CMAR.S268928]

17 **Liu H**, Li C, Zhao Z, Guan X, Yang M, Liu Z, Tang Y, Jiang Z, Wang X. Safety and Long-Term Effect Assessment of Neoadjuvant Chemoradiotherapy for Elderly Patients With Locally Advanced Rectal Cancer: A CHN Single-Center Retrospective Study. *Technol Cancer Res Treat* 2020; **19**: 1533033820970339 [PMID: 33161830 DOI: 10.1177/1533033820970339]

18 **Faria SC**, Sagebiel T, Patnana M, Cox V, Viswanathan C, Lall C, Qayyum A, Bhosale PR. Tumor markers: myths and facts unfolded. *Abdom Radiol (NY)* 2019; **44**: 1575-1600 [PMID: 30498924 DOI: 10.1007/s00261-018-1845-0]

19 **Mendis S**, To YH, Tie J. Biomarkers in Locally Advanced Rectal Cancer: A Review. *Clin Colorectal Cancer* 2022; **21**: 36-44 [PMID: 34961731 DOI: 10.1016/j.clcc.2021.11.002]

20 **Alix-Panabières C**, Pantel K. Liquid Biopsy: From Discovery to Clinical Application. *Cancer Discov* 2021; **11**: 858-873 [PMID: 33811121 DOI: 10.1158/2159-8290.CD-20-1311]

21 **Dizdarevic E**, Hansen TF, Jakobsen A. The Prognostic Importance of ctDNA in Rectal Cancer: A Critical Reappraisal. *Cancers (Basel)* 2022; **14** [PMID: 35565381 DOI: 10.3390/cancers14092252]

22 **Wang Y**, Yang L, Bao H, Fan X, Xia F, Wan J, Shen L, Guan Y, Wu X, Xu Y, Shao Y, Sun Y, Tong T, Li X, Cai S, Zhu J, Zhang Z. Utility of ctDNA in predicting response to neoadjuvant chemoradiotherapy and prognosis assessment in locally advanced rectal cancer: A prospective cohort study. *PLoS Med* 2021; **18**: e1003741 [PMID: 34464382 DOI: 10.1371/journal.pmed.1003741]

23 **Gao C**, Fang L, Li JT, Zhao HC. Significance and prognostic value of increased serum direct bilirubin level for lymph node metastasis in Chinese rectal cancer patients. *World J Gastroenterol* 2016; **22**: 2576-2584 [PMID: 26937145 DOI: 10.3748/wjg.v22.i8.2576]

24 **Jiang D**, Shi J, Yuan M, Duan X, Li L, Li Q. Levels of serum bilirubin in small cell lung cancer and non-small cell lung cancer patients. *Cell Mol Biol (Noisy-le-grand)* 2018; **64**: 71-76 [PMID: 29808804]

25 **Liu X**, Meng QH, Ye Y, Hildebrandt MA, Gu J, Wu X. Prognostic significance of pretreatment serum levels of albumin, LDH and total bilirubin in patients with non-metastatic breast cancer. *Carcinogenesis* 2015; **36**: 243-248 [PMID: 25524924 DOI: 10.1093/carcin/bgu247]

26 **Sun H**, He B, Nie Z, Pan Y, Lin K, Peng H, Xu T, Chen X, Hu X, Wu Z, Wu D, Wang S. A nomogram based on serum bilirubin and albumin levels predicts survival in gastric cancer patients. *Oncotarget* 2017; **8**: 41305-41318 [PMID: 28476041 DOI: 10.18632/oncotarget.17181]

27 **Vítek L**. [Role of bilirubin in the prevention of cardiovascular diseases and cancer]. *Cas Lek Cesk* 2016; **155**: 10-14 [PMID: 27088786]

28 **Ma Y**, Shi L, Lu P, Yao S, Xu H, Hu J, Liang X, Wei S. Creation of a Novel Nomogram Based on the Direct Bilirubin-To-Indirect Bilirubin Ratio and Lactate Dehydrogenase Levels in Resectable Colorectal Cancer. *Front Mol Biosci* 2021; **8**: 751506 [PMID: 34746234 DOI: 10.3389/fmolb.2021.751506]

World Journal of Gastrointestinal Oncology

Submit a Manuscript: https://www.f6publishing.com

World J Gastrointest Oncol 2022 November 15; 14(11): 2238-2252

DOI: 10.4251/wjgo.v14.i11.2238

ISSN 1948-5204 (online)

ORIGINAL ARTICLE

Observational Study

Features of gastric cancer by anatomic subsite in northern China: A multi-center Health Science Report database study

Rui-Ze Qu, Yan-Peng Ma, Xiao-Yuan Bao, Li-Yuan Tao, Xin Zhou, Si-Yi Lu, Yi Zhang, Bing-Yan Wang, Fei Li, Lin Tuo, Zhi-Peng Zhang, Wei Fu

Specialty type: Gastroenterology and hepatology

Provenance and peer review: Unsolicited article; Externally peer reviewed.

Peer-review model: Single blind

Peer-review report's scientific quality classification

Grade A (Excellent): 0
Grade B (Very good): 0
Grade C (Good): C, C, C
Grade D (Fair): 0
Grade E (Poor): 0

P-Reviewer: Dilek ON, Turkey; Kinami S, Japan; Li L, New Zealand

Received: August 5, 2022
Peer-review started: August 5, 2022
First decision: September 29, 2022
Revised: October 5, 2022
Accepted: October 27, 2022
Article in press: October 27, 2022
Published online: November 15, 2022

Rui-Ze Qu, Yan-Peng Ma, Xin Zhou, Si-Yi Lu, Yi Zhang, Bing-Yan Wang, Fei Li, Zhi-Peng Zhang, Wei Fu, Department of General Surgery, Cancer Center, Peking University Third Hospital, Beijing 100191, China

Xiao-Yuan Bao, Medical Informatics Center, Peking University Health Science Center, Beijing 100191, China

Li-Yuan Tao, Research Center of Clinical Epidemiology, Peking University Third Hospital, Beijing 100191, China

Lin Tuo, Department of Hospital Management, Peking University Health Science Center, Beijing 100191, China

Corresponding author: Wei Fu, MD, Chief Doctor, Professor, Department of General Surgery, Cancer Center, Peking University Third Hospital, No. 49 North Garden Road, Haidian District, Beijing 100191, China. fuwei@bjmu.edu.cn

Abstract

BACKGROUND

The features of gastric cancer based on the anatomic site remain unknown in northern China patients.

AIM

To analyze gastric cancer features and associated trends based on the anatomical site in northern China patients.

METHODS

This cross-sectional study used incident gastric cancer case data from 10 Peking University-affiliated hospitals (2014 to 2018). The clinical and prevailing local features were analyzed.

RESULTS

A total of 10709 patients were enrolled, including antral (42.97%), cardia (34.30%), and stomach body (18.41%) gastric cancer cases. Cancer in the cardia had the highest male:female ratio, proportion of elderly patients, and patients with complications, including hypertension, diabetes, cerebrovascular, and coronary diseases (P < 0.001). gastric cancer involving the antrum showed the lowest

proportion of patients from rural areas and accounted for the highest hospitalization rate and cost (each $P < 0.001$). The proportion of patients with cancer involving the cardia increased with an increase in the number of gastroesophageal reflux disease cases during the same period ($P < 0.001$). Multivariate analysis revealed that tumor location in the cardia increased the risk of in-hospital mortality ($P = 0.046$). Anatomical subsite was not linked to postoperative complications.

CONCLUSION
The features of gastric cancer based on the anatomical site differ between northern China and other regions, both globally and within the country. Social factors may account for these differences and should affect policy-making and clinical practice.

Key Words: Feature; Gastric cancer; Anatomical site; Northern China

Core Tip: Cancer in the cardia has the highest male:female ratio, proportion of elderly patients, and patients with complications including hypertension, diabetes, cerebrovascular, and coronary diseases. Gastric cancer in the antrum has the lowest proportion of patients from rural areas and accounts for the highest hospitalization rate and cost. The proportion of patients with cancer in the cardia increases with an increase in the number of gastroesophageal reflux disease cases during the same period. Tumor location in the cardia increases the risk of in-hospital mortality. Anatomical subsite is not linked to postoperative complications.

Citation: Qu RZ, Ma YP, Bao XY, Tao LY, Zhou X, Lu SY, Zhang Y, Wang BY, Li F, Tuo L, Zhang ZP, Fu W. Features of gastric cancer by anatomic subsite in northern China: A multi-center Health Science Report database study. *World J Gastrointest Oncol* 2022; 14(11): 2238-2252
URL: https://www.wjgnet.com/1948-5204/full/v14/i11/2238.htm
DOI: https://dx.doi.org/10.4251/wjgo.v14.i11.2238

INTRODUCTION

Gastric cancer is among the most common digestive malignant tumors worldwide and is predicted to have 27600 incident cases and cause 11010 deaths in the United States of America[1]. It ranks fifth among cancer diagnoses (1089103 cases) and fourth in gross mortality (768793 cases) worldwide[2]. China is among the regions with the highest gastric cancer incidence, reporting over 450000 new cases and 300000 deaths[3]. China may account for approximately half of the annual incidence of gastric cancer in Eastern Asia[4]. High mortality rates are a major concern for gastric cancer. Gastric cancer-related disability-adjusted life-years are the third-highest worldwide[4], accounting for 24.2% of cases with a 5-year overall survival (OS) rate[5]. In this cohort, the 5-year OS of patients with stage IV disease is lower than 4%[6].

A few studies have demonstrated differences in clinical and epidemiological features of this tumor type based on its presence in the anatomical subsites of the stomach. These subsites are usually divided into cardia (including adjacent gastroesophageal junction) and non-cardia locations, including the gastric body and antrum[7]. The constituent ratio of patients with gastric cancer in the cardia tends to be relatively high in Western countries, including the United States of America and the United Kingdom[7-10]. However, this same constituent ratio decreases in some Asian countries, including Japan, with a significant increase in the number of patients with gastric cancer in the stomach corpus[11]. The divergent trends could result from different etiologies for cardia and non-cardia subsites of gastric cancer; *e.g.*, non-cardia gastric cancer (specifically, antral gastric cancer) is directly associated with *Helicoibacter pylori* (*H. pylori*)-induced atrophic gastritis and accompanying hypochlorhydria[12,13]. In contrast, cancer involving the cardia (including cancers of the gastroesophageal junction) is closely related to gastroesophageal reflux disease (GERD)[14]. Gastric tumors at different anatomic locations may be distinct clinical entities[15].

Environmental and lifestyle factors affect the burden of gastric cancer. Smoking is an important risk factor in male patients[16], and a high-sodium diet is associated with gastric cancer in Eastern Asian patients, particularly in Chinese patients[4]. The incidence rates and distribution patterns of gastric cancer differ across various geographic regions[17], including within China. Despite the rise in the ratio of patients with cancer at the cardia of the stomach and the concomitant reduction among those with gastric cancer involving the antrum in the Chinese population, the rates of antral gastric cancer vary from 20% to 50%[18,19]. Both trends may result from a divergence in risk factors, including variations in

environmental influences and eating habits that differ among regions; these factors may also determine differences among tumors at different locations[18]. However, few population-based studies have been conducted in China on this topic[18,19], and analyses of data from northern China are lacking. Herein, we aimed to examine the clinical features of gastric cancer at different anatomical sites in patients from northern China. We also aimed to examine the associated variability and trends.

MATERIALS AND METHODS

Data source

Patient information was obtained from the Health Science Report (HSR) database of Peking University-affiliated hospitals[20,21]. As a patient-level database consisting of hospitalized populations from 10 comprehensive tertiary hospitals affiliated with Peking University, the HSR database is managed by the Department of Hospital Management, Peking University Health Science Center, including patients covering all of China (mainly from northern China), and handles 2097347 gastric cancer patients. HSRs are submitted annually by the hospitals, as determined by the guidelines of the National Health Commission of the People's Republic of China. A system developed by the Medical Information Center of Peking University Health Science Center was applied for integration, storage, management, analysis, and display of the data, and controls for safety and quality were embedded in each layer. Demographic and clinical characteristics of selected patients were extracted, including the corresponding International Classification of Diseases 10 edition (ICD-10) codes, demographic characteristics (age, sex, and others), hospitalization information (route of admission, hospital stay, costs, among others), diagnosis, operation type, and pathological information. Ethical approval was obtained from the Ethics Committee of Peking University Third Hospital (IRB00006761-M2019387). The written informed consent requirement was waived because of the retrospective nature of the study.

Study population

According to the accessibility and quality of data, patients registered from January 1, 2014, to December 31, 2018, were chosen for analysis[20]. Individuals who (1) had pathology records with a diagnosis of gastric cancer, (2) were hospitalized in at least one of the included hospitals, and (3) had one or more sets of complete hospitalization records were included in the analysis. Patients who had (1) no pathological diagnosis or (2) tumors in the stomach that had metastasized from other organs were excluded from the analysis. Anonymization of personal information was conducted for data privacy protection.

Identification of gastric cancer

ICD-10 codes were implemented for facilitated identification, and gastric cancer was designated as C16.0-4 as per published research[19]. Descriptive medical phrases were also applied to query for gastric/cardia/esophagogastric junction/non-cardia/body/antrum/pylorus cancer in the possible linguistic expressions in the Chinese language. Due to differences in anatomical, biological, and clinical characteristics by different subsites in gastric cancer, the selected patients were further divided according to tumor anatomical locations into gastric cancer involving the cardia (ICD-10 code: C16.0), gastric cancer involving the body (ICD-10 codes: C16.1-2), gastric cancer involving the antrum (ICD-10 codes: C16.3-4), and gastric cancers of multiple foci (ICD-10 code: C16.8). For cases without exact diagnosis on anatomical site (ICD-10 code: C16.5-6 and C16.9), diagnosis description and pathological results were screened by two senior gastroenterologists. Patients with unidentifiable subsites were categorized as "other type". A fuzzy string-matching algorithm was also applied with the listed medical phrases to search for more potential patients to avoid omission. Validation was applied to the classification strategy. Data from a total of 1000 gastric cancer patients were extracted stochastically each time after primary selection, with a respective manual review of the diagnosis by two senior gastroenterologists for detection with the help of R (version 3.5.1), and the final consistency rate was over 99%.

Statistical analysis

The screened gastric cancer patients were classified by searching for different keywords on clinical, diagnostic, and surgical data with R (version 3.5.1). Only incident cases, which were identified as patients who were pathologically diagnosed through surgery and/or endoscopy for pathology (the gold standard for gastric cancer diagnosis), were defined as the study population. Those with multiple hospitalization records were identified by health care card numbers, and only their first visits were included to avoid duplication. The composition ratio of each anatomical subsite was calculated separately, and clinical characteristics, including age, sex, hospitalization costs, hospitalization stay, admission mode, and disease-related complications, were calculated based on tumor location. Alternation trends for some factors within the study period were calculated. According to worldwide guidelines that recommend endoscopy screening for gastric cancer from the age of 50 years, patients were categorized into age groups of ≤ 49 years, 50-74 years, and ≥ 75 years, and the age group of 50-74

years was further analyzed by dividing into four groups with 5-year increments. Patients with records of surgery (including laparoscopic or open tumor resection and excluding endoscopy and endoscopic resection) were selected, and the short-term postoperative complications, including anastomotic leakage, anastomotic hemorrhage, abdominal hemorrhage, abdominal infection, gastroparesis, incision infection, incision hemorrhage, incision dehiscence, and pancreatic fistula, were indexed.

Continuous variables are expressed as means ± SD, and categorical variables are expressed as frequencies and proportions. Student's t-test was used to compare continuous variables, and the chi-squared test was used to compare categorical variables. SPSS (SPSS Inc., Armonk, Chicago, IL, United States, version 26.0) was used for all statistical analyses, and a two-sided test was considered statistically significant at P value of < 0.05.

The association between gastric cancer and risk of in-hospital death or short-term postoperative complications was examined in the involved gastric cancer patients (postoperative complications were examined in patients who had undergone surgery) by performing a multivariate analysis adjusted for sex, age, anatomical subsite, complications (including hypertension, diabetes, cerebrovascular disease, coronary disease, reflux syndrome, anemia, and hypoproteinemia), and operation (for analysis of in-hospital mortality). Logistic regression was used in indicators with occurrence higher than 5%, and Poisson regression was used in indicators with occurrence lower than 5%. Knots were used according to the principle of minimized Akaike information criterion. Adjusted odds and transformed odds ratios (aORs) were used to estimate the absolute risks (probabilities) with 95% confidence intervals (CIs).

RESULTS

Basic information

Patients selected from the database originated from 10 affiliated hospitals of Peking University across nearly all provinces of China, while most came from northern China. In the aggregate, 2097347 hospitalizations between January 1, 2014, and December 31, 2018, were eligible (including 289561, 309776, 462175, 490020, and 545815 annual hospitalizations, respectively). After further selection, 10709 incident gastric cancer cases were chosen, including 2608, 2429, 2614, 2744, and 2811 cases from 2014 to 2018, respectively. A total of 72.71% of the patients were men. Patients originated nationwide but were mainly from northern China and Beijing, Inner Mongolia, and Hebei (Supplementary Figure 1). The average age of the patients with incident gastric cancer was 61.18 years ± 11.91 years (95%CI: 60.96-61.41). The mean hospitalization cost was 55.70 (95%CI: 54.79-56.60) thousand RMB (approximately 8.77 thousand USD).

Anatomical distribution of gastric cancer

A total of 4602 (42.97%), 3673 (34.30%), 1972 (18.41%), 386 (3.61%), and 76 (0.71%) cases were antrum, cardia, gastric body, multiple site, and unclear site gastric cancer, respectively (Figure 1A). Among 10,247 cases extracted for proportion calculation, the ratios of the gastric antrum, cardia, and body cancers were 44.91%, 35.85%, and 19.24%, respectively (Figure 1B). Data from cases from different regions worldwide were collected from previous studies, and the proportions of cardia and non-cardia (including body and antrum) cases were recalculated (Table 1).

Clinical features of gastric cancer based on anatomical sites

Gastric cardia, body, and antrum cancer cases were extracted for clinical feature analysis, and the body and antrum cases were further classified as "non-cardia cancer" for additional analyses. Both cardia and non-cardia cancers showed a higher proportion of male patients, while the male:female ratio in cardia cancer cases was approximately 5:1; it was approximately 2:1 in non-cardia cancer cases (Table 1, Figure 2A and B, P < 0.001 both in the comparison of the three subsites and of cardia and non-cardia cancer cases). The average age of patients with gastric cardia, body, and antrum cancers were 63.98, 57.57, and 60.32 years, respectively (Table 2, P < 0.001). After dividing the cases into three age subgroups (≤ 49 years, 50-74 years, and ≥ 75 years), both cardia and non-cardia cancers at the three anatomical subsites showed most patients in the age group of 50-74 years. However, non-cardia cancer was more prevalent among patients younger than 50 years, and cardia cancer was more prevalent among patients older than 75 years (Figure 2C and D, P < 0.001 both in three subsites and in cardia and non-cardia cancer cases). Due to the location of the involved hospitals, most patients came from urban areas, while gastric antrum cancer accounted for the lowest proportion of patients from the rural area compared to those from the upper subsites. This finding was further verified through insurance information: patients with cardia cancer had a higher proportion of rural medical insurance settlement (Table 2, P < 0.001, respectively). In addition, gastric cardia cancer had the largest proportion, and gastric body cancer had the lowest proportion of patients with hypertension, diabetes, cerebrovascular disease, and coronary disease (Table 2, P < 0.001, P = 0.03, P = 0.01, and P < 0.001 for hypertension and diabetes, respectively). Moreover, 11.46% of gastric cardia cancer patients had a combined diagnosis of GERD, which was higher than the proportion of non-cardia cancer patients, which included gastric body and antrum cancers (Table 2, P < 0.001). Non-cardia cancer cases accounted for a greater

Table 1 Summary of reported proportion of cardia and non-cardia (including body and antrum) cancer worldwide

Region	Ref.	Period		Anatomical site ratio (%)[1]		
				Cardia	Non-Cardia	
					Body	Antrum
East Asia	Northern China	This article	2014-2018	35.85%	19.24%	44.91%
	Southwest China	Liu *et al*[19], 2016	2008-2012	37.15%	10.30%	52.55%
	Northwest China	Zhou *et al*[18], 2008	1993-2004	35.78%	28.00%	36.22%
	Japan	Koizumi *et al*[11], 2018	2013-2015	9.82%	53.58%	36.60%
West Asia	Northwest Iran	Derakhshan *et al*[29], 2004	2000-2003	44.78%	26.19%	29.03%
North America	The USA	Camargo *et al*[7], 2011	1999-2007	41.41%	11.13%	47.46%
Europe	Central Switzerland	Schmassmann *et al*[26], 2009	1982-2007	26.02%	73.98%	
	Spain	Aragonés *et al*[27], 2010	1980-2004	26.67%	73.33%	
	Netherland	Holster *et al*[28], 2014	1973-2011	31.82%	30.30%	37.88%

[1]Proportions of cardia and non-cardia (including body and antrum) were recalculated.
USA: United States.

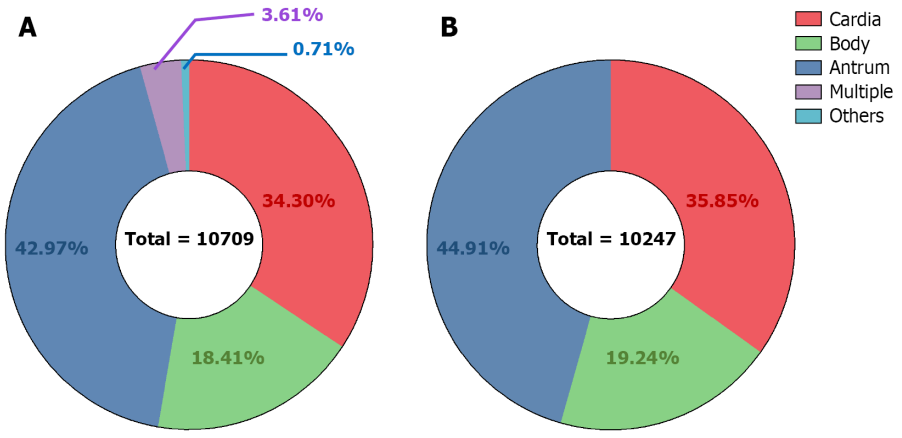

DOI: 10.4251/wjgo.v14.i11.2238 **Copyright** ©The Author(s) 2022.

Figure 1 Anatomical distribution of gastric cancer among the study population. A: All involved patients; B: Gastric cardia, body, and antrum.

proportion of anemia and hypoproteinemia than cardia cancer cases (for anemia: 8.16% for gastric body cancer patients and 7.13% for antrum cancer patients; for hypoproteinemia: 4.56% for gastric body cancer patients and 3.78% for antrum cancer patients) (Table 2, P = 0.009 and 0.005, respectively). A higher proportion of obstruction syndrome was found in antrum cancer patients than in the other groups (Table 2, P < 0.001). Detailed P values of the pairwise comparisons among the three subsites are shown in Supplementary Table 1.

Hospitalization features of gastric cancer based on anatomical sites

Gastric body cancer cases had the lowest emergency admission rate. No significant difference was found between the emergency proportion of the cardia and antrum cancers (Table 2, P = 0.007 in total, and P = 0.121 between the antrum and cardia cancers). Gastric antrum cancer led to the longest hospitalization duration among the three anatomical subsites; in contrast, gastric cardia cancer had the shortest hospitalization (Table 2, P < 0.001). Gastric antrum cancer had the highest total hospitalization (78.41 ± 54.69 thousand CNY, 95%CI: 76.83-79.98) and surgery costs [30.84 ± 20.43 thousand CNY, (95%CI: 30.24-31.43)], and cardia cancer had the lowest [total hospitalization: 50.33 ± 50.68 thousand CNY, (95%CI: 48.69-51.97); surgery: 17.86 ± 22.69 thousand CNY, (95%CI: 17.12-18.62)] (Supplementary Table 2, P < 0.001 for both total hospitalization and surgery costs). The detailed P values among the three subsites are shown in Supplementary Table 3.

Table 2 Clinical and hospitalizing features on gastric cancer patients based on anatomic site subgroups

Variables			Cardia (*n* = 3673)	Body (*n* = 1972)	Antrum (*n* = 4602)	*P* value
Clinical features	Basic information	Gender				< 0.001
		Male	3046 (82.93%)	1264 (64.10%)	3140 (68.23%)	
		Female	627 (17.07%)	708 (35.90%)	1462 (31.77%)	
		Age (yr)				< 0.001
		≤ 49	266 (7.24%)	479 (24.29%)	809 (17.58%)	
		50-74	536 (78.16%)	158 (67.70%)	585 (69.71%)	
		≥ 75	2871 (14.60%)	1335 (8.01%)	3208 (12.71%)	
		Mean (mean ± SD)	63.98 ± 10.21 (63.65, 64.31)	57.57 ± 12.68 (57.04, 58.10)	60.32 ± 12.06 (59.97, 60.67)	< 0.001
		Patient source				< 0.001
		Urban	3000 (81.68%)	1633 (82.81%)	3969 (86.25%)	
		Rural	673 (18.32%)	339 (17.19%)	633 (13.75%)	
		Insurance Source				< 0.001
		MIUE	1499 (40.81%)	906 (45.94%)	2004 (43.55%)	
		MIUR	179 (4.88%)	98 (4.97%)	205 (4.45%)	
		NRCMI	673 (18.32%)	302 (15.31%)	627 (13.62%)	
		Own expense	885 (24.09%)	476 (24.14%)	1121 (24.36%)	
		Others	437 (11.90%)	190 (9.64%)	645 (14.02%)	
	Complications	Hypertension				< 0.001
		No	2630 (71.60%)	1550 (78.60%)	3470 (75.40%)	
		Yes	1043 (28.40%)	422 (21.40%)	1132 (24.60%)	
		Diabetes				0.03
		No	3213 (87.48%)	1767 (89.60%)	4093 (88.94%)	
		Yes	460 (12.52%)	205 (10.40%)	509 (11.06%)	
		GERD				< 0.001
		No	3252 (88.54%)	1886 (95.64%)	4387 (95.33%)	
		Yes	421 (11.46%)	86 (4.36%)	215 (4.67%)	
		Cerebrovascular disease				0.01
		No	3488 (94.96%)	1895 (96.10%)	4430 (96.26%)	
		Yes	185 (5.04%)	77 (3.90%)	172 (3.74%)	
		Coronary disease				< 0.001
		No	3353 (91.29%)	1843 (93.46%)	4309 (93.63%)	
		Yes	320 (8.71%)	129 (6.54%)	293 (6.37%)	
		Obstruction				< 0.001
		No	3616 (98.45%)	1952 (98.99%)	4136 (89.87%)	
		Yes	57 (1.55%)	20 (1.01%)	466 (10.13%)	
		Anemia				0.009
		No	3451 (93.96%)	1811 (91.84%)	4274 (92.87%)	
		Yes	222 (6.04%)	161 (8.16%)	328 (7.13%)	
		Hypoproteinemia				0.005
		No	3566 (97.09%)	1882 (95.44%)	4428 (96.22%)	

	Yes	107 (2.91%)	90 (4.56%)	174 (3.78%)	
Hospitalization features	Admission route				0.007
	Emergency	100 (2.72%)	28 (1.42%)	101 (2.20%)	
	Non-emergency	3573 (97.28%)	1944 (98.58%)	4501 (97.80%)	
	Stay (d) (mean ± SD)	13.41 ± 12.17 (13.02, 13.80)	14.08 ± 12.24 (13.57, 14.59)	16.89 ± 12.24 (16.53, 17.24)	< 0.001

MIUE: Medical insurance for urban employees; MIUR: Medical insurance for urban residents; NRCMI: New rural cooperative medical insurance; GERD: Gastroesophageal reflux disease.

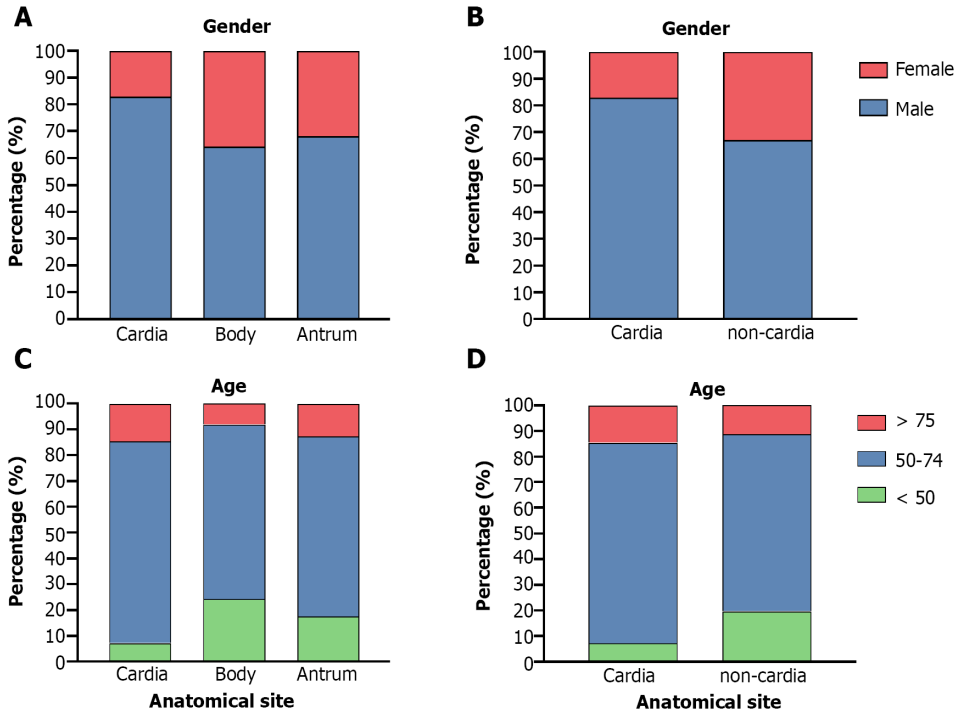

DOI: 10.4251/wjgo.v14.i11.2238 **Copyright** ©The Author(s) 2022.

Figure 2 Sex and age distribution among the different anatomical subsites of gastric cancer. A: Sex distribution for the three anatomical subsites; B: Sex distribution for the cardia and non-cardia cases; C: Age distribution for the three anatomical subsites; D: Age distribution for the cardia and non-cardia cancer cases.

Clinical features of gastric cancer during 2014-2018 based on anatomical sites

Gastric cardia and antrum cancers were chosen to examine the annual alternation in proportion between 2014 and 2018, combined with the proportion trend analysis of related complications, GERD, and *H. pylori* infection-related diseases (HIRD). A general trend of the increasing proportion of gastric cardia cancer was observed (ranging from 26.77% to 28.59%), along with an increase in the combined diagnosis of GERD (Figure 3A, $P < 0.001$). The complication ratio of GERD ranged from 6.99% to 15.11%, which is slightly higher than that in a previous report on Chinese patients[19]. A general decrease in trend was found for gastric cancers in the 5-year period, accompanied by an increase in the combined diagnostic proportion of HIRD (Figure 3B, $P = 0.014$), and the ratio of HIRD was lower than that in previous reports[22,23].

According to the World Health Organization, the age boundary between middle and old age is 60 years, and the cutoff between old and advanced age is 75 years in the Asia-Pacific region. Therefore, a detailed study based on anatomical subsites was conducted for the 50-74 years age group at increments of every 5 years to observe age-related trends. A significant decrease was found in the proportion of patients with gastric cardia cancer in the 55-59 years age group, with increasing trends between the 60-64 and 65-69 years age groups (Figure 3C, $P = 0.02$). For non-cardia cancer, although a slight increase was found in the 70-74 years age group, no significant difference was found in the five age groups (Figure 3D, $P = 0.086$).

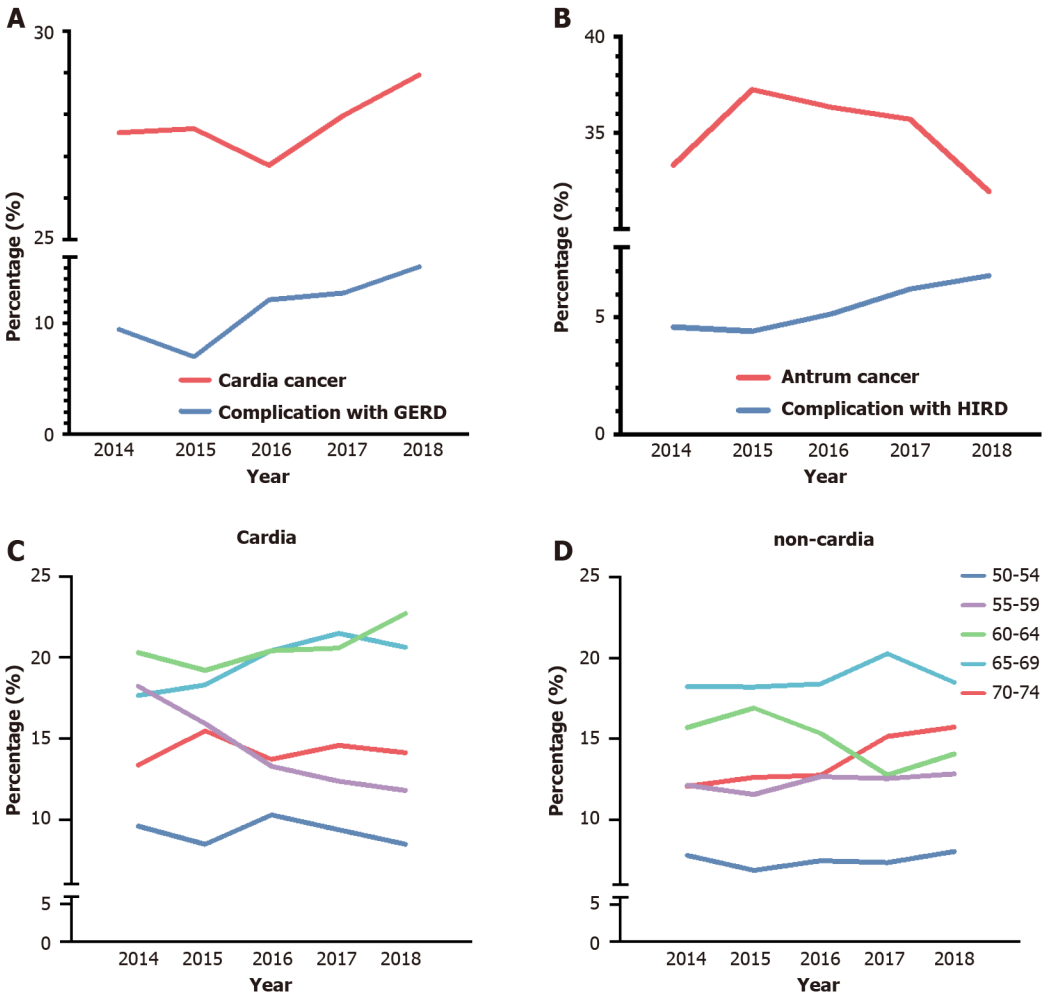

DOI: 10.4251/wjgo.v14.i11.2238

Figure 3 Alternation trends in combined diagnosis, age, and constituent ratio according to the anatomical subsite of gastric cancer during the study period. A: Percentage change in cardia cancer along with the complication of gastroesophageal reflux disease; B: Percentage change in gastric antrum cancer along with the complication of *Helicoibacter pylori* (*H. pylori*) infection-related diseases; C: Age changes among patients with cardia cancer aged 50-74 years, after stratification of patients into five age subgroups; D: Age changes among patients with non-cardia cancer aged 50-74 years, after stratification into five age subgroups. GERD: Gastroesophageal reflux disease; HIRD: *H. pylori* infection-related diseases.

Hospitalization clinical outcomes of gastric cancer based on anatomical sites

In-hospital mortality and short-term postoperative complication rates reflect the prognosis of patients and the quality and safety of medical treatment. In this study, a total of 92 (0.86%) gastric cancer-related deaths were detected, including 37 (1.01%) patients with gastric cardia cancer, 13 (0.66%) with gastric body cancer, and 33 (0.72%) with antrum cancer (P = 0.243 among the three subsites, Supplementary Table 4).

A total of 6,956 patients (6749 cancers at the three anatomical subsites) had a history of surgery during hospitalization. Among them, 605 (8.70%) had short-term postoperative complications, including 158 (8.55%) cardia cancer cases, 109 (9.08%) body cancer cases, and 324 (accounted for 8.76%) antrum cancer cases (P = 0.876 among the three subsites, Supplementary Table 3).

Validation of risk factors on hospitalization clinical outcomes

Multivariable regression analysis was performed to further explore the association between anatomical subsite and patient in-hospital clinical outcomes, including in-hospital mortality in all patients and postoperative complications in patients who had undergone surgery. Other vital factors, such as sex, age, operation (in the analysis of in-hospital mortality), and complications, were also included in the analysis. In-hospital mortality was associated with the anatomical sites, among which cardia cancer had a higher risk (aOR 1.75, 95%CI: 1.01-3.04, P = 0.046). It was also associated with age increase (aOR 1.03, 95%CI: 1.01-1.06, P = 0.001) and increased risks of complications, including anemia (aOR 2.37, 95%CI: 1.39-4.06, P = 0.002), hypoproteinemia (aOR 5.44, 95%CI: 3.09-9.59, P < 0.001), obstruction syndrome (aOR 5.59, 95%CI: 3.26-9.59, P < 0.001), and reflux syndrome (aOR 1.92, 95%CI: 1.13-3.28, P = 0.017) (Figure 4A). The higher risk of postoperative complications was not associated with anatomical sites

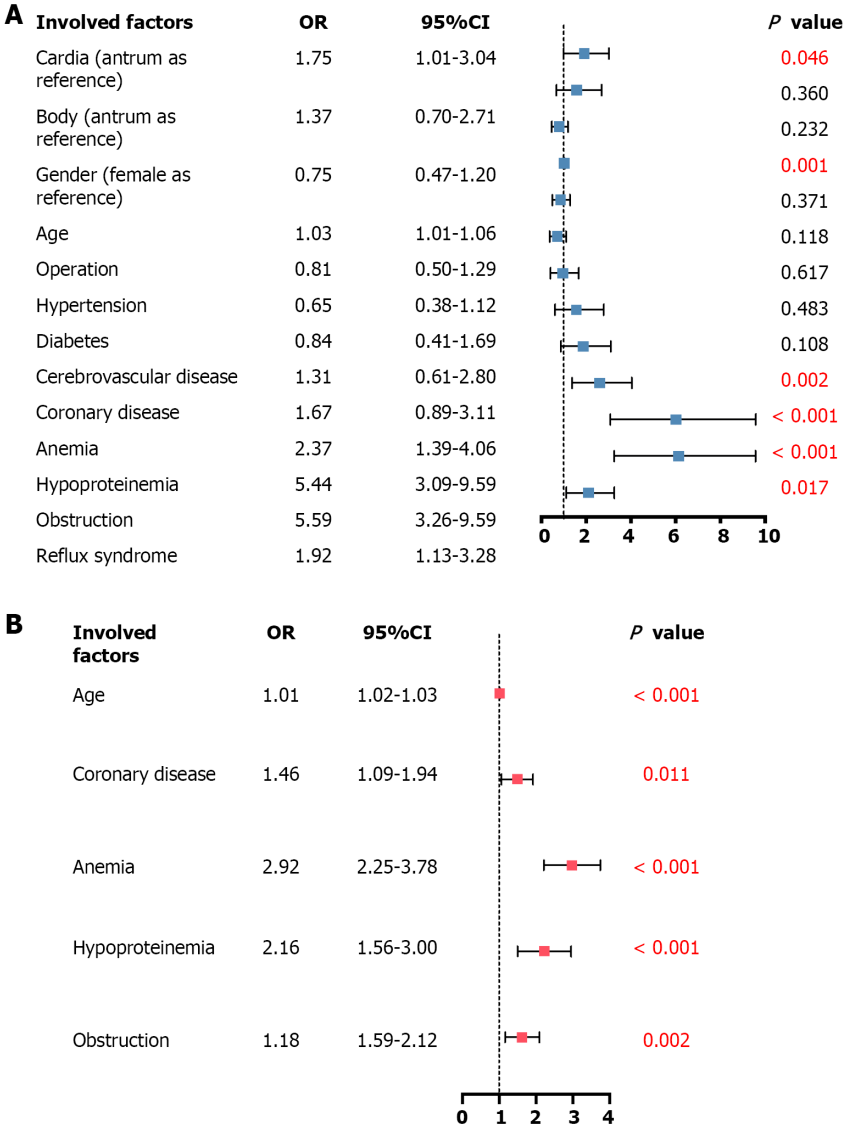

DOI: 10.4251/wjgo.v14.i11.2238 **Copyright** ©The Author(s) 2022.

Figure 4 Multivariable regression analysis on the relationship between hospitalization clinical outcomes and risk factors, including anatomical subsite. A: Validation of risk factors on in-hospital death through Poisson regression; B: Validation of risk factors on short-term postoperative complications through logistic regression.

(aOR 0.979, 95%CI: 0.79-1.21, $P = 0.846$); however, it was associated with age increase (aOR 1.01, 95%CI: 1.02-1.03, $P < 0.001$) and increased risks of complications, including coronary disease (aOR 1.46, 95%CI: 1.09-1.94, $P = 0.011$), anemia (aOR 2.92, 95%CI: 2.25-3.78, $P < 0.001$), hypoproteinemia (aOR 2.16, 95%CI: 1.56-3.00, $P < 0.001$), and obstruction syndrome (aOR 1.18, 95%CI: 1.59-2.12, $P = 0.002$) (Figure 4B).

DISCUSSION

In this study, we first examined the epidemiologic features of gastric cancer in northern China based on anatomical subsites, showing a higher male ratio, older age distribution, older age-related trend, increasing proportion, close relationship with GERD, and increased risk of in-hospital mortality in gastric cardia cancer than in other types. This cancer site was also associated with younger age distribution, increased likelihood of residence in the city, and decreasing trends in the proportion of antral cancer. Overall, the constituent ratio of gastric cardia cancer in northern China was higher than the average level in China (18-27%)[24,25] and Europe (26-31%)[26-28] and lower than that in North America and West Asia (both > 40%)[7,29]. Compared to previous reports in China, the constituent ratio of gastric cardia cancer in this study was slightly higher than that in the Gansu Province (northwest China)[18] and lower than that in southwest China[19] but showed high inner similarity compared with other global regions (Supplementary Table 5). Similarly, the proportion of antral gastric cancer is in the mid-level worldwide[24]. Regionality is a typical phenomenon in both cardia and non-cardia (including

gastric body and antrum) cancers and is generally considered to be linked to race, unique eating habits, and the environment[17,30].

Gastric cardia cancer may account for a large proportion of all gastric cancers in countries/regions with a low incidence of gastric cancer[31,32], contributing to better control of some risk factors of non-cardia cancer, including *H. pylori* infection. However, with a higher incidence of gastric cancer in China, the proportion of cardia cancer in this study was also higher, compared with that in European countries [26-28]. One major reason might be the high prevalence of smoking in China, which is considered a major risk factor for cardia cancer-related risk factors, including GERD and cardia cancer[33,34]. In this study, five times more men than women had gastric cardia cancer; this ratio was higher than the global (by approximately 3:1)[25] and China-based (by approximately 4:1) values[24], further suggesting the effect of smoking, showing sex-based differences. Furthermore, a higher proportion of upper gastric cancer, including cardia cancer, has been found in rural residents (including those with rural medical insurance) that are usually considered to have a higher smoking prevalence[35]. Therefore, more attention should be paid to the implementation of smoking cessation policies, especially those targeting men and rural areas, to help prevent cardia cancer. The sex-based difference between cardia and non-cardia cancers could also be traced to the epidemiology of Epstein-Barr virus-associated gastric cancer (EBVaGC)[36]. The relationships among EBVaGC, cardia cancer, and male sex were tested in a meta-analysis, with a male to female ratio of approximately 2-3:1[37].

In this study, cardia cancer cases increased annually and proportionally to the cases at other subsites and concurrent GERD ratio, which was also found in southwest China[19]. Smoking, which is a risk factor for GERD and subsequent gastric cardia cancer, may contribute to this trend. The implementation of tobacco-controlling policies in China, specifically in northern and southwestern regions, remains insufficient, with a reported ratio of 60.2%-61.8% of adults in northern China who are passive smokers [34]. Moreover, the lifestyle among Chinese people, including youth, has been westernized[38]. Increased ingestion of animal-source foods has made obesity one of the main public health issues in China, especially in developed cities, and was shown to be a risk factor for both GERD and cardia cancer by increasing abdominal pressure and prolonging nocturnal acid exposure[39-41]. Reducing smoking and obesity may help prevent further increases in gastric cardia cancer rates as the Chinese population ages.

Association between higher in-hospitalization mortality and cardia anatomical subsite was found in this study, rather than non-cardia sites, in multivariable regression analysis after adjusting for age, sex, and basic complications. The rates of postoperative complications were comparable among the anatomical sites. The older age distribution and more severe previous complication status among cardia cancer patients in this study may account for the correlation with the increased risk of in-hospital mortality, as they affect surgical safety[42]. Moreover, the non-significant short-term postoperative complication risk difference among the anatomical sites might reflect the establishing of techniques in gastric cancer surgery, ensuring the safety of cardia cancer surgeries by helping achieve adequate anastomotic tension and blood supply[43]. The preoperative management of basic diseases may help improve recovery rates and safety profile.

H. pylori is a major risk factor for non-cardia cancer[22], especially for that located in the antrum[25]. The incidence of *H. pylori* infection is relatively low in northern China, which may account for the reported proportions of non-cardia cancers[44]. Eating habits are key factors in *H. pylori* infection. The constituent ratio of antrum cancer was higher in southwest China compared to our results[19], which could be correlated with the habit of spicy food consumption in this region, which might increase the incidence of *H. pylori* infection[45,46]. A generally decreasing trend of antral cancer proportion in the present study might be attributed to the popularization of screening, including that for gastric cancer and HIRD[47]. However, the proportion of malignancies located in the antrum was higher than that in some Western countries, including northern America, which could be attributed to the high virulence of *H. pylori* bacterial strains in East Asian populations[48]. Moreover, the hospitalization duration and financial burden remain significant in gastric antrum cancer, as observed in the present study; this finding may be related to the complex surgical methods involved and high complication rates[49]. The approximately 10-times higher incidence of obstruction in antrum cancer than in other cancer sites may affect treatment efficiency[50]. This finding suggests that further screening and radical cure of both *H. pylori* and antrum cancer are required in the future[51].

This study had several limitations. First, due to the data source used, which covers medical centers but not an entire region or province, this study involved patients from northern China. Second, detailed anatomic data were not available in some cases in the HSRs, resulting in the creation of the category named "other types", and the anatomical information based on the "upper, middle, and lower" classification could not be re-traced. Third, due to the absence of some information in HSRs, including laboratory test results, imaging findings, or long-term prognostic information, the detailed figures, including tumor stage and patient prognosis, could not be extracted; the detailed operative procedures, details on the economic status of the patients (*e.g.*, salary), and lifestyles were also not available, making it difficult to construct specific characteristics and risk factor features of gastric cancer patients in northern China, and should be further testified in the future. Fourth, the combined diagnosis proportion of HSRs was much lower than that in previous studies[22,23]. This reflects the defects of some HSRs that missed such diagnoses and the diagnostic failure of some clinicians that missed *H. pylori* infections,

resulting in omissions. Finally, the results of the multivariate analysis should be further validated in more cohorts to increase their credibility.

CONCLUSION

In summary, this is the first study to report the composition ratio characteristics and changes in gastric cancer trends based on anatomical sites in patients in northern China. This study examined plausible explanations for these findings. Large-scale screening programs for gastric cancer and infection, increasing awareness and prevention of risk factors, reducing smoking and obesity, as well as patient stratification for treatment based on anatomical sites are required to reduce the burden of gastric cancer.

ARTICLE HIGHLIGHTS

Research background

Gastric cancer is among the most common digestive malignant tumors worldwide. China is among the regions with the highest gastric cancer incidence. Differences in clinical and epidemiological features of this tumor type based on its presence in the anatomical subsites of the stomach have been reported.

Research motivation

Few population-based studies have been conducted in China to determine differences among tumors at different locations, and analyses of data from northern China are lacking.

Research objectives

To examine the clinical features of gastric cancer at different anatomical sites in patients from northern China. We also aimed to examine the associated variability and trends.

Research methods

We conducted a cross-sectional study used incident gastric cancer case data from 10 Peking University-affiliated hospitals, and the clinical and prevailing local features were analyzed.

Research results

Ten thousand seven hundred and nine patients were enrolled, including antral, cardia, and stomach body gastric cancer cases. Cancer in the cardia had the highest male:female ratio, proportion of elderly patients, and patients with complications, including hypertension, diabetes, cerebrovascular, and coronary diseases ($P < 0.001$). gastric cancer involving the antrum showed the lowest proportion of patients from rural areas and accounted for the highest hospitalization rate and cost (each $P < 0.001$). The proportion of patients with cancer involving the cardia increased with an increase in the number of gastroesophageal reflux disease (GERD) cases during the same period ($P < 0.001$). Multivariate analysis revealed that tumor location in the cardia increased the risk of in-hospital mortality ($P = 0.046$). Anatomical subsite was not linked to postoperative complications.

Research conclusions

In this study, we first examined the epidemiologic features of gastric cancer in northern China based on anatomical subsites, showing a higher male ratio, older age distribution, older age-related trend, increasing proportion, close relationship with GERD, and increased risk of in-hospital mortality in gastric cardia cancer than in other types. This cancer site was also associated with younger age distribution, increased likelihood of residence in the city, and decreasing trends in the proportion of antral cancer. Overall, the constituent ratio of gastric cardia cancer in northern China was higher than the average level in China and Europe, and lower than that in North America and West Asia. Compared to previous reports in China, the constituent ratio of gastric cardia cancer in this study was slightly higher than that in the northwest China and lower than that in southwest China but showed high inner similarity compared with other global regions. Similarly, the proportion of antral gastric cancer is in the mid-level worldwide. Regionality is a typical phenomenon in both cardia and non-cardia (including gastric body and antrum) cancers and is generally considered to be linked to race, unique eating habits, and the environment.

Research perspectives

This is the first study to report the composition ratio characteristics and changes in gastric cancer trends based on anatomical sites in patients in northern China. This study examined plausible explanations for these findings. Large-scale screening programs for gastric cancer and infection, increasing awareness and prevention of risk factors, reducing smoking and obesity, as well as patient stratification for

treatment based on anatomical sites are required to reduce the burden of gastric cancer.

ACKNOWLEDGEMENTS

We acknowledge the Department of Hospital Management from Peking University Health Science Center for the usage permission of database, and the Medical Information Center from Peking University Health Science Center for assistance with data analysis.

FOOTNOTES

Author contributions: Qu RZ, Ma YP and Bao XY contributed equally; Fu W, Zhang ZP, and Tuo L contributed equally to this article; Fu W and Zhang ZP contributed to conceptualization; Qu RZ, Ma YP, Tao LY, and Bao XY contributed to data curation; Qu RZ, Ma YP, and Tao LY contributed to formal analysis; Fu W and Zhang ZP contributed to funding acquisition and supervision; Qu RZ and Ma YP contributed to investigation; Bao XY and Tuo L contributed to methodology; Fu W, Zhang ZP, and Tuo L contributed to project administration and resources; Bao XY and Tuo contributed to software; Ma YP, Zhou X, Wang BY, Li F, Lu SY, and Zhang Y contributed to validation; Qu RZ, Ma YP, and Bao XY contributed to visualization; Qu RZ and Ma YP contributed to writing-original draft; Fu W, Zhang ZP, Tuo L, Qu RZ, Ma YP, and Zhou X contributed to writing-review & editing.

Supported by the National Natural Science Foundation of China, No. 81972702, No. 91959110, and No. 62173005.

Institutional review board statement: The study was reviewed and approved by the Ethics Committee of Peking University Third Hospital (Approval No. IRB00006761-M2019387).

Informed consent statement: Written informed consent was waived because of the retrospective nature of the study.

Conflict-of-interest statement: The authors declare that they have no conflicts of interest.

Data sharing statement: The datasets analyzed during the current study are stored in the Medical Information Center, Peking University Health Science Center, and are not available for the public owing to privacy protection, but could be accessed on reasonable request.

STROBE statement: The authors have read the STROBE Statement—checklist of items, and the manuscript was prepared and revised according to the STROBE Statement—checklist of items.

Country/Territory of origin: China

ORCID number: Wei Fu 0000-0001-5248-7891.

S-Editor: Chen YL
L-Editor: A
P-Editor: Chen YL

REFERENCES

1 **Siegel RL**, Miller KD, Jemal A. Cancer statistics, 2020. *CA Cancer J Clin* 2020; **70**: 7-30 [PMID: 31912902 DOI: 10.3322/caac.21590]
2 **Sung H**, Ferlay J, Siegel RL, Laversanne M, Soerjomataram I, Jemal A, Bray F. Global Cancer Statistics 2020: GLOBOCAN Estimates of Incidence and Mortality Worldwide for 36 Cancers in 185 Countries. *CA Cancer J Clin* 2021; **71**: 209-249 [PMID: 33538338 DOI: 10.3322/caac.21660]
3 **Chen W**, Zheng R, Baade PD, Zhang S, Zeng H, Bray F, Jemal A, Yu XQ, He J. Cancer statistics in China, 2015. *CA Cancer J Clin* 2016; **66**: 115-132 [PMID: 26808342 DOI: 10.3322/caac.21338]
4 **Ocvirk S**, O'Keefe SJD. Dietary fat, bile acid metabolism and colorectal cancer. *Semin Cancer Biol* 2021; **73**: 347-355 [PMID: 33069873 DOI: 10.1016/j.semcancer.2020.10.003]
5 **Berrino F**, De Angelis R, Sant M, Rosso S, Bielska-Lasota M, Coebergh JW, Santaquilani M; EUROCARE Working group. Survival for eight major cancers and all cancers combined for European adults diagnosed in 1995-99: results of the EUROCARE-4 study. *Lancet Oncol* 2007; **8**: 773-783 [PMID: 17714991 DOI: 10.1016/s1470-2045(07)70245-0]

6 **Thrumurthy SG**, Chaudry MA, Chau I, Allum W. Does surgery have a role in managing incurable gastric cancer? *Nat Rev Clin Oncol* 2015; **12**: 676-682 [PMID: 26260039 DOI: 10.1038/nrclinonc.2015.132]

7 **Camargo MC**, Anderson WF, King JB, Correa P, Thomas CC, Rosenberg PS, Eheman CR, Rabkin CS. Divergent trends for gastric cancer incidence by anatomical subsite in US adults. *Gut* 2011; **60**: 1644-1649 [PMID: 21613644 DOI: 10.1136/gut.2010.236737]

8 **Crane SJ**, Locke GR 3rd, Harmsen WS, Diehl NN, Zinsmeister AR, Melton LJ 3rd, Romero Y, Talley NJ. Subsite-specific risk factors for esophageal and gastric adenocarcinoma. *Am J Gastroenterol* 2007; **102**: 1596-1602 [PMID: 17459024 DOI: 10.1111/j.1572-0241.2007.01234.x]

9 **Dolan K**, Sutton R, Walker SJ, Morris AI, Campbell F, Williams EM. New classification of oesophageal and gastric carcinomas derived from changing patterns in epidemiology. *Br J Cancer* 1999; **80**: 834-842 [PMID: 10360663 DOI: 10.1038/sj.bjc.6690429]

10 **Kocher HM**, Linklater K, Patel S, Ellul JP. Epidemiological study of oesophageal and gastric cancer in south-east England. *Br J Surg* 2001; **88**: 1249-1257 [PMID: 11531876 DOI: 10.1046/j.0007-1323.2001.01847.x]

11 **Koizumi S**, Motoyama S, Watanabe N, Matsuhashi T, Iijima K. Chronological Changes in the Gastric Cancer Subsite in Akita, Japan: The Trends from the Data of a Hospital-Based Registration System. *Tohoku J Exp Med* 2018; **246**: 131-140 [PMID: 30369514 DOI: 10.1620/tjem.246.131]

12 **Uemura N**, Okamoto S, Yamamoto S, Matsumura N, Yamaguchi S, Yamakido M, Taniyama K, Sasaki N, Schlemper RJ. Helicobacter pylori infection and the development of gastric cancer. *N Engl J Med* 2001; **345**: 784-789 [PMID: 11556297 DOI: 10.1056/NEJMoa001999]

13 **Hansen S**, Vollset SE, Derakhshan MH, Fyfe V, Melby KK, Aase S, Jellum E, McColl KE. Two distinct aetiologies of cardia cancer; evidence from premorbid serological markers of gastric atrophy and Helicobacter pylori status. *Gut* 2007; **56**: 918-925 [PMID: 17317788 DOI: 10.1136/gut.2006.114504]

14 **Derakhshan MH**, Malekzadeh R, Watabe H, Yazdanbod A, Fyfe V, Kazemi A, Rakhshani N, Didevar R, Sotoudeh M, Zolfeghari AA, McColl KE. Combination of gastric atrophy, reflux symptoms and histological subtype indicates two distinct aetiologies of gastric cardia cancer. *Gut* 2008; **57**: 298-305 [PMID: 17965056 DOI: 10.1136/gut.2007.137364]

15 **Brown LM**, Devesa SS. Epidemiologic trends in esophageal and gastric cancer in the United States. *Surg Oncol Clin N Am* 2002; **11**: 235-256 [PMID: 12424848 DOI: 10.1016/s1055-3207(02)00002-9]

16 **Kumar S**, Metz DC, Ellenberg S, Kaplan DE, Goldberg DS. Risk Factors and Incidence of Gastric Cancer After Detection of Helicobacter pylori Infection: A Large Cohort Study. *Gastroenterology* 2020; **158**: 527-536.e7 [PMID: 31654635 DOI: 10.1053/j.gastro.2019.10.019]

17 **Russo AE**, Strong VE. Gastric Cancer Etiology and Management in Asia and the West. *Annu Rev Med* 2019; **70**: 353-367 [PMID: 30355265 DOI: 10.1146/annurev-med-081117-043436]

18 **Zhou Y**, Zhang Z, Wu J, Ren D, Yan X, Wang Q, Wang Y, Wang H, Zhang J, Zhu X, Yang Y, Luo C, Guo X, Tang C, Qiao L. A rising trend of gastric cardia cancer in Gansu Province of China. *Cancer Lett* 2008; **269**: 18-25 [PMID: 18501504 DOI: 10.1016/j.canlet.2008.04.013]

19 **Liu K**, Yang K, Zhang W, Chen X, Zhang B, Chen Z, Chen J, Zhao Y, Zhou Z, Chen L, Hu J. Changes of Esophagogastric Junctional Adenocarcinoma and Gastroesophageal Reflux Disease Among Surgical Patients During 1988-2012: A Single-institution, High-volume Experience in China. *Ann Surg* 2016; **263**: 88-95 [PMID: 25647058 DOI: 10.1097/SLA.0000000000001148]

20 **Qu R**, Ma Y, Tao L, Bao X, Zhou X, Wang B, Li F, Lu S, Tuo L, Zhan S, Zhang Z, Fu W. Features of colorectal cancer in China stratified by anatomic sites: A hospital-based study conducted in university-affiliated hospitals from 2014 to 2018. *Chin J Cancer Res* 2021; **33**: 500-511 [PMID: 34584375 DOI: 10.21147/j.issn.1000-9604.2021.04.07]

21 **Qu R**, Ma Y, Zhang Z, Fu W. Increasing burden of colorectal cancer in China. *Lancet Gastroenterol Hepatol* 2022; **7**: 700 [PMID: 35809603 DOI: 10.1016/S2468-1253(22)00156-X]

22 **Yang L**, Kartsonaki C, Yao P, de Martel C, Plummer M, Chapman D, Guo Y, Clark S, Walters RG, Chen Y, Pei P, Lv J, Yu C, Jeske R, Waterboer T, Clifford GM, Franceschi S, Peto R, Hill M, Li L, Millwood IY, Chen Z; China Kadoorie Biobank Collaborative Group. The relative and attributable risks of cardia and non-cardia gastric cancer associated with Helicobacter pylori infection in China: a case-cohort study. *Lancet Public Health* 2021; **6**: e888-e896 [PMID: 34838195 DOI: 10.1016/S2468-2667(21)00164-X]

23 **Wang RT**, Wang T, Chen K, Wang JY, Zhang JP, Lin SR, Zhu YM, Zhang WM, Cao YX, Zhu CW, Yu H, Cong YJ, Zheng S, Wu BQ. Helicobacter pylori infection and gastric cancer: evidence from a retrospective cohort study and nested case-control study in China. *World J Gastroenterol* 2002; **8**: 1103-1107 [PMID: 12439934 DOI: 10.3748/wjg.v8.i6.1103]

24 **Colquhoun A**, Arnold M, Ferlay J, Goodman KJ, Forman D, Soerjomataram I. Global patterns of cardia and non-cardia gastric cancer incidence in 2012. *Gut* 2015; **64**: 1881-1888 [PMID: 25748648 DOI: 10.1136/gutjnl-2014-308915]

25 **Arnold M**, Ferlay J, van Berge Henegouwen MI, Soerjomataram I. Global burden of oesophageal and gastric cancer by histology and subsite in 2018. *Gut* 2020; **69**: 1564-1571 [PMID: 32606208 DOI: 10.1136/gutjnl-2020-321600]

26 **Schmassmann A**, Oldendorf MG, Gebbers JO. Changing incidence of gastric and oesophageal cancer subtypes in central Switzerland between 1982 and 2007. *Eur J Epidemiol* 2009; **24**: 603-609 [PMID: 19669623 DOI: 10.1007/s10654-009-9379-y]

27 **Aragonés N**, Izarzugaza MI, Ramos M, Chirlaque MD, Almar E, Martínez C; Oesophago-gastric Cancer Working Group. Trends in oesophago-gastric cancer incidence in Spain: analysis by subsite and histology. *Ann Oncol* 2010; **21** Suppl 3: iii69-iii75 [PMID: 20427363 DOI: 10.1093/annonc/mdq083]

28 **Holster IL**, Aarts MJ, Tjwa ET, Lemmens VE, Kuipers EJ. Trend breaks in incidence of non-cardia gastric cancer in the Netherlands. *Cancer Epidemiol* 2014; **38**: 9-15 [PMID: 24309073 DOI: 10.1016/j.canep.2013.11.001]

29 **Derakhshan MH**, Yazdanbod A, Sadjadi AR, Shokoohi B, McColl KE, Malekzadeh R. High incidence of adenocarcinoma arising from the right side of the gastric cardia in NW Iran. *Gut* 2004; **53**: 1262-1266 [PMID: 15306582 DOI: 10.1136/gut.2003.035857]

30 **Saumoy M**, Schneider Y, Shen N, Kahaleh M, Sharaiha RZ, Shah SC. Cost Effectiveness of Gastric Cancer Screening According to Race and Ethnicity. *Gastroenterology* 2018; **155**: 648-660 [PMID: 29778607 DOI:

10.1053/j.gastro.2018.05.026]

31 **Ferro A**, Peleteiro B, Malvezzi M, Bosetti C, Bertuccio P, Levi F, Negri E, La Vecchia C, Lunet N. Worldwide trends in gastric cancer mortality (1980-2011), with predictions to 2015, and incidence by subtype. *Eur J Cancer* 2014; **50**: 1330-1344 [PMID: 24650579 DOI: 10.1016/j.ejca.2014.01.029]

32 **Rauf A**, Khalil AA, Rahman UU, Khalid A, Naz S, Shariati MA, Rebezov M, Urtecho EZ, de Albuquerque RDDG, Anwar S, Alamri A, Saini RK, Rengasamy KRR. Recent advances in the therapeutic application of short-chain fatty acids (SCFAs): An updated review. *Crit Rev Food Sci Nutr* 2022; **62**: 6034-6054 [PMID: 33703960 DOI: 10.1080/10408398.2021.1895064]

33 **Engel LS**, Chow WH, Vaughan TL, Gammon MD, Risch HA, Stanford JL, Schoenberg JB, Mayne ST, Dubrow R, Rotterdam H, West AB, Blaser M, Blot WJ, Gail MH, Fraumeni JF Jr. Population attributable risks of esophageal and gastric cancers. *J Natl Cancer Inst* 2003; **95**: 1404-1413 [PMID: 13130116 DOI: 10.1093/jnci/djg047]

34 **Wang M**, Luo X, Xu S, Liu W, Ding F, Zhang X, Wang L, Liu J, Hu J, Wang W. Trends in smoking prevalence and implication for chronic diseases in China: serial national cross-sectional surveys from 2003 to 2013. *Lancet Respir Med* 2019; **7**: 35-45 [PMID: 30482646 DOI: 10.1016/S2213-2600(18)30432-6]

35 **Yang G**, Fan L, Tan J, Qi G, Zhang Y, Samet JM, Taylor CE, Becker K, Xu J. Smoking in China: findings of the 1996 National Prevalence Survey. *JAMA* 1999; **282**: 1247-1253 [PMID: 10517427 DOI: 10.1001/jama.282.13.1247]

36 **Naseem M**, Barzi A, Brezden-Masley C, Puccini A, Berger MD, Tokunaga R, Battaglin F, Soni S, McSkane M, Zhang W, Lenz HJ. Outlooks on Epstein-Barr virus associated gastric cancer. *Cancer Treat Rev* 2018; **66**: 15-22 [PMID: 29631196 DOI: 10.1016/j.ctrv.2018.03.006]

37 **Murphy G**, Pfeiffer R, Camargo MC, Rabkin CS. Meta-analysis shows that prevalence of Epstein-Barr virus-positive gastric cancer differs based on sex and anatomic location. *Gastroenterology* 2009; **137**: 824-833 [PMID: 19445939 DOI: 10.1053/j.gastro.2009.05.001]

38 **Global Burden of Disease Cancer Collaboration**, Fitzmaurice C, Allen C, Barber RM, Barregard L, Bhutta ZA, Brenner H, Dicker DJ, Chimed-Orchir O, Dandona R, Dandona L, Fleming T, Forouzanfar MH, Hancock J, Hay RJ, Hunter-Merrill R, Huynh C, Hosgood HD, Johnson CO, Jonas JB, Khubchandani J, Kumar GA, Kutz M, Lan Q, Larson HJ, Liang X, Lim SS, Lopez AD, MacIntyre MF, Marczak L, Marquez N, Mokdad AH, Pinho C, Pourmalek F, Salomon JA, Sanabria JR, Sandar L, Sartorius B, Schwartz SM, Shackelford KA, Shibuya K, Stanaway J, Steiner C, Sun J, Takahashi K, Vollset SE, Vos T, Wagner JA, Wang H, Westerman R, Zeeb H, Zoeckler L, Abd-Allah F, Ahmed MB, Alabed S, Alam NK, Aldhahri SF, Alem G, Alemayohu MA, Ali R, Al-Raddadi R, Amare A, Amoako Y, Artaman A, Asayesh H, Atnafu N, Awasthi A, Saleem HB, Barac A, Bedi N, Bensenor I, Berhane A, Bernabé E, Betsu B, Binagwaho A, Boneya D, Campos-Nonato I, Castañeda-Orjuela C, Catalá-López F, Chiang P, Chibueze C, Chitheer A, Choi JY, Cowie B, Damtew S, das Neves J, Dey S, Dharmaratne S, Dhillon P, Ding E, Driscoll T, Ekwueme D, Endries AY, Farvid M, Farzadfar F, Fernandes J, Fischer F, G/Hiwot TT, Gebru A, Gopalani S, Hailu A, Horino M, Horita N, Husseini A, Huybrechts I, Inoue M, Islami F, Jakovljevic M, James S, Javanbakht M, Jee SH, Kasaeian A, Kedir MS, Khader YS, Khang YH, Kim D, Leigh J, Linn S, Lunevicius R, El Razek HMA, Malekzadeh R, Malta DC, Marcenes W, Markos D, Melaku YA, Meles KG, Mendoza W, Mengiste DT, Meretoja TJ, Miller TR, Mohammad KA, Mohammadi A, Mohammed S, Moradi-Lakeh M, Nagel G, Nand D, Le Nguyen Q, Nolte S, Ogbo FA, Oladimeji KE, Oren E, Pa M, Park EK, Pereira DM, Plass D, Qorbani M, Radfar A, Rafay A, Rahman M, Rana SM, Søreide K, Satpathy M, Sawhney M, Sepanlou SG, Shaikh MA, She J, Shiue I, Shore HR, Shrime MG, So S, Soneji S, Stathopoulou V, Stroumpoulis K, Sufiyan MB, Sykes BL, Tabarés-Seisdedos R, Tadese F, Tedla BA, Tessema GA, Thakur JS, Tran BX, Ukwaja KN, Uzochukwu BSC, Vlassov VV, Weiderpass E, Wubshet Terefe M, Yebyo HG, Yimam HH, Yonemoto N, Younis MZ, Yu C, Zaidi Z, Zaki MES, Zenebe ZM, Murray CJL, Naghavi M. Global, Regional, and National Cancer Incidence, Mortality, Years of Life Lost, Years Lived With Disability, and Disability-Adjusted Life-years for 32 Cancer Groups, 1990 to 2015: A Systematic Analysis for the Global Burden of Disease Study. *JAMA Oncol* 2017; **3**: 524-548 [PMID: 27918777 DOI: 10.1001/jamaoncol.2016.5688]

39 **Patti MG**. An Evidence-Based Approach to the Treatment of Gastroesophageal Reflux Disease. *JAMA Surg* 2016; **151**: 73-78 [PMID: 26629969 DOI: 10.1001/jamasurg.2015.4233]

40 **Pan XF**, Wang L, Pan A. Epidemiology and determinants of obesity in China. *Lancet Diabetes Endocrinol* 2021; **9**: 373-392 [PMID: 34022156 DOI: 10.1016/S2213-8587(21)00045-0]

41 **Camilleri M**, Malhi H, Acosta A. Gastrointestinal Complications of Obesity. *Gastroenterology* 2017; **152**: 1656-1670 [PMID: 28192107 DOI: 10.1053/j.gastro.2016.12.052]

42 **D'Journo XB**, Boulate D, Fourdrain A, Loundou A, van Berge Henegouwen MI, Gisbertz SS, O'Neill JR, Hoelscher A, Piessen G, van Lanschot J, Wijnhoven B, Jobe B, Davies A, Schneider PM, Pera M, Nilsson M, Nafteux P, Kitagawa Y, Morse CR, Hofstetter W, Molena D, So JB, Immanuel A, Parsons SL, Larsen MH, Dolan JP, Wood SG, Maynard N, Smithers M, Puig S, Law S, Wong I, Kennedy A, KangNing W, Reynolds JV, Pramesh CS, Ferguson M, Darling G, Schröder W, Bludau M, Underwood T, van Hillegersberg R, Chang A, Cecconello I, Ribeiro U Jr, de Manzoni G, Rosati R, Kuppusamy M, Thomas PA, Low DE; International Esodata Study Group. Risk Prediction Model of 90-Day Mortality After Esophagectomy for Cancer. *JAMA Surg* 2021; **156**: 836-845 [PMID: 34160587 DOI: 10.1001/jamasurg.2021.2376]

43 **Ojima T**, Nakamura M, Hayata K, Kitadani J, Katsuda M, Takeuchi A, Tominaga S, Nakai T, Nakamori M, Ohi M, Kusunoki M, Yamaue H. Short-term Outcomes of Robotic Gastrectomy vs Laparoscopic Gastrectomy for Patients With Gastric Cancer: A Randomized Clinical Trial. *JAMA Surg* 2021; **156**: 954-963 [PMID: 34468701 DOI: 10.1001/jamasurg.2021.3182]

44 **Liu WZ**, Xie Y, Lu H, Cheng H, Zeng ZR, Zhou LY, Chen Y, Wang JB, Du YQ, Lu NH; Chinese Society of Gastroenterology, Chinese Study Group on Helicobacter pylori and Peptic Ulcer. Fifth Chinese National Consensus Report on the management of Helicobacter pylori infection. *Helicobacter* 2018; **23**: e12475 [PMID: 29512258 DOI: 10.1111/hel.12475]

45 **Hwang MK**, Bode AM, Byun S, Song NR, Lee HJ, Lee KW, Dong Z. Cocarcinogenic effect of capsaicin involves activation of EGFR signaling but not TRPV1. *Cancer Res* 2010; **70**: 6859-6869 [PMID: 20660715 DOI: 10.1158/0008-5472.CAN-09-4393]

46 **López-Carrillo L**, López-Cervantes M, Robles-Díaz G, Ramírez-Espitia A, Mohar-Betancourt A, Meneses-García A,

López-Vidal Y, Blair A. Capsaicin consumption, Helicobacter pylori positivity and gastric cancer in Mexico. *Int J Cancer* 2003; **106**: 277-282 [PMID: 12800206 DOI: 10.1002/ijc.11195]

47 **Lee YC**, Chiang TH, Chou CK, Tu YK, Liao WC, Wu MS, Graham DY. Association Between Helicobacter pylori Eradication and Gastric Cancer Incidence: A Systematic Review and Meta-analysis. *Gastroenterology* 2016; **150**: 1113-1124.e5 [PMID: 26836587 DOI: 10.1053/j.gastro.2016.01.028]

48 **Yamaoka Y**. Helicobacter pylori typing as a tool for tracking human migration. *Clin Microbiol Infect* 2009; **15**: 829-834 [PMID: 19702588 DOI: 10.1111/j.1469-0691.2009.02967.x]

49 **So JB**, Rao J, Wong AS, Chan YH, Pang NQ, Tay AYL, Yung MY, Su Z, Phua JNS, Shabbir A, Ng EKW. Roux-en-Y or Billroth II Reconstruction After Radical Distal Gastrectomy for Gastric Cancer: A Multicenter Randomized Controlled Trial. *Ann Surg* 2018; **267**: 236-242 [PMID: 28383294 DOI: 10.1097/SLA.0000000000002229]

50 **Grunwald D**, Cohen J, Bartley A, Sheridan J, Chuttani R, Sawhney MS, Pleskow DK, Berzin TM, Mizrahi M. The location of obstruction predicts stent occlusion in malignant gastric outlet obstruction. *Therap Adv Gastroenterol* 2016; **9**: 815-822 [PMID: 27803736 DOI: 10.1177/1756283x16667893]

51 **de Martel C**, Georges D, Bray F, Ferlay J, Clifford GM. Global burden of cancer attributable to infections in 2018: a worldwide incidence analysis. *Lancet Glob Health* 2020; **8**: e180-e190 [PMID: 31862245 DOI: 10.1016/S2214-109X(19)30488-7]

World Journal of Gastrointestinal Oncology

Submit a Manuscript: https://www.f6publishing.com

World J Gastrointest Oncol 2022 November 15; 14(11): 2253-2265

DOI: 10.4251/wjgo.v14.i11.2253

ISSN 1948-5204 (online)

CASE REPORT

A rare synchrony of adenocarcinoma of the ampulla with an ileal gastrointestinal stromal tumor: A case report

Venkata Vinod Kumar Matli, Gazi B Zibari, Gregory Wellman, Poornima Ramadas, Sudha Pandit, James Morris

Specialty type: Oncology

Provenance and peer review: Unsolicited article; Externally peer reviewed.

Peer-review model: Single blind

Peer-review report's scientific quality classification

Grade A (Excellent): 0
Grade B (Very good): B
Grade C (Good): C
Grade D (Fair): 0
Grade E (Poor): E

P-Reviewer: Frosio F, Italy; Li W, China; Pan Y, China

Received: July 11, 2022
Peer-review started: July 11, 2022
First decision: August 19, 2022
Revised: September 15, 2022
Accepted: October 2, 2022
Article in press: October 2, 2022
Published online: November 15, 2022

Venkata Vinod Kumar Matli, Department of Internal Medicine, Christus Highland Medical Center, Shreveport, LA 71106, United States

Gazi B Zibari, Division of Hepatobiliary Surgery, Willis-Knighton Health System, Shreveport, LA 711103, United States

Gregory Wellman, Department of Gastrointestinal and Liver Pathology, Christus Highland Medical Center, Shreveport, LA 71105, United States

Poornima Ramadas, Division of Hematology and Oncology, Louisiana State University Health Sciences Center, Shreveport, LA 71103, United States

Sudha Pandit, James Morris, Division of Gastroenterology and Hepatology, Louisiana State University Health Sciences Center, Shreveport, LA 71103, United States

Corresponding author: Venkata Vinod Kumar Matli, MD, Attending Doctor, Department of Internal Medicine, Christus Highland Medical Center, 1455 E Bert Kouns Industrial Loop Christus Highland Medical Center, Shreveport, LA 71106, United States.
vmatli@soundphysicians.com

Abstract

BACKGROUND

This is a unique case of a patient who was found to have two extremely rare primary malignancies synchronously, *i.e.*, an ampullary adenocarcinoma arising from a high-grade dysplastic tubulovillous adenoma of the ampulla of Vater (TVAoA) with a high-grade ileal gastrointestinal stromal tumor (GIST). Based on a literature review and to the best of our knowledge, this is the first report of this synchronicity. Primary ampullary tumors are extremely rare, with an incidence of four cases *per* million population, which is approximately 0.0004%. Distal duodenal polyps are uncommon and have a preponderance of occurring around the ampulla of Vater. An adenoma of the ampulla (AoA) may occur sporadically or with a familial inheritance pattern, as in hereditary genetic polyposis syndrome such as familial adenomatous polyposis syndrome (FAPS). We report a case of a 77-year-old male who was admitted for painless obstructive jaundice with a 40-pound weight loss over a two-month period and who was subsequently diagnosed with two extremely rare primary malignancies, *i.e.*, an adenocarcinoma of the ampulla arising from a high-grade TVAoA and a high-grade ileal GIST found synch-ronously.

CASE SUMMARY

A 77-year-old male was admitted for generalized weakness with an associated weight loss of 40 pounds in the previous two months and was noted to have painless obstructive jaundice. The physical examination was benign except for bilateral scleral and palmar icterus. Lab results were significant for an obstructive pattern on liver enzymes. Serum lipase and carbohydrate antigen-19-9 levels were elevated. Computed tomography (CT) of the abdomen and pelvis and magnetic resonance cholangiopancreatography were consistent with a polypoid mass at the level of the common bile duct (CBD) and the ampulla of Vater with CBD dilatation. The same lesions were visualized with endoscopic retrograde cholangiopancreatography. Histopathology of endoscopic forceps biopsy showed TVAoA. Histopathology of the surgical specimen of the resected ampulla showed an adenocarcinoma arising from the TVAoA. Abdominal and pelvic CT also showed a coexisting heterogeneously enhancing, lobulated mass in the posterior pelvis originating from the ileum. The patient underwent ampullectomy and resection of the mass and ileo-ileal side-to-side anastomosis followed by chemoradiation. Histopathology of the resected mass confirmed it as a high-grade, spindle cell GIST. The patient is currently on imatinib, and a recent follow-up positron emission tomography (PET) scan showed a complete metabolic response.

CONCLUSION

This case is distinctive because the patient was diagnosed with two synchronous and extremely rare high-grade primary malignancies, *i.e.*, an ampullary adenocarcinoma arising from a high-grade dysplastic TVAoA with a high-grade ileal GIST. An AoA can occur sporadically and in a familial inheritance pattern in the setting of FAPS. We emphasize screening and surveillance colonoscopy when one encounters an AoA in upper endoscopy to check for FAPS. An AoA is a premalignant lesion, particularly in the setting of FAPS that carries a high risk of metamorphism to an ampullary adenocarcinoma. Final diagnosis should be based on a histopathologic study of the surgically resected ampullary specimen and not on endoscopic forceps biopsy. The diagnosis of AoA is usually incidental on upper endoscopy. However, patients can present with constitutional symptoms such as significant weight loss and obstructive symptoms such as painless jaundice, both of which occurred in our patient. Patient underwent ampullectomy with clear margins and ileal GIST resection. Patient is currently on imatinib adjuvant therapy and showed complete metabolic response on follow up PET scan.

Key Words: Tubulovillous adenoma of the ampulla of Vater; Ampullary adenocarcinoma; Gastrointestinal stromal tumor; Ampullary polyp; Small bowel mesenchymal tumor; Case report

Core Tip: This case is distinctive because the patient was diagnosed with two synchronous and extremely rare high-grade primary malignancies, *i.e.*, an ampullary adenocarcinoma arising from a high-grade dysplastic tubulovillous adenoma of the ampulla of Vater (TVAoA) with a high-grade ileal gastrointestinal stromal tumor (GIST). Based on a literature review, this is the first report of an ampullary adenocarcinoma coexisting with an ileal GIST. AoA may occur sporadically or in a familial inheritance pattern, as in the setting of familial adeno-matous polyposis syndrome (FAPS). We emphasize the need for screening and surveillance colonoscopy when one encounters an AoA in upper endoscopy to check for FAPS. TVAoA is a premalignant lesion, particularly in the setting of FAPS, and carries a high risk for metamorphism to an ampullary adenocarcinoma.

Citation: Matli VVK, Zibari GB, Wellman G, Ramadas P, Pandit S, Morris J. A rare synchrony of adenocarcinoma of the ampulla with an ileal gastrointestinal stromal tumor: A case report. *World J Gastrointest Oncol* 2022; 14(11): 2253-2265

URL: https://www.wjgnet.com/1948-5204/full/v14/i11/2253.htm

DOI: https://dx.doi.org/10.4251/wjgo.v14.i11.2253

INTRODUCTION

Solitary adenomas involving the ampulla of Vater (AoV) account for 5% of gastrointestinal tumors, and most are found incidentally on endoscopy[1]. Adenomas of the ampulla of Vater (AoAs) may be sporadic, as in our case, or follow a familial inheritance pattern, as in the setting of familial

adenomatous polyposis syndrome (FAPS). Although these lesions are rare, the study of AoA is essential, as they are premalignant, and the risk of progression to an adenocarcinoma is high[1].

We report the case of a 77-year-old male who presented with generalized weakness along with associated decreased appetite and a 40-pound weight loss for approximately two months and who was found to have a solitary high-grade tubulovillous adenoma of the ampulla of Vater (TVAoA); the initial diagnosis was a high-grade TVAoA. However, the diagnosis ultimately changed to an ampullary adenocarcinoma arising from a TVAoA. The patient also had a coexisting small bowel gastrointestinal stromal tumor (GIST). This case is unique because of the synchronicity of two extremely primary malignancies, *i.e.*, an ampullary adenocarcinoma arising from a high-grade dysplastic TVAoA with a high-grade ileal GIST. There is a scarcity of literature on this topic, and we feel it is interesting to discuss the diagnosis, management, and follow-up associated with this case.

CASE PRESENTATION

Chief complaints

The patient was a 77-year-old Caucasian male who presented with generalized weakness and decreased appetite associated with a weight loss of approximately 40 pounds in the last 2 months.

History of present illness

This patient had a medical history significant for essential hypertension, type 2 diabetes mellitus, and hyperlipidemia, and he presented with generalized weakness with decreased appetite associated with a weight loss of approximately 40 pounds in the prior 2 mo. He denied any abdominal pain, nausea, vomiting, or diarrhea but noted that recently his urine had become dark and his skin had become yellowish in color.

History of past illness

The patient had a medical history significant for essential hypertension, type 2 diabetes mellitus, and hyperlipidemia.

Personal and family history

He denied smoking tobacco, alcohol use, or any kind of illicit drug abuse. Family history was insignificant.

Physical examination

The patient's vital signs were stable. The physical examination was significant for scleral and palmar icterus. No lymph nodes were palpable. The rest of the physical examination findings were benign.

Laboratory examinations

Complete blood counts were normal. A comprehensive metabolic panel revealed a serum sodium level of 128 mmol/L, creatinine level of 1.5 mg/dL, and lipase level of 1904 U/L, which decreased to 755 U/L on the day of discharge. The hepatitis panel was negative. Liver function tests are shown in Table 1, and tumor markers are shown in Table 2.

Imaging examinations

Contrast-enhanced computed tomography (CT) of the abdomen and pelvis showed a polypoid, soft tissue mass at the level of the distal common bile duct (DCBD)/AoV measuring approximately 9 mm with resultant intra- and extrahepatic biliary dilatation (Figure 1A and B). The CBD measured 15 mm in diameter, and cystic lesions measuring up to 1 cm were noted in the tail of the pancreas. There was a heterogeneously enhanced lobulated mass with punctate calcifications in the posterior pelvis likely originating from the serosal surface of the pelvic small bowel (Figure 1C and D). Magnetic resonance cholangiopancreatography (MRCP) (Figure 2) showed a polypoid mass again noted at the level of the DCBD/AoV. It measured approximately 2.3 cm × 2.0 cm × 1.7 cm with a slightly prominent pancreatic duct measuring 6 mm in diameter. Given his CT and MRCP findings, medical gastroenterology and general surgery experts were consulted. He underwent endoscopic retrograde cholangiopancreatography (ERCP), which showed abnormal papillae with polypoid masses (Figure 3). Sphincterotomy and deep cannulation procedures were performed and confirmed by fluoroscopy. It showed CBD dilatation, and there was an abrupt cutoff at the distal aspect. The general surgery consultant recommended biopsy of the pelvic mass for probable metastatic disease. The patient underwent positron emission tomography (PET), which showed an endo-biliary stent in the region of the papilla, a 1.7 cm ampullary mass with intense fluorodeoxyglucose (FDG) avidity (Figure 4A) and an oval-shaped, well-defined FDG-avid lesion measuring approximately 6 cm × 3 cm (Figure 4B), with a small punctate area of calcification present within the lesion located deep in the pelvis along the posterior margin of the small bowel loops. No FDG-avid lymph nodes were identified. No lytic or blastic FDG lesions were observed.

Table 1 Liver function tests

Liver function tests	On admission	On discharge
ALT	299	196
AST	122	75
ALP	848	754
Total Bilirubin	5.9	2.6
Direct Bilirubin	4.2	2.0
Albumin	3.0	2.6

AST: Aspartate aminotransferase, ALT: Alanine aminotransferase, ALP: Alkaline phosphatase. AST/ALT/ALP = U/Liter.

Table 2 Tumor markers

Tumor marker	Result	Normal range
CEA	0.99	0.01-4.00
CA-19	454	0.00-37

CEA: Carcinoembryonic antigen, ng/mL; CA-19: Carbohydrate antigen-19, U/mL.

Histopathology of the ampullary mass that was biopsied on endoscopy showed a tubulovillous adenoma with high-grade dysplasia (Figure 5).

MULTIDISCIPLINARY EXPERT CONSULTATION

Gazi B. Zibari, MD, FACS, Academic Chairman of the Dept of Surgery, Program Director of Surgery Residency, Director, John C. McDonald Regional Transplant & Hepato-Pancreato-Biliary Center, Willis Knighton Health System.

This case was discussed at the hepatobiliary multidisciplinary conference, and all images and paths were discussed. It was recommended for the patient to undergo resection of both the ampullary mass and small bowel lesions. The patient was an ideal candidate for the Whipple procedure, even robotically/laparoscopically. However, the patient only consented to ampullectomy, not to the Whipple procedure. The patient underwent duodenal exploration and was found to have a broad ampullary polypoid lesion that was not amenable to endoscopic resection. However, endoscopic ultrasound and intraoperative ultrasound did not reveal any evidence of pancreatic invasion. We advanced a Fogarty catheter *via* the cystic duct through the ampulla down to the duodenum. The ampullary mass was excised with a negative margin as well as negative peri-pancreatic/peri-duodenal nodes *per* frozen section (Figure 6A and B).

Subsequently, a pedunculated ileal GIST was found approximately 150 cm proximal to the ileocecal valve. This was resected *en bloc* with a loop of small bowel. There was no associated mesenteric adenopathy. Subsequently, side-to-side small bowel anastomoses were created (Figure 6C).

With an adenocarcinoma in the specimen and a close margin on permanent section, the patient did not undergo the Whipple procedure, and the patient also wished to undergo chemotherapy and was therefore scheduled to see medical and radiation oncology experts.

Surgical pathology

Histopathology of the sections of the ampullary mass (Figure 7A and B) demonstrated a 1.5 cm invasive adenocarcinoma arising from a high-grade dysplastic TVAoA. The tumor invaded the muscularis propria of the duodenum. The tumor invaded 1 mm of the pancreas but did not invade the pancreatic parenchyma. In the intact specimen, no tumor was present at the surgical margins of the resection. Given the likelihood that nonmarginal tissue may be exposed to thermal artifacts, the margins of resection were deemed to be free of tumors.

Histopathology of the sections of the small bowel mass (Figure 7C and D) demonstrated a high-grade, GIST spindle cell type, with 15 mitoses *per* 5 square millimeters. A series of special stains (Figure 7E) with working controls was performed. The tumor cells were positive for DOG-1 and CD 117, consistent with a GIST.

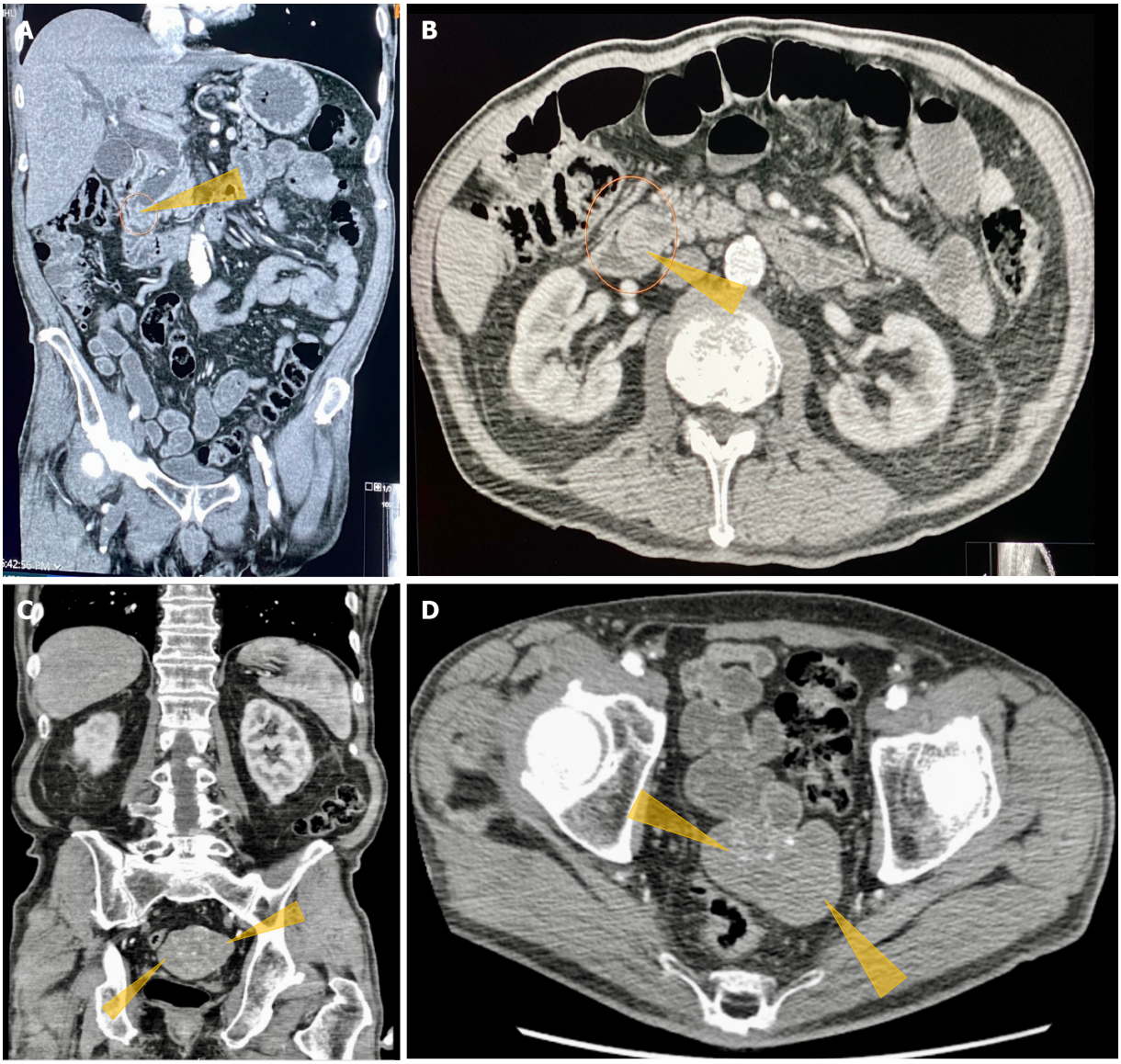

DOI: 10.4251/wjgo.v14.i11.2253 **Copyright** ©The Author(s) 2022.

Figure 1 Computerized tomography of the abdomen and pelvis with contrast images. A: Computerized tomography (CT) abdomen and pelvis with contrast. Coronal section shows obstructed distal common bile duct (CBD) due to a 9 mm polypoid intraluminal (pointed yellow arrows) lesion in the distal CBD; B: CT of the abdomen and pelvis with contrast. Axial section shows polypoid, soft tissue mass at the level of distal common bile duct (pointed yellow arrows); C: CT of the abdomen and pelvis with contrast. Heterogeneously enhanced lobulated mass with punctate calcifications (pointed yellow triangles) in the posterior pelvis originating from the serosal surface of the pelvic small bowel; D: CT of the abdomen and pelvis with contrast. Axial section shows a heterogeneously enhanced lobulated mass with punctate calcifications (pointed yellow triangle) in the posterior pelvis originating from the serosal surface of the pelvic small bowel.

FINAL DIAGNOSIS

The final diagnosis was a T2N0M0 adenocarcinoma of the ampulla arising from a high-grade TVAoA coexisting with a T3N0M0 high-grade ileal GIST.

TREATMENT

As mentioned above in the multidisciplinary expert consultation, the patient underwent surgical ampullectomy, ileal GIST resection with ileo-ileal side to side anastomosis. The patient was scheduled for chemoradiation as recommended by medical oncologist.

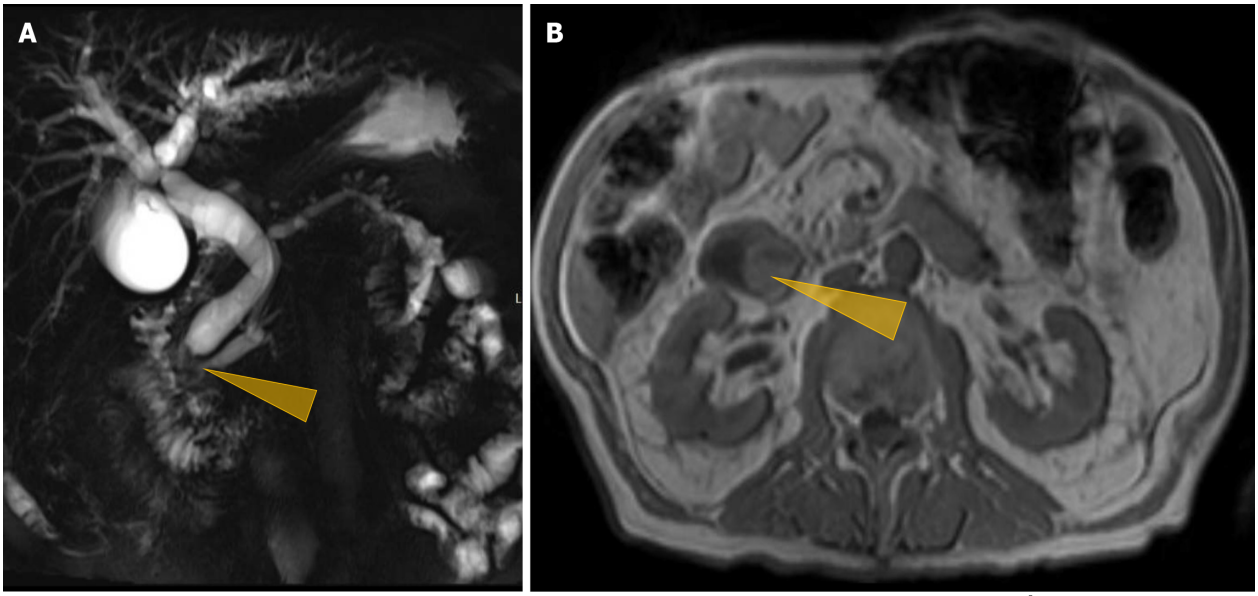

DOI: 10.4251/wjgo.v14.i11.2253 **Copyright** ©The Author(s) 2022.

Figure 2 Magnetic resonance cholangiopancreaticography imaging studies. A: Magnetic resonance cholangio pancreaticography image showing intra and extrahepatic biliary dilatation and a polypoid mass was noted at the level of the distal common bile duct (CBD)/ampulla of Vater (Pointed yellow triangle). It measured approximately 2.3 cm × 2.0 cm × 1.7 cm with a slightly prominent pancreatic duct measuring 6 mm in diameter. Common bile duct was measured 14 mm in diameter; B: Magnetic resonance imaging of the abdomen showing a polypoid mass (pointed yellow triangle) at the level of the CBD.

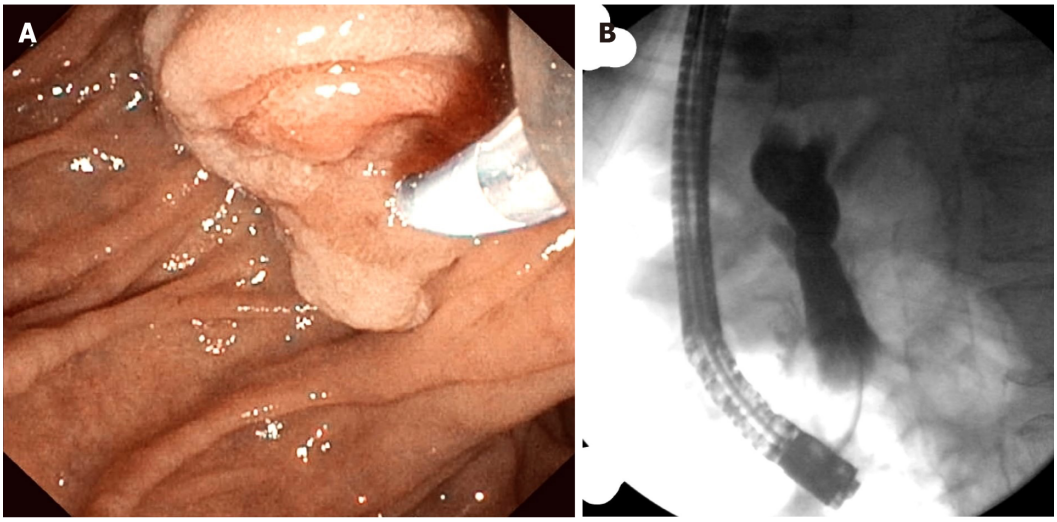

DOI: 10.4251/wjgo.v14.i11.2253 **Copyright** ©The Author(s) 2022.

Figure 3 Endoscopic retrograde pancreatography studies. A: The patient had abnormal papilla with a polypoid mass. Sphincterotomy and deep cannulation procedures were performed and confirmed by fluoroscopy. endoscopic retrograde cholangiopancreatography (ERCP) showed common bile duct (CBD) dilatation, and there was an abrupt cutoff at the distal aspect; B: ERCP fluoroscopy. Fluoroscopy showed CBD dilatation, and there was an abrupt cutoff at the distal aspect.

OUTCOME AND FOLLOW-UP

Surveillance CT of the chest, abdomen and pelvis w/contrast on three months after surgery showed no findings for metastatic disease (Figure 8).

After three weeks of recovery from ampullectomy, the patient underwent five and half weeks of external beam radiation therapy with concurrent chemotherapy with 5-fluorouracil. He is currently on an adjuvant therapy of imatinib (400 mg *per* oral daily) for the GIST. His repeat PET scan performed on August 2022 showed a complete metabolic response (16).

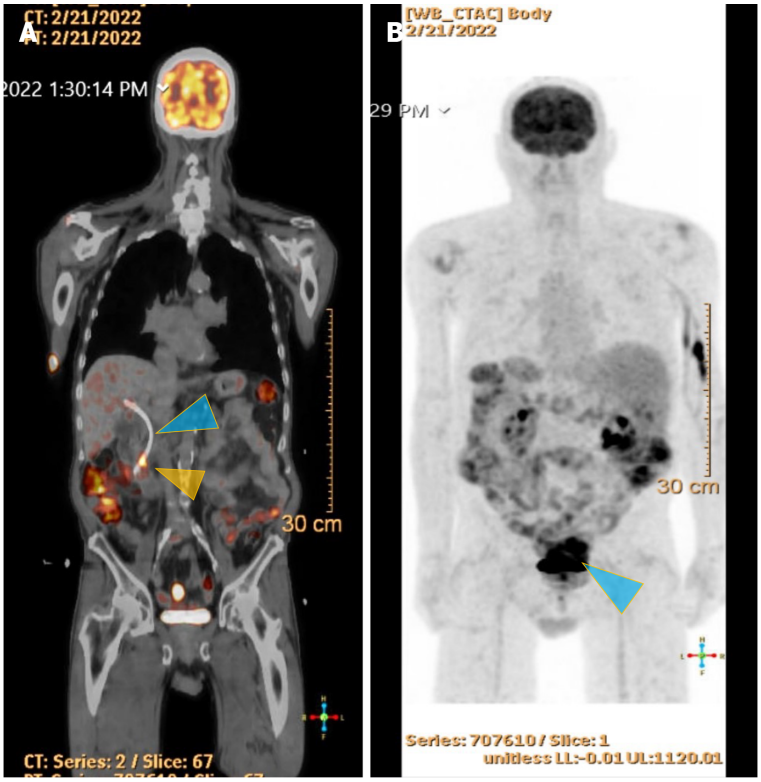

DOI: 10.4251/wjgo.v14.i11.2253 **Copyright** ©The Author(s) 2022.

Figure 4 18F-Flurodeoxyglucose positron emission tomography scan studies. A: Shows an end-obiliary stent in the region of the papilla (blue triangle) and a 1.7 cm ampullary mass with intense fluorodeoxyglucose (FDG) avidity(yellow triangle); B: Shows an oval-shaped, well-defined, FDG-avid lesion measuring approximately 6 cm × 3 cm with a small, punctate area of calcification was present in the lesion located deep in the pelvis along the posterior margin of small bowel loops (blue triangle) with intense FDG avidity.

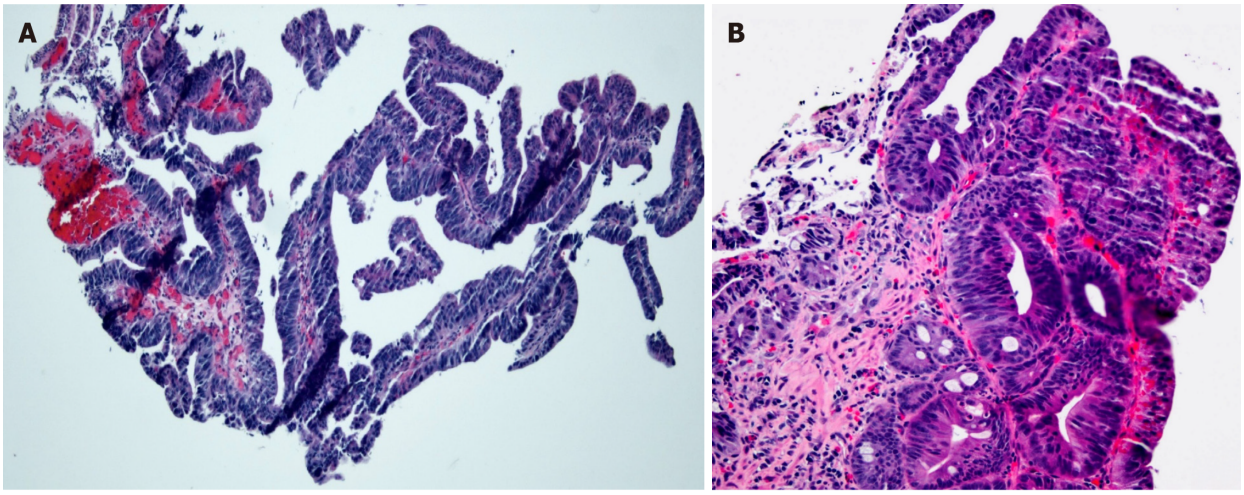

DOI: 10.4251/wjgo.v14.i11.2253 **Copyright** ©The Author(s) 2022.

Figure 5 Histopathology of endoscopic biopsy. A: Medium-power photomicrograph demonstrating dysplastic glandular epithelium with a tubulovillous architecture (hematoxylin and eosin stain, 100 × original magnification); B: High-power photomicrograph showing high-grade glandular dysplasia (hematoxylin and eosin stain, 200 × original magnification).

DISCUSSION

This is a unique case of a patient who was found to have two extremely primary malignancies synchronously, *i.e.*, an ampullary adenocarcinoma arising from a high-grade dysplastic TVAoA with a high-grade ileal GIST. Based on a literature review and to the best of our knowledge, this is the first report of this synchronicity. Primary ampullary tumors are extremely rare, with an incidence of four cases *per* million population, which is approximately 0.0004%. Distal duodenal polyps are uncommon and have a preponderance of occurring around the ampulla of Vater. Duodenal polyps are found in

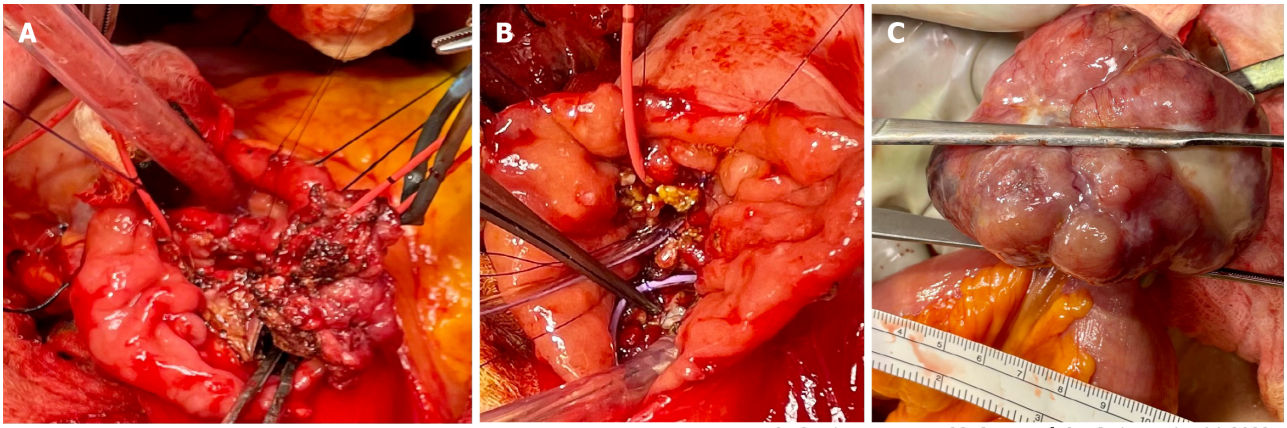

DOI: 10.4251/wjgo.v14.i11.2253 **Copyright** ©The Author(s) 2022.

Figure 6 Intraoperative images. A: A broad base ampullary mass with red Fogarty catheter was advanced from the cystic duct down through the ampulla to the duodenum; B: The ampullary mass was excised, and two internal stents were placed in the bile duct and pancreatic duct in addition to the red Fogarty catheter in the bile duct; C: Pedunculated gastrointestinal stromal tumor arising from the small bowel approximately 150 cm proximal to the ileocecal valve.

4.6% of patients referred for upper endoscopy[2]. Duodenal polyps occur more frequently in the ampulla than in the distal duodenum. Because of the widespread use of upper endoscopy, the incidence of ampullary tumors has been increasing.

Adenomas are the most common ampullary tumors. AoAs can occur as sporadic in a familial inheritance pattern, such as in the setting of FAPS. Two essential points prompted us to write this case report. Firstly, when an AoA is found on upper endoscopy, patients should be sent for screening and periodic surveillance colonoscopy for FAPS. Secondly, AoAs are premalignant lesions can progress to an ampullary adenocarcinoma, which should be identified early for appropriate management and improved outcome. An AoA in the setting of FAPS has a high risk for progression to an ampullary adenocarcinoma. Compared with non-FAPS patients, these patients have an approximately 124-fold increased risk of progression[3]. The diagnosis of an AoA is usually incidental. However, some patients present with obstructive symptoms, such as painless jaundice associated with weight loss, which occurred in our patient due to CBD obstruction[3]. This results in pancreatitis due to pancreatic duct obstruction[3]. When there are constitutional symptoms such as weight loss, an in-depth work-up is needed to evaluate the potential malignant transformation of an AoA. Endoscopic forceps biopsy is only diagnostic in 64% of cases. Diagnostic accuracy is greater when histopathological studies are performed on surgical specimens. Therefore, a final diagnosis should only be made when surgical pathology is available[3,4].

Ampullary carcinoma is the 2nd most common periampullary regional cancer and metastasizes locally in the abdomen and to the liver. Distant metastasis is less common, but there are case reports describing skeletal and brain metastases[1]. Carcinoma of the ampulla of Vater is a rare tumor accounting for approximately 0.2% of all gastrointestinal malignancies, with an estimated incidence of < 6 cases *per* million people *per* year[1]. AoAs and adenocarcinomas originate from the glandular epithelium of the AoV[5]. The cell of origin of these cancers is the epithelial covering of the distal parts of the CBD, pancreatic duct, and periampullary duodenum. Histological subtypes that are common are mucinous, signet ring cell, neuroendocrine, and undifferentiated carcinomas.

A study by Seifert *et al*[6] revealed that 30% of ampullary adenomas progressed to ampullary adenocarcinomas, which were found during surgery or on follow-up. It also showed that 41.2% of surgically resected ampullary adenocarcinoma patients had residual well-differentiated adenomatous tissue[6].

The next step after diagnosis is established is staging. The usual imaging modalities are CT of the chest, abdomen, and pelvis, MRCP, endoscopic ultrasound, and endoscopic intraductal ultrasound. If there is any biliary tree abnormality in the CT or MRCP, then ERCP plays an important role. ERCP can be diagnostic for determining the extent of the spread of the tumor followed by sphincterotomy and stent placement to facilitate pancreaticobiliary drainage[3].

Incidental and small adenomas may not need any treatment, but high-grade dysplastic tubulovillous adenomas require definitive treatment due to the potential risk of progression to an adenocarcinoma[5].

Management of an ampullary adenocarcinoma:

The patient had a broad-based adenoma in the ampulla, and ampullectomy could have been performed robotically, but it would have been performed for a longer time, and we were concerned about negative margins. On the other hand, a robotic Whipple procedure is possible, but the patient did not agree to that procedure.

In regards to the ileal GIST, minimally invasive surgical resection and robotic resection are available options, although rupture of the tumor may be a potential complication. We have done many of these

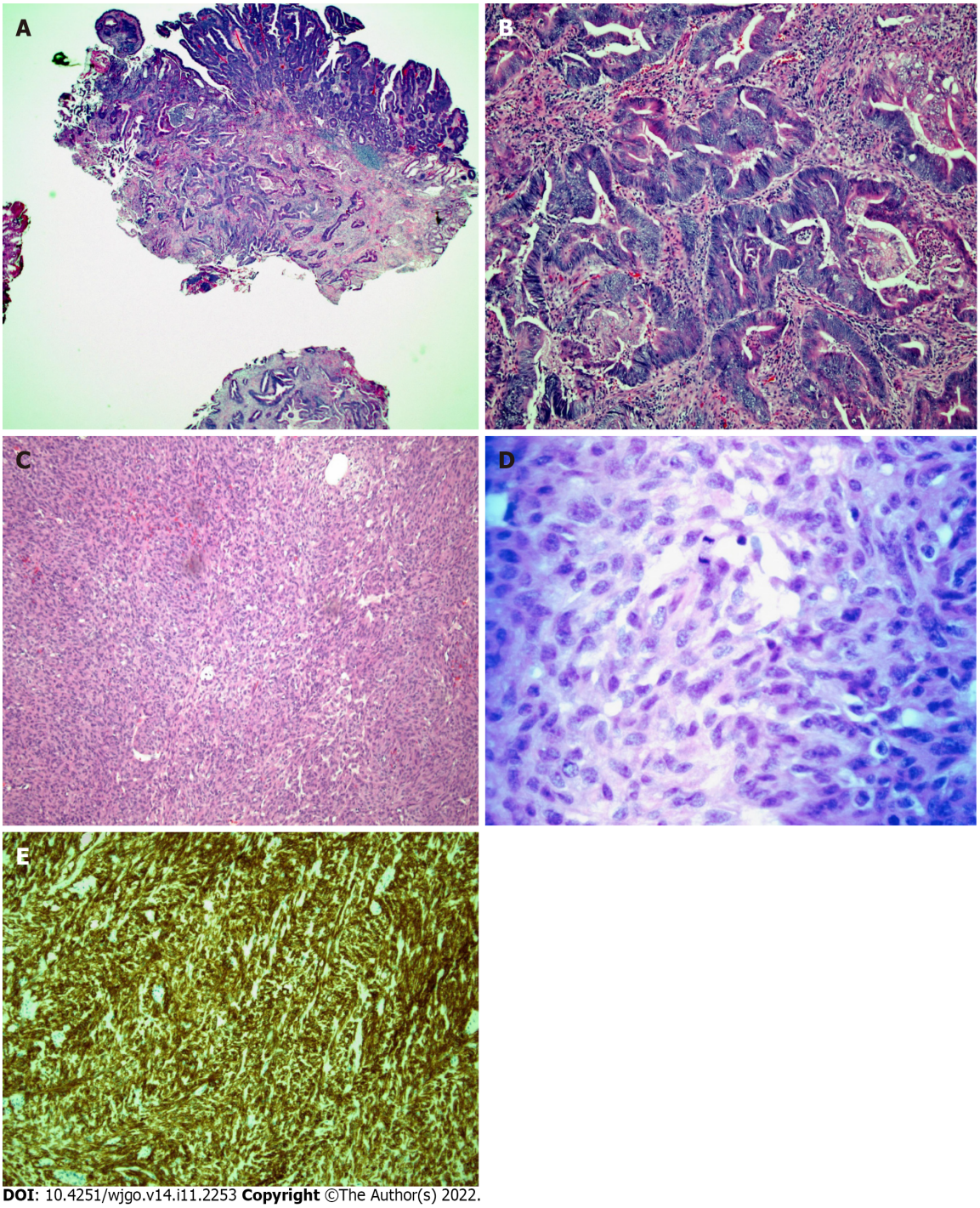

DOI: 10.4251/wjgo.v14.i11.2253

Figure 7 Histopathology of the surgically resected ampullary mass and ileal mass. A: Low-power micrograph of invasive adenocarcinoma arising from a tubulovillous adenoma with high-grade dysplasia in the ampullary region (hematoxylin and eosin stain, original magnification 20 ×); B: High-power micrograph of ampullary mass showing malignant glands (hematoxylin and eosin stain, original magnification 100 ×); C: Low-power photomicrograph of ileal mass showing the spindle cell morphology of a gastrointestinal stromal tumor (GIST) (hematoxylin and eosin stain, 100 × original magnification); D: A high-power view of cellular mitosis within the ileal GIST (hematoxylin and eosin stain, 600 × original magnification) showed 15 mitoses *per* 5 square millimeters; E: Immunohistochemical staining for CD117 showing strong and diffuse cytoplasmic immunoreactivity confirming GIST (hematoxylin and eosin stain, 100 × original magnification).

procedures and have never had a rupture at our facility; in fact, robotic articulation does help to maneuver the tumor without traumatizing it. Therefore, we can perform both ampullectomy, duodenal polyp excision and GIST with minimally invasive surgery either robotically or laparoscopically; some at our facility prefer robotic procedures because of the ease of anastomosis and articulation of the robot. With the Whipple procedure, we can obtain clear margins, but duodenal/ampullary lesions are more challenging because of the risk of positive margins.

An overview of the management of ampullary adenomas and ampullary carcinomas is described in Table 3.

Table 3 Endoscopic

Endoscopic			Surgical	
Curative	Palliative	Surveillance	Trans-duodenal ampullectomy	Radical or Whipple's resection
Endoscopic snare polypectomy or piecemeal polypectomy	Invasive ampullary adenocarcinoma	FAPS	Benign ampullary adenomas that are difficult to operate on endoscopically[7]. The advantage of this is less morbidity and mortality and alternative access to ampullary tumor resection[7]	Ampullary adenocarcinoma. Radical resection if tumor burden in the duct is high

FAPS: Familial adenomatous polyposis syndrome.

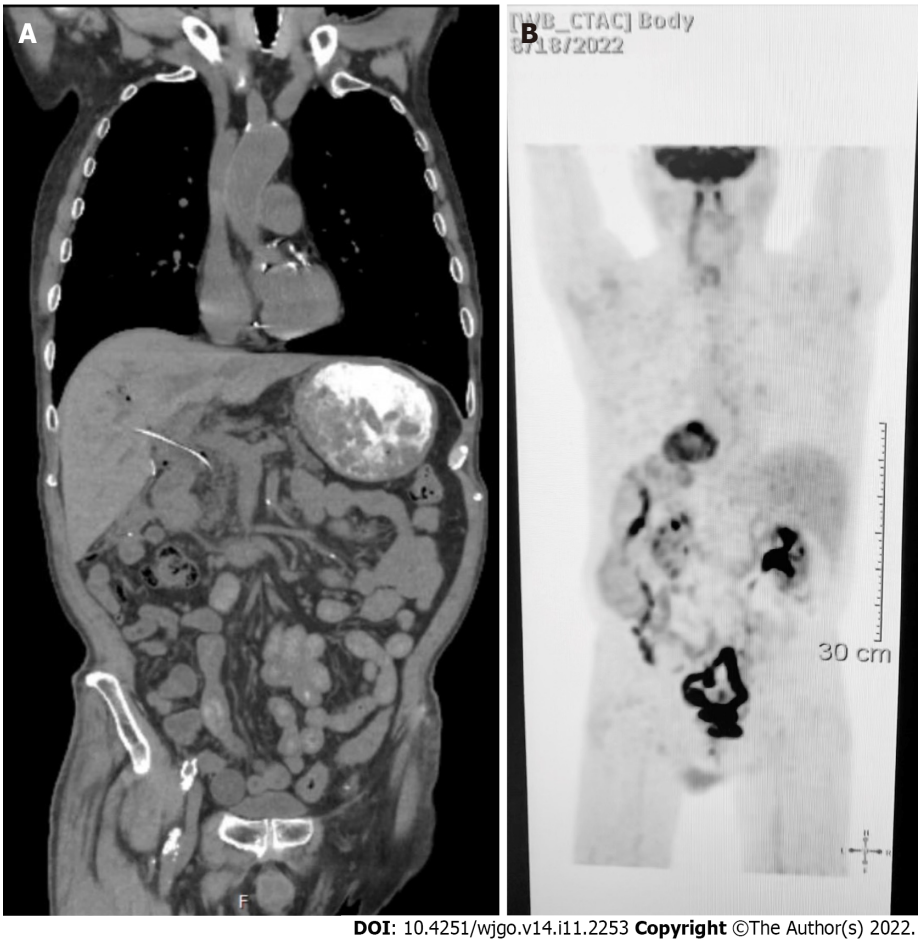

DOI: 10.4251/wjgo.v14.i11.2253 **Copyright** ©The Author(s) 2022.

Figure 8 Follow up computed tomography and positron emission tomography scan studies. A: Surveillance computed tomography of the chest, abdomen and pelvis w/contrast on three months after surgery showed no findings for metastatic disease; B: Follow-up positron emission tomography scan showing a complete metabolic response.

GISTs are rare tumors comprising 3% of gastrointestinal tumors but are the most common mesenchymal tumors of the GI tract[4]. The most common sites are the stomach (60%) and small bowel (30%)[2,3]. These are sporadic tumors, unlike ampullary adenomas. Some studies report that the incidence significantly varies from 0.4 to 2.0 cases *per* 100000 *per* year, with a slight male preponderance and a median age of 60-65 years[7-9].

GISTs are malignant mesenchymal tumors whose cell of origin is the myenteric interstitial cells of Cajal; they are also known as pacemaker cells of the GI tract and are found in the proximal muscles surrounding the intermuscular plexus of the GI tract. They are soft tissue sarcomas of the GI tract, but they differ in genetics, pathogenesis, clinical presentation, and management[4].

Most GISTs have universal expression of c-KIT/CD117. DOG-1 is another novel marker and can be seen in c-kit-negative cases. The mitotic rate can predict the risk of recurrence.

In 1998, a breakthrough was achieved when the tyrosine kinase receptor mutation c-kit was identified [10]. The most common mutations in GISTs are located in c-KIT exon 11 in approximately 65% of cases and exon 9 in approximately 10%. GISTs with exon 11 mutations are more sensitive to the tyrosine kinase inhibitor imatinib than those with exon 9 mutations.

Platelet-derived growth factor alpha (PDGFRA) mutations account for approximately 5%-10% of cases. Mutations are located on exons 12, 14, and 18. It is important to identify the D842 V2V mutation in exon 18, as this mutation confers resistance to imatinib. Avapritinib is the preferred treatment for GISTs with this mutation[4].

Other rare GIST mutations are BRAF and NTRK gene rearrangements, which carry therapeutic implications. Histopathological diagnosis depends upon morphological and immunochemical analysis of the tumor. Immunochemistry is usually positive for CD117(KIT) and/or DOG-1 in 95% of patients. Five percent of GISTs are negative for CD117 and/or DOG-1[8].

Mutational analysis of GISTs is important, as it has good predictive value for sensitivity to targeted therapy, as noted previously, and prognosis. The European Society for Medical Oncology practice guidelines recommend testing for mutations as a part of the diagnostic workup for all high-risk GISTs. GISTs negative for KIT/PDGFRA require subsequent immunochemical testing for succinate dehydrogenase complex subunit-B.

Management of GISTs includes multidisciplinary consultation with pathologists, radiologists, surgeons, medical oncologists, and gastroenterologists, *etc.*, to achieve better outcomes.

Standard management of a localized GIST is complete surgical resection or excision without dissection of clinically negative lymph nodes. The goal is to excise the tumor with negative margins. Tumors greater than 2 cm in size should be biopsied and surgically resected. If less than 2 cm in size, surveillance *via* endoscopic ultrasound can be performed. However, if lesions are suspicious, then they should be surgically resected. Small GISTs located in the upper and lower GI tract can be resected endoscopically by a surgeon who has endoscopic expertise.

Systemic therapy is performed as a neoadjuvant or adjuvant based on tumor size and other characteristics and is the main strategy for the management of advanced/metastatic disease (Tables 4 and 5).

The first-line treatment for KIT exon-9-mutated GISTs is imatinib (800 mg daily), whereas avapritinib (300 mg daily) is the first-line treatment for GISTs with PDGFRA exon 18 D842 V2V mutation[8]. The imatinib dose can be escalated from 400 mg to 800 mg when there is disease progression. Second-line therapy with sunitinib (50 mg daily) is recommended when there is intolerance to imatinib or progressive disease. Regorafenib (160 mg daily) is generally the third-line therapy for patients unresponsive to imatinib and sunitinib. Ripretinib (150 mg daily) is approved in patients who have received prior treatment with three or more kinase inhibitors, including imatinib.

National Comprehensive Cancer Network guidelines recommend follow-up with history and physical and imaging studies every 3 to 6 mo for the first 5 years and then annually after complete resection of GISTs. Relapse to the liver and peritoneum can occur, but distant metastasis to bone and other sites is rare.

The coexistence of the malignancies described in this case is extremely rare, and to our knowledge, this is the first reported case in the literature. Mazur and Clark[10] first published the term GIST in 1983; initially, we considered GISTs as neoplasms of smooth muscle cells and called them gastrointestinal smooth muscle tumors[10]. There have been case reports in the literature reporting GISTs occurring with other histologically diverse parallel primary malignancies. There have been reported occurrences of GISTs of the gastric antrum with colorectal adenocarcinomas[11] and duodenal GISTs with rectal adenocarcinomas[12]. There has been increasing evidence of coexistent, contemporaneous GISTs with other neoplasms of the breast, digestive tract, liver and urogenital system[7,13,14].

CONCLUSION

This case is distinctive because the patient was diagnosed with two synchronous and extremely rare high-grade primary malignancies, *i.e.*, an ampullary adenocarcinoma arising from a high-grade dysplastic TVAoA with a high-grade ileal GIST. An AoA can occur sporadically and in a familial inheritance pattern in the setting of FAPS. We emphasize screening and surveillance colonoscopy when one encounters an AoA in upper endoscopy to check for FAPS. An AoA is a premalignant lesion, particularly in the setting of FAPS that carries a high risk of metamorphism to an ampullary adenocarcinoma. Final diagnosis should be based on a histopathologic study of the surgically resected ampullary specimen and not on endoscopic forceps biopsy. The diagnosis of AoA is usually incidental on upper endoscopy. However, patients can present with constitutional symptoms such as significant weight loss and obstructive symptoms such as painless jaundice, both of which occurred in our patient. Patient underwent ampullectomy with clear margins and ileal GIST resection. Patient is currently on imatinib adjuvant therapy and showed complete metabolic response on follow up PET scan.

Table 4 Management of Localized gastrointestinal stromal tumors

Imatinib-sensitive mutation					Imatinib-insensitive mutation
Uncomplicated (No major complications expected with surgery)		Complicated (Major complications expected with surgery)			See Table 5
Surgery (Resection of tumor with negative margins)		Preoperative imatinib for 6 mo			
Low/Intermediaterisk	High risk	Tumor negative or microscopically positive margins feasible		Tumor negative or microscopically positive margins not feasible	
Follow-up	Adjuvant treatment with imatinib for 36 mo	Low/Intermediaterisk Follow-up	High risk Adjuvant imatinib for 36 mo	Manage as advanced GIST or metastatic GIST	

GIST: Gastrointestinal stromal tumors.

Table 5 Management of advanced or metastatic gastrointestinal stromal tumors

Imatinib-sensitive mutations			Imatinib-insensitive mutations				
KIT mutations (except exon-9 variety)	Exon-9 KIT mutations		PDGFRA842 V2V mutation	BRAF mutation	NTRK translocation	SDHB	All other mutations
Imatinib 400 mg daily	Imatinib 800 mg daily		Avapritinib	BRAF inhibitor	NTRK inhibitorentrectiniblaro-trectinib	Customized management	Sunitinib
Imatinib responsive	Imatinib unresponsive						
Surgery of the residual disease and continue imatinib for life	Excision and ablation of progressing lesion	Add and continue sunitinib if responsive					

ACKNOWLEDGEMENTS

The authors express their deepest appreciation to Manish Dhawan MD, Department of Hematology and Oncology and Dustin Hadley, Physician assistant, Department of Gastroenterology, Christus Highland Medical Center, who provided insightful comments about this research.

FOOTNOTES

Author contributions: Matli VVK obtained all the required data and drafted the article after literature review; Wellman G was a gastrointestinal and liver pathologist, reviewed the slides and revised the article; Ramadas P, medical oncologist, revised the article; Pandit S, gastroenterologist, reviewed the literature and revised the article; Zibari GB, hepatobiliary surgeon and Morris J, gastroenterologist and hepatologist, critically revised the article and approved the final version of the article.

Informed consent statement: Written informed consent was obtained from the patient for the publication of this article and any accompanying images.

Conflict-of-interest statement: All the authors report no relevant conflicts of interest for this article.

CARE Checklist (2016) statement: The authors have read the care checklist (2016), and the manuscript was prepared and revised according to the care checklist (2016).

Country/Territory of origin: United States

ORCID number: Venkata Vinod Kumar Matli 0000-0002-9678-4537; Gazi B Zibari 0000-0001-7689-4299; Gregory Wellman 0000-0001-6891-8211; Poornima Ramadas 0000-0002-7547-2315; Sudha Pandit 0000-0002-5220-0755; James Morris 0000-0002-9989-3966.

S-Editor: Fan JR
L-Editor: A
P-Editor: Zhang XD

REFERENCES

1 **Voutsadakis IA**, Doumas S, Tsapakidis K, Papagianni M, Papandreou CN. Bone and brain metastases from ampullary adenocarcinoma. *World J Gastroenterol* 2009; **15**: 2665-2668 [PMID: 19496199 DOI: 10.3748/wjg.15.2665]
2 **Joensuu H**, Hohenberger P, Corless CL. Gastrointestinal stromal tumour. *Lancet* 2013; **382**: 973-983 [PMID: 23623056 DOI: 10.1016/S0140-6736(13)60106-3]
3 **Kadado KJ**, Abernathy OL, Salyers WJ, Kallail KJ. Gastrointestinal Stromal Tumor and Ki-67 as a Prognostic Indicator. *Cureus* 2022; **14**: e20868 [PMID: 35145775 DOI: 10.7759/cureus.20868]
4 **Sugiyama Y**, Sasaki M, Kouyama M, Tazaki T, Takahashi S, Nakamitsu A. Current treatment strategies and future perspectives for gastrointestinal stromal tumors. *World J Gastrointest Pathophysiol* 2022; **13**: 15-33 [PMID: 35116177 DOI: 10.4291/wjgp.v13.i1.15]
5 **Sun JH**, Chao M, Zhang SZ, Zhang GQ, Li B, Wu JJ. Coexistence of small cell neuroendocrine carcinoma and villous adenoma in the ampulla of Vater. *World J Gastroenterol* 2008; **14**: 4709-4712 [PMID: 18698690 DOI: 10.3748/wjg.14.4709]
6 **Seifert E**, Schulte F, Stolte M. Adenoma and carcinoma of the duodenum and papilla of Vater: a clinicopathologic study. *Am J Gastroenterol* 1992; **87**: 37-42 [PMID: 1728122]
7 **Nilsson B**, Bümming P, Meis-Kindblom JM, Odén A, Dortok A, Gustavsson B, Sablinska K, Kindblom LG. Gastrointestinal stromal tumors: the incidence, prevalence, clinical course, and prognostication in the preimatinib mesylate era--a population-based study in western Sweden. *Cancer* 2005; **103**: 821-829 [PMID: 15648083 DOI: 10.1002/cncr.20862]
8 **Casali PG**, Blay JY, Abecassis N, Bajpai J, Bauer S, Biagini R, Bielack S, Bonvalot S, Boukovinas I, Bovee JVMG, Boye K, Brodowicz T, Buonadonna A, De Álava E, Dei Tos AP, Del Muro XG, Dufresne A, Eriksson M, Fedenko A, Ferraresi V, Ferrari A, Frezza AM, Gasperoni S, Gelderblom H, Gouin F, Grignani G, Haas R, Hassan AB, Hindi N, Hohenberger P, Joensuu H, Jones RL, Jungels C, Jutte P, Kasper B, Kawai A, Kopeckova K, Krákorová DA, Le Cesne A, Le Grange F, Legius E, Leithner A, Lopez-Pousa A, Martin-Broto J, Merimsky O, Messiou C, Miah AB, Mir O, Montemurro M, Morosi C, Palmerini E, Pantaleo MA, Piana R, Piperno-Neumann S, Reichardt P, Rutkowski P, Safwat AA, Sangalli C, Sbaraglia M, Scheipl S, Schöffski P, Sleijfer S, Strauss D, Strauss SJ, Hall KS, Trama A, Unk M, van de Sande MAJ, van der Graaf WTA, van Houdt WJ, Frebourg T, Gronchi A, Stacchiotti S; ESMO Guidelines Committee, EURACAN and GENTURIS. Gastrointestinal stromal tumours: ESMO-EURACAN-GENTURIS Clinical Practice Guidelines for diagnosis, treatment and follow-up. *Ann Oncol* 2022; **33**: 20-33 [PMID: 34560242 DOI: 10.1016/j.annonc.2021.09.005]
9 **Søreide K**, Sandvik OM, Søreide JA, Giljaca V, Jureckova A, Bulusu VR. Global epidemiology of gastrointestinal stromal tumours (GIST): A systematic review of population-based cohort studies. *Cancer Epidemiol* 2016; **40**: 39-46 [PMID: 26618334 DOI: 10.1016/j.canep.2015.10.031]
10 **Mazur MT**, Clark HB. Gastric stromal tumors. Reappraisal of histogenesis. *Am J Surg Pathol* 1983; **7**: 507-519 [PMID: 6625048 DOI: 10.1097/00000478-198309000-00001]
11 **Hussein MR**, Alqahtani AS, Mohamed AM, Assiri YI, Alqahtani NI, Alqahtani SA, Ali HM, Elyas AAA, Al-Shraim MM, Hussain SS, Abu-Dief EE. A Unique Coexistence of Rectal Adenocarcinoma and Gastric Antral Gastrointestinal Stromal Tumor: A Case Report and Minireview. *Gastroenterology Res* 2021; **14**: 340-347 [PMID: 35059068 DOI: 10.14740/gr1482]
12 **Hakozaki Y**, Sameshima S, Tatsuoka T, Okuyama T, Yamagata Y, Noie T, Oya M, Fujii A, Ueda Y, Shimura C, Katagiri K. Rectal carcinoma and multiple gastrointestinal stromal tumors (GIST) of the small intestine in a patient with neurofibromatosis type 1: a case report. *World J Surg Oncol* 2017; **15**: 160 [PMID: 28835241 DOI: 10.1186/s12957-017-1231-3]
13 **Vassos N**, Agaimy A, Hohenberger W, Croner RS. Coexistence of gastrointestinal stromal tumours (GIST) and malignant neoplasms of different origin: prognostic implications. *Int J Surg* 2014; **12**: 371-377 [PMID: 24632413 DOI: 10.1016/j.ijsu.2014.03.004]
14 **Waidhauser J**, Bornemann A, Trepel M, Märkl B. Frequency, localization, and types of gastrointestinal stromal tumor-associated neoplasia. *World J Gastroenterol* 2019; **25**: 4261-4277 [PMID: 31435178 DOI: 10.3748/wjg.v25.i30.4261]

World Journal of Gastrointestinal Oncology

Submit a Manuscript: https://www.f6publishing.com

World J Gastrointest Oncol 2022 November 15; 14(11): 2266-2272

DOI: 10.4251/wjgo.v14.i11.2266

ISSN 1948-5204 (online)

CASE REPORT

Silent advanced large cell neuroendocrine carcinoma with synchronous adenocarcinoma of the colon: A case report

Hyeon Seok Baek, Sang Wook Kim, Soo Teik Lee, Ho Sung Park, Seung Young Seo

Specialty type: Oncology

Provenance and peer review: Unsolicited article; Externally peer reviewed.

Peer-review model: Single blind

Peer-review report's scientific quality classification

Grade A (Excellent): 0
Grade B (Very good): 0
Grade C (Good): C, C, C, C
Grade D (Fair): 0
Grade E (Poor): 0

P-Reviewer: Liu J, China; Liu Z, China; Niu JK, China; Tanabe H, Japan

Received: July 22, 2022
Peer-review started: July 22, 2022
First decision: August 19, 2022
Revised: August 31, 2022
Accepted: October 12, 2022
Article in press: October 12, 2022
Published online: November 15, 2022

Hyeon Seok Baek, Sang Wook Kim, Soo Teik Lee, Seung Young Seo, Department of Internal Medicine, Research Institute of Clinical Medicine of Jeonbuk National University-Biomedical Research Institute of Jeonbuk National University Hospital, Jeonju-si 56445, Jeollabuk-do, South Korea

Ho Sung Park, Department of Pathology, Jeonbuk National University Medical School, Jeonju-si 56445, Jeollabuk-do, South Korea

Corresponding author: Seung Young Seo, MD, PhD, Professor, Department of Internal Medicine, Research Institute of Clinical Medicine of Jeonbuk National University-Biomedical Research Institute of Jeonbuk National University Hospital, 20 Geonji-ro, Deokjin-gu, Jeonju-si 56445, Jeollabuk-do, South Korea. bear7905@jbnu.ac.kr

Abstract

BACKGROUND

Large cell neuroendocrine carcinoma (LCNEC) accounts for about 0.25% of colorectal cancer patients. Furthermore, synchronous LCNEC and adenocarcinoma coexistence in the colon is very rare. LCNEC are usually aggressive and have a poor prognosis. Usually, colorectal LCNEC patients complain of abdominal symptoms such as pain, diarrhea or hematochezia because it is often diagnosed as an advanced disease that accompanies metastatic lesions.

CASE SUMMARY

We describe a case of relatively asymptomatic synchronous LCNEC and colon adenocarcinoma. A 62-year-old male patient visited our hospital due to anemia detected by a local health check-up. He did not complain of melena, hematochezia or abdominal pain. Physical examination was unremarkable and his abdomen was soft, nontender and nondistended with no palpable mass. Laboratory tests revealed anemia with hemoglobin 5.1 g/dL. Colonoscopy revealed an ulcerofungating lesion in the ascending colon and about a 1.5 cm-sized large sessile polyp in the sigmoid colon. Endoscopic biopsy of the ascending colon lesion revealed the ulcerofungating mass that was LCNEC and endoscopic mucosal resection at the sigmoid colon lesion showed a large polypoid lesion that was adenocarcinoma. Multiple liver, lung, bone and lymph nodes metastasis was found on chest/abdominal computed tomography and positron emission tomography. The patient was diagnosed with advanced colorectal LCNEC with liver, lung, bone and lymph node metastasis (stage IV) and synchronous colonic adenocarcinoma metastasis. In this case, no specific symptom except anemia was

observed despite the multiple metastases. The patient refused systemic chemotherapy and was discharged after transfusion.

CONCLUSION
We report a case of silent LCNEC of the colon despite the advanced state and synchronous adenocarcinoma.

Key Words: Large cell neuroendocrine carcinoma; Colon; Synchronous; Adenocarcinoma; Case report

Core Tip: Large cell neuroendocrine carcinoma (LCNEC) account for about 0.25% of colorectal cancer patients. Furthermore, LCNEC with synchronous or metachronous adenocarcinoma in the colon has been reported in only a few cases. We report the diagnostic experience of a 62-year-old patient with advanced LCNEC in the colon and synchronous adenocarcinoma metastasis but no definitive symptoms except anemia. We suggest the possibility of an association between the two types of primary colon cancer. Therefore, if a patients diagnosed with LCNEC in the colon, appropriate screening tests are required. Further studies are needed on the pathogenesis of the two primary cancers.

Citation: Baek HS, Kim SW, Lee ST, Park HS, Seo SY. Silent advanced large cell neuroendocrine carcinoma with synchronous adenocarcinoma of the colon: A case report. *World J Gastrointest Oncol* 2022; 14(11): 2266-2272
URL: https://www.wjgnet.com/1948-5204/full/v14/i11/2266.htm
DOI: https://dx.doi.org/10.4251/wjgo.v14.i11.2266

INTRODUCTION

Large cell neuroendocrine carcinoma (LCNEC) accounts for about 0.25% of colorectal cancer patients [1]. Patients with colorectal LCNEC are usually found to be in an advanced stage with metastasis at the time of diagnosis[2]. Furthermore, LCNEC with synchronous or metachronous adenocarcinoma in the colon has been reported in only a few cases[3,4].

The symptoms of colorectal LCNEC are not different from those of conventional colonic adenocarcinoma. Patients with colorectal LCNEC usually present with abdominal symptoms such as abdominal pain, diarrhea, hematochezia or tenesmus. Paraneoplastic and carcinoid syndromes which have resulted from excessive hormone production, may rarely be a clinical presentation[5]. Contrast enhanced computed tomography (CT) and magnetic resonance imaging are useful for initial diagnosis and staging of disease in patients with gastroenteropancreatic neuroendocrine tumors (NETs)[6]. However, there are no specific characteristic imaging findings of colorectal LCNEC.

The diagnosis of LCNEC is based on pathologic findings. Histologic features of LCNEC are trabecular growth, organoid nesting, rosettes and perilobular palisading patterns. The tumor cells are generally large and shows moderate to abundant cytoplasm. Nucleoli are often detected and their presence facilitates distinction from small cell carcinoma. Several immunohistochemical markers such as synaptophysin, chromogranin and neural cell adhesion molecule (CD56) are useful for confirmation of neuroendocrine differentiation. However, one positive marker is enough if the staining is clearcut[7].

Here, we report on a case of advanced LCNEC (stage IV) in the colon and synchronous adenocarcinoma metastasis in a patient with no specific symptoms except anemia. This case report was approved by the Institutional Review Board of Jeonbuk National University Hospital (IRB No. CUH 2022-07-002), and the patient has signed the informed consent for publication of the case (date of the consent: 2022-04-14).

CASE PRESENTATION

Chief complaints

A 62-year-old male patient visited the hospital for anemia detected by a local health check-up.

History of present illness

He denied abdominal symptoms such as pain, diarrhea and hematochezia.

History of past illness
His medical history was unremarkable.

Personal and family history
He was a non-smoker and non-alcohol drinker and had no significant family history.

Physical examination
Physical examination was unremarkable.

Laboratory examinations
Laboratory tests revealed anemia with hemoglobin 5.1 g/dL and a normal liver function test. Serum carcinoembryonic antigen (3.01 ng/mL) and carbohydrate antigen 19-9 (< 9.0 U/mL) were also within normal limits.

Imaging examinations
Esophagogastroduodenoscopy and colonoscopy were performed to find the cause of anemia. Colonoscopy revealed a circumferential ulcerofungating mass in the ascending colon and a biopsy was performed (Figure 1A). Furthermore, about a 1.5 cm-sized large sessile polyp was seen in the sigmoid colon and endoscopic mucosal resection was performed (Figure 1B). Advanced ascending colon cancer was suspected and the patient underwent a chest/abdominopelvic CT. The abdominopelvic CT showed irregular wall thickening over a length of about 10 cm in the ascending colon with regional fat stranding and multiple pericolic lymph node enlargements, thickening and nodularity in the adjacent peritoneum. Moreover, numerous low-density lesions with a maximal 8.7 cm diameter in both the liver lobe (Figure 2A). The chest CT showed left supraclavicular lymph node enlargement (Figure 2B) and a tiny nodule of about 6 mm in the right lung upper lobe.

In the pathology report, an ulcerofungating mass in the ascending colon was confirmed as LCNEC, and a large polypoid lesion in the sigmoid colon was confirmed as adenocarcinoma (Figure 3). The LCNEC showed strong immunoreactivity for synaptophysin. The mitotic index was > 30/10HPF and the Ki-67 index was 65.7%, suggesting a poor prognosis. Both the LCNEC and colonic adenocarcinoma showed positive immunohistochemical stain for CK20.

Positron emission tomography revealed abnormal fluorodeoxyglucose uptake at the ascending colon with enlarged lymph nodes at the adjacent mesentery and hematogenous metastasis in the liver, lung, bones, peritoneum and supraclavicular lymph node (Figure 4).

FINAL DIAGNOSIS
The patient was diagnosed with advanced colorectal LCNEC with liver, lung, bone and lymph nodes metastasis (stage IV) and synchronous colonic adenocarcinoma metastasis.

TREATMENT
Systemic chemotherapy was considered but the patient refused treatment and was discharged.

OUTCOME AND FOLLOW-UP
At 3 mo after diagnosis, the patient received the best supportive care and was still alive.

DISCUSSION
Gastroenteropancreatic neuroendocrine neoplasms (NENs) occur in the neuroendocrine cells of the gastroenteropancreatic tract and are also known as carcinoids and islet cell tumors. Well-differentiated NENs are classified as NETs G1 or G2. NET G1 can be identical with carcinoid. The term NEC refers to all poorly differentiated NENs. NEC is classified into minor and large cell variants[8]. Most NETs are carcinoids and have a better prognosis than conventional adenocarcinomas.

On the other hand, LCNEC is known to be an aggressive disease and have a poor prognosis[9]. However, in this case, the patient had no abdominal symptoms such as melena, hematochezia or pain despite the advanced LCNEC with multiple metastases. Moreover, no progressive LCNEC-associated symptoms except asymptomatic anemia were observed in this case.

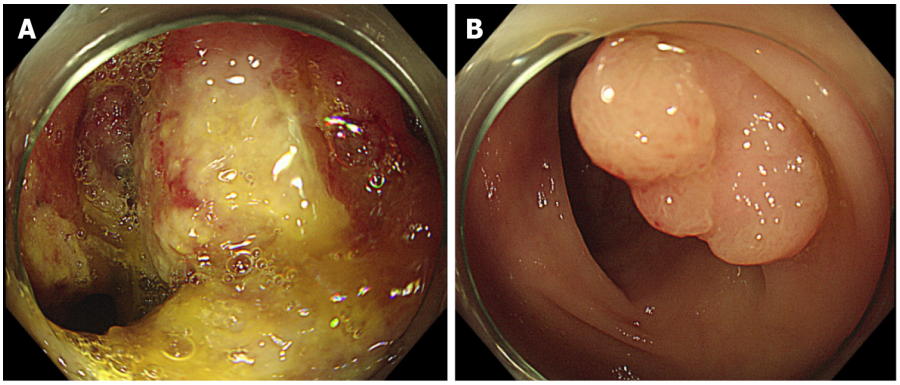

DOI: 10.4251/wjgo.v14.i11.2266 **Copyright** ©The Author(s) 2022.

Figure 1 Colonoscopy images. A: Ulcerofungating lesion involving the luminal circumference in the ascending colon; B: About a 1.5 cm sized sessile polyp in the sigmoid colon.

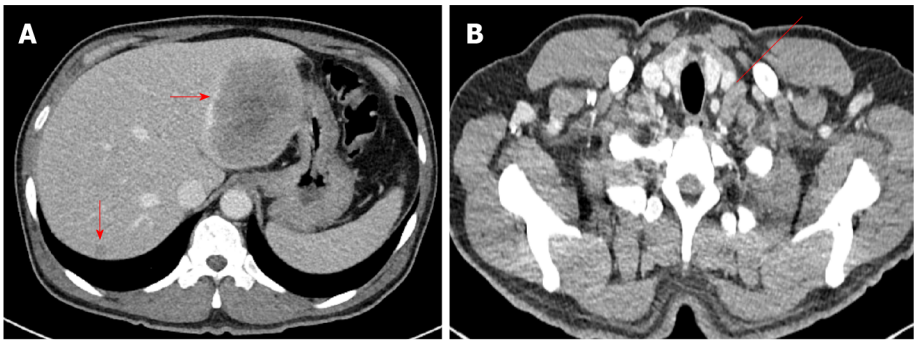

DOI: 10.4251/wjgo.v14.i11.2266 **Copyright** ©The Author(s) 2022.

Figure 2 Abdominopelvic computed tomography and chest computed tomography images. A: Low density lesion of about 8.7 cm in the left lobe of the liver, and several smaller lesions in the right lobe of the liver (arrow); B: Left supraclavicular lymph node enlargement (line).

The prognosis of colorectal LCNEC is poor. Colorectal LCNEC is a highly aggressive neoplasm with a high mortality rate[10], and 36% of LCNEC patients had distant metastasis at the time of diagnosis. The liver is the most involved organ in metastatic disease[11]. In this case, multiple metastatic lesions in the liver, lungs, bones, peritoneum and lymph nodes were noted at the diagnosis.

LCNEC with synchronous or metachronous adenocarcinoma in the colon has been reported only in a few cases. The pathophysiological association between neuroendocrine carcinoma and adenocarcinoma is still unclear. Some suggest a possible association in the pathogenesis of the colorectal NET and adenocarcinoma[12,13]. CK20 is known as a common marker in colorectal adenocarcinoma. Kato *et al* [13] reported a CK20 positive colonic LCNEC which is accompanied by synchronous colorectal adenocarcinoma. This report suggested different types of gastrointestinal neoplasm might originate from a common stem cell clone which might share a similar genetic mutation(s) during early oncogenesis. In our case, an immunohistochemical stain for CK20 was performed on the colonic LCNEC and adenocarcinoma, and both were confirmed to be immunoreactive (Figures 3G and 3H), supporting the theory of Kato *et al*[13]. Therefore, when LCNEC of the colon is diagnosed, it can be accompanied by synchronous or metachronous colonic adenocarcinoma and a close examination of the remaining colon is required. In addition, colonoscopy follow-up should be considered.

The primary treatment of colorectal LCNEC is surgery if R0 resection is possible[14]. When complete resection is impossible, a debulking procedure and cytoreductive therapy or systemic chemotherapy should be considered[15]. LCNEC is similar to small cell neuroendocrine carcinoma (SCNEC) in histogenesis, biology and clinical behavior. For patients with locally advanced or metastatic disease, extrapolation from the treatment paradigms for both non-SCNEC and SCNEC, with chemoradiation and chemotherapy in stage III, and chemotherapy and palliative radiation in stage IV, seems reasonable. Regarding drug choice for systemic chemotherapy, regimens based on efficacy in SCNEC such as etoposide and a platinating agent are preferred[16]. There are no established guidelines for patients diagnosed with LCNEC with synchronous adenocarcinoma of the colon, but chemotherapy can be considered depending on which disease is predominant. In this case, LCNEC was considered a more predominant lesion than adenocarcinoma and a chemotherapy with a combination of cisplatin and etoposide was considered, but the patient refused.

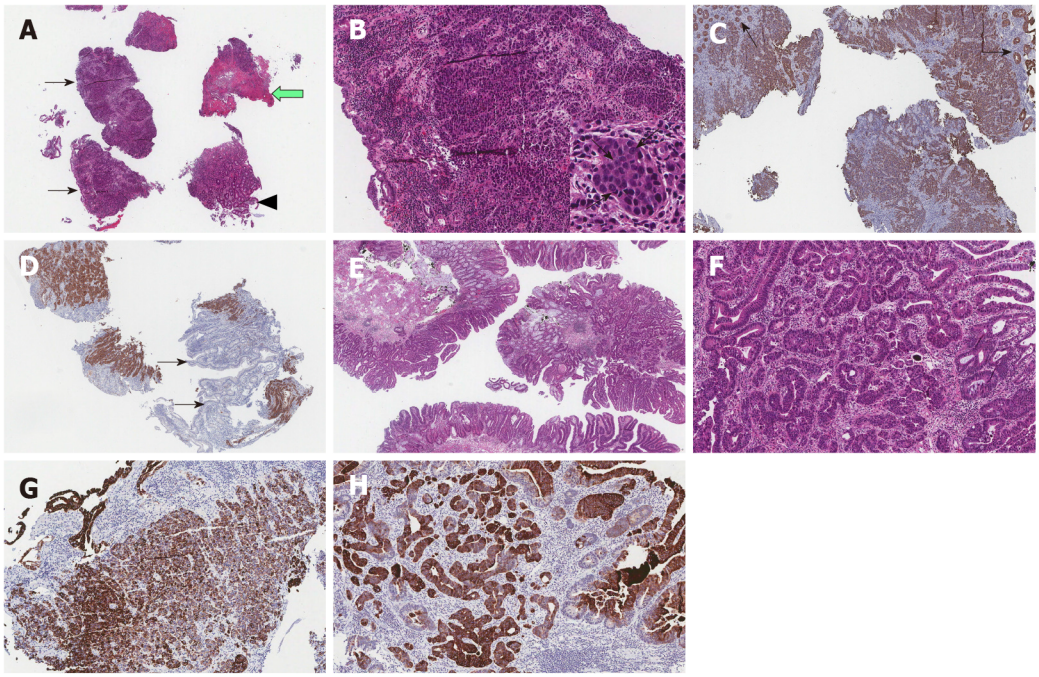

DOI: 10.4251/wjgo.v14.i11.2266 **Copyright** ©The Author(s) 2022.

Figure 3 Histologic and immunohistochemical findings of colonic large cell neuroendocrine carcinoma. Histologic findings of colonic adenocarcinoma. Immunohistochemical stain for CK20 in both colonic large cell neuroendocrine carcinoma and colonic adenocarcinoma. A: Low power view of biopsy specimen reveals several tissue fragments mainly consisted of tumor (black arrows), ulcer debris (white arrow), and non-neoplastic colonic mucosa (arrowhead) (HE, × 20); B: Medium power view displays invasive tumor cells forming organoid structures such as cords or small nests (HE, × 100). Tumor cells display severe atypia and have round nuclei, sometimes with prominent nucleoli (arrows), and moderate amounts of cytoplasm, with high mitotic rate (Inset, HE, × 400); C: Infiltrating tumor cells are identified by immunohistochemical stain for cytokeratin (CK, × 100). Note the non-neoplastic mucosal glands (arrows) that are separated from the tumor; D: Tumor cells show strong immunoreactivity for neuroendocrine marker (synaptophysin, × 100). Note the non-neoplastic mucosal glands (arrows) are negative for neuroendocrine marker; E: Low power view of biopsy specimen reveals colonic epithelial proliferative lesion forming tubular and papillary structures (HE, × 20); F: Medium power view displays invasive growth of tumor cells that form irregular branching and budding of glands (HE, × 100); G: Infiltrating tumor cells of colonic large cell neuroendocrine carcinoma are immunoreactive for CK20 (× 100); H: Invasive tumor glands of colonic adenocarcinoma are also immunoreactive for CK20 (× 100).

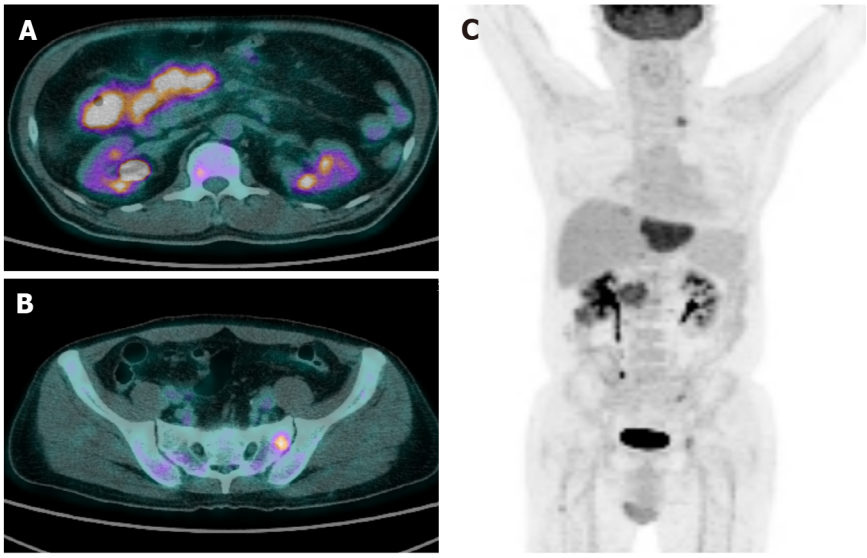

DOI: 10.4251/wjgo.v14.i11.2266 **Copyright** ©The Author(s) 2022.

Figure 4 Positron emission tomography images. A: Abnormal fluorodeoxyglucose uptake at the ascending colon with enlarged lymph nodes at the adjacent mesentery; B and C: Hematogenous metastasis in the liver, lung, bones, peritoneum, supraclavicular lymph node.

CONCLUSION

In conclusion, we report on a case of silent LCNEC of the colon despite the advanced state and

synchronous adenocarcinoma, suggesting the possibility of an association between the two types of primary colon cancer. In patients diagnosed with LCNEC in the colon, there is a possibility of synchronous or metachronous adenocarcinoma after surgical treatment, so appropriate screening tests are required. Further studies are needed on the pathogenesis of the two primary cancers.

FOOTNOTES

Author contributions: Baek HS analyzed clinical data and drafted the manuscript; Lee ST, Kim SW, Seo SY advised and reviewed the manuscript; Park HS performed the pathologic review.

Informed consent statement: Informed written consent was obtained from the patient regarding the publication of this report and accompanying images.

Conflict-of-interest statement: All the authors report no relevant conflicts of interest for this article.

CARE Checklist (2016) statement: The authors have read the CARE Checklist (2016), and the manuscript was prepared and revised according to the CARE Checklist (2016).

Country/Territory of origin: South Korea

ORCID number: Hyeon Seok Baek 0000-0002-8959-302X; Sang Wook Kim 0000-0001-8209-540X; Soo Teik Lee 0000-0002-2975-053X; Ho Sung Park 0000-0002-4879-874X; Seung Young Seo 0000-0003-2018-0013.

S-Editor: Wang JJ
L-Editor: Filipodia
P-Editor: Wang JJ

REFERENCES

1 **Bernick PE**, Klimstra DS, Shia J, Minsky B, Saltz L, Shi W, Thaler H, Guillem J, Paty P, Cohen AM, Wong WD. Neuroendocrine carcinomas of the colon and rectum. *Dis Colon Rectum* 2004; **47**: 163-169 [PMID: 15043285 DOI: 10.1007/s10350-003-0038-1]
2 **Minocha V**, Shuja S, Ali R, Eid E. Large cell neuroendocrine carcinoma of the rectum presenting with extensive metastatic disease. *Case Rep Oncol Med* 2014; **2014**: 386379 [PMID: 25225617 DOI: 10.1155/2014/386379]
3 **Park JS**, Kim L, Kim CH, Bang BW, Lee DH, Jeong S, Shin YW, Kim HG. Synchronous large-cell neuroendocrine carcinoma and adenocarcinoma of the colon. *Gut Liver* 2010; **4**: 122-125 [PMID: 20479925 DOI: 10.5009/gnl.2010.4.1.122]
4 **Lin KH**, Chang NJ, Liou LR, Su MS, Tsao MJ, Huang ML. Metachronous adenocarcinoma and large cell neuroendocrine carcinoma of the colon. *Formos J Surg* 2018; **51**: 76 [DOI: 10.4103/fjs.fjs_2_17]
5 **Vilallonga R**, Espín Basany E, López Cano M, Landolfi S, Armengol Carrasco M. [Neuroendocrine carcinomas of the colon and rectum. A unit's experience over six years]. *Rev Esp Enferm Dig* 2008; **100**: 11-16 [PMID: 18358055 DOI: 10.4321/s1130-01082008000100003]
6 **Sahani DV**, Bonaffini PA, Fernández-Del Castillo C, Blake MA. Gastroenteropancreatic neuroendocrine tumors: role of imaging in diagnosis and management. *Radiology* 2013; **266**: 38-61 [PMID: 23264526 DOI: 10.1148/radiol.12112512]
7 **The International Agency for Research on Cancer**, Travis WD, Brambilla E, Muller-Hermelink HK, Harris CC. Pathology and Genetics of Tumours of the Lung, Pleura, Thymus and Heart (IARC WHO Classification of Tumours) 1st Edition. Switzerland: World Health Organization, 2004
8 **Schott M**, Klöppel G, Raffel A, Saleh A, Knoefel WT, Scherbaum WA. Neuroendocrine neoplasms of the gastrointestinal tract. *Dtsch Arztebl Int* 2011; **108**: 305-312 [PMID: 21629514 DOI: 10.3238/arztebl.2011.0305]
9 **Emory RE Jr**, Emory TS, Goellner JR, Grant CS, Nagorney DM. Neuroendocrine ampullary tumors: spectrum of disease including the first report of a neuroendocrine carcinoma of non-small cell type. *Surgery* 1994; **115**: 762-766 [PMID: 8197570]
10 **Staren ED**, Gould VE, Jansson DS, Hyser M, Gooch GT, Economou SG. Neuroendocrine differentiation in "poorly differentiated" colon carcinomas. *Am Surg* 1990; **56**: 412-419 [PMID: 2368984]
11 **Aytac E**, Ozdemir Y, Ozuner G. Long term outcomes of neuroendocrine carcinomas (high-grade neuroendocrine tumors) of the colon, rectum, and anal canal. *J Visc Surg* 2014; **151**: 3-7 [PMID: 24412088 DOI: 10.1016/j.jviscsurg.2013.12.007]
12 **Lipka S**, Hurtado-Cordovi J, Avezbakiyev B, Freedman L, Clark T, Rizvon K, Mustacchia P. Synchronous Small Cell Neuroendocrine Carcinoma and Adenocarcinoma of the Colon: A Link for Common Stem Cell Origin? *ACG Case Rep J* 2014; **1**: 96-99 [PMID: 26157837 DOI: 10.14309/crj.2014.13]

13 **Kato T**, Terashima T, Tomida S, Yamaguchi T, Kawamura H, Kimura N, Ohtani H. Cytokeratin 20-positive large cell neuroendocrine carcinoma of the colon. *Pathol Int* 2005; **55**: 524-529 [PMID: 15998383 DOI: 10.1111/j.1440-1827.2005.01864.x]

14 **Pascarella MR**, McCloskey D, Jenab-Wolcott J, Vala M, Rovito M, McHugh J. Large cell neuroendocrine carcinoma of the colon: A rare and aggressive tumor. *J Gastrointest Oncol* 2011; **2**: 250-253 [PMID: 22811859 DOI: 10.3978/j.issn.2078-6891.2011.026]

15 **Arnold R**. Endocrine tumours of the gastrointestinal tract. Introduction: definition, historical aspects, classification, staging, prognosis and therapeutic options. *Best Pract Res Clin Gastroenterol* 2005; **19**: 491-505 [PMID: 16183523 DOI: 10.1016/j.bpg.2005.03.006]

16 **Glisson BS**, Moran CA. Large-cell neuroendocrine carcinoma: controversies in diagnosis and treatment. *J Natl Compr Canc Netw* 2011; **9**: 1122-1129 [PMID: 21975912 DOI: 10.6004/jnccn.2011.0093]

World Journal of Gastrointestinal Oncology

Submit a Manuscript: https://www.f6publishing.com

World J Gastrointest Oncol 2022 November 15; 14(11): 2273-2287

DOI: 10.4251/wjgo.v14.i11.2273

ISSN 1948-5204 (online)

CASE REPORT

Surgical management of monomorphic epitheliotropic intestinal T-cell lymphoma followed by chemotherapy and stem-cell transplant: A case report and review of the literature

Abdul Saad Bissessur, Ji-Chun Zhou, Ling Xu, Zhao-Qing Li, Si-Wei Ju, Yun-Lu Jia, Lin-Bo Wang

Specialty type: Oncology

Provenance and peer review: Unsolicited article; Externally peer reviewed.

Peer-review model: Single blind

Peer-review report's scientific quality classification

Grade A (Excellent): A
Grade B (Very good): B, B
Grade C (Good): 0
Grade D (Fair): 0
Grade E (Poor): 0

P-Reviewer: Basson MD, United States; Paparoupa M, Deutschland; Piltcher-da-Silva R, Brazil

Received: July 26, 2022
Peer-review started: July 26, 2022
First decision: August 8, 2022
Revised: August 22, 2022
Accepted: October 11, 2022
Article in press: October 11, 2022
Published online: November 15, 2022

Abdul Saad Bissessur, Ji-Chun Zhou, Ling Xu, Zhao-Qing Li, Si-Wei Ju, Lin-Bo Wang, Department of Surgical Oncology, Sir Run Run Shaw Hospital, Zhejiang University School of Medicine, Hangzhou 310006, Zhejiang Province, China

Yun-Lu Jia, Department of Medical Oncology, First Affiliated Hospital, Zhejiang University School of Medicine, Hangzhou 310006, Zhejiang Province, China

Corresponding author: Lin-Bo Wang, Doctor, MBBS, MD, PhD, Attending Doctor, Chief Doctor, Director, Professor, Surgical Oncologist, Department of Surgical Oncology, Sir Run Run Shaw Hospital, Zhejiang University School of Medicine, No. 3 Eastern Qingchun Road, Hangzhou 310006, Zhejiang Province, China. linbowang@zju.edu.cn

Abstract

BACKGROUND

Monomorphic epitheliotropic intestinal T-cell lymphoma (MEITL) is a rare and rapidly progressive intestinal T-cell non-Hodgkin lymphoma associated with a very poor prognosis and a median survival of 7 mo. Advances in the identification of MEITL over the last two decades have led to its recognition as a separate entity. MEITL patients, predominantly male, typically present with vague and nonspecific symptoms and diagnosis is predominantly confirmed at laparotomy. Currently, there are no standardized treatment protocols, and the optimal therapy remains unclear.

CASE SUMMARY

We report a case of MEITL that was initially considered to be gastrointestinal stromal tumor (GIST) and Imatinib was administered for one cycle. The 62-year-old man presented with abdominal pain, abdominal distension, and weight loss of 20 pounds. Within 2 wk, the size of the mass considerably increased on computed tomography scans. The patient underwent surgery followed by chemotherapy with CHOP (cyclophosphamide, doxorubicin, vincristine, and prednisone) and stem-cell transplant. A correct diagnosis of MEITL was established based on postoperative pathology. Immunophenotypically, the neoplastic cells fulfilled the diagnostic criteria for MEITL as they were $CD3^+$, $CD4^+$, $CD8^+$, $CD56^+$, and $TIA\text{-}1^+$.

CONCLUSION

Given that MEITL has no predisposing factor and presents with vague symptoms with rapid progression, the concomitant presence of abdominal symptoms and B

symptoms (weight loss, fever, and night sweats) with hypoalbuminemia, anemia, low lymphocytic count and endoscopic findings of diffuse infiltrating type lesions should alert physicians to this rare disease, especially when it comes to Asian patients. Immediate laparotomy should then be carried out followed by chemotherapy and stem-cell transplant.

Key Words: Monomorphic epitheliotropic intestinal T-cell lymphoma; Gastrointestinal stromal tumor; Immunophenotypically; Chemotherapy; Stem-cell transplant; Case report

Core Tip: Monomorphic epitheliotropic intestinal T-cell lymphoma (MEITL) is a rare and rapidly progressive intestinal T-cell non-Hodgkin lymphoma. Currently, there is no standardized treatment or diagnostic protocols for MEITL. Chemotherapy followed by stem-cell transplant postoperatively has shown promising results in terms of remission and progression free survival. Since MEITL is associated with a poor prognosis and high recurrence, it is crucial that the oncologist should follow and monitor any relapsing signs.

Citation: Bissessur AS, Zhou JC, Xu L, Li ZQ, Ju SW, Jia YL, Wang LB. Surgical management of monomorphic epitheliotropic intestinal T-cell lymphoma followed by chemotherapy and stem-cell transplant: A case report and review of the literature. *World J Gastrointest Oncol* 2022; 14(11): 2273-2287
URL: https://www.wjgnet.com/1948-5204/full/v14/i11/2273.htm
DOI: https://dx.doi.org/10.4251/wjgo.v14.i11.2273

INTRODUCTION

Monomorphic epitheliotropic intestinal T-cell lymphoma (MEITL), formerly known as enteropathy-associated T-cell lymphoma type II (EATL type II), is a rare non-Hodgkin primary lymphoma of the gastrointestinal tract arising from intraepithelial T-cells[1].

Previously, EATL was recognized as a single entity of small intestinal lymphoma and was termed as enteropathy-type T-cell lymphoma. But in 2008, the World Health Organization (WHO) classified the disease into two subtypes: (1) EATL type I, which comprises of 80%-90% of all cases; and (2) EATL type II, accounting for 10%-20% (a rather monomorphic variant)[2]. EATL accounted for 5.4% of all lymphomas based on an international survey[3].

However, after 2008, studies revealed noteworthy and remarkable clinical and pathological differences between the two types of lymphoma aforementioned. As a result, the WHO redefined these lymphomas as distinct and separate entities: Type I EATL was then termed as enteropathy-associated T-cell lymphoma and type II, owing to its distinctive nature, was designated as MEITL[4]. The nomenclature and classification are illustrated in Figure 1.

The geographic distribution of EATL and MEITL varies: EATL is seen more often in areas with a high prevalence of celiac disease (particularly Northern Europe) whereas MEITL has a broader geographic distribution and is seen in regions where celiac disease is rare, particularly in Asian countries[2,4]. The findings of a study conducted in Asia which included 38 cases of MEITL suggested that intestinal T-cell lymphomas might be merely MEITL in Asian patients[5].

Male predominance (ratio 2.6:1.0) has been observed in MEITL and the median age of onset is 58 years old, with the small intestine as the most commonly involved site[6]. Upon consultation, MEITL patients typically present with vague and nonspecific symptoms such as abdominal pain, fatigue, weight loss, small bowel perforation, diarrhea, and gastrointestinal (GI) obstruction[2,5,7]. Low albumin, increased lactate dehydrogenase (LDH), and elevated C-Reactive protein (CRP) have been observed in most studies of MEITL cases[2,5].

Tumor cells with a monomorphic shape, an epitheliotropic pattern, $CD8^+$, and $CD56^+$ are the diagnostic criteria for MEITL and serve to distinguish them from other types of T-cell lymphoma[8].

The vagueness of symptoms and/or lack of all symptoms at presentation make the initial diagnosis of T-cell lymphoma challenging. In addition, primary diagnosis of MEITL can be delayed until further investigation due to the similar symptoms/imaging manifestations to those of other GI cancers. Another challenge that may be encountered is intestinal obstruction and perforation. Thus, diagnosis is predominantly confirmed at laparotomy[9].

Herein, we present a case of MEITL, the treatment approach, and follow-up result. This case report and literature review will provide an up-to-date insight into the management of MEITL. Because of a relatively poor prognosis and a median survival of only 7 mo[5], weight loss, elevated LDH and CRP, and low albumin should alert the physician especially when it comes to Asian patients. No standardized

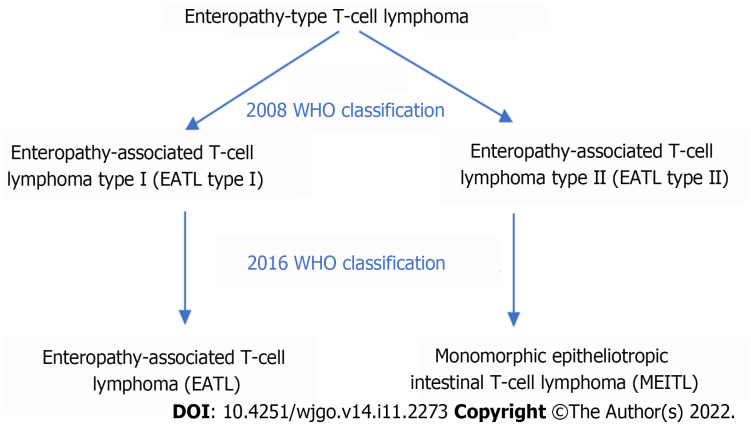

DOI: 10.4251/wjgo.v14.i11.2273

Figure 1 Evolution of classification of monomorphic epitheliotropic intestinal T-cell lymphoma.

treatment is yet established for MEITL due to the rarity of the disease. However, surgical resection followed by chemotherapy and/or autologous stem cell transplantation has been demonstrated to have better outcomes compared to surgery alone. In addition, new clinical trials using novel regimen of IVE/MTX (ifosfamide, vincristine, etoposide/methotrexate) followed by autologous stem cell transplant have proven significantly better outcomes with a 65% complete remission and 60% 5-year survival rate [10].

CASE PRESENTATION

Chief complaints

A 62-year-old man visited our hospital with a 2-mo history of abdominal pain and distension.

History of present illness

The patient had persistent epigastric pain half an hour after eating, which alleviated after a few hours. The patient's bowel habits varied between constipation and diarrhea. His symptoms gradually aggravated. He reported a weight loss of 20 pounds.

History of past illness

The patient had no history of other illnesses such as hypertension, diabetes, or heart disease. He had a full positron emission tomography (PET)/computed tomography (CT) scan in the previous year which revealed no abnormality, highlighting the rapid and aggressive progression of the disease.

At an outside hospital, the patient underwent a gastroscopy which showed chronic superficial gastritis and a colonoscopy which revealed multiple colorectal polyps and proctitis. Half a month later, he came to our hospital for further treatment and diagnosis.

Personal and family history

The patient had no significant personal and family history.

Physical examination

Physical abdominal examination revealed abdominal distension on inspection and decreased bowel sounds on auscultation. On palpation, a 15-cm mass could be felt. The mass had a clear boundary and an irregular shape. The abdomen was soft and deep palpation revealed left lower abdominal tenderness.

Laboratory examinations

Laboratory tests and blood workouts revealed an elevated level of CRP at 163.5 mg/L, normal lactate dehydrogenase at 180 IU/L, albumin at 36.2 g/L, lymphocytic percentage at 0.58%, and hemoglobin at 113 g/L. Other laboratory results are shown in Table 1. Tumor markers were all within the normal ranges (Table 2).

Imaging examinations

The patient had two CT scans 2 wk apart at our hospital. An increase in the size of the mass was observed on the second CT scan, with significant necrosis (Figure 2). The size of the mass on the first and second CT scans was estimated to be approximately 85 mm × 74 mm × 107 mm and 113 mm × 97 mm ×

Table 1 Patient's laboratory results of blood chemistry

Item	Result	Reference value
White blood cell count (× 10^9/L)	7.8	3.5-9.5
Neutrophils (%)	88.2	40.0-75.0
Eosinophils (%)	0.6	0.4-0.8
Basophils (%)	0.3	0.0-1.0
Lymphocytes (%)	0.58	1.10-3.20
Monocytes (%)	0.28	0.10-0.60
Red blood cell count (× 10^{12}/L)	3.87	4.30-5.80
Hemoglobin (g/L)	113	130-175
Mean corpuscular volume (fL)	88.6	82.0-100.0
Platelet count (× 10^9/L)	380	125-350
Hematocrit (%)	0.34	0.11-0.28
Lactate dehydrogenase (IU/L)	180	120-250
C-reactive protein (mg/L)	163.5	< 6.0
Direct bilirubin (umol/L)	2.7	0.0-4.0
Indirect bilirubin (umol/L)	7.90	0.00-22.00
Creatine kinase (U/L)	45	50-310
Total protein (g/L)	67.7	65.0-85.0
Albumin (g/L)	36.2	40.0-55.0
Globulin (g/L)	31.4	25.0-35.0
Glucose (mmol/L)	6.34	4.30-5.90

Table 2 Tumor markers

Marker	Result	Reference value
CA211	1.05	0.0-3.3
SCC	1.08	0.0-1.5
CA724	1.36	0.0-6.9
CA242	4.89	0.0-20.0
CA125	31.51	< 35.0
CA-153	12.87	< 25.0
CEA	1.97	0.0-5.0
CA19-9	18.57	< 37.0

146 mm, respectively. Local mesenteric lymph nodes were enlarged.

FURTHER DIAGNOSTIC WORK-UP

The patient was consulted at the General Surgery Department of our hospital and gastrointestinal stromal tumor (GIST) was initially considered due to the imaging presentation of the tumor (Figure 2) and the associated symptoms. Gleevec (Imatinib) was administered as empirical neoadjuvant targeting therapy. He had 5-8 times of diarrhea/d after oral administration of Gleevec.

While the patient was on Gleevec, his symptoms further aggravated, with a higher accumulation of pelvic fluid accompanied with fever (maximum of 37.9 °C). As intestinal perforation and peritonitis were suspected, and the patient underwent emergency surgery.

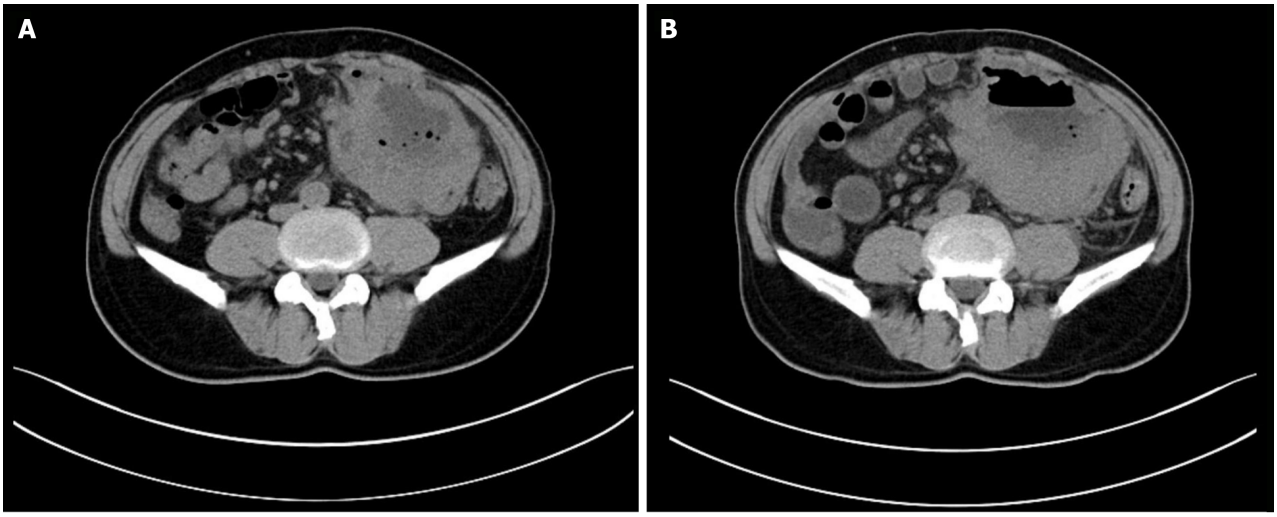

DOI: 10.4251/wjgo.v14.i11.2273 **Copyright** ©The Author(s) 2022.

Figure 2 Computed tomography images. A: First computed tomography (CT) scan; B: Second CT scan 2 wk later. Multiple enlarged mesenteric lymph nodes and apparent necrosis were noted on the second CT scan.

Postoperative immunohistochemistry findings revealed CD3 (+), CD20 (-), CD21 (residual FDC +), CD138 (-), Kappa (+), Lambda (+), Ki-67 (80%), CD117 (-), CD4 (+), CD5 (-), CD7 (+), CD8 (+), CD30 (-), CD10 (-), PD-1 (-), CK-PAN (-), GranzymeB (+), TIA-1 (+), and CD56 (+) (Figure 3). Epstein-Barr virus (EBV)-encoded RNA (EBER) *in situ* hybridization was negative. The results are listed in Table 3.

FINAL DIAGNOSIS

Based on postoperative immunohistochemistry findings, the final diagnosis was MEITL.

TREATMENT

The patient underwent surgery followed by chemotherapy and stem-cell transplant.

Intraoperative findings

The size of the mass was estimated to be 15 cm × 14 cm × 10 cm and the margin was not clear. The texture was hard. Superficial purulent exudation was observed. The tumor had inflammatory adhesions with the mesentery of the small intestine, descending colon, and transverse colon. The relationship between the tumor and left psoas major muscle and left ureter was unclear. Specimens were sent for further pathology diagnosis after tumor resection.

OUTCOME AND FOLLOW-UP

After surgery and before systemic treatment, ^{18}F-fluorodeoxyglucose (FDG) PET/CT scan (Figure 4) revealed no remarkable abnormalities, no abnormal density focus, and no significant increase or decrease in radioactivity uptake. There was no significant thickening and increase of radioactivity uptake in the anastomotic intestinal wall. The metabolism of FDG was increased in the middle abdomen subcutaneously. Several large lymph nodes were spotted in the left abdominal mesenteric area, with the largest measuring 1.1 cm × 1.6 cm. The standardized uptake value (SUV) of the left mesentery was 1.6. An increase in the metabolism of FDG was also noted in the ascending colon.

In addition, the patient underwent a bone marrow biopsy, which showed no overt morphologic or flow cytometry evidence of T-cell lymphoma or metastatic malignancy (Figure 5).

A month after surgery, the patient was started on chemotherapy with CHOP (cyclophosphamide, doxorubicin, vincristine, and prednisone), scheduled for four cycles, every 3 wk. After chemotherapy, the patient underwent stem-cell transplant. Between surgery and the first cycle of CHOP chemotherapy, the patient developed an itchy rash on his hands which subsequently relieved after his first chemotherapy cycle.

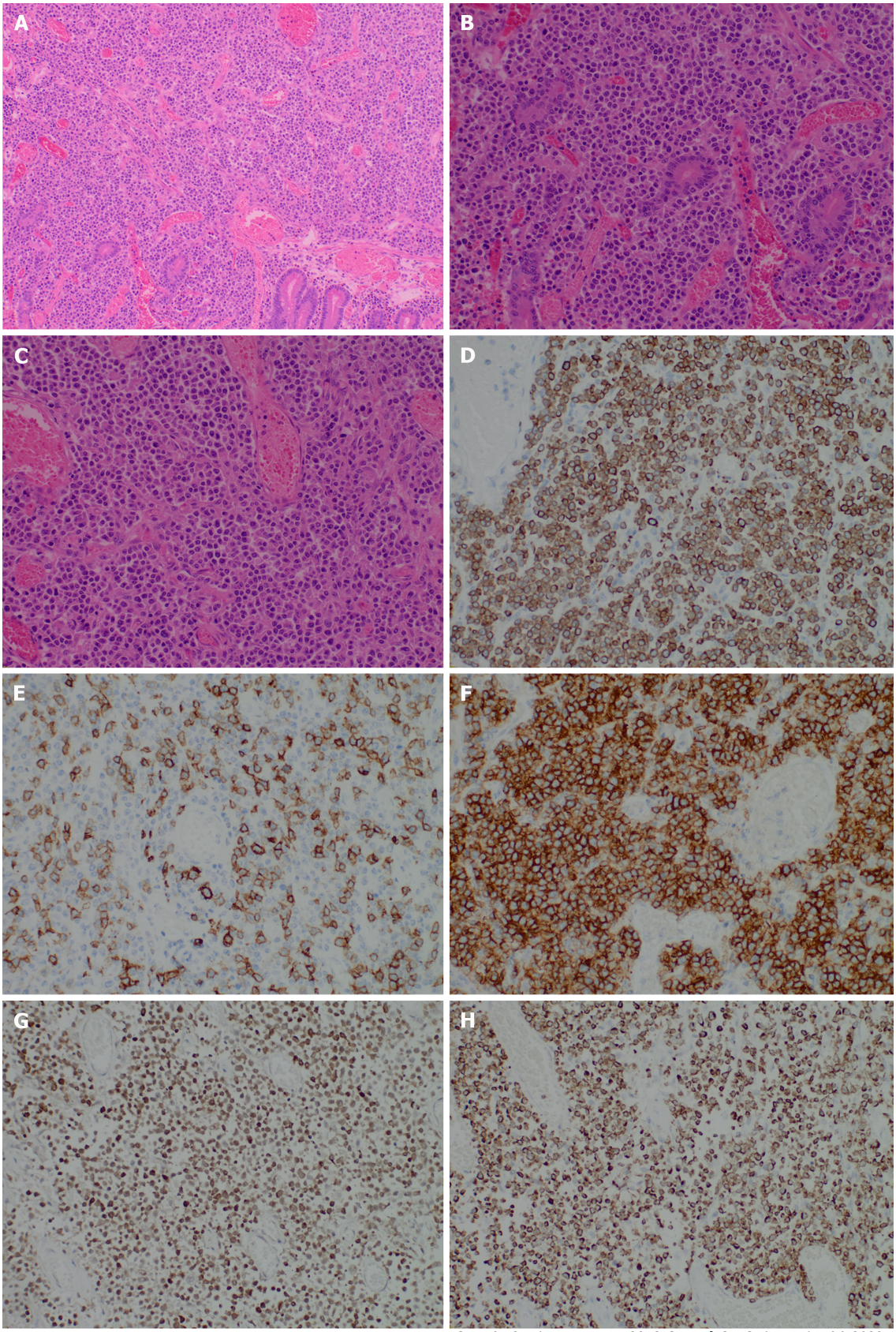

DOI: 10.4251/wjgo.v14.i11.2273

Figure 3 Pathologic and immunohistochemistry findings. A and B: Low magnification (A) (× 40, H&E) and high magnification (B) (× 200, H&E) images of lymphocytes demonstrating an epitheliotropic pattern; C: The shape of lymphoma cells is uniform throughout, emphasizing the monomorphism; D-H: The tumor cells were positive for CD3 (D), CD8 (E), CD56 (F), Granzyme B (G), and TIA-1 (H). (C-H, magnification × 200).

Table 3 Panel of immunohistochemical stains

IHC stain	Result
CD3	+
CD4	+
CD5	-
CD7	+
CD8	+
CD30	-
CD56	+
CD117	-
CD138	-
Ki-67	80%
Kappa	+
Lambda	+
PD-1	-
CK-PAN	-
TIA-1	+
Granzyme B	+
EBER ISH	-

IHC: Immunohistochemistry; EBER: Epstein-Barr virus-encoded RNA.

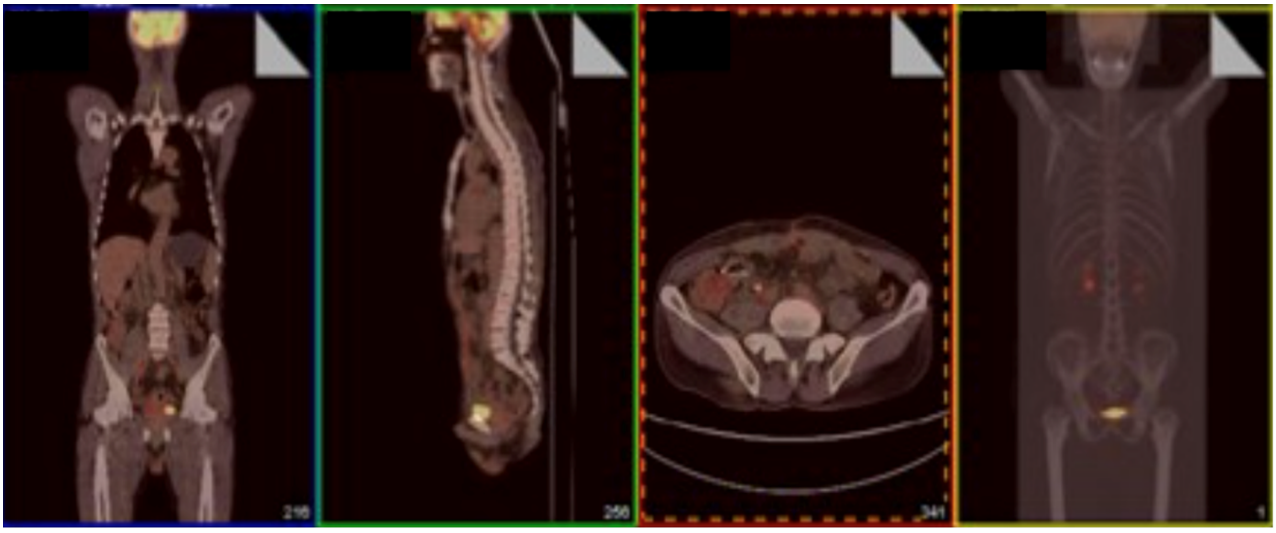

DOI: 10.4251/wjgo.v14.i11.2273

Figure 4 Postoperative positron emission tomography scan.

Regarding the staging of MEITL, gastrointestinal lymphomas follow the Lugano staging system[11], which is tabulated in Table 4. Our patient was staged as having IIE disease.

DISCUSSION

Consistent with our case, it was reported that the most common site of involvement is the small intestine, particularly the jejunum followed by the ileum and duodenum; rarely it could also involve the colon and stomach[12]. Metastasis to mesenteric lymph nodes is common[13]. Our patient had several

Table 4 The Lugano staging system

Stage		Features
I		Tumor confined to small bowel: Single or multiple primary lesions
II	II	Para-intestinal nodal involvement
	II-1	Involving mesenteric, aortic, caval, pelvic, or inguinal nodes
	II-2	With penetration of serosa involving adjacent organs or tissues
	E (IIE, II-1E, II-2E)	Tumor extending into abdomen from primary small bowel site
III		NO stage III
IV		Disseminated extranodal sites or supra-diaphragmatic nodal involvement

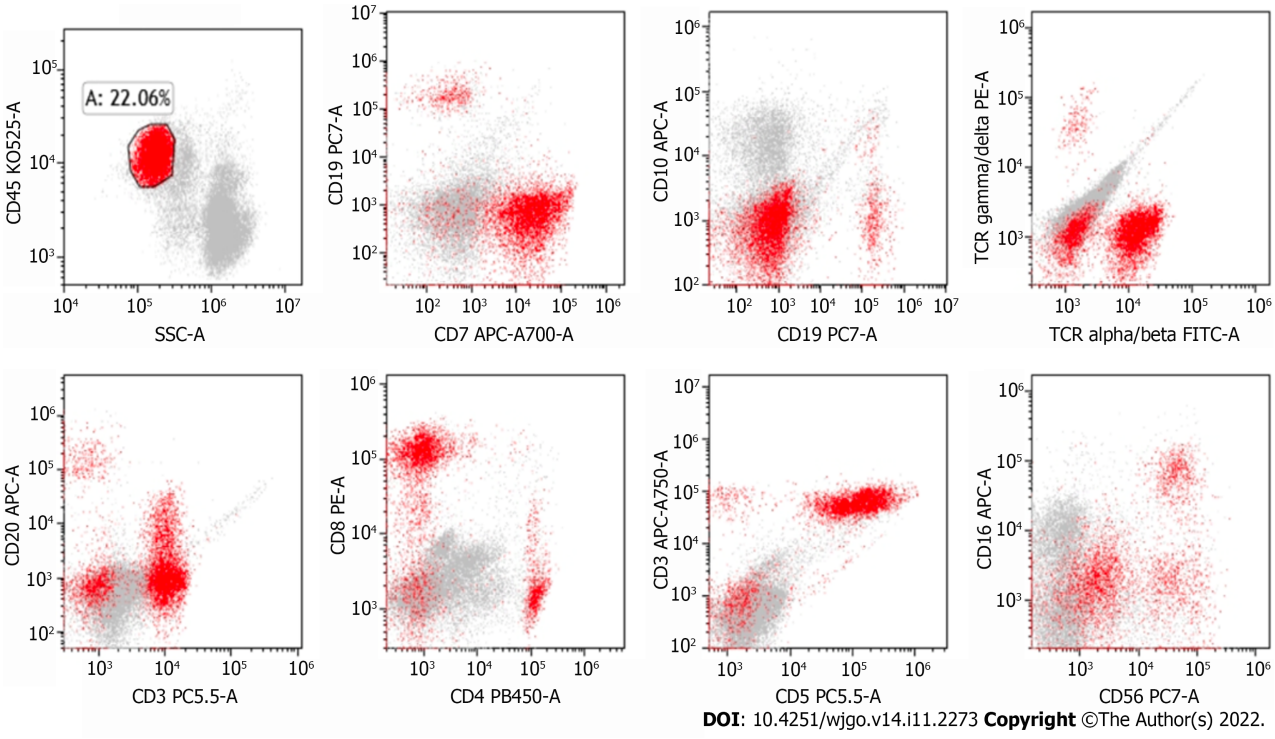

DOI: 10.4251/wjgo.v14.i11.2273 **Copyright** ©The Author(s) 2022.

Figure 5 A (approximately 22.06% of non-erythroid cells) mature lymphocyte population (mainly T cells, with a small amount of B and NK cells).

enlarged mesenteric lymph nodes observed on CT but they were due to lymphoid hyperplasia rather than metastasis. Regarding imaging modalities, obstruction is not common in the small bowel. Multifocal involvement and perforation are more prevalent[14]. Necrosis, reported not to be usual in MEITL[6,8], was observed in our case (Figure 6).

The pattern of presenting symptoms greatly varied among previous studies, with abdominal pain being the most commonly reported symptom. Our patient presented with a 2-mo history of abdominal pain, abdominal distension, and weight loss. However, abdominal pain has a wide range of diagnoses which can pose a great challenge in diagnosing MEITL upon clinical presentation. Weight loss, despite being regarded as a B symptom, has not been found to be an exclusive symptom when it came to diagnosis of MEITL in Asian patients[5,6]. In contrast to classic EATL which can be suspected in sudden worsening of abdominal pain and diarrhea in a previously diagnosed celiac disease patient, MEITL has not been found to have any predisposing factor and was rather known to be sporadic. Clinically, diagnosis of MEITL is more challenging and delayed because of the low index of clinical suspicion and a vague inconsistent display of symptoms that can be easily confused with other malignancies[15-17].

Low albumin, elevated LDH, abnormally high CRP, low hemoglobin, and abnormal lymphocyte count are common laboratory abnormalities detected[2,5,10,16]. Our patient had all the listed laboratory abnormalities except for a normal LDH level.

In this case, based on postoperative pathology reports, other malignancies such as poorly differentiated adenocarcinoma, B-cell lymphoma, and GIST were easily excluded because of the expression of only T-cell markers by monoclonal tumor cells. In addition, negative staining for CD20[18,19] and

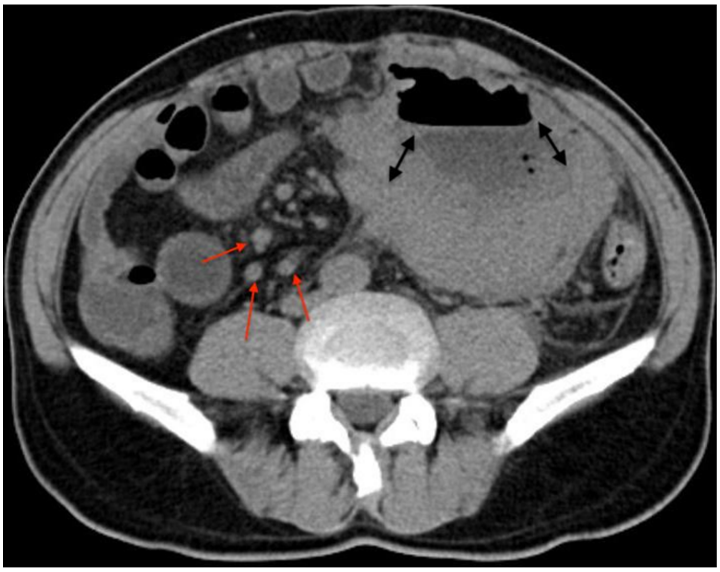

DOI: 10.4251/wjgo.v14.i11.2273

Figure 6 Computed tomography. Red arrows indicate enlarged mesenteric lymph nodes; double headed-arrows indicate necrosis.

CD117[20] excluded B-cell lymphomas and GIST, respectively. The positive staining for CD56 and CD8 led to the diagnosis of MEITL and not the classical EATL form[2,3,9,21]. The panel of immunohistochemistry markers was consistent with MEITL. EBER *in situ* hybridization was negative, thus excluding the possibility of natural killer/T-cell lymphoma which most commonly presents as a facial mass, with a small percentage involving the GI tract[22,23].

Despite having been demonstrated to be negative in several papers and studies for the occurrence of MEITL[17,24], CD4 was found be positive in our case. One of the largest multicenter studies of MEITL analyzed 38 patients where $CD4^+CD8^+$ rate was as low as 19%[5]. $CD4^+CD8^+$, however, supports the cellular origin of MEITL being type 'A' intestinal T-cells[6].

A literature review about the endoscopic findings of MEITL revealed a higher tendency of diffuse infiltrating type lesions compared to ulcerative and polypoid lesions. In a study of nine MEITL patients [25], the endoscopic examination findings were: Six (67%) diffuse infiltrating type lesions (colitis-like or proctocolitis-like); two (22%) polypoid type lesions; and one (11%) ulcerative type lesion. Another study of endoscopic findings of 15 cases of MEITL[26] showed eight (53%) ulcero-infiltrative type lesions and two ulcerative type lesions.

Currently, there are no standardized treatment or diagnostic protocols for MEITL. Being a very rare entity, there exist very few trials and regimens in regards to MEITL, with some having more promising results in eligible patients. Historically, MEITL has been treated with surgery, chemotherapy, autologous stem cell transplant, or their combination. Several studies hypothesized that chemotherapy with or without surgery delivered better outcomes than surgery alone[21,27]. Moreover, different chemotherapy regimens have been investigated over the last decade[3,10,16,28], resulting in different prognoses (Table 5)[29-64].

Despite anthracycline-based regimens being associated with better survival rates than other therapies or no therapy at all[3], Sieniawski *et al*[10] compared a novel regimen with anthracycline-based regimen. The novel regimen begins with one course of CHOP (cyclophosphamide, doxorubicin, vincristine, and prednisone), followed by three courses of IVE/MTX (ifosfamide, vincristine, etoposide alternating with intermediate-dose methotrexate). Autologous stem-cell transplantation (ASCT) was then performed 3 wk after the last cycle of IVE/MTX. They found that the novel regimen had a better response (lower mortality and higher remission). Chiadamide combined with chemotherapy also slightly improved the survival time in two patients, with a mean survival time of 16 mo[45]. The planned regimen for our patient was four cycles of CHOP every 3 wk, followed by stem cell transplant.

Given that (1) MEITL has no predisposing factor; (2) the diagnosis of MEITL is predominantly made at laparotomy; (3) a bulky tumor and elevated serum LDH and CRP levels are risk factors significantly associated with a worse prognosis, and (4) MEITL has no standardized treatment, the concomitant presence of abdominal pain and systemic symptoms (weight loss, fever, and night sweating) together with laboratory parameters indicative for hypoalbuminemia, anemia (low hemoglobin), increased CRP, and low lymphocytic count and endoscopic findings of diffuse infiltrating type lesions can be regarded as highly suspicious features of MEITL and should alert physicians to this rare disease and opt for immediate laparotomy.

Table 5 Details of previously published case reports

Ref.	Gender/age	Chief complaint	Treatment	Prognosis
Chen *et al*[29]	M/60	Abdominal pain	Emergency surgery followed by CHOP + IVE/MTX + SCT, followed by ASCT	CR; liver recurrence 2.5 years later refractory to GDP regimen. Passed away 2 wk after recurrence
Ishibashi *et al*[30]	M/60	Diarrhea and 10 kg weight loss in 17 mo	CHASE followed by SCT	3 years
	F/40	Diarrhea and 6 kg weight loss in 3 mo	THP-COP followed by surgery 10 mo later	2 mo after surgery
	F/50	Abdominal distension	CHOP + high-dose MTX + SCT	9 mo
	M/70	Nausea	SMILE	9 mo
Aiempanakit *et al*[31]	M/67	Diarrhea for 4 mo and 15 kg weight loss over 3 mo	Anthracycline-based regimen	2 mo
Antoniadu *et al*[32]	M/76	Severe dyspnea	N/A	5 d
Aoyama *et al*[33]	M/85	Fever and diarrhea	CHOP followed by DeVIC	Not stated but deceased subsequently due to progressive disease
Pan *et al*[34]	F/67	Abdominal pain	1 cycle of CEOP	3.7 mo
Liu *et al*[35]	F/48	Abdominal pain, distension, vomiting, watery diarrhea, weight loss	Unspecified chemotherapy	1 mo after chemotherapy initiation
Ozaka *et al*[36]	F/68	Melena and mild anemia	8 cycles of CHOP	Achieved complete remission and was still alive at the time of publication (68 mo after diagnosis)
Kasinathan *et al*[37]	F/70	Abdominal pain and vomiting for 4 wk	2 cycles of CHOP, followed by 2 cycles of GDP	Developed gastrointestinal bleeding and succumbed 4 wk after initiation of GDP
Mago *et al*[38]	M/59	SOB for 1 mo, abdominal distension for 2 wk	1 cycle of CHOEP	Passed away within few days after tumor lysis syndrome
Nato *et al*[39]	F/43	Abdominal distension, 2 mo history of early satiety and nausea	4 cycles of GDP achieving a PR, CR was achieved after CBT conditioned with total body irradiation, cyclophosphamide, and cytarabine	Cognitive impairment (7 mo post transplantation) was improved after 3 cycles of MPV and whole brain radiotherapy and passed away 6 mo later
Pan *et al*[40]	M/63	Diffuse abdominal pain for 1 mo	Emergency surgery followed by 2 cycles of CHOP	2 mo
	M/47	Diarrhea, dyspnea, orthopnea, weight loss for 1 year	1 dose of L-asparaginase, etoposide, and decadron regimen followed by emergency surgery, adjuvant chemotherapy included etoposide, methylprednisolone, high-dose cytarabine, and cisplatin	9 mo
Umino *et al*[41]	M/41	Diarrhea and epigastric pain for 1 mo	3 neoadjuvant cycles of ICE followed by autologous SCT	13 mo
Ferran *et al*[42]	F/45	Cutaneous lesions followed by abdominal perforation after chemotherapy initiation	6 neoadjuvant cycles of CHOP and 1 cycle of SMILE followed by surgery. 1 adjuvant cycle L-GEMOX	8 mo
Aoki *et al*[43]	F/77	Abdominal discomfort, night sweats, and fever for 1 mo	EPOCH for 6 mo	Still alive 1 year after diagnosis
Soardo *et al*[44]	M/65	2-wk history of weight gain, increased abdominal volume with progressive mild dyspnea, and fever in the last 2 d	Emergency laparotomy	1 mo postoperatively
Liu *et al*[45]	M/61	Upper abdominal pain and black stool for 2 mo	Partial excision of small intestine and chidamide-based combination regimen	15 mo
	F/35	Abdominal distension for 1 mo	Sigmoid colostomy followed by chidamide-based combination therapy	17 mo

Samuel *et al*[46]	M/62	Hypovolemic shock secondary to severe chronic diarrhea and 100 pounds lost over a year	Chemotherapy	1 mo
Ikeda *et al*[47]	M/61	3 episodes of ileal strangulation within 4 mo of gastrectomy	Ileal resection followed by 2 cycles of CHOP and 1 cycle of ICE	3 mo
Lenti *et al*[48]	F/63	Diarrhea and 10 kg weight loss in 6 mo	Surgery followed by a single course of CHOP	27 mo
	M/58	Diarrhea and 5 kg weight loss	Surgery	4 mo
Broccoli *et al*[49]	M/65	Petechiae at both limbs, acute abdominal pain, diarrhea, and clinical signs of bowel perforation	Emergency resection of 9 cm of small bowel	6 mo
Tabata *et al*[50]	M/72	Ileum perforation…severe constipation after 21 mo in CR	Emergency resection followed by anthracycline-based regimen chemotherapy (CR for 21 mo), paltrexate therapy was administered during recurrence	In CR after 52 mo
Fisher *et al*[51]	F/60	Abdominal pain, diarrhea, and 30 pounds of weight loss over 3 mo	EOCH chemotherapy (subsequently developing a large lymphoma 6 mo after therapy initiation)	N/A
Tian *et al*[8]	M/58	Abdominal pain, diarrhea, and weight loss over 3 mo	1 course of CHOP	Died subsequently after the first cycle due to bone marrow suppression
	F/64	Abdominal pain and diarrhea for 5 years	5 wk of adjuvant chemotherapy consisting of romidepsin with Revlimid followed by laparotomy involving small bowel bypass	3 mo
Kubota *et al*[52]	M/41	Diarrhea for 1 mo and intermittent abdominal pain	Resection followed by CHOP and 3 cycles of ICE resulted in CR	Repeated intrathecal chemotherapy and high-dose chemotherapy followed by ASCT achieved CR
Gentille *et al*[53]	F/70	Intermittent abdominal pain, nausea, vomiting and diarrhea for 14 mo. 50 pounds of weight loss	Right hemicolectomy followed by 5 cycles of EPOCH (with PEG-asparaginase added in the last cycle)	Developed abdominal pain 15 mo after initial therapy, subsequently passing away around 20 mo after initial diagnosis
Sato *et al*[54]	F/52	Diarrhea and anorexia for 8 wk + 6 kg weight loss	CHOP followed by stem-cell transplant	Unknown
Kakugawa *et al*[55]	M/65	Watery diarrhea for 14 mo	8 cycles of CHOP followed by 5 cycles of ESHAP	Still alive 67 mo post chemotherapy
Felipe-Silva *et al*[56]	M/78	Diarrhea for 2 mo + 20 kg weight loss	Surgical resection followed by 2 cycles of CHOP, which was changed to COP	6 mo
Okumura *et al*[57]	F/66	Abdominal distension for 1 mo presenting with acute abdomen	Surgical resection followed by high dose chemotherapy and SCT	Still alive at the time of publication, in complete remission
Yang *et al*[58]	M/39	Acute onset of lower abdominal pain and diffuse peritonitis	Surgical resection	Unknown
Fukushima *et al*[59]	M/60	Severe diarrhea	CHOP	1 year
Liong *et al*[60]	M/50	Diarrhea for 6 mo, presenting with acute abdomen due to intestinal perforation	Surgical resection followed by CHOP	4 mo
Noh *et al*[61]	M/68	Nausea and vomiting for 6 mo + 25 kg weight loss	Surgical resection followed by chemotherapy (unspecified)	Unknown
Hashimoto *et al*[62]	M/64	Diarrhea for several months	Chemotherapy (unspecified)	Unknown
Liu *et al*[63]	F/43	Upper abdominal pain and weight loss for 3 mo	4 cycles of CHOEP and 2 cycles of DHAP followed by surgery	11 mo after diagnosis, 1 d after surgery due to septic shock
Fukushima *et al*[64]	F/68	Upper abdominal pain and nausea	Laparoscopic intestinal resection followed by auto-peripheral blood SCT	22 mo without recurrence; passed away 1 mo after duodenal recurrence in 23rd mo

M: Male; F: Female; CHOP: Cyclophosphamide, doxorubicin, vincristine, prednisolone; IVE: Ifosfamide, vincristine, and etoposide; MTX: Methotrexate;

SCT: Stem cell transplant; CHASE: Cyclophosphamide, cytarabine, etoposide, dexamethasone; GDP: Gemcitabine, dexamethasone and cisplatin; THP-COP: Pirarubicin, cyclophosphamide, vincristine and prednisolone; SMILE: Dexamethasone, methotrexate, ifosfamide, L-asparaginase and etoposide; DeVIC: Etoposide, ifosfamide, and carboplatin; CEOP: Cyclophosphamide, epirubicin, vincristine, and prednisolone; SOB: Shortness of breath; CHOEP: Cyclophosphamide, doxorubicin, vincristine, etoposide, and prednisone; PR: partial response; CR: Complete response; CBT: Cord blood transplantation; MPV: Methotrexate, procarbazine, vincristine; ICE: Ifosfamide, carboplatin, and etoposide; L-GEMOX: Gemcitabine, oxaliplatin, asparaginase, dexamethasone; EPOCH: Etoposide, prednisolone, oncovin, cyclophosphamide, hydroxydaunorubicin; ICE: Ifosfamide, carboplatin and etoposide; ESHAP: Etoposide, methylprednisolone, cytarabine, cisplatin; DHAP: Dexamethasone, high dose cytarabine, platinol.

Fluorine-2-fluorodeoxyglucose positron emission tomography (^{18}F-FDG PET) has been proven to be the most useful diagnostic modality in the staging and follow-up for recurrence of aggressive lymphomas. A study of 12 MEITL cases[65] examined by PET concluded that MEITL is not restricted to the gut; many different anatomical sites were involved at presentation or at relapse with the infiltration of thoracic structures in 50% of the cases and central nervous system involvement in 25% of the cases. Our patient, however, had no abnormalities, no abnormal density focus, and no significant increase or decrease in radioactivity uptake on his whole body ^{18}F-FDG PET scan after surgery and before his chemotherapy. The increase in metabolism of FDG in the middle abdomen subcutaneously is considered to be postoperative changes. Inflammation was considered for the increase in metabolism of FDG in the ascending colon. An increase in uptake of FDG is not distinct for malignancy; benign infectious and inflammatory processes as well as treatment-induced inflammatory changes can also account for an increase in FDG uptake[66]. In regards to uptake of FDG on PET scans in the setting of MEITL, clinicians must be careful as infectious and inflammatory processes can also lead to an increase.

As GIST was highly suspected as the primary diagnosis, no endoscopic biopsy was planned due to the risk of intraabdominal bleeding and tumor rupture (increasing risk of dissemination and metastasis). However, after the mass was found to be significantly enlarged within 2 wk while on Gleevec, emergency surgery after acute abdomen (perforation and acute peritonitis) was performed and specimens were sent for pathology examination. This is consistent with previous studies, which showed that EATL and MEITL have been preponderantly diagnosed at laparotomy[16,21]. In the study by Sieniawski *et al*[21], 52 out of 57 patients underwent emergency laparotomy and Gale *et al*[16] reported that diagnosis was made at laparotomy in 25 out of 31 patients.

CONCLUSION

Understanding MEITL as an entity can be dismaying for both patients and physicians. Diagnosis should be correlated to clinical symptoms while the final diagnosis is mainly based on the pathological features and immunophenotypes. Since MEITL is associated with a poor prognosis and high recurrence, it is crucial that the oncologist should follow and monitor any relapsing signs. In the occurrence of a rapidly growing malignant tumor in the small intestine (otherwise not explained by any other pathologic processes), vague gastrointestinal symptoms, and a poor suspicion of diagnosis due to lack of specific tests accompanied by elevated C-reactive protein, elevated LDH, hypoalbuminemia, anemia, and low lymphocytic count, we suggest emergent laparotomy and specimens to be sent for pathology. Based on our case' relatively favorable prognosis and the cases reported in the literature, surgical resection followed by chemotherapy and stem-cell transplant leads to a better prognosis and should be recommended as the standard treatment protocol.

FOOTNOTES

Author contributions: Bissessur AS and Zhou JC wrote this paper; Bissessur AS conducted literature review; Xu L, Li ZQ, Ju SW, and Jia YL contributed in data acquisition and manuscript preparation; Jia YL, Zhou JC, and Wang LB were responsible for patient care and data analysis; Zhou JC and Wang LB substantively reviewed the manuscript; all authors read and approved the final manuscript.

Informed consent statement: Informed written consent was obtained from the patients for the publication of this report and any accompanying images.

Conflict-of-interest statement: The authors declare that they have no conflict of interest to disclose.

CARE Checklist (2016) statement: The authors have read the CARE Checklist (2016), and the manuscript was prepared and revised according to the CARE Checklist (2016).

Country/Territory of origin: China

ORCID number: Abdul Saad Bissessur 0000-0003-4422-5511; Ji-Chun Zhou 0000-0002-0727-4034; Ling Xu 0000-0001-7259-4731; Zhao-Qing Li 0000-0001-7373-7562; Si-Wei Ju 0000-0001-5228-5384; Yun-Lu Jia 0000-0003-2213-7561; Lin-Bo Wang 0000-0001-6594-8722.

S-Editor: Chen YL
L-Editor: Wang TQ
P-Editor: Cai YX

REFERENCES

1 **Isaacson PG**. Gastrointestinal lymphoma. *Hum Pathol* 1994; **25**: 1020-1029 [PMID: 7927306 DOI: 10.1016/0046-8177(94)90060-4]
2 **Campo E**, Swerdlow SH, Harris NL, Pileri S, Stein H, Jaffe ES. The 2008 WHO classification of lymphoid neoplasms and beyond: evolving concepts and practical applications. *Blood* 2011; **117**: 5019-5032 [PMID: 21300984 DOI: 10.1182/blood-2011-01-293050]
3 **Delabie J**, Holte H, Vose JM, Ullrich F, Jaffe ES, Savage KJ, Connors JM, Rimsza L, Harris NL, Müller-Hermelink K, Rüdiger T, Coiffier B, Gascoyne RD, Berger F, Tobinai K, Au WY, Liang R, Montserrat E, Hochberg EP, Pileri S, Federico M, Nathwani B, Armitage JO, Weisenburger DD. Enteropathy-associated T-cell lymphoma: clinical and histological findings from the international peripheral T-cell lymphoma project. *Blood* 2011; **118**: 148-155 [PMID: 21566094 DOI: 10.1182/blood-2011-02-335216]
4 **Swerdlow SH**, Campo E, Pileri SA, Harris NL, Stein H, Siebert R, Advani R, Ghielmini M, Salles GA, Zelenetz AD, Jaffe ES. The 2016 revision of the World Health Organization classification of lymphoid neoplasms. *Blood* 2016; **127**: 2375-2390 [PMID: 26980727 DOI: 10.1182/blood-2016-01-643569]
5 **Tse E**, Gill H, Loong F, Kim SJ, Ng SB, Tang T, Ko YH, Chng WJ, Lim ST, Kim WS, Kwong YL. Type II enteropathy-associated T-cell lymphoma: a multicenter analysis from the Asia Lymphoma Study Group. *Am J Hematol* 2012; **87**: 663-668 [PMID: 22641357 DOI: 10.1002/ajh.23213]
6 **Tan SY**, Chuang SS, Tang T, Tan L, Ko YH, Chuah KL, Ng SB, Chng WJ, Gatter K, Loong F, Liu YH, Hosking P, Cheah PL, Teh BT, Tay K, Koh M, Lim ST. Type II EATL (epitheliotropic intestinal T-cell lymphoma): a neoplasm of intra-epithelial T-cells with predominant CD8αα phenotype. *Leukemia* 2013; **27**: 1688-1696 [PMID: 23399895 DOI: 10.1038/leu.2013.41]
7 **Chan JK**, Chan AC, Cheuk W, Wan SK, Lee WK, Lui YH, Chan WK. Type II enteropathy-associated T-cell lymphoma: a distinct aggressive lymphoma with frequent γδ T-cell receptor expression. *Am J Surg Pathol* 2011; **35**: 1557-1569 [PMID: 21921780 DOI: 10.1097/PAS.0b013e318222dfcd]
8 **Tian S**, Xiao SY, Chen Q, Liu H, Ping J. Monomorphic epitheliotropic intestinal T-cell lymphoma may mimic intestinal inflammatory disorders. *Int J Immunopathol Pharmacol* 2019; **33**: 2058738419829387 [PMID: 30757928 DOI: 10.1177/2058738419829387]
9 **Ferreri AJ**, Zinzani PL, Govi S, Pileri SA. Enteropathy-associated T-cell lymphoma. *Crit Rev Oncol Hematol* 2011; **79**: 84-90 [PMID: 20655757 DOI: 10.1016/j.critrevonc.2010.06.006]
10 **Sieniawski M**, Angamuthu N, Boyd K, Chasty R, Davies J, Forsyth P, Jack F, Lyons S, Mounter P, Revell P, Proctor SJ, Lennard AL. Evaluation of enteropathy-associated T-cell lymphoma comparing standard therapies with a novel regimen including autologous stem cell transplantation. *Blood* 2010; **115**: 3664-3670 [PMID: 20197551 DOI: 10.1182/blood-2009-07-231324]
11 **Rohatiner A**, d'Amore F, Coiffier B, Crowther D, Gospodarowicz M, Isaacson P, Lister TA, Norton A, Salem P, Shipp M. Report on a workshop convened to discuss the pathological and staging classifications of gastrointestinal tract lymphoma. *Ann Oncol* 1994; **5**: 397-400 [PMID: 8075046 DOI: 10.1093/oxfordjournals.annonc.a058869]
12 **Lee HJ**, Im JG, Goo JM, Kim KW, Choi BI, Chang KH, Han JK, Han MH. Peripheral T-cell lymphoma: spectrum of imaging findings with clinical and pathologic features. *Radiographics* 2003; **23**: 7-26; discussion 26 [PMID: 12533636 DOI: 10.1148/rg.231025018]
13 **Gopalakrishna H**, Al-Abdouh A, Nair G, Bekele A. Incidental Diagnosis of Monomorphic Epitheliotropic Intestinal T-Cell Lymphoma: A Case Report. *Cureus* 2020; **12**: e10084 [PMID: 33005508 DOI: 10.7759/cureus.10084]
14 **Ghai S**, Pattison J, Ghai S, O'Malley ME, Khalili K, Stephens M. Primary gastrointestinal lymphoma: spectrum of imaging findings with pathologic correlation. *Radiographics* 2007; **27**: 1371-1388 [PMID: 17848697 DOI: 10.1148/rg.275065151]
15 **Di Sabatino A**, Biagi F, Gobbi PG, Corazza GR. How I treat enteropathy-associated T-cell lymphoma. *Blood* 2012; **119**: 2458-2468 [PMID: 22271451 DOI: 10.1182/blood-2011-10-385559]
16 **Gale J**, Simmonds PD, Mead GM, Sweetenham JW, Wright DH. Enteropathy-type intestinal T-cell lymphoma: clinical features and treatment of 31 patients in a single center. *J Clin Oncol* 2000; **18**: 795-803 [PMID: 10673521 DOI: 10.1200/JCO.2000.18.4.795]
17 **Ondrejka S**, Jagadeesh D. Enteropathy-Associated T-Cell Lymphoma. *Curr Hematol Malig Rep* 2016; **11**: 504-513 [PMID: 27900603 DOI: 10.1007/s11899-016-0357-7]
18 **Martelli M**, Ferreri AJ, Agostinelli C, Di Rocco A, Pfreundschuh M, Pileri SA. Diffuse large B-cell lymphoma. *Crit Rev Oncol Hematol* 2013; **87**: 146-171 [PMID: 23375551 DOI: 10.1016/j.critrevonc.2012.12.009]

19 **Paro MM**, Siftar Z, Kardum-Skelin I, Sustercić D, Nazor A, Flegar-Mestrić Z, Jaksić B. Flow cytometry immunophenotyping (FCI) of fine needle aspirates (FNAs) of lymph nodes. *Coll Antropol* 2010; **34**: 359-365 [PMID: 20698103]

20 **Hirota S**, Isozaki K, Moriyama Y, Hashimoto K, Nishida T, Ishiguro S, Kawano K, Hanada M, Kurata A, Takeda M, Muhammad Tunio G, Matsuzawa Y, Kanakura Y, Shinomura Y, Kitamura Y. Gain-of-function mutations of c-kit in human gastrointestinal stromal tumors. *Science* 1998; **279**: 577-580 [PMID: 9438854 DOI: 10.1126/science.279.5350.577]

21 **Sieniawski MK**, Lennard AL. Enteropathy-associated T-cell lymphoma: epidemiology, clinical features, and current treatment strategies. *Curr Hematol Malig Rep* 2011; **6**: 231-240 [PMID: 21912848 DOI: 10.1007/s11899-011-0097-7]

22 **Cai Q**, Cai J, Fang Y, Young KH. Epstein-Barr Virus-Positive Natural Killer/T-Cell Lymphoma. *Front Oncol* 2019; **9**: 386 [PMID: 31139570 DOI: 10.3389/fonc.2019.00386]

23 **Wang L**, Liu Y, Lin XY, Yu JH, Miao Y, Qiu XS, Wang EH. A case of enteropathy-associated T-cell lymphoma (type I) arising in stomach without refractory celiac disease. *Diagn Pathol* 2012; **7**: 172 [PMID: 23217032 DOI: 10.1186/1746-1596-7-172]

24 **Weindorf SC**, Smith LB, Owens SR. Update on Gastrointestinal Lymphomas. *Arch Pathol Lab Med* 2018; **142**: 1347-1351 [PMID: 30407861 DOI: 10.5858/arpa.2018-0275-RA]

25 **Ishibashi H**, Nimura S, Hirai F, Harada N, Iwasaki H, Kawauchi S, Oshiro Y, Matsuyama A, Nakamura S, Takamatsu Y, Yonemasu H, Shimokama T, Takeshita M. Endoscopic and clinicopathological characteristics of colorectal T/NK cell lymphoma. *Diagn Pathol* 2020; **15**: 128 [PMID: 33087157 DOI: 10.1186/s13000-020-01044-5]

26 **Kim DH**, Lee D, Kim JW, Huh J, Park SH, Ha HK, Suh C, Yoon SM, Kim KJ, Choi KD, Ye BD, Byeon JS, Song HJ, Jung HY, Yang SK, Kim JH, Myung SJ. Endoscopic and clinical analysis of primary T-cell lymphoma of the gastrointestinal tract according to pathological subtype. *J Gastroenterol Hepatol* 2014; **29**: 934-943 [PMID: 24325295 DOI: 10.1111/jgh.12471]

27 **Nijeboer P**, Malamut G, Mulder CJ, Cerf-Bensussan N, Sibon D, Bouma G, Cellier C, Hermine O, Visser O. Enteropathy-associated T-cell lymphoma: improving treatment strategies. *Dig Dis* 2015; **33**: 231-235 [PMID: 25925928 DOI: 10.1159/000369542]

28 **Daum S**, Ullrich R, Heise W, Dederke B, Foss HD, Stein H, Thiel E, Zeitz M, Riecken EO. Intestinal non-Hodgkin's lymphoma: a multicenter prospective clinical study from the German Study Group on Intestinal non-Hodgkin's Lymphoma. *J Clin Oncol* 2003; **21**: 2740-2746 [PMID: 12860953 DOI: 10.1200/JCO.2003.06.026]

29 **Chen Y**, Tan SY, Petersson BF, Khor YM, Gopalakrishnan SK, Tan D. Occult recurrence of monomorphic epitheliotropic intestinal T-cell lymphoma and the role of MATK gene expression in diagnosis. *Hematol Oncol* 2017; **35**: 852-855 [PMID: 26948059 DOI: 10.1002/hon.2288]

30 **Ishibashi H**, Nimura S, Kayashima Y, Takamatsu Y, Aoyagi K, Harada N, Kadowaki M, Kamio T, Sakisaka S, Takeshita M. Multiple lesions of gastrointestinal tract invasion by monomorphic epitheliotropic intestinal T-cell lymphoma, accompanied by duodenal and intestinal enteropathy-like lesions and microscopic lymphocytic proctocolitis: a case series. *Diagn Pathol* 2016; **11**: 66 [PMID: 27457239 DOI: 10.1186/s13000-016-0519-x]

31 **Aiempanakit K**, Amatawet C, Chiratikarnwong K, Auepemkiate S, Kayasut K, Suwiwat S, Apinantriyo B. Erythema multiforme-like cutaneous lesions in monomorphic epitheliotropic intestinal T-cell lymphoma: a rare case report. *J Cutan Pathol* 2017; **44**: 183-188 [PMID: 27862162 DOI: 10.1111/cup.12864]

32 **Antoniadou F**, Dimitrakopoulou A, Voutsinas PM, Vrettou K, Vlahadami I, Voulgarelis M, Korkolopoulou P, Kafasi N, Mikou P. Monomorphic epitheliotropic intestinal T-cell lymphoma in pleural effusion: A case report. *Diagn Cytopathol* 2017; **45**: 1050-1054 [PMID: 28681573 DOI: 10.1002/dc.23772]

33 **Aoyama Y**, Tsunemine H, Zushi Y, Maruoka H, Goto Y, Kodaka T, Itoh T, Takahashi T. Colonal monomorphic epitheliotropic intestinal T-cell lymphoma with novel phenotype of cytoplasmic CD3 expression. *J Clin Exp Hematop* 2018; **58**: 102-106 [PMID: 29657256 DOI: 10.3960/jslrt.18002]

34 **Pan ST**, Ko YH, Tan SY, Chuang SS. Primary cutaneous peripheral T-cell lymphoma with a late relapse solely in the ileum mimicking monomorphic epitheliotropic intestinal T-cell lymphoma. *Pathol Res Pract* 2018; **214**: 2106-2109 [PMID: 30477646 DOI: 10.1016/j.prp.2018.10.002]

35 **Liu C**, Feng L, Sun X. Monomorphic Epitheliotropic Intestinal T-Cell Lymphoma: A Rare Case of Diffuse Ulcers in the Intestine. *Clin Gastroenterol Hepatol* 2021; **19**: e121-e122 [PMID: 32668339 DOI: 10.1016/j.cgh.2020.07.011]

36 **Ozaka S**, Inoue K, Okajima T, Tasaki T, Ariki S, Ono H, Ando T, Daa T, Murakami K. Monomorphic epitheliotropic intestinal T-cell lymphoma presenting as melena with long-term survival: A case report and review of literature. *World J Gastroenterol* 2021; **27**: 6501-6510 [PMID: 34720538 DOI: 10.3748/wjg.v27.i38.6501]

37 **Kasinathan G**. Monomorphic epitheliotropic intestinal T-cell lymphoma of the duodenum: an aggressive disease. *Hematol Transfus Cell Ther* 2021; **43**: 518-520 [PMID: 32536535 DOI: 10.1016/j.htct.2020.04.005]

38 **Mago S**, Mavilia M, Forouhar F, Vaziri H. Small bowel T-cell lymphoma: a MEITL-ing diagnosis. *Clin J Gastroenterol* 2021; **14**: 1071-1083 [PMID: 33881752 DOI: 10.1007/s12328-021-01417-3]

39 **Nato Y**, Miyazaki K, Imai H, Nakano E, Kageyama Y, Ino K, Fujieda A, Matsumoto T, Tawara I, Tanaka K, Yamaguchi M, Katayama N. Early central nervous system relapse of monomorphic epitheliotropic intestinal T-cell lymphoma after cord blood transplantation. *Int J Hematol* 2021; **114**: 129-135 [PMID: 33646526 DOI: 10.1007/s12185-021-03107-9]

40 **Pan ST**, Wang RC, Su YZ, Hsieh YC, Chuang SS. Lymphomatous effusion of monomorphic epitheliotropic intestinal T-cell lymphoma is characterized by azurophilic granules and is a dismal sign: Report of two new cases with literature review. *Diagn Cytopathol* 2021; **49**: E247-E252 [PMID: 33387400 DOI: 10.1002/dc.24690]

41 **Umino A**, Kubota Y, Honda-Yoshigai M, Okazaki T, Yoshihara Y, Wakayama K, Kawasaki S, Kusaba K, Kimura S, Sueoka E. Monitoring of tumor cells by flow cytometry permits rapid evaluation of disease progression in monomorphic epitheliotropic intestinal T-cell lymphoma. *Cytometry B Clin Cytom* 2021; **100**: 454-456 [PMID: 33259698 DOI: 10.1002/cyto.b.21977]

42 **Olmos-Alpiste F**, Vázquez I, Gallardo F, Sánchez-Gonzalez B, Colomo L, Pujol RM. Monomorphic Epitheliotropic Intestinal T-Cell Lymphoma With Secondary Cutaneous Involvement: A Diagnostic Challenge. *Am J Dermatopathol* 2021; **43**: 300-304 [PMID: 33264131 DOI: 10.1097/DAD.0000000000001855]

43 **Aoki Y**, Sujino T, Takabayashi K, Mutakuchi M, Emoto K, Hosoe N, Ogata H, Kanai T. Various Endoscopic Features in Monomorphic Epitheliotropic Intestinal T-Cell Lymphoma. *Case Rep Gastroenterol* 2021; **15**: 312-322 [PMID: 33790720 DOI: 10.1159/000513902]

44 **Soardo G**, Castaldo V, Donnini D, Uzzau A, Pizzolitto S, Sechi LA. Monomorphic Epitheliotropic Intestinal T Cell Lymphoma of the Appendix: a Case Report and Review of Literature. *J Gastrointest Cancer* 2020; **51**: 688-694 [PMID: 31970655 DOI: 10.1007/s12029-020-00363-6]

45 **Liu TZ**, Zheng YJ, Zhang ZW, Li SS, Chen JT, Peng AH, Huang RW. Chidamide based combination regimen for treatment of monomorphic epitheliotropic intestinal T cell lymphoma following radical operation: Two case reports. *World J Clin Cases* 2020; **8**: 1278-1286 [PMID: 32337203 DOI: 10.12998/wjcc.v8.i7.1278]

46 **Samuel R**, Krill T, Merwat S. Monomorphic Epitheliotropic Intestinal T cell Lymphoma: a Rare Cause of Chronic Diarrhea. *J Gastrointest Cancer* 2019; **50**: 1051-1054 [PMID: 30761475 DOI: 10.1007/s12029-019-00210-3]

47 **Ikeda C**, Maruyama D, Oka H, Fujino T, Maeshima AM, Matsushita H. Bone marrow involvement by monomorphic epitheliotropic intestinal T-cell lymphoma. *Br J Haematol* 2019; **187**: 10 [PMID: 31240703 DOI: 10.1111/bjh.16073]

48 **Lenti MV**, Biagi F, Lucioni M, Di Sabatino A, Paulli M, Corazza GR. Two cases of monomorphic epitheliotropic intestinal T-cell lymphoma associated with coeliac disease. *Scand J Gastroenterol* 2019; **54**: 965-968 [PMID: 31361171 DOI: 10.1080/00365521.2019.1647455]

49 **Broccoli A**, Bertuzzi C, Fiorentino M, Morigi A, Stefoni V, Agostinelli C, Argnani L, Cavo M, Zinzani PL. *BRAF* V600E-positive monomorphic epitheliotropic intestinal T-cell lymphoma complicating the course of hairy cell leukemia. *Onco Targets Ther* 2019; **12**: 4807-4812 [PMID: 31354304 DOI: 10.2147/OTT.S202061]

50 **Tabata R**, Tabata C, Okamura M, Takei Y, Ohshima K. Successful treatment of monomorphic epitheliotropic intestinal T cell lymphoma with pralatrexate. *Ann Hematol* 2019; **98**: 1301-1303 [PMID: 30173289 DOI: 10.1007/s00277-018-3491-6]

51 **Fisher A**, Yousif E, Piper M. Truth lies below: A case report and literature review of typical appearing polyps yet with an atypical diagnosis. *World J Gastrointest Endosc* 2019; **11**: 54-60 [PMID: 30705732 DOI: 10.4253/wjge.v11.i1.54]

52 **Kubota Y**, Kusaba K. Monomorphic epitheliotropic intestinal T-cell lymphoma involving the central nervous system. *Blood* 2018; **131**: 1765 [PMID: 29650734 DOI: 10.1182/blood-2017-11-819136]

53 **Gentille C**, Qin Q, Barbieri A, Ravi PS, Iyer S. Use of PEG-asparaginase in monomorphic epitheliotropic intestinal T-cell lymphoma, a disease with diagnostic and therapeutic challenges. *Ecancermedicalscience* 2017; **11**: 771 [PMID: 29062389 DOI: 10.3332/ecancer.2017.771]

54 **Sato Y**, Ono M, Sagawa T, Takimoto R, Hirakawa M, Ohnuma H, Sato T, Iyama S, Murase K, Miyanishi K, Kobune M, Kato J. Endoscopic findings of enteropathy-type T-cell lymphoma by double-balloon enteroscopy and capsule endoscopy. *Dig Endosc* 2010; **22**: 243-245 [PMID: 20642619 DOI: 10.1111/j.1443-1661.2010.00989.x]

55 **Kakugawa Y**, Terasaka S, Watanabe T, Tanaka S, Taniguchi H, Saito Y. Enteropathy-associated T-cell lymphoma in small intestine detected by capsule endoscopy. *Leuk Lymphoma* 2012; **53**: 1623-1624 [PMID: 22242819 DOI: 10.3109/10428194.2012.656633]

56 **Felipe-Silva A**, de Campos FPF, de Medeiros RSS, Lourenção RM, Zerbini MCN. Enteropathy-associated T-cell lymphoma (type II): a Brazilian case report. *Autops Case Rep* 2012; **2**: 31-36 [PMID: 31528569 DOI: 10.4322/acr.2012.014]

57 **Okumura K**, Ikebe M, Shimokama T, Takeshita M, Kinjo N, Sugimachi K, Higashi H. An unusual enteropathy-associated T-cell lymphoma with MYC translocation arising in a Japanese patient: a case report. *World J Gastroenterol* 2012; **18**: 2434-2437 [PMID: 22654438 DOI: 10.3748/wjg.v18.i19.2434]

58 **Yang Y**, Batth SS, Chen M, Borys D, Phan H. Enteropathy-associated T cell lymphoma presenting with acute abdominal syndrome: a case report and review of literature. *J Gastrointest Surg* 2012; **16**: 1446-1449 [PMID: 22528568 DOI: 10.1007/s11605-012-1878-6]

59 **Fukushima M**, Kawanami C, Inoue S, Imai Y, Inokuma T. Enteropathy-associated T-cell lymphoma diagnosed and followed-up by using double-balloon enteroscopy. *Gastrointest Endosc* 2013; **78**: 361-362, discussion 363 [PMID: 23541443 DOI: 10.1016/j.gie.2013.02.033]

60 **Liong CC**, Ravindran S, Gnana Kumar G, Chin EF, Koh PS, Chan WK. Enteropathy-associated T-cell lymphoma: An extremely rare cause of chronic diarrhoea. *Med J Malaysia* 2016; **71**: 88-90 [PMID: 27326953]

61 **Noh CK**, Roh J, Lee KJ. Monomorphic epitheliotropic intestinal T cell lymphoma presenting in weblike feature. *Gastrointest Endosc* 2019; **89**: 891-892 [PMID: 30576648 DOI: 10.1016/j.gie.2018.12.009]

62 **Hashimoto R**, Matsuda T. Gastrointestinal: Endoscopic findings of monomorphic epitheliotropic intestinal T-cell lymphoma. *J Gastroenterol Hepatol* 2019; **34**: 311 [PMID: 30225983 DOI: 10.1111/jgh.14474]

63 **Liu Z**, He L, Jiao Y, Wang H, Suo J. Type II enteropathy-associated T cell lymphoma in the duodenum: A rare case report. *Medicine (Baltimore)* 2020; **99**: e20050 [PMID: 32501967 DOI: 10.1097/MD.0000000000020050]

64 **Fukushima M**, Honda T, Komatsu N, Sasaki R, Ozawa E, Miuma S, Miyaaki H, Irie J, Okano S, Nakao K. Initial and advanced endoscopic findings of monomorphic epitheliotropic intestinal T-cell lymphoma in the duodenum: A case report. *DEN open* 2022; **2**: e118 [PMID: 35873525 DOI: 10.1002/deo2.118]

65 **Chan TSY**, Lee E, Khong PL, Tse EWC, Kwong YL. Positron emission tomography computed tomography features of monomorphic epitheliotropic intestinal T-cell lymphoma. *Hematology* 2018; **23**: 10-16 [PMID: 28581364 DOI: 10.1080/10245332.2017.1335979]

66 **Rahman WT**, Wale DJ, Viglianti BL, Townsend DM, Manganaro MS, Gross MD, Wong KK, Rubello D. The impact of infection and inflammation in oncologic ^{18}F-FDG PET/CT imaging. *Biomed Pharmacother* 2019; **117**: 109168 [PMID: 31334700 DOI: 10.1016/j.biopha.2019.109168]

World Journal of Gastrointestinal Oncology

Submit a Manuscript: https://www.f6publishing.com

World J Gastrointest Oncol 2022 November 15; 14(11): 2288-2294

DOI: 10.4251/wjgo.v14.i11.2288

ISSN 1948-5204 (online)

CASE REPORT

Surgical treatment of liver inflammatory pseudotumor-like follicular dendritic cell sarcoma: A case report

Li-Yue Fu, Jiu-Liang Jiang, Meng Liu, Jun-Jun Li, Kai-Ping Liu, Hai-Tao Zhu

Specialty type: Oncology

Provenance and peer review: Unsolicited article; Externally peer reviewed.

Peer-review model: Single blind

Peer-review report's scientific quality classification

Grade A (Excellent): 0
Grade B (Very good): 0
Grade C (Good): C, C, C
Grade D (Fair): 0
Grade E (Poor): 0

P-Reviewer: Lin J, China; Sahin TT, Turkey

Received: August 16, 2022
Peer-review started: August 16, 2022
First decision: September 23, 2022
Revised: September 28, 2022
Accepted: October 17, 2022
Article in press: October 17, 2022
Published online: November 15, 2022

Li-Yue Fu, Jiu-Liang Jiang, Meng Liu, Kai-Ping Liu, Clinical School, Guizhou Medical University, Guiyang 550001, Guizhou Province, China

Jun-Jun Li, Hai-Tao Zhu, Department of Hepatobiliary Surgery, Affiliated Hospital of Guizhou Medical University, Guiyang 550001, Guizhou Province, China

Corresponding author: Hai-Tao Zhu, PhD, Doctor, Professor, Surgeon, Department of Hepatobiliary Surgery, Affiliated Hospital of Guizhou Medical University, No. 28 Guiyi Road, Yunyan District, Guiyang 550001, Guizhou Province, China. 205429734@qq.com

Abstract

BACKGROUND

Inflammatory pseudotumor-like follicular dendritic cell sarcoma (IPT-like FDCS) is rare with a low malignant potential. Hepatic IPT-like FDCS has similar clinical features to hepatocellular carcinoma (HCC), making it extremely difficult to distinguish between them in clinical practice. We describe the case of a young female patient diagnosed with HCC before surgery, which was pathologically diagnosed as IPT-like FDCS after the left half of the liver was resected. During 6 mo of follow-up, the patient recovered well with no signs of recurrence or metastasis.

CASE SUMMARY

A 23-year-old female patient with a 2-year history of hepatitis B presented to the Affiliated Hospital of Guizhou Medical University. She was asymptomatic at presentation, and the findings from routine laboratory examinations were normal except for slightly elevated alpha-fetoprotein levels. However, ultrasonography revealed a 3-cm diameter mass in the left hepatic lobe, and abdominal contrast-enhanced computed tomography revealed that the tumor had asymmetrical enhancement during the arterial phase, which declined during the portal venous phase, and had a pseudo-capsule appearance. Based on the findings from clinical assessments and imaging, the patient was diagnosed with HCC, for which she was hospitalized and had undergone laparoscopic left hepatectomy. However, the tumor specimens submitted for pathological analyses revealed IPT-like FDCS. After surgical removal of the tumor, the patient recovered. In addition, the patient continued to recover well during 6 mo of follow-up.

CONCLUSION

Hepatic IPT-like FDCS is difficult to distinguish from HCC. Hepatectomy may provide beneficial outcomes in non-metastatic hepatic IPT-like FDCS.

Key Words: Hepatocellular carcinoma; Liver; Pseudotumor-like follicular dendritic cell sarcoma; Surgery; Tumor; Case report

Core Tip: Inflammatory pseudotumor-like follicular dendritic cell sarcoma (IPT-like FDCS) is a type of FDCS with low malignant potential. We investigated the clinical and pathological characteristics, diagnosis, and treatment in a 23-year-old woman diagnosed with hepatic IPT-like FDCS. She underwent laparoscopic left hepatectomy, with an uneventful postoperative course. It is difficult to distinguish hepatic IPT-like FDCS from hepatocellular carcinoma based on clinical features. Therefore, most patients with hepatic IPT-like FDCS are found after surgery. However, surgery may be the best treatment option for patients with hepatic IPT-like FDCS. At present, no abnormality has been found in the patient during the 6-mo follow-up.

Citation: Fu LY, Jiang JL, Liu M, Li JJ, Liu KP, Zhu HT. Surgical treatment of liver inflammatory pseudotumor-like follicular dendritic cell sarcoma: A case report. *World J Gastrointest Oncol* 2022; 14(11): 2288-2294
URL: https://www.wjgnet.com/1948-5204/full/v14/i11/2288.htm
DOI: https://dx.doi.org/10.4251/wjgo.v14.i11.2288

INTRODUCTION

Follicular dendritic cell sarcoma (FDCS) is a rare tumor with nonspecific clinical features. FDCS cannot be diagnosed based on clinical findings alone; therefore, its diagnosis depends on pathological examinations of surgically resected tumor specimens. Pathologically, most FDCSs express at least two FDC markers, including CD21, CD35, and CNA-42. There are two morphologic variants of this tumor: Conventional and inflammatory pseudotumor (IPT)-like[1]. The etiology and pathogenesis of IPT-like FDCS are not clear. Its occurrence may coincide with Epstein-Barr virus (EBV) infection, because in cases with confirmed IPT-like FDCS, the positive rate of Epstein-Barr encoding region (EBER) through *in situ* hybridization was as high as 92.1%[2]. EBV-encoded small RNA exists in all tumor cells, and hybridization imprinting tests confirmed that the virus exists in the form of a monoclonal free body, suggesting that EBV infection occurred before FDC tumor proliferation. CD21, the receptor molecule expressed on the surface of FDC, is the receptor of EBV; therefore, scholars speculate that EBV plays an important role in tumor formation. IPT-like FDCS cells are irregularly arranged and IPT-like FDCS presents with lymphocytic infiltrate, with a positive *in situ* hybridization test for (EBV)-encoded RNA [3]. Most IPT-like FDCSs affect the liver and spleen. Herein, we report a rare case of a female patient with liver IPT-like FDCS in the context of hepatitis B virus infection. We investigated the clinical and pathological characteristics, diagnosis, and treatment of IPT-like FDCS.

CASE PRESENTATION

Chief complaints

A 23-year-old female patient with an underlying hepatitis B virus infection presented, with no symptoms, at the Affiliated Hospital of Guizhou Medical University.

History of present illness

She was asymptomatic.

History of past illness

She had received entecavir as treatment for her hepatitis B infection 2 years previously.

Personal and family history

The patient had an unremarkable personal and family history.

Physical examination

There were no significant findings on initial physical examination.

Laboratory examinations

Laboratory analyses provided the following findings: Hemoglobin, 134 g/L; white blood cell count, 5.23 × 10^9 cells/L; platelet count, 149 × 10^9 cells/L; red blood cell count, 4.50 × 10^9 cells/L; anti-HB test results, positive; serum levels of albumin, 50.40 g/L; aspartate aminotransferase level, 39.50 U/L; alanine aminotransferase level, 23.80 U/L; alkaline phosphatase level, 80 U/L; total bilirubin level, 15.40 μmol/L; direct bilirubin level, 5.20 μmol/L; total bilirubin level, 10.20 μmol/L; hepatitis B viral DNA, 2.35e+01 IU/mL (normal ≤ 10 UI/mL); and alpha-fetoprotein (AFP) level, 12.31 ng/mL (normal = 0.00–7.00 ng/mL).

Imaging examinations

Ultrasonography revealed a 3-cm diameter mass in the left hepatic lobe (Figure 1), necessitating the performance of abdominal contrast-enhanced computed tomography (CT). CT showed asymmetrical tumor enhancement during the arterial phase; however, the enhancement declined during the portal venous phase, and the tumor had a pseudo-capsule appearance (Figure 2).

FINAL DIAGNOSIS

We initially diagnosed the disease as hepatocellular carcinoma (HCC) based on the findings from clinical, laboratory, and imaging assessments.

TREATMENT

After discussion with the radiologist, early hepatocellular carcinoma was highly suspected according to the imaging signs and clinical manifestations. There was no other adjuvant treatment for the patient according to the preoperative comprehensive evaluation. Therefore, the patient underwent laparoscopic left hepatectomy.

OUTCOME AND FOLLOW-UP

Postoperative pathological analysis showed a large number of medium to small lymphocytes distributed in the liver space-occupying lesion area, and an unequal number of spindle or epithelial cells, and histiocyte-like cells, were distributed alternately. Further, hepatic lobule structure was found in the surrounding liver tissue, some small lymphocytes had infiltrated the portal area, and a few small cells were found in the hepatic sinuses.

Immunohistochemical staining showed that the tumor specimen was positive for CD2, CD3, CD5, CD7, CD8, and TIA-1 in all lymphocytes. A portion of the tissue specimen was CD4 positive. Furthermore, positive expressions of CD21, CD35, Ki-67 (30%), and SMA were observed in a portion of the specimen with spindle-epithelioid tumor cells. *In situ* hybridization test was only positive for EBV-encoded RNA in spindle-epithelioid tumor cells (Figure 3). Based on these pathological findings, the patient was diagnosed with IPT-like FDCS. During the 6-mo postoperative follow-up period, the patient had no signs of recurrence or metastasis (Figure 4).

DISCUSSION

Although IPT-like FDCS is a special type of FDCS, it exhibits characteristic features comparable to those of conventional FDCS[4]. More than 60 cases of IPT-like FDCS have been reported in English literature, mainly located in the liver (more than 20 cases)[5-8] and spleen (more than 30 cases)[9-12], and to a lesser extent in the colon (6 cases)[13-15], lungs (1 case)[16], and pancreas (1 case)[17]. The tumor mainly occurs in middle-aged and elderly people, with a female-to-male ratio of 2.2:1, and a median age of 56.5 years[18].

To date, all reported patients with IPT-like FDCS in the liver presented with fever, jaundice, abdominal pain, and/or anemia as the initial clinical manifestations. In addition, other case reports highlighted paraneoplastic arthritis as an initial clinical manifestation[19,20]. However, the patient in the present case did not experience any clinical manifestations prior to the hospital visit, which shows the peculiarity of the disease in clinical practice. In our case, contrast-enhanced CT showed an asymmetrical tumor enhancement and decline during the arterial and portal venous phases, respectively, with a pseudo-capsule appearance of the tumor; these findings corroborated with those of previous studies[21].

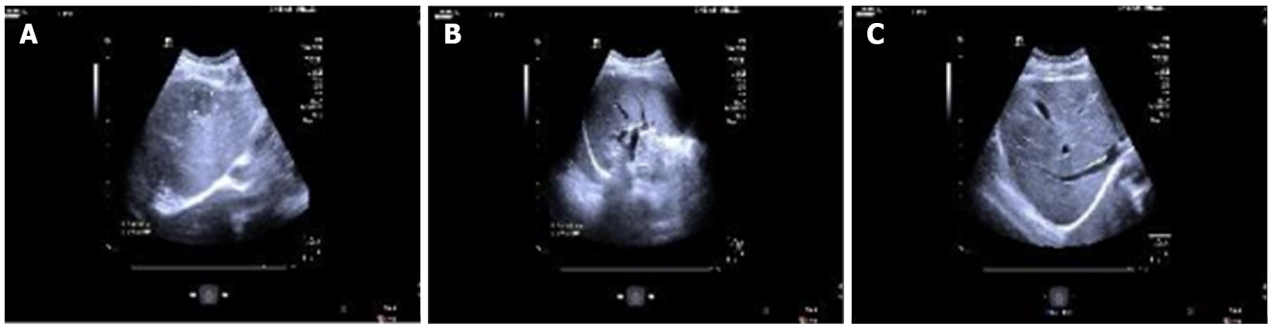

DOI: 10.4251/wjgo.v14.i11.2288 **Copyright** ©The Author(s) 2022.

Figure 1 Ultrasonography before surgery. A: A hypoechoic nodule, about 26 mm × 22 mm in size; B: The nodule with a regular shape, clear boundary, and homogeneous internal echo; C: It can be seen in S4 of the liver.

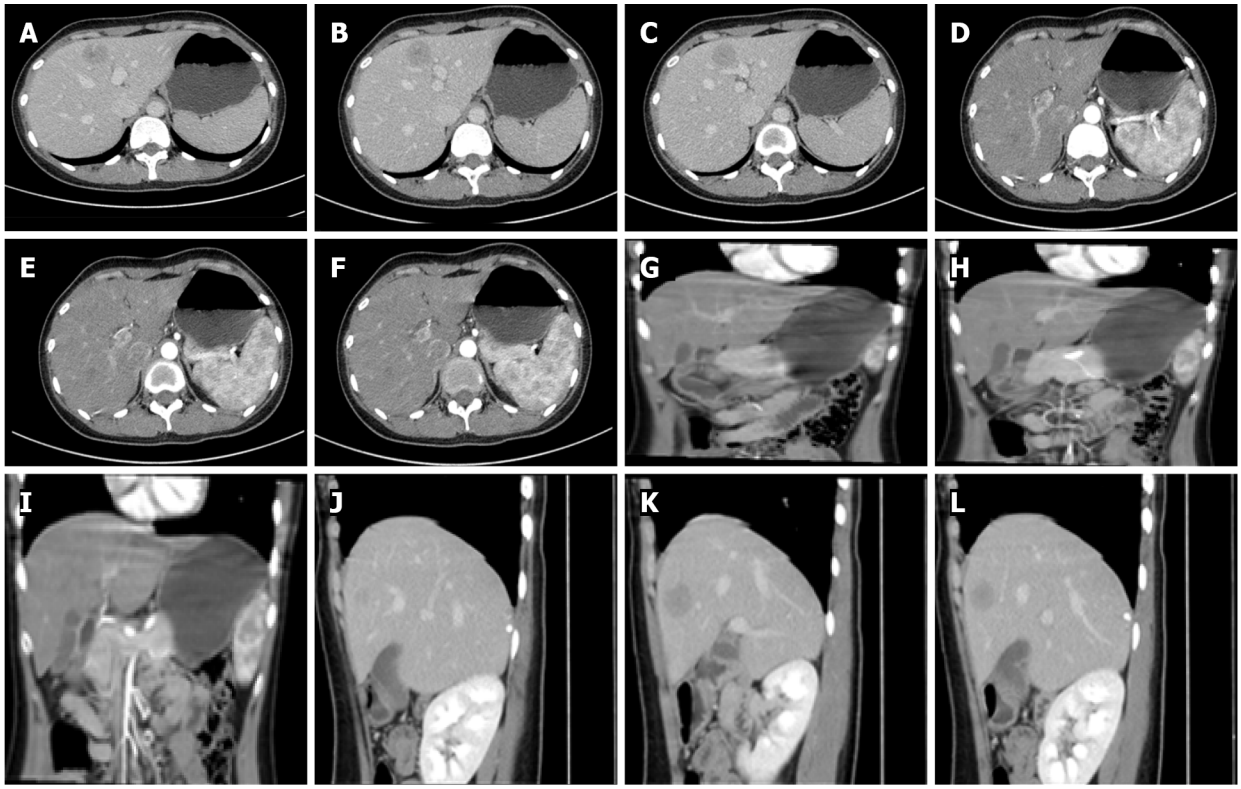

DOI: 10.4251/wjgo.v14.i11.2288 **Copyright** ©The Author(s) 2022.

Figure 2 Abdominal contrast-enhanced computed tomography before surgery. Nodular abnormal enhancement foci (about 27 mm × 26 mm) can be seen in the left inner lobe of the liver, showing uneven and obvious enhancement in the arterial phase and weakening in the venous phase, and a pseudo-capsule can be seen surrounding it. A-F: Axial position; G-I: Coronal position; J-L: Sagittal position.

Because the imaging manifestations of IPT-like FDCS of the liver are nonspecific, CT usually shows low-density nodule enhancement, which is characterized by non-uniform enhancement in the arterial phase and resolution in the delayed phase. Some highly differentiated HCCs can also show resolution in the delayed phase; therefore, hepatic inflammatory pseudotumor (HIPT)-like FDCS should also be differentiated from HCC with internal necrosis *via* imaging findings. HCC with internal necrosis often has peripheral structural invasion, accompanied by cirrhosis and portal hypertension, and may have tumor thrombus formation. HCC is the most common malignant tumor of the liver. The patient had chronic viral hepatitis, AFP elevation, and imaging findings suggestive of HCC. These signs are consistent with the general clinical manifestations of HCC. Therefore, we should pay attention to the possibility of this disease in addition to the huge mixed echo mass in the liver. If IPT-like FDCS is suspected, it is important to perform routine puncture biopsy. Puncture biopsy is a feasible preoperative diagnostic method for IPT-like FDCS, but many false negative cases have been encountered due to the smaller amount of obtained puncture tissue. Its definitive diagnosis mainly relies on immunohistochemical and *in situ* hybridization analyses of surgically obtained tumor specimens.

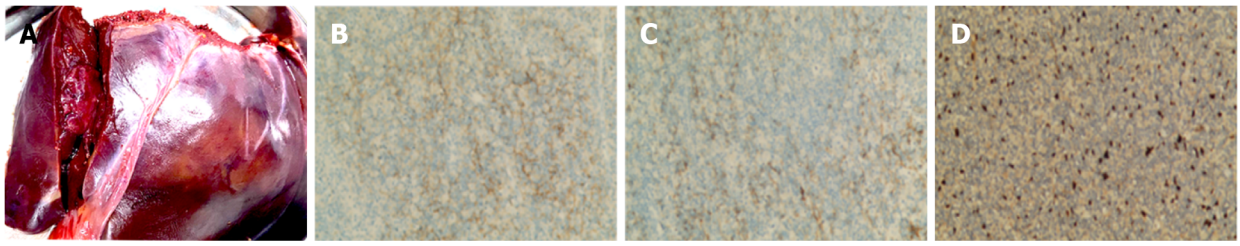

DOI: 10.4251/wjgo.v14.i11.2288 **Copyright** ©The Author(s) 2022.

Figure 3 Immunohistochemical staining and *in situ* hybridization test. A: Tissue specimens; B and C: Immunohistochemical results: Proliferative histiocytes CD21 (+), CD35 (+), D2-40 (-), and SMA (+), focal. Lymphocyte hepatocyte (+), CD3 (diffuse), CD20 (-), CD79 α (-), CD10 (-), bcl-2 (-), CD5 (+), CD19 (+), Sox11 (-), CD56 (-), CD4 (+), partial, CD8 (+), minority, cyclin D1 (-), TIA (+), Granzyme B (-), CD2 (+), CD7 (+), bcl-6 (-), MUMI (-), CD30 (scattered transformed large cells), and TCR-R (-). Ki-67 (about 25%+); D: *In situ* hybridization results: Some cells showed EBER+, positive control +. EBER: Epstein-Barr encoding region.

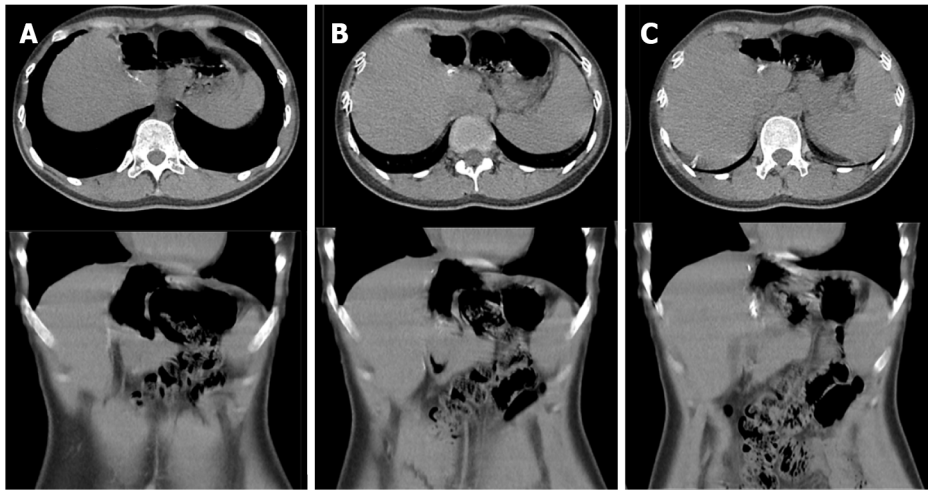

DOI: 10.4251/wjgo.v14.i11.2288 **Copyright** ©The Author(s) 2022.

Figure 4 Abdominal computed tomography after 6 mo of follow-up. A: After 6 mo of follow-up, the abdominal computed tomography re-examination; B: The re-examination showed that no nodular or strip-shaped high-density shadow in the liver; C: There was no abnormality in the left lobe of the liver.

Apart from HCC, pathological analyses should be performed to distinguish HIPT-like FDCS from other diseases such as HIPT and primary liver lymphoma because the symptoms and imaging findings of HIPT are nonspecific. The histopathological characteristics of HIPT include the presence of inflammatory lesions consisting of diffused and dense hyalinized collagenosis with inflammatory cells, compact foamy histiocyte proliferation, as well as lymphocyte and plasma cell infiltration[22]. In primary liver lymphoma, clinical features are nonspecific as well, and histological analyses demonstrate infiltrations limited to the liver. Among the types of lymphoma, diffuse large B-cell lymphoma is the most common type noted[23,24]. HIPT-like FDCS shows a contrasting lymphocyte infiltration pattern compared with that of FDCS, immunohistochemical analyses show positive expression of one of the FDCS markers (CD21, CD35, CD23, or CNA42) in tumor cells, and *in situ* hybridization testing is positive for EBV-encoded RNA in spindle-epithelioid tumor cells. Clinicians can better diagnose HIPT-like FDCS *via* pathological examinations of surgically resected tissue specimens.

In summary, HIPT-like FDCS displays combined characteristics of chronic inflammation and malignant tumors on imaging. The final diagnosis is dependent on pathology, which shows that the tumor cells express CD21, CD23, CD35, SMA, and other markers, or do not express these antigens, but are EBER positive. HCC, HIPT, and primary liver lymphoma should be considered in the differential diagnosis.

In the treatment of HIPT-like FDCS, complete resection of tumor is the best treatment, but there is still dispute about whether conventional radiotherapy and chemotherapy are needed after surgery. Chemotherapy and/or radiotherapy can be used for patients with recurrence or surgery that cannot be cured[25-27]. The review found that the incidence of HIPT-like FDCS is very low, as are the recurrence and metastasis rate and mortality rate of previously reported liver cases; 4 cases recurred or metastasized, the recurrence rate was 11.8%, and the mortality rate was 2.9%. The remaining cases survived well[2]. In the present case, HIPT-like FDCS was found to be an indolent malignant tumor with no sign of relapse or metastasis noted during the follow-up.

CONCLUSION

HIPT-like FDCS is extremely difficult to distinguish from HCC due to their similar clinical features. In addition, surgical resection may provide better long-term outcomes in patients with indolent malignant HIPT-like FDCSs.

ACKNOWLEDGEMENTS

The authors thank Clinical Medical School, Guizhou Medical University, and the Hepatobiliary Department, Affiliated Hospital of Guizhou Medical University.

FOOTNOTES

Author contributions: Fu LY contributed to manuscript writing and editing and data collection; Jiang JL, Liu M, Li JJ, and Liu KP contributed to data analysis; Zhu HT contributed to conceptualization and supervision; all authors have read and approved the final manuscript.

Supported by Guizhou Medical University and Affiliated Hospital of Guizhou Medical University.

Informed consent statement: Written informed consent was obtained from the patient for publication of this report and any accompanying images.

Conflict-of-interest statement: All the authors report no relevant conflicts of interest for this article.

CARE Checklist (2016) statement: The authors have read the CARE Checklist (2016), and the manuscript was prepared and revised according to the CARE Checklist (2016).

Country/Territory of origin: China

ORCID number: Li-Yue Fu 0000-0002-3479-6372; Jiu-Liang Jiang 0000-0002-3479-6356; Hai-Tao Zhu 0000-0002-5388-9021.

S-Editor: Fan JR
L-Editor: A
P-Editor: Fan JR

REFERENCES

1 **Pileri SA**, Grogan TM, Harris NL, Banks P, Campo E, Chan JK, Favera RD, Delsol G, De Wolf-Peeters C, Falini B, Gascoyne RD, Gaulard P, Gatter KC, Isaacson PG, Jaffe ES, Kluin P, Knowles DM, Mason DY, Mori S, Müller-Hermelink HK, Piris MA, Ralfkiaer E, Stein H, Su IJ, Warnke RA, Weiss LM. Tumours of histiocytes and accessory dendritic cells: an immunohistochemical approach to classification from the International Lymphoma Study Group based on 61 cases. *Histopathology* 2002; **41**: 1-29 [PMID: 12121233 DOI: 10.1046/j.1365-2559.2002.01418.x]

2 **Ge R**, Liu C, Yin X, Chen J, Zhou X, Huang C, Yu W, Shen X. Clinicopathologic characteristics of inflammatory pseudotumor-like follicular dendritic cell sarcoma. *Int J Clin Exp Pathol* 2014; **7**: 2421-2429 [PMID: 24966952]

3 **Cheuk W**, Chan JK, Shek TW, Chang JH, Tsou MH, Yuen NW, Ng WF, Chan AC, Prat J. Inflammatory pseudotumor-like follicular dendritic cell tumor: a distinctive low-grade malignant intra-abdominal neoplasm with consistent Epstein-Barr virus association. *Am J Surg Pathol* 2001; **25**: 721-731 [PMID: 11395549 DOI: 10.1097/00000478-200106000-00003]

4 **Cazzola M**. Introduction to a review series: the 2016 revision of the WHO classification of tumors of hematopoietic and lymphoid tissues. *Blood* 2016; **127**: 2361-2364 [PMID: 27069255 DOI: 10.1182/blood-2016-03-657379]

5 **Aparicio Serrano A**, Castro Rodríguez J, Gallego Jiménez E, Barrera Baena P. Inflammatory pseudotumor-like follicular dendritic cell sarcoma of the liver. *Rev Esp Enferm Dig* 2021; **113**: 378-379 [PMID: 33371694 DOI: 10.17235/reed.2020.7602/2020]

6 **Lu SS**, Wang Z, Zhao S, Liu WP. [Hepatic inflammatory pseudotumor-like follicular dendritic cell sarcoma with paravertebral metastasis and recurrence: report of a case]. *Zhonghua Bing Li Xue Za Zhi* 2021; **50**: 958-960 [PMID: 34344089 DOI: 10.3760/cma.j.cn112151-20210325-00234]

7 **Pascariu AD**, Neagu AI, Neagu AV, Băjenaru A, Bețianu CI. Hepatic inflammatory pseudotumor-like follicular dendritic cell tumor: a case report. *J Med Case Rep* 2021; **15**: 410 [PMID: 34321082 DOI: 10.1186/s13256-021-02957-5]

8 **Jin K**, Li MN, Li S, Li J, Chen N. [Hepatic inflammatory pseudotumor-like follicular dendritic cell sarcoma]. *Zhonghua Gan Zang Bing Za Zhi* 2020; **28**: 172-174 [PMID: 32164072 DOI: 10.3760/cma.j.issn.1007-3418.2020.02.015]

9 **Hang JF**, Wang LC, Lai CR. Cytological features of inflammatory pseudotumor-like follicular dendritic cell sarcoma of spleen: A case report. *Diagn Cytopathol* 2017; **45**: 230-234 [PMID: 27775241 DOI: 10.1002/dc.23626]

10 **Kwon H**. Inflammatory pseudotumor-like follicular dendritic cell tumor of the spleen. *Turk J Gastroenterol* 2018; **29**: 128-130 [PMID: 29391320 DOI: 10.5152/tjg.2018.17220]

11 **Li X**, Shi Z, You R, Li Y, Cao D, Lin R, Huang X. Inflammatory Pseudotumor-Like Follicular Dendritic Cell Sarcoma of the Spleen: Computed Tomography Imaging Characteristics in 5 Patients. *J Comput Assist Tomogr* 2018; **42**: 399-404 [PMID: 29287022 DOI: 10.1097/RCT.0000000000000700]

12 **Gong QX**, Fan QH, Zhou ZS, Zhang ZH, Yu MN, Wang Z, Wang C, Zhang WM. [Inflammatory pseudotumor-like follicular dendritic cell tumor of spleen]. *Zhonghua Bing Li Xue Za Zhi* 2008; **37**: 40-44 [PMID: 18509984]

13 **Kazemimood R**, Saei Hamedani F, Sharif A, Gaitonde S, Wiley E, Giulianotti PC, Groth JV. A Rare Case of Epstein-Barr Virus Negative Inflammatory Pseudotumor-like Follicular Dendritic Cell Sarcoma Presenting as a Solitary Colonic Mass in a 53-Year-Old Woman; Case Report and Review of Literature. *Appl Immunohistochem Mol Morphol* 2017; **25**: e30-e33 [PMID: 27299190 DOI: 10.1097/PAI.0000000000000405]

14 **Pan ST**, Cheng CY, Lee NS, Liang PI, Chuang SS. Follicular Dendritic Cell Sarcoma of the Inflammatory Pseudotumor-like Variant Presenting as a Colonic Polyp. *Korean J Pathol* 2014; **48**: 140-145 [PMID: 24868227 DOI: 10.4132/KoreanJPathol.2014.48.2.140]

15 **Shi QY**, Zheng Z, Wu HY, Chen JY, Fan XS. [Colonic inflammatory pseudotumor-like follicular dendritic cell sarcoma: report of a case]. *Zhonghua Bing Li Xue Za Zhi* 2022; **51**: 138-140 [PMID: 35152634 DOI: 10.3760/cma.j.cn112151-20210727-00531]

16 **He H**, Xue Q, Tan F, Yang L, Wang X, Gao Y, Mao Y, Mu J, Wang D, Zhao J, Zhao L, Gao S. A rare case of primary pulmonary inflammatory pseudotumor-like follicular dendritic cell sarcoma successfully treated by lobectomy. *Ann Transl Med* 2021; **9**: 77 [PMID: 33553370 DOI: 10.21037/atm-20-4965]

17 **Mograbi M**, Stump MS, Luyimbazi DT, Shakhatreh MH, Grider DJ. Pancreatic Inflammatory Pseudotumor-Like Follicular Dendritic Cell Tumor. *Case Rep Pathol* 2019; **2019**: 2648123 [PMID: 31885993 DOI: 10.1155/2019/2648123]

18 **Kiryu S**, Takeuchi K, Shibahara J, Uozaki H, Fukayama M, Tanaka H, Maeda E, Akahane M, Ohtomo K. Epstein-Barr virus-positive inflammatory pseudotumour and inflammatory pseudotumour-like follicular dendritic cell tumour. *Br J Radiol* 2009; **82**: e67-e71 [PMID: 19325041 DOI: 10.1259/bjr/66918927]

19 **Martins PN**, Reddy S, Martins AB, Facciuto M. Follicular dendritic cell sarcoma of the liver: unusual presentation of a rare tumor and literature review. *Hepatobiliary Pancreat Dis Int* 2011; **10**: 443-445 [PMID: 21813397 DOI: 10.1016/s1499-3872(11)60076-3]

20 **Levi Sandri GB**, Colasanti M, Vennarecci G, Ettorre GM. Paraneoplastic arthritis as first symptom of a liver inflammatory pseudotumor-like follicular dendritic cell sarcoma. *Liver Int* 2016; **36**: 1392 [PMID: 27125361 DOI: 10.1111/liv.13148]

21 **Xu L**, Ge R, Gao S. Imaging features and radiologic-pathologic correlations of inflammatory pseudotumor-like follicular dendritic cell sarcoma. *BMC Med Imaging* 2021; **21**: 52 [PMID: 33731032 DOI: 10.1186/s12880-021-00584-6]

22 **Horiuchi R**, Uchida T, Kojima T, Shikata T. Inflammatory pseudotumor of the liver. Clinicopathologic study and review of the literature. *Cancer* 1990; **65**: 1583-1590 [PMID: 2155699 DOI: 10.1002/1097-0142(19900401)65:7<1583::aid-cncr2820650722>3.0.co;2-l]

23 **Lizarralde E**, Martínez P, Ibañez T, Gutiérrez A. Primary hepatic lymphoma and primary biliary cirrhosis. *Am J Gastroenterol* 2000; **95**: 562-563 [PMID: 10685781 DOI: 10.1111/j.1572-0241.2000.t01-1-01811.x]

24 **Delshad SD**, Ahdoot JJ, Portocarrero DJ. Primary hepatic lymphoma. *Clin Gastroenterol Hepatol* 2010; **8**: e49-e50 [PMID: 19948244 DOI: 10.1016/j.cgh.2009.11.014]

25 **Zhang BX**, Chen ZH, Liu Y, Zeng YJ, Li YC. Inflammatory pseudotumor-like follicular dendritic cell sarcoma: A brief report of two cases. *World J Gastrointest Oncol* 2019; **11**: 1231-1239 [PMID: 31908727 DOI: 10.4251/wjgo.v11.i12.1231]

26 **Choe JY**, Go H, Jeon YK, Yun JY, Kim YA, Kim HJ, Huh J, Lee H, Shin DH, Kim JE. Inflammatory pseudotumor-like follicular dendritic cell sarcoma of the spleen: a report of six cases with increased IgG4-positive plasma cells. *Pathol Int* 2013; **63**: 245-251 [PMID: 23714251 DOI: 10.1111/pin.12057]

27 **Zhao M**, Du X, OuYang B, Li M, Yang H. Inflammatory pseudotumor-like follicular dendritic cell sarcoma mimicking a colonic polyp. *J Gastrointest Surg* 2021; **25**: 2429-2430 [PMID: 33674906 DOI: 10.1007/s11605-021-04961-y]

World Journal of Gastrointestinal Oncology

Submit a Manuscript: https://www.f6publishing.com

World J Gastrointest Oncol 2022 November 15; 14(11): 2295-2301

DOI: 10.4251/wjgo.v14.i11.2295

ISSN 1948-5204 (online)

CASE REPORT

Rare squamous cell carcinoma of the jejunum causing perforated peritonitis: A case report

Lin Xiao, Lie Sun, Ji-Xin Zhang, Yi-Sheng Pan

Specialty type: Surgery

Provenance and peer review: Unsolicited article; Externally peer reviewed.

Peer-review model: Single blind

Peer-review report's scientific quality classification

Grade A (Excellent): A
Grade B (Very good): B
Grade C (Good): 0
Grade D (Fair): 0
Grade E (Poor): 0

P-Reviewer: Haddadi S, Algeria; Şahin EA, Turkey

Received: September 2, 2022
Peer-review started: September 2, 2022
First decision: September 19, 2022
Revised: September 25, 2022
Accepted: October 17, 2022
Article in press: October 17, 2022
Published online: November 15, 2022

Lin Xiao, Lie Sun, Yi-Sheng Pan, Department of General Surgery, Peking University First Hospital, Beijing 100034, China

Ji-Xin Zhang, Department of Pathology, Peking University First Hospital, Beijing 100034, China

Corresponding author: Yi-Sheng Pan, MD, Doctor, Department of General Surgery, Peking University First Hospital, No. 8 Xishiku Street, Beijing 100034, China.
bdyypanyisheng@163.com

Abstract

BACKGROUND

Adenocarcinoma has the highest incidence among malignant tumors of the small intestine (SI). Squamous cell carcinoma (SCC) often occurs in organs covered with squamous epithelium. Primary or metastatic SCC originating from the SI is very rare, with very few cases reported in the literature.

CASE SUMMARY

This case report involves a 69-year-old man who developed abdominal pain after lunch. After admission, an abdominal computed tomography scan revealed perforation of the alimentary canal and multiple abnormal low-density lesions in the liver. During laparotomy, an approximately 4 cm × 3 cm-sized solid tumor was found in the jejunum, located 30 cm from the Treitz ligament, with a perforation. An intestinal segment of approximately 15 cm was removed, including the perforated portion. The pathological result was SCC. In combination with liver imaging, a diagnosis of SI SCC with multiple liver metastases was considered. The patient died from hepatic failure 1 mo after the operation.

CONCLUSION

SI tumors are very rare compared to those originating in other digestive organs. Due to its insidious onset, the diagnosis of this disease is usually delayed. Clinicians must pay close attention to digestive symptoms such as persistent abdominal pain and melena.

Key Words: Squamous cell carcinoma; Jejunal perforation; Peritonitis; Abdominal computed tomography scan; Case report

Core Tip: Squamous cell carcinoma (SCC) in the small bowel is a rare pathologic category. Clinical symptoms are not evident, and it is challenging to determine whether it is the small intestine's primary or metastatic SCC. This paper describes a 69-year-old male patient diagnosed with SCC of the small intestine and hepatic metastases. Effective diagnosis and early treatment are vital in improving the prognosis of malignant small bowel tumors. Radical resection should be undertaken if no metastases are found.

Citation: Xiao L, Sun L, Zhang JX, Pan YS. Rare squamous cell carcinoma of the jejunum causing perforated peritonitis: A case report. *World J Gastrointest Oncol* 2022; 14(11): 2295-2301
URL: https://www.wjgnet.com/1948-5204/full/v14/i11/2295.htm
DOI: https://dx.doi.org/10.4251/wjgo.v14.i11.2295

INTRODUCTION

Small intestinal (SI) tumors are very rare compared to other digestive organs[1]. The incidence of small bowel tumors accounts for only 0.6% of all malignant tumors, including about 1%-3% of gastrointestinal malignancies[2]. Previous studies of malignant tumors have reported that approximately 30% to 50% are adenocarcinoma, 25% to 30% are carcinoid, and 15% to 20% are lymphoma[3]. Primary squamous cell carcinoma (SCC) of the SI is extremely rare, with only a few reports in the literature[4-8]. This paper describes a surgically treated patient with SCC arising from the jejunum with perforated peritonitis and multiple liver metastases.

CASE PRESENTATION

Chief complaints

The patient's main complaints were epigastric pain after eating, nausea and vomiting, and then gradually full abdominal distension.

History of present illness

The patient developed epigastric pain and nausea half an hour after lunch. He then began vomiting; the vomitus was the stomach contents. Finally, he experienced full abdominal distension.

History of past illness

The patient was diagnosed with hypertension and diabetes, which were well-controlled with oral medications.

Personal and family history

The patient had no history of SCC, and his family was negative for cancer.

Physical examination

After admission, the patient's blood pressure was 125/71 mmHg, heart rate was 89 bpm, and body temperature was 36.7 °C. Abdominal tenderness, rebounding pain, muscle tension, and acute peritonitis were noted. Notably, no enlarged lymph nodes were found during the physical examination.

Laboratory examinations

Blood analysis revealed a white blood cell count of 10.96 × 10^9/L, hemoglobin concentration of 124 g/L, neutrophil count of 8.96 × 10^9/L, and hypersensitive C-reactive protein level of 53 mg/L. Creatinine (141.7 Umol/L), albumin (40 g/L), alanine aminotransferase, and aspartate aminotransferase levels were normal. His glucose level was 15.6 mmol/L, prothrombin international normalized ratio was 1.14, and D-dimer was 0.77 mg/L.

Imaging examinations

A computed tomography (CT) scan showed that the SI wall of the left upper abdomen was irregularly thickened, and free gas appeared in the abdominal cavity. Multiple round low-density nodules of varying sizes can be seen in the liver parenchyma (Figure 1).

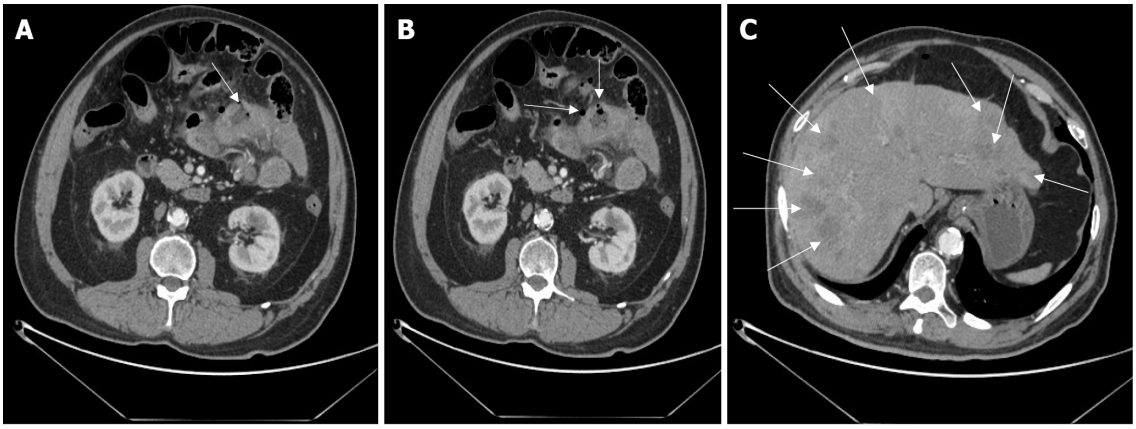

DOI: 10.4251/wjgo.v14.i11.2295

Figure 1 Abdominal computed tomography images. A: Uneven thickening of the small intestinal wall with viscus perforation (arrow); B: Free gas outside the intestine but in the abdomen (arrows); C: The liver parenchyma had multiple round low-density nodules of varying sizes (arrows).

FINAL DIAGNOSIS

Postoperative pathology showed an approximately 4 cm × 3 cm × 1 cm-sized ulcerative tumor of the SI from the jejunum, which had infiltrated the entire thickness of the intestinal wall. Tumor cells presented as a poorly differentiated carcinoma, growing in nests, and intracellular dyskeratosis was visible (Figure 2A and B). No tumor cells were seen in the corresponding mesenteric adipose tissue and lymph nodes. Immunohistochemical findings demonstrated strong positivity for cytokeratin and antioncogene P40 (Figure 2C and D). These results were consistent with a diagnosis of SCC.

TREATMENT

Laparotomy revealed that the SI was extensively edematous. A mass-like lesion about 4 cm in diameter with perforation (Figure 3) was identified. An intestinal segmental resection of about 15 cm, including the perforation site and the corresponding mesentery, was removed. An end-to-end intestinal anastomosis was performed, and the abdominal cavity was flushed with physiological saline solution.

OUTCOME AND FOLLOW-UP

The surgery was completed successfully. Palliative chemotherapy combined with immunotherapy was recommended, according to the opinion of chemotherapy specialists. Due to the patient's poor physical condition, his family refused further treatment and only relieved his pain. The patient was discharged on postoperative day 6. However, he had advanced-stage malignancy and died from hepatic failure 1 mo after the operation.

DISCUSSION

The SI represents the longest part of the digestive tract, accounting for about 75% of the total length of the gastrointestinal canal and more than 90% of the mucosal surface. However, malignant tumors rarely develops in the SI[9]. The unique environment in the small bowel, including complex factors such as pH, immune function, and various enzymes, may be related to the low incidence of small bowel tumors [10]. Small bowel tumors are rare globally, and according to the "age standard of the world population", the global incidence rate is less than 1.0 per 100000, ranging from 0.3 to 2.0[11]. SCC is even rarer among SI malignancies. Generally, SCC occurs in parts of the body covered by squamous epithelium, such as the skin, oral cavity, esophagus, and cervix. Some organs not covered by squamous epithelium can develop SCC through squamous epithelial metaplasia, such as the bronchus and gallbladder. SCC of the SI is extremely rare compared to other gastrointestinal tumors, accounting for approximately 2% among 1312 specimens of SI tumors[12]. More commonly, SCC detected in the intestine represents metastatic cancer from other organs. Lung cancer commonly metastasizes to the SI[13-15]. Other cancers known to metastasize to the SI include mandibular gingiva, esophagus, and cervix cancers[16-20]. Metastatic SCC of the SI is 2.5 times more common than primary SCC of the SI at autopsy[21].

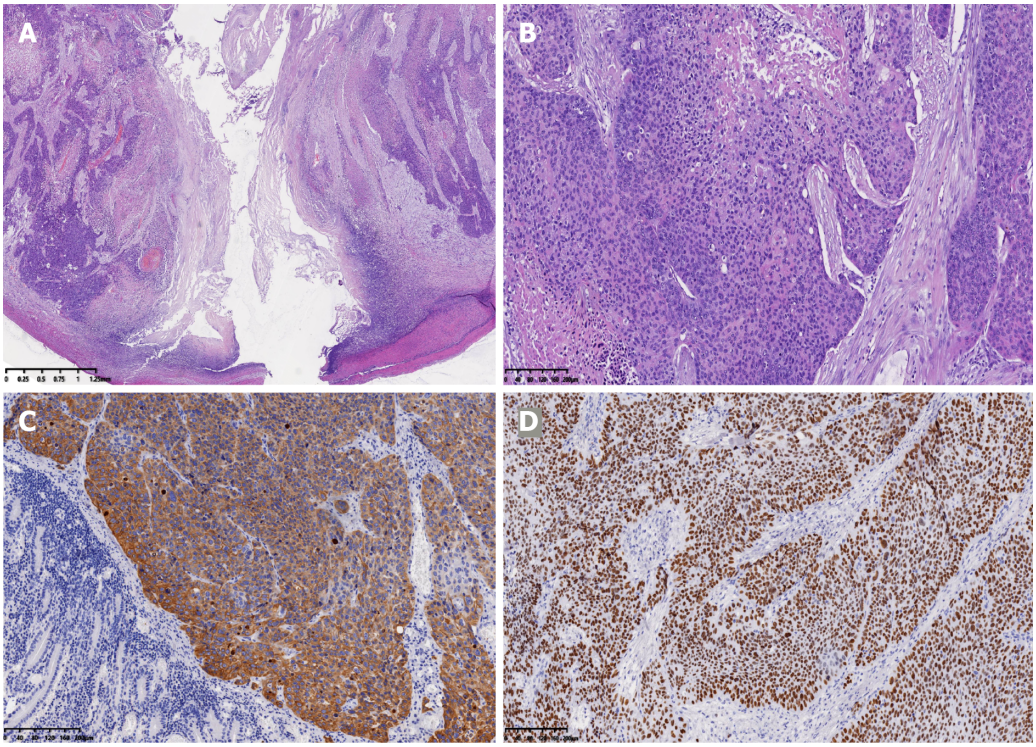

DOI: 10.4251/wjgo.v14.i11.2295 **Copyright** ©The Author(s) 2022.

Figure 2 Pathological and immunohistochemical findings. A and B: Pathological findings from surgical specimen. The lesion showed a serosal penetration (A), with diffuse and nested growth of tumor cells and intracellular dyskeratosis being visible (B); C and D: Immunochemistry demonstrated that the staining for cytokeratin-5/6 and antioncogene P40 was strongly positive.

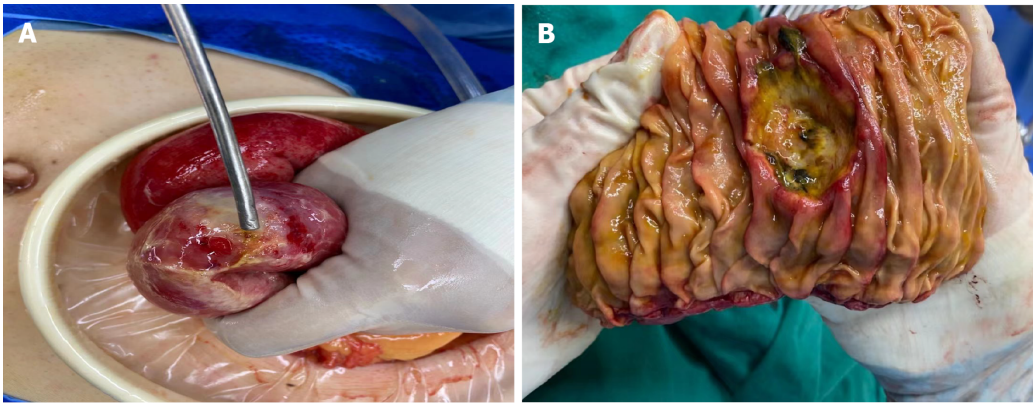

DOI: 10.4251/wjgo.v14.i11.2295 **Copyright** ©The Author(s) 2022.

Figure 3 Exploratory laparotomy results. A: The perforation of a jejunal segment with a purulent surface was noted; B: The enteric cavity showed a deep ulcer lesion.

The origin of primary SCC of the SI may be related to the malignant transformation of undifferentiated basal cells of the SI mucosal epithelium. There are three possible mechanisms of SCC developing in the SI: (1) Pluripotent stem cells differentiate into malignant squamous cells; (2) malignant transformation of ectopic squamous epithelium; and (3) malignant changes in squamous metaplasia caused by chronic mucosal damage[22]. These three pathways were supported by Platt *et al*[23]. The diagnosis of SCC must be rigorous, and key considerations are: (1) The characteristics of a malignant tumor, such as apparent atypia and nested distribution; (2) the characteristics of the epithelial cells, such as the formation of a keratinized pearl; (3) lack of glandular components and glandular epithelium; and (4) no evidence of involvement of primary SCC of other organs. Pathologically, it is challenging to identify tumor cells as a primary or metastatic feature of SCC in the SI, especially when metastatic tumors reach mucosal surfaces[24]. For rare SCC of the SI, when the histology is atypical and the cytokeratin and intercellular bridge structure are not obvious, it should be distinguished from carcinoids in the SI. Immunohistochemistry and neuroendocrine granules can be used to make such a

differentiation.

In this case study, the patient was admitted to hospital with acute abdominal pain. Emergency surgery was performed because of peritonitis due to jejunal perforation, identified by relevant imaging and physical examinations. Postoperative pathology revealed disorderly growth of the squamous epithelial cells in large nests with pink keratin in the center. Immunohistochemical findings demonstrated that staining for cytokeratin-5/6 and antioncogene P40 was both strongly positive. Additionally, no other tissues or organs yield positive findings, including the respiratory, alimentary, and urogenital tracts.

In contrast, computed tomography imaging identified multiple low-density masses in the liver. The patient had no history of SCC, so a diagnosis of SCC of the SI, adenocarcinoma, and carcinoids is excluded. Despite showing multiple lesions on liver imaging, the patient refused to undergo contrast-enhanced MRI or liver puncture for pathology, due to poor physical condition. The multiple liver metastases of SI SCC *via* hematogenous spread were the considered diagnosis and may be related to the liver's perfusion of the portal vein system. There is currently no postoperative adjuvant therapy for small bowel SCC other than surgical resection worldwide. Chemotherapy (taxanes and platinums) combined with immunotherapy was recommended, referring to the treatment for esophageal and lung SCC, but with no evidence support. The patient's family refused further medical treatment due to his poor physical condition and only relieved his pain. He died from hepatic failure 1 mo after the operation.

Neoplasms of the SI are rare, and several different histological types of cancer can occur in the SI. The clinical symptoms are not specific. It is challenging to access the SI *via* conventional endoscopy, making the diagnosis of SI tumors difficult. Most patients are hospitalized for complications of the disease, with surgical R0 resections challenging because of the advanced stages of the disease at diagnosis. Capsule endoscopy is considered the best way to visualize the entire SI. It is also considered the first diagnostic method for gastrointestinal bleeding of unknown origin after a negative upper gastrointestinal endoscopy and colonoscopy. Many advances have been made in the clinical treatment of adenocarcinoma as well as stromal and neuroendocrine tumors arising from the SI[25]. As SI squamous tumors are rare, more extensive cases and studies are necessary to achieve a well-designed clinical trial. The comprehensive treatment of SI SCC is challenging and requires further medical research. Once a small bowel tumor is diagnosed, radical resection should be performed as soon as possible, representing resections of at least 10 cm of the involved region and the corresponding mesenteric lymph nodes to improve overall survival[26].

CONCLUSION

Malignant tumors of the SI are uncommon cancers and are easily misdiagnosed in the clinic. Therefore, most small bowel tumors are in the advanced stages when patients are admitted to the hospital. Early detection and diagnosis are of great significance for the optimal prognosis of patients. Clinicians should pay close attention to the symptoms of patients presenting with acute abdominal pain, such as acute peritonitis, bowel obstruction, and intussusception, during clinical diagnosis and treatment. Surgical resection is currently the most effective treatment for malignant SI tumors. It is also necessary to treat the patient's underlying disease to assist them in restoring their health. Further clinical studies and reports of similar cases are required to improve our knowledge of SCC in the SI and ensure the best clinical outcomes.

FOOTNOTES

Author contributions: Xiao L collected the patient data and drafted the manuscript; Sun L revised the manuscript; Zhang JX performed image processing and wrote the manuscript; all authors read and approved the final manuscript.

Informed consent statement: Informed written consent was obtained from the patient for publication of this report and any accompanying images.

Conflict-of-interest statement: The authors declare that they have no conflict of interest to disclose.

CARE Checklist (2016) statement: The authors have read the CARE Checklist (2016), and the manuscript was prepared and revised according to the CARE Checklist (2016).

Country/Territory of origin: China

ORCID number: Lin Xiao 0000-0001-8644-1568; Lie Sun 0000-0001-5609-530X; Ji-Xin Zhang 0000-0002-4682-4985; Yi-Sheng Pan 0000-0001-7256-5017.

S-Editor: Chen YL
L-Editor: Wang TQ
P-Editor: Chen YL

REFERENCES

1 **Siegel RL**, Miller KD, Jemal A. Cancer statistics, 2015. *CA Cancer J Clin* 2015; **65**: 5-29 [PMID: 25559415 DOI: 10.3322/caac.21254]
2 **Sarosiek T**, Stelmaszuk M. [Small intestine neoplasms]. *Pol Merkur Lekarski* 2018; **44**: 45-48 [PMID: 29498365]
3 **Gill SS**, Heuman DM, Mihas AA. Small intestinal neoplasms. *J Clin Gastroenterol* 2001; **33**: 267-282 [PMID: 11588539 DOI: 10.1097/00004836-200110000-00004]
4 **Sun DS**, Shin OR, Ku YM, Kim YS, Seo KJ. Squamous cell carcinoma of the small bowel manifesting as a jejunal perforation: a case report. *Int J Clin Exp Pathol* 2014; **7**: 6345-6349 [PMID: 25337289]
5 **Battal M**, Bostancı O, Basak T, Kartal K, Ekiz F. Pure squamous cell carcinoma of the duodenum. *Case Rep Surg* 2015; **2015**: 714640 [PMID: 25785220 DOI: 10.1155/2015/714640]
6 **Bao Y**, Zhong ZX, Yu YW. Squamous cell carcinoma of small intestine: a case report. *Chin Med Sci J* 2014; **29**: 239-241 [PMID: 25429750 DOI: 10.1016/s1001-9294(14)60078-x]
7 **Nandedkar SS**, Trivedi KK, Malukani K. Primary squamous cell carcinoma of the small intestine. *J Cancer Res Ther* 2013; **9**: 739-740 [PMID: 24518732 DOI: 10.4103/0973-1482.126477]
8 **Mumtaz S**, Ahmad Z, Fatima S, Qureshi A. Squamous cell carcinoma in the small intestine. *BMJ Case Rep* 2011; **2011** [PMID: 22696720 DOI: 10.1136/bcr.01.2011.3762]
9 **Pan SY**, Morrison H. Epidemiology of cancer of the small intestine. *World J Gastrointest Oncol* 2011; **3**: 33-42 [PMID: 21461167 DOI: 10.4251/wjgo.v3.i3.33]
10 **Condino G**, Aratari A, Papi C, Catarci M. Gastrointestinal bleeding and severe anaemia: An uncommon presentation of small bowel carcinoma complicating ileal Crohn's disease. *Dig Liver Dis* 2015; **47**: 899-900 [PMID: 26205829 DOI: 10.1016/j.dld.2015.06.011]
11 **Schottenfeld D**, Beebe-Dimmer JL, Vigneau FD. The epidemiology and pathogenesis of neoplasia in the small intestine. *Ann Epidemiol* 2009; **19**: 58-69 [PMID: 19064190 DOI: 10.1016/j.annepidem.2008.10.004]
12 **Terada T**. Malignant tumors of the small intestine: a histopathologic study of 41 cases among 1,312 consecutive specimens of small intestine. *Int J Clin Exp Pathol* 2012; **5**: 203-209 [PMID: 22558474]
13 **Costa RS**, Vieira AL, Costa JM, Fernandes B, Ferreira A. Metastatic small bowel occlusion as initial presentation of squamous cell carcinoma of the lung. *Turk J Gastroenterol* 2019; **30**: 492-494 [PMID: 30460901 DOI: 10.5152/tjg.2018.18419]
14 **Yamada H**, Akahane T, Horiuchi A, Shimada R, Shibuya H, Hayama T, Nozawa K, Ishihara S, Matsuda K, Watanabe T. A case of lung squamous cell carcinoma with metastases to the duodenum and small intestine. *Int Surg* 2011; **96**: 176-181 [PMID: 22026313 DOI: 10.9738/1380.1]
15 **Yuksel O**, Uyar P, Sahin TT, Demirhan B. Small bowel perforation due to metastatic lung squamous cell carcinoma. *Saudi Med J* 2007; **28**: 631-633 [PMID: 17457493]
16 **Okamura T**, Beppu T, Tokumaru T, Yamada M, Sugiyama T, Koide N, Tani M, Kaneko M, Hamahata A, Nishimura Y, Fukuda T. Cancer of the mandibular gingiva metastasizing to the small intestine. *Auris Nasus Larynx* 2019; **46**: 479-482 [PMID: 30170905 DOI: 10.1016/j.anl.2018.08.006]
17 **Li R**, Chen Z, Wen Q. Metastatic squamous cell carcinoma from hand skin causing small bowel obstruction: an unusual case presentation. *World J Surg Oncol* 2014; **12**: 166 [PMID: 24885006 DOI: 10.1186/1477-7819-12-166]
18 **Wang M**, Patel J, Casey TT, Kieffer R, Dunn GD. Metastatic squamous cell carcinoma from the esophagus occurring as small bowel obstruction. *South Med J* 1985; **78**: 884-886 [PMID: 3925568 DOI: 10.1097/00007611-198507000-00030]
19 **Hulecki SJ**, Klein FA, Davis JE. Squamous cell carcinoma of cervix metastatic to ileal loop. *Urology* 1985; **26**: 579-580 [PMID: 4071870 DOI: 10.1016/0090-4295(85)90366-8]
20 **Deshpande SH**, Kini S, Nawalkar PR, Pandya JS. Metastasis of carcinoma of buccal mucosa to small intestine causing ileal perforation. *BMJ Case Rep* 2019; **12** [PMID: 31748358 DOI: 10.1136/bcr-2019-231449]
21 **Disibio G**, French SW. Metastatic patterns of cancers: results from a large autopsy study. *Arch Pathol Lab Med* 2008; **132**: 931-939 [PMID: 18517275 DOI: 10.5858/2008-132-931-MPOCRF]
22 **Wang FD**, Wang ZW, Xue HD, Wu HW, Zhang Y, Yu JC, Jin ZY. Primary Squamous Cell Carcinoma of the Small Intestine: Pathogenesis and Clinical Features. *Chin Med J (Engl)* 2016; **129**: 2131-2133 [PMID: 27569244 DOI: 10.4103/0366-6999.189067]
23 **Platt CC**, Haboubi NY, Schofield PF. Primary squamous cell carcinoma of the terminal ileum. *J Clin Pathol* 1991; **44**: 253-254 [PMID: 2013630 DOI: 10.1136/jcp.44.3.253]
24 **Estrella JS**, Wu TT, Rashid A, Abraham SC. Mucosal colonization by metastatic carcinoma in the gastrointestinal tract: a potential mimic of primary neoplasia. *Am J Surg Pathol* 2011; **35**: 563-572 [PMID: 21412071 DOI: 10.1097/PAS.0b013e318211b3d2]

25 **Puccini A**, Battaglin F, Lenz HJ. Management of Advanced Small Bowel Cancer. *Curr Treat Options Oncol* 2018; **19**: 69 [PMID: 30397729 DOI: 10.1007/s11864-018-0592-3]

26 **Xie X**, Zhou Z, Song Y, Dang C, Zhang H. Surgical Management and Prognostic Prediction of Adenocarcinoma of Jejunum and Ileum. *Sci Rep* 2017; **7**: 15163 [PMID: 29123252 DOI: 10.1038/s41598-017-15633-w]

Published by **Baishideng Publishing Group Inc**
7041 Koll Center Parkway, Suite 160, Pleasanton, CA 94566, USA
Telephone: +1-925-3991568
E-mail: bpgoffice@wjgnet.com
Help Desk: https://www.f6publishing.com/helpdesk
https://www.wjgnet.com